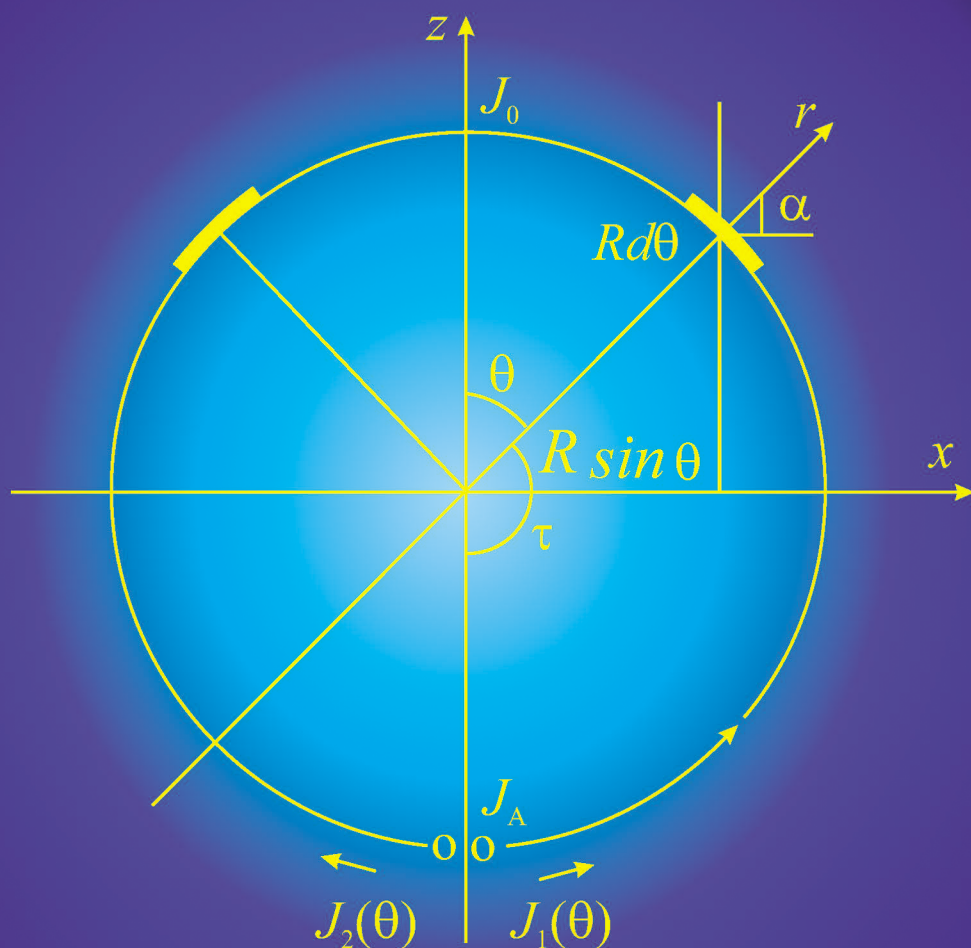


# ANTENNAS

From the Theory of Long Lines to Integral Equations

BORIS LEVIN



CRC Press  
Taylor & Francis Group

A SCIENCE PUBLISHERS BOOK

# ANTENNAS

---

From the Theory of Long Lines to Integral Equations

---

**Boris Levin**

Formerly Professor Holon Institute of Technology  
Holon, Israel



**CRC Press**

Taylor & Francis Group

Boca Raton London New York

---

CRC Press is an imprint of the  
Taylor & Francis Group, an **informa** business

A SCIENCE PUBLISHERS BOOK

First edition published 2025  
by CRC Press  
2385 NW Executive Center Drive, Suite 320, Boca Raton FL 33431  
and by CRC Press  
4 Park Square, Milton Park, Abingdon, Oxon, OX14 4RN

Copyright: © 2025 Boris Levin

*CRC Press is an imprint of Taylor & Francis Group, LLC*

Reasonable efforts have been made to publish reliable data and information, but the author and publisher cannot assume responsibility for the validity of all materials or the consequences of their use. The authors and publishers have attempted to trace the copyright holders of all material reproduced in this publication and apologize to copyright holders if permission to publish in this form has not been obtained. If any copyright material has not been acknowledged please write and let us know so we may rectify in any future reprint.

Except as permitted under U.S. Copyright Law, no part of this book may be reprinted, reproduced, transmitted, or utilized in any form by any electronic, mechanical, or other means, now known or hereafter invented, including photocopying, microfilming, and recording, or in any information storage or retrieval system, without written permission from the publishers.

For permission to photocopy or use material electronically from this work, access [www.copyright.com](http://www.copyright.com) or contact the Copyright Clearance Center, Inc. (CCC), 222 Rosewood Drive, Danvers, MA 01923, 978-750-8400. For works that are not available on CCC please contact [mpkbookspermissions@tandf.co.uk](mailto:mpkbookspermissions@tandf.co.uk)

*Trademark notice:* Product or corporate names may be trademarks or registered trademarks and are used only for identification and explanation without intent to infringe.

*Library of Congress Cataloging-in-Publication Data (applied for)*

ISBN: 978-1-032-58215-3 (hbk)  
ISBN: 978-1-032-58217-7 (pbk)  
ISBN: 978-1-003-44906-5 (ebk)

DOI: 10.1201/9781003449065

Typeset in Times New Roman  
by Prime Publishing Services

# Preface

=====

This book with an unusual title is devoted to the author's favorite topic - to the use of the theory of long lines in technical electrodynamics.

The objects studied by physics have different sizes: point, linear, volumetric. In particular, the main object of mechanics is a point. Radio physics also considers objects of different sizes. Elements of an electrical circuit: resistance, capacitor, inductor—as a rule, are considered point. The three listed elements form a resonant circuit—a kind of symbol of radio engineering. The objects considered by different scientific specialties differ in accordance with their subject matter. Concentrated loads are the main objects of electrostatics, electrical engineering, of transmitting and receiving circuits. The simplicity of the characteristics of a single element facilitates the calculation of circuits consisting of these elements.

Applied (technical) electrodynamics, unlike electrostatics, studies electromagnetic fields created by moving charges. The main objects of electrodynamics are extended elements, the simplest of which is a two-wire long line. Accordingly, in the qualitative analysis of the problems under consideration, in the case of electrodynamics, the main attention is paid to the properties of various variants of long lines.

Volumetric objects are the most complex. They occupy the surrounding space or part of this space. Such an object is an electromagnetic field. As is known, the theory of electromagnetism was created by Maxwell on the base of Faraday's all-round experiments, including the structure of field lines proposed by him. Maxwell's ingenious conjecture that along with the conduction current there is a displacement current led to the creation of a system of equations generalizing the known equations of electrical engineering. King wrote briefly and exactly about first antennas and first steps of antenna engineering in the article "The linear antenna—eighty years of progress".

The electromagnetic field theory proposed by Maxwell required the use of the most complex areas of mathematics, including mathematical analysis, set theory, variational and vector calculus. The use of integral and integral-differential equations for current and the expansion of their solutions into series has become a standard technique for analyzing the electrical characteristics of radiators. Mathematical programming is the necessary element of an antenna synthesis.

The new book on antenna analysis and synthesis takes an unusual approach and relies heavily on the long line theory. The application of this theory to the analysis of processes in antennas is not new, but is usually considered only as an auxiliary method. It is regarded insufficiently rigorous compared to the method of integral equations, when analyzing processes in known and proposed antennas, as well as



fields in the surrounding space. The specialists prefer to rely on numerical results of solving integral equations. Amateurs, as a rule, are limited to simple equivalent circuits, consisting of lumped elements.

The application of the theory of long lines, the dimensions of which are many times greater than the wavelength and are comparable to the distance to the infinitely remote surface of zero potential, corresponds to the physical content of antenna problems. In this case, the mathematical apparatus is greatly simplified. The result obtained with help of this theory has, as a rule, an approximate character, but is close to a rigorous solution, if it based on an understanding of the problem. At the same time, the nature of the solution dependence on individual parameters and the possibility of obtaining the desired characteristics are clarified. This result differs significantly from the calculation of randomly selected device options, which is known as a trial-and-error method. Unfortunately, the widespread use of the moments method did not change the results of a random choice and did not permit to solve separate problems.

For example, despite long attempts, it was not possible to apply the method of integral equations to a circular loop antenna with dimensions comparable to the wavelength. The theory of long lines makes it possible to solve such problems. Using the theory of long lines allows us to get an approximate solution (see Chapter 4).

Let us consider still a few examples.

Calculation of the radiation resistance of antennas by the method of Poynting vector requires to execute the intricate integration, since the dependence of the field on the distance to the observation point at an arbitrary angle  $\vartheta$  has a complex character. For  $\theta = \pi/2$  the formula for the field is simple. If we consider that the radiated power is determined on the infinitely distant spherical surface and the dimensions of the antenna are small compared with the distance to this surface, i.e., one can assume that the distance between any point of the antenna and this surface is constant, then the task is greatly simplified (see Chapter 3).

As is known, for a long time there was a contradiction between the reciprocity theorem and the method of induced emf. In the first formulation of the method of induced emf, the integrand was the product of two complex conjugate quantities  $EJ^*$ . The reciprocity theorem denies the fact of complex conjugacy. The problem became clearer when the equivalent long line was applied in the method of induced emf to calculate the resistance of losses caused by the skin effect, and this resistance turned out to be negative (see Chapter 3).

The physical approach to the problem makes it possible to explain the reason for the contradiction between the reciprocity theorem and the first formulation of the method of induced emf. Essentially, the reciprocity theorem states that the power transmitted from one antenna to another is independent of the direction of transmission, and the value of power is equal to  $EJ$  (to the product of the electric field and the current). Losses introduce a negative component into the magnitude of the electric field, which, in the presence of an asterisk, increases the power introduced by the source. This means that its presence is an obvious error, and the cause of the error is the use of reactive power, which has no physical meaning.

The law of energy conservation speaks of the conservation of instantaneous power, which consists of active power (radiation and losses) and oscillating power that passes from one region of space to another and from one reactance (for example,

an inductance) to another (to a capacitance, for example). This implies the need to analyze the oscillating power as a real physical quantity. The use of the concept of oscillating power led to the creation of the second formulation of the induced emf method, coincided with the result based on the reciprocity theorem. The second formulation permits to take into consideration the losses in the antenna and in the medium surrounding the antenna (see Chapter 3).

The solution of the integral equation for the current in the antenna is reduced to the calculation of the terms of the series. The first term of the series depends on the magnitude of the external emf. Each subsequent member of the series is caused with the appearance of an additional emf created by the previous member of the series [for the current]. Understanding this cause and communication allows us to calculate the new terms of the series and its total sum. A new method for solving the Leontovich's integral equation for current along a linear radiator made it possible to calculate the total sum of the series for a current and can be applied to other integral equations and to the analogical problems (see Chapter 4).

The combined application of the method of complex potentials and the theory of long lines allows solving many problems of calculating capacitances and long lines, the wires of which are located along the generatrices of three-dimensional structures (see Chapter 6). The introduction of an infinitely distant surface of zero potential is a natural addition to the theory of long lines and to the method of complex potentials. This addition allows us to solve the problems of energy flow distribution in the space surrounding the wires of a long line and the elements of a microstrip antenna, and to suggest the rigorous method for calculating the characteristics of a microstrip antenna (see Chapter 7).

We remember that through 20 years after Maxwell formulated his famous equations, which have established the foundations of classical electrodynamics, Henry Hertz experimentally proved the existence of wave phenomena predicted by these equations. Hertz, who preferred Helmholtz's theory of electrostatic and electrodynamic forces, during its experimental verification concluded that Maxwell's approach was correct, simplified his system of equations and became the first person to observe the process of transmission of electromagnetic oscillations between two open circuits. To this he was using a spark gap, which excited damped oscillations in a wire of length 60 cm with metal plates at the ends. Experiment of Hertz gave a start to the future stormy development of radio engineering.

The system of expressions for electromagnetic field, complemented with boundary conditions on the surface of some or other antenna, allows to write the equation for a current in the antenna wire. Solving this equation and finding the current distribution along the wire, one can determine the electrical characteristics of a radiator. But in the first decades after Hertz' works the researches were interested in other matters. Engineers were trying to solve the problem of a signal reception. Among them names of Marconi and Popov are best known. In 1894, 23-year-old Rutherford made a device for receiving radio signals, which was based on demagnetizing of a bunch of needles, and even demonstrated it to Marconi, and the latter undertook to improve it. The transmission problem was solved by the invention of radio tubes. And the power of radio tubes began to grow from year to year.

The radio technology developed in three directions and led to the creation of radio receivers, radio transmitters and antennas. The calculation of processes in receivers and transmitters turned out to be simpler, since it in the first approximation considered circuits consisting from the same concentrated loads, but in the case of transmitters it was complicated by using of high powers. At the same time, scientific problems were not limited to the calculation of loads. For example, mathematical difficulties were associated with the calculation of transients based on the application of the Laplace transform (operational calculus). Basically, the calculations were reduced to the Kirchhoff equations. The analysis of electromagnetic vector fields required the use of functions such as gradient, divergence and curl (to simplify this utilization, a special quantity “nabla” had to be introduced) and extensive use of integral equations for the current. The theory of equivalent long lines greatly facilitated the approach to these problems, but did not eliminate the need for their rigorous solution. Repeated attempts have been made to simplify the solution of complex problems, limiting themselves to replacing complex antennas with simple equivalents such as an “elementary dipole”. But, as King pointed out, such a method bypasses the main issues of antenna problems and does not solve them.

As follows from what has been said, the proposed book extensively applies the partial equivalence of antennas and corresponding long lines. Results obtained by rigorous methods are compared with approximate ones, this allows to expand the scope of approximate methods, in particular, using them to analyze the influence of individual parameters on antenna characteristics. An appropriate analysis is sometimes necessary and does not follow from the numerical results obtained by the method of moments.

In addition to what has been said about the content of the book, it is worth dwelling on the sharp jump in the development of antenna technology in the middle of the last century and the explosive wave of new results obtained after this jump. The development of any new technology has a stepwise character. In the middle of the last century, it might seem that the development of antenna technology has stopped. The induced emf method confidently took over the calculation of the electrical characteristics of antennas. Unfortunately, it was insufficiently rigorous and precise and did not allow analyzing complex radiators.

In 1941, Stratton’s famous book “The Theory of Electromagnetism” was published, which was later named golden one. In this book, as a rigorous method for analyzing a straight linear antenna, it was recommended to use a method based on calculating the eigenfunctions of a spheroid (a prolate ellipsoid with an eccentricity slightly different from unity). This proposal was clearly pessimistic, because the calculation of spheroidal functions is complicated, and the method gives an approximate result and is applicable practically only to one simplest antenna. Therefore, it might seem that the powerful blast wave that soon arose and was concerned with to creation and solution of integral equations for currents in antennas became a kind of reaction to this pessimistic forecast. Nevertheless, the work on the calculation method using spheroidal eigenfunctions was brought to the known numerical results, like the known ones, and forever forgotten due to the limited possibilities of theirs use.

A second attempt to use a spheroid was made to calculate the field of a linear antenna mounted on a support in the form of rod (after an unsuccessful attempt to use a hemisphere as the equivalent of a rod). Experimental verification showed that the hemisphere and hemispheroid are not suitable for the role of equivalents. Calculating the radiation pattern of a linear radiator with an elevated feed point gives much more accurate results.

Since then, books on antennas begin with an analysis of a direct linear radiator, as the calculation of a complex radiator can be performed by dividing it into simple elements. A straight, perfectly conducting filament with a very small radius or a tube with a finite radius are taken as models. The conduction current  $J(z)$  flows along the filament and the tube. When the radiator is excited by one generator, the current distribution is sinusoidal, like the current distribution in a uniform two-wire long line. This assumption is based on the simple idea that the current distribution along the metal wires of an open at the end two-wire line does not change significantly, when the wires are separated in different directions. The validity of this approach is confirmed by the measurement results. The solution of integral equations for the current in the straight radiator shows that the sinusoidal distribution is the first approximation to the true distribution.

The wave that arose in the middle of the last century led to a powerful advance of the theory and to the development of many new antenna options. As can be seen from what has been said, the use of a complex mathematical apparatus of integral equations became the source of the blast wave. The development of computer technology has maintained the powerful character of the wave for a long time. Using King's terminology, we can say that the appearance of the wave was the beginning of another 80-year stage of progress in the development of antenna theory and technology. The goal of researchers and engineers was to solve the problems left by the previous generation and to develop the new designs of antennas. But it does not make sense to describe the results of this development in the introduction, because the whole book is devoted to this.

This book begins with a description of the properties of long lines, equivalent to metal and impedance antennas, and antenna analysis methods based on calculating the characteristics of long lines. The book presents and sequentially describes both known and new results. In the sections devoted to the use of integral equations for the current in a linear metal radiator, the main attention is paid to the Leontovich's equation. An important advantage of this equation is the simplicity of the solution and the absence of the argument  $\varphi$  in it, because the integration over  $\varphi$  already performed. The refined solution made it possible to determine the total sum of the series for the current, which is close to the known solution including only the first terms (maintaining the fundamental conclusions made earlier). The results of the synthesis of different types of antennas with capacitive loads are presented, which made it possible to implement Hallen's hypothesis about the usefulness of applying such loads to create an in-phase current distribution in antennas and to obtain required characteristics.

During the blast wave, along with linear radiators, the methods for calculating loop antennas were actively developed. Unfortunately, it was not possible to write and solve an integral equation for the current in a loop of arbitrary shape and size.

Apparently, Leontovich's co-author M. Levin achieved maximum results by applying the theory of long lines to a circular loop. But his work did not appear in the open press. The author of this book has taken the liberty to repeat the results of his famous namesake (see Chapter 4).

The special chapter is devoted to the application of the complex potential method. New results include the widespread use of this method in relation to the calculation of capacitive structures in homogeneous and inhomogeneous media, to analysis of antenna directional patterns and field flows of electrical fields between antenna elements and in the surrounding space. In particular, the analysis of flows of electrical fields made it possible to substantiate a rigorous method for analyzing microstrip antennas, whose are distinguished by their simplicity and wide range of applications. [A method for calculating a large loop antenna based on the theory of long lines is proposed.] The characteristics of antennas in various conditions of their installation are considered and compared. The results of the use of multi-floors structures that provide radiation in the direction perpendicular to the antenna axis, and structures that make it possible to reduce the mutual influence of antennas located at different heights on a common mast are described.

The book covers a wide variety of the antennas proposed by the designers, including linear radiators with constant and changing along the length surface impedance, with constant and switching loads, with resistive covering and the absorbers, multi-wire, and multi-radiator antennas, folded and multi-folded designs, for different frequency ranges, for underground communication. New methods for analyzing and synthesizing antennas are proposed, including the method of electrostatic analogy, methods for reducing three-dimensional problems to flat ones. It is considered the results of applying the methods of compensation, of the struggles with interference caused by the influence of moving metal objects etc. The method of electrostatic analogy provides an increase of the directivity of director-type antennas and promises to reduce the dimensions of the log-periodic antennas.

The author also tried to define more exactly, correct, and explain many of the previously obtained results and to include in the new book detailed links to materials previously published in various sources, for which there is not enough space in the new book.

The proposed book is a natural addition to the known monographs. It is intended for professionals, who are engaged in the development, placement, and exploitation of antennas and for lecturers, teachers, students, advisors, etc. The contents of the book can be used for university courses.

# Contents

<i>Preface</i>	iii
<b>1. From Straight Radiators to Long Lines</b>	<b>1</b>
1. Electromagnetic Field	1
2. Sinusoidal Currents of Radiators	4
3. Equivalent Long Line	10
4. Multi-wire and Multi-radiator Structures of Antennas	15
5. Folded Radiators	23
6. Folded Radiators with Wires of Different Length	29
7. Multi-folded Radiators	35
8. Antenna with Meander Load	41
References	51
<b>2. Impedance and Complementary Antennas</b>	<b>53</b>
1. Radiator with Inductive Surface Impedance	53
2. Impedance Folded Radiators	65
3. Principles of Similarity and Duality	73
4. Impedance Magnetic Antennas	80
5. Radiators with Resistive Surface Impedance	86
6. Principle of Complementarity and Self-complementary Antennas	92
7. Antenna on Pyramid Edges	99
8. Self-complementary Antennas with Rotational Symmetry	106
References	117
<b>3. Antenna Analysis Based on Long Lines' Theory</b>	<b>119</b>
1. Hertz Dipole	119
2. Method of Poynting and Resistance of an Antenna Radiation	121
3. Measurement of an Antenna Gain in a Fresnel Zone	140
4. Oscillating Power Theorem	149
5. Method of Induced Emf and an Antenna Reactance	152
6. Loss Resistance in the Ground	161
7. Loss Resistance in the Wires	172
8. Reciprocity Theorem	175
References	181
<b>4. Integral Equations for Radiators' Currents</b>	<b>183</b>
1. Hallen's Equations	183
2. Leontovich's Equation	186

3. Method of constants' Variation	190
4. Integral Equation for Two Metal Radiators	198
5. Radiators with Distributed Loads	203
6. Integral Equations for a System of Radiators	213
7. Loop Antenna with Large Dimensions	217
8. Shapes of Small Loop Antenna	223
9. Not Linear Structures	230
10. Emergency Load	234
References	239
<b>5. The Problems of Analysis</b>	<b>241</b>
1. Generalized Method of Induced Emf	241
2. Effect of Volume Metal Designs on Antenna Characteristics	246
3. Influence of Installation Site	254
4. Method of Complex Potential	268
5. Piecewise Homogeneous Media	273
6. Characteristics of Directivity of Antennas Arrays	280
7. Calculating Directivity Factor with Help of Main Directional Patterns	288
8. Anechoic Chambers	292
9. Turn of the Directional Pattern	297
10. Method of Compensation and a Cell Phone	300
11. New Antenna for a Personal Cellular Phone	313
12. Struggle with Environmental Influences	321
References	327
<b>6. Application of Method of Complex Potential</b>	<b>329</b>
1. Symmetrical Cable of Delay and Coaxial Chamber for Calibrating Measuring Devices	329
2. Calculation of Capacitances	334
3. Intersecting Wires on the Boundary of Two Mediums	340
4. Capacitances in a System of a Few Conductors	344
5. A Long Line from Converging Straight Wires and a Slotted Antenna on a Cone	346
6. Field of a Long Line from Converging Parabolic Wires	358
7. Distribution of Energy Flow between the Wires of the Long Line and Antenna	367
8. Reflector Arrays from Microstrip Antennas	376
References	383
<b>7. Synthesis Problems</b>	<b>384</b>
1. In-phase Current Distribution	384
2. Method of Mathematical Programming	400
3. Application of Results to Concrete Tasks	405
4. Method of Electrostatic Analogy	415
5. New Options of Log-periodic Antennas	422
6. Curvilinear Radiator	434

7. Director-type Antenna	441
8. Microstrip Antennas with In-phase Current Distribution	446
References	449
<b>8. Some Types of Antennas and Cables</b>	<b>450</b>
1. Loop and Folded Antennas with Capacitors	450
2. Multi-tiered Antennas	457
3. Antennas for Underground Communication	466
4. Antenna for Coast Radio Center	471
5. Ship's Antennas for Medium Frequency Waves	474
6. Short-wave Antennas	482
7. Antennas of Meter and Decimeter Waves	495
8. Reciprocal Coupling between Coaxially Disposed Radiators	496
9. Multi-wire Cables	506
References	516
<i>Types of Antennas</i>	<b>519</b>
<i>Index</i>	<b>520</b>





# Taylor & Francis

Taylor & Francis Group

<http://taylorandfrancis.com>

# From Straight Radiators to Long Lines

## 1. Electromagnetic Field

The simplest radiators are symmetric and asymmetric electric radiators of finite length (Fig. 1). A symmetrical radiator (dipole) is a straight-line conductor, whose currents in points symmetrical about its center are equal in magnitude and have the same direction. To create such a current distribution, an electromotive force (emf) source is included in the radiator middle, which divides the radiator into two arms with the same length  $L$  (Fig. 1a). An asymmetrical radiator is a straight conductor, excited by emf source displaced from its middle (Fig. 1b). A special case of an asymmetric radiator is a monopole (Fig. 1c). This is a conductor with an emf at the base, established perpendicular to a metallic surface. The metallic surface radiation replaces the radiation of the lower arm of the dipole. All these radiators are widely used in antenna technology. In addition, more complex antennas can be analyzed by breaking them into simple elements in the form of symmetrical or asymmetrical radiators. The significance of the theory of simple radiators relates to this.

The modern theory of antennas is based on Maxwell's equations—the basic equations of electrodynamics. The first two of them in the differential form appear as

$$\text{curl } \vec{H} = \vec{j} + \frac{\partial \vec{D}}{\partial t}, \quad \text{curl } \vec{E} = -\frac{\partial \vec{B}}{\partial t}, \quad (1.1)$$

where  $\vec{H}$  is a vector of magnetic field strength,  $\vec{j}$  is a vector of volume density of conduction current,  $\vec{D}$  is a vector of electric displacement,  $t$  is time,  $\vec{E}$  is a vector of electric field strength,  $\vec{B}$  is a vector of magnetic induction. Hereinafter the International System of Units is used. The equation (1.1) are to be complemented with an equation of continuity

$$\text{div } \vec{j} = \frac{\partial \rho}{\partial t}, \quad (1.2)$$

where  $\rho$  is a volume density of an electrical charge.

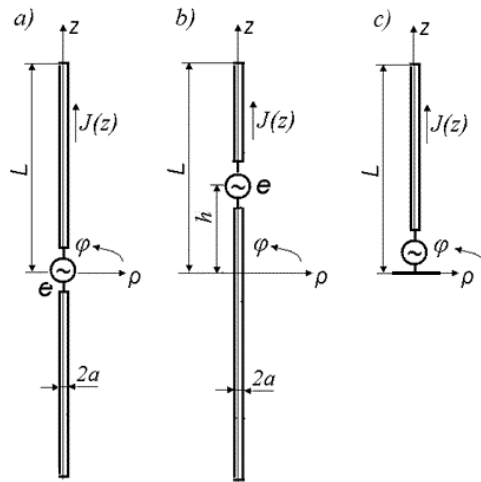


Fig. 1: Symmetrical (a) and asymmetrical (b) metal radiators and monopole (c) from cylindrical wires.

Usually, two more equations are included into a system of Maxwell's equations:

$$\operatorname{div} \vec{D} = \rho, \operatorname{div} \vec{B} = 0, \quad (1.3)$$

but they follow from the equations (1.1) and (1.2) [1].

The equation (1.1) interconnect the electromagnetic fields and current in free space. Both currents and electric and magnetic components of fields exist jointly only. From (1.1) и (1.2) it follows for a harmonic field time-varying as  $\exp(j\omega t)$  and an isotropic medium ( $D = \epsilon E$ ,  $B = \mu H$ ) that

$$\operatorname{curl} \vec{H} = \vec{j} + j\omega \epsilon \vec{E}, \operatorname{curl} \vec{E} = -j\omega \mu \vec{H}, \operatorname{div} \vec{j} + j\omega \rho = 0. \quad (1.4)$$

The antenna field is created by the power received from the radio transmitter. This means that radiation of an antenna is result of the influence of another medium. In order to take it into account consideration, the set of equations in accordance with the equivalence theorem should include extraneous (external) currents and fields as the original sources of excitation. They are introduced into the quantities  $\vec{j}$ ,  $\vec{E}$  and  $\vec{H}$  in the capacity of summands. Their nature and placement depend on the model of the area near a generator, which is commonly called the 'excitation zone'. The total electromagnetic field of an antenna is equal to a sum of the fields produced by the excitation zone and the fields produced by the wires' currents, arising when the source is turned on. As a rule, on the great distance from the antenna the first field is substantially less than the second one and can be neglected.

Maxwell's equations for electromagnetic field, which for any antenna are complemented with boundary conditions, allow to write the equation for the current in the conductors of an antenna, to find the current distribution along these conductors and to determine the electrical characteristics of the radiator.

An investigation of an electromagnetic field can be simplified by introducing auxiliary functions, which are called potentials. The auxiliary vector field (vector potential) is introduced by means of confrontation the mathematical expression  $\text{div curl } \vec{A} = 0$ , where  $\vec{A}$  is an arbitrary vector, and the second equation of (1.3). At that it is not difficult to verify that the vector  $\vec{B}$  can be presented as a curl (rotor) of some vector  $\vec{A}$ :

$$\vec{B} = \text{curl } \vec{A}. \quad (1.5)$$

Yet, equality (1.5) determines the vector  $\vec{A}$  ambiguously. To define it unambiguously, one should also specify the value of  $\text{div } \vec{A}$ . Substituting (1.5) into the second equation of system (1.4) and using mathematical identity of

$$\text{curl grad } U = 0,$$

where  $U$  is an arbitrary scalar function (a scalar potential of field), we get

$$\vec{E} = -j\omega\vec{A} - \text{grad } U. \quad (1.6)$$

Substituting (1.5) and (1.6) into the first equation of system (1.4) and considering the mathematical identity

$$\text{curl curl } \vec{A} = \text{grad div } \vec{A} - \Delta \vec{A},$$

we are finding:

$$\Delta \vec{A} + \omega^2 \mu \epsilon \vec{A} - \text{grad}(\text{div } \vec{A} + j\omega \mu \epsilon U) = -\mu \vec{j}. \quad (1.7)$$

Let us define  $\text{div } \vec{A}$  in such a way as to simplify the last expression as far as possible. For this purpose, we will put

$$\text{div } \vec{A} = -j\omega \mu \epsilon U. \quad (1.8)$$

This equality is known as the calibration condition, or Lorentz's condition. In accordance with (1.7) and (1.8),

$$\vec{A} + k^2 \vec{A} = -\mu \vec{j}, \quad (1.9)$$

where  $k = \omega\sqrt{\mu\epsilon}$  is a wave propagation constant in the medium surrounding the antenna. Equation (1.9) is called the vector wave equation. Its solution allows us to find the vector potential  $\vec{A}$ , and then the electric and magnetic fields of the antenna. Indeed, according to (1.5), (1.6) and (1.8)

$$\vec{E} = -j\frac{\omega}{k^2}(\text{grad div } \vec{A} + k^2 \vec{A}) = -j\omega\vec{A} - j\frac{1}{\omega\mu\epsilon} \nabla(\nabla \cdot \vec{A}), \quad \vec{H} = \frac{1}{\mu} \text{curl } \vec{A} = \frac{1}{\mu} \nabla \times \vec{A}. \quad (1.10)$$

If the electromagnetic field sources are distributed continuously in a certain region  $V$ , and the surrounding medium is a homogeneous isotropic dielectric, then the solution of an equation (1.9) for harmonic field has the form

$$\vec{A} = \frac{\mu}{4\pi} \iiint_{(V)} \vec{J} \frac{e^{-jkR}}{R} dV, \quad (1.11)$$

where  $R$  is the distance from the observation point (in the medium) to the point of integration (in the area  $V$ ). The expression (1.11) can be written as

$$\vec{A} = \mu \iiint_{(V)} \vec{J} G dV, \quad (1.12)$$

where  $G = \frac{\exp(-ikR)}{4\pi R}$  is the Green's function.

In accordance with (1.8), (1.12) and the continuity equation, we will obtain a similar expression for the scalar potential:

$$U = j \frac{1}{\omega\epsilon} \iiint_{(V)} G \operatorname{div} \vec{J} dV = \frac{1}{\epsilon} \iiint_{(V)} \rho G dV. \quad (1.13)$$

It should be noted that the region  $V$ , where the sources of the electromagnetic field are located, can be multiply connected (if, for example, one must regard radiation of several antennas or a few metal bodies are located close to one antenna).

Presented results, obtained with help of expressions for the volumetric derivatives of the scalar and vector fields, are given in accordance with Chapter 2 of the book [2] (Thiele G.A. Wire antennas). A parallel variant based on the use of the operator  $\nabla$ , is presented in accordance with the book [3].

## 2. Sinusoidal Currents of Radiators

We will consider the variants of radiators from the particular case when the source of the electromagnetic field is the electric current, having axial symmetry and located parallel to the  $z$  axis in a certain region  $V$ :

$$j = j_z \vec{e}_z, j_z = j_z(z) = \operatorname{const}(\varphi). \quad (1.14)$$

Here, the cylindrical system of coordinates  $(\rho, \varphi, z)$  is used, with unit vectors (orts)  $\vec{e}_\rho, \vec{e}_\varphi, \vec{e}_z$  along the axes. As seen from (1.12), the vector potential in this case has only the component  $A_z$ :

$$\vec{A} = A_z(\rho, z) \vec{e}_z, \quad (1.15)$$

i.e.,

$$\operatorname{div} \vec{A} = \frac{dA_z}{dz}, \operatorname{grad} \operatorname{div} \vec{A} = \frac{\partial^2 A_z}{\partial \rho \partial z} \vec{e}_\rho + \frac{\partial^2 A_z}{\partial z^2} \vec{e}_z, \operatorname{curl} \vec{A} = -\frac{\partial A_z}{\partial \rho} \vec{e}_\varphi,$$

and in accordance with (1.10)

$$E_z(\rho, z) = -j \frac{\omega}{k^2} (k^2 A_z + \frac{\partial^2 A_z}{\partial z^2}), E_\rho(\rho, z) = -\frac{j\omega}{k^2} \frac{\partial^2 A_z}{\partial \rho \partial z}, H_\varphi(\rho, z) = -\frac{1}{\mu} \frac{\partial A_z}{\partial \rho},$$

$$E_\varphi = H_z = H_\rho = 0. \quad (1.16)$$

Obviously, if the distribution of current  $\vec{J}(z)$  along the radiator is known, one can calculate the electromagnetic field of the current with the help of presented formulas. If the antenna is excited at some point (e.g.,  $z = 0$ ) by a generator with concentrated emf  $e$ , the antenna input impedance at the driving point is

$$Z_A = \frac{e}{J(0)}, \quad (1.17)$$

and in order to determine this impedance, it is enough to know the current magnitude at the corresponding point. When calculating the power absorbed in the load of a receiving antenna also it is need to know the current magnitude. Thus, the current distribution along an antenna is a very important characteristic.

As a simple and clear model of a vertical linear radiator, one can use a straight perfectly conducting filament, coinciding with the  $z$  axis (Fig. 2a), along which the conduction current  $\vec{J}(z)$  flows. Current density  $\vec{J}(s, z)$  is related to this current by a relation

$$\vec{J}(z) = \iint_{(s)} \vec{J}(s, z) ds, \quad (1.18)$$

where  $s$  is the filament cross-section. From (1.12) and (1.16)

$$A_z(\rho, z) = \mu \int_{-L}^L J(z') G dz', E_z(\rho, z) = \frac{1}{j\omega\epsilon} \int_{-L}^L J(z') \left( k^2 G + \frac{\partial^2 G}{\partial z^2} \right) dz'. \quad (1.19)$$

Here  $G = G_1 = \exp(-jkR_1)/(4\pi R_1)$ , distance  $R_1$  from observation point  $M$  to integration point  $P$  is equal to  $R_1 = \sqrt{(z - z')^2 + \rho^2}$ .

In the considered model the radiator radius is zero. The model of a radiator shaped as a straight circular thin-wall cylinder (tube) with radius  $a$  (Fig. 2b) has finite dimensions. Both ends of the cylinder are left open, without covers, in order that the current as before had only a longitudinal component. The surface density of current along the cylinder is  $J_s(z) = J(z)/2\pi a$ . Since a volume element in the cylindrical system of coordinates is equal to  $dV = \rho d\rho d\varphi dz$ , and  $\rho = a$  on the cylinder surface, then, in accordance with (1.12) and (1.16),

$$A_z(\rho, z) = \frac{\mu}{2\pi} \int_{-L}^L J(z') \int_0^{2\pi} G d\varphi' dz', E_z(\rho, z) = \frac{1}{2\pi j\omega\epsilon} \int_{-L}^L J(z') \int_0^{2\pi} \left( k^2 G + \frac{\partial^2 G}{\partial z^2} \right) d\varphi' dz', \quad (1.20)$$

where  $G = G_2 = \exp(-jkR_2)/(4\pi R_2)$ , distance  $R_2$  from observation point  $M$  to integration point  $P$  is equal to  $R_2 = \sqrt{(z - z')^2 + \rho^2 + a^2 - 2a\rho \cos\varphi'}$ . In particular, if the observation point is located on the radiator surface,  $R_2 = \sqrt{(z - z')^2 + 4a^2 \sin^2 \varphi/2}$ .

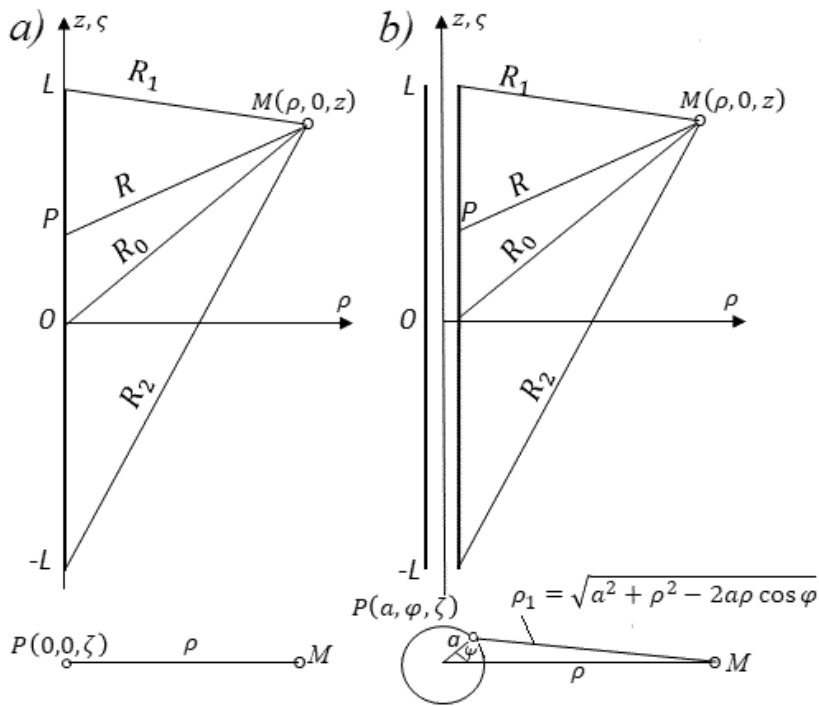


Fig. 2: The dipole models in the shape of a straight filament (a) and a thin-wall circular cylinder (b).

As said above, the knowledge of a current distribution along the radiator allows us to determine all its electrical characteristics. An assumption that this distribution has a sinusoidal form played an important role in the theory of antennas. The sinusoidal form is confirmed by a character of expressions (1.16), (1.19) and (1.20) for a vertical (longitudinal along  $z$  axis) component of an electric field created by the antenna current. Partly this assumption was based on measurement results. But mainly it is based on a simple understanding that the sinusoidal current distribution existing in the two-wire long line open at the end does not change significantly, if the wires are spread apart and located at an angle to each other. Later on, in the derivation and solution of integral equations for currents in radiators, it was rigorously shown that the sinusoidal distribution is the first approximation to the true current distribution along the antenna, and from this point of view, its use is quite reasonable and has a reliable justification.

We will suppose that the linear current along a symmetrical cylindrical radiator (see Fig. 1a) obeys the law

$$J(z) = I_n \frac{\sin k(L - |z|)}{\sin kL}. \quad (1.21)$$

If we use a perfectly conducting filament as a model of a symmetrical radiator, then in accordance with (1.19)

$$E_z = \frac{1}{4\pi j\omega\epsilon} \int_0^L J(z') \left( k^2 + \frac{\partial^2}{\partial z'^2} \right) \left( \frac{e^{-jkr}}{R} + \frac{e^{-jkr_+}}{R_+} \right) dz'. \quad (1.22)$$

This expression takes into account the symmetry of the currents in the radiator arms. Accordingly, if to replace at the lower arm the variable  $-\zeta$  by the variable  $\zeta$  and to use designations  $R = \sqrt{(z + \zeta)^2 + \rho^2}$  and, then, because

$$\frac{\partial R}{\partial \zeta} = -\frac{\partial R}{\partial z}, \frac{\partial R_+}{\partial \zeta} = \frac{\partial R_+}{\partial z}, \frac{\partial^2 R}{\partial \zeta^2} = \frac{\partial^2 R}{\partial z^2}, \frac{\partial^2 R_+}{\partial \zeta^2} = \frac{\partial^2 R_+}{\partial z^2},$$

we obtain

$$E_z = \frac{1}{4\pi j\omega\epsilon} \int_0^L J(\zeta) \frac{\partial^2}{\partial \zeta^2} \left[ \frac{\exp(-jkR)}{R} + \frac{\exp(-jkR_+)}{R_+} \right] d\zeta + \frac{k^2}{4\pi j\omega\epsilon} \int_0^L J(\zeta) \left[ \frac{\exp(-jkR)}{R} + \frac{\exp(-jkR_+)}{R_+} \right] d\zeta.$$

Twice integrating the first term of the expression by parts, we find

$$E_z = \frac{1}{4\pi j\omega\epsilon} \left\{ \int_0^L \left[ \frac{d^2 J(\zeta)}{d\zeta^2} + k^2 J(\zeta) \right] \left[ \frac{\exp(-jkR)}{R} + \frac{\exp(-jkR_+)}{R_+} \right] d\zeta + J(\zeta) \frac{\partial}{\partial \zeta} \left[ \frac{\exp(-jkR)}{R} + \frac{\exp(-jkR_+)}{R_+} \right] \Big|_0^L - \frac{dJ(\zeta)}{d\zeta} \left[ \frac{\exp(-jkR)}{R} + \frac{\exp(-jkR_+)}{R_+} \right] \Big|_0^L \right\}. \quad (1.23)$$

If the current along the radiator is distributed in accordance with (1.21), the first multiplier in the integrand and hence the first term of the expression (1.23) is zero. As it is easy to be convinced, the second summand is zero too, since its first multiplier becomes zero at  $\zeta = L$  and the second multiplier vanishes at  $\zeta = 0$ . The derivative of the current distribution function is equal to

$$\frac{dJ(\zeta)}{d\zeta} = -kJ(0) \frac{\cos k(L - |\zeta|)}{\sin kL} \text{sign} \zeta, \quad (1.24)$$

where *sign*  $\zeta$  means sign of  $\zeta$ . As result, we obtain

$$E_z = -j \frac{30J(0)}{\epsilon_r \sin kL} \left[ \frac{\exp(-jkR_1)}{R_1} + \frac{\exp(-jkR_2)}{R_2} - 2 \cos kL \frac{\exp(-jkR_0)}{R_0} \right]. \quad (1.25)$$

Here it is taken into consideration that  $\frac{k}{4\pi\omega\epsilon_0} = 30$ . The distances between the observation point M and the upper and lower ends and the radiator middle are equal respectively to  $R_1 = \sqrt{(z + L)^2 + \rho^2}$ ,  $R_2 = \sqrt{(z - L)^2 + \rho^2}$ ,  $R_0 = \sqrt{z^2 + \rho^2}$  (Fig. 2a).

If the current distribution along the antenna has a stepped character, and there are voltage jumps at the boundaries of the segments, i.e., function  $\partial J / \partial \zeta$  has a discontinuity, then

$$E_z = \frac{1}{4\pi j\omega\epsilon} \left\{ \frac{2\exp(-jkR_0)}{R_0} \frac{dJ(0)}{d\zeta} - \left[ \frac{\exp(-jkR_{11})}{R_{11}} + \frac{\exp(-jkR_{12})}{R_{12}} \right] \frac{dJ(L)}{d\zeta} + \sum_{m=1}^M \left[ \frac{\exp(-jkR_{m1})}{R_{m1}} - \frac{\exp(-jkR_{m2})}{R_{m2}} \right] \left[ \frac{dJ(l_m + 0)}{d\zeta} - \frac{dJ(l_m - 0)}{d\zeta} \right] \right\}, \quad (1.26)$$



where  $R_0 = \sqrt{a^2 + \zeta^2}$ ,  $R_{m1} = \sqrt{a^2 + (l_m - \zeta)^2}$ ,  $R_{m2} = \sqrt{a^2 + (l_m + \zeta)^2}$ ,  $\frac{dJ(l_m + 0)}{d\zeta}$  and  $\frac{dJ(l_m - 0)}{d\zeta}$  are values of derivatives to the right and left of the point  $z = l_m$ ,  $a$  is an antenna radius in the point  $\zeta$ ,  $M$  is the number of such discontinuities in each arm of the antenna.

As can be seen from (1.16), if the electric current, which excites the electromagnetic field, is directed in parallel to the  $z$  axis and has axial symmetry, then together with  $E_z$ , the normal component of the electric field  $E_\rho$  and the tangential component of the magnetic field  $H_\phi$  also do not equal to zero. These components can be calculated similarly to  $E_z$ , i.e., in accordance with (1.16). However, it is easier to use the first Maxwell's equation. Let's write this equation in a cylindrical coordinate system:

$$-\frac{\partial H_\phi}{\partial z} = j\omega\epsilon E_\rho, \quad \frac{1}{\rho} \frac{\partial}{\partial \rho} (\rho H_\phi) = j\omega\epsilon E_z + j_z. \quad (1.27)$$

Since  $\frac{\partial}{\partial \rho} [\exp(-jkR_i)] = \frac{k_\rho}{jR_i} \exp(-jkR_i)$ , where  $i = 0, 1, 2$ , then (1.25) can be rewritten as

$$E_z = \frac{30J(0)}{k_\rho \epsilon_r \sin kL} \frac{\partial}{\partial \rho} [\exp(-jkR_1) + \exp(-jkR_2) - 2 \cos kL \exp(-jkR_0)].$$

Comparing this expression with the second equation in (1.27) and considering that in an arbitrary point  $M$   $i_z = 0$ , we find:

$$H_\phi = j \frac{J(0)}{4\pi\rho \sin kL} [\exp(-jkR_1) + \exp(-jkR_2) - 2 \cos kL \exp(-jkR_0)]. \quad (1.28)$$

Substituting (1.28) into the first expression of (1.27), we get

$$E_\rho = j \frac{30J(0)}{\epsilon_r \rho \sin kL} \left[ \frac{(z-L)\exp(-jkR_1)}{R_1} + \frac{(z+L)\exp(-jkR_2)}{R_2} - 2z \cos kL \frac{\exp(-jkR_0)}{R_0} \right]. \quad (1.29)$$

If we use the radiator model in the form of a straight circular cylinder, then when calculating the field, one should proceed from the expression (1.20). Repeating the arguments and carrying out calculations similar to the case with a perfectly conducting thread, we find instead of (1.25)

$$E_z = -j \frac{30J(0)}{2\pi\epsilon_r \sin kL} \int_0^{2\pi} \left[ \frac{\exp(-jkR_1)}{R_1} + \frac{\exp(-jkR_2)}{R_2} - 2 \cos kL \frac{\exp(-jkR_0)}{R_0} \right] d\phi, \quad (1.30)$$

where  $R_1 = \sqrt{(z-L)^2 + \rho^2 + a^2 - 2a\rho\cos\varphi}$ ,  $R_2 = \sqrt{(z+L)^2 + \rho^2 + a^2 - 2a\rho\cos\varphi}$ ,  $R_0 = \sqrt{z^2 + \rho^2 + a^2 - 2a\rho\cos\varphi}$  are distances from the observation point to points on

the radiator surface in the upper, lower and middle cross-sections of the radiator, respectively (Fig. 2b). As for the other components of the electromagnetic field ( $H_\varphi$  and  $E_\rho$ ), their calculation is complicated by the fact that  $\frac{\partial}{\partial \rho} [\exp(-jkR_i)] = \frac{k(\rho - a \cos \varphi)}{jR_i} \exp(-jkR_i)$ . Therefore, the field  $E_z$  cannot be represented in the form similar to (1.27).

Expressions (1.25) and (1.30) for the fields  $E_z$ , created by the currents flowing in radiator models in the form of a straight ideally conducting filament and a straight circular tubes are valid for arbitrary observation points, including those lying on the radiator surface. It is easy to be convinced, however, that the tangential component of the electric field does not vanish when substituting  $\rho = 0$  into the first expression and to substitute  $\rho = a$  into the second one. On the contrary, at the indicated values of  $\rho$ , the value  $E_z$  sometimes becomes maximum.

In Fig. 3 the typical curves presented in the book [4] for the real and imaginary components of the field  $E_z$  are given as function of  $z$  coordinate. The curves are constructed in accordance with the expression (1.25), i.e., for a perfectly conductive filament. When the length of the radiator arm is equal to  $L = \lambda/4$ , both components of the field (real and imaginary) are continuous curves. It can be seen from the figure that the real component of the field is almost constant along the entire radiator, while the imaginary component increases indefinitely at radiator ends. This increase is associated with the decrease to zero of the distances  $R_{1(2)} = L \pm z$ , located in the denominators of first and second terms of the square bracket in expression (1.25). The third term with  $R_0$  in the denominator in this case does not give the maximum, because  $\cos kz = 0$ . But, with a small change in the radiator length both curves change (see dotted line). The unlimited growth of the curve is caused by the fact that in this model the radiator radius is zero.

From this it follows that in a metal tube or a filament with a sinusoidal current, the field is not identical to the field of the tube excited in the middle by a concentrated emf in the form of a narrow slot. To ensure a sinusoidal current distribution, it is necessary to create a continuous emf along the radiator, coincident in shape and opposite in sign to the curves shown in Fig. 3.

However, the approximate sinusoidal current distribution along the radiator creates the electromagnetic field in the surrounding space, which is close to the actual field, including the near zone. Indeed, as can be seen from (1.28) and (1.29),

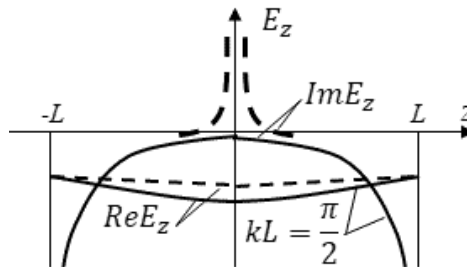


**Fig. 3:** The real ( $Re E_z$ ) and imaginary ( $Im E_z$ ) components of the electric field strength tangent to the radiator surface.

the components of the field  $H_\phi$  and  $E_\rho$  on the antenna surface are inversely proportional to the radius  $a$  of the antenna and increase infinitely with decreasing radius to zero, while the field  $E_z$ , defined in accordance with (1.25) remains finite almost everywhere with the exception of the ends of the radiator and the point of excitation, i.e., electric field lines approach the axis of the radiator almost at a right angle, as it should be near a metal surface.

Here so much attention was paid to the sinusoidal distribution of the current along the radiator because this distribution was used for a long time for two purposes; firstly, for antennas calculation and secondly, for the powers' calculation. The antennas calculation was based on comparing the antenna current and the current in the equivalent long line. The powers' calculation was based on equality the source power and the power passing through a closed surface surrounding an antenna.

### 3. Equivalent Long Line

As already mentioned, the current distribution along the antenna mainly determines its characteristics. Therefore, a significant role in the development of the calculating antennas method was played by comparing the properties of radiators with the properties of two-wire long lines. The simplest metal radiators are shown in Fig. 1. The circuit of a long line equivalent to a symmetrical metal radiator (Fig. 1a) is presented in Fig. 4. An infinitesimal element of such a line with length  $dz$  contains an inductance  $d\Lambda = \Lambda_1 dz$  and a capacitance  $C = C_1 dz$ . Here  $\Lambda_1$  and  $C_1$  are the inductance and the capacitance per unit length of the line.

Let us start with the option of a symmetrical metal radiator (dipole) excited by a generator connected in its center. An inductance of an element  $dz$  is equal to the sum of inductances of elements of both wires, and the capacitance of this element (the capacitance between the wires) is half a capacitance between an element of each wire and a surface located between wires and dividing an antenna into two identical structures. In the case of a grounded metal radiator (monopole) with a generator at the base, an inductance of an element  $dz$  is equal to an inductance of a wire element, and a capacitance of an element  $dz$  is equal to a capacitance between a wire element and an infinitely distant surface of zero potential:

$$C_1 = 2\pi\epsilon/\ln(2L/a).$$

The current distribution in the wires of a metal dipole with arms of length  $L$  little differs from the current distribution in the wires of a two-wire metal long line open

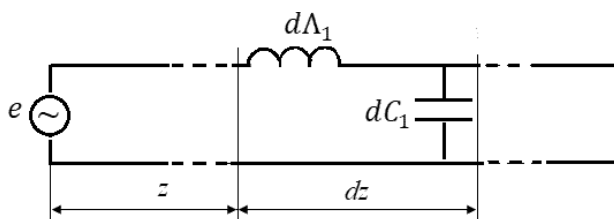


Fig. 4: Long line, equivalent to a metal radiator.

at the end with the same length. The essential difference between them is only the fact that a long line with a small distance between the parallel wires weakly radiates. The tangential component of the electric field on the surface of the metal wires of an antenna and of an equivalent long line is equal to zero, i.e., the boundary conditions on the surface of each metallic wire are

$$E_z(a, z) + K(z) = 0, -L \leq z \leq L. \quad (1.31)$$

Here  $E_z(a, z)$  is the tangential component of the electric field,  $K(z)$  is the extraneous (external) emf. The current distribution  $J(z)$  must satisfy the condition of no current at the ends of the antenna

$$J(\pm L) = 0.$$

Expression (1.31) is a mathematical record of the fact, according to which the resulting field, which is equal to the sum of the external field and the field created by the radiator current, is equal to zero on a perfectly conducting metal surface. External emf is usually given as a  $\delta$ -function:

$$K_1(z) = e\delta(z), K_2(z) = e\delta(z - h).$$

The input impedance of a two-wire long line open at the end in the first approximation is equal to the reactive component of the input impedance of the corresponding antenna:

$$Z_i = -jW_l \cot kL.$$

Here  $W_l$  is the wave impedance of the line,  $L$  is its length. If the generator is displaced from the center of the antenna by a distance  $h$ , then the input impedance of the long line is equal to the sum of the impedances of the lines located on different sides of the generator. In the case of a dipole, these are lines with length  $L - h$  and  $L + h$ , open at the end, in the case of a monopole these are the line with length  $L - h$  open at the end and the line with length  $h$  closed at the end.

The equations for currents and voltages in metal wires of a long line are called telegraph equations. These equations are much simpler than the equations for currents and voltages in metal radiators. They can be used to analyze both two-wire and one-wire long lines, located above an infinite metal surface—conductive earth. In the general case the number of parallel wires in the radiator can be significantly more than two. They form a structure of electrically connected lines located in parallel or perpendicular to the ground surface.

The theory of coupled lines developed by A.A. Pstolkors [5] underlies the analysis of antennas and cables consisting of parallel wires. This theory allows considering structures from  $N$  closely spaced parallel wires, taking into account the influence of the earth. An asymmetric line of two wires in the form of a horizontal folded radiator with a gap (see Fig. 5) is the simplest example of such a structure.

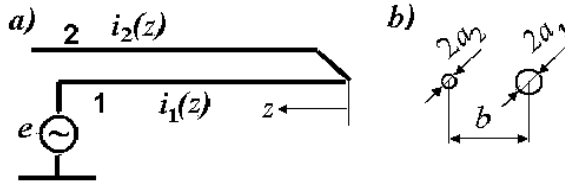


**Fig. 5:** The asymmetrical line, which is equivalent to a horizontal folded radiator with the gap: (a) circuit, (b) cross-section.

In the case of two parallel wires, the telegraph equations for the current and voltage in wires 1 and 2 of this line are written in the form

$$\begin{aligned} -\frac{\partial u_1}{\partial z} &= jX_{11} i_1 + jX_{12} i_2, \quad u_1 = j \frac{1}{k^2} \left( X_{11} \frac{\partial i_1}{\partial z} + X_{12} \frac{\partial i_2}{\partial z} \right), \\ -\frac{\partial u_2}{\partial z} &= jX_{22} i_2 + jX_{12} i_1, \quad u_2 = j \frac{1}{k^2} \left( X_{22} \frac{\partial i_2}{\partial z} + X_{12} \frac{\partial i_1}{\partial z} \right). \end{aligned} \quad (1.32)$$

Here  $u_i$  is a potential of wire  $i$  relative to the ground,  $i_i$  is a current along wire  $i$ , and  $X_{ik} = \omega L_{ik}$  is the self- or mutual inductive impedance per unit length.

The two left equations of this set are based on the fact that the decrease of voltages at segment  $dz$  of each wire is the result of the emf influence. The emfs are induced by the self-currents and by the currents of adjacent wires. The other two equations are written on the basis of continuity equations connecting charges and potentials.

Dependence of the current on coordinate  $z$  is adopted in the form  $\exp(\gamma z)$ , where  $\gamma$  is the propagation constant. Differentiation of the right equations and substitution them into the left equations permits to obtain a set of homogeneous equations, which shows that propagation constant  $\gamma$  in the system of two metal wires is equal to  $k$ . The solution of the equations set is searched in the form

$$U_i = A_i \cos kz + jB_i \sin kz.$$

Assuming  $z = 0$  in order to determine constant quantities  $A$  and  $B$ , we obtain

$$i_{1(2)} = I_{1(2)} \cos kz + j \left[ \frac{U_{1(2)}}{W_{11(22)}} - \frac{U_{2(1)}}{W_{12(21)}} \right] \sin kz, \quad u_{1(2)} = U_{1(2)} \cos kz + j \sum_{s=1}^2 \rho_{1(2)s} I_s \sin kz, \quad (1.33)$$

where  $I_{1(2)}$  and  $U_{1(2)}$  are the current and potential at the beginning of wire 1 or 2 (at point  $z=0$ ),  $W_{1(2)s}$  and  $\rho_{1(2)s}$  are the electrostatic and electrodynamics wave impedances between wire 1 or 2 and wire  $S$ .

In the general case the number of wires can be significantly greater than two. The theory of coupled lines is a basis of the analysis of antennas consisting of parallel wires. This theory allows us to analyze multi-wire structures of antennas and cables. As an example, in Fig. 6 an option of a horizontal load of the antenna is shown. The wires of such a load are connected with each other in parallel and form the structure from electrically coupled lines located parallel to the earth. An increase in the number of wires leads to an increase in capacitance and a decrease in the reactive

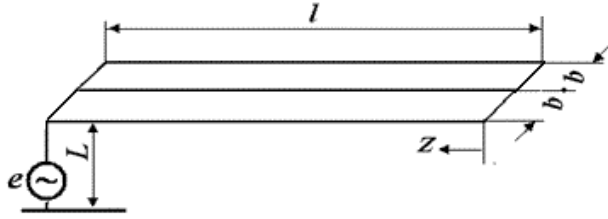


**Fig. 6:** Horizontal load of the antenna in the shape of a three in parallel-connected wires located parallel to the earth.

impedance of such a load. As a result, the effective height of the vertical antenna and its resistance of the radiation increase.

If the structure consists of  $N$  parallel metal wires located above the earth, expressions for the current and the potential of wire  $n$  have the form

$$i_n = I_n \cos kz + j \left[ \frac{2U_n}{W_{nn}} - \sum_{s=1}^N \frac{U_s}{W_{ns}} \right] \sin kz, \quad u_n = U_n \cos kz + j \sum_{s=1}^N \rho_{ns} I_s \sin kz, \quad (1.34)$$

where  $I_n$  and  $U_n$  are the current and potential at the beginning of wire  $n$  (at point  $z = 0$ ) respectively,  $W_{ns}$  and  $\rho_{ns}$  are the electrostatic and electrodynamics wave impedances between wires  $n$  and  $s$ :

$$\rho_{ns} = \alpha_{ns}/c, \quad W_{ns} = \begin{cases} 1/(c\beta_{ns}), & n = s, \\ -1/(c\beta_{ns}), & n \neq s. \end{cases} \quad (1.35)$$

Here,  $\alpha_{ns}$  is the potential coefficient (with allowance for a mirror image in the perfectly conducting ground surface),  $\beta_{ns}$  is the coefficient of electrostatic induction, and  $c$  is the light velocity. The coefficients  $\beta_{ns}$  and  $\alpha_{ns}$  are related with relationship  $\beta_{ns} = \Delta_{ns}/\Delta_N$ , where  $\Delta_N = |\alpha_{ns}|$  is  $N \times N$  determinant, and  $\Delta_{ns}$  is the cofactor of the determinant  $\Delta_N$ .

For an asymmetrical line of two wires, we can write

$$\frac{1}{W_{11}} = \frac{\rho_{22}}{\rho_{11\rho_{22}} - \rho_{12}^2}, \quad \frac{1}{W_{22}} = \frac{\rho_{11}}{\rho_{11\rho_{22}} - \rho_{12}^2}, \quad \frac{1}{W_{12}} = \frac{\rho_{12}}{\rho_{11\rho_{22}} - \rho_{12}^2},$$

i.e.,

$$\left( \frac{1}{W_{12}} - \frac{1}{W_{11}} \right) : \left( \frac{1}{W_{12}} - \frac{1}{W_{22}} \right) = \frac{\rho_{22} - \rho_{12}}{\rho_{11} - \rho_{12}} = g. \quad (1.36)$$

If the wires of an asymmetrical line have unequal lengths, or the concentrated loads are included in the wires, the line must be divided on the segments. The expressions for the current and potential of wire  $n$  at segment  $m$  take the form:

$$i_n^{(m)} = I_n^{(m)} \cos kz_m + j \left[ \frac{2U_n^{(m)}}{W_{nn}^{(m)}} - \sum_{s=1}^N \frac{U_s^{(m)}}{W_{ns}^{(m)}} \right] \sin kz_m, \quad u_n^{(m)} = U_n^{(m)} \cos kz_m + j \sum_{s=1}^N \rho_{ns}^{(m)} I_s^{(m)} \sin kz_m, \quad (1.37)$$

where  $I_n^{(m)}$  and  $U_n^{(m)}$  are the current and potential of wire  $n$  at the beginning of segment  $m$  (at point  $z_m = 0$ ) respectively,  $M$  is the number of segments  $m$ , and  $W_{ns}^{(m)}$  and  $\rho_{ns}^{(m)}$  are the electrostatic and electrodynamics wave impedances between wires  $n$  and  $s$  at segment  $m$ . These equations generalize the expressions (1.34).

To solve the set of equations, the boundary conditions are used. They are based on the absence of currents at the free ends of wires, the continuity of the current and potential along each wire, the abrupt changes of a potential in the points of connecting loads and generator  $e$ . Calculating the current magnitude  $J(0)$  at the feed point permits to find the input impedance of an asymmetrical line,

$$Z_i = e/J(0).$$

It is equal approximately to the reactive impedance of the antenna, whose equivalent is the given asymmetrical line. One can find the antenna impedance more accurately, if antenna is treated as a linear radiator, the current along which is equal to the total current along the line.

During the calculation of an antenna input impedance, one needs, as a rule, to find field  $E_\zeta$  on the antenna surface. And it should be kept in mind that, although the current function  $J(\zeta)$  is continuous along the entire length of the antenna and sinusoidal at each segment, function  $dJ/d\zeta$  may have a jump on the segment boundaries.

The equations (1.37) contain wave impedances  $W_{ns}^{(m)}$  and  $\rho_{ns}^{(m)}$ , the equations (1.36) contain similar magnitudes. The magnitudes of the wave impedances are calculated through the potential coefficients. These coefficients are determined by the method of an average potentials in accordance with the actual mutual location of antenna wires. The simplest variant of these method is the Howe's method. As is shown in [6], the mutual potential coefficient of two parallel wires with equal lengths, whose dimensions and position are given in Fig. 7, is determined as

$$\alpha_{ns} = \alpha(L, l, b)/(2\pi\epsilon), \quad (1.38)$$

where

$$\alpha(L, l, b) = \frac{1}{2L} \left[ (L+l) \operatorname{sh}^{-1} \frac{L+l}{b} + (L-l) \operatorname{sh}^{-1} \frac{L-l}{b} - 2L \operatorname{sh}^{-1} \frac{l}{b} - \sqrt{(L+l)^2 + b^2} - \sqrt{(L-l)^2 + b^2} + 2\sqrt{l^2 + b^2} \right], \quad (1.39)$$

i.e.,  $\rho_{ns} = \alpha_{ns}/c = \alpha(L, l, b)/(2\pi\epsilon_0 \epsilon_r c) = 60 \alpha(L, l, b)/\epsilon_r$ .

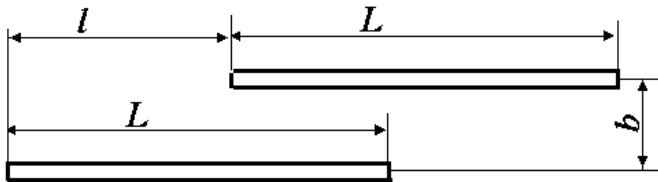


Fig. 7: The mutual location of two wires.

As already mentioned, the calculation method based on the application of telegraph equations was proposed for the calculation of antenna structures consisting of parallel horizontal wires. In the course of its use, it became clear that this method can be used in order to calculate the characteristics of radiators consisting of parallel wires perpendicular to the ground, taking into account the mirror image in the conductive surface of the ground, i.e., this method permits to investigate the properties of multi-wire vertical structures. That dramatically increased the possibilities for calculating various antennas options and became a powerful incentive for the widespread application of the given method.

If the parallel wires are located upright, i.e., perpendicular to conductive ground, then a potential coefficient of conductor  $n$  at segment  $m$  with the account of a mirror image is equal to

$$\alpha_{nn}^{(m)} = \alpha[l_m - l_{m+1}, 0, a_n^{(m)}] - \alpha[l_m - l_{m+1}, l_m + l_{m+1}, a_n^{(m)}], \quad (1.40)$$

where  $l_m$  and  $l_{m+1}$  are the boundary coordinates of segment  $m$ ,  $a_n^{(m)}$  is the radius of wire  $n$  at segment  $m$ . The mutual potential coefficient between wires  $n$  and  $s$  at segment  $m$  is

$$\alpha_{ns}^{(m)} = \alpha[l_m - l_{m+1}, 0, b_{ns}^{(m)}] - \alpha[l_m - l_{m+1}, l_m + l_{m+1}, b_{ns}^{(m)}]. \quad (1.41)$$

Here  $b_{ns}^{(m)}$  is the distance between the axes of wires  $n$  and  $s$  at segment  $m$ . The circuit of one possible option of a multi-radiator antenna is presented in Fig. 8a as an example of such a structure. The circuit of an equivalent long line is given in Fig. 8b.

Summing up, it should be said that a consistent generalization of the results allows us to move from the telegraph equation for a uniform long line to the system of telegraph equations for a structure of stepped long lines that are in parallel located in space and consist of uniform lines with different geometric dimensions. The wave propagation constant in each long line coincides with the wave propagation constant in free space.

It is necessary to note the great usefulness of the theory of coupled lines. This theory allows us to find the current distribution in each wire. As is known, in the first approximation, the current distribution along a linear radiator coincides with the current distribution along a uniform long line. This allows further use of the current distribution along the wires of the line to calculate the active component and to refine the reactive component of the input impedance of the antennas by means the method of induced emf.

#### 4. Multi-wire and Multi-radiator Structures of Antennas

One of the methods for improving the electrical characteristics of antennas is based on the use of several parallel wires and linear radiators in one design. This Section is devoted to them.

Let's start with multi-wire structures. To increase the level of matching of the antenna with the cable in a wide frequency range, it is necessary to reduce the input





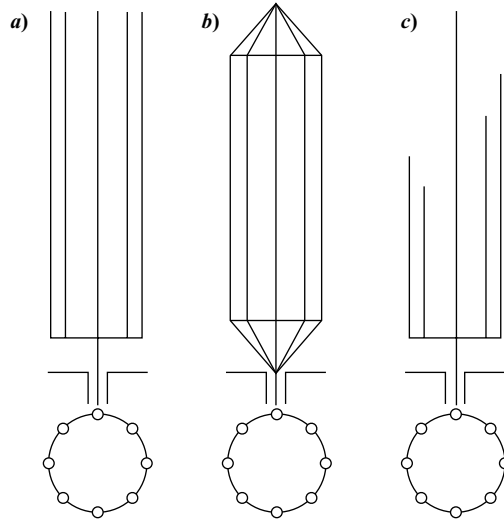


**Fig. 9:** Multi-wire (a, b) and multi-radiator (c) antennas.

multi-wire radiator and by an equivalent metal tube are the same, if their lengths are identical. As can be seen from (1.42), the radius of the equivalent radiator is much larger than the radius  $a$  of a single wire. Accordingly, the antenna wave impedance  $W_R$  and consequently the reactive component  $X_A$  of its input impedance decrease.

From the identity of fields in the far zone, generally speaking, the identity of the remaining electrical characteristics, for example, of the input impedances, does not follow. The input impedances of a multi-wire and an equivalent thick radiator are confronted with each other in [7]. At that the multi-wire radiator (see Fig. 9a) consists from identical linear radiators with the same exciting emf and the same currents. As the calculations show, a form of curves for the input impedance of a multi-wire antenna and an equivalent radiator is the same, but the first ones are shifted toward larger values of  $L/\lambda$ . If  $N$  increases, this shift decreases. The current distribution depends on  $N$  and differs from the current distribution along the thin linear radiator (with  $N = 1$ ): the current of an individual wire decreases, the wave propagation constant along the antenna grows and approaches to the propagation constant of an equivalent radiator.

Similar data for a cage antenna were obtained in [8]. The calculation results for such an antenna excited by a two-wire long line (Fig. 10) are given in [9]. Indicated in the figure the dimensions of an antenna and a long line (in meters) are equal:  $L = 12.5$ ,  $b = 0.25$ ,  $a = 1.5 \cdot 10^{-3}$ ,  $\theta = 45^\circ$ . Each arm of the radiator is formed by eight wires ( $N = 8$ ), a wave impedance of the line is equal to  $W_l = 350$  Ohm. The calculation takes into account the spatial coupling between the radiator wires and the feed line and also the effect of a line end. In this case, the input impedance of an antenna is understood as the impedance of the load, which, being connected instead of an antenna to the line end, creates in the arbitrary cross-section of the line outside the excitation zone such the wave mode, as when connecting an antenna. The mentioned load is equal to the input impedance of an antenna, which is determined

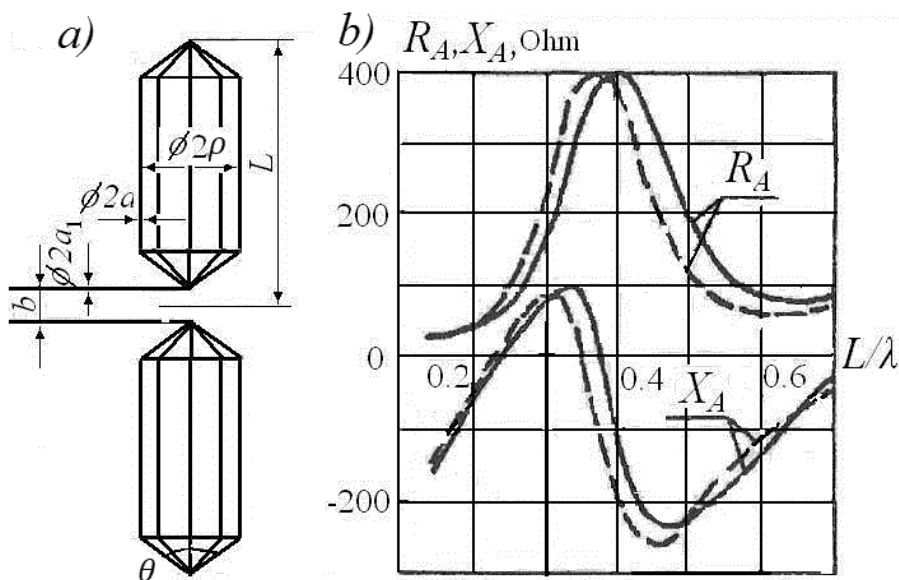


Fig. 10: Cage antenna, excited by a two-wire line: a - circuit, b - input impedance.

in accordance with the results of a measuring when a measuring device connected to the feed line outside the excitation zone.

The solid line in Fig. 10 shows the impedance of a cage antenna, the dotted line shows the impedance of an equivalent cylindrical radiator with a radius determined by formula (1.42).

Multi-wire antennas are used, as a rule, for the operation in one frequency band, although this band can be quite wide. The antenna consisting from a few radiators can operate in several frequency bands. In this respect, it is analogous to multi-folded structures. One possible variant of a multi-radiator antenna, which has found practical application, is given in Fig. 11a. Its equivalent long line is presented in Fig. 11b. The antenna is described in [10].

The antenna consists of a central radiator 1 with a complex impedance load  $Z_0$  and the side radiators 2 located around a radiator 1 along the cylinder generatrices and connected to the base of this radiator. The impedance load is a distinguishing feature of the given antenna. It is included to provide on the low segment of antenna an operation mode, close to the running wave mode. Such a mode is created between the generator and the load. It allows to raise the level of matching and to obtain the desired directional pattern in the vertical plane. As a load, a special power absorber is used. The multi-radiator antenna without a load has high characteristics in the vicinity of series resonances of individual radiators, but to reduce the spatial coupling between the radiators and to obtain similar characteristics in a continuous range one must sharply reduce the spatial coupling between the radiators. Combining the two details: a complex load and a multi-radiator structure promises additional opportunities.

To calculate the antenna characteristics, a program based on the method of moments can be used. Another method of calculation, requiring less computer time

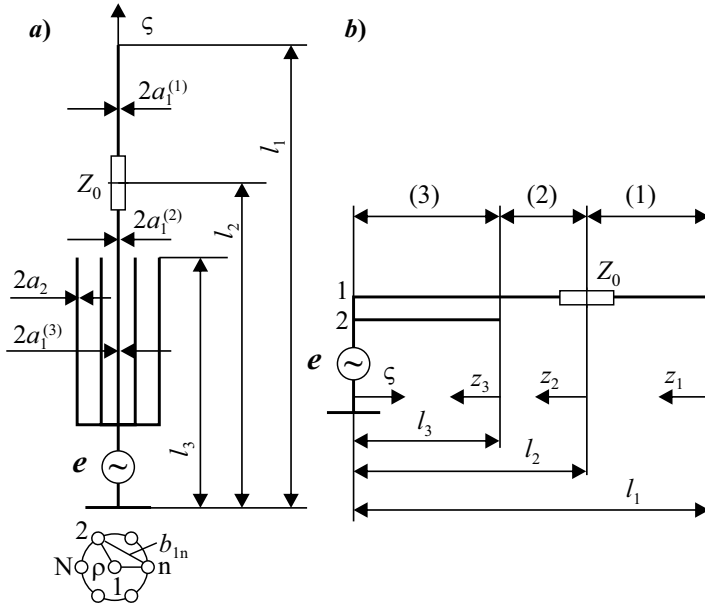


**Fig. 11:** Multi-radiator antenna with a complex impedance load (a) and an equivalent asymmetrical line (b).

and having more physical visibility, is described in [11]. In it, for simplicity, it is assumed that the geometrical dimensions of the side radiators are the same, and the radiators are evenly distributed around the circumference of the cylinder. Such a variant also permits to tune the antenna. The result of the solution slightly depends on the uniformity of the radiators placement. But the calculation also can be executed in the general case, e.g., for different lengths of radiators.

The chosen variant of a calculation allows to simplify the problem by reducing the asymmetrical line to a two-wire line, and to obtain a solution for the current in an explicit form. The first wire of the asymmetric line is the central radiator, and the second wire is formed by a system of  $N - 1$  side radiators ( $N$  is the total number of radiators). Since the wires of the line have different lengths, and one of them has an impedance load, the line should be divided into three sections. Expressions for the current and potential on a segment  $m$  of a wire  $n$  of an asymmetrical line have a form analogous to the expressions (1.37), with  $n = 1, 2, m = 1, 2, 3$ . The antenna circuit is presented in Fig. 11b. The wire numbers are given at the left ends of the wires, the segment numbers are indicated in round brackets in the middle of each segment.

The boundary conditions for the two-wire asymmetric line shown in Fig. 11b, are written as

$$i_1^{(1)} \Big|_{z_1=0} = i_2^{(3)} \Big|_{z_3=0} = 0, i_1^{(1)} \Big|_{z_1=l_1-l_2} = i_1^{(2)} \Big|_{z_2=0}, i_1^{(2)} \Big|_{z_2=l_2-l_3} = i_1^{(3)} \Big|_{z_3=0},$$

$$u_1^{(1)} \Big|_{z_1=l_1-l_2} = u_1^{(2)} - i_1^{(2)} Z_0 \Big|_{z_2=0}, u_1^{(2)} \Big|_{z_2=l_2-l_3} = u_1^{(3)} \Big|_{z_3=0}, u_1^{(3)} \Big|_{z_s=l_s} = u_2^{(3)} \Big|_{z_3=l_3} = e. \quad (1.43)$$

These conditions mean the absence of the current at the free ends of the wires and the continuity of current and potential along each wire, except for the point where the load is placed and the potential jump takes place. Substituting (1.37) to (1.43) and solving the resulting system of equations, we find:

$$\begin{aligned}
 I_1^{(1)} = I_2^{(3)} = 0, \quad I_1^{(2)} = j \frac{U_1^{(1)}}{\rho_{11}^{(1)}} \sin k(l_1 - l_2), \quad I_2^{(3)} = j \frac{U_1^{(1)} \sin k(l_1 - l_2) \sin k(l_{1e} - l_3)}{\rho_{11}^{(1)} \sin k(l_{1e} - l_2)}, \\
 U_1^{(2)} = \frac{U_1^{(1)} \rho_{11}^{(2)} \sin k(l_1 - l_2) \cot k(l_{1e} - l_3)}{\rho_{11}^{(1)}}, \quad U_1^{(3)} = \frac{U_1^{(1)} \rho_{11}^{(2)} \sin k(l_1 - l_2) \cos k(l_{1e} - l_3)}{\rho_{11}^{(1)} \sin k(l_{1e} - l_2)}, \\
 U_2^{(3)} = \frac{U_1^{(1)} \rho_{11}^{(2)} \sin k(l_1 - l_2) \cos k(l_{1e} - l_3)}{\rho_{11}^{(1)} \sin k(l_{1e} - l_2)} \left[ 1 - \frac{\rho_{11}^{(3)} - \rho_{12}^{(3)}}{\rho_{11}^{(2)}} \tan k(l_{1e} - l_3) \tan kl_3 \right], \\
 U_1^{(1)} = -e \rho_{11}^{(1)} \sin k(l_{1e} - l_2) \cdot \\
 \left\{ \rho_{11}^{(3)} \sin k(l_1 - l_2) \sin k(l_{1e} - l_3) \sin kl_3 \left[ 1 - \frac{\rho_{11}^{(2)}}{\rho_{11}^{(3)}} \cot k(l_{1e} - l_3) \cot kl_3 \right] \right\}^{-1}.
 \end{aligned}$$

Here it is taken into account that  $W_{11}^{(1)} = \rho_{11}^{(1)}$ ,  $W_{11}^{(2)} = \rho_{11}^{(2)}$ , and  $l_{1e}$  is a complex quantity determined from expression  $Z_0 - j\rho_{11}^{(1)} \cot k(l_1 - l_3) = -j\rho_{11}^{(2)} \cot k(l_{1e} - l_3)$ . The total current along the antenna is a function of the coordinate  $\zeta = l_m - z_m$  (Fig. 11b):

$$J(\zeta) = \sum_{n=1}^M i_n^{(m)} = \begin{cases} j \frac{U_1^{(1)}}{\rho_{11}^{(1)}} \sin k(l_1 - |\zeta|), & l_2 \leq |\zeta| \leq l_1, \\ j \frac{U_1^{(1)}}{\rho_{11}^{(1)}} D_1 \frac{\sin k(l_{1e} - |\zeta|)}{\sin k(l_{1e} - l_3)}, & l_3 \leq |\zeta| \leq l_2, \\ j \frac{U_1^{(1)}}{\rho_{11}^{(1)}} [D_1 \cos k(l_3 - |\zeta|) + D_2 \sin k(l_3 - |\zeta|)], & 0 \leq |\zeta| \leq l_3, \end{cases} \quad (1.44)$$

where

$$\begin{aligned}
 D_1 &= \frac{\sin k(l_1 - l_2) \sin k(l_{1e} - l_3)}{\sin k(l_{1e} - l_2)}, \\
 D_2 &= \rho_{11}^{(2)} \frac{\sin k(l_1 - l_2) \cos k(l_{1e} - l_3)}{\sin k(l_{1e} - l_2)} \left\{ \frac{1}{W_{11}^{(3)}} - \frac{1}{W_{12}^{(3)}} + \left[ \frac{1}{W_{22}^{(3)}} - \frac{1}{W_{12}^{(3)}} \right] \right. \\
 &\quad \left. \left[ 1 - \frac{\rho_{11}^{(3)} - \rho_{12}^{(3)}}{\rho_{11}^{(3)}} \tan k(l_{1e} - l_3) \tan kl_3 \right] \right\}.
 \end{aligned}$$

Input impedance of an asymmetrical line

$$Z_l = e/(J(0)). \quad (1.45)$$

This expression, taking into account (1.44), permits to approximately determine a reactive impedance of a multi-radiator antenna—similar to how an expression for an input impedance of an equivalent two-wire long line permits to approximately determine a reactive impedance of a linear radiator. In order to determine the input impedance of an antenna more precisely, one must consider a linear radiator, the current along which is equal to the total current along the multi-radiator antenna. In accordance with the second formulation of the method of induced emf, the input impedance of considering antenna is

$$Z_A = -\frac{1}{J^2(0)} \left[ \int_0^{l_1} E_\zeta J(\zeta) d\zeta - Z_0 J^2(l_2) \right], \quad (1.46)$$

where  $E_\zeta$  is the tangential component of an electric field created by the current  $J(\zeta)$  on the radiator surface along its axis. The free term in the square brackets of this expression is the power in a complex load  $Z_0$ . Near the parallel resonance, this expression gives a large error, and it should be replaced by

$$Z_A = e/[2J(0) + \frac{1}{e} \int_0^{l_1} E_\zeta(J) d\zeta - \frac{1}{e} Z_0 J^2(l_2)].$$

The field  $E_\zeta$  is calculated by the usual way. The function  $J(\zeta)$  is continuous in all interval of integration, and it is a sinusoid on each section. However, the function  $dJ/d\zeta$  has a discontinuity at the segments' boundaries, i.e., it is necessary to consider the difference in the derivatives on both sides of this discontinuity. With allowance for jumps of the derivative we obtain instead (1.30):

$$E_z(J) = -j \frac{15}{k} \left\{ \frac{2 \exp(-jkR_0)}{R_0} \frac{dJ(0)}{dz} - \left[ \frac{\exp(-jkR_{11})}{R_{11}} + \frac{\exp(-jkR_{12})}{R_{12}} \right] \frac{dJ(J_1)}{dz} + \right. \\ \left. \sum_{m=2}^3 \left[ \frac{\exp(-jkR_{m1})}{R_{m1}} + \frac{\exp(-jkR_{m2})}{R_{m2}} \right] \left[ \frac{dJ(l_m + 0)}{dz} - \frac{dJ(l_m - 0)}{dz} \right] \right\},$$

where  $R_0 = \sqrt{a^2 + z^2}$ ,  $R_{m1} = \sqrt{a^2 + (l_m - z)^2}$ ,  $R_{m2} = \sqrt{a^2 + (l_m + z)^2}$ ,  $a$  is the radiator radius at point  $z$ ,  $dJ(l_m + 0)/dz$  and  $dJ(l_m - 0)/dz$  are the values of derivative on the right and left from the point  $z = l_m$ .

The resistance of an antenna radiation is

$$R_\Sigma = R_A - R_{load}, \quad (1.47)$$

where  $R_A$  is the active component of the input impedance and  $R_{load}$  is the loss resistance on the antenna input, which is caused by a load  $z_0 = R_0$ , i.e.,

$$R_{load} = Re \frac{J^2(l_2) R_0}{J^2(0)} \quad (1.48)$$

In accordance with the theorem on oscillating power, the oscillating power  $P$ , created by the source, is equal to  $P = P_1 + P_2$ , where  $P_1 = J^2(0)(R_\Sigma + jX_A)$  is an oscillating power passing through the surface of an antenna,  $P_2 = J^2(l_2) R_0$  is the oscillating power in the load, i.e.,  $P = J^2(0)(R_A + jX_A)$  where

$$R_A = Re \frac{P_1 + P_2}{J^2(0)} = Re \frac{P_1}{J^2(0)} + Re \frac{J^2(l_2)R_0}{J^2(0)}.$$

These expressions are based on the equalities (1.47) and (1.48).

The magnitudes of wave impedances  $\rho_{ns}^{(m)}$  and  $W_{ns}^{(m)}$ , which are used in the expression (1.44) for the total current of the multi-radiator antenna, are determined by the potential coefficients. For an asymmetrical line of two wires with different lengths, divided into three sections, these magnitudes are equal

$$\rho_{ns}^{(m)} = \frac{\alpha_{ns}^{(m)}}{c}, \frac{1}{W_{11}^{(3)}} = \frac{\rho_{22}^{(3)}}{\Delta}, \frac{1}{W_{12}^{(3)}} = \frac{\rho_{12}^{(3)}}{\Delta}, \frac{1}{W_{22}^{(3)}} = \frac{\rho_{11}^{(3)}}{\Delta}$$

where  $\Delta = \rho_{11}^{(3)}\rho_{22}^{(3)} - [\rho_{12}^{(3)}]^2$ . Potential coefficients are calculated by the method of average potentials, based on the actual location of the antenna wires. Taking into account the mirror image, we obtain

$$\alpha_{ns}^{(m)} = \frac{1}{2\pi\epsilon} \left\{ \alpha \left[ l_m - l_{m+1}, 0, b_{ns}^{(m)} \right] - \alpha \left[ l_m - l_{m+1}, l_m + l_{m+1}, b_{ns}^{(m)} \right] \right\}, \quad (1.49)$$

where  $\alpha(L, l, b)$  is the mutual potential coefficient for two parallel wires as shown in Fig. 7. Its magnitude is determined by the expression (1.38). The parameter  $b_{ns}^{(m)}$  in expression (1.49) is the distance between the axes of wires  $n$  and  $s$  of the segment  $m$ .

More precisely, the antenna impedance can be found by considering a linear radiator, the current along which is equal to the total current along the multi-radiator antenna. For the first wire of an asymmetrical long line the equation (1.38), in which  $n = 1$ , is valid:

$$\alpha_{11}^{(m)} = \frac{1}{2\pi\epsilon} \left\{ \alpha \left[ l_m - l_{m+1}, 0, a_1^{(m)} \right] - \alpha \left[ l_m - l_{m+1}, l_m + l_{m+1}, a_1^{(m)} \right] \right\}.$$

Here  $a_1^{(m)}$  is radius of a central radiator on a segment  $m$ . The potential coefficient of the second wire of the long line is equal to its potential at  $Q_1 = 0, Q_2 = 1$  ( $Q_i$  is the charge per unit length of the wire  $i$ ), and the charge  $Q_2$  is evenly distributed among the side radiators due to the symmetry:  $q_n = Q(N-1)$ . Therefore

$$\alpha_{22}^{(3)} = \sum_{n=2}^N \alpha_{2n} \frac{q_n}{Q_2} = \frac{1}{N-1} \sum_{n=2}^N \alpha_{2n}, \quad (1.50)$$

where  $\alpha_{2n} = \frac{1}{2\pi\epsilon} [\alpha(l_3, 0, b_n) - \alpha(l_3, l_3, b_n)]$  is the mutual potential coefficient between the second and  $n$  radiators, and

$$b_n = \begin{cases} 2\rho \sin \frac{\pi(n-2)}{N-1}, & 3 \leq n \leq N, \\ a_2, & n = 2. \end{cases}$$

Here  $\rho$  is the radius of a cylinder, along the generatrices of which side radiators are located,  $a_2$  is the radius of the side radiator. The mutual potential coefficient between the first and second wire of the long line is equal to the potential of the first wire at  $Q_1 = 0, Q_2 = 1$ , i.e.,

$$\alpha_{12}^{(3)} = \sum_{n=2}^N \alpha_{1n} \frac{q_n}{Q_2} = \alpha_{1n}, \quad (1.51)$$

where  $\alpha_{1n} = \frac{1}{2\pi\epsilon} [\alpha(l_3, 0, \rho) - \alpha(l_3, l_3, \rho)]$  is the mutual potential coefficient between the first and  $n$  radiator.

Figure 12 presents the characteristics of the multi-radiator antenna shown in Fig. 11. This antenna has six side radiators. Their dimensions (in meters) are equal to  $l_1 = 10, l_2 = 7, l_3 = 6.5, a_2 = 0.01, a_1^{(1)} = 0.007, a_1^{(2)} = a_1^{(3)} = 0.02, \rho = 0.15$ . Load  $Z_0$  represents a parallel connection of a resistor with a resistance  $R = 200$  Ohm and a coil with an inductance  $\Lambda = 14 \mu H$ . The experimental values, which are presented in Fig. 12 together with the calculated curves, coincide well with them.

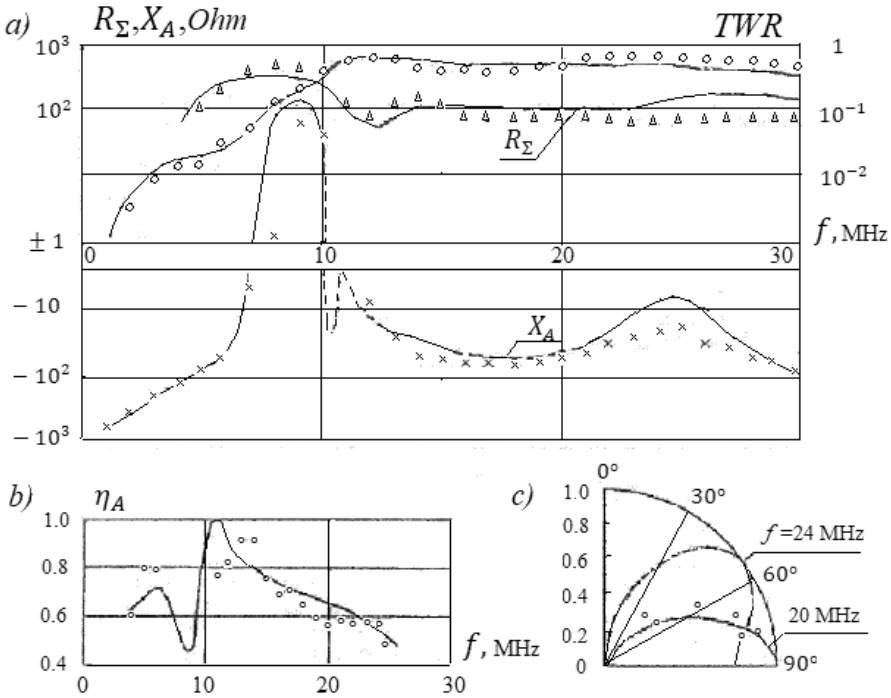
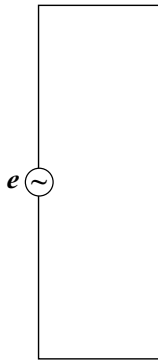


Fig. 12: Characteristics of the multi-radiator antenna.

## 5. Folded Radiators

As already was said, the theory of coupled lines is a base of the analysis for antennas consisting of parallel wires. The asymmetrical line of two vertical wires situated above ground is an equivalent of a folded antenna.





**Fig. 13:** Symmetric folded radiator.

Symmetric and asymmetric antennas from the parallel wires, located on a distance, which is small in comparison with the lengths of the waves and the wires, are used widespread together with conventional linear radiators. The simplest version of such radiator is symmetric antenna of two thin wires of the identical diameter, which is excited in the middle of one of the wires (Fig. 13). This antenna is called the folded radiator. Two asymmetrical options of such a radiator are shown in Fig. 14. In the first option the second (unexcited) wire shorted to the ground (Fig. 14a), in the second option there is a gap between this wire and the ground (Fig. 14b). In the general case the diameters of wires forming the radiator are not the same. The wires of an asymmetric radiator may be connected or not connected with each other on the upper end and have a different length (Fig. 14c). The radiator may be executed in a shape of coaxial structure (Fig. 14d).

An advantage of antenna consisting of parallel conductors is firstly the fact that it is substantially shorter than the linear antenna intended for operating at the same frequency. Selection of an option and dimensions of such antenna provides additional degrees of freedom for obtaining the desired electrical characteristics, for example, for improving matching with signal source (with generator or cable). One can say that the folded radiators combine the functions of radiation and matching.

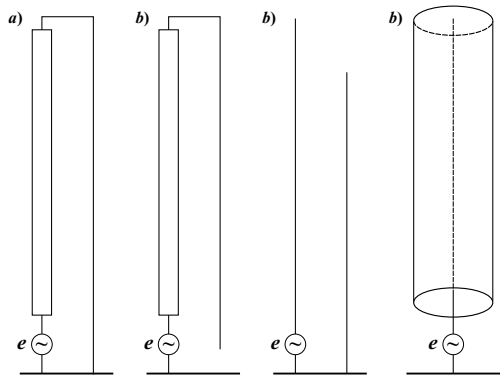


**Fig. 14:** Asymmetric folded radiators with a ground connection (a) and a gap (b) in the second wire, with wires of different length (c) and in a shape of coaxial structure (d).

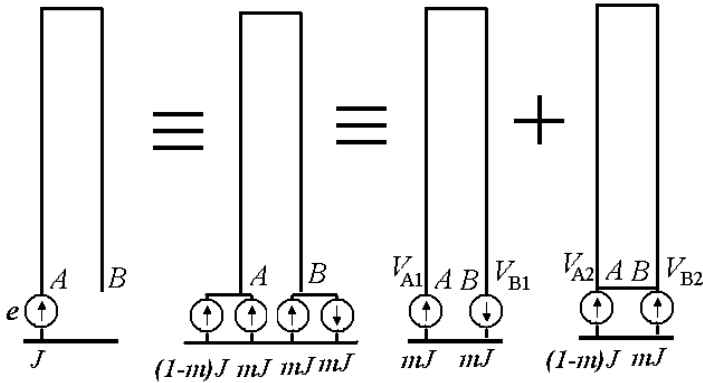


Fig. 15: Calculation of the folded radiator with a gap.

The two-wire long line open at the end is a useful analog of a conventional linear radiator. This line allows finding the current distribution along an antenna wire. An analog of folded radiator is a line of two wires (Fig. 5). In the general case the number of wires can be significantly greater than two. They form the structure from electrically coupled lines. In accordance with the theory of a coupled lines, we will consider the method of calculating folded antennas, using as an example an asymmetric folded radiator with a gap in an unexcited wire (see Fig. 14b). In this gap between the free end of an antenna and the ground we will connect in parallel two generators of a current with equal magnitude ( $mJ$ ) and opposite sign (Fig. 15). Also, we divide the main generator with a current  $J$  onto two parallel generators of a current with identical sign and different magnitude:  $mJ$  and  $(1 - m)J$ .

The voltage at the point  $A$  in accordance with the principle of superposition is equal to the sum of the voltages created in it by all generators. Therefore, as shown in Fig. 15, the circuit of the folded radiator may be split into two circuits, with two generators in each circuit. The voltages at point  $A$ , created in each of these circuits, are calculated and summed up. The currents of the wires of the first circuit have the opposite phases, i.e., given voltages are equal in magnitude and opposite in direction. This means that the first circuit is a two-wire long line, short-circuited at the end. The currents of the wires of the second circuit are in phase, i.e., the potentials of the points of both wires located at the same height (including the points near antenna base) are identical. This means that the second circuit is a linear radiator (monopole), excited at the base.

As shown in Section 3, an asymmetric two-wire line located above the ground and depicted in Fig. 5 is equivalent of a folded radiator. Currents and potentials of these wires are defined by the set of equations (1.33). Electrostatic and electrodynamics wave impedances included in these equations are calculated in accordance with expressions (1.35). As follows from the first equation of the set (1.33), in considered long line there are only anti-phase currents ( $i_1 = -i_2$ ), if the following conditions are met:

$$I_1 = -I_2, \quad U_1/W_{11} - U_2/W_{12} = -(U_2/W_{22} - U_1/W_{12}),$$

whence in accordance with (1.36)  $U_1 = -U_2/g$ . From the second equation of (1.33) and the equality (1.36) it follows that the ratio of potentials of the points located on the different wires in the same cross-section is equal to  $u_1/u_2 = U_1/U_2 = -1/g$ . This means that the voltages in points  $A$  and  $B$  of short-circuited two-wire line are related by the equality

$$V_{A1}/V_{B1} = -1/g. \quad (1.52)$$

If only in-phase currents exist in an asymmetric line, the potentials of wires in the same cross-section of line should be equal along the entire length of the line ( $u_1 = u_2$ ), i.e.,

$$U_1 = U_2, \rho_{11} I_1 + \rho_{12} I_2 = \rho_{12} I_1 + \rho_{22} I_2,$$

whence  $I_1 = gI_2$ . This means that the currents of wires in each cross-section of the monopole (including the base) are related by a relationship

$$i_1/i_2 = J_{A2}/J_{B2} = g. \quad (1.53)$$

From (1.52) and (1.53), we obtain

$$(V - V_{A1})/V_{A1} = (J - J_{B2})/J_{B2} = g.$$

Here  $V = V_{A1} - V_{B1}$  is the voltage at the input of the line, and  $J = J_{A2} + J_{B2}$  is the current at the base of the folded radiator, which is equal to the total current (to the current of the generator). From here

$$V_{A1}/V = J_{B2}/J = m = 1/(1 + g). \quad (1.54)$$

From (1.54) and Fig. 13 it is seen that  $m$  is a fraction of the in-phase current in the right wire of the monopole.

In the first circuit (in the short-circuited two-wire line) the voltage at the point  $A$  is

$$V_{A1} = mV = m^2 J_{Z1},$$

where  $Z_1 = jW_1 \tan kL$  is the input impedance of the line,  $W_1$  is its wave impedance. In the second circuit (in the monopole) this voltage is

$$V_{A2} = JZ_e(a_e),$$

where  $Z_e(a_e)$  is the input impedance of the asymmetric linear radiator of height  $L$  with an equivalent radius  $a_e$ . Dividing the total voltage at the point  $A$  by the current of the generator, we find the input impedance of the folded radiator with a gap:

$$Z_A = (V_{A1} + V_{A2})/J = Z_e(a_e) + jm^2 W_1 \tan kL. \quad (1.55)$$

As it follows from this expression, the input impedance the folded radiator with a gap is a series connection of the monopole and the short-circuited two-wire long line, i.e., it is equal to a sum of their input impedances (see Fig. 16).

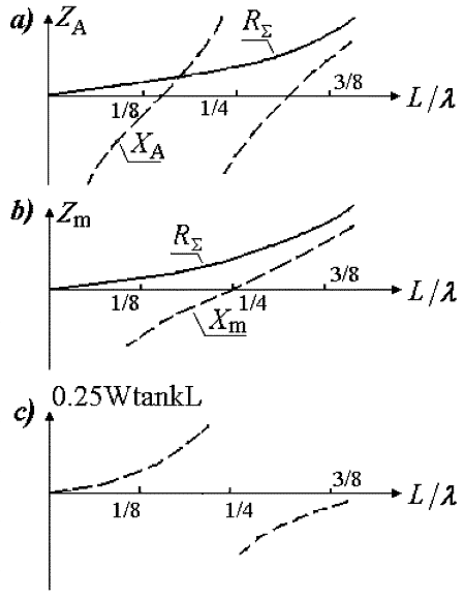


**Fig. 16:** Input impedance of the folded radiator with a gap (a), of the monopole (b) and of the long line (c).

Similarly, the input impedance of the folded radiator with the grounded second wire in contrast to a folded radiator with a gap is a parallel connection of an input impedances of a monopole and a short-circuited long line, i.e., it has more complex character:

$$Y_A = j \frac{1}{W_l \tan kK} + \frac{p^2}{Z_e(a_e)} \quad (1.56)$$

where  $p = 1 - m = g/(1 + g)$  is the fraction of the in-phase current in a left wire of the radiator. To obtain this expression, one must include in a right wire of a folded radiator in series two generators of voltage, which have the equal magnitudes ( $pe$ ) and opposite signs. Also, one must divide the main generator (with electromotive force  $e$ ) on two consistently connected generators of voltage with electromotive forces  $pe$  and  $(1 - p)e$  and with the same signs. Further, the circuit of the folded radiator is divided into two circuits—the short-circuited two-wire line and the monopole. At that the currents in the base of the left wire created in each of these circuits are calculated and summed up.

Expression (1.56) was obtained in [12], where the procedure of calculating the folded radiator with wires of different diameters and the ground connection of the second wire is given. If the folded radiator is formed by two identical thin wires with radii  $a = a_1 = a_2 \ll b$  (here  $b$  is the distance between wires axes—see Fig. 5), then

$$m = p = 0.5, g = 1, a_e = \sqrt{ab}, W_l = 120 \ln(b/a). \quad (1.57)$$

For wires with different radii, we have

$$p = 1 - m = \frac{\ln(b/a_2)}{2 \ln(b/\sqrt{a_1 a_2})}, a_e = \exp \left[ \frac{\ln a_1 \ln a_2 - \ln^2 b}{2 \ln(\sqrt{a_1 a_2}/b)} \right], a = \frac{\ln(b/a_2)}{\ln(b/a_1)},$$

$$W_1 = 120 \ln \frac{b}{\sqrt{a_1 a_2}}. \quad (1.58)$$

In the general case,

$$m = C_{22}/(C_{11} + C_{22}), \quad (1.59)$$

where  $C_{22}$  is the self-capacitance of the right wire, and  $C_{11}$  is the self-capacitance of the left wire. From (1.54) and (1.58) it follows that the currents in the wires of the monopole are proportional to self-capacitances of the wires, and potentials of the wires of the long line are proportional to reactances  $X_n = -1/(\omega C_m)$  between the wires and the ground.

The limiting case ( $m = 1, C_{11} = 0$ ) is shown in Fig. 14d. Here the folded radiator is designed as a segment of a coaxial line, which is open at the bottom and closed at the top. According to (1.55)

$$Z_A = Z_e(a_e) + jW_1 \tan kL,$$

where  $W_1 = 60 \ln(a_2/a_1)$ . If the outer conductor of a coaxial line is shorted to ground, then according to (1.56)  $Y_A = -j/(W_1 \tan kL)$ . Thus, in extreme cases, expressions (1.55) and (1.56) give a sufficiently obvious result.

As can be seen from (1.54) and (1.55), the replacement of a linear radiator by a folded radiator changes significantly the input impedance of the antenna. Folded radiator with a gap, if the length of this radiator is less than a quarter of a wave length, contains the inductive reactance of a short-circuited line. This inductive reactance is connected in series with the input impedance of the monopole and compensates its capacitive reactance. Therefore, when the height of a linear and a folded radiator are the same, the frequency of a first parallel resonance of the folded radiator is close to the frequency of the first series resonance of the linear radiator. Accordingly, the frequency of the first series resonance of the folded radiator is substantially lower than the frequency of the first series resonance of a linear radiator, approximately twice. Figure 16 shows typical active and reactive components of the input impedance of the folded radiator with a gap and the wires of equal diameter (a) and also the input impedances of its elements: of a monopole (b) and of a long line (c).

As already said, input impedance of the folded radiator with the grounded second wire has complex character. However, this option allows to transform an active component of a monopole input impedance. Indeed, according to (1.56) the input admittance of the folded radiator at the resonant frequency of a monopole is

$$Y_A = \frac{R_e(a_e) + jp^2 W_1 \tan kL}{jR_e(a_e) W_1 \tan kL},$$

i.e., neglecting the first term of a numerator as against the second term and substituting the value  $p$  in accordance with (1.57), we obtain

$$R_A \approx \frac{R_e(a_e)}{p^2} = R_m(a_e) \left[ 1 + \frac{\ln(b/a_1)}{\ln(b/a_2)} \right]^2. \quad (1.60)$$

Selection of the wires' radii permits increasing a level of matching such antenna with a cable or a generator.

It is necessary to say a few words about the physical meaning of the obtained results. It is obvious that in the free space two closely spaced parallel wires, along which equal currents flow in opposite directions, do not radiate the signal, since the fields of wires are mutually canceled each other. The conductive metallic surface (ground), on which antenna is installed, causes appearance of displacement currents between the wires and ground (they are shown by dotted lines in Fig. 17) and decreasing the conduction currents in parallel wires with increasing distance from the ground. Displacement currents are the cause of the summand's emergence in the input impedance of the antenna, analogous to the resistance of radiation.

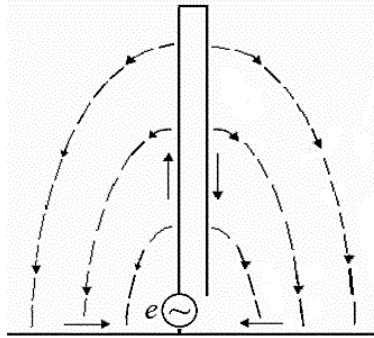


Fig. 17: Displacement and conduction currents in the folded radiator.

## 6. Folded Radiators with Wires of Different Length

The previous Section is devoted to folded radiators consisting of wires with equal lengths. Procedure of calculating currents in these radiators and long lines from parallel wires with equal length is based on the theory of electrically coupled lines. In order to determine the input impedance of a folded antenna, its circuit is divided into a linear radiator and a two-wire long line. If a folded radiator consists of wires with different length (see Fig. 14c), its structure may be similarly split into a line and a radiator, but the method of calculating currents in the line and the radiator becomes not obvious. The described problem is considered in [13]. But it is not the only task of this type.

An example of an antenna with two parallel wires of different lengths is given in Fig. 18a. As can be seen from the figure, this structure is distinguished from the structure shown in Fig. 5 and consists of two segments. The lengths of the upper and lower segments are equal respectively to  $l = l_1 - l_2$  and  $l_2 = L$ . Here  $l_1$  is the length of

a longer wire, and  $l_2$  is the length of a shorter wire. The lower segment is made in the form of two parallel wires of the same length with the identical cross-section, for example, with the circular cross-section of the radius  $a$ . Capacitance between two thin wires located in a homogeneous medium with permittivity  $\varepsilon$  per unit length of the wire is equal to

$$C_0 = \pi\varepsilon/\ln(b/a), \quad (1.61)$$

where  $b$  is the distance between the wires' axes. This capacitance determines the wave impedance of the line's lower segment.

Influence of the upper segment of the line on its input impedance is taken into account by means of calculating the capacitance between upper segment of the long wire (with length  $l$ ) and the short wire. We shall define an input impedance of the line with wires of different length as an input impedance of the line from short wires with capacitive load at the end. The electrostatic structure in this case consists of three conducting elements designated in Fig. 18a as (1), (2) and (3).  $C$  is the capacitance between elements (2) and (3) in the presence of element (1). It is not equal to the capacitance between isolated elements (2) and (3) in the absence of element (1). For this reason, let us find the necessary capacitance as the difference of two capacitances:

$$C = C_1 - C_0L, \quad (1.62)$$

where  $C_1$  is the total capacitance between the long and short wire, and  $C_0L$  is the capacitance between the wires of the lower segment. At that  $C_1$  is the capacitance of an electrically neutral system from two conductors (for example, [4]):

$$C_1 = (\alpha_{11} + \alpha_{22} - 2\alpha_{12})^{-1}. \quad (1.63)$$

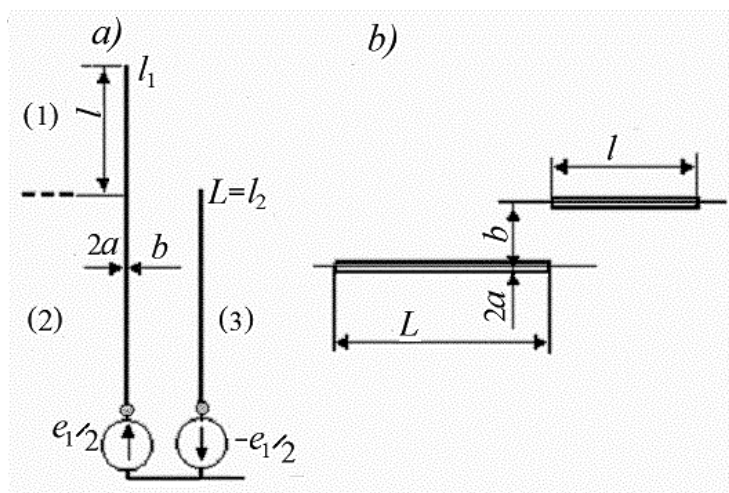


Fig. 18: Long line with wires of different length (a) and its capacitive load (b).

Here  $\alpha_{11}$  and  $\alpha_{22}$  are potential coefficients of the short and long wires,  $\alpha_{12}$  is mutual potential coefficient between these wires. They are calculated by the following formulas:

$$\alpha_{11} = \frac{1}{2\pi\epsilon L} \{ \ln[L/a + \sqrt{1 + (L/a)^2}] + a/L - \sqrt{1 + (a/L)^2} \},$$

$$\alpha_{22} = \frac{1}{2\pi\epsilon(L+l)} \{ \ln[(L+l)/a + \sqrt{1 + (L+l)^2/a^2}] + a/(L+l) - \sqrt{1 + a^2/(L+l)^2} \}$$

$$\alpha_{12} = \frac{1}{4\pi\epsilon(L+l)} \{ \ln[(L + \sqrt{L^2 + b^2})/b] + \frac{L+l}{L} \ln[(L+l + \sqrt{(L+l)^2 + b^2})/b] - \frac{l}{L} \ln[(l + \sqrt{l^2 + b^2})/b] + \frac{l}{L} [-\sqrt{L^2 + b^2} + \sqrt{l^2 + b^2} - \sqrt{(L+l)^2 + b^2} + b] \}.$$

Since  $\frac{L}{a}, \frac{l}{a} \gg 1$ , then  $\alpha_{11} = \frac{1}{2\pi\epsilon L} \left( \ln \frac{2L}{a} - 1 \right)$ ,  $\alpha_{22} = \frac{1}{2\pi\epsilon(L+l)} \left[ \ln \frac{2(L+l)}{a} - 1 \right]$ .

Sometimes inequalities  $L/b, l/b \gg 1$  is not valid. In this case:

$$\alpha_{12} = \frac{1}{4\pi\epsilon(L+l)} \left[ \ln \frac{2L}{b} + \ln \frac{2(L+l)}{b} - \frac{l}{L} \ln \frac{2l}{b} - 2 \right].$$

Calculations show that the capacitance  $C$  is small as compared with the capacitance  $C_0 L$ . If, for example,  $L = 7.5$ ,  $b = 1.0$ ,  $2a = 0.05$ , wires are in the air, i.e.,  $\epsilon = 1/(36\pi \cdot 10^9)$ , and the length  $l$  of an upper segment changes from 1 to 4 (all dimensions are in centimeters), then  $C_0 L = 7.07$  pF, and  $C$  changes from 0.05 to 0.1 pF. Thus, the additional length  $l$  creates capacitive load at the end of the two-wire line, and this load is equivalent to lengthening the long line by a segment with a length

$$l_0 = \frac{1}{k} \cot^{-1} \frac{1}{\omega C W_l}, \quad (1.64)$$

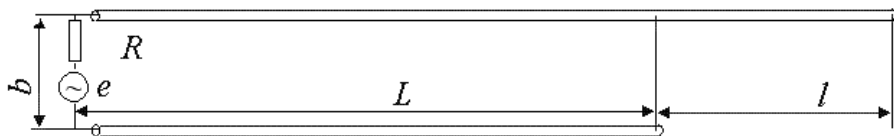
where  $W_l$  is the wave impedance of the long line. The calculation results, demonstrated the values of capacitance  $C$  and the equivalent segment lengths  $l_0$  for the mentioned dimensions at 1 GHz are given in Table 1. It is easily convinced that the capacitance between the elements (1) and (3) in the absence of the element (2) is substantially greater than the capacitance  $C$  presented in Table 1.

These calculations were verified by numerical simulation with the help of CST program. The model of structure, which was applied at this simulation, is shown in Fig. 19, where  $e$  is a generator with output impedance  $R = 50$  Ohm. The simulation results for the lengthened segment, denoted as  $l_{01}$ , are also presented in Table 1. Since the distance  $b$  between the wires is finite, then the dimensions  $l_0$  and  $l_{01}$  for  $l = 0$ , obtained on the basis of approximate theory of two-wire long line, differ from 0. The cause of this fact are self capacitances of the wires. In order to clearly demonstrate an effect of the magnitudes  $l$  on lengthening segment, dimensions  $l_0$  and  $l_{01}$  were decreased by their values at  $l = 0$ .



**Table 1:** Magnitudes of Lengthening and Capacitive Loads.

$l$ , cm	$2a = 0.05$ cm			$2a = 0.2$ cm		
	$l_0$ , cm	$l_{01}$ , cm	$C$ , pF	$l_0$ , cm	$l_{01}$ , cm	$C$ , pF
0.0	0	0	0.020	0	0	0.047
0.5	0.22	0.19	0.037	0.21	0.15	0.073
1.0	0.41	0.39	0.050	0.37	0.30	0.093
1.5	0.56	0.52	0.063	0.49	0.45	0.108
2.0	0.69	0.86	0.073	0.58	0.61	0.119
2.5	0.80	1.10	0.081	0.65	0.79	0.128
3.0	0.90	1.38	0.089	0.71	1.00	0.135
3.5	0.98	1.66	0.095	0.75	1.24	0.140
4.0	1.05	1.94	0.101	0.78	1.48	0.144
4.5	1.12	2.17	0.107	0.81	1.64	0.148

**Fig. 19:** The circuit of the simulation of the two-wire long line with wires of different lengths.

As it is seen from Table 1, the calculation and simulation results agree well for  $l \leq 0.1 \lambda$ . Results show that the input impedance of a line with wires of unequal lengths differs comparatively weakly from the input impedance of a two-wire line, whose length is equal to the shorter wire.

Similar result at  $2a = 0.2$  cm is given also in Table 1.

In accordance with given results one can write for the current distributions along the wires of line:

$$\begin{aligned}
 i_1(z) &= \begin{cases} I_0 \sin kl_0 \sin k(L + l - z)/\sin kl, & L \leq z \leq L + l, \\ I_0 \sin k(L + l_0 - z), & 0 \leq z \leq L, \end{cases} \\
 i_2(z) &= \begin{cases} 0, & L \leq z \leq L + l, \\ -I_0 \sin k(L + l_0 - z), & 0 \leq z \leq L, \end{cases} \quad (1.65)
 \end{aligned}$$

where  $I_0$  is the current of a generator. A long line with equal length of wires located in free space can radiate only in the case when the distance between the wires is not too small compared with the wave length. As it follows from expressions (1.65) for the currents, in the case of wires with unequal length, the source of radiation is the additional length  $l$  of a longer wire.

The obtained results allow to consider another problem—calculating input impedance of a linear radiator (monopole) composed of two parallel wires with different lengths (Fig. 20a). Figure 20b shows an equivalent asymmetric long line for such structure.

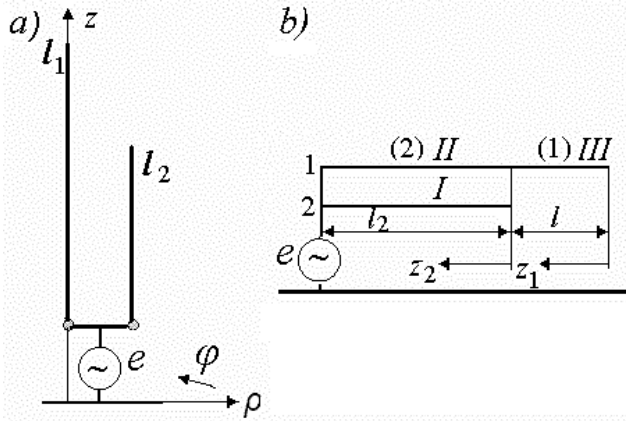


**Fig. 20:** Monopole, formed by the wires of different lengths (a), and equivalent to it long line (b).

In this case it is necessary to divide the long line into two segments, as shown in Fig. 20b. The segment 1 has one wire; the segment 2 consists of two wires. The segment number is indicated in brackets, the number of wires is indicated in its base. The currents and potentials along the segment  $m$  of the  $n$ th wire are given by (1.37), where  $n = 1, 2, m = 1, 2$ . If the distance between the wires is small in comparison with the wires' lengths, one can consider that

$$\rho_{nn}^{(m)} = \text{const}(n) = \rho_1^{(m)}, \rho_{ns}^{(m)} = \text{const}(n) = \rho_2^{(m)},$$

$$W_{nn}^{(m)} = \text{const}(n) = W_1^{(m)}, W_{ns}^{(m)} = \text{const}(n) = W_2^{(m)}.$$

The zero currents at the ends of the wires and the continuity of the current and potential along each wire permit to write the boundary conditions:

$$i_1^{(1)} \Big|_{z_1=0} = i_2^{(2)} \Big|_{z_2=0} = 0; i_1^{(1)} \Big|_{z_1=l} = i_2^{(2)} \Big|_{z_2=0}; u_1^{(1)} \Big|_{z_1=l} = u_1^{(2)} \Big|_{z_2=0}; u_1^{(2)} \Big|_{z_2=l_2} = u_2^{(2)} \Big|_{z_2=l_2} = e.$$

In accordance with these boundary conditions

$$I_1^{(1)} = I_1^{(1)} = 0, I_1^{(2)} = j \frac{U_1^{(1)}}{W_1^{(1)}} \sin kl, U_1^{(2)} = U_1^{(1)} \cos kl, U_1^{(2)}$$

$$= U_1^{(1)} \left[ \cos kl_2 - \frac{\rho_1^{(2)} - \rho_2^{(2)}}{W_1^{(1)}} \sin kl_2 \tan kl_2 \right],$$

$$U_1^{(1)} = \frac{e}{\cos kl \cos kL_2} \left[ 1 - \frac{\rho_1^{(2)}}{W_1^{(1)}} \tan kl \tan kL_2 \right]^{-1}.$$

The current distribution along the first and the second segment of the longer wire and along the shorter wire is respectively

$$i_1^{(1)} = j \frac{U_1^{(1)}}{W_1^{(1)}} \sin k(l_1 - z); i_1^{(2)} = j U_1^{(1)} \left\{ \frac{\sin kl \cos kz_2}{W_1^{(1)}} + \cos kl \left[ \frac{1}{W_1^{(2)}} - \frac{1}{W_2^{(2)}} \left\langle 1 - \frac{\rho_1^{(2)} - \rho_2^{(2)}}{W_1^{(1)}} \right\rangle \tan kl \tan kL_2 \right] \sin kz_2 \right\};$$

$$i_2^{(2)} = j U_1^{(1)} \cos kl \left\{ \frac{1}{W_1^{(2)}} - \frac{1}{W_2^{(2)}} \left[ 1 - \frac{\rho_1^{(2)} - \rho_2^{(2)}}{W_1^{(1)}} \right] \tan kl \tan kL_2 \right\} \sin kz_2. \quad (1.66)$$

The total current along the second segment is

$$i_1^{(2)} + i_2^{(2)} = j U_1^{(1)} \left\{ \frac{\sin kl \cos k(l_2 - z)}{W_1^{(1)}} \cos kl \left[ \frac{1}{W_1^{(2)}} - \frac{1}{W_2^{(2)}} \left\langle 1 - \frac{\rho_1^{(2)} - \rho_2^{(2)}}{W_1^{(1)}} \right\rangle \tan kl \tan kL_2 \right] \sin k(l_2 - z) \right\}. \quad (1.67)$$

These expressions show that the current distribution along each segment of the monopole is sinusoidal, i.e., it is similar to the current distribution along a monopole consisting of two segments with different wave impedances (for example, with different wire diameters).

Let us write the expression for the total current along the monopole in the form

$$J_{Am}(z) = \sum_{n=1}^M i_n^{(m)}(z), \quad l_{m+1} \leq z \leq l_m, \quad (1.68)$$

where

$$i_n^{(m)}(z) = A_{nm} \cos k(l_m - z) + j B_{nm} \sin k(l_m - z).$$

In accordance with (1.66)

$$A_{11} = A_{21} = A_{22} = B_{21} = 0, \quad B_{11} = \frac{U_1^{(1)}}{W_1^{(1)}}, \quad A_{12} = j \frac{U_1^{(1)}}{W_1^{(1)}} \sin kl,$$

$$B_{12} = B_{22} = U_1^{(1)} \cos kl \left[ \frac{1}{W_1^{(2)}} - \frac{1}{W_2^{(2)}} \left\langle 1 - \frac{\rho_1^{(2)} - \rho_2^{(2)}}{W_1^{(1)}} \right\rangle \tan kl \tan kL_2 \right]. \quad (1.69)$$

The input reactance of the monopole is equal to the input impedance of the equivalent line:

$$jX_A = Z_l = \frac{e}{J_A(0)} = -j \frac{[W_1^{(1)} - \rho_1^{(2)} \tan kl \tan kL_2] \cos^2 kl_2}{\tan kl \cos^2 kL_2 + DW_1^{(1)} \sin 2kl_2}, \quad (1.70)$$

where

$$D = \frac{1}{W_1^{(2)}} - \left[ 1 - \frac{\rho_1^{(2)} - \rho_2^{(2)}}{W_1^{(1)}} \right] \frac{\tan kl \tan kL_2}{W_2^{(2)}}.$$

The radiation resistance of the monopole is equal to

$$R_\Sigma = 40k^2 h_e^2, \quad (1.71)$$

where  $h_e$  is the effective height of the monopole given by

$$\begin{aligned} h_e &= \frac{1}{kJ(0)} \sum_{m=1}^2 \{ (A_{1m} + A_{2m}) \operatorname{sinc}(l_m - l_{m+1}) + j(B_{1m} + B_{2m}) [1 - \cos k(l_m - l_{m+1})] \} = \\ &= \frac{jU_1^{(1)}}{kJ(0)W_1^{(1)}} \{ 1 + \sin kL \sin kL_2 + \cos kl [2DW_1^{(1)} (1 - \cos kl_2) - 1] \}. \end{aligned} \quad (1.72)$$

These expressions define the currents along each wire of asymmetric radiator and allow more accurately calculate its input impedance. Considering that an antenna is linear radiator and the current along it is equal to a total current of both wires, it is possible to find the input impedance, for example, by the method of induced emf (second formulation). During calculating the tangential component of the electric field, one must take into account the discontinuity of the current derivative on the segment boundaries.

## 7. Multi-folded Radiator

As said in Section 5, asymmetric folded radiator consisting of two parallel wires, upper ends of which are connected to each other, combines the functions of radiation and matching. In folded radiator with a gap, if the length of the radiator is less than a quarter of wave length, capacitive impedance of a monopole is compensated by inductive impedance of short-circuited long line. If in the folded radiator the second wire is shorted to a ground, the long line, connected in parallel with input impedance of linear antenna, changes the radiator resistance, transforms it.

Multi-folded radiator (Fig. 21) consists of several folded radiators connected in series with each other and gives more opportunities to obtain new circuits and connections (series and parallel ones) and new results in this direction. Such a radiator is a group of parallel wires connected in pairs at the top and bottom so that to form a system of coupled and connected in series elongated loops (two-wire long lines). In the particular case when the number of wires is two, this antenna becomes a folded radiator.

If the transverse dimensions of multi-folded radiator are small in comparison with its height  $L$  and the wave length  $\lambda$ , then, as is shown in the article [14], devoted to research of electromagnetic oscillations in systems of parallel thin wires, the current in each wire of such a system can be divided into in-phase and anti-phase components, and the entire system may be reduced to an aggregate of linear radiator and non-radiating long lines.

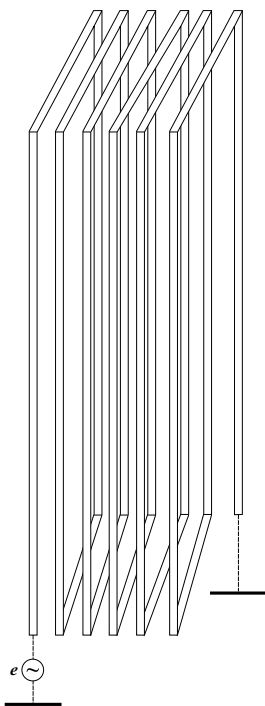


**Fig. 21:** Multi-folded radiator.

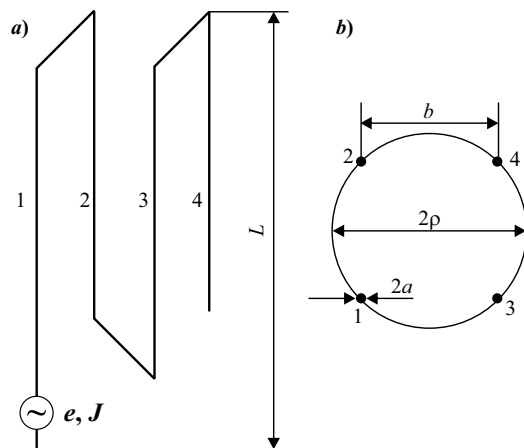


**Fig. 22:** Two-folded radiator with a gap: a – circuit, b – cross-section.

The calculating method of such antenna may be considered using an example of a two-folded radiator with a gap (Fig. 22).

At first, we must divide the two-folded antenna onto a radiator and long lines. For that, into the gap between the free end of the antenna and the ground we include in parallel two generators of the current, that are equal in magnitude ( $mJ$ ) and opposite in sign (Fig. 23). Here  $J$  is the current of the main generator. We divide

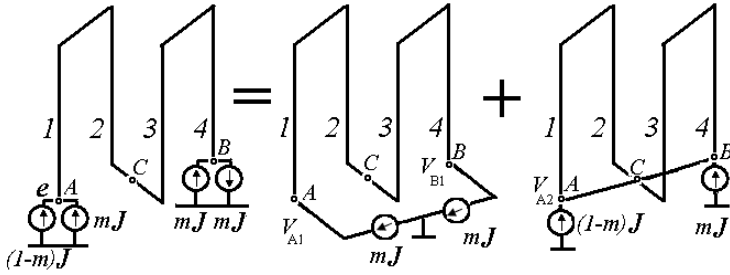


Fig. 23: To the calculation of a two-folded radiator with a gap.

the main generator onto two generators of the currents that are identical in direction and different in magnitude, with currents  $mJ$  and  $(1 - m)J$ . The total current of the generator as a result does not change; the current in the gap is zero as before.

According to the superposition principle a voltage at point  $A$  is equal to a sum of voltages, produced by all generators. Therefore, as it is shown in Fig. 23, one can divide the circuit of the two-folded antenna onto two circuits, with two generators in each one. The voltages at point  $A$ , created in each of these circuits, are calculated and summed.

In the first auxiliary circuit the generators are identical and connected in series. Therefore, the voltage between the point  $A$  and the ground is

$$V_{A1} = V/2 = 0.5mJZ_1, \quad (1.73)$$

where  $V = V_{A1} - V_{B1}$  is the input voltage, and  $Z_1$  is the impedance of a complicated long line. More precisely, there are two coupled lines with the same distance  $b\sqrt{2}$  between wires and the equal wave impedances  $W_1 = 120 \ln(b\sqrt{2}/a)$ . One of these lines is a load for the other line. In the first approximation it could be consider that it is a united two-wire line with the wave impedance  $W_1$ , bended in the middle at an angle  $180^\circ$ . If to calculate the input impedance of a first circuit with help of the theory of electrically coupled lines, then the wave impedance of the complicated line will be equal to the value  $W_2 = W_3 W_4 / (W_4 - W_3)$  where

$$W_3 \approx 80 \ln b/a, \quad W_4 = 240 \ln [b/(a\sqrt{2})].$$

It is easy to make sure that for small radius of wires ( $b \gg a$ )  $W_2 \approx W_1 \approx 120 \ln b/a$ .

The points  $A$  and  $B$  in the second auxiliary circuit are connected with each other as equipotential points. It means that  $m = 1/2$ , if the wires diameters are identical. The second circuit is the folded radiator, in which each "conductor" consists of two parallel wires (1 and 4, 2 and 3 respectively). This circuit can also be divided into two ones: the four-wire line of length  $L$ , shorted at the end, and the asymmetric radiator (monopole) of height  $L$ . The wave impedance of the line is equal to  $W_5 = 60 \ln(b/a\sqrt{2})$ . Equivalent radius of the monopole from four wires, located along the cylinder generatrixes (the wire radius is  $b/a\sqrt{2}$ ) is equal to  $a_e = \sqrt[4]{ab^3\sqrt{2}}$ . Input impedance of the second circuit is

$$Z_{A2} = Z_m(a_e) + j0.25W_5 \tan kL.$$

This input impedance is calculated by means of the same procedure of dividing the initial circuit onto two circuits (monopole and the long line) and summing the voltages. For the voltage between point A and the ground in the second circuit one can write

$$V_{A2} = \mathcal{J}[Z_m(a_e) + j0.25W_5 \tan kL], \quad (1.74)$$

i.e., the input impedance of the entire antenna

$$Z_A = Z_m(a_e) + j0.25W_2 \tan 2kL + j0.25W_5 \tan kL. \quad (1.75)$$

This impedance is presented in Fig. 24, which shows the input impedances of the antenna and its components. The input impedance of the considered antenna is a series connection of the monopole and two lines with length  $L$  and  $2L$  shorted at the end. The wave impedances of these lines are close to values

$$W(n) \approx \frac{120}{n} \ln b/a,$$

where  $n$  is the number of wires in each 'conductor' of the line.

From expression (1.75) and Fig. 24 it follows that the radiation's resistance of the two-folded antenna with a gap is equal to the radiation's resistance of the monopole with the same height. The reactive component of the input impedance has additional resonances. The first parallel resonance is caused by a parallel resonance of the long line with length  $2L$ , i.e., its frequency is half the frequency of the first series resonance of an ordinary monopole with the same height. The frequency of the first series resonance of the antenna is even smaller (but not necessarily two times).

Due to increase of the wires' quantity and a corresponding increase of the length of a total antenna wire, the number of resonances in a concrete frequency range increase. For example, if the number of folded radiators connecting in series with each other is equal to  $N = 2^n$ , then for the antenna with a gap we obtain similarly to (1.75)

$$Z_A = Z_m(a_e) + j0.25 \sum_{m=0}^n W(2^m) \tan (NkL/2^m), \quad (1.76)$$

where  $a_e = \sqrt[2N]{2Nap^{2N-1}}$  is the equivalent radius of the monopole, consisting of  $2N$  wires, which are located along the generatrices of the cylinder with the radius  $\rho$  (if  $N$  grows, the equivalent radius tends to  $\rho$ ). The frequency of the first parallel resonance of the antenna (i.e., of its second resonance) is  $N$  times lower than the frequency of the first series resonance of an ordinary monopole with the same height. Such a character of the input impedance allows, firstly, to use multi-folded antenna in the range of longer waves, and secondly, when it is necessary, to tune the antenna onto several frequencies.

If  $N$ -folded antenna with shorting to ground has the wires of identical diameters (see Fig. 21, dotted line), its input admittance is

$$Y_A = \frac{1}{120 \ln(b/a) \tan NkL} + \frac{1}{4Z_{N/2}}, \quad (1.77)$$

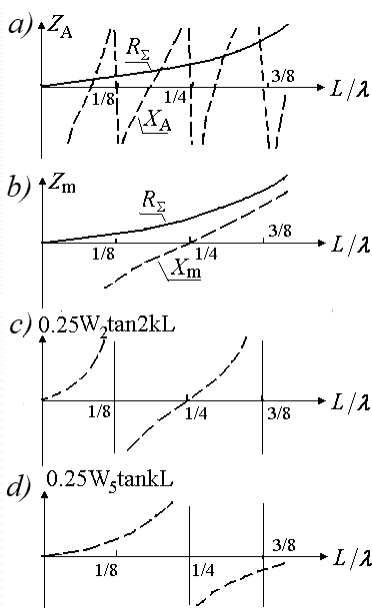


**Fig. 24:** Impedance of two-folded antenna (a) and of its components: monopole (b), long line of length  $2L$  (c), long line of length  $L$  (d).

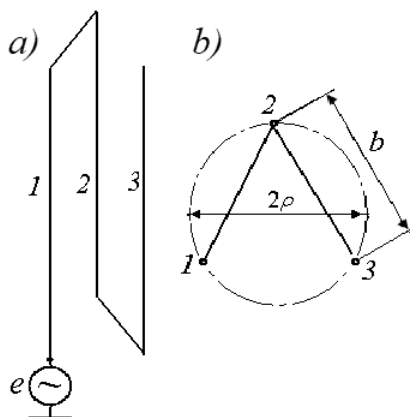


**Fig. 25:** Three-wire antenna: a – circuit, b – cross-section.

where  $Z_{N/2}$  is the input impedance of the  $N/2$ -folded antenna with a gap and with "conductors" from two wires. This result generalizes expression (1.56) and was obtained similarly.

In the case of odd number of antenna wires the calculation becomes more complicated. For example, a radiator of three wires (Fig. 25) may be divided onto a three-wire line and a monopole of a height  $L$  (Fig. 26). Potentials of all wires in each cross-section of a second circuit (monopole) must be the same. In accordance with (1.59), the magnitude  $m$  depends on the capacitance relation of two antenna branches. The right branch consists of two wires, and its capacitance is twice as much.



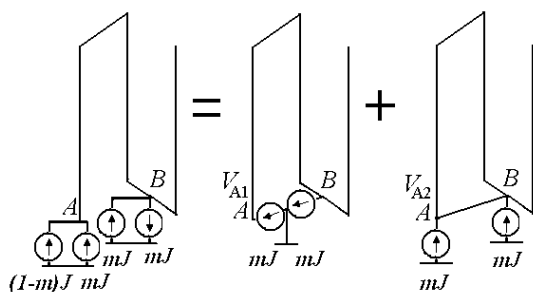


Fig. 26: To the calculation of three-wire folded antenna with a gap.

From here it follows that  $m = 2/3$ . One can show, using the theory of electrically coupled lines that an impedance of a line from the identical three wires (of a first circuit) is equal to

$$Z_l = j80 \ln(b/a) \frac{1}{\cot 2kK + \cot kL}.$$

In this circuit there are only anti-phase currents, and their sum is equal to zero in each cross-section. Sum of potentials in an arbitrary cross-section also is zero, i.e.

$$V_{A1} = -2V_{B1} = 2V/3,$$

where  $V = V_{A1} - V_{B1}$  is the voltage at the input of the long line. From here the impedance of the three-wire antenna is

$$Z_A = \frac{V_{A1} + V_{A2}}{J} = Z_m(a_e) + j80 \ln(b/a) \frac{1}{\cot 2kL + \cot kL}.$$

Equivalent radii of the three-wire monopole and the three-folded radiator are equal accordingly to  $a_e = \sqrt[3]{ab^2}$  and  $a_e = \sqrt[6]{6ab^5}$ . If the number of folded radiators is  $N = 3 \cdot 2^n$ , then

$$Z_A = Z_m(a_e) + j0.25 \sum_{m=0}^n W(2^m) \tan(NkL/2^m) + j0.33 W(2^n) \frac{1}{\cot 2kL + \cot kL}. \quad (1.78)$$

The value of  $a_e$  is given above.

Multi-folded antennas can play an important role in solving a problem of creating weak fields near a transmitting antenna. This problem is relevant when near the transmitting antenna is a body that is sensitive to an electromagnetic field, and it is necessary to protect this body from the field, not shielding it from an external space. This situation arises when one must solve the problems of electromagnetic compatibility and when protect people from irradiation.

An idea of protection from the electromagnetic field with help of screening, i.e., by means of using a shadowing effect, appears obvious. But practically this approach is not realizable. The near field has no ray structure. Therefore, the shadow formed behind the metal screen has the dimensions close to the screen dimensions.

For example, the screen for protection of the user's head from irradiation must have the dimensions, which is substantially larger than the dimension of the cellular phone.

More acceptable results are given by another principle—by the principle of mutual compensation of fields created by different radiators in a given area. This method is used to protect the equipment near power lines. In a special option of this method for creating a compensating field and a 'dark spot', an additional radiator is used, which is excited by the same source of energy, which feeds the main radiator [15]. The method is based on a rapid decrease of the near field with increasing the distance from the radiator. The field of a weak radiator located nearer to the given area has the same value as the field of a main radiator. In this case, a small field, as a rule, practically does not affect the shape of the directional pattern, since, near the antenna, the radiated field flows around the 'dark spot'.

Such an antenna is an asymmetrical dipole, one arm of which is made as a metal plate and other arm is a multi-folded structure. This structure ensures the anti-phase current in the antenna and hence creates the small auxiliary field, which compensates the main field at a compensation point and forms around this point an area of a weak field (a dark spot). Contribution of this arm to the radiation is small. But the reactance of the monopole is close to zero, if the plate length is close to a resonant length. To ensure matching with a cable or generator, the multi-folder structure should have a series resonance at the first operation frequency. In the operation frequency band, the reactance of a multi-folded structure permits to compensate the reactance of a monopole.

## 8. Antenna with Meander Load

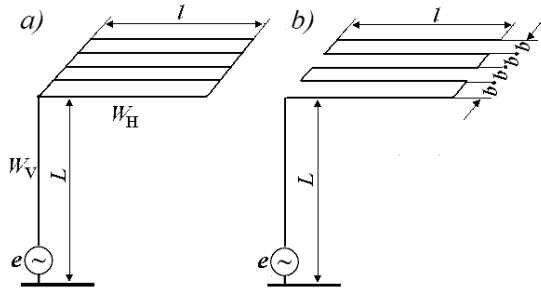
In this Section we consider an example of using multi-folded structure in the form of the meander. This structure is applied in the capacity of a horizontal load of a vertical wire antenna. The antenna with meander load is analyzed by means of the theory of coupled lines. As is known, the horizontal load serves for increasing an effective height of the antenna by changing a current distribution along a radiating vertical wire. The equivalent length of the horizontal segment of an antenna is equal to

$$l_e = \frac{1}{k} \tan^{-1} \left( \frac{W_H}{W_V} \cot kL \right) \approx \frac{W_V l}{W_H}. \quad (1.79)$$

As is seen from (1.79), an equivalent length of the horizontal segment is inversely proportional to its wave impedance  $W_H$  and directly proportional to its length  $l$  and also to a wave impedance  $W_V$  of a vertical segment. Therefore, the horizontal load usually fabricated in the form of several parallel wires, connected with each other at the ends (Fig. 27a).

In Fig. 27b the antenna circuit is shown, where wires of a horizontal load are connected with each other in series [16]. In this circuit, a current path along a load is lengthened, i.e., an equivalent length of a load is increased. The antenna was called in accordance with the shape of a horizontal load.

An increase in the equivalent length of the load makes it possible to increase the effective height of the antenna. As can be seen from the above, in this case the structure of the wires is used not to create an antenna with several series resonances

Fig. 27: Inverted  $L$  antenna (a) and antenna with meander load (b).

and, accordingly, a high matching level at several operating frequencies, but to obtain a qualitative communication at one frequency. It should be remembered that inverted  $L$  antennas are widely used on ships of the marine fleet, where the problem of increasing effective height of the antenna is acute.

As already mentioned, in order to calculate the input impedance of the load, one can use the theory of coupled parallel long lines located above the infinite metal surface. The current and the potential of each wire of an asymmetric line consisting of  $N$  parallel wires are determined by expressions (1.34). The wave impedances between the wires are  $\rho_{ns}$  and  $W_{ns}$ . For example, determining the input impedance of three-wire load, shown in Fig. 28, begins with writing the boundary conditions for the currents and potentials:

$$\begin{aligned} u_1(0) &= u_2(0), & i_1(0) + i_2(0) &= 0, & i_3(0) &= 0, \\ u_2(l) &= u_3(l), & i_2(l) + i_3(l) &= 0, & u_1(l) &= e. \end{aligned} \quad (1.80)$$

It is supposed that the radii of wires are small as compared to the distances  $b$  between them. Since the height  $L$  of their suspension is commensurable with the wire length  $l$ , the method of average potentials is used to determine the potential coefficients. Taking into account mirror image, we get:

$$\alpha_{11} = \alpha_{22} = \alpha_{33} = \alpha_1 / (2\pi\epsilon), \quad (1.81)$$

where

$$\alpha_1 = \ln(l/a) - 0.307 - \sinh^{-1}(l/2L) + \sqrt{1 + (2L/l)^2} - 2L/l.$$

Similarly

$$\alpha_{12} = \alpha_{21} = \alpha_{23} = \alpha_{32} = \epsilon_2 / (2\pi\epsilon), \quad \alpha_{13} = \alpha_{31} = \alpha_3 / (2\pi\epsilon).$$

where

$$\alpha_2 = \sinh^{-1}(l/b) - \sqrt{1 + (b/l)^2} + b/l - \sinh^{-1}(l/\sqrt{4L^2 + b^2}) + \sqrt{1 + (4L^2 + b^2/l^2)} - \sqrt{4L^2 + b^2/l^2},$$

and  $\alpha_3$  turns out from  $\alpha_2$ , if we replace  $b$  by  $2b$ . Since the distance

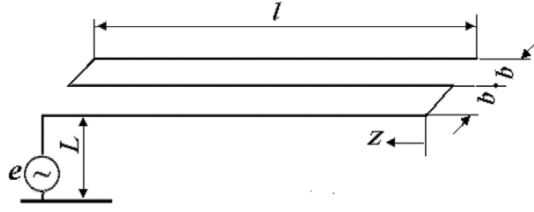


Fig. 28: Meander load of three wires.

between neighboring wires of the load is small in comparison with  $L$  and  $l$ , we will accept to simplify calculations

$$\alpha_2 = \alpha_3. \quad (1.82)$$

This assumption does not cause significant error because  $\sinh^{-1} x = \ln(x + \sqrt{x^2 + 1})$ , i.e., the error has logarithmic character. The error is justified also since the length of the connecting bridges at the load ends can be taken into account in the used method only indirectly (by means of replacing  $l$  by  $l + b$ ). From the mentioned expressions we obtain

$$\rho_{ns} = \begin{cases} \rho_1, & n = s, \\ \rho_2, & n \neq s, \end{cases} \quad (1.83)$$

where  $\rho_1 = 60 \alpha_1$ ,  $\rho_2 = 60 \alpha_2$ . Taking into account relationship between coefficients  $\beta_{ns}$  and  $\alpha_{ns}$ , we get that

$$W_{ns} = \begin{cases} W_1 = 1/(c\beta_{11}), & n = s, \\ W_2 = -1/(c\beta_{12}), & n \neq s, \end{cases}$$

and for three-wire load

$$\frac{1}{W_1} = \frac{\rho_1 + \rho_2}{(\rho_1 - \rho_2)(\rho_1 + 2\rho_2)}, \quad \frac{1}{W_2} = \frac{\rho_2}{(\rho_1 - \rho_2)(\rho_1 + 2\rho_2)}. \quad (1.84)$$

Substituting expressions (1.34) for the current and potential into the boundary conditions (1.80) and taking into account (1.83) and (1.84), we obtain:

$$\begin{aligned} U_2 = U_1, \quad I_2 = -I_1, \quad I_3 = 0, \quad U_3 = U_1 + j(\rho_2 - \rho_1)I_1 \tan kl, \\ I_1 = j \frac{2U_1 \tan kl}{\rho_1 + 2\rho_2 - \rho_1 \tan^2 kl}, \quad U_1 = e \frac{\rho_1 + 2\rho_2 - \rho_1 \tan^2 kl}{\cos kl[\rho_1 + 2\rho_2 + (2\rho_2 - 3\rho_1)\tan^2 kl]}. \end{aligned}$$

From here the input impedance of three-wire load is

$$Z_3 = \frac{u_1(l)}{i_1(l)} = -j \cot kl \frac{\rho_1 + 2\rho_2 + (2\rho_2 - 3\rho_1)\tan^2 kl}{3 - \tan^2 kl}. \quad (1.85)$$

In order to test the effect of the adopted assumption (1.82) on the result of calculating electrical characteristics of the antenna we shall consider the option with  $\rho_3 = 60 \alpha_3$ . In this case the electrodynamics wave impedances are equal to

$$W_{11} = W_{33} = \frac{(\rho_1 - \rho_2)(\rho_1^2 + \rho_1 \rho_3 - 2\rho_2^2)}{\rho_1^2 - \rho_2^2}, \quad W_{22} = \frac{\rho_1^2 + \rho_1 \rho_3 - 2\rho_2^2}{\rho_1 + \rho_3},$$

$$W_{13} = W_{31} = \frac{(\rho_1 - \rho_3)(\rho_1^2 + \rho_1 \rho_3 - 2\rho_2^2)}{\rho_1 \rho_3 - \rho_2^2}, \quad W_{12} = W_{21} = W_{23} = W_{32} = \frac{\rho_1^2 + \rho_1 \rho_3 - 2\rho_2^2}{\rho_2},$$

and expression for  $Z_3$  will take the form

$$Z_3 = -j \frac{A + B \tan^2 kl}{C + D \tan^2 kl} \cot kl, \quad (1.86)$$

where

$$A = 2 \left[ \frac{1}{W_{11}} - \frac{3}{W_{12}} + \frac{1}{W_{22}} - \frac{1}{W_{13}} \right]^{-1}, \quad B = A(2\rho_{12} - \rho_{11} - \rho_{13}) \left( \frac{1}{W_{11}} - \frac{1}{W_{12}} \right) + 2(\rho_{12} - \rho_{11}),$$

$$C = 2 + A \left( \frac{1}{W_{11}} - \frac{1}{W_{12}} - \frac{1}{W_{13}} \right), \quad D = (2\rho_{12} - \rho_{11} - \rho_{13})$$

$$\left[ \frac{2}{W_{13}} + A \left( \frac{1}{W_{11}} - \frac{1}{W_{12}} - \frac{1}{W_{13}} \right) \left( \frac{1}{W_{11}} - \frac{1}{W_{12}} \right) \right].$$

As calculation results show, impedances  $Z_3$ , calculated in accordance with (1.85) and (1.86) for real antennas differ from each other by no more than 1–2 per cent, i.e., the use of the approximate expressions for  $\rho_{ns}$  and  $W_{ns}$  weakly effects on the calculation result, if the inequality  $a \ll b \ll l$  is valid. At the same time, the application of this approximation greatly simplifies the calculation and allows to use it for load from any number of wires.

In this case determinant  $\Delta_N$  in the expression for  $\beta_{ns}$  is written in the form

$$\Delta_N = \begin{vmatrix} \alpha_1 & \alpha_2 & \alpha_2 & \dots & \alpha_2 \\ \alpha_2 & \alpha_1 & \alpha_2 & \dots & \alpha_2 \\ \alpha_2 & \alpha_2 & \alpha_1 & \dots & \alpha_2 \\ \dots & \dots & \dots & \dots & \dots \\ \alpha_2 & \alpha_2 & \alpha_2 & \dots & \alpha_1 \end{vmatrix}. \quad (1.87)$$

It is easy to check and to be convinced that for  $N$ , equal to 1, 2, 3

$$\Delta_N = (\alpha_1 - \alpha_2)^{N-1} [\alpha_1 - (N-1)\alpha_1]. \quad (1.88)$$

The method of mathematic induction permits to prove that this expression is valid for any positive integer  $N$ . For that it is necessary to show that the rightness of

this expression for the determinant  $\Delta_N$  means its rightness for the determinant  $\Delta_{N+1}$ . We expand the determinant by the elements of the first line:

$$\Delta_{N+1} = \alpha_1 \Delta_N + \alpha_2 \sum_{r=2}^{N+1} (-1)^{r+1} M_{1r} = \alpha_1 \Delta_N - N \alpha_2 D_N. \quad (1.89)$$

Here  $M_{1r}$  is minor of the determinant  $\Delta_{N+1}$ ,  $D_N = M_{12}$  is the determinant of the  $N$ th order:

$$D_N = \begin{vmatrix} \alpha_2 & \alpha_2 & \alpha_2 & \dots & \alpha_2 \\ \alpha_2 & \alpha_1 & \alpha_2 & \dots & \alpha_2 \\ \alpha_2 & \alpha_2 & \alpha_1 & \dots & \alpha_2 \\ \dots & \dots & \dots & \dots & \dots \\ \alpha_2 & \alpha_2 & \alpha_2 & \dots & \alpha_1 \end{vmatrix}.$$

For this determinant the expression similar to expression (1.89), is true:

$$D_N = \alpha_2 \Delta_{N-1} - (N-1) \alpha_2 D_{N-1}.$$

At the same time in accord with (1.87)

$$\Delta_N = \alpha_1 \Delta_{N-1} - (N-1) \alpha_2 D_{N-1}.$$

From the last two equalities

$$D_N = \Delta_N + (\alpha_2 - \alpha_1) \Delta_{N-1}.$$

Substituting into this expression the value  $\Delta_N$  from (1.88) and the value  $\Delta_{N-1}$ , which in accord with (1.88) is equal to  $\Delta_{N-1} = (\alpha_1 - \alpha_2)^{N-2} [\alpha_1 - (N-2) \alpha_2]$ , we obtain

$$D_N = \alpha_2 (\alpha_1 - \alpha_2)^{N-1}.$$

From here in accordance with (1.89)

$$\Delta_{N+1} = \alpha_1 (\alpha_1 - \alpha_2)^{N-1} [\alpha_1 + (N-1) \alpha_2] - N \alpha_2^2 (\alpha_1 - \alpha_2)^{N-1} = (\alpha_1 - \alpha_2)^N (\alpha_1 + N) \alpha_2,$$

as required. Since

$$\Delta_{ns} = \begin{cases} \Delta_{n-1}, & n = s, \\ (-1)^{n+s} \alpha_2 (\alpha_1 - \alpha_2)^{N-2}, & n \neq s, \end{cases}$$

i.e., in accordance with expression for  $\beta_{ns}$  electrostatic wave impedances are equal to

$$W_1 = (\rho_1 - \rho_2) \frac{\rho_1 + (N-1) \rho_2}{\rho_1 + (N-1) \rho_2}, \quad W_2 = (\rho_1 - \rho_2) \frac{\rho_1 + (N-1) \rho_2}{\rho_2},$$

Boundary conditions for currents and potentials of N-wire load differ for an even and odd number of wires. For an odd number of wires, when  $N = 2m-1$ , the boundary conditions are:

$$\begin{aligned} u_{2n-1}(0) &= u_{2n}(0), \quad i_{2n-1}(0) + i_{2n}(0) = 0, \quad i_{2m-1}(0) = 0, \\ u_{2n}(l) &= u_{2n+1}(l), \quad i_{2n}(l) + i_{2n+1}(l) = 0, \quad u_1(l) = e. \end{aligned}$$

In this case, as shown in [17], the input impedance of the load is

$$Z_{2m-1} = \frac{u_1(l)}{i_1(l)} = -j(\rho_1 - \rho_2) \tan \beta \frac{2(A_m + A_{m-1} - 1) + H_{2m-1} [1 - A_m - A_{m-1} + (B_m + B_{m-1})/(2M \sin^2 \beta)]}{2(A_{m-1} - A_m) + H_{2m-1} [A_m - A_{m-1} + (B_{m-1} + B_m)/(2M \sin^2 \beta)]} \quad (1.90)$$

where

$$\begin{aligned} \beta &= kL, \quad A_m = m + 2 \sum_{r=1}^{m-1} r \cos 2(m-r)\beta, \quad B_m = \cos 2m\beta, \\ M &= \frac{\rho_2}{\rho_1 + 2(m-1)\rho_2}, \quad H_{2m-1} = (1 - 4M \sin^2 \beta) / \sum_{s=0}^{m-1} (B_s - 2M_s A \sin^2 \beta). \end{aligned}$$

Similarly, for an even number of wires ( $N = 2m$ )

$$Z_{2m} = -j(\rho_1 - \rho_2) \tan \beta \frac{4M \tan^2 \beta (C_m + C_{m-1} - \cos^2 \beta) + H_{2m} (D_m + D_{m-1})}{4M \tan^2 \beta (C_{m-1} - C_m) + H_{2m} (D_{m-1} - D_m)}, \quad (1.91)$$

where

$$\begin{aligned} C_m &= m + \sum_{r=0}^{m-1} (2r+1) \cos 2(m-r)\beta, \quad D_m = \frac{\cos 2(m+1)\beta}{\cos \beta}, \\ H_{2m} &= \left[ 1 - 4M \tan^2 \beta \sum_{s=0}^{m-1} C_s \right] / \sum_{s=0}^{m-1} D_s, \end{aligned}$$

For the sake of convenience of a calculation, numerators, and denominators of expressions (1.90) and (1.91) can be presented as an expansion in powers of the quantity  $\tan^2 \beta$  [16].

In Table 2 expressions for calculating the load impedances with different numbers of wires are given. If  $\tan \beta < 1$ , the calculation accuracy in accordance with (1.91) and with expressions, presented in Table 2, is determined by the number of calculated terms. If  $\beta \ll 1$ , then limiting in (1.91) by the first two terms of the numerator and denominator, we find:

$$Z_N = -j \frac{\rho_1 + (N-1)\rho_2}{N\beta} \left\{ 1 - \frac{N\beta^2 [N_{\rho_1} + (N-1)\rho_2]}{3[\rho_1 + (N-1)\rho_2]} \right\}. \quad (1.92)$$

Table 2: Impedances of Loads.

Number of wires	Expressions for calculating
2	$-0.5j \cot \beta [\rho_1 + \rho_2 + (\rho_2 - \rho_1) \tan^2 \beta]$
3	$-j \frac{\cot \beta}{3 - \tan^2 \beta} [\rho_1 + 2\rho_2 + (2\rho_2 - 3\rho_1) \tan^2 \beta]$
4	$-j \frac{\cot \beta}{4(1 - \tan^2 \beta)} [\rho_1 + 3\rho_2 - 2(3\rho_1 - \rho_2) \tan^2 \beta + (\rho_1 - \rho_2) \tan^4 \beta]$
5	$-j \frac{\cot \beta}{5 - 10 \tan^2 \beta + \tan^4 \beta} [\rho_1 + 4\rho_2 - 10\rho_1 \tan^2 \beta + (5\rho_1 - 4\rho_2) \tan^4 \beta]$
6	$-j \frac{\cot \beta}{2(1 - 3 \tan^2 \beta)(3 - \tan^2 \beta)} \cdot$ $[\rho_1 + 5\rho_2 - 5(3\rho_1 + \rho_2) \tan^2 \beta + 3(5\rho_1 - 3\rho_2) \tan^4 \beta - (\rho_1 - \rho_2) \tan^6 \beta]$

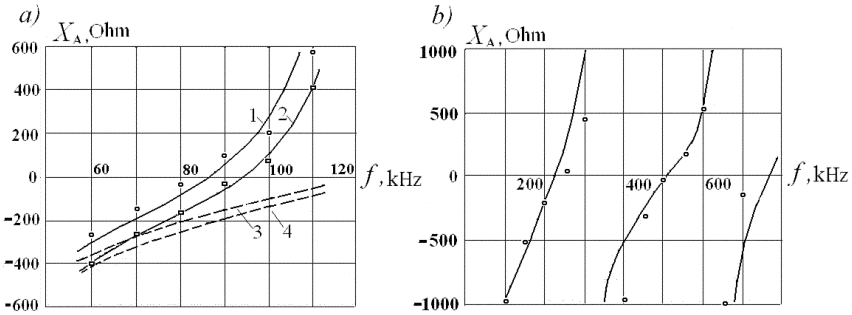


Fig. 29: Reactance of antennas with meander load of four (a) and six (b) wires.

This expression is true also for the odd number of wires.

Knowing the load impedance, one can determine all electrical characteristics of the antenna.

Figure 29a shows the calculated curves and the results of experimental verification for the same antenna with different distance between wires. This experiment was performed on a model. Dimensions of the antenna (in meters):  $L = 200$ ,  $l = 300$ ,  $a = 0.1$ . The number of wires in the load is equal to four. The distance  $b$  between the wires' axes of a first antenna load (curve 1) is equal to 5, of the second load (curve 2) to 2. In Fig. 29b the results of calculation and experimental verification are presented for an antenna with load of six wires. Dimensions of the antenna:  $L = 50$ ,  $l = 70$ ,  $b = 1.54$ ,  $a = 0.004$ . And the coincidence with the experiment is good in both cases.

For comparison, the input reactance of the inverted L antennas with the same sizes is given in the figure by dotted lines (curves 3 and 4). As can be seen from the figures, the use of meander load increases the electrical length of the antenna and shifts its resonances in the direction of low frequencies.

Figure 30a presents the calculated curves and experimental values of the input impedance for similar antenna (curve 1) with six wires in the load and with



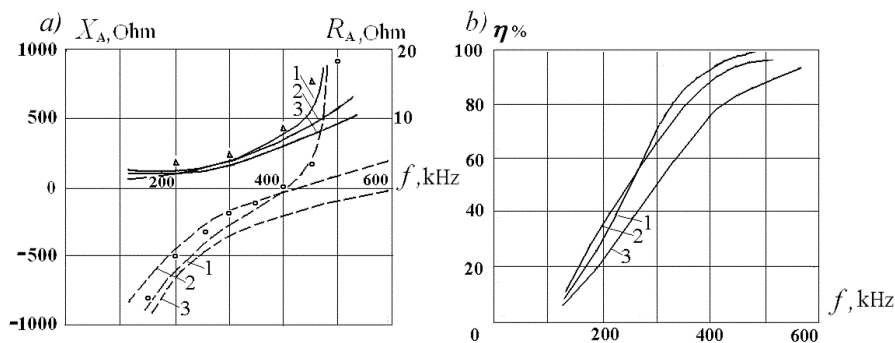


Fig. 30: Input impedance (a) and efficiency (b) of antenna with meander load and inverted-L antennas with different length of load.

dimensions:  $L = 50$ ,  $l = 45$ ,  $b = 1.54$ ,  $a = 0.025$ . For comparison, the input impedance of the inverted L antennas with the same height and with the length of the horizontal load 90 and 45 m (curves 2 and 3) are given. In Fig. 30b the calculated efficiency of these antennas is given. As seen from the figure, in the range of 200–500 kHz efficiency of the antenna with meander load is substantially higher than the efficiency of the inverted L antenna of the same size and is comparable with the efficiency of such antenna, which has the load with a double length of the wire.

The use of antenna with meander load in media frequency range allows reducing a size of a plot, which the antenna occupies, an area of the grounding and a price of construction.

The first specimen of this antenna was put into operation in 1983 in the town Pavlovo on the radio center of the Baltic Shipping Company. In 1987, the radio center of commercial sea port in Ventspils (Latvia) was equipped with three antennas. The effectiveness of the new antenna has been tested by measuring the field's strength, produced by new antennas in comparison with the inverted L antenna. Antennas were operating with the same transmitter. Tests have shown that the field created by the antenna with a meander load is greater in 1.5–1.6 times. This is equivalent to increasing the transmitter power in 2.3–2.6 times.

The correct selection of elements of antenna construction requires calculation of currents and voltages arising therein. For example, the magnitudes of the voltages between the wires ends and the ground determine the choice of insulators, on which the load is suspended. Diameters of wires depend on the maximum currents, etc.

We regard in particular the load consisting from the three wires using condition (1.82) for simplifying calculation. As shown former, by substituting the boundary conditions (180) in the equations (1.34) for the currents and potentials along the load wires, we obtain

$$i_1(z) = I \sin(2\beta + kz),$$

where

$$I = j \frac{U_1}{\cos^2 \beta (\rho_1 + 2\rho_2 - \rho_1 \tan^2 \beta)} = j \frac{e}{\cos^3 \beta [\rho_1 + 2\rho_2 - (3\rho_1 - 2\rho_2) \tan^2 \beta]}.$$

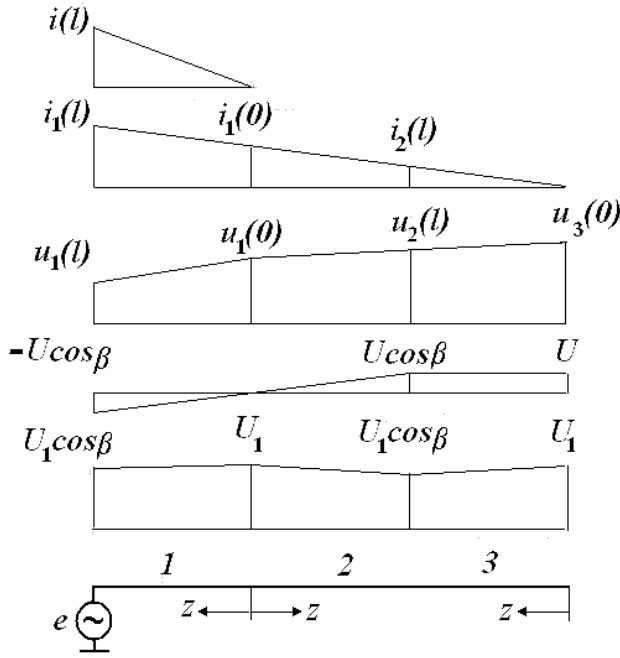


Fig. 31: Currents and potentials along the wires of the load.

Similarly

$$i_2(z) = -I \sin(2\beta + kz), i_3(z) = I \sin kz.$$

The total current in the load wires is

$$i(z) = \sum_{n=1}^3 i_n(z) = I(2 \cos 2\beta + 1) \sin kz, \quad (1.93)$$

i.e., current is distributed along coordinate  $z$  in accordance with sinusoidal law.

Figure 31 shows the current distribution  $i_1(l)$  along the wires of three-wire load in accordance with (1.93). If to straighten mentally the load wire, it will be seen that the current of the wire and the total current are distributed in accordance with sinusoidal law. Sinusoidal law of the current distribution along the load wire remains valid for a greater number of wires. For example, if a load consists of the four wires,

$$i_1(z) = I \sin(3\beta + kz), i_2(z) = -I \sin(3\beta - kz), i_3(z) = I \sin(\beta + kz), i_4(z) = -I \sin(\beta - kz),$$

where

$$I = j \frac{U_1}{\cos^3 \beta [\rho_1 + 3\rho_2 - (3\rho_1 + \rho_2) \tan^2 \beta]} \\ = j \frac{e}{\cos^4 \beta [\rho_1 + 3\rho_2 - 2(3\rho_1 - 2\rho_2) \tan^2 \beta + (\rho_1 - \rho_2) \tan^4 \beta]}.$$

Potential does not submit to this law. The expressions give for the potential another result:

$$u_1(z) = U_1 \cos kz + j(\rho_1 - \rho_2) I_1 = U_1 \cos kz - U \cot \alpha,$$

where

$$U = \frac{2e(\rho_1 - \rho_2)\tan^2 \beta}{\cos \beta [\rho_1 + 2\rho_2 - (3\rho_1 - 2\rho_2)\tan^2 \beta]}.$$

Similarly

$$u_2(z) = U_1 \cos kz + U \cot \beta \sin kz, \quad u_3(z) = U_1 \cos kz + U \cos kz.$$

Thus, the potential of the load wire is the sum of two terms. Both terms and its sum are shown in Fig. 31.

The results of calculating the input current of the load (for different number  $N$  of wires) and the potential at the end of the load are given in the Tables 3 and 4. The presented magnitudes of a current and a potential are maximal for all frequency range up to the series resonance. Therefore, in accordance with these magnitudes it is possible and need to choose the diameters of the wires and the type of insulators.

Figure 32 gives as an example the calculated values of the maximum potentials and currents of the load for an antenna with the dimensions:  $L = 50$ ,  $l = 45$ ,  $b = 1.54$ ,  $a = 0.025$ . The number of wires in the load is  $N = 6$ . The maximum potential is determined with respect to the voltage  $e$  on the input of a load and to emf at the antenna input. The maximum current is specified with respect to emf  $e$  and to the input current  $J_A$  of the antenna. It is taken into consideration that

$$e_A = e \frac{\cos k(L + l_e)}{\cos k l_e}, \quad J_A = i_1(l) \frac{\sin(L + l_e)}{\sin k l_e},$$

where  $l_e = \frac{1}{k} \tan^{-1}(-jW/Z_N)$  is an equivalent length of the load with input impedance  $Z_N^k$ .

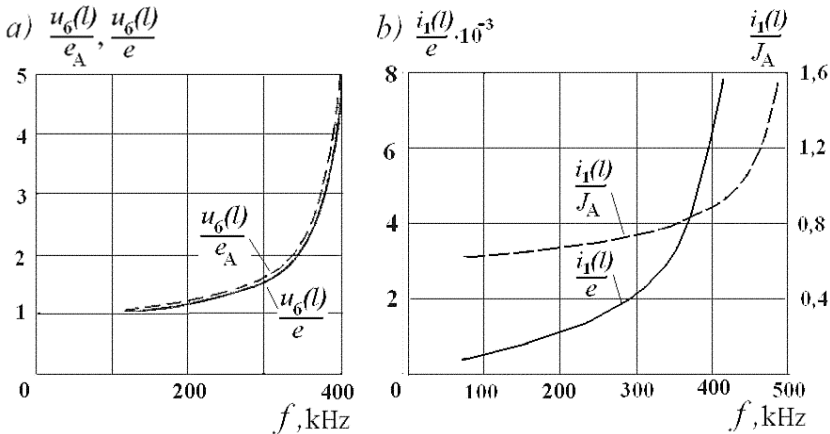


Fig. 32: Maximum potential (a) and maximum current (b) as functions of frequency.

**Table 3:** Input Current of the Load.

Number of wires	$i_{max}$
1	$j \frac{e \sin \beta}{\rho_1 \cos \beta}$
2	$j \frac{e \sin 2\beta}{\cos^2 \beta [\rho_1 + \rho_2 + (\rho_2 - \rho_1) \tan^2 \beta]}$
3	$j \frac{e \sin 3\beta}{\cos^3 \beta [\rho_1 + 2\rho_2 - (3\rho_1 - 2\rho_2) \tan^2 \beta]}$
4	$j \frac{e \sin 4\beta}{\cos^4 \beta [\rho_1 + 3\rho_2 - 2(3\rho_1 - \rho_2) \tan^2 \beta + (\rho_1 - \rho_2) \tan^4 \beta]}$
5	$j \frac{e \sin 5\beta}{\cos^5 \beta} [\rho_1 + 4\rho_2 - 10\rho_1 \tan^2 \beta + (5\rho_1 - 4\rho_2) \tan^4 \beta]$
6	$j \frac{e \sin 6\beta}{\cos^6 \beta} [\rho_1 + 5\rho_2 - 5(3\rho_1 + \rho_2) \tan^2 \beta + 3(5\rho_1 - 3\rho_2) \tan^4 \beta - (\rho_1 - \rho_2) \tan^6 \beta]$

**Table 4:** Potential on the End of Load Wire.

Number of wires	$u_{max}$
1	$u_1(0) \frac{e}{\cos \beta}$
2	$u_2(l) = \frac{e[\rho_1 + \rho_2 + (\rho_1 - \rho_2) \tan^2 \beta]}{\rho_1 + \rho_2 + (\rho_2 - \rho_1) \tan^2 \beta}$
3	$u_3(0) = \frac{e[\rho_1 + 2\rho_2 + (\rho_1 - 2\rho_2) \tan^2 \beta]}{\cos \beta [\rho_1 + 2\rho_2 + (2\rho_2 - 3\rho_1) \tan^2 \beta]}$
4	$u_4(l) = \frac{e[\rho_1 + 3\rho_2 + 2(\rho_1 - 3\rho_2) \tan^2 \beta + (\rho_1 - \rho_2) \tan^4 \beta]}{\rho_1 + 3\rho_2 - 2(3\rho_1 - 2\rho_2) \tan^2 \beta + (\rho_1 - \rho_2) \tan^4 \beta}$
5	$u_5(0) = \frac{e[\rho_1 + 4\rho_2 + 2(\rho_1 - 6\rho_2) \tan^2 \beta + \rho_1 \tan^4 \beta]}{\cos \beta [\rho_1 + 4\rho_2 - 10\rho_1 \tan^2 \beta + (5\rho_1 - 4\rho_2) \tan^4 \beta]}$
6	$u_6(l) = \frac{e[\rho_1 + 5\rho_2 + (3\rho_1 - 23\rho_2) \tan^2 \beta + 3(\rho_1 + \rho_2) \tan^4 \beta + (\rho_1 - \rho_2) \tan^6 \beta]}{\rho_1 + 5\rho_2 - 5(3\rho_1 + \rho_2) \tan^2 \beta + 3(5\rho_1 - 3\rho_2) \tan^4 \beta - (\rho_1 - \rho_2) \tan^6 \beta}$

## References

- [1] Stratton, J.A. (1941). Electromagnetic Theory. New York: McGraw-Hill.
- [2] Mittra, R. (Editor). (1973). Computer Techniques for Electromagnetics. Oxford. New York: Pergamon Press.
- [3] Balanis, C.A. (2005). Antenna Theory: Analysis and Design. New York: Wiley & Sons.
- [4] Markov, G.T. and Sazonov, D.M. (1975). Antennas. Moscow: Energy (in Russian).
- [5] Pistolkors, A.A. (1947). Antennas. Moscow: Sviyazizdat (in Russian).

- [6] Iossel, Yu. Ya., Kochanov, E.S. and Strunsky, M.G. (1981). Calculation of Electrical Capacitance. Leningrad: Energoisdat (in Russian).
- [7] Belousov, S.P. and Kliger, G.A. (1982). Analysis of wire radiators. Proc. of Radio Institute, 3: 5–11 (in Russian).
- [8] Popovic, B.D. and Surutka, J.V. (1972). Cylindrical cage antenna. Nachrichtentechn. Fachber, 45: 51 (in German).
- [9] Pantic, Z.Z. (1979). Cage-dipole antenna driven by a two-wire line. Archiv fur Electronic and Ubertragungs Technics, 33(7/8): 329–330 (in German).
- [10] Vershkov, M.V. and Mirotvorsky, O.B. (1990). Ships Antennas. Leningrad: Shipbuilding (in Russian).
- [11] Levin, B.M. and Mirotvorsky, O.B. (1986). Multi-radiator antenna with a resistor. Antennas, 33: 94–100 (in Russian).
- [12] Kusnezov, V.D. (1955). Shunt radiators. Radiotechnics, 10: 57–65 (in Russian).
- [13] Levin, B.M. (2013). A long line and a nonsymmetric oscillator with wires of different length. Radiotechnics and Electronics Engineering, 58(1): 48–55 (in Russian).
- [14] Leontovich, M.A. (1945). Theory of forced electromagnetic oscillations in thin conductors of arbitrary cross-sections with its applications to calculations of some antennas. Proc. of MPSS Institute, 1:1 (in Russian).
- [15] Bank, M. and Levin, B. (2007). The development of the cellular phone antenna with a small radiation of human organism tissues. IEEE Antennas Propagation Magazine, 49(4): 65–73.
- [16] Vershkov, M.V., Levin, B.M. and Fraiman, S.S. (1972). Antenna with meander load. Proc. of MF Institute, 151: 73–80 (in Russian).
- [17] Levin, B.M. (1976). Meander load with arbitrary number of wires. Proc. of MF Institute, 216: 130–139 (in Russian).

# Impedance and Complementary Antennas

## 1. Radiator with Inductive Surface Impedance

Chapter 1 uses a method for analyzing metal antennas based on comparing their electrical characteristics with those of equivalent long lines. We will apply a similar approach to an analysis of the electrical characteristics of impedance antennas. These antennas are the linear radiators with nonzero boundary conditions on the surface. One can determine the current distribution along the radiator with help of the integral equation for the current. But the laws of a current distribution along radiator wires and along the wires of the equivalent line (or of system of lines) are identical. The advantage of equivalent lines is the maximum simplicity in finding the distribution law and the efficiency of applying the obtained results to designing radiators with required characteristics.

The impedance long line (Fig. 1) is a similar analogue of an impedance antenna as a customary long line is an analogue of a metal one. Unlike a metal antenna, the boundary condition on the surface of the wire with distributed surface impedance has the form

$$\frac{E_z(a, z) + K(z)}{H_\varphi(a, z)} = Z(Z), -L \leq z \leq L, \quad (2.1)$$

where  $E_z(a, z)$  is the tangential component of an electric field on the antenna surface,  $H_\varphi(a, z)$  is the azimuthal component of a magnetic field on this surface,  $K(z)$  is the

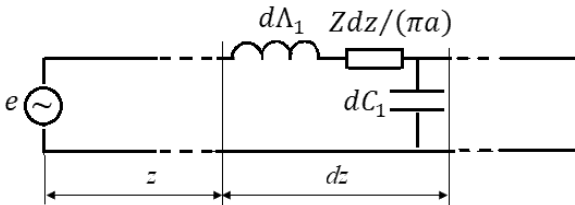


Fig. 1: Long line, equivalent to a radiator with constant surface impedance.

exciting external (extraneous) emf.  $Z(z)$  is the surface impedance, which in general case depends on coordinate  $z$  (it is assumed that the antenna axis coincides with  $z$  axis of a cylindrical coordinate system).

An example of an impedance radiator is a metal rod with a shell made from a magnetodielectric. Let the rod length be  $L$ , the rod radius be  $a_1$ , and the outer radius of the shell be  $a$ . As shown in [1], the boundary conditions of the presented type are valid, if the field structure in one of the media (for example, in the magneto-dielectric shell) does not depend on the structure of the field in another medium (in surrounding space). Radiators, on whose surface the boundary conditions (2.1) are fulfilled and the surface impedance substantially changes the current distribution along the antenna, are called radiators with non-zero (impedance) boundary conditions, or simply impedance radiators.

In accordance with the equivalence theorem, when considering electromagnetic fields in a free space surrounding the radiator, an antenna should be replaced by a field on its surface. Later one can operate only with fields. But for clarity and simplicity of reasoning, it is expedient in accordance with [1] mentally to put a metal coat on the antenna surface. In this case the surface density  $\vec{J}_s$  of a total linear electric current  $\vec{J}(z)$  along the metal coat of a radiator is related to the strength  $\vec{H}$  of the magnetic field by an expression

$$\vec{J}_s = [\vec{e}_\rho, \vec{H}], \quad (2.2)$$

where  $\vec{e}_\rho$  is the unit vector directed along the axis  $\rho$ .

Unlike a metal radiator, the tangential component  $E_z$  of an electric field on the surface of an impedance radiator is not equal to zero, thus leading to an additional voltage drop  $dU_1$  on each element  $dz$  of the wire. Using the boundary condition (2.1) and taking into consideration expression for  $H_\phi(a, z)$ , we obtain for the voltage drop on the wire  $dU_1 = \frac{Z(z)}{2\pi a} J(z)dz$  and for the voltage drop of the line

$$dU = 2dU_1 = \frac{Z(z)}{\pi a} J(z)dz.$$

Factor 2 takes into consideration that the radiator consists of two wires. Thus, an infinitesimal element  $dz$  of the equivalent line contains in addition to an inductance  $d\Lambda_1 = \Lambda_1 dz$  and a capacitance  $dC = C_1 dz$  also, an impedance  $Z(z)dz/(\pi a)$ . Telegraph equations for such a line have a form

$$-\frac{dU}{dz} = \left( j\omega\Lambda_1 - \frac{Z}{\pi a} \right) J(z), \quad -\frac{dJ(z)}{dz} = j\omega C_1 U(z),$$

whence

$$\frac{d^2 J(z)}{dz^2} + k_1^2 J(z) = 0, \quad \frac{d^2 U(z)}{dz^2} + k_1^2 U(z) = 0, \quad (2.3)$$

where

$$k_1^2 = k^2 - jZ\omega C_1/(\pi a). \quad (2.4)$$

Here  $k_1$  is the wave propagation constant in the radiator and in the equivalent two-wire long line,  $C_1$  is the capacitance between the radiator arms and between the wires of the long line per unit of their length.

This capacitance is half as much as the capacitance  $C_0$  between each wire and the surface of zero potential. Because the total length  $2L$  is the maximum dimension of the radiator, which is significantly larger than other dimensions, one should consider that in the first approximation the surface of zero potential is placed at a distance  $2L$  from the radiator and that the capacitance  $C_0$  is equal to the self-capacitance of a long wire with length  $2L$  and radius  $a$ , i.e.,

$$C_0 = \frac{2\pi\epsilon_0}{\ln(2L/a)} = 4\pi\epsilon_0\chi, \quad C_1 = C_0/2 = 2\pi\epsilon_0\chi, \quad (2.5)$$

whence

$$k_1^2 = k^2 - j2\omega\epsilon_0\chi Z/a = k^2 - j2k\chi Z/(aZ_0). \quad (2.6)$$

Here  $\chi = \frac{1}{2\ln(2L/a)}$  is a small parameter of the thin antennas' theory,  $Z_0 = \sqrt{\mu_0/\epsilon_0} = 120\pi$  is a wave impedance of the free space. Solving equations (2.3) in the ordinary way, we find the current  $J(z)$  and the wave impedance  $W_l$  of an impedance line, open at the end:

$$J(z) = J(0) \sin k_1 (L - z) / \sin k_1 L; \\ W_l = \frac{\omega\Lambda_1 - j(Z/\pi a)}{k_1} = \frac{k_1}{\omega C_1} = 120 \frac{k_1}{k} \ln \frac{2L}{a}. \quad (2.7)$$

Surface impedance allows us to obtain the current distribution in the radiator with a propagation constant, which significantly differs from the propagation constant in the air already in the first approximation. Such an antenna called an impedance antenna. The choice of impedance provides an additional degree of freedom in the process of optimizing the antennas characteristics.

In presented expressions  $J(0)$  is the generator current. Thus, from the above it follows that the radiator with the constant surface impedance in a first approximation can be considered as the equivalent long line differing from a customary long line by the presence of the surface impedance  $Z/\pi a$  per unit length. The current in the radiator is distributed according to a sinusoidal law, its propagation constant  $k_1$  differs from a propagation constant  $k$  in a metal antenna. The wave impedance of the impedance radiator is greater than the wave impedance  $W_l$  of a metal antenna by a factor  $k_1/k$ . The input impedance of an open at the end two-wire long line with a constant surface impedance is equal to

$$Z_l = -j \frac{k_1}{k} W_l \cot k_1 L. \quad (2.8)$$

If the power point in a symmetrical and grounded asymmetric impedance radiator (in an impedance dipole and monopole) is shifted, the input impedance of



equivalent impedance lines changes in the same way as the input impedance of a customary metal line.

An antenna with a constant surface impedance is a particular case of a radiator with impedance changing along the antenna. From general considerations, it is clear, that if the constant impedance allows expansion of antenna possibilities, then its change along the antenna will provide an additional degree of freedom and allow greater achievement. If the surface impedance changes along the antenna (more precisely, if its magnitude is piecewise constant), the equivalent long line is non-uniform line, in other words, it is a stepped line (see Fig. 2). Such a radiator can be realized as a structure from  $2N$  uniform segments with length  $l_m$ , different magnitudes of the surface impedance  $Z^{(m)}$  at the segments and correspondingly with different values of the wave impedance  $W_m$ , current  $J_m$  and voltage  $U_m$ . On each segment, a surface impedance is constant (Fig. 3).

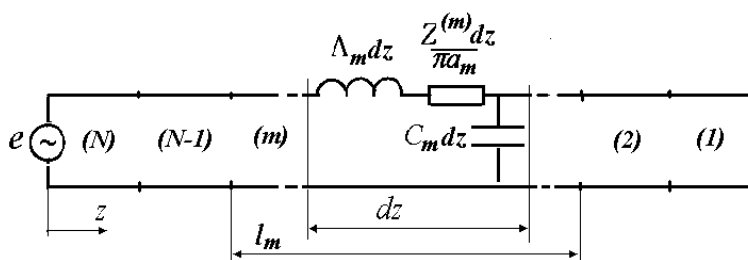


Fig. 2: Stepped long line equivalent to a radiator with piecewise constant surface impedance.

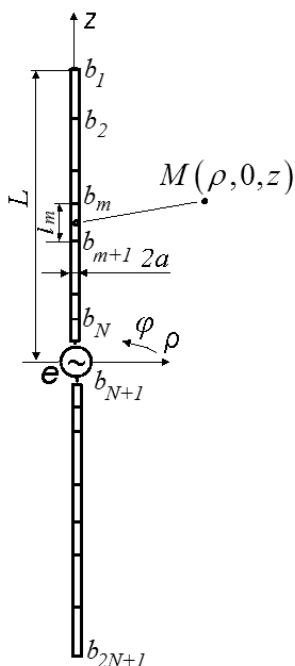


Fig. 3: Radiator with changing impedance.

We will assume that the antenna radius  $a$  is much smaller than the wave length  $\lambda$  and the antenna length  $2L$  and that in this case the current distribution along each antenna segment has in the first approximation a sinusoidal character. Let the antenna be symmetric. Comparison of each pair of the identical segments of an antenna and a corresponding segment of an equivalent line allows us to obtain expressions for the propagation constant  $k_m$  and the wave impedance  $W_m$ , similar to (2.6) and (2.7).

From the theory of long lines, it is known that on each segment of the stepped line

$$u_m = U_m \cos(k_m z_m + \varphi_m), J_m = jI_m \sin(k_m z_m + \varphi_m), I_m = U_m/W_m. \quad (2.9)$$

Because voltage and current along the stepped long line, equivalent to the radiator, are continuous:

$$u_m|_{z_m=0} = u_{m-1}|_{z_{m-1}=l_{m-1}}, J_m|_{z_m=0} = J_{m-1}|_{z_{m-1}=l_{m-1}},$$

this allows us to express the amplitude and phase of a current and a voltage in any segment through the amplitude and phase of the previous segment

$$I_m = I_{m+1} \frac{\sin(k_{m-1} l_{m-1} + \varphi_{m-1})}{\sin \varphi_m}, U_m = U_{m-1} \frac{\cos(k_{m-1} l_{m-1} + \varphi_{m-1})}{\cos \varphi_m}. \quad (2.10)$$

If to divide the left and right parts of the first expressions (2.10) onto the corresponding parts of the second expression and to use (2.7) and (2.9), we find:

$$\tan \varphi_m = \frac{k_m}{k_{m-1}} \tan (k_{m-1} l_{m-1} + \varphi_{m-1}). \quad (2.11)$$

Equalities (2.10) and (2.11) allow us to express the amplitude and phase of the current on any segment through one of the currents and the parameters of segments:

$$I_m = I_N \prod_{p=m+1}^N \frac{\sin \varphi_p}{\sin(k_{p-1} l_{p-1} + \varphi_{p-1})},$$

$$\varphi_m = \tan^{-1} \left\{ \frac{k_m}{k_{m-1}} \tan \left[ k_{m-1} l_{m-1} + \tan^{-1} \left\{ \frac{k_m}{k_{m-1}} \tan \left( k_{m-2} l_{m-2} + \dots + \tan^{-1} \left( \frac{k_2}{k_1} \tan k_1 \right) \dots \right) \right\} \right] \right\}. \quad (2.12)$$

The last expression is valid also for the segment  $N$ , if to adopt that  $\prod_{p=N+1}^N = 1$ . Since the current of the generator is

$$J(0) = J_N \sin (k_N l_N + \varphi_N),$$

then

$$I_m = A_m J(0), \quad (2.13)$$

where

$$A_m = \prod_{p=N+1}^N \sin \varphi / (\prod_{p=m}^N \sin(k_p l_p + \varphi_p)).$$

Expressions (2.9) together with (2.12) and (2.13) present the approximate laws of voltage and current distribution along the radiator with piecewise constant surface impedance. The input voltage and the input current of the line are respectively equal to

$$e = U_N \cos(k_N l_N + \varphi_N), \quad J(0) = jI_N \sin(k_N l_N + \varphi_N),$$

i.e., the input impedance of the stepped long line is

$$Z_l = e/J(0) = -jW_N \cot(k_N l_N + \varphi_N).$$

The required value of the surface impedance and the given law of its change along the radiator can be realized by means of concentrated loads, connected in an antenna wire. Consider a monopole of a height  $L$  with  $N$  loads  $Z_m$  (Fig. 4). Let loads be located uniformly along an antenna at distance  $b$  from each other. If the distance  $b$  is small ( $kb \ll 1$ ), the current distribution along an antenna practically does not change, if the concentrated loads are replaced by continuous surface impedance  $Z(z)$  distributed across a length of each segment. Assume that the surface impedance of antenna segment  $m$  is constant and equal to  $Z^{(m)}$ . Then

$$Z^m = bZ^{(m)}/(2\pi a_m) \quad (2.14)$$

where  $a_m$  is radius of this segment.

The above results apply to impedance antennas regardless of how the impedance is created. Consider specific options for impedance antennas. The first impedance antennas were the radiators with inductive surface impedance. They were fabricated in the form of a vertical cylindrical spiral and compared with a straight metal radiator of the same height. Their characteristics and prospects of use were reviewed by Brown [2]. Calculations and experiments have shown that an inductive surface impedance essentially increases an electrical length of the antenna and leads to a little increase in radiation's resistance.

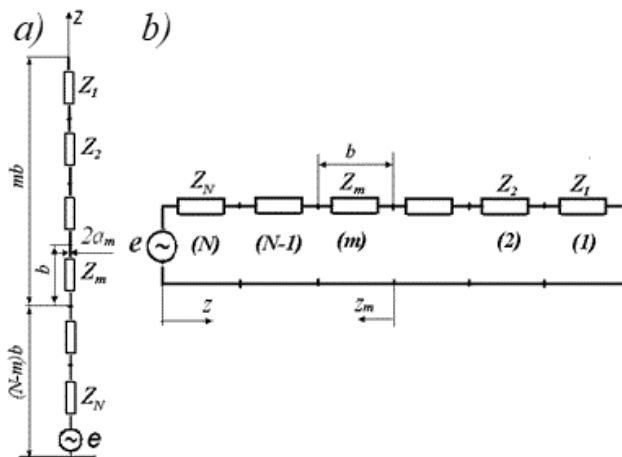


Fig. 4: An antenna (a) and equivalent to it long line (b) with several concentrated loads.

Later the version of the radiator shown in Fig. 5 has been extensively researched. This antenna is a vertically located metal rod of a radius  $a_1$ , surrounded by a ferrite shell of a radius  $a$  with absolute permeability  $\mu$  and absolute permittivity  $\varepsilon$ .

The field structure inside the antenna will not change, if the ferrite shell is cut into horizontal rings, between which infinitely thin and perfectly conductive equidistant metal disks are placed, connected to the metal rod (Fig. 6a). If the distances between the disks are small in comparison with the wavelength in ferrite, the antenna structure can be represented as a set of radial lines shorted by the metal rod.

In order to determine the surface impedance of a given antenna, one must calculate an input impedance  $Z_{in}$  of a radial line. A voltage and a current on the input of a radial line are equal respectively to  $U(\rho) = AJ_0(m\rho) + BY_0(m\rho)$  and to  $J(\rho) = j\frac{1}{W_p} [AJ_1(m\rho) + BY_1(m\rho)]$ . Here  $\rho$  is a line length,  $W_p = 120\pi\sqrt{\mu_r/\varepsilon_r}h/(2\pi a)$  is its wave impedance,  $J_0$ ,  $Y_0$ ,  $J_1$  and  $Y_1$  are Bessel functions,  $m$  is the wave propagation constant in ferrite,  $\mu_r$  and  $\varepsilon_r$  are the relative permeability and permittivity of ferrite and  $h$  is the ring thickness. Taking into consideration that in an antenna center  $U|_{\rho=a_1} = 0$ , we find

$$Z_p = \frac{U(\rho)}{i(\rho)} \Big|_{\rho=a} = -jW_p \frac{Y_0(ma)J_0(ma_1) - J_0(ma)Y_0(ma_1)}{Y_1(ma)J_0(ma_1) - J_1(ma)Y_0(ma_1)} \quad (2.15)$$

Since  $U(a) = hE_z(a)$  and  $J(a) = 2\pi aH_\phi(a)$ , the surface impedance is

$$Z = E_z/H_\phi|_{\rho=a} = 2\pi aZ_p/h. \quad (2.16)$$

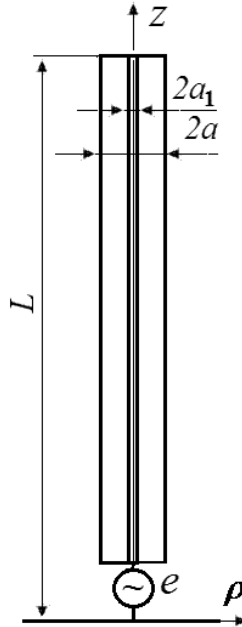
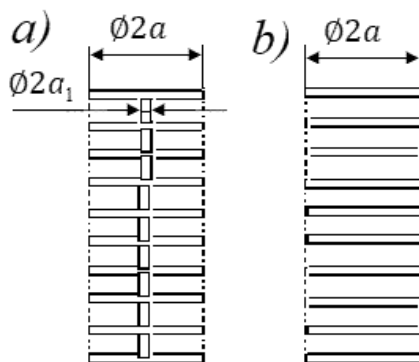


Fig. 5: Radiator in the form of a metal rod with a magneto-dielectric shell.



**Fig. 6:** Antennas with a ferrite shell and a metal rod (a) or horizontal discs (b).

An analogous result can be obtained by considering the diffraction of a converging cylindrical wave on a circular infinitely long cylinder. If the antenna diameter is small in comparison with the wavelength in ferrite, i.e.,  $ma \ll 1$ , then

$$Z = j120\pi\mu_r ka \ln(a/a_1), \quad (2.17)$$

and in accordance with (6)

$$k_1 = k \sqrt{1 + \mu_r \ln(a/a_1)/\ln(2L/a)}. \quad (2.18)$$

As it follows from (2.17), the surface impedance of thin antennas is directly proportional to the quantity  $\mu_r$  and does not depend on  $\varepsilon_r$ . Thus, to ensure a significant slowing in a thin shell, it is necessary to choose a magneto-dielectric with a high  $\mu_r$  (ferrite). At first, hoping to achieve high slowing, researchers tried to use dielectric materials. As a rule, they were deeply disappointed with the obtained results. As for the propagation constant of the wave along the antenna in the form of a metal rod with a ferrite shell, it is always greater than in the air.

It is necessary to emphasize that the main result of slowing is a decrease of resonant frequencies of an antenna that permits hope for decrease in its length. This result was obtained by calculation, confirmed by an experiment, and largely stimulated the work on expanding the frequency range of antennas. In Fig. 7 the calculated curves and experimental values are given for components of an input impedance of three asymmetrical radiators. Their parameters are presented in Table 1. The resistance of radiation is determined by subtracting from the active component of input impedance firstly the usual losses and secondly the losses in a ferrite shell. The losses in a shell are determined by means of substitution of a complex magnetic permeability  $\mu_r = \mu_1 - j\mu_2$  of ferrite, the second term of this expression defines losses. Calculations were completed in the range of decimeter waves for antennas with a height of 1–2 m with the slowing from 2.3 to 5. The antenna efficiency depends on the frequency, increases with its increase and is equal near 50 per cent for option 1 and near 80 per cent for option 2.

The experimental method for determining the resistance of radiation is based on measuring the same signals received with help of an investigated and a reference

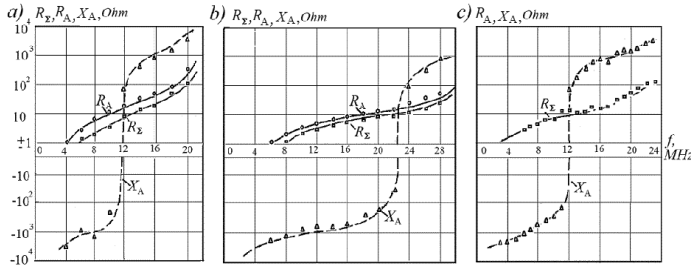


Fig. 7: Input impedance of first (a), second (b) and third (c) variant of antenna with ferrite shell.

Table 1: Parameters of Asymmetrical Radiators.

Option	$L(m)$	$a(m)$	$a_1(m)$	$\mu_r$	$\varepsilon_r$	$k_1/k$
1	2.0	0.021	0.007	40	10	3.0
2	1.5	0.15	0.007	25	10	2.3
3	1.0	0.021	0.007	100	10	5.0

antenna. The ratio of the effective lengths of both antennas is determined by the ratio of the received signals. As a reference antenna, a linear metal radiator of equal height is used. If the effective length of the reference antenna is known, it is not difficult to find an effective length and a radiation's resistance of the investigated antenna. This method has high accuracy and allows us to divide the active component of the input impedance into the radiation's resistance and the loss resistance.

The experimental results are given in Fig. 7 by circles, squares, and triangles. They are quite close to the calculation results. Some discrepancy at high frequencies is due to an increase in the magnitude  $\mu_2$ , that was considered constant in the calculations.

As a second option of an impedance radiator with a ferrite shell let us consider a thin antenna in the form of a set of equidistant and parallel metal disks (Fig. 6b). The absence of an internal metal rod significantly changes the characteristics of the radiator. In this case the current in the point  $\rho = 0$  is zero and the surface impedance  $Z$  is equal to

$$Z = -j 240 / (ka_2 \varepsilon_r),$$

i.e.,  $k_1^2 = k^2 - j 4\chi / (\varepsilon_r a_2^2)$ , and in contrast to the previous option, the resonant frequency does not decrease, but rather sharply increases (except the shell with very large dielectric permittivity).

In Fig. 8 the radiation's resistance and the reactive component of input impedance are presented for two asymmetrical antennas with a ferrite shell and geometric dimensions (in meters):  $L = 2.0$ ,  $a_1 = 0.007$ ,  $a = 0.021$ . The relative ferrite permittivity is close to 10, and the relative magnetic permeability as a function of  $z$  coordinate is shown in the figure. In Fig. 8a the shell covers the upper part of the metal rod and in Fig. 8b the lower part. As can be seen from the figures, in the second variant, the series resonance is shifted towards low frequencies. The experimental values are given by circles and triangles. The coincidence of the experiment with the calculation is satisfactory.

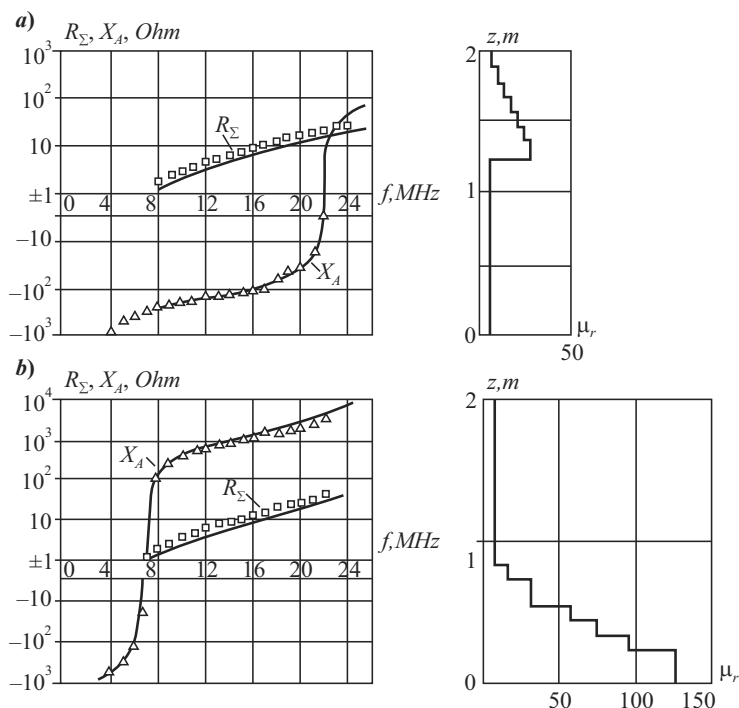


**Fig. 8:** Input characteristics of antennas with a piecewise constant surface impedance.

The theoretical and experimental investigations described above were accomplished mainly in the sixties of the last century. The articles [1] and [3] became a stimulus of these works. The first results were obtained by a group of authors led by E. A. Glushkovsky. These articles [4–6] were published in 1967–1968. Similar results were presented in [7–9] and described in detail in the book [10]. The investigations clearly confirmed that the ferrite coating changes the propagation constant of a wave along the radiator and the current distribution along its axis, i.e., it changes all electrical characteristics of the antenna. But these results did not lead to a serious expansion of the operation frequency band of antennas, since the basic task was not solved: it was not possible to find the dependence of the surface impedance on the coordinate along the radiator (along the equivalent long line) in order to improve efficiently its electrical characteristics in the given frequency range. The reason of this circumstance was using inductive surface impedance and appropriate loads. Hallen quite rightly suggested that capacitive loads are required to ensure high electrical performance.

In the course of work to determine the effect of separate elements of an antenna on its input characteristics in order to expand the frequency range, it was proposed to analyze the antenna with a constant frequency of the first (series) resonance [6]. The input reactance of such an antenna was determined at different variants of changing surface impedance along an antenna length in the form

$$X_A = 60k_0 X/(k\chi), \quad (2.19)$$

where in accordance with (2.12)

$$X = -\frac{k_N}{k_0} \cot \left\{ Mk_N l_N + \tan^{-1} \left[ \frac{k_N}{k_{N-1}} \tan \left( Mk_{N-1} l_{N-1} \cdots + \tan^{-1} \left( \frac{k_2}{k_1} \tan l_1 \right) \right) \right] \right\}.$$

As is seen from the last expression, the magnitude  $X$  depends only on the ratio between different propagation constants, but not on their absolute magnitudes. This expression uses the following notation:  $k_0 = \pi/(2L)$  is the propagation constant along the antenna with a constant surface impedance,  $k_m$  is the propagation constant along the stepped antenna in the arbitrary segment  $m$  with length  $l_m$ ,  $M = \frac{f}{f_1}$  is the relative frequency,  $f$  is the frequency,  $f_1$  is the frequency of the first resonance. The expression for  $X$  contains magnitudes

$$Mk_m l_m = \frac{k_m}{k_0} \cdot \frac{Ml_m \pi}{i(\rho)}.$$

Here the magnitude  $\frac{Ml_m \pi}{i(\rho)}$  is a constant factor of the segment  $m$ . The magnitude  $Mk_m l_m$  is equal to the product of a ratio  $k_m/k_0$  on this constant factor. Thus, at a given relative frequency  $M$  the reactance  $X$  depends only on the ratio  $k_i/k_0$ . When these magnitudes are changed, the frequency of the first resonance does not change:

$$X_A|_{M=1} = X|_{M=1} = 0. \quad (2.20)$$

Since the resulting equation is transcendental, we will consider it successively for radiators with a different number of segments with the same length. Let's start with two segments: first, in accordance with (2.20), we will define the magnitude  $k_2/k_0$  as a function of  $k_i/k_0 = k_1/k_0$ . This dependence is given in Fig. 9.

In Fig. 10 the curves for the reactance  $X$  are plotted depending on the relative frequency  $M$  for each point of Fig. 9. From the Fig. 10 one can see that at  $M > 1$  curves pass closer to the abscissa axis, if  $k_1 < k_0 < k_2$ . The best option is option with  $k_1 = 0$ . This means that on the segment near the free end of the antenna, the surface impedance should be equal to zero.

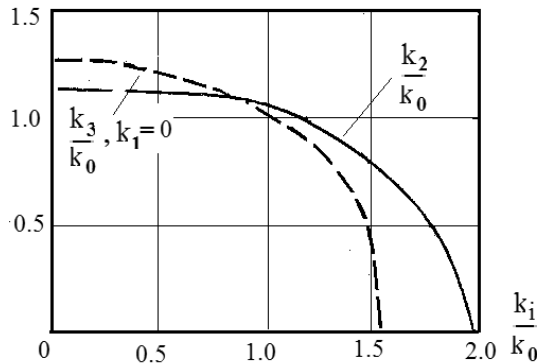


Fig. 9: The relationship between propagation constants of different segments at  $X_A|_{M=1} = 0$ .



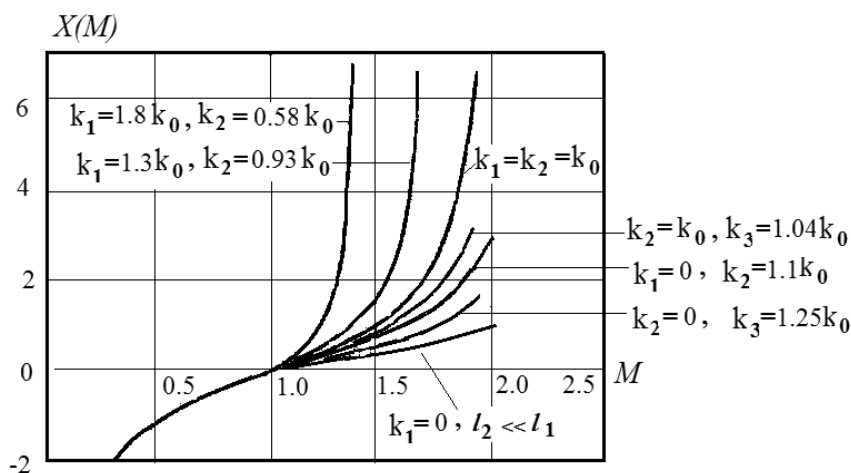


Fig. 10: Reactance  $X(M)$  of an antenna for constant frequency of the first resonance.

Proceeding on this result, in an antenna of three segments of equal length, we can put  $k_1 = 0$ . For this variant in Fig. 9, the ratio  $k_3/k_0$  is presented as a function of  $k_1/k_0 = k_2/k_0$ , and in Fig. 10 the curves are given for the reactance  $X(M)$ . The calculation again shows that one must concentrate the surface impedance near the generator. Therefore, as a next step, it is expedient to consider the radiator from two sections of different lengths  $l_1$  and  $l_2$ , where  $l_1 \cong L$ ,  $l_2 \ll l_1$ ,  $k_1 \ll k_0$ . Analysis again shows that the lower reactance  $X(M)$  is obtained for the smaller length  $l_2$ . This result corresponds to a conventional wire antenna with a coil at the base.

Rigorous analysis reveals the obvious incorrectness of an obtained result, but the cause of the error was determined only over time. In the course of solving this problem, only the inductive option of the surface impedance was considered, and this option does not allow us to provide the required result.

As a second example of the analysis we will consider the influence of the loads on the shape of an antenna's directional pattern. Considering the problem of synthesizing antennas with loads, my opponent studied the directional patterns of antenna, consistently increasing the number of loads in the radiator. After switching on the first load, the directional pattern changed significantly; after switching on the second load, it changed slightly and after switching on the third load, the change became invisible. He published an article in which he concluded that increasing the number of loads does not affect directional pattern. In this work two mistakes were made: first, the comparison of figures without their mathematical processing is unacceptable; secondly, if to increase the number of loads to ten, the quantity will pass into quality and the effect of loads on the directional pattern will be very appreciable.

Errors of this type, which sometimes even well-known scientists admit, are discussed in detail in the book [11]. They require a thoughtful study of the results and a careful approach to conclusions.

## 2. Impedance Folded Radiators

Folded radiator, on whose surface in contrast to metal radiator non-zero boundary conditions are performed, is called by impedance folded radiator. Non-zero boundary conditions have the form (2.1).

They are valid, if the structure of a field in one of a media (in the antenna shell) does not depend on a field structure in a different environment (surrounding space). Use of the surface impedance (or concentrated loads) creates an additional degree of freedom and permits to expand opportunities of the antenna [1]. The asymmetric versions of the impedance folded radiator similarly the metal folded radiators are located perpendicular to the ground surface. The unexcited wires of these radiators may be having a gap or be shorted to the ground. Both variants are shown in Fig. 11.

The calculation of an impedance folded radiator, like calculation of the metal folded radiator, is based on the theory of coupled lines [12]. For two-wire impedance long line, consisting of located above ground wires with impedance coating the telegraph equations generalizing equations (1.32) are correct:

$$\begin{aligned} -\frac{\partial u_1}{\partial z} &= j(X_{11} + Q_1) i_1 + jX_{12} i_2, \quad u_1 = j \frac{1}{k^2} \left( X_{11} \frac{\partial i_1}{\partial z} + X_{12} \frac{\partial i_2}{\partial z} \right), \\ -\frac{\partial u_2}{\partial z} &= j(X_{22} + Q_2) i_2 + jX_{12} i_1, \quad u_2 = j \frac{1}{k^2} \left( X_{22} \frac{\partial i_2}{\partial z} + X_{12} \frac{\partial i_1}{\partial z} \right). \end{aligned} \quad (2.21)$$

Here, as in Section 1.3,  $u_i$  is the potential of the wire  $i$  relative to ground,  $i_i$  is the current along the wire  $i$ ,  $X_{ik} = \omega \Lambda_k$  is the self or mutual inductive impedance per unit length. Besides that,  $jQ_i = Z_i/(2\pi a_i)$  is additional impedance per unit length created by surface impedance  $Z_i$ .

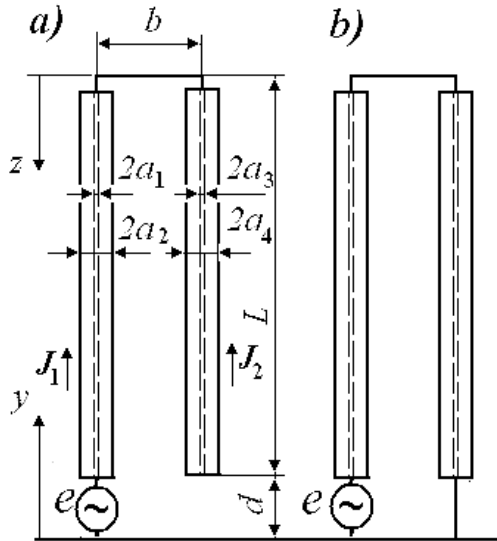


Fig. 11: Impedance folded radiators: a – the second wire has a gap, b – the second wire shorted to the ground.

The two left equations of the set (2.21) are based as in the case of the metal wires on the fact that the decrease of potential at segment  $dz$  of each wire is the result of the influence of emfs, which are created by the own current and by the current of adjacent wire. The other two equations are based on the electrostatic equations relating charges and potentials in accordance with the equation of continuity. The dependence of a current on coordinate  $z$  is adopted in the form  $\exp(\gamma z)$ .

In accordance with the law of electrostatics, which connects charges and potentials, at the boundaries of segments

$$dJ_m(b_m)/dz = dJ_{m-1}(b_m)/dz.$$

Differentiating the right pair of equations and substituting them into the left equations, we find:

$$\left(X_{11} + Q_1 + \frac{\gamma^2}{k^2} X_{11}\right) i_1 + X_{12} \left(1 + \frac{\gamma^2}{k^2}\right) i_2 = 0, \left(X_{22} + Q_2 + \frac{\gamma^2}{k^2} X_{22}\right) i_2 + X_{12} \left(1 + \frac{\gamma^2}{k^2}\right) i_1 = 0. \quad (2.22)$$

In order to this set of uniform equations has a solution, it is necessary to satisfy the condition

$$\gamma_{1(2)}^2 = -k_2^2 - \frac{\omega}{2} [G_1 \beta_{11} + Q_2 \beta_{22} \mp \sqrt{(Q_1 \beta_{11} - Q_2 \beta_{22})^2 + 4Q_1 Q_2 \beta_{12}^2}]. \quad (2.23)$$

Here

$$\beta_{11} = \frac{k^2 X_{22}}{\omega(X_{11} X_{22} - X_{12}^2)}, \beta_{12} = -\frac{k^2 X_{12}}{\omega(X_{11} X_{22} - X_{12}^2)}, \beta_{22} = -\frac{k^2 X_{11}}{\omega(X_{11} X_{22} - X_{12}^2)}$$

are coefficients of electrostatic induction. Thus, a system of two impedance wires located above the ground has two different propagation constants. If the impedance is purely reactive, they are equal to

$$k_{1(2)} = \sqrt{-\gamma_{1(2)}^2}.$$

We seek a solution in the form

$$u_1 = A \cos k_1 z + jB \sin k_1 z + C \cos k_2 z + jD \sin k_2 z. \quad (2.24)$$

The ratio of the currents obtained from (2.22) is substituted in the first equation of (2.21):

$$i_1 = j \frac{k^2 + \gamma^2}{\gamma^2 Q_1} \frac{du_1}{dz} = a_1 (B \cos k_1 z + jA \sin k_1 z) + a_2 (D \cos k_2 z + jC \sin k_2 z), \quad (2.25)$$

where  $a_i = (k^2 - k_i^2)/k_i Q_i = -1/W_i$ . From (2.25) and similar relationship between  $i_2$  and  $u_2$  one can obtain

$$\frac{du_2}{dz} : \frac{du_1}{dz} = \frac{Q_2 i_2}{Q_1 i_1}. \quad (2.26)$$

i.e.,

$$u_2 = b_1 (A \cos k_1 z + jB \sin k_1 z) + b_2 (D \cos k_2 z + jC \sin k_2 z), \quad (2.27)$$

and  $b_i = \frac{Q_2}{Q_1} \frac{k^2(X_{11} + Q_1) - k_i^2 X_{11}}{(k_i^2 - k^2) X_{12}}$ . Finally, from (2.26) and (2.25) it follows that

$$i_2 = a_1 c_1 (B \cos k_1 z + jA \sin k_1 z) + a_2 c_2 (D \cos k_2 z + jC \sin k_2 z), \quad (2.28)$$

where  $c_i = b_i Q_1 / Q_2$ .

Setting  $z = 0$ , we find that  $A = U_{11}$ ,  $D = I_{11}/a_1$ ,  $C = U_{12}$ ,  $B = I_{12}/a_2$ , where  $U_{11}$ ,  $U_{12}$ ,  $I_{11}$ ,  $I_{12}$  are fractions of voltages and currents at a beginning of the first wire (near load), which correspond to phase constants  $k_1$  and  $k_2$ . Considering that the current flowing from the generator to the load, i.e., in the direction of reduction  $z$ , is a positive current, we rewrite (2.24), (2.25), (2.27) and (2.28), taking into account the defined coefficients:

$$\begin{aligned} u_1 &= U_{11} \cos k_1 z + U_{12} \cos k_2 z + j(W_1 I_{11} \sin k_1 z + W_2 I_{12} \sin k_2 z), \\ i_1 &= I_{11} \cos k_1 z + I_{12} \cos k_2 z + j\left(\frac{U_{11}}{W_1} \sin k_1 z + \frac{U_{12}}{W_2} \sin k_2 z\right), \\ u_2 &= b_1 U_{11} \cos k_1 z + b_2 U_{12} \cos k_2 z + j(b_1 W_1 I_{11} \sin k_1 z + b_2 W_2 I_{12} \sin k_2 z), \\ i_2 &= c_1 I_{11} \cos k_1 z + c_2 I_{12} \cos k_2 z + j\left(c_1 \frac{U_{11}}{W_1} \sin k_1 z + c_2 \frac{U_{12}}{W_2} \sin k_2 z\right). \end{aligned} \quad (2.29)$$

One must emphasize the important conclusion, which follows directly from (2.29). Currents and potentials of both wires are connected by rigid relationships. These relationships depend not on the details of combining antenna elements into an overall structure (not in accordance with so-called boundary conditions). They depend on the wires' diameters and the surface impedances. Therefore, changing the boundary conditions (for example, the point of connecting emf, points of load placement and magnitudes of loads) it is impossible to create in-phase or anti-phase currents in the wires of the impedance folded radiator (by contrast to metal folded radiators). Accordingly, the input impedance of such impedance radiator cannot be presented as an aggregate of impedance lines and impedance radiators, which connected in parallel or in series. As it will be shown further, the only exception is the folded radiators consisting of identical wires.

We apply these results to the calculating input impedance of a folded radiator with a gap in second (unexcited) wire (see Fig. 11a). The boundary conditions for this variant have the form:

$$i_1(0) + i_2(0) = 0, u_1(0) = u_2(0), i_2(L) = 0, u_1(L) = e. \quad (2.30)$$

Substituting (2.29) into (2.30), we find

$$\begin{aligned}
 I_{12} &= -I_{11} + \frac{1+c_1}{1+c_2}, \quad U_{11} = -U_{11} \frac{1-b_1}{1-b_2}, \quad I_{11} = -jd_1 \frac{U_{11}}{W_1}, \\
 e &= U_{11} \left( \cos k_1 L - \frac{1-b_1}{1-b_2} \cos k_2 L \right) + I_{11} \left( W_1 \sin k_1 L - W_2 \frac{1+c_1}{1+c_2} \sin k_2 L \right), \\
 d_1 &= \tan k_1 L \left[ 1 - \frac{W_1 (1-b_1) c_2 \sin k_2 L}{W_2 (1-b_2) c_1 \sin k_1 L} \right] : \left[ 1 - \frac{c_2 (1+c_1) \cos k_2 L}{c_1 (1+c_2) \cos k_1 L} \right]. \quad (2.31)
 \end{aligned}$$

Then the input impedance of an impedance line is

$$\begin{aligned}
 X_{ii} &= \frac{e}{ji_1(L)} = \\
 &= \frac{1 - \frac{(1-b_1) \cos k_2 L}{(1-b_2) \cos k_1 L} + d_1 \tan k_1 L \left[ 1 - \frac{W_2 (1+c_1) \sin k_2 L}{W_1 (1+c_2) \sin k_1 L} \right]}{1 - \frac{W_1 (1-b_1) c_2}{W_2 (1-b_2) c_1} - d_1 \cot k_1 L \left[ 1 - \frac{(1+c_1) \cos k_2 L}{(1+c_2) \cos k_1 L} \right]}. \quad (2.32)
 \end{aligned}$$

Expression (2.32) makes it possible to determine approximately reactive component of the input impedance of the impedance folded radiator (similarly to the fact as formula for the input impedance of an equivalent long line allows to determine a reactive component of an input impedance of the metal radiator). The antenna input impedance can be found more precisely by the method of induced electromotive force. Equating the oscillating power passing through a closed surface surrounding the antenna and the oscillating power of the source, we obtain (for asymmetric radiator):

$$Z_A = -\frac{1}{j_1^2(0)} \int_0^L E_y J(y) dy, \quad (2.33)$$

where  $E_y$  is a field on the antenna surface,  $J_1(0)$  is a current of a generator and  $J(y) = J_1(y) + J_2(y)$  is a total current of an antenna as function of coordinate  $y = L - z$  (Fig. 11a).

Expression (2.33) is a generalization of the method of induced emf for the folded radiator. In the folded radiator with a gap, a total input current of the antenna coincides with a generator current. In the folded radiator with an unexcited wire shorted to a ground this coincidence is absent. Near parallel resonance, where the method of induced emf gives the wrong result, for the folded radiator with a gap one must use the expression

$$Z_A = e \left[ 2J_1(0) + \frac{1-b_1}{e \int_0^L E_y(y) dy} \right], \quad (2.34)$$

and the total current of this antenna is equal to

$$J(y) = j(1 + c_1) \frac{U_{11}}{W_1} \cdot \left\{ \sin k_1 (L - |y|) - \frac{W_1 (1 - b_1) (1 + c_2)}{W_2 (1 - b_2) (1 + c_1)} \sin k_2 (L - |y|) - d_1 [\cos k_1 (L - |y|) - \cos k_2 (L - |y|)] \right\}. \quad (2.35)$$

The field in the far region taking a mirror image into account is

$$E_\theta = \frac{60k(1 + c_1) U_{11} \exp(-jkr) \sin \theta}{W_1 r} \left[ \frac{\Theta_1 (\cos \theta)}{k^2 \cos^2 \theta - k_1^2} - \frac{\Theta_2 (\cos \theta)}{k^2 \cos^2 \theta - k_2^2} \right], \quad (2.36)$$

where

$$\Theta_i (\cos \theta) = k_i e_i [\cos (kL \cos \theta) - \cos k_i L] + d_i [k \cos \theta \sin (kL \cos \theta) - k_i \cos k_i L],$$

$$e_1 = 1, e_2 = \frac{W_1 (1 - b_1) (1 + c_2)}{W_2 (1 - b_2) (1 + c_1)}.$$

An effective length of asymmetric radiator is

$$h_e = \frac{k_2 (1 - \cos k_1 L) - e_2 k_1 (1 - \cos k_2 L) - d_1 (k_2 \sin k_1 L - k_1 \sin k_2 L)}{k_1 k_2 [\sin k_1 L - e_2 \sin k_2 L - d_1 (\cos k_1 L - \cos k_2 L)]}. \quad (2.37)$$

Thus, the calculation of the folded radiator with non-zero boundary conditions is divided into two stages. First, the current distribution along the antenna wires is determined using the theory of asymmetric lines; afterwards electrical characteristics of the antenna are calculated. In order to calculate the far field, the total current of an antenna is used. Input impedance of an antenna is calculated by the method of induced electromotive force, or by solving integral equation. Coefficients  $W_i$ ,  $b_i$ ,  $c_i$ ,  $k_i$  depend on the inductive reactances  $X_{ik} = \omega p_{ik}/c^2$  per unit length, where  $p_{ik}$  are the potential coefficients, which are determined by a method of an average potential (for example, by method of Howe), in accordance with the actual location of the antenna wires.

Practically important special cases, when the surface impedance on one of the wires of the folded radiator is equal to zero, are of particular interest. Main characteristics of folded antennas with a gap, if one or another wire is purely metallic, are given in Table 2. One must note that in the calculation of the difference  $k_1^2 - k^2$  it is necessary to expand it into the series of Maclaurin.

If the radiator is made up of two identical wires ( $Q_1 = Q_2$ ,  $a_2 = a_4$ ), then

$$k_1 = \sqrt{k^2 + \omega Q_1 (\beta_{11} + \beta_{12})} = k \sqrt{1 + Q_1 / (X_{11} + X_{12})},$$

$$k_2 = \sqrt{k^2 + \omega Q_1 (\beta_{11} - \beta_{12})} = k \sqrt{1 + Q_1 / (X_{11} - X_{12})},$$

**Table 2:** Characteristics of Folded Radiators with a Gap.

Value	$Q_2 = 0$	$Q_1 = 0$
$k_1$	$k$	$k$
$k_2$	$k\sqrt{1 + \frac{Q_1 X_{22}}{X_{11} X_{22} - X_{12}^2}}$	$k\sqrt{1 + \frac{Q_2 X_{11}}{X_{11} X_{22} - X_{12}^2}}$
$k_1^2 - k^2$	$Q_2 \frac{k^2}{X_{22}}$	$Q_1 \frac{k^2}{X_{11}} - Q_2 \frac{k^2 X_{12}^2}{X_{11}^3}$
$X_{ii}$	$-\frac{k_2 Q_1}{k_2^2 - k^2} \cdot \frac{F_1 + F_2}{F_3 + F_4} \cot kL,$ <p>where <math>F_1 = 1 + \frac{(X_{22} - X_{12}) \cos k_2 L}{X_{12} \cos k_2 L},</math></p> $F_2 = d_1 \tan kL \left\{ 1 - \frac{k_2 k Q_1 \sin k_2 L}{[(k_2^2 - k^2)(X_{12} - X_{11}) + k_2 Q_1] \sin kL} \right\},$ $F_3 = \frac{(X_{22} - X_{12}) \sin k_2 L}{X_{12} \sin kL},$ $F_4 = d_1 \tan kL \frac{k_2 X Q_1 \sin k_2 L}{[(k_2^2 - k^2)(X_{12} - X_{11}) + k^2 Q_1] \sin kL},$	$-X_{11} \frac{1 + d_1 \tan kL}{k(1 - d_1 \tan kL)} \cot kL$
$d_1$	$\left\{ 1 + \frac{X_{22} - X_{12}}{k_2 k Q_1 X_{12}} [(k_2^2 - k^2) X_{11} + k^2 Q_1] \frac{\sin k_2 L}{\sin kL} \right\} /$ $\left[ 1 + \frac{(k_2^2 - k^2) X_{11} - k^2 Q_1}{(k_2^2 - k^2)(X_{12} - X_{11}) + k^2 Q_1} \cdot \frac{\cos k_2 L}{\cos kL} \right]$	$-\frac{(k_2^2 - k^2)(X_{11} - X_{12})^2}{k_2 k Q_2 X_{11}} \cot kL$
$e_2$	$\frac{X_{12} - X_{22}}{k_2 k Q_1 X_{12}} [(k_2^2 - k^2)(X_{12} + X_{11}) + k^2 Q_1]$	$-\frac{(k_2^2 - k^2)(X_{11} - X_{12})^2}{k_2 k Q_2 X_{11}}$

whence  $b_1 = c_1 = 1$ ,  $b_2 = c_2 = -1$ ,  $d_1 = 0$ , i.e., expressions (29) take the form

$$\begin{aligned}
 u_1 &= U_{11} \cos k_1 z + U_{12} \cos k_2 z + j(W_1 I_{11} \sin k_1 z + W_2 I_{12} \sin k_2 z), \\
 i_1 &= I_{11} \cos k_1 z + I_{12} \cos k_2 z + j \left( \frac{U_{11}}{W_1} \sin k_1 z + \frac{U_{12}}{W_2} \sin k_2 z \right), \\
 u_2 &= U_{11} \cos k_1 z + U_{12} \cos k_2 z + j(W_1 I_{11} \sin k_1 z + W_2 I_{12} \sin k_2 z), \\
 i_2 &= I_{11} \cos k_1 z - I_{12} \cos k_2 z + j \left( \frac{U_{11}}{W_1} \sin k_1 z - \frac{U_{12}}{W_2} \sin k_2 z \right). \quad (2.38)
 \end{aligned}$$

This means that in this case, irrespective of the boundary conditions for the currents and voltages, their components with the propagation constant  $k_1$  are equal in magnitude and opposite in sign (anti-phase wave). Accordingly, the input impedance of the folded radiator with a gap (see Fig. 11a) can be presented as an aggregate of input impedances of two-wire line and monopole:

$$X_{ii} = -W_m \cot k_1 L + \frac{1}{4} W_{ii} \tan k_2 L, \quad (2.39)$$

where  $W_m = W_1/2 = k_1/[2kc(\beta_{11} + \beta_{12})] = k_1/(2kcC_{11})$  is the wave impedance of the impedance linear radiator consisting of two parallel wires, and  $W_l = 2W_2 = \frac{2k_2}{kc(\beta_{11} - \beta_{12})} = \frac{k_2}{kc(C_{12} + C_{11}/2)}$  is the wave impedance of an impedance long line also consisting of two wires located symmetrically relatively surface of zero potential (ground). Magnitudes  $C_{11}$  and  $C_{12}$  in these expressions are partial capacitances.

For the folded radiator with the second wire shorting to ground (see Fig. 11b) instead of the third boundary condition (2.30) we have

$$u_2(L) = 0. \quad (2.40)$$

Therefore, instead of the third equation of the set (2.31), we obtain

$$I_{11} = -jd_2 \frac{U_{11}}{W_{11}}, \quad (2.41)$$

where

$$d_2 = -\cot k_1 L \left[ 1 + \frac{b_2(1-b_1) \cos k_2 L}{b_1(1-b_2) \cos k_1 L} \right] / \left[ 1 - \frac{W_2 b_2(1+c_1 \sin k_2 L)}{W_1 b_1(1+c_2 \sin k_1 L)} \right],$$

and  $d_2$  will take the place of the coefficient  $d_1$  in expressions for electrical characteristics of the radiator.

When  $Q_2 = 0$ , coefficient  $d_2$  is equal to  $d_2 = -\cot kL$ . When  $Q_1 = 0$ ,

$$d_2 = -\cot kL \left[ 1 + \frac{(X_{11} - X_{12}) \cos k_2 L}{X_{12} \cos kL} \right] \left[ 1 - \frac{k_2 k Q_2 X_{11} \sin k_2 L}{(k_2^2 - k^2) X_{12} (X_{11} - X_{12}) \sin k_1 L} \right]^{-1}.$$

When  $Q_1 = Q_2$ ,  $a_2 = a_4$ ,

$$Y_{il} = \frac{1}{W_1 \tan k_2 L} - \frac{1}{4W_m \cot k_1 L}. \quad (2.42)$$

When  $Q_1 = Q_2 = 0$ , i.e.,  $k_1 = k_2 = k$ , equalities (2.41) and (2.42) are transformed into expressions (1.55) and (1.56).

As an example, in Fig. 12 the model of the impedance folded radiator is presented. One wire of this radiator is made in the form of a rod with a ferrite coating (relative magnetic permeability of the coating is 10), and the other wire is made in the form of a metal tube. Dimensions of a model are given in millimeters.

The calculated curves and experimental values of active  $R_A$  and reactive  $X_A$  components of the input impedance of the impedance folded radiators are given in Figs. 13 and 14. In different variants the generator is connected to different wires, the second wire is connected or not connected to the ground, wires of different diameter are used. The coincidence of the calculated and experimental results is quite satisfactory. As is seen from the figures, the radiator characteristics are substantially changed, if one or other wire is excited. Using slowing coating allows to decrease the resonant frequencies by a factor of 2–2.5.



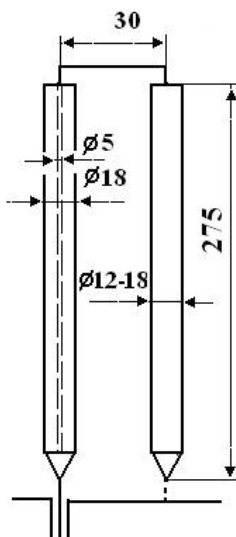


Fig. 12: Model of the impedance folded radiator.

Comparing the characteristics of impedance and metal folded antennas, it is easy to see that both impedance antennas and metal ones allow to significantly decrease the resonant frequencies in comparison with linear antennas of the same height. In the case of impedance antennas, there is an additional degree of freedom for choosing a resonant frequency, which depends on the dielectric permittivity and magnetic permeability of the coating material.

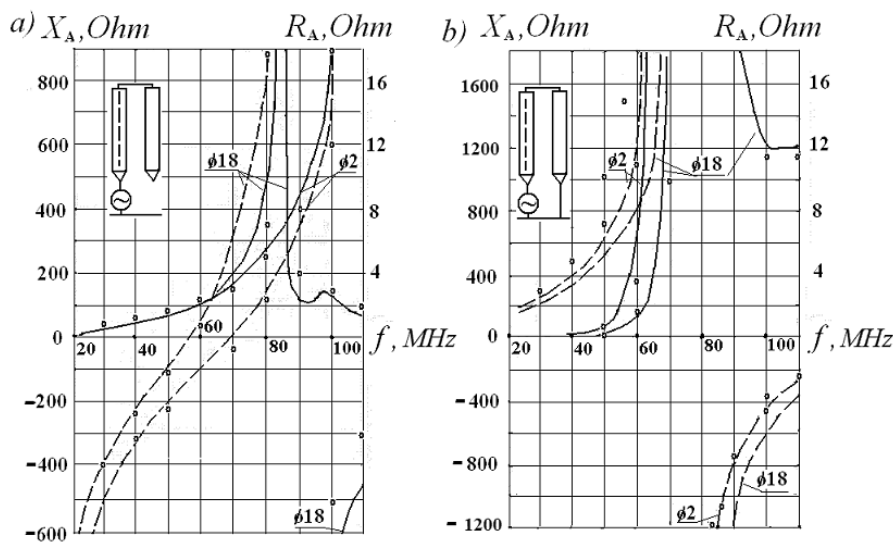


Fig. 13: Input impedance of the impedance folded radiator with excited impedance wire:  
a – with a gap, b – with a shorting to the ground.

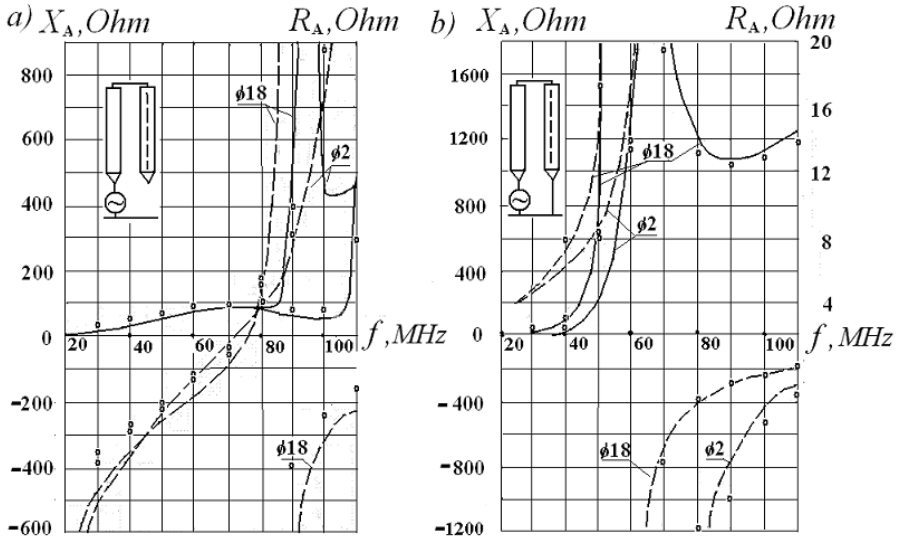


Fig. 14: Input impedance of the impedance folded radiator with excited metal wire:  
a – with a gap, b – with a shorting to the ground.

### 3. Principles of Similarity and Duality

This Section is devoted to the principles of electrodynamics similarity and duality. As is known, antennas with the shape defined by angular dimensions, e.g., conic radiators of infinite length, satisfy the principle of electrodynamics similarity. In this case, a change of the scale does not lead to a change of antenna characteristics, i.e., the radiator shape and its dimensions in wavelengths are the same at different frequencies.

Relationships of similarity follow from Maxwell equations. For the harmonic field created by an antenna in surrounding space, one can write in accordance with (1.1)

$$\text{curl} \vec{H} = (\sigma + j\omega\epsilon) \vec{E}, \text{curl} \vec{E} = -j\omega\mu \vec{H}. \quad (2.43)$$

Similarly, at another frequency

$$\text{curl} \vec{H}' = (\sigma' + j\omega'\epsilon') \vec{E}', \text{curl} \vec{E}' = -j\omega'\mu' \vec{H}', \quad (2.44)$$

Here

$$\vec{E}' = k_E \vec{E}, \vec{H}' = k_H \vec{H}, \omega' = k_\omega \omega, \epsilon' = k_\epsilon \epsilon, \mu' = k_\mu \mu, \sigma' = k_\sigma \sigma, l' = k_l l,$$

where  $k_E, k_H, k_\omega, k_\epsilon, k_\mu, k_\sigma, k_l$  are the coefficients, interrelating various magnitudes at different frequencies, and  $l$  is the distance (arbitrary linear coordinate). The said coefficients are called coefficients of modeling, since the use of similarity principle

allows us to study antennas characteristics by means of numerical or experimental simulation.

If to substitute these coefficients into (2.44) and to take into account the linearity of magnitudes and of operator  $\text{curl}\vec{A}$ , where  $\vec{A}$  is an arbitrary vector, then the resulting equations will coincide with equations (2.43), i.e.,  $k_H = k_\sigma k_E k_p$ ,  $k_H = k_\omega k_\epsilon k_p$ ,  $k_E = k_\omega k_\mu k_H k_p$ . If  $k_\epsilon = k_\mu = 1$ , then  $k_H/k_E = k_\sigma k_l = k_\omega k_l = 1/(k_\omega k_l)$ , whence  $k_\omega k_l = 1$ ,  $k_H = k_E$ ,  $k_\sigma k_l = 1$ . From these expressions it follows that the electromagnetic field at different frequencies will be the same, if the electrical dimensions of an antenna (the ratio of linear dimensions to the wavelength) at different frequencies coincide and the material conductivity is inversely proportional to magnitude  $k_p$ , i.e., increases with a frequency.

Self-complementary and log-periodic antennas, which belong to the class of frequency-independent antennas, consist from the radiators with coinciding characteristics. More precisely, their characteristics change weakly, if an operation frequency changes. The log-periodic antenna is an antenna array. It consists of a few dipoles of the same shape and different dimensions, which are connected in a single structure. The self-complementary antenna of several dipoles with the same shape and dimensions is also antenna array, although its elements are not parallel to each other.

Principle of similarity is applicated in studying antennas models. When the geometrical dimensions of a model are smaller than dimensions of the original in  $N$  times, it is necessary to increase the signal frequency and the conductivity of model material in  $N$  times. Since  $k_H = k_E$ , i.e., relationship of the currents and voltages remains the same, the resistances should remain the same, whereas the capacitances of capacitors and the inductances of inductors, which are used in the model, should be smaller in  $N$  times.

As a rule, it is not impossible to increase the conductivity of material in  $N$  times, i.e., the resistances of an antenna and of a model as well as the characteristics depending on them (e.g., efficiency, Q-factor, gain) substantially distinguished from each other.

When analyzing the characteristics of slot antennas, the principle of duality of Pistolors [13] is used. In accordance with this principle, a linear metal radiator has an analogue - a slot antenna. An ideal slot antenna, analogous to a perfectly conducting metal radiator, is understood as a slot cut in an infinitely thin ideally conducting plate of unlimited dimensions. The duality principle states that if an electromagnetic field of frequency  $f$  is excited by means an ideal slot antenna, then the vectors  $\vec{E}$  and  $\vec{H}$  of this field in the slot and the surrounding space will coincide (taking into account the direction) with vectors of fields  $\vec{H}_1$  and  $-\vec{E}_1$  of the ideal metal plate having the same shape and dimensions

$$\vec{E} = \vec{H}_1, \vec{H} = -\vec{E}_1,$$

provided that the current density  $J$  on the plate and the tangential component  $E_t$  at a similar point of the slot are related by the expression

$$J = E_t \sqrt{-\mu_0/\epsilon_0}.$$

To prove the principle of duality, we will consider a volume  $V$ , surrounded by a surface  $S$ . Let in this volume the medium is characterized by magnetic permeability  $\mu = \mu_0$ , dielectric permittivity  $\varepsilon = \varepsilon_0$  and conductivity  $\sigma = 0$ . We write the electromagnetic field in this volume in accordance with Maxwell's equations (1.4) in the form

$$\text{curl} \vec{H} = j\omega\varepsilon_0 \vec{E}, \text{curl} \vec{E} = -j\omega\mu_0 \vec{H}. \quad (2.45)$$

If to perform the substitution of variables in these equations

$$\vec{E}_1 = \sqrt{\varepsilon_0} \vec{E}, \vec{H}_1 = \sqrt{\mu_0} \vec{H}, \quad (2.46)$$

it is easy to be convinced that  $\vec{E}_1$  and  $\vec{H}_1$  are also electric and magnetic vectors of field, but they are expressed in another units, since they were multiplied by the same constant factor. After changing the variables, we arrive at the equations

$$\text{curl} \vec{H}_1 = j\omega\sqrt{\varepsilon_0\mu_0} \vec{E}_1, \text{curl} \vec{E}_1 = -j\omega\sqrt{\varepsilon_0\mu_0} \vec{H}_1, \quad (2.47)$$

These equations for  $\vec{E}_1$  and  $\vec{H}_1$  are the same (symmetrical). Therefore, both fields in the volume  $V$  coincide, if the boundary conditions on the surface  $S$  coincide.

The picture of electric and magnetic fields in the case of an ideal slot antenna and in the case of a metal plate located in free space is given in the book [14]. Figure 15 demonstrates a picture of a field of an ideal slot antenna, and Fig. 16 shows a picture of fields of a metal plate. The solid lines in the figures indicate the direction of the electric vector, and the dashed lines indicate the direction of the magnetic one. In the case of a slot antenna a half-space, bounded by an ideally conducting plane and a hemisphere of large radius centered at a slot center, is taken as the volume  $V$ . In the case of a metal antenna, the volume  $V$  is located between a hemisphere centered at the center of the plate and a plane coinciding with the plate.

From the above pictures the identity of the boundary conditions follows. They confirm the identity of the fields when they are mutually replaced. As follows from the results of the transition from expressions (2.45) to formulas (2.47), in order to calculate the magnetic field strength  $\vec{H}$  of the slot antenna, based on the known strength  $\vec{E}$  of the electric field of the metal plate, it is necessary to perform a substitution of variables in accordance with (2.46), and after that to replace  $E$  with  $H$  and  $H$  with  $E$ . It is believed that width of the slot and the metal plate are the same and equal to  $d$ . The current flows along both sides of the plate and is equal to  $J(0) = 2 \int_0^d H_x dx$ .

As is known, the electric field of a metal radiator is equal to

$$E_{\theta_e} = 120\pi H_{\theta_e} = j30kl_e J(0) \frac{\exp(-jkR)}{R} F(\theta, \varphi), \quad (2.48)$$

where  $l_e$  is the effective length,  $J(0)$  is an antenna input current,  $R$  is a distance to an observation point,  $F(\theta, \varphi)$  is the directional pattern. Accordingly, the magnetic field of the one-sided slot is

$$H_{\theta_s} = -j60kl_e U_s \frac{\exp(-jkR)}{R\mu_0/\varepsilon_0} F(\theta, \varphi). \quad (2.49)$$

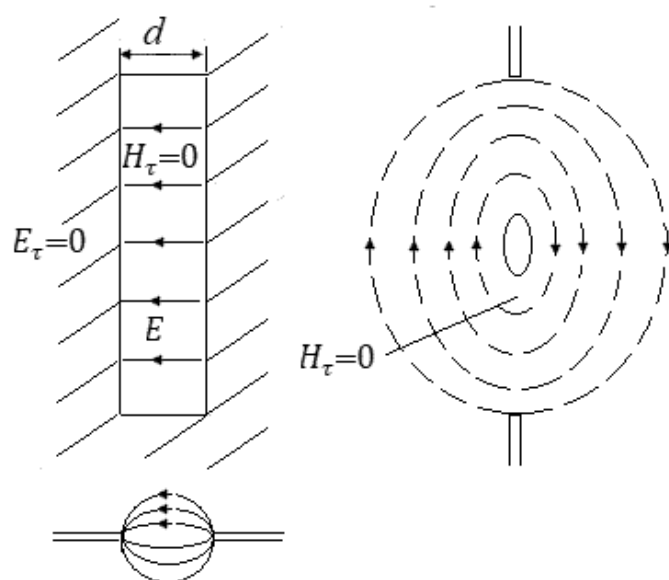


Fig. 15: Fields of an ideal slot antenna.

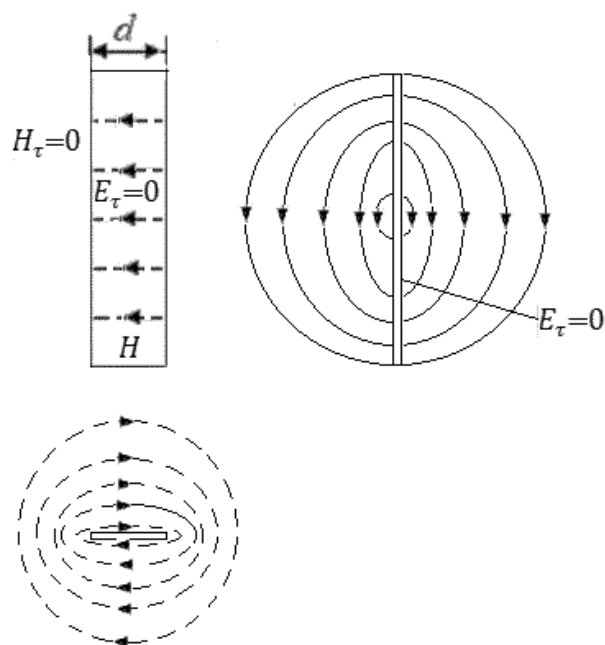


Fig. 16: Fields of a metallic plate.

Here  $U_s = \int_0^d E_{ts}$  is the voltage at the slot center. From this expression one can see that we are considering the radiation of a one-sided slot. At that, since  $\mu_0/\varepsilon_0 = (120\pi)^2$ , then

$$E_{\varphi s} = 120\pi H_{\theta s} = -j \frac{30kl_e U_s}{60\pi} \frac{\exp(-jkR)}{R} F(\theta, \varphi). \quad (2.50)$$

From (2.48) and (2.50) it seen that the field of an ideal slot antenna differs from the field of a metal radiator, firstly, by polarization (the radiator field consists of  $E_{\theta e}$  and  $H_{\varphi e}$ , and the field of a slot antenna consists from  $H_{\theta s}$  and  $-E_{\varphi s}$ ), and secondly, by a constant factor. In the case of a radiator the field is proportional to the value  $J(0)$ , in the case of a one-sided slot—to the value  $U_s/(60\pi)$ , in the case of a double-sided slot—to the value  $U_s/(120\pi)$ . Summing up results of comparing the fields of a metal radiator and an ideal double-sided slot and taking into account the dependence of the fields on the magnitudes  $J(0)$  and  $U_s/(120\pi)$ , we can say that the value  $U_s/(120\pi)$  is a kind of analogue of the current  $J(0)$ . This analogue will be used further.

The electromagnetic fields of an ideal slot antenna and a metal radiator are the same not only in the far zone, but also in near and other zones of the antennas. Since the distribution of voltage along the slot and current along the metal radiator is the same both in the longitudinal and transverse directions, it can be argued that the input conductivity  $Y_{s1}$  of a one-sided slot and the input conductivity  $Y_{s2}$  of a double-sided slot are greater than the input impedance of a metal radiator by  $1/(60\pi)^2$  times and by  $1/(120\pi)^2$  times respectively, i.e., are equal to

$$Y_{s1} = Z_e/(60\pi)^2, \quad Y_{s2} = Z_e/(120\pi)^2,$$

This means, for example, that in accordance with the theory of long lines, the conductivity of a one-sided slot antenna is

$$Y_s = [R_{\Sigma e} - j W_e \cot k l]/(60\pi)^2. \quad (2.51)$$

Metal and slot radiators are sources of electromagnetic fields. But in the case of a metal radiator, we are primarily talking about the strength of the electric field, and in the case of a slot antenna about the strength of the magnetic field. For this reason, the name of the magnetic radiator was assigned to the slot antenna, in contrast to the electric radiator in the form of a metal rod or plate. For the same reason the value  $U_s/(120\pi)$  was called magnetic current.

As shown in [15], the integral equation for a voltage  $U$  between the faces of a slot, cut in a non-planar metal screen, coincides in appearance with the equation for a current in an equivalent metal antenna of analogous shape and dimensions. However, the operator  $G(U)$ , incoming into this equation, which is directly proportional to  $U$ , depends on the screen shape, i.e., in general case it differs from the operator  $G(J)$  for a rectilinear metal antenna located in free space. Therefore, the question of the electrical characteristics of the slots cut in non-planar screens of different shape remains open.

Analysis of the characteristics of slot antennas located in three-dimensional space on circular metal structures [16] created new perspectives in solving the described

problem. He pointed out options of slots in non-planar screens, the characteristics of which coincide with the characteristics of metal radiators. These are for example self-complementary slotted antennas. In particular, it is a symmetrical two-sided slot antenna, located on a circular metal cone of an infinite length and excited on the cone top (Fig. 17a).

In accordance with the duality principle, the active resistance of a double-sided slot antenna cut into a flat perfectly conducting metal screen of unlimited dimensions and infinitesimal thickness is equal to

$$R_{\Sigma s} = \frac{(120\pi)^2}{R_{\Sigma e}}. \quad (2.52)$$

Here  $R_{\Sigma e}$  is the resistance of a metal radiator with a similar shape and dimensions. This expression is obtained as a result of comparing the powers radiated by both antennas. If to compare with each other the oscillating power created by these radiators, one can get a similar expression for the input impedances of the radiators:

$$Z_s = \frac{(120\pi)^2}{Z_e}. \quad (2.53)$$

One of radiators (slotted) is called by magnetic in accordance with the nature of its current, the other radiator (metallic)—by electric one.

Let us move from the V-shaped magnetic radiator (Fig. 17b) to the slot antenna (Fig. 17c). To do this, we divide each arm of the magnetic radiator by means of a metal surface in a form of a circular cone passing through an arms axis. Since the magnetic field lines of the radiator coincide with the surface having the shape of a circular cone, the field of the radiator at that does not change. The metal surface divides the magnetic radiator into two radiators. They are located on different sides from this surface, inside and outside the conic solid angle. Since in this case the magnetomotive force  $e_m$ , exciting the radiator, and oscillating power  $P = e_s J_s$ , created by the radiator, do not change, the fraction of the magnetic current  $J_s$  in each of the new radiators is equal to the fraction of the power radiated into its part of a space.

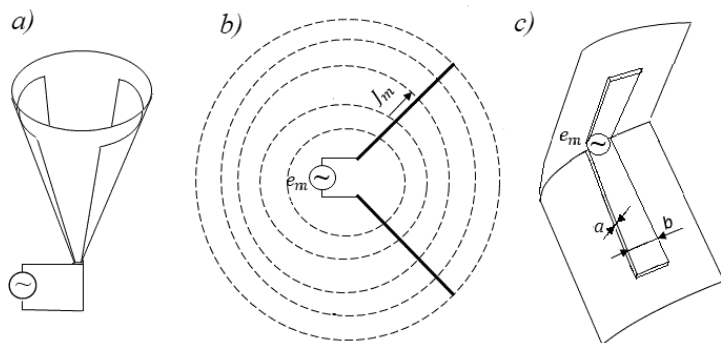


**Fig. 17:** Slot antenna on a circular metal cone (a) and transition from magnetic radiator (b) to slot antenna (c).

Let  $m$  is the fraction of power inside the solid angle, and  $(1-m)$ —outside it. Then the input admittance of the magnetic radiator located inside the cone is equal to

$$Y_1 = eS/(mJ_s) = Y/m,$$

where  $Y = 1/Z_s$  is the total admittance of the original radiator. As can be seen from Fig. 17c, the cross-section of the magnetic radiator with a current  $sJ_M$  has the thickness  $a$  and trapezoidal shape with a base  $b$ , and  $b \gg a$ . Such a radiator is equivalent to a one-sided slot of width  $b$ . The second radiator is equivalent to a similar one-sided slot. Its current is equal to  $(1-m)J_s$ . Its input admittance is

$$Y_2 = \frac{e_s}{(1-m)J_s} = Y/(1-m).$$

If to replace both slots by one double-sided slot and to assume that its admittance is equal to the sum of the admittances of both slots, then

$$Y_s = Y_1 + Y_2 = Y/[m(1-m)]. \quad (2.54)$$

The input impedance of the double-sided slot with the account of (2.53) and (2.54) is equal to

$$Z_s = 1/Y_s = m(1-m)/Y = (120\pi)^2 m(1-m)/Z_e. \quad (2.55)$$

If the shape and dimensions of a slot radiator are identical to the shape and dimensions of a metal one, then

$$Z_s = Z_e = 120\pi \sqrt{m(1-m)}, \quad (2.56)$$

The input impedance of the slot is actually the input impedance of the metal radiator located near the slot, or the input impedance of a uniform two-wire line. With increasing the length of the two-wire line, its input impedance tends to the wave impedance, which for the identical width of the slot and the metal radiator is equal to  $60\pi$ . Comparison of this fact with the expression (2.56) shows that the magnitude  $m$  is equal to 0.5 for any angle of the cone aperture. This means that the power radiated inside a solid angle is equal to the power radiated outside it.

A special case of the considered transition is the transition from a straight vertical magnetic radiator to a vertical slot. This slot and a flat metal radiator are the complementary antennas. In this case, the slot antenna is located in an infinite vertical metal plane, and the coincidence of the operators  $G(U)$  and  $G(J)$  is beyond doubt. Both operators are linear. In the considered general case (Fig. 17a), the operators also have the same shape, but the straight arms of the magnetic V-radiator are located at an angle to each other, and its operator  $G(J)$  is not linear. Such a slot antenna, without doubt, is similar to metal V-radiator. V-radiator and radiator, shown in Fig. 17c, differ from each other only in that one of them is electric and the other is magnetic.

If the slot antenna is located on the faces of the pyramid, the surface of which, in contrast to the surface of rotation, is not smooth, then it cannot be complementary, and its operator differs from both mentioned operators.



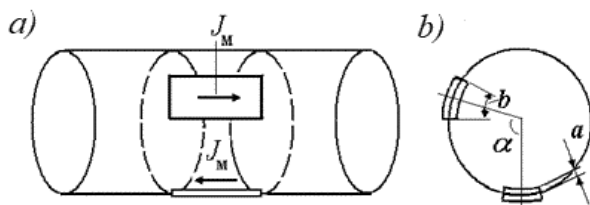


Fig. 18: Two parallel magnetic radiators (a) and two slot antennas (b).

As is said earlier, slot antennas located on circular metal surfaces (i.e., cut in the indicated surfaces) operate as slot antennas, complementary to metal ones. Such surfaces are the surfaces of circular cones and paraboloids, as well as the surfaces of circular cylinders. In this regard, we will consider the structure of two identical magnetic radiators located on the surface of a metal cylinder and excited in anti-phase (Fig. 18a). Magnetic radiators are implemented in the form of slot antennas. In this case, the operators of slot antennas are linear and coincide with the operators of linear metal radiators. Half the power of each antenna is radiated into the internal volume of the cylinder.

A similar situation, as shown in [16], takes place in the case of two parallel infinitely long filaments, whose linear charge densities are the same in magnitude and opposite in sign. Half of the energy flow along a long line of two parallel wires propagates inside an imaginary circular cylinder passing through these wires. The second half passes outside. With a great deal of confidence, it can be argued that a similar situation holds true for wires of finite length, even though the current magnitude varies along the wire. More on this it is said in Section 6.7.

The slot antennas shown in Fig. 18 create the system of two anti-phase radiators located along the generatrices of a circular cylinder. It can be any generatrices, with an arbitrary arc length between radiators around the circumference of the cylinder. The input impedance of each radiator is equal to

$$Z_A = Z_{11} - Z_{12},$$

where  $Z_{11}$  is the self-impedance of each radiator, and  $Z_{12}$  is the mutual impedance between the radiators. In the case of thin radiators, the directional pattern of the array from two radiators is determined only by the distance between them and does not depend on the angle between the slots' planes, i.e., a metal surface is only a structure, on which slots are located.

## 4. Impedance Magnetic Antennas

As said in the previous Section, a slot antenna is a practical embodiment of a magnetic radiator, and the characteristics of a slot antenna can be determined in accordance with the duality principle, based on the analogy between an electric and magnetic radiator. The impedance magnetic radiator should be considered the same analogue

of an impedance electric radiator. On the surface of this antenna non-zero boundary conditions are satisfied. As is shown in [1], that are conditions of the type

$$\frac{H_z(a, z) + K_1(z)}{E_\varphi(a, z)} = -\frac{1}{Z_1(z)}, \quad -L \leq z \leq L. \quad (2.57)$$

Here  $E_\varphi(a, z)$  and  $H_z(a, z)$  are the azimuthal component of the electric field and the longitudinal component of the magnetic field, respectively,  $K_1(z)$  is the extraneous emf, and  $Z_1(z)$  is the surface impedance, which in general case depends on coordinate  $z$ .

In this case the telegraph equations have the form

$$-\frac{dU_m}{dz} = \left( j\omega\Lambda_1 + \frac{1}{aZ} \right) J_m(z), \quad \frac{dJ_m(z)}{dz} = j\omega C_1 U_m(z),$$

whence

$$\frac{d^2 J_m(z)}{dz^2} + k_1^2 J_m(z) = 0,$$

where

$$k_1^2 = k^2 + j \frac{\omega C_0}{2aZ_1}.$$

In accordance with (2.1), in the case of a metal antenna with an inductive surface impedance, the second term in this expression is equal to  $-jZ\omega C_1/(\pi a)$ . The cross-section of this radiator is the circle. The slot antenna has the shape of a strip, i.e., in the last expression  $\pi$  should be replaced by 2. The surface impedance  $Z$  in accordance with (2.57) must be replaced by  $-\frac{1}{Z_1(z)}$ .  $C_0$  is the capacitance between the radiator and the surface of zero potential is equal to  $C_0 = \frac{2\pi\epsilon_0}{\ln(2L/a)} = 4\pi\epsilon_0\chi$ . The shape of the cross-section changes the small parameter  $\chi$ , but does not affect the general form of the equation for the current. Substituting these results into an expression for  $k_1^2$ , we get

$$k_1^2 = k^2 - j 2\pi k\chi/(aZ_0 Z_1),$$

i.e.,

$$k_1 = \sqrt{k^2 - j2\pi k\chi/(aZ_0 Z_1)},$$

where  $Z_0 = 120 \pi$  is the wave impedance of the free space. A propagation constant would have such a magnitude in a metal radiator with given dimensions and surface impedance. In the case of a double-sided slot the magnetic current is equal to the conditional value  $J_m = U_s/Z_0$ . In order to go to real values, each current should be

multiplied by  $Z_0$ , and the square of the current by  $Z_0^2$ . Accordingly, for the propagation constant along the impedance slot antenna shown in Fig. 19 we get

$$k_1 = \sqrt{k^2 - j2\pi k \chi Z_0 / (a Z_1)}, \quad (2.58)$$

which completely coincides with the magnitude obtained in [1] in the derivation of the integral equation for  $U_s$ . Of essential interest is the case when the surface impedance is large enough to change the current distribution along the antenna and the equivalent line already in the first approximation in  $\chi$ . Such an example is the problem of natural oscillations of a rectangular trough [1]. The trough is considered as a narrow slot in a flat screen, uniformly loaded with distributed impedance  $Z_1$ , the magnitude of which is equal to the ratio  $E/H$  at the input of a short-circuited rectangular waveguide (Fig. 19a). Since in the first approximation the current distribution is sinusoidal, the impedance is created by fields of the type,  $TE_0$ , i.e.,

$$E_y/H_z = -jZ_1 (k/\gamma) \tan \gamma d,$$

where  $\gamma$  is the wave propagation constant with allowance for the surface impedance,  $d$  is a depth of the trough. If to write an equation for the natural frequencies of the trough oscillation, then one can interpret a uniformly loaded slot as a section of a long line with the capacitors connected in parallel to this line (Fig. 19b). Such a magnetic antenna is called the impedance one.

Impedance magnetic antennas also include the antenna in the form of a straight magnetodielectric rod (Fig. 20a) and the antenna in the form of a straight circular metal cylinder with a narrow longitudinal slot (Fig. 20b). Both antennas are excited by a wire loop located around the central section. As a result, the loop is loaded by an impedance equal to

$$Z_M = 1/Y = U_{ind}/J(0) = Z_0^2/Z_e. \quad (2.59)$$

Here  $U_{ind}$  is the induced voltage,  $J(0)$  is the loop current. The loop current is the magnetomotive force  $e_M$  applied at the point of excitation, and the induced voltage is proportional to magnetic current of the loop.

The input impedance  $Z_e$  of comparatively short radiator with a total length  $2L < \lambda/2$  and a radius  $a$  can be calculated by means of expression

$$Z_e = 80 \left( \frac{k}{k_1} \right)^2 \tan^2 \frac{k_1 L}{2} - j120 \left( \ln \frac{2L}{a} - 1 \right) \cot k_1 L. \quad (2.60)$$

Analysis of the characteristics of a magnetic radiator in a form of a magnetic rod (Fig. 20a) begins with the calculation of the surface impedance [16]. If a magnetic rod fabricated from a ferrite, its surface impedance can be determined, as shown in Section 1, by replacing the rod with a set of radial lines or by solving the diffraction problem of a cylindrical wave converging on the surface of the rod. As a result, we find

$$Z = \frac{E_\varphi}{H_z} \Big|_{\rho=a} = j120\pi \sqrt{\mu_r/\epsilon_r} \frac{J_1(ma)}{J_0(ma)} \quad (2.61)$$

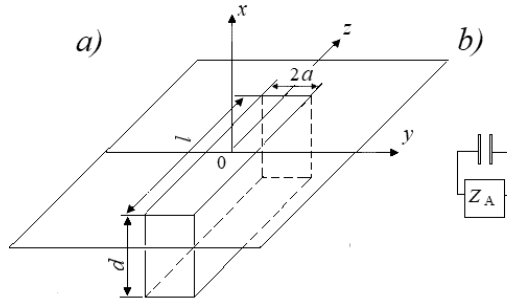


Fig. 19: Slotted antenna in the form of a loaded slot (a) and its equivalent circuit (b).

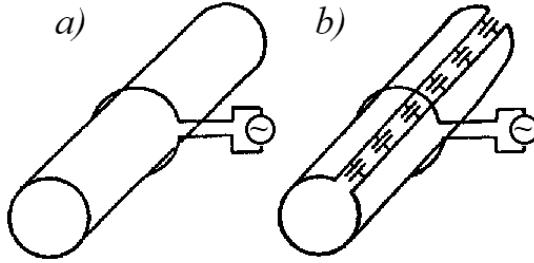


Fig. 20: The impedance magnetic radiators in a form of a magnetic rod (a) and a metal cylinder with a slot (b).

where  $m$  is the wave propagation constant in the ferrite,  $J_1(ma)$  and  $J_0(ma)$  are the Bessel functions. In the case of thin rods ( $ma \ll 1$ ) the surface impedance and propagation constant are equal to

$$Z = j60\pi\mu_r ka, \quad k_1 = \sqrt{k^2 - 2\left(\mu_r a^2 \ln \frac{2L}{a}\right)}. \quad (2.62)$$

The last expression permits to define the condition of magnetic current propagation along the rod

$$\mu_r \geq \frac{k^2 a^2}{2} \ln \frac{2L}{a}.$$

The equal sign in this expression corresponds to the critical wavelength  $\lambda_0$ :

$$\lambda_0 = 2\pi a \sqrt{\ln \frac{2L}{a} / (2\mu_r)}.$$

At  $\lambda > \lambda_0$  the magnetic current is damped, at  $\lambda < \lambda_0$  it spreads along the antenna. If  $\mu_r$  increases infinitely, the ferrite rod becomes an ideal magnetic radiator. Unfortunately, such ferrites do not exist, and the magnetic permeability of the rod is additionally reduced due to the demagnetizing factor. If to increase the diameter of the ferrite rod, then the expressions for the surface impedance and the wave propagation constant along the rod will change, but the properties of the antenna as a whole will change slightly. As shown in [17], when  $\lambda = \lambda_0$ , the directional pattern of the ferrite rod,

excited by the loop, changes (at low frequencies it coincides with the directional pattern of the loop, at higher frequencies it coincides with the directional pattern of the impedance radiator).

The second option of impedance magnetic radiator is a narrow slot cut in a circular metal cylinder. From the general expression for  $k_1$  it follows that the propagation constant of the magnetic current along the radiator is real, if the surface impedance is capacitive in nature. To do this, along a narrow slot of the cylinder it is need to include several capacitors. Then the surface impedance will be created by parallel connection of the capacitor capacitance and the cylinder inductance.

Inductive impedance of a metal cylinder with a length  $L$  and a radius  $\rho$  in accordance with (2.60) is

$$j\omega\Lambda = Z \frac{2\pi\rho}{L} = \frac{j120\pi^2 k\rho^2 \mu_r}{L}.$$

The total impedance (inductance plus capacitance) is equal to

$$Z_+ = j\omega\Lambda / (1 - f^2/f_0^2),$$

where  $f_0$  is the frequency of a parallel resonance. The cross-section perimeter of the slot with a width  $a$  is equal to  $2a$ . Because the total load of the slot antenna is  $Z_+$ , its surface impedance is

$$Z = Z_+ \cdot L/a.$$

Accordingly, the propagation constant is

$$k_1 = \sqrt{k^2 - j\pi k \chi Z_0 / (aZ)} = \sqrt{k^2 - \chi(1 - f^2/f_0^2)/(\rho^2 \mu_r)}.$$

Equating to zero the radicand, we obtain an equation that allows us to determine the critical frequency for a wave, propagating along the slot. This frequency is equal to  $f_0$ . If the frequency is less than  $f_0$ , the magnetic current does not propagate along such a slot antenna. If  $f = f_0$  and accordingly  $k_1 = k$ , the slot represents an ideal magnetic radiator. The frequency increase leads to a sharp increase of a propagation constant, when many of current half-waves is placed along an antenna, and their fields cancel each other. When the operation frequency is close to the critical one  $f_0$ , i.e., in the narrow frequency range near  $f_0$ , the antenna has high efficiency.

The input impedance introduced by the rod antenna into the exciting loop is defined by the expression (2.59), where  $Z_e$  is taken from (2.60).

The impedance magnetic radiator in the form of a circular metal cylinder with a narrow longitudinal slot and capacitors located along the slot has found use as a receiving antenna for the *VHF* range [18]. The author treated the antenna developed by him as a loop and calculated the insertion active component of its input impedance in the resonance point in accordance with expression

$$R = Z_0^2 / (80k^2 L^2),$$

i.e., he considered that the resistance introduced into a loop is equal to the resistance of an elementary magnetic dipole (Hertz dipole). This insertion resistance is  $\pi^2/4$

times smaller than given in (2.60) and can be considered as a first approximation that does not use the sinusoidal distribution of the magnetic current and the resonant nature of the input impedance of a magnetic radiator.

Figure 21 shows the results of calculations and measurements of input impedance of a metal cylinder with a narrow longitudinal slot and with capacitors. The main dimensions (in meters) are:  $2L = 2.0$ ,  $\rho = 0.11$ ,  $2a = 0.03$ . The capacity is created by capacitors with the capacitance 51 pF located from each other at a distance  $b = 0.025$  m. Curve 1 is the measurement result for the loop, curves 2 and 3 are the result of calculation and measurement of an antenna. Figure 22 shows the fields of a loop and an antenna in the far zone at the same loop current in the loop depending on the frequency. In Figure 23 experimental results are given for an antenna with dimensions (in meters)  $2a = 0.01$ ,  $\rho = 0.021$ ,  $b = 0.02$  and with capacitors, which capacitance is equal to 25 pF. The results are showing, how the frequency of a first resonance changes with changing an antenna length  $2L$ .

Returning to [18], it should be said that the author created a new antenna without being carried away by its features and without wasting time on useless theorizing. In this case, it is impossible not to recognize the fairness of this approach, given the venerable age of the antenna. But this topic needs comments. Any radiator can be considered, using different level of understanding of a problem. The simplest approach to calculating the input impedance of the antenna is to consider it as a resonant circuit consisting of lumped elements: a capacitor, an inductor and a resistor, the magnitude of which depends on radiation and losses. The second approach considers the antenna as a structure of infinite length. Of course, in many cases this approach is simpler. But a result close to the truth requires analyzing the antenna as a radiator of a finite length.

Speaking frankly about such a controversial issue at the risk of running into harsh criticism, I want to quote King, who wrote in [19]: "Since the time of Hertz,

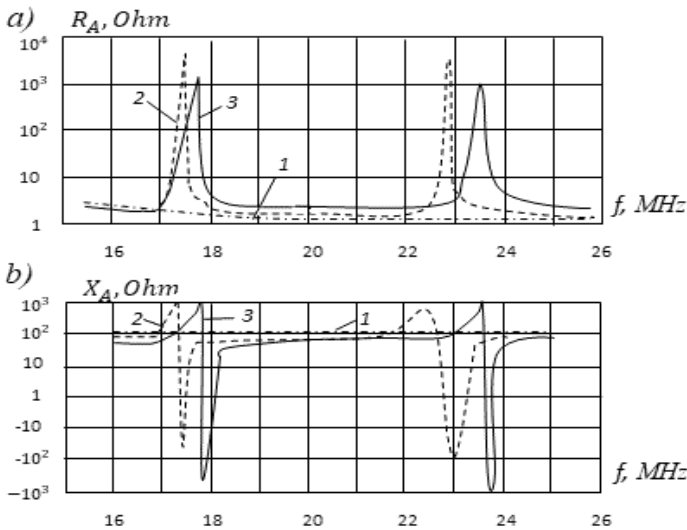


**Fig. 21:** Active (a) and reactive (b) components of the input impedance for radiator in the form of a metal cylinder with a slot : 1 – loop, experiment, 2 – antenna, calculation, 3 – antenna, experiment).

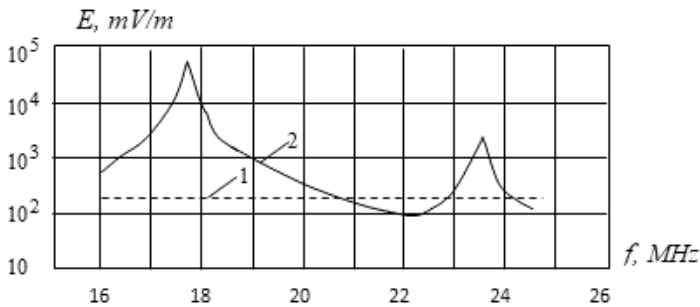


**Fig. 22:** Dependence of the field in the far zone on the frequency for the loop (1) and a metal cylinder with a slot (2), experiment.

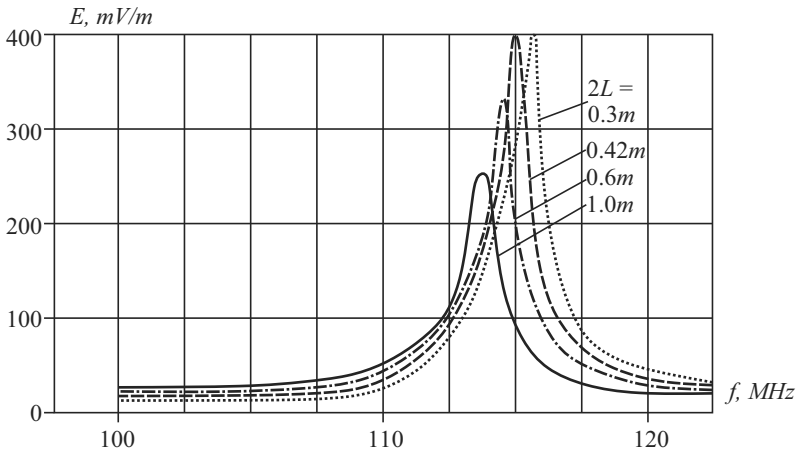


**Fig. 23:** Dependence of the first resonance frequency of the slot antenna on the cylinder length  $2L$ .

the infinitely small dipole replaces too complex for analysis, but physically feasible antennas in studies associated with the location of sources in different environments ... It should be noted that this method bypasses the main issues of antenna problems and does not solve them."

As an example of an overly cautious approach to the analysis of not too complicated questions, it is expedient to recall how we usually perceive the phrase that the current does not propagate along a given conductor. This fact does not mean that the given wire does not radiate. This fact only means that the current exponentially decays. The length of the section with decaying current may be sufficient to create a signal of the desired magnitude.

## 5. Radiators with Resistive Surface Impedance

The antennas considered in the previous sections of a chapter are radiators with reactive surface impedance. Their main difference from metal radiators is a change in the wave propagation constant along the antenna. Another variant of a surface

impedance is resistive coating. This coating slightly effects on the magnitude of the propagation constant, but leads to a smooth attenuation of the current amplitude along the antenna. As an example, let us consider transparent antennas. Analysis of the properties of such antennas, performed by means of Leontovich's equation, significantly helps to determine their capabilities and to speed up the process of their development and application.

Let's start with the necessary information about transparent antennas. The creation of these antennas became possible thanks to working out of thin transparent conductive films. Such antennas have unconditional merits. First, they can be made invisible. Secondly, they can be used in the capacity of screens for projecting different images—both still (photos) and moving (for example, TV transmission). This option of additional use is especially important for small receiving devices, that is, for operation at high radio frequencies.

Thin films of ITO (Indium-Tin-Oxide), placed on high-quality glass substrates, are electrically conductive and optically transparent at ultrahigh and superhigh frequencies. This allows us to use them as flat antennas for mobile communications and other applications. The optical transparency of the ITO film as a function of its resistivity is presented in Fig. 24 taken from [20]. Verification shows that the transparency coefficient increases with increasing resistivity of the film and is close to 95% if the resistivity of the film is greater than 5 Ohms/square.

The impact of the limitations imposed by the low conductivity of the *ITO* film is becoming clear, if to consider the dependence of its specific surface impedance  $R_{sq1}$  on the film thickness  $d$ . In accordance with the boundary condition of Leontovich, if the metal film thickness  $d$  is greater than a penetration depth  $\delta$ , the film resistivity is equal to

$$R_{sq} = 1/(\sigma\delta) \text{ Ohm}, \quad (2.63)$$

where  $\sigma$  is its specific conductivity with respect to constant current (in  $S/m$ ). The penetration depth is given by the formula

$$\delta = 1/\sqrt{\pi f k \mu \sigma}. \quad (2.64)$$

Here  $f$  is frequency (in Hz),  $\mu = \mu_0 = 4\pi \cdot 10^{-7}$  F/m is the absolute permeability. If the thickness  $d$  of the metal film is much smaller than the penetration depth  $\delta$ , the film's sheet resistivity is equal to

$$R_{sq1} = R_{sq} \delta/d = 1/(\sigma d). \quad (2.65)$$

The specific resistivity of ITO films is substantially greater than the specific resistivity of printed circuit boards and metal antennas, where copper and aluminum are used. For example, the specific resistivity of the transparent film CEC005P is equal to 4.5 Ohm/square. The specific conductivities of copper and aluminum are respectively  $5.8 \cdot 10^7$  and  $3.5 \cdot 10^7$  S/m, and hence, in accordance with (2.63) and (2.64), the specific resistivity of a copper plate, whose thickness is greater than the penetration depth, at frequencies 1 and 5 GHz, is equal to  $6.9 \cdot 10^{-3}$  and  $18.4 \cdot 10^{-3}$  respectively (the specific resistivity of an aluminum plate with analogous thickness



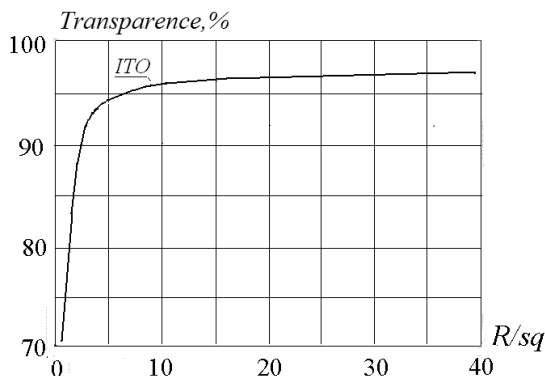


Fig. 24: Example of the film transparency at the frequency 0.545 GHz.

at these frequencies is equal to  $4.2 \cdot 10^{-3}$  and  $11.1 \cdot 10^{-3}$  respectively). That means, the resistivity of ITO transparent film is greater by several orders than the resistivity of copper and aluminum, i.e., the conductive films are different from materials, commonly used in antennas (copper, aluminum), by a decrease of conductivity. This fact significantly changes the properties of radiators.

For comparative analysis of antennas made of materials with high and low conductivity, it is necessary to apply methods for solving the corresponding boundary value problems of electrodynamics. These methods are divided into direct numerical and approximate analytical. The conclusion of specialists on the results of these methods application in prolonged researches is clearly formulated in [21]: “The undoubted advantage of analytical methods is that they are physically clearer in comparison with numerical methods. Analytical methods allow us to determinate the effect of device parameters on its individual characteristics.”

In recent years, transparent antennas have been the subject of many works. However, these works were aimed mainly at determining and improving the properties of materials. Physical processes in transparent antennas, their electrical characteristics, and the difference of these characteristics from characteristics of metal antennas with a high conductivity as a rule do not consider.

For understanding physical processes in antenna, the knowledge of a current distribution along its axis has great importance. One must also understand that if the current does not propagate along the wire (decays), then the field, which it creates, is small, but not equal to zero. The knowledge of a current distribution law allows us to define all main characteristics of antennas and serves as the basis for its analysis. This postulate remains valid in spite of elaboration of such calculation programs as program CST, since firstly these programs basically allow to calculate input characteristics (and characteristics dependent on them). Calculating the distribution of a current by means of these programs is difficult problem. Secondly, such a program does not allow us to understand the reasons for distribution change, to take them into account and to use in the antenna design.

The described below method despite its apparent simplicity makes it possible to significantly improve the agreement of calculation with the experiment. The transparent antenna is an antenna with non-zero (impedance) boundary conditions.

The current along it can be calculated in accordance with the telegraph equation (2.3). This equation is valid, if a surface impedance of an antenna is large enough to change a wave propagation constant along the antenna already in the first approximation. In this case it is necessary first to consider the surface impedance  $R_{sq1}$ , created by losses in the transparent film. The antenna width  $b$  is less important and has a smaller effect on the characteristics of the antenna.

The presence of a distributed resistive load means that the current along the radiator has a sinusoidal character with a slowly decreasing amplitude

$$J(z) = J(0) e^{-\alpha z} \sin kz. \quad (2.66)$$

Substituting the surface impedance  $Z = R_{sq1}$  into the equation (2.3) for the current in the free oscillation mode, we get

$$\frac{d^2 J(z)}{dz^2} + k^2 J(z) = \frac{k\chi J(z) R_{sq1}}{60\pi a}.$$

Taking into account expression (2.66) we find

$$\frac{dJ(z)}{dz} = J(z)(-\alpha + k \cot kz), \quad \frac{d^2 J(z)}{dz^2} = J(z)(\alpha^2 - k^2 - 2k\alpha \cot kz), \text{ i.e.}$$

$$J(z)(\alpha^2 - 2k\alpha \cot kz) = \frac{k\chi J(z) R_{sq1}}{60\pi a},$$

where

$$\alpha = \frac{k}{\tan kz} \pm \sqrt{\left(\frac{k}{\tan kz}\right)^2 + \frac{k\chi R_{sq1}}{60\pi a}} \quad (2.67)$$

Let, for example,  $R_{sq1} = 4.5 \text{ OM}$ ,  $a = 0.006 \text{ m}$ ,  $\chi \approx 0.12$ . On the frequency  $f = 5 \text{ GHz}$  the wave length  $\lambda$  is equal to  $0.06 \text{ m}$  and the propagation constant is  $k \cong 105$ , i.e.,  $\tan kz$  tends to infinity, and

$$\alpha = \sqrt{\frac{k\chi R_{sq1}}{60\pi a}} \cong 7.1.$$

In Fig. 25 the current distributions of two radiators with the same dimensions are compared. One radiator is made from the metal with a perfect conductivity, and another radiator is made from film CEC005P. The dimensions of the radiators in millimeters are given in Fig. 25a. The curve of the current (see Fig. 25b) along a metal antenna is denoted by number 1, the curve of the current along a transparent antenna is denoted by number 2. As is seen from Fig. 25b, the current in the metal antenna with perfect conductivity does not decrease. The current of the transparent antenna decays rapidly and decreases 5 times at a distance  $0.23 \text{ m}$  from the source and 10 times at a distance  $0.33 \text{ m}$  from the source. These distances are close to the calculation results.

Therefore, the current along the transparent antenna axis is distributed over sinusoidal law, but the sinusoid amplitude is decreased in accordance with exponential

law. If  $\alpha L = 2$ , where  $L$  is the arm length of an antenna, the amplitude of the current along the arm length is decreased by  $e^2$  times, where  $L$  is the base of the natural logarithms, i.e., current is almost zero. If  $\alpha L > 2$ , the operating length of the antenna is even shorter. The performed analysis leads to an important conclusion: the length of the radiating segment of the antenna in a first approximation is independent on frequency. This means that increasing the antenna length in order to ensure operation on lower frequencies is useless. The input impedance of such an antenna does not have a sharp resonance, and the effective length of the antenna is small.

In accordance with the results of the calculation, the experimental verification was carried out on an antenna model of small height (Fig. 26, dimensions are given in millimeters). The radiator is made of CEC005P film. The measurements show that this model has stable characteristics in the frequency range 2.5–4.5 GHz and higher, close to calculated results. But the exponential decrease of current leads to a signal that is created by an antenna section located near the power point, and in the rest part of an antenna there is practically no current. Therefore, the input impedance of such an antenna does not have a resonance, and the effective length of the antenna is small in comparison with the effective length of a monopole manufactured from a metal with high conductivity.

Losses in a transparent antenna is one of the reasons for its low efficiency. The low level of matching of the transparent antenna with the cable leads to an additional reduction in efficiency of the antenna. Therefore, to increase this efficiency, it is first necessary to ensure a smooth transition from the central conductor of the cable to the transparent film forming the antenna. For example, one should place between them a plate with a variable width (a metal triangle with a base equal to the radiator width).

This triangle allows creation of even distribution of current across the entire antenna width that increases the total current and the radiated signal. In order that the current distribution to be uniform and the reflection coefficient is minimal on the boundary of rectangular and triangular sections and in the point of cable addition, the wave impedances of these sections and the cable should be close to each other. Accordingly, the triangular section of the described model must be fabricated from the same film. But, as a rule, this is not enough.

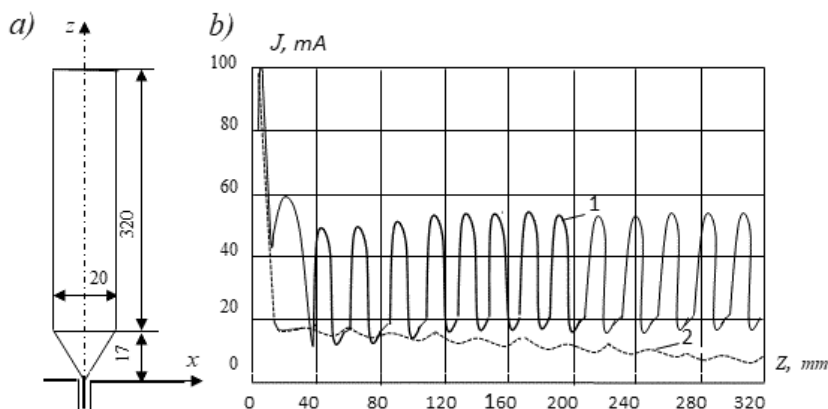


Fig. 25: Current distribution along the metal (1) and transparent (2) radiators on a frequency 5 GHz.

The wave impedance of the radiator can be reduced, if it is made in the form of a self-complementary antenna consisting of the flat metal radiators. In Fig. 27 two asymmetrical self-complementary antennas with one and two flat cones are shown. In Fig. 28 reflectivity of three flat antennas are presented: for antenna with a triangular section, shown in Fig. 25a (curve 1), for antenna with one transparent cone (Fig. 27a) and arm length equal to  $L = 0.045$  m (curve 2) and for antenna with two transparent cones (Fig. 27b) and the same arm length (curve 3). As can be seen from Fig. 28, an antenna with two cones provides a smooth change of reflectivity over a wide frequency range. This result demonstrates a significant advantage of the third option.

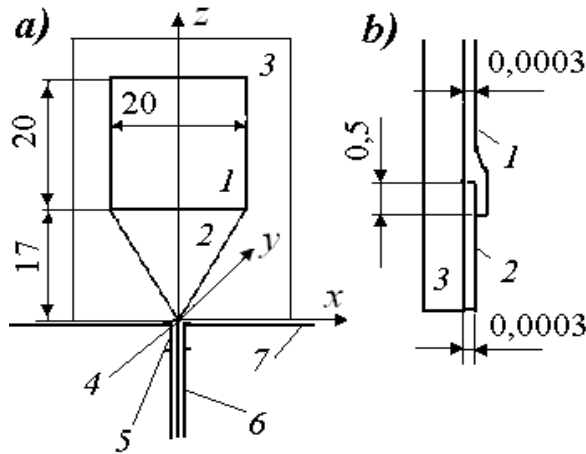


Fig. 26: A front view (a) and cross-section (b) of flat transparent antenna:

1 – transparent film, 2 – metal triangle, 3 – glass substrate, 4 – soldering point, 5 – connector, 6 – cable, 7 – disc.

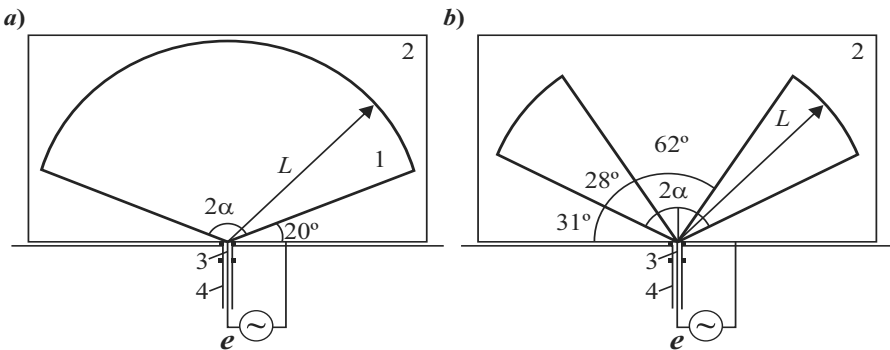
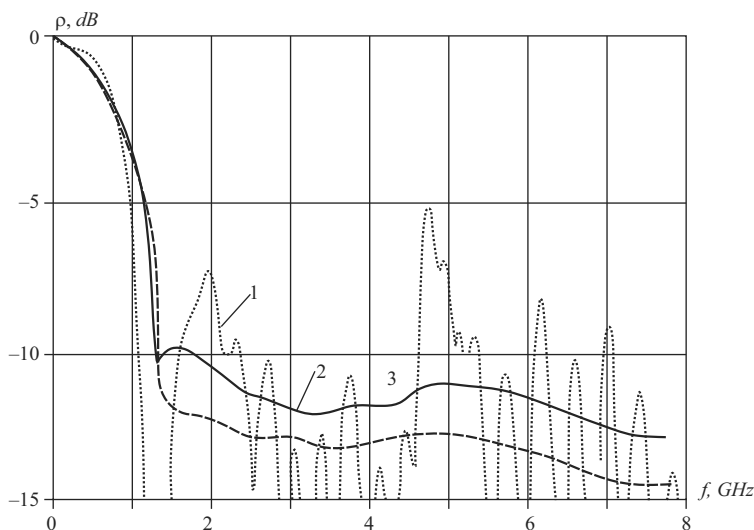


Fig. 27: Asymmetrical self-complementary antennas with one (a) and two (b) flat cones:

1 – transparent film, 2 – glass substrate, 3 – connector, 4 – cable.



**Fig. 28:** Reflection coefficients of antennas with transparent triangle (curve 1), with one transparent cone (curve 2) and with two transparent cones (curve 3).

## 6. Principle of Complementarity and Self-complementary Antennas

As was said, a symmetry of Maxwell's equations with respect to the quantities  $\sqrt{\epsilon_0} \vec{E}$  and  $\sqrt{\mu_0} \vec{H}$  lead to existence of metal (electric) and slot (magnetic) radiators, which create fields of identical form in accordance with the duality principle. The complementarity principle follows from the principle of duality and speaks about an interconnection between scattering properties of metal and slot radiators. If the metal and slot antennas are placed nearby on the infinite flat metal sheet (it is assumed that the sheet is infinitely thin and has infinite conductivity), and these antennas occupy the entire sheet, the antennas are called complementary [22, 23]. The input impedances of such antennas are related by the expression

$$Z_s = (60\pi)^2 / Z_e. \quad (2.68)$$

Here magnitude is input impedance of the slot radiator, equal to input impedance of the adjacent metal radiator, which occupies the rest of the infinite sheet. Magnitude  $Z_e$  is input impedance of the metal radiator, the shape, and dimensions of which coincide with the shape and dimensions of the slot. If these antennas have the same shape and dimensions, they are called self-complementary and

$$Z_s = Z_e = 60\pi, \quad (2.69)$$

i.e., the input impedance of each radiator is independent of frequency, purely active and equal to a wave impedance  $60\pi$ . These properties are partially preserved, if dimensions of a metal sheet are finite.

In 1957 Rumsey formulated the constructive feature of the frequency independent antennas as follows: if the shape of the antenna is such that it could be specified entirely by angles, its performances do not depend on frequency [24]. Special properties of such structures make them unique. The first considered structure of such an antenna is presented in Fig. 29a. It consists of metal and slot symmetrical radiators of the same shape and dimensions. This antenna differs from the self-complementary by finite dimensions of the structure. If to replace her triangular metal surfaces by wires dispersing out of the feed point (out of the triangle vertex), the antenna will take a form shown in Fig. 29b. Her characteristics are close to characteristics of the antenna presented in Fig. 29a.

Antennas consisting of a metal and slot radiators of the same shape and dimensions should not necessarily be flat. For example, antennas placed on the surface of a circular cone, which is shown in Fig. 30, satisfy this principle. As indicated in [25], if the structure of a conical two-thread spiral the angular widths of the metal strip and the slot are the same, then we can talk about the self-complementary structure consisting from the identical sections of cone surface. One section is covered with a metal shell and the other one is free from it.

In the general case, an expression like to (2.68), is valid for the input impedance of a symmetrical bilateral slot antenna of arbitrary shape and dimensions, located on a circular metal cone of infinite length and excited in its vertex (Fig. 31). This expression is based on the duality principle, follows from a comparison of the radiated powers, and was derived in Section 3.

Performed analysis shows that the choice of the surface for the placement of the self-complementary radiated structures is not random. That is a surface of revolution, in particular a circular cone, which in the limit turns into a plane. This result was for the first time obtained in [26]. The shape of the metal and slot radiators located on a circular cone, can be different—similarly to the shape of radiators located on the plane. In the simplest case, the radiator boundary coincides with the cone generatrix (see Fig. 30a). Question of the coefficient  $m$  in the general case stays open.

The metal radiator located on a circular cone may be directed at an acute angle  $\theta_0$  to the ground. This allows to increase dimensions (the arm length) and directivity of the antenna, using supports of the given height. In order for the dimensions of the metal and the slot radiators to coincide, the distance between supports should be twice of their height. Then the points A and B and their mirror images coincide with the vertices of a square (see Fig. 30a).

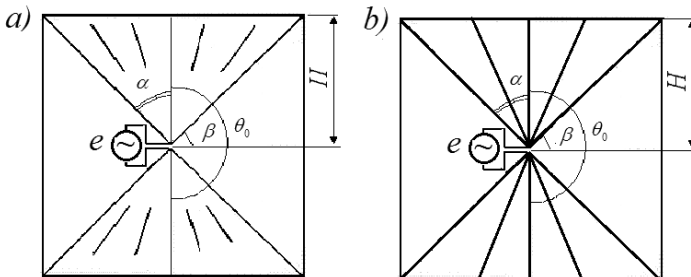
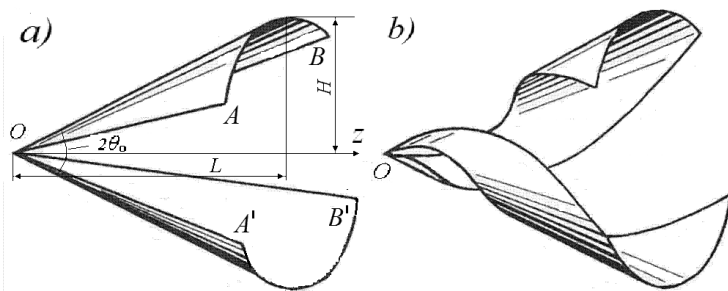
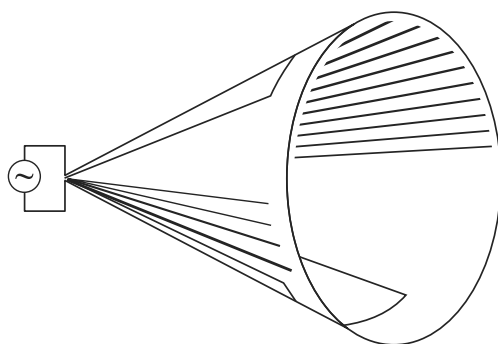


Fig. 29: Flat self-complementary radiators from metal sheets (a) and wires (b).



**Fig. 30:** Self-complementary radiators located on a conic surface.



**Fig. 31:** Slot on a surface of a circular cone.

The conical problem exemplifies the three-dimensional problem of calculating the electric field of charged bodies. Such problems are difficult. They are getting simplified if all the quantities characterizing the field depend only on two coordinates. In this case, the field is called a plane-parallel. It is of interest to use the results of solving a two-dimensional problem for the calculation of the field in a three-dimensional problem, when the metal bodies' position resembles a two-dimensional version. In this case the surfaces of the conductive bodies coincide with the surfaces of equal potential and the electrostatic problem solution in accordance with the uniqueness theorem must satisfy Laplace's equation.

Conical and cylindrical problems are compared with each other in [27], where it is shown that the Laplace's equation stays valid in transition from one problem to another, if the replaced variables are related by equalities:

$$\rho = \tan(\theta/2), \quad \varphi_c = \varphi. \quad (2.70)$$

Here  $\rho$  and  $\varphi_c$  are cylindrical coordinates,  $\theta$  and  $\varphi$  are spherical coordinates. An example of a cylindrical problem is a circular metal cylinder with cut in it the longitudinal slots of a constant width. The conical problem is a problem of two converging shells. The capacitance per unit length and the wave impedance of the cylindrical line (see, e.g., [28] or [29]) are equal to

$$C = \varepsilon K(\sqrt{1-k^2})/K(k), \quad W = 120\pi K(k)/K(\sqrt{1-k^2}), \quad (2.71)$$

where  $K(k)$  is a complete elliptic integral of the first kind with argument  $k = \tan^2(\beta/2)$ , and  $\beta$  is an angular half-width of a slot. Thus,  $C$  and  $W$  depend in a first problem only on a slot angular width  $2\beta$  and in a second problem on a shell angular width  $2\alpha = \pi - 2\beta$ . Since they do not depend on the cylinder radius, expressions for  $C$  and  $W$  are valid for conical shells forming the conical line.

Magnitudes  $C$  and  $W$  are constant along the conical line, i.e., the long line is uniform. It is known that when the line length increases, the input impedance  $Z_i$  of such a line tends towards its wave impedance. Input impedance of the line excited at the cone vertex tends towards the magnitude

$$Z_i(k) = 120\pi K(k)/K(\sqrt{1-k^2}). \quad (2.72)$$

Described conic structure is on the one hand a long line and on the other hand it is a metal V-radiator, whose arms perform in the form of converging shells located along the surface of a circular cone. Finally, this same structure can be regarded as a symmetrical slot V-antenna cut in the conic screen. If  $Z_e(2\alpha)$  is the input impedance of the metal V-radiator with the arm angular width  $2\alpha$ , and  $Z_s(2\beta)$  is the input impedance of the slot V-antenna with the arm angular width  $2\beta$ , then it follows that

$$Z_e(2\alpha) = Z_s(2\beta) = Z_i(k) = 120\pi K(k)/K(\sqrt{1-k^2}). \quad (2.73)$$

If the angular width of a metal shell and a slot is the same, i.e.,  $2\beta = 2\alpha = \pi/2$ , then

$$k = \tan^2(\pi/8) = 0.172, K(k)/K(\sqrt{1-k^2}) = 0.5,$$

and consequently

$$Z_e(\pi/2) = Z_s(\pi/2) = Z_i(0.172) = 60\pi. \quad (2.74)$$

Let the metal shell and the slot have different widths. It is necessary to keep in mind that the input impedance of the slot is the input impedance of the shell located next to the slot. If the shell width is  $2\alpha = \pi/3$ , and the slot width is  $2\beta = \pi/3$ , then

$$k = \tan^2(\pi/12) = 0.0718, K(k)/K(\sqrt{1-k^2}) = 0.391,$$

i.e.,  $Z_e(2\pi/3) = Z_s(\pi/3) = 120\pi \cdot 0.391$ . If the slot and shell widths are equal to  $2\beta = 2\pi/3$  and  $2\alpha = \pi/3$ , then

$$k = \tan^2(\pi/6) = 0.333, K(k)/K(\sqrt{1-k^2}) = 0.641,$$

i.e.,

$$Z_e(\pi/3) = Z_s(2\pi/3) = 120\pi \cdot 0.641.$$

Therefore,

$$Z_e(2\pi/3) \cdot Z_s(2\pi/3) = (120\pi)^2 \cdot 0.391 \cdot 0.641 = (60\pi)^2. \quad (2.75)$$



Expressions (2.75) and (2.56) show how impedances of a slot and a metal radiator identical to slot in shape and dimensions are related to each other. It is easy to be convinced that this relation is valid for radiators of any width. As is seen from (2.75) and (2.74), the value  $m$  in both cases is equal to  $1/2$ , i.e., the same power is radiated into the cone and out regardless of the angular width of the cone and the slots. From this it follows that the conic radiator creates a directional radiation and its directivity is maximum along the axis of its aperture.

Two options of the slots cut in a metal cone are shown in Fig. 30. In the first one, the slot boundary coincides with the generatrix of a cone. In the second one, the slot boundary is a spiral line and the cone with the slots forms a two-turn spiral, excited at the vertex. Strictly speaking, formulas (2.73)–(2.75) are valid only for the first version of the slot. However, if the widths of the shells and the slots are the same in both versions, one can be convinced that the capacitances per unit length and the wave impedances, and therefore the input impedances of the radiators, are the same for both versions, if a circular cone with symmetrical slots has an infinite length.

The magnetic radiator, which considered in Section 3, locates along the surface of magnetic field strength. This surface can be a curved one. For example, it can have the shape of a parabola. Then a metallic surface, which coincides with the surface of the magnetic field strength, will have a shape of a circular paraboloid with a vertex at the point of excitation (Fig. 32a). In the general case, that is a surface of revolution with a curved generatrix. On such a surface as well as on a circular cone also it is possible to place the self-complementary radiators, to which expression (2.56) is applicable. If radiators are not self-complementary, equality (2.55) is valid.

Parabolic and cylindrical problems are compared with each other in [30], where it is shown that the Laplace's equation in transition from one problem to other stays valid, if the replaced variables are related by equalities:

$$\rho = \sigma, \varphi_c = \psi. \quad (2.76)$$

Here  $\rho$  and  $\varphi_c$  are the cylindrical coordinates,  $\sigma$  and  $\psi$  are the parabolic coordinates. Hence, the Laplace's equation holds true in transition from the parabolic problem to the cylindrical one, if expressions (2.76) are valid. The analysis of such a structure is facilitated by the use of the parabolic system of orthogonal curvilinear coordinates  $(\sigma, \tau, \psi)$  [31]. In this structure coordinate surfaces are confocal paraboloids of rotation ( $\sigma = \text{const}$ ,  $\tau = \text{const}$ ) with focuses at the coordinates' origin and half-planes ( $\psi = \text{const}$ ) passing through the axis of rotation (see Fig. 32b). Rectangular coordinates are related to parabolic coordinates by the expressions:

$$x = \sigma\tau \cos \psi, y = \sigma\tau \sin \psi, z = (\tau^2 - \sigma^2)/2. \quad (2.77)$$

The wires are located along the paraboloid surface, or more exactly along the curves of intersection of this surface by half-planes passing through the axis of rotation ( $\sigma = \text{const}$ ,  $\psi = \text{const}$ ). The variables transformation in accordance with (2.76) results in the mapping of parabolic surface  $\tau = \text{const}$  (for arbitrary  $\tau$ ) onto the plane  $(\rho, \varphi_c)$ . The line of this surface intersection with any paraboloid  $\sigma = \text{const}$  is transformed into a circumference.

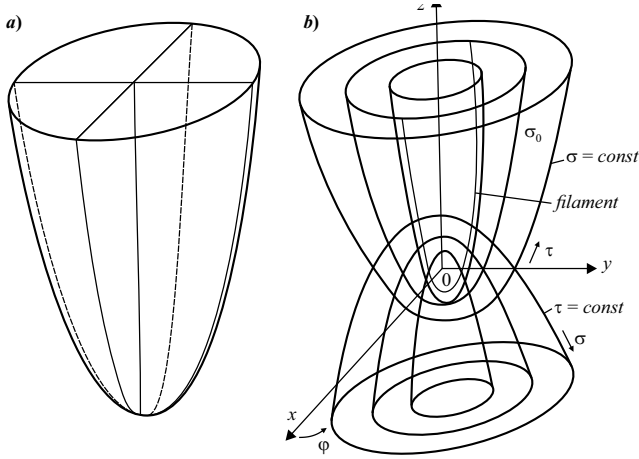


Fig. 32: Paraboloid of rotation (a), and parabolic coordinates system (b).

The case of two charged converging shells of angular width  $2\alpha$  located along the surface of a paraboloid is of specific interest since it demonstrates the placement of metal and slot antennas of finite width on surfaces of revolution. The two-dimensional problem in the form of a long line from two coaxial cylindrical shells corresponds to this case. In the parabolic line as in the conic line magnitudes  $C$  and  $W$  are constant. Hence the line is uniform and expressions (2.71) and (2.72) are valid for it. If the widths of a slot and a metal shell are the same, the expression (2.74) is valid also. If the paraboloid axis is placed horizontally, then the metal radiator, as a similar radiator on a circular cone, is located at an acute angle to the ground, and that allows to increase an arm length and an antenna directivity at the given height of supports.

The reciprocal comparison of the arm lengths of different self-complementary radiators of the same height with each other shows that the arm length of a flat radiator is equal to  $S_f = H$ . The arm length of a conic radiator depends on an angle  $\theta_0$  (see Fig. 30) and is equal to  $S_c = H/\sin \theta_0$ . In particular, if  $\theta_0 = 30^\circ$ ,  $S_c = 2H$ . The arm length of a parabolic radiator is calculated by a known formula

$$S_p = \sqrt{z_1(z_1 + p/2)} + p/2 \operatorname{sh}^{-1} \sqrt{2z_1/p}. \quad (2.78)$$

Here (Fig. 33)  $z_1 = z + z_0$  is the length of a paraboloid from the vertex to an antenna aperture,  $|z_0| = -H^2/2(L + l)$  is a distance from a vertex to origin,  $p = (L + l) H^2/[2L(L + l) + H^2]$  is a parabolic parameter,  $l = \sqrt{L^2 + H^2}$ . In particular, if  $\theta_0 = 30^\circ$ ,  $S_p = 2.2H$ . This value is more by 10.2 per cent than  $S_c$ , including 7.7 per cent at the expense of increasing the length by the segment  $z_0$ . If  $\theta_0 = 15^\circ$ ,  $S_f = H$ , as before, the magnitudes  $S_c$  and  $S_p$  are, respectively,  $3.86H$  and  $4.04H$ . Thus, a paraboloid has the maximum arm length.

For comparison, Fig. 34 shows an active ( $R_A$ ) and reactive ( $X_A$ ) components of an input impedance for a flat, conical, and parabolic antenna, depending on the ratio  $\lambda/H$  of a wavelength to an antenna height. The angle at a cone vertex and the angle between straight lines connecting the focus of a paraboloid with aperture boundaries are equal to  $30^\circ$ . In Fig. 35 and 36 reflectivity  $\rho$  and standing wave ratio (SWR) of

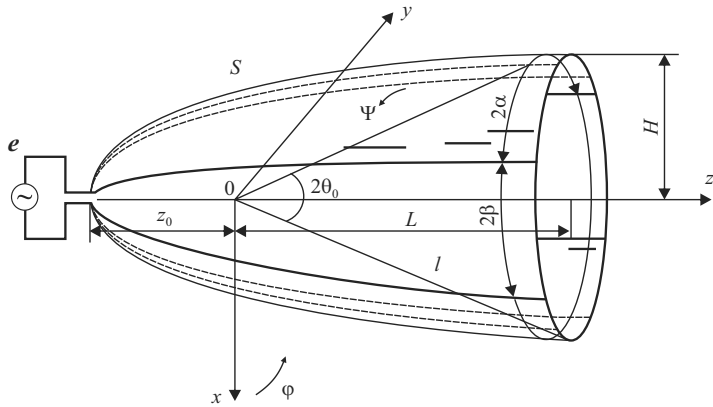


Fig. 33: Paraboloid of radiation.

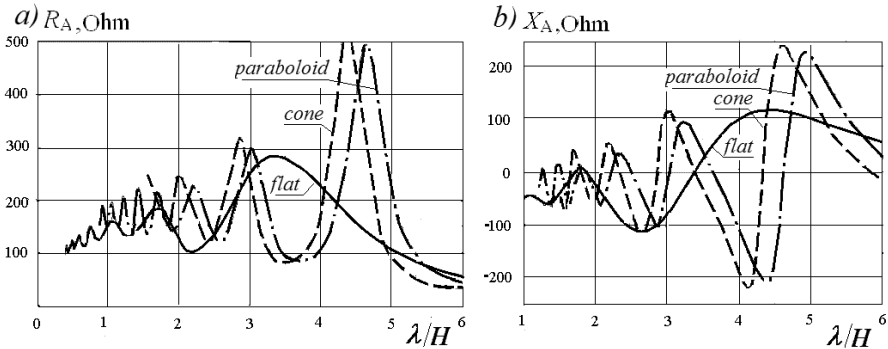


Fig. 34: Input impedance of a flat, conical, and parabolic antenna, depending on the ratio  $\lambda/H$  of a wave length to an antenna height.

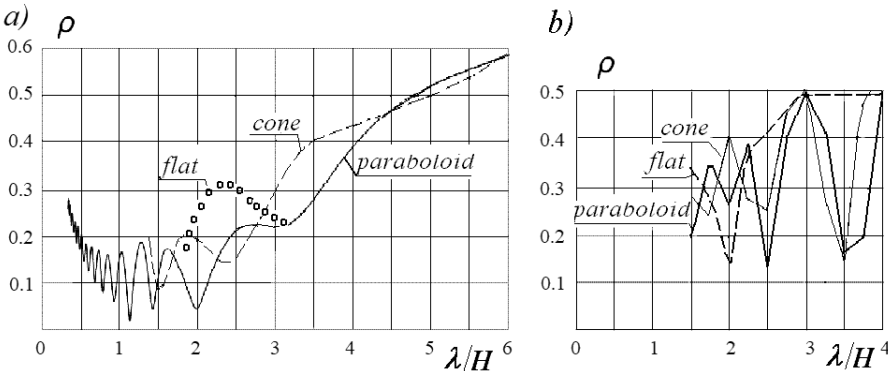
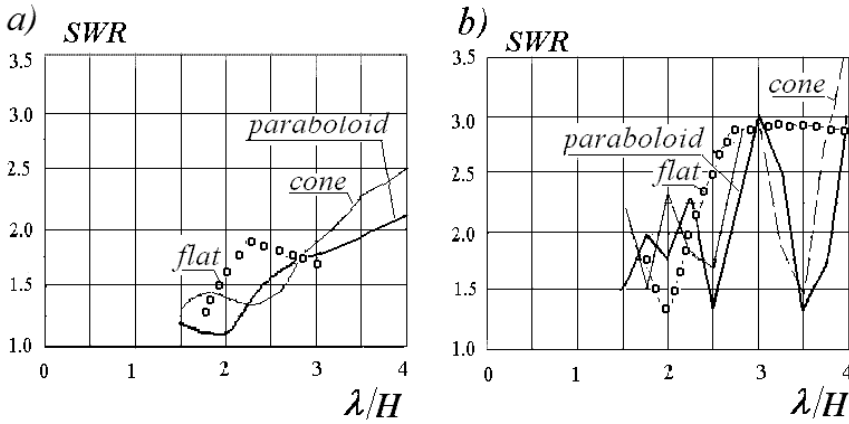


Fig. 35: Reflection coefficient of a flat, conical, and parabolic antenna in a cable with a wave impedance of  $60 \pi$  (a) and 100 Ohm (b).

the identical antennas are given depending on the ratio  $\lambda/H$  in a cable with a wave impedance  $60 \pi$  Ohm (a) and 100 Ohm (b).

Calculations and experiments show that increase in the electrical length of a generatrix improves characteristics of the radiator (matching with the cable,



**Fig. 36:** Standing wave ratio (SWR) of a flat, conical and parabolic antenna in a cable with a wave impedance of  $60\pi$  (a) and 100 Ohm (b).

**Table 3:** Gain and Efficiency of Different Radiators.

$\lambda/H$	Gain at $\theta_0$					Efficiency at $\theta_0$				
	flat	cone		Paraboloid		flat	cone		paraboloid	
	90°	30°	15°	30°	15°	90°	30°	15°	30°	15°
1	2.8	16.1	17.8	11	12.4	0.97	0.96	0.98	0.98	0.98
2	1.9	4.7	4.9	4.2	6.8	0.91	0.96	0.98	0.96	0.97
2.5	2.3	3.4	3.4	3.5	5.3	0.92	0.98	0.95	0.95	0.97
3	1.9	2.5	2.5	2.8	4.4	0.93	0.90	0.91	0.95	0.95

directivity) and reduces the angle of inclination of the main lobe of a directional pattern (Table 3).

## 7. Antenna on Pyramid Faces

Analysis shows that the characteristics of antenna located along the faces of a horizontally lying pyramid are close to the characteristics of antenna located along the surface of a horizontal circular cone or paraboloid. Increase in the arm length of such an antenna allows us to improve the electrical characteristics of the antenna compared to characteristics of flat self-complementary radiator with the same height or to reduce its height at the same characteristics. The simple shape of an antenna located along the pyramid faces compared to antennas located on the surfaces of rotation facilitates the construction of large antennas for the medium-wave range (for example, for broadcasting). It is advisable to use these antennas also in the short-wave range, especially on vehicles.

The previous sections consider flat and three-dimensional (volumetric) radiators that have a shape of self-complementary radiators but differ from them by finite dimensions. The inclined volumetric radiator of the same height can operate at lower frequencies than the vertical flat radiator. But in order to substantially reduce

the operating frequency, it is necessary to increase the antenna dimensions and to simplify the design. The metal surfaces of the antennas are usually replaced by the structures from thin wires. First of all, it is important for three-dimensional antennas. Such structures for asymmetric versions of antennas with wires located along conical and parabolic surfaces are shown, for example, in Fig. 37.

Similar structures, whose wires are located along faces of regular or irregular pyramids with a horizontal axis are presented in Fig. 38. Taking into account a mirror image in the ground, one can consider that these radiators are symmetrical. An electric radiator (dipole) consists of two flat metal cones, located along the upper and lower pyramid faces. The magnetic radiator consists of two slots located along the side faces.

To simplify the calculation of these constructions, one can replace the radiator arms from the wires by the metal plates in the shape of a flat triangles (Fig. 39). These antennas look like to self-complementary antennas, but they are differing from

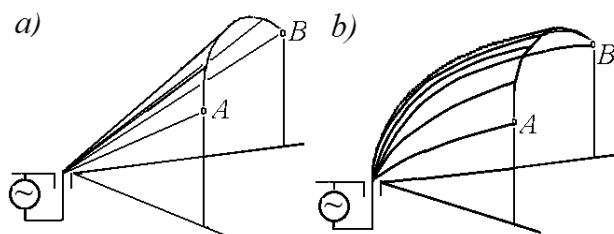


Fig. 37: Antennas with wires located on conical (a) and parabolic (b) surfaces.

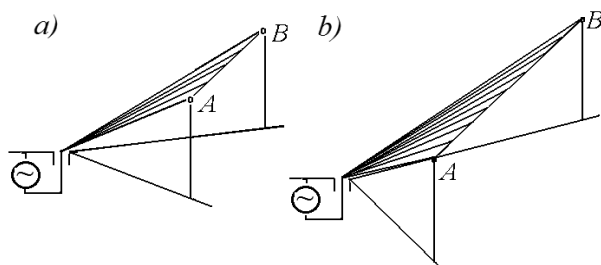


Fig. 38: Antennas with wires located along faces of a regular (a) and irregular (b) pyramids.

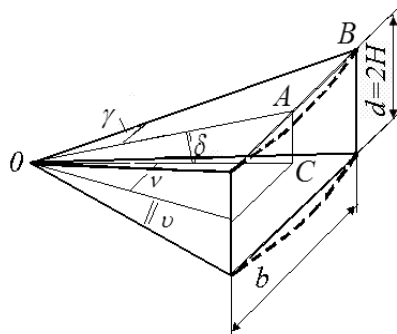


Fig. 39: An antenna from two flat triangle metal plates.

such antennas, because their surfaces do not coincide with the smooth surfaces of rotation. Such structures do not have axial symmetry. Therefore, expressions (2.75) and (2.76) in this case do not apply.

Their characteristics are close to the characteristics of volumetric self-complementary antennas. Since their electrical lengths are larger than those of flat antennas with the same height, they can be used for broadcasting at low and medium frequencies. For an approximate analysis of such antenna, primarily for calculating the wave and input impedances, one can use the proximity of their structure to the structure of an antenna located on a circular cone.

For calculating input impedances of these radiators, one can apply a method based on calculating the wave impedance of a uniform line of infinite length. As in the case of wave impedance of the earlier considered conical line with a circular cross-section, the wave impedance of the pyramid is defined by angles at its vertex. This impedance depends on the ratio of magnitudes  $b$  and  $d$  ( $b$  is the length of a triangle base and  $d$  is the distance between the plates) and does not depend on absolute values of these magnitudes. The ratio  $b/d$  is constant along a line, i.e., this long line is uniform, and its input impedance with increasing line length tends towards the wave impedance  $W$ .

Capacitance per unit length of this line in the first approximation is equal to the capacitance per unit length of a line from two metal flat cones with an angle  $2\gamma$  at the vertex, which lie in the planes located at an angle  $2\delta$  to one another [27]. A flat cone differs from a triangular plate by that the base of an isosceles triangle is replaced by an arc of a circumference with as center in point  $O$  (the boundaries of the flat cones are shown in Fig. 39 by a dotted line). In this case the capacitance  $C_l$  per unit length and the wave impedance  $W$  are calculated in accordance with (2.71), but  $k$  is equal, as is shown in [27], to

$$k = [(1 - \sin \gamma)/(1 + \sin \gamma)]^{\pi/2\delta}. \quad (2.79)$$

At that  $\tan \gamma = AB/A_0$ ,  $\sin \delta = AC/A_0$ ,  $\tan \gamma/\sin \delta = AB/AC = b/d$ . If a pyramid is regular, i.e.,  $b = d$ , then  $\tan \gamma/\sin \delta = 1$ . The wave impedance  $W$  is a function of the ratio  $b/d$  and angle  $\gamma$ . If, for example,  $b/d = 1$ , i.e., dimensions of metal and slot radiators are the same, then an increase  $\gamma$  from  $15^\circ$  to  $30^\circ$  (and correspondingly an increase  $\delta$  from  $15.5^\circ$  to  $35.3^\circ$ ) leads to an increase  $W$  from 42.3 to 45 Ohm. The input impedance of such radiators is smaller  $60\pi$ , but it does not depend on the frequency, if the pyramid length tends towards infinity.

An electric radiator (dipole) of such an antenna consists of two flat metal cones, located along an upper and lower faces of a pyramid. Its input impedance  $Z_e$  is equal to impedance of the metal radiator, which is identical to the slot in shape and dimensions. If, for example,  $b/d = 1$  and  $\gamma = 15^\circ$  (accordingly  $\delta = 15.6^\circ$ ), then  $k = 0.0467$  and  $Z_e = 42.2\pi$ . The input impedance  $Z_s$  of the magnetic radiator is equal to input impedance of the metal radiator located next to the slot. In this case  $\gamma = 15.6^\circ$  and  $\delta = 15^\circ$ , i.e.,  $k = 0.1923$  and  $Z_s = 63\pi$ . Accordingly,  $Z_e Z_s = (51.6\pi)^2$ . If  $b/d = 2$ ,  $\gamma = 30^\circ$ , then  $\delta = 45^\circ$ ,  $k = 0.111$ ,  $Z_e = 52.6\pi$ . If  $\delta = 30^\circ$ , then  $\gamma = 45^\circ$ ,  $k = 0.00505$  and  $Z_s = 28.22\pi$ , i.e.,  $Z_e Z_s = (38.5\pi)^2$ . As the calculations show, in the given case the product  $Z_e Z_s$  depends on the ratio  $b/d$ , but it is always smaller than  $(60\pi)^2$ . The smaller

angle  $\gamma$ , the closer wave impedance of the radiator located along the pyramid sides to the wave impedance of the conical radiator with the same angular width.

The electrical characteristics of symmetrical antennas located on a regular pyramid with  $\gamma = \delta = 15^\circ$  are shown by solid curves in Figs. 40 to 42, and in Table 4, depending on the ratio  $\lambda/H$ , where  $\lambda$  is the wavelength,  $H$  is the antenna height. Each antenna arm was modeled as a thin triangular metal sheet with a height  $H$  and a thickness  $0.01H$ . The gap between the arms at the pyramid vertex was  $0.01H$ . The antenna characteristics are calculated by means of the CST program. The active and reactive components of the input impedance for the antenna located along the sides of a regular pyramid with an angle  $30^\circ$  at the vertex are shown in Fig. 40. Reflectivity and standing wave ratio (*SWR*) in cables with wave impedance  $W_c = 60\pi$  (a) and 100 Ohm (b) are shown in Fig. 41 and 42 respectively.

These figures show also the analogical characteristics for a conical antenna with the same angle at the vertex. One can see that the characteristics of these antennas are similar, but not identical. Here also results of measuring an antenna mock-up located on the pyramid are given. They confirm the calculations.

The electrical characteristics of an antenna located along the faces of an irregular pyramid are shown in Figs. 43 to 45 and in Table 4. The pyramid has a rectangular cross-section. An angular width of a metal and a slot radiator is  $60^\circ$  and  $30^\circ$  respectively. For comparison, in these figures the characteristics of an antenna located on a pyramid with a square cross section are given. It can be seen from Fig. 43 that *SWR* of an antenna located on an irregular pyramid is larger when using a coaxial cable with a wave impedance  $W_c = 60\pi$  Ohm and is less when  $W_c = 100$  Ohm.

The results of these calculations show that properties of self-complementary radiators are not always preferable in comparison to properties of radiators with similar dimensions. As can be seen from Fig. 43, an increase of the angular width of the metal radiator increases the current along it and reduces active and reactive component of the input impedance, hence approximating its value to a wave impedance of a standard cable. If an asymmetric antenna uses a special cable with a wave impedance  $W_c = 30\pi = 94$  Ohm, then at the main frequency the antenna located on the regular pyramid will be better matched to the cable. If a standard cable with  $W_c = 50$  Ohm is used, an asymmetric antenna located along the faces of an irregular pyramid is better matched.

This result is easily explained. As is shown in Section 6, the wave impedance of the radiator located along the pyramid sides can be calculated in accordance with (2.71). On the other hand, this expression allows us to determinate an angular width of an antenna, which provides optimum matching with a cable at a given wave impedance of a cable and a known vertical angle on a pyramid vertex. For example, if the cable wave impedance is 100 Ohm (in the case of symmetrical antenna) and it is necessary to obtain the same magnitude of the antenna wave impedance, in accordance with the mentioned formula, the following relation must be fulfilled:

$$\frac{K(\sqrt{1-k^2})}{K(k)} = \frac{120\pi}{100} = 3.770.$$

Function  $K(k)$  for small values of an argument  $k$  is close to the value 1.57, i.e.,  $k(\sqrt{1-k^2}) = 5.919$ . From the tables we find that  $\sqrt{1-k^2} = 89.383^\circ$ , and  $k = 0.01196$ .

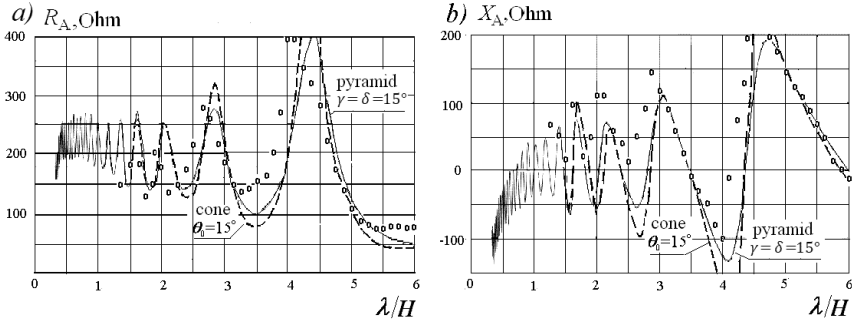


**Fig. 40:** Input impedance of an antenna, located on a regular pyramid, and a conical antenna depending on the ratio  $\lambda/H$ .

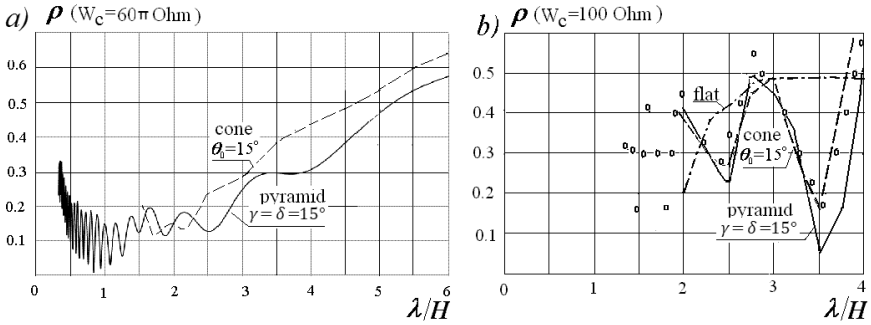


**Fig. 41:** Reflectivity of an antenna, located on regular pyramid, and of a conical antenna in a cable with a wave impedance of  $60\pi$  (a) and 100 Ohm (b).

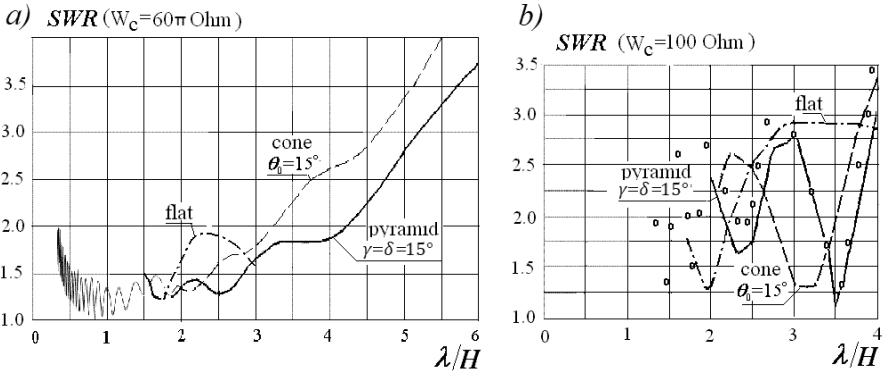


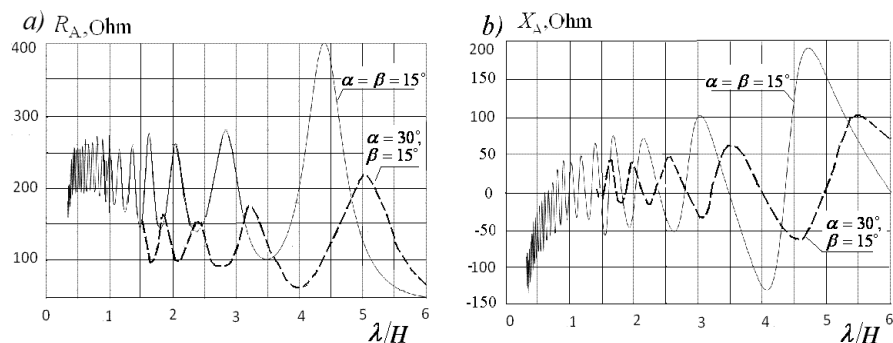
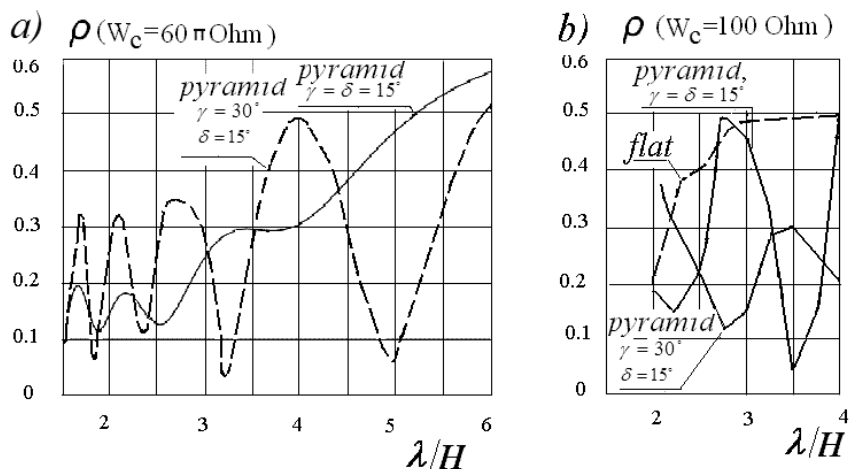
**Fig. 42:** Standing wave ratio of an antenna, located on regular pyramid, and of a conical antenna in a cable with a wave impedance of  $60\pi$  Ohm (a) and 100 Ohm (b).

If, for example,  $\delta = 15^\circ$ , then from (2.71)  $\gamma = 20.7^\circ$ . Similarly, in order to match a conic self-complementary antenna with a standard cable, whose wave impedance is smaller than the antenna wave impedance, one must increase the angular width of the metal radiator.



**Table 4:** Gain and Efficiency of Symmetrical Antennas, located on Pyramid Faces

$\lambda/H$	Gain		Efficiency	
	$\gamma = \delta = 15^\circ$	$\gamma = 30^\circ, \delta = 15^\circ$	$\gamma = \delta = 15^\circ$	$\gamma = 30^\circ, \delta = 15^\circ$
1	23.3	17.6	0.97	0.98
2	6.56	10.2	0.98	0.95
2,5	5.21	6.87	0.98	0.95
4	4.08	5.5	0.93	0.94

**Fig. 43:** Input impedance of antennas, located on a regular ( $\gamma = \delta = 15^\circ$ ) and irregular ( $\gamma = 30^\circ, \delta = 15^\circ$ ) pyramid.**Fig. 44:** Reflectivity of antennas, located on a regular ( $\gamma = \delta = 15^\circ$ ) and irregular ( $\gamma = 30^\circ, \delta = 15^\circ$ ) pyramid, in cables with wave impedance  $W_c = 60\pi$  (a) and  $W_c = 100$  Ohm (b).

The typical characteristics of conic self-complementary antennas and of antennas, located on the pyramid faces, are presented in figures. In Fig. 46 the calculated curves and experimental values (circles) of  $R_A$  and  $X_A$  are given for conic antennas with different angles  $2\theta_0$ . In Fig. 47  $SWR$  of the conic and flat antennas are compared with each other, and it is demonstrated advantage of the conic antennas. In Fig. 48 pattern factors are presented for symmetrical antennas located along the

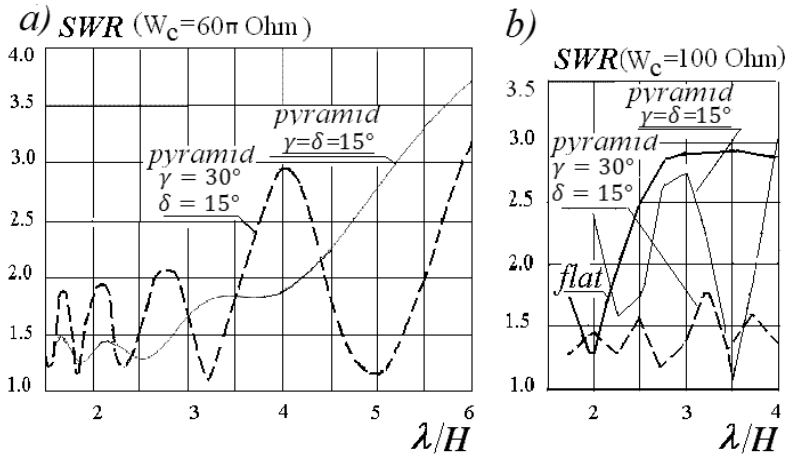


Fig. 45: SWR of antennas, located on a regular ( $\gamma = \delta = 15^\circ$ ) and irregular ( $\gamma = 30^\circ$ ,  $\delta = 15^\circ$ ) pyramid, in cables with wave impedance  $W_c = 60\pi$  (a) and  $W_c = 100 \text{ Ohm}$  (b).

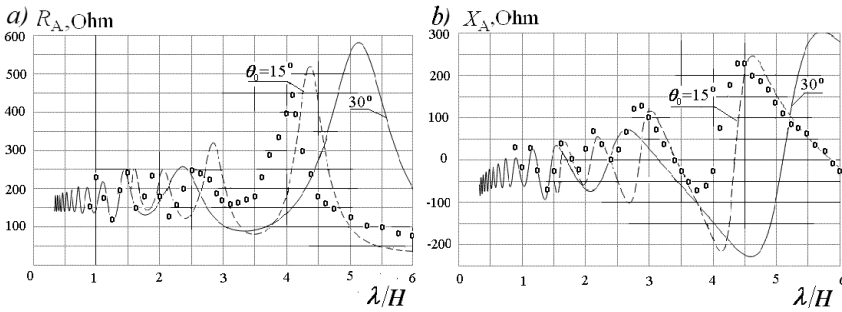


Fig. 46: Active (a) and reactive (b) components of input impedances of a symmetrical conic antennas with the angle  $60^\circ$  and  $30^\circ$  at vertex.

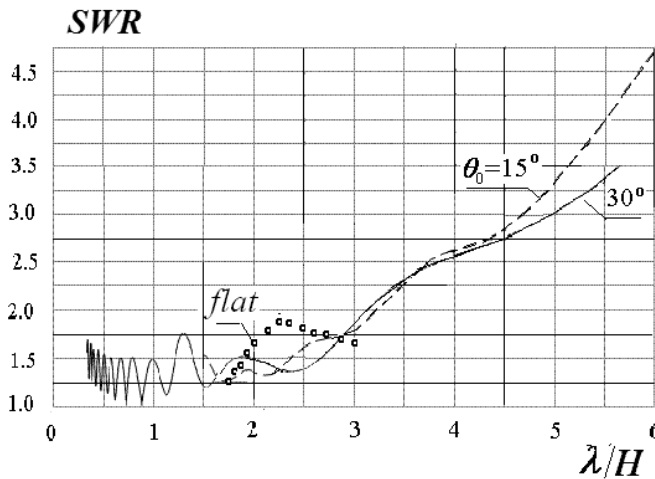


Fig. 47: Standing wave ratio of a symmetrical conic antennas with an angle  $60^\circ$  and  $30^\circ$  at vertex.

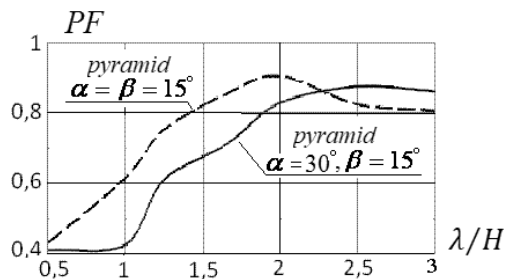


Fig. 48: Pattern factors of the symmetrical antennas located on the pyramid faces.

faces of regular and irregular pyramid (in this case within the angular sector from  $60^\circ$  to  $90^\circ$ ). The results of the calculation were checked on mock-ups placed in an anechoic chamber.

## 8. Self-complementary Antennas with Rotational Symmetry

Antennas with rotational symmetry are a most complex variant of self-complementary antennas. They consist of several metal radiators and the same number of slots. Two antennas with rotational symmetry are shown in Fig. 49. Both antennas have finite dimensions. Each antenna consists of four symmetrical radiators of the same size and shape: two metallic and two slots. In the first antenna (Fig. 49a) the arm of each radiator has a shape of a flat cone. This is a circular sector, the left and right sides of which coincide with the radii and the base with the outer boundary of the structure. In the second antenna (Fig. 49b), the boundaries of the radiators do not coincide with radii. The radiators have a log-periodic structure. Antennas with radiators in a shape of flat cones are simpler and their properties will be considered depending on the number of cones and variants of connecting the antenna to a generator or a cable. The properties of an antenna shown in Fig. 50b are similar, although there are additional details.

Let's consider variants of antennas with different numbers of symmetrical metal radiators (dipoles). Antennas with one metal dipole are presented in Fig. 50. They have different widths depending on the angle at the flat cone vertex:  $135^\circ$  (a),  $90^\circ$  (b),  $45^\circ$  (c),  $22.5^\circ$  (d). Antennas with two metal dipoles are given in Fig. 51. They differ from each other by a circuit of connection with the generator poles. The cones connected with each other by a thin line are connected to the same pole: adjacent cones in variant a are connected; one cone in variant b is connected with the other cone bypassing the third cone; three cones in variant c are connected with one pole and the fourth cone is connected with another pole. The properties of diverse variants are different. In Fig. 52 different circuits of connection to the generator are demonstrated for an antenna with four metal dipoles.

The main parameters of the considered antenna variants are given in Table 5. These are angle  $\theta_0$  between the axes of metal dipoles, the angular half-width  $\alpha$  of a metal dipole and the angular half-width  $\beta$  of a slot (it is equal to  $\beta = \theta_0/2 - \alpha$ ). The table gives the numbers of Figures for different antennas, the ratio  $C_l$  of the capacitance per unit length of each antenna to the absolute permittivity of the air,

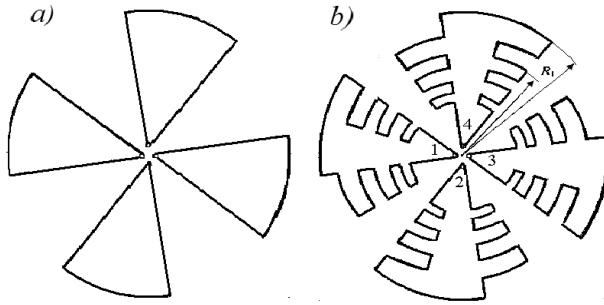


Fig. 49: Antennas from flat conic (a) and log-periodic (b) metal plates.

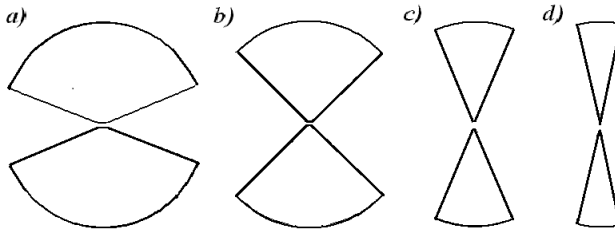


Fig. 50: Flat antennas with one metal radiator.

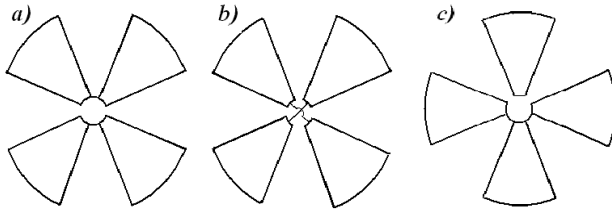


Fig. 51: Flat antennas with two metal radiators.

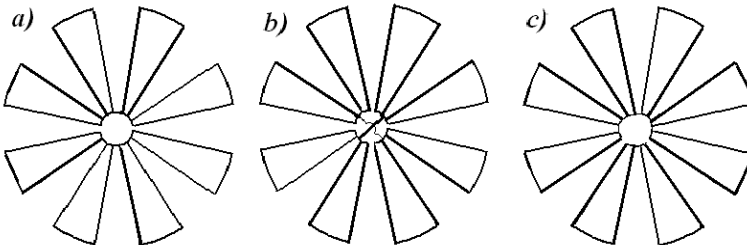


Fig. 52: Flat antennas with four metal radiators.

and the antenna wave impedance  $W_1$ . The magnitude  $W_2$  is the wave impedance of a three-dimensional antenna. About this, see further.

From this table it follows that the input impedance of each antenna variant is constant in the first approximation, i.e., the current distribution along the antenna is close to the current distribution along an equivalent long line. As already said, the input impedance of a uniform line without losses with increasing its length tends

**Table 5:** Parameters and Wave Impedances of Antennas with Rotation Symmetry.

Dipoles number	Fig.	$\theta_0$	$\alpha$	$\beta$	$C_l/\varepsilon_0$	$W_1$	$W_2$
1	2.50a	180°	67.5°	22.5°	2.94	$40.8\pi$	$40.8\pi$
	2.50b	180°	45°	45°	2	$60\pi$	$60\pi$
	2.50c	180°	22.5°	67.5°	1.35	$88.7\pi$	$88.7\pi$
	2.50d	90°	11.25°	78.75°	1.04	$115.4\pi$	
2	2.51a	90°	22.5°	22.5°	4	$17.8\pi$	$20.4\pi$
	2.51b	90°	22.5°	22.5°	8	$15\pi$	$19\pi$
	2.51c	90°	22.5°	22.5°	5.35	$22.4\pi$	$26.5\pi$
4	2.52a	45°	11.25°	11.25°	12	$9.9\pi$	$8.4\pi$
	2.52b	45°	11.25°	11.25°	24	$7.5\pi$	$9.1\pi$
	2.52c	45°	11.25°	11.25°	13.04	$10.6\pi$	$10.6\pi$

towards its wave impedance. Similarly, the input impedance of the studied flat antenna changes: as the length of each antenna arm increases, its input impedance tends towards its wave impedance. If the antenna has a self-complementary structure, then its wave impedance is equal to  $60\pi$ . As its length increases, the input impedance of the antenna tends towards  $60\pi$  in accordance with expression (2.69).

In Fig. 53 curves show active and reactive components of input impedances for three antennas. They demonstrate how, with decreasing  $\lambda/L$  ( $\lambda$  is a wavelength,  $L$  is an arm length of an antenna), the value  $X_A$  approaches to zero and  $R_A$  to the wave impedance. Option 1 in Fig. 53 corresponds to an antenna with one metal radiator, option 2 corresponds to an antenna with two such radiators, and each pole of the generator is connected to two adjacent plates. Option 3 corresponds to the same antenna when the plates are connected to the generator pole bypassing the third plate.

As can be seen from Fig. 53, the input characteristics of antennas consisting of metal and slot radiators of the same shape and dimensions, if these antennas are located on a small metal sheet, are far from the characteristics of self-complementary antennas. The input impedance of the antenna shown in Fig. 29a slowly converges to the results, promised by expression (2.69). Similar results are obtained, if to compare input impedances of small-sized antennas with the values given in Table 5. The obvious closeness of the indicated magnitudes occurs when the structure dimensions are comparable with the wavelength. As an example, one can present results of using antennas with a single metal radiator in the high-frequency antenna array [32]. In these antennas, triangular metal surfaces are replaced by wires that diverge from a feed point—a triangle vertex (Fig. 29b). Each plate is replaced by five wires. The antenna size depends on the width of the frequency range: the wider the range, the longer the necessary length  $H$  of the antenna arm. Let the required level of traveling-wave ratio ( $TWR$ ) in the cable be greater than 0.6, and the frequency overlap ratio is equal to  $k_f = 2$ . In that case an arm length  $H$  on the upper  $f_1$ , lower  $f_2$  and central  $f_3 = \sqrt{f_1 f_2}$  frequency of a range is equal to  $0.3\lambda$ ,  $0.6\lambda$  and  $0.42\lambda$ . If  $k_f = 10$ , the arm length at similar frequencies is  $0.5\lambda$ ,  $5\lambda$  and  $1.6\lambda$ . At the same time, multi-stepped transformers were used in the feed lines of antenna array, which ensure the required level of

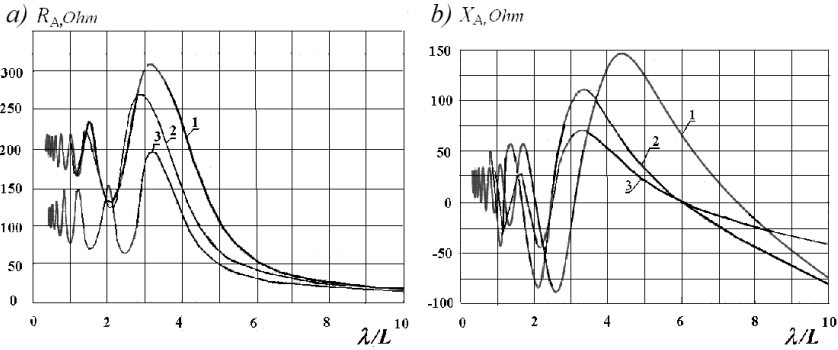


Fig. 53: Active (a) and reactive (b) components of an input impedances of flat antennas.

matching. This significantly alleviates the problem of selecting the wave impedances of feed lines.

As can be seen from the table, the described antennas have very different wave impedances, including small ones. Proximity of wave impedances of antennas and cables is a necessary condition for the antennas' efficiency. Known antenna variants do not satisfy this condition, since their wave impedances often are substantially greater than the wave impedances of standard cables. Small wave impedances of new radiators should facilitate the task of matching and expanding the use of self-complementary antennas.

In asymmetric structures, where the metal dipoles forming an antenna are replaced by monopoles located above the conducting surface (ground), the wave impedance is half as many. In Fig. 54 the circuits of connecting monopoles with generators are given. They are like to the circuits of connecting dipoles shown in Fig. 51a and 51c.

The method of calculating a simple self-complementary antenna with a single metal radiator was proposed by Carrel [27]. It is based on the conformal transformation of geometric figures. Transformation on a plane is called by conformal, if as a result of it the angles between any two intersecting lines remain unchanged and the lengths of all infinitesimal segments passing through a given point of the plane change by the same number of times. Under such a transformation, the capacitance preserves its magnitude. The method of conformal transformations in particular is used for calculating the capacitance of a system of wires by means of replacing the original structure with a structure whose capacitance is known.

Before applying this method, it is necessary to reduce the problem to a flat task. This problem is simplified if to move from a spherical coordinate system to a cylindrical one. When the coordinate system is changed in accordance with the uniqueness theorem, Laplace's equation must remain valid. As shown in [27], this condition is satisfied, if in transition from a spherical coordinate system to a cylindrical one the replaced variables are related by the equalities::

$$\rho = \tan(\theta/2), \varphi_c = \varphi, \quad (2.80)$$

where  $\rho$  and  $\varphi_c$  are cylindrical coordinates,  $\theta$  and  $\varphi$  are spherical ones.

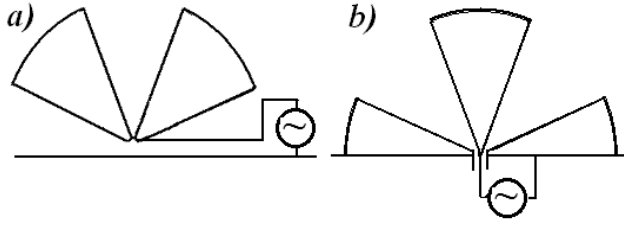


**Fig. 54:** Connecting asymmetric antennas to a generator.

The structure, described in [27], in the shape of two arms, is shown in Fig. 55a. As a result of coordinate system's transformation in accordance with (2.80), each radial line becomes a point and the entire structure is transformed into two identical 'cuts' in the form of two segments of horizontal line (see Fig. 55b). Further the Schwarz-Christoffel's transform maps this structure on to a rectangle, whose two opposite vertical sides are plates of a flat capacitor having an infinite width. Capacitance of a capacitor per unit width is equal to

$$C_l = \varepsilon_0 K(\sqrt{1-k^2})/K(k), \quad (2.81)$$

where  $\varepsilon_0 = 10^{-9}/(36\pi)$  is the absolute permittivity of the surrounding medium,  $K(k)$  and  $K(\sqrt{1-k^2})$  are complete elliptic integrals of the first kind from arguments  $k$  and  $\sqrt{1-k^2}$ , and  $k$  is equal to

$$k = \frac{\sin(\theta_0/2) - \sin \alpha}{\sin(\theta_0/2) + \sin \alpha}. \quad (2.82)$$

If the axial lines of arms (see Fig. 55a) coincide, then

$$k = (1 - \sin \alpha)/(1 + \sin \alpha). \quad (2.83)$$

The basic variant described in [27] is identical to the variant shown in Fig. 29b, where  $\alpha = \beta = \frac{\pi}{4}$ . In this case  $k = 0.1716$ ,  $K(k) = 0.5K(\sqrt{1-k^2})$ , i.e., according to (2.82), the capacitance of capacitor per unit width is equal to  $C_l = 2\varepsilon_0$ , and the antenna impedance is

$$W = 120\pi K(k)/K(\sqrt{1-k^2}) = 120\pi\varepsilon_0/C_l, \quad (2.84)$$

i.e.,  $W = 60\pi$ .

In the case of two metal radiators (Fig. 56a) let us go in accordance with the conditions (2.80) from the spherical to the cylindrical coordinate system (Fig. 56b). As a transition results, the  $n$ -th radial line (the line numbers are indicated with Arabic numerals) transforms to the point with the coordinate  $\rho_n$ . The point numbers coincide with the line numbers. The general expression for the magnitude  $\rho_n$  has the form

$$\rho_n = \tan \{0.5[(2m-1)\theta_0/2 \pm \alpha]\}, \quad (2.85)$$

where  $m = 1, 2, \dots$ . The sign  $-$  refers to the odd, and the sign  $+$  to the even values of  $n$ . Since  $\alpha = \beta = \frac{\pi}{8}$ , i.e., the slot and cone have the same width, then  $\rho_n = \tan [(2n-1)\alpha/2]$ .

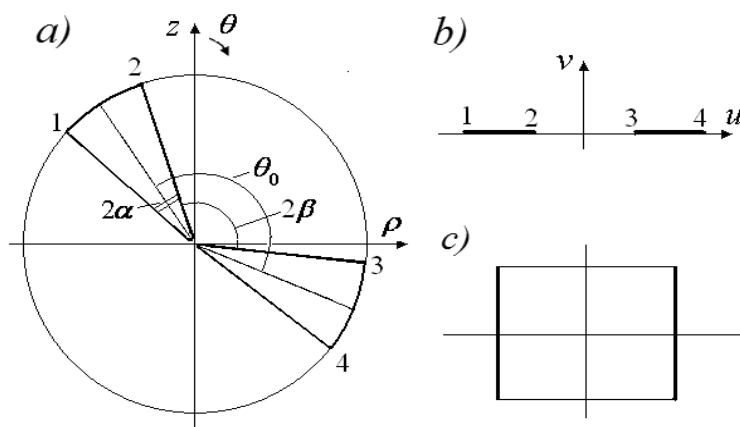


Fig. 55: Radiator of two flat metal cones (a), transition to two 'slits' (b), Schwarz-Christoffel's transformation (c).

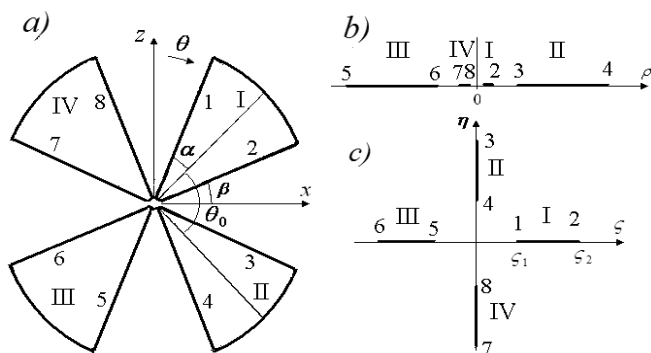


Fig. 56: Flat antenna of two metal radiators (a), transition to the cylindrical (b) and rectangular (c) coordinate system.

The general view of the transformed structure is given in Fig. 56b. This is a horizontal line with four slots ('cuts') connecting points with numbers  $2n - 1$  and  $2n$ .

As can be seen from the above, the described method allows to solve the problem for a metal radiator of arbitrary angular width with arbitrary angles between the axial lines of the arms. But in the case of two metal radiators, the described technique leads to four straight slits, in the case of  $N$  dipoles, to  $2N$  slits. This makes possible to calculate several capacitances, but it does not allow bringing them together into one capacitance. Besides that, Fig. 56b does not consider the relative position of elements. Therefore, in order to consider such a structure of several metal radiators, it is necessary to transit to rectangular coordinate system (Fig. 2.56c). For this aim, one can use the expression

$$\xi_n = \sqrt{\tan(2 \tan^{-1} \rho_n)}. \quad (2.86)$$



The antenna consists of four identical flat metal cones evenly spaced along the circumference, i.e., separated by the same slots. The slot's numbers are shown in the figure in Roman numerals. The total angular width of the cone and the adjacent slot is equal to  $\theta_0 = 2(\alpha + \beta) = \pi/2$ . In accordance with (2.86) other  $\zeta_1 = 0.6436$ ,  $\zeta_2 = 1.5538$ , other coordinates are similar.

As already mentioned, the generator poles can be connected to different elements. In Fig. 57 there are three connection options. The cones connected with each other by a thin line are connected to the same pole of the generator. One pole is marked with a sign '+', the other with a sign '-'. In the first option (Fig. 57a) two neighboring metal cones are connected to each pole, in the second option (Fig. 57b) the cones are connected to each pole bypassing a third cone. In the third option (Fig. 57c), three cones are connected to one pole and one cone to another pole.

The dashed line in Fig. 57a is the symmetry axis of the structure. This is zero potential line. The capacitance between the poles on both sides of the line consists of two pairs of different capacitances. The capacitances of the first pair are formed by flat cones with coincident axes. They are calculated in accordance with expressions (2.83) and (2.81), and each one is equal to  $C_{11} = 1.36\epsilon_0$ . Capacitances of the second pair are capacitances between the cones with mutually perpendicular axes. As shown in [28], the value of such capacitance can be obtained by means of a quadrant shown in Fig. 58a. This value is twice as large as calculated by formula (2.81), if  $k$  is equal to

$$k = \sqrt{\frac{(a^2 + c^2)(b^2 + d^2)}{(a^2 + d^2)(b^2 + c^2)}}.$$

Here  $a, b, c, d$  are the coordinates of the slots' ends in Fig. 58a. In our case  $a = c$ ,  $b = d$ , i.e.,

$$k = 2ab/(a^2 + b^2). \quad (2.87)$$

In accordance with (2.86) and (2.87)  $a = \zeta_1$ ,  $b = \zeta_2$ ,  $k = 0.7071$ , i.e.,  $K(k) = K(\sqrt{1 - k^2}) = 1.8541$ , and the capacitance between the cones with mutually perpendicular axes (see Fig. 58a) is equal to  $C_{12} = 2\epsilon_0$ . The total input capacitance of the first antenna variant is  $C_1 = 2(C_{11} + C_{12})_{\epsilon_0} = 6.73\epsilon_0$ .

It is not difficult to be convinced that in the second variant of connecting metal cones with the generator poles, the capacitance consists of four elements  $C_{12}$ , i.e.,  $C_2 = 8\epsilon_0$ . Thus, the wave impedances of the first and second variants are  $17.8\pi$  and  $15\pi$  respectively. In the third variant, the capacitance between one metal cone and three others consists of two parts. The first of these is the capacitance between a single cone and two side ones of the three. It is equal, as is not hard to see,  $C_{31} = 4\epsilon_0$ . The capacitance between two identical radiators is equal to  $C_{11} = 1.36\epsilon_0$ , i.e., the total capacitance is  $C_3 = 5.36\epsilon_0$ , and the wave impedance is  $W = 22.4\pi$ .

As already said, proximity of wave impedances of antennas and cables is a necessary condition for the antennas' efficiency. To accomplish this condition, one must change the width of metal radiators. In the case of a first option of connecting four metal plates with the generator, if use the structure with  $\alpha = 14^\circ$  and  $\beta = 31^\circ$ , then, as calculations show,  $W = 32\pi$ . The wave impedances of a similar asymmetric antenna shown in Fig. 54a is equal to  $W \approx 16\pi \approx 50 \text{ Ohm}$ .

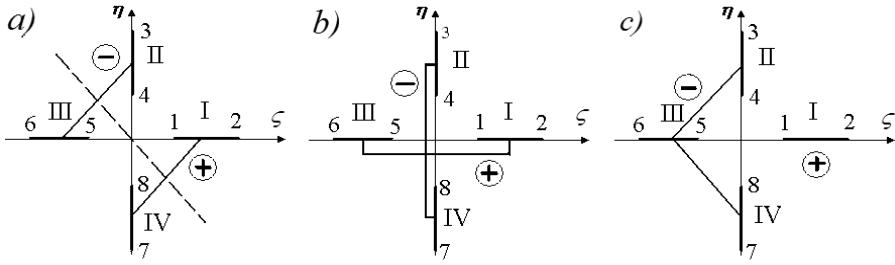


**Fig. 57:** Three options of antenna connection to generator poles: two neighboring cones (a) and two cones through one (b) are connected to each pole, three cones are connected to first pole and one to second (c).

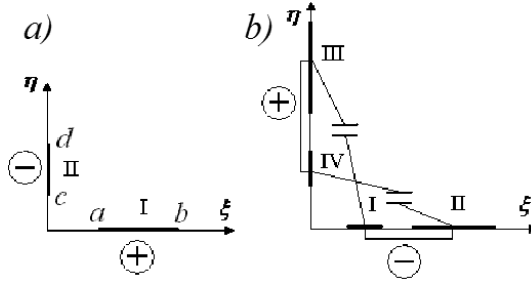


**Fig. 58:** Quadrants for calculating capacitance of antennas with two (a) and four (b) dipoles.

Calculating wave impedances of antennas from four metal radiators can be carried out in a similar manner. As shown in Fig. 52, there are three possible options for connecting flat cones to the poles of the generator. In the first variant of connection, the total capacitance consists of four capacitances  $C_{11} = 1.04 \varepsilon_0$  (each capacitance is formed by flat cones with coincident axes, cone width is  $22.5^\circ$ ) and four capacitances  $C_{12} = 2\varepsilon_0$  (each capacitance is formed by flat cones with mutually perpendicular axes, located in two quadrants with two capacitances in either quadrant, see Fig. 58b). The total capacitance is  $C_1 = 12.2 \varepsilon_0$ , the wave impedance is  $W = 9.9 \pi$ . In the second variant the total capacitance consists of eight capacitances  $C_{12} = 2\varepsilon_0$  between flat cones with mutually perpendicular axes, located in four mentioned quadrants. The total capacitance is  $C_2 = 16\varepsilon_0$ , the wave impedance is  $W = 7.5 \pi$ . In the third variant, the capacitance  $C_3$  consists of two capacitances  $C_{11}$ , two capacitances  $C_{12}$  and four capacitances between flat cones, located at different angles to each other; total  $C_3 = 11 \varepsilon_0$ . The wave impedance is  $W = 10.6 \pi$ .

A step forward with respect to simple vertical antennas in the form of a flat metal dipole with a plate of angular width equal to a slot angular width was made as a result of creating the flat self-complementary antennas with rotation symmetry. They are located in a vertical plane and an axis of their circular symmetry coincides with a perpendicular to this plane, i.e., it is horizontal. Another step forward is the development of three-dimensional (volumetric) antennas. Their appearance became possible when it was proved that the antenna based on the complementarity principle can be placed not only on the plane, but also on the surface of rotation; for example, on the surface of a circular cone or paraboloid located around the horizontal axis.

Comparison of conic and cylindrical problems in [27]) showed that one problem reduces to another, if replaced variables satisfy conditions (2.80) that were

formulated for conic and cylindrical coordinate systems with the coincident vertical axes. Comparison of these problems shows [30] that their equivalence takes place, if the variables satisfy the conditions

$$\rho = \sigma, \varphi_c = \varphi, \quad (2.88)$$

where  $\rho$  and  $\varphi_c$  are cylindrical coordinates,  $\sigma$  and  $\varphi$  are parabolic. In the conic problem (Fig. 59a) an exciting emf is located at a cone vertex and radiator arms are located along its surface. Boundaries of each arm coincide with cone generatrices. Angular dimensions of the arcs along the aperture, which correspond to the metal radiator and the slot, are designated as  $2\alpha$  and  $2\beta$ . A paraboloid (Fig. 59b) has a similar shape of an aperture.

A rigorous analysis (see [26]) shows that input impedances of metal and slot radiators located on an infinite circular cone or paraboloid related to each other by the expression (2.68). For  $\alpha = \beta$ , the expression (2.69) is valid. This is natural, since their structure can be considered as two-wire long lines, and these lines are uniform, i.e., in this respect, they do not differ from the corresponding line located on the surface of a circular cylinder with a constant radius of cross section. Therefore, if  $\alpha = \beta$ , then the expressions (2.81), (2.83) and (2.84) are valid for conical and similar parabolic antennas. If  $\alpha \neq \beta$ , then  $k$  is calculated in accordance with (2.82).

As shown in Section 6, the conic structure with one symmetrical slot has properties similar to a flat structure with a similar slot. In general case the relation analogous to expression (2.69) is true for a volumetric structure with arbitrary number of symmetrical slots, located at a circular metal cone or paraboloid of infinite length and excited on its vertex.

In conical problem not only axes of different cones coincide with a common symmetry axis, but the vertexes of these cones also coincide with each other. Unlike this, in the parabolic problem, the vertexes of different paraboloids are shifted along the common axis, so that each paraboloid is located separately. Capacitance per unit length measured along the axis of the cone and paraboloid, and also wave impedance of each antenna, are determined by the same formulas. But, if the apertures of the cone and the paraboloid are identical, i.e., their heights are equal to each other, the length of a parabolic generatrix is more than the length of a conic generatrix and accordingly, an effective height of the parabolic antenna is more. And, of course, effective heights and side lengths of both volumetric antennas are much more than

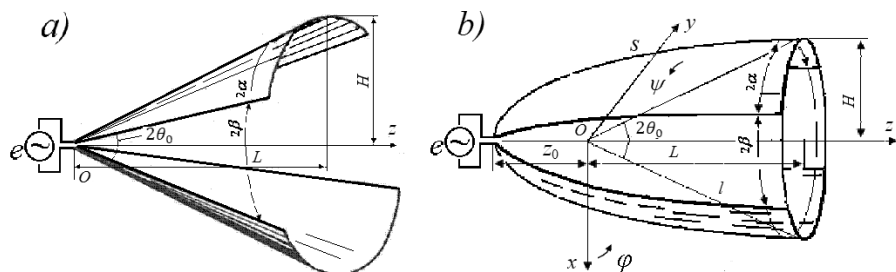


Fig. 59: Volumetric antennas on cone (a) and paraboloid (b).

the effective height and the side boundary length of the flat antenna with the same geometric height. Therefore, they have for a given frequency and height the higher effectiveness in comparison with a flat antenna.

In Fig. 35 and 36 reflectivity  $\rho$  and  $SWR$  of symmetrical antennas located along surfaces of the circular paraboloid, the circular cone and the vertical flat antenna are presented. The angle  $2\theta_0$  at cone vertex and the angle  $2\theta_0$  between opposite focal radius-vectors of the paraboloid are equal to  $30^\circ$ . The wave impedances of cables are equal to  $60 \pi$  Ohm. These graphs allow comparison of electrical characteristics of antennas with each other. They confirm the advantage of parabolic and conic antennas over flat antenna in a predetermined frequency range.

Three-dimensional antennas, as well as flat antennas, can consist of several metal and slot radiators connected in parallel to each other. They can also be named antennas with rotational symmetry. An example of such conical antenna is given in Fig. 60a. This antenna, as well as a flat antenna, shown in Fig. 49a, consists of two metal dipoles. When calculating its characteristics, we go, first, to the plane problem using, conditions (2.70). Since all points of each its generatrix are located at the same angle  $\theta$  to the axis  $z$ , in consequence of the transformation they will fall into a common point and the metal plate will become a section of the circumference (Fig. 61b). If the plates have the same width and are separated by slots of the same width, then the coordinates of the initial  $(x_{m1}, y_{m1})$  and final  $(x_{m2}, y_{m2})$  points of these sections are determined by the expressions

$$x_{m1(2)} = \rho \cos \varphi_{m1(2)}, \quad y_{m1(2)} = \rho \sin \varphi_{m1(2)}, \quad (2.89)$$

where in accordance with (2.80) the quantity  $\rho$  is  $\rho = \tan(\theta/2)$  ( $\theta/2$  is half angle at the cone vertex) and  $\varphi_m$  is the angle  $\varphi$  measured along the circumference from the axis  $x$  to the point  $m$ . It is equal to  $\varphi_m = (2m - 1) \varphi_0/2 \pm \alpha$ , where magnitudes of angles  $\varphi_0$  and  $\alpha$  are clear from Fig. 60, signs ‘-’ and ‘+’ correspond to the beginning and end of the segment.

As in the case of similar flat antennas, three options are possible for connecting different antenna elements to the generator poles (Fig. 61). The plates connected to each other by a thin line are connected to the same generator pole. One pole is marked with a sign ‘+’, the other with a sign ‘-’. In the first (Fig. 61a) and the second (Fig. 61b) option, two metal plates are connected to each pole: in the first case they are neighboring plates, in the second, the plates are connected bypassing a third plate. In the third option (Fig. 61c) one plate is connected to one pole, and three plates to other one.

The axis  $x$  in Fig. 61a and 61b is the axis of system symmetry. This is zero potential line. An antenna capacitance between the poles with both sides of the line consist of two pairs of different capacitances. The capacitances of first pair are formed by sections of a circumference (arcs) with coinciding symmetry axes (see Fig. 61). They are calculated in accordance with (2.83) and (2.81), and capacitance is equal to  $C_{11} = 1.364\epsilon_0$ .

The capacitances of second pair are capacitances between arcs located in neighboring quadrants (Fig. 60c). Each arc is the circumference segment of a radius  $\rho$ . If to introduce the function  $z = x + jy$ , where  $x = \rho \cos \varphi$ ,  $y = j\rho \sin \varphi$ , then  $z$  at each

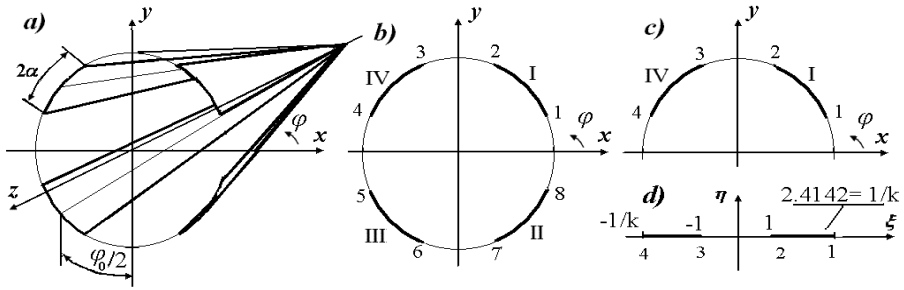


**Fig. 60:** Conical antenna with two metal radiators: a – general form, b – transition to a plane problem, c – symmetry division, d – conformal mapping.

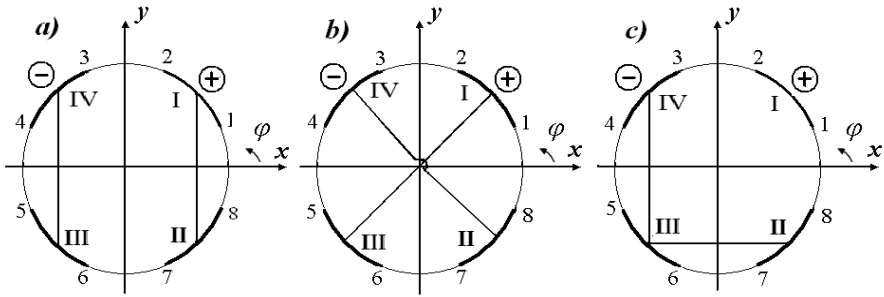


**Fig. 61:** Three options of connecting the antenna to the generator poles.

point of the arc is equal to  $z = \rho (\cos \varphi + j \sin \varphi)$ . Let angular widths of a metal plate and a slot be same. Then arc I is located between points with coordinates  $x_1 = \rho \cos \varphi_1$ ,  $y_1 = j\rho \sin \varphi_1$  and  $x_2 = \rho \cos \varphi_2$ ,  $y_2 = j\rho \sin \varphi_2$ , where  $\varphi_1 = 22.5^\circ$ ,  $\varphi_2 = 67.5^\circ$ . Using conformal mapping in the form

$$\zeta = jz/\rho + \rho/(jz), \quad (2.90)$$

where  $\zeta = \xi + j\eta$ ,  $z = x + jy$ , we obtain

$$\zeta = j(\cos \varphi + j \sin \varphi) - j/(\cos \varphi + j \sin \varphi) = 2 \sin \varphi, \quad (2.91)$$

i.e., in the plane  $\zeta$  the arc section becomes the axis segment between the points  $\xi_1 = 2 \sin \varphi_1 = 0.765$  and  $\xi_2 = 2 \sin \varphi_2 = 1.848$  (Fig. 60d). Similarly, the second arc section is transformed and becomes the segment between points 3 and 4. Dividing the points coordinates to  $\xi_2$ , we obtain the values given in Fig. 60d, from which it follows that in this case  $k = 0.41$ . Using the Schwarz-Christoffel's mapping, we find, in accordance with (2.88), that the capacitance of a structure shown in Fig. 58c is equal to  $C_{12} = 1.583\varepsilon_0$ .

Accordingly, the total antenna capacitance for the first variant of its connection to the generator poles is equal to  $C_1 = 2C_{11} + 2C_{12} = 5.9 \varepsilon_0$  and the wave impedance is  $W = 20.4 \pi \text{ Ohm}$ .

The capacitance of the second antenna variant consists of four capacitances  $C_{12}$  between arcs located in neighboring quadrants (Fig. 61b) and is equal to  $C_2 = 6.3\varepsilon_0$ .

This means that the wave impedance of the second variant is  $W = 19 \pi \text{ Ohm}$ . In the third variant, the capacitance between one arc and three others consists of two parts. The first part is the capacitance between a single arc and two side arcs. As is not hard to be convinced, it is equal to  $2 C_{12} = 3.17 \varepsilon_0$ . The capacitance between two arcs with coinciding axes is equal to  $C_{11} = 1.364 \varepsilon_0$ , i.e., the total power is equal to  $C_3 = 4.53 \varepsilon_0$  and the wave impedance is  $W = 26.5 \pi \text{ Ohm}$ .

Calculation of wave impedances of antennas from four metal radiators can be performed in a similar way. As shown in Fig. 52, here one can also separate three main options of connecting boards to the generator poles. In the first and second connection option, the capacitances of four pairs of arcs with coinciding symmetry axes are included in full capacitance (each capacitance is equal to  $C_{11} = 1.04 \varepsilon_0$ ), in the third variant it is necessary to take into account the capacitances of two such pairs. The calculation is complicated by the need to take into account mutual capacitances not only between neighboring, but also remote arcs. This circumstance can be considered by increasing the angles  $\varphi_1$  and  $\varphi_2$  respectively, but this solution has an approximate character.

The calculation gives the following results. The total capacitance of the first connection variant is equal to  $C_1 = 14.3 \varepsilon_0$ , the second— $C_2 = 13.2 \varepsilon_0$ , the third— $C_3 = 11.3 \varepsilon_0$ . The wave impedance of the first variant is  $W = 8.4 \pi \text{ Ohm}$ , of the second— $W = 9.1 \pi \text{ Ohm}$  and of the third— $W = 10.6 \pi \text{ Ohm}$ . The wave impedances  $W_2$  of three-dimensional antennas located on conical and parabolic surfaces of rotation are given in Table 5 and allow comparing them with the wave impedances  $W_1$  of flat antennas. They are the same in antennas with one metal radiator and are a little more in antennas with two and four radiators.

The obtained results show that the class of self-complementary antennas is much wider than what was previously thought. This class should be supplemented, firstly, by structures consisting of several metal and slot radiators, and, secondly, by three-dimensional structures located on the surfaces of rotation, in particular on the surfaces of a circular cone or paraboloid. Comparison of cylindrical, conical and parabolic problems allows to determine the relationship between variables that ensure their mathematical equivalence.

The proximity of the values of wave impedances of cables and antennas is a necessary condition for the efficiency of antennas. The known variants of self-complementary antennas do not satisfy this condition, since their wave impedances are greater than the wave impedances of standard cables. The antennas considered here have different wave impedances, including a significantly smaller one. This makes it much easier to reconcile in a wide frequency range and expand the scope of self-complementary antennas. Three-dimensional radiators increase substantially the efficiency of the antennas of the same height.

## References

- [1] Miller, M.A. (1954). Application of uniform boundary conditions to the theory of thin antennas. *Journal of Technical Physics*, 24(8): 1483–1495 (in Russian).
- [2] Brown, G.H. (1936). A critical study of the characteristics of broadcast antennas as affected by antenna current distribution. *Proc. IRE*, 24(1): 48–81.

- [3] Leontovich, M.A. and Levin, M.L. (1944). On the theory of oscillations excitation in the linear radiators. *Journal of Technical Physics*, 14(9): 481–506 (in Russian).
- [4] Glushkovsky, E.A., Levin, B.M. and Rabinovich, E.Ya. (1967). Integral equation for the current in thin impedance radiator. *Radiotechnics*, 22(12): 18–23 (in Russian).
- [5] Glushkovsky, E.A., Izrailit, A.B., Levin, B.M. and Rabinovich, E. Ya. (1968). Methods of calculating linear impedance radiators. *Radiotechnics*, 23(1): 40–46 (in Russian).
- [6] Glushkovsky, E.A., Izrailit, A.B., Levin, B.M. and Rabinovich, E. Ya. (1967). Linear antennas with surface impedance changing along its length. *Antennas*, 2: 154–165 (in Russian).
- [7] Popovic, B.D. (1973). Theory of cylindrical antennas with lumped impedance loadings. *Radio and Electronic Engineer*, 43(3): 243–248 (in German).
- [8] Ovsyanikov, V.V. (1975). The use of lumped reactance for reducing dimensions of vibrator antennas. *Proc. Electrodynamics and microwave physics of University in Dnepropetrovsk*, 4: 138–144 (in Russian).
- [9] Ovsyanikov, V.V. (1985). *Monopole and Dipole Antennas with Reactive Loads*. Moscow: Radio and Communication (in Russian).
- [10] Levin, B.M. (1998). *Monopole and Dipole Antennas for Marine-Vehicle Radio Communications*. S.-Petersburg: Абрис (in Russian).
- [11] Finck, L.M. (1984). *Signals, Interferences. Mistakes ... Notes on Some Surprises, Paradoxes and Errors in the Theory of Communication*. Moscow: Radio and Communication (in Russian).
- [12] Levin, B.M. (1976). Impedance folded radiator. *Antennas*, 23: 80–90 (in Russian).
- [13] Pistolkors, A.A. (1948). Theory of the circular diffraction antenna. *Proc. of IRE*, 36(1): 56–60.
- [14] Fradin, A.Z. (1977). *Antenna-Feeder Devices*. Moscow: Communication (in Russian).
- [15] Pheld, Ya. N. (1948). *Fundamentals of the Theory of Slot Antennas*. Moscow: Sovetskoye Radio (in Russian).
- [16] Glushkovsky, E.A., Levin, B.M. and Rabinovich, E. Ya. (1969). Thin magnetic impedance antennas. *Antennas*, 5: 108–120 (in Russian).
- [17] Pistolkors, A.A. (1947). *Proc. of Research Institute of Communications*, 5(40): 3 (in Russian).
- [18] Schefer, G. (1963). *Archive der Elektrischen Übertragung*, 6: 289 (in German).
- [19] King, R.W.P. (1967). The linear antenna—eight ears of progress. *Proc. of IRE*, 55(1): 2–16.
- [20] Guan, N., Furuya, H., Delaune, D. and Ito, K. (2008). Antennas made of transparent conductive films. *Piers Online*, 4(1): 116–120.
- [21] Nesterenko, M.V. (2010). Analytical methods in the theory of thin impedance vibrators. *Progress in Electromagnetic Research*, B(21): 299–328 (in Russian).
- [22] Booker, H.G. (1946). Slot aerials and their relation to complementary wire aerials (Babinet's principle). *Journal of the Institution of Electrical Engineers, Part IIIA*(4): 620–626.
- [23] Mushlake, Y. (1996). *Self-Complementary Antennas: Principle of Self-Complementarity for Constant Impedance*. London: Springer.
- [24] Rumsey, V.H. (1957). Frequency independent antennas. 1957 IRE National Convention Record, Part 1: 114–118.
- [25] Rumsey, V.H. (1966). *Frequency Independent Antennas*. Academic Press.
- [26] Levin, B.M. and Markov, V.G. (1997). *Method of complex potential and antennas*. S.-Petersburg: Ship Electrical Engineering and Communication (in Russian).
- [27] Carrel, R.L. (1958). The characteristic impedance of two infinite cones of arbitrary cross-section. *IEEE Transactions on Antennas and Propagation*, AP-6(2): 197–201.
- [28] Iossel, Yu. Ya., Kochanov, E.S. and Strunsky, M.G. (1981). *Calculation of Electrical Capacitance*. Leningrad: Energoisdat (in Russian).
- [29] Buchholz, H. (1957). *Elektrische und Magnetische Potentialfelder*. Berlin (in German).
- [30] Levin, B.M. (2013). *The Theory of Thin Antennas and Its Use in Antenna Engineering*. Bentham Science Publishers.
- [31] Korn, G. and Korn, T. (1961). *Mathematical Handbook for Scientists and Engineers*. New York, Toronto, London: McGraw-Hill.
- [32] Belousov, S.P., Gurevich, R.V., Kliger, G.A. and Kuznetsov, B.D. (1979). *Antennas for Broadcasting and Radio Communication, Part 1. Shortwave Antennas*. Moscow: Communication (in Russian).

# Antenna Analysis Based on Long Lines' Theory

## 1. Hertz Dipole

In antenna theory the concept of a Hertz dipole is widely used. This is an elementary electric radiator in the form of a thin rectilinear filament with a current. The length  $b$  of a filament is small compared to the wavelength  $\lambda$  ( $b \ll \lambda$ ), and the amplitude and phase of the current are the same along its entire length:

$$J(z, t) = \text{const} \cdot e^{j\omega t}.$$

Here  $z$  is the coordinate along the dipole,  $t$  is the time,  $\omega$  is the circular frequency. If the line of current coincides with  $z$  axis, then in the spherical coordinate system the fields' components of the Hertz dipole are equal to

$$\begin{aligned} E_r &= -j60kJb \cos\theta \left[ \frac{1}{k^2r^2} + \frac{1}{kr} \right] \frac{\exp(-jkr)}{r}, \\ E_\theta &= -j30kJb \sin\theta \left[ \frac{1}{k^2r^2} + j\frac{1}{kr} - 1 \right] \frac{\exp(-jkr)}{r}, \\ H_\phi &= -j kJb \sin\theta \left[ j\frac{1}{kr} - 1 \right] \frac{\exp(-jkr)}{4\pi r}. \end{aligned} \quad (3.1)$$

In a rectangular coordinate system, the vertical component of the field is

$$E_z = E_r \cos\theta - E_\theta \sin\theta = -j30Jb \left( \frac{\partial^2}{\partial z^2} + k^2 \right) \frac{\exp(-jkr)}{kr}. \quad (3.2)$$

In these expressions, the factor  $e^{j\omega t}$ , which demonstrates monochromatic oscillations, is absent. Fields and currents are considered as functions of spatial coordinates at the same moment in time.



The field of the Hertz dipole is conditionally divided into three zones: the near, or induction zone ( $kr \ll 1$ ), the far, or radiation zone ( $kr \gg 1$ ), and the intermediate zone ( $kr \sim 1$ ). In the induction zone, each component of the field, i.e.,  $E_r$ ,  $E_\theta$ ,  $H_\varphi$ , is defined mainly by a summand with the largest power of the magnitude  $1/(kr)$ . Therefore, the electric field is inversely proportional to the third power and the magnetic field—to the second power of a distance  $r$ . The electric and magnetic fields in this zone differ in phase with each other by  $90^\circ$ .

In the radiation zone, the fields are defined by the terms with the smallest power of magnitude  $1/kr$ . The values  $E_\theta$  and  $H_\varphi$  are inversely proportional to the first power of a distance  $r$ , and  $E_r$ —to the second power. Neglecting the value  $E_r$  compared to  $E_\theta$  we obtain the following expressions for the field components in the radiation zone:

$$E_\theta = -j30kIb \sin \theta \frac{\exp(-jkr)}{r}, H_\varphi = E_\theta / 120\pi, E_r \approx E_\varphi = 0, H_r = H_\theta = 0. \quad (3.3)$$

From expressions (3.3) it can be seen that at large distances from the Hertz dipole, a spherical electromagnetic wave is formed with the following features:

- 1) points with the same field phase are located on a sphere with radius  $r = \text{const}$ , the center of which coincides with the dipole center,
- 2) the phases of an electric and magnetic fields are the same,
- 3) the field has a linear polarization,
- 4) the ratio of the electric vector  $E_\theta$  to the magnetic  $H_\varphi$  is equal to  $Z_0 = \sqrt{\mu_0/\epsilon_0} = 120 \pi \text{ Ohm}$ . The magnitude  $Z_0$  is called the wave impedance of free space.

In connection with the symmetry of Maxwell's equations with respect to electric and magnetic fields, in electrodynamics it is customary to speak about electric and magnetic dipoles, although real magnetic charges do not exist. The circular electric current creates a magnetic field, the structure of which coincides with the structure of the electric field created by two opposite electric charges of the same magnitude (by the electric dipole). Therefore, a flat circular loop of small (compared to the wavelength) radius with a current of constant amplitude and phase is called an elementary magnetic radiator. Such a radiator is used to excite an impedance magnetic antenna in the form of a rod (see Section 4).

The dependences of radiation fields  $E_\theta$  and  $H_\varphi$  on angular coordinates  $\theta$  and  $\varphi$  are called the directional patterns of these fields. Due to the complexity of the image of volume figures, they are replaced by planar figures, which are the cross-sections of the specified volumetric figures by planes passing through their central points. Usually, directional patterns are normalized to unity. As is seen from (3.3), the directional pattern of Hertz dipole in the vertical plane is

$$F(\theta, \varphi) = \sin \theta. \quad (3.4)$$

Along with the directional patterns the integral characteristics of the directivity in the form of numbers are widely used. These numerical characteristics are called a directivity and a gain. The directivity  $D$  is understood as a ratio of radiation intensity in the direction of a main maximum to the average value of radiation intensity in all directions. A simple calculation allows us to determine the directivity of the

Hertz dipole. Let the power flow through the unit area of a spherical surface in the direction of maximum radiation is equal to  $P_m$ . In an arbitrary direction, the flow does not depend on  $\varphi$  and, in accordance with (3.3), is equal to  $P_m \sin^2 \theta$ . For the total flow through a spherical surface, we obtain

$$P = P_m \int_0^{2\pi} d\varphi \cdot 2 \int_0^{\pi/2} \sin^2 \theta \cdot d\theta = 4\pi P_m \cdot \frac{2}{3},$$

i.e., the average flow through a unit area is  $P_0 = P/4\pi = \frac{2}{3} P_m$ , and respectively  $D = P/P_0 = \frac{3}{2}$ .

To account for losses in an antenna, the concept of a gain is used. The gain  $G$  is understood as the ratio of the radiation intensity of a real antenna in the direction of the main maximum to the average radiation intensity of this antenna in the absence of losses in it (when an entire power created by a transmitter is radiated). The gain is equal to

$$G = \eta D, \quad (3.5)$$

where  $\eta$  is the efficiency factor.

The important antenna characteristic is the pattern factor (PF), which is equal to an average radiation level in the required range of angles. For example, to increase the distance of radio communication, signals must be radiated along the earth's surface, mostly between angles  $\theta$ , equal to  $60^\circ$  and  $90^\circ$ . The share of power radiated in this angular sector can serve by an antenna quality measure. The pattern factor in the vertical plane is

$$PF = \frac{1}{K} \sum_{k=1}^K F(\theta_k), \quad (3.6)$$

where  $F(\theta_k)$  is the magnitude of normalized vertical directional pattern at an angle  $\theta_k$  in an angular sector from  $\theta_1$  to  $\theta_k$ . If the directivity of an antenna is large, but maximum is located outside the necessary angular sector, then its increase is not just useless for increasing the communication range, but as a rule is harmful, because it leads to the signal decrease under the required angles.

## 2. Method of Poynting and Resistance of an Antenna Radiation

Resistance of radiation and active component of the input impedance are important characteristics of any radiator. A matching level of the transmitter with the antenna and a losses level during transfer, i.e., a quantity of power given off by a signal source, depend on this magnitude. These characteristics of the radiator can be determined proceeding from the relationship of power created by the source of emf and power passing through a closed surface surrounding the antenna. Two methods of calculation are based on this relationship: the method of Poynting and the method of induced emf. In the capacity of the closed surface in the Poynting method the spherical surface is usually used. The cylindrical surface as a rule is used in the method of induced emf. Such a cylinder with height  $2h$  and radius  $b$ , along the axis of which the symmetric radiator is located, is shown in Fig. 1.

The article [1], published in 1884, is devoted to the calculation of the power of the radiated signal. In this article it is shown that the power flow density coming out of a volume bounded by a closed surface is determined by the Poynting vector

$$\vec{P} = [\vec{E}, \vec{H}], \quad (3.7)$$

more precisely, by a projection of this vector on the normal to the corresponding surface. For the side surface and the upper cover of the cylinder, these projections on the normal have the form

$$P_\rho = -E_z H_\varphi, P_z = E_\rho H_\varphi.$$

Let us combine the cylindrical closed surface with the radiator surface, by putting  $h = L$ ,  $b = a$ . Then, with a small radius of the radiator, the power flows passing through the cover and the bottom of the cylinder will also be small. If the radiator is a thin filament with a radius tending to zero, then the integrals over its upper and lower bases (the cover and the bottom of the cylinder) will tend to zero. If the radiator has the shape of a circular cylinder with a finite radius, then these integrals also tend to zero, since the longitudinal current inside the cylinder decays rapidly, i.e., when  $\rho < a$ , the tangential component of the magnetic field  $H_\varphi$  in both bases is close to zero.

Therefore, the power passing through a closed surface is determined only by an integral along the lateral surface of the cylinder:

$$P = -\int_{-L}^L \int_0^{2\pi} E_z H_\varphi a d\varphi dz = p_\rho, \quad (3.8)$$

and its magnitude  $P_\rho$  does not depend on the coordinate  $\varphi$ , since the components of the electromagnetic field do not depend on  $\varphi$ . At that the power is understood as the

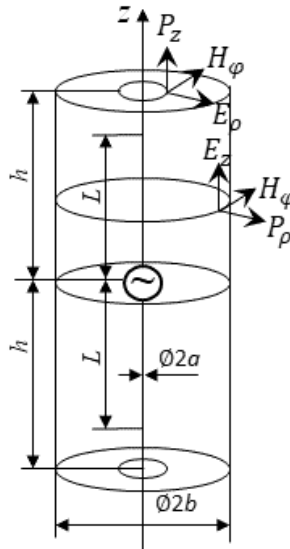


Fig. 1: Closed surface around a radiator.

so-called active power, equal to the average value over the oscillation period. Therefore, the power is equal to the product of two real quantities (without an asterisk).

Poynting method allows us to determine the resistance of antenna radiation with help of calculating the power passing through the spherical closed surface, in the center of which an antenna is located. We will consider that the sphere radius  $R$  is so large that the sphere is located in the far zone of an antenna, and a field passing through it has the character of a plane wave. In a plane wave, the vectors  $\vec{E}$  and  $\vec{H}$  are mutually perpendicular, and their ratio  $E/H$  is equal to  $Z_0$  ( $Z_0 = 120 \pi$  is the wave impedance of a free space). The given relation can be easily verified by comparing expressions (1.25) and (1.28) for  $E_z$  and  $H_\phi$ . This means that the active power is proportional to the square of an electric field strength, i.e.,  $P = E_\theta^2/Z_0$ , where  $E_\theta$  is the component of an electric field strength, tangent to the sphere surface.

In the general case, electric and magnetic fields of an antenna are defined by an expression (1.10) and depend on a vector-potential  $\vec{A}$ , which is a function of currents in the region  $V$ . Let a symmetric linear radiator (dipole) located along  $z$  axis is a source of field, and a perfectly conductive filament is used as the radiator model. The current of this radiator is distributed in accordance with a sinusoidal law (1.21), i.e., is equal to

$$J(z) = I_0 \frac{\sin k(L - |z|)}{\sin kL} = J(0) \sin k(L - |z|).$$

One can consider that its field consists of the sum of fields of elementary radiators (Hertz dipoles), directed at the same angle. The elementary radiator  $n$  is a filament of a length  $l_n$  with unaltered current  $J_{n0}$ . The field of such a radiator in a far zone in the horizontal direction, perpendicular to its axis, is

$$E_\theta = j \frac{60kL J(0) \exp(-jkR_0) \sin\theta}{\varepsilon_r R_0}.$$

Here  $k = \omega\sqrt{\mu\varepsilon}$  is the wave propagation constant in the environment,  $\omega$  is the circular frequency of the signal,  $\mu$  and  $\varepsilon$  are permeability and permittivity of the medium respectively ( $\varepsilon = \varepsilon_r \varepsilon_0$ , where  $\varepsilon_r$  is relative permittivity of the medium, and  $\varepsilon_0$  is absolute permittivity of the air).

Let us compare the fields of a symmetric linear radiator and the Hertz dipole in the indicated direction. We will assume that the fields are the same, if the area under the current curve of the linear radiator coincides with the sum of areas under the current curves of the Hertz dipoles, equivalent to the segments of the linear radiator. It is known that the first of these areas is equal to

$$S_1 = 2 \frac{I_0}{\sin kL} \int_0^L \sin k(L - z) dz = \frac{2(1 - \cos kL)}{k \sin kL} \frac{2}{k} \tan \frac{kL}{2}. \quad (3.9)$$

For the second magnitude, one can write

$$S_2 = \sum_{n=1}^N J_{n0} l_n.$$

Here  $N$  is the number of segments,  $n$  is the segment number. The magnitude  $S_1$  in accordance with the method used to obtain it, is customary called by the equivalent effective length  $l_e$  of the linear radiator.

To determine the magnitude of a field at an arbitrary angle  $\theta$  to the antenna, it is necessary to consider the difference of distances from the central and other points of the antenna to the observation point (Fig. 2a). This difference is called the path difference, it is equal to  $r = z \cos \theta$ . For the field of a symmetric radiator located along  $z$  axis with the center at the origin, we obtain

$$E_\theta = j \frac{30k \exp(-jkR) \sin \theta}{\varepsilon_r R} \int_{-L}^L J(z) \exp(jkz \cos \theta) dz. \quad (3.10)$$

In the case of a sinusoidal current distribution along the radiator, we find

$$E_\theta = j \frac{60I_0}{\varepsilon_r \sin kL} \frac{\exp(-jkR)}{R} \frac{\cos(kL \cos \theta) - \cos kL}{\sin \theta}. \quad (3.11)$$

Here, the last multiplier determines the directional pattern of the radiator in a vertical plane.

Using the expression for the antenna field in an arbitrary direction, one can determine the active power radiated by the antenna and passing through the surface of the sphere:

$$P = \frac{R_0^2}{120\pi} \int_0^{2\pi} d\varphi \int_0^{2\pi} \frac{E_\theta^2}{R_0^2} \sin \theta d\theta.$$

Dividing this power to the square of the current at the output of the generator, we find the resistance of the antenna radiation:

$$R_\Sigma = \frac{P}{J^2(0)}. \quad (3.12)$$

This method of determining the resistance of radiation is widely known as Poynting method. The calculations commonly are performing by numerical methods.

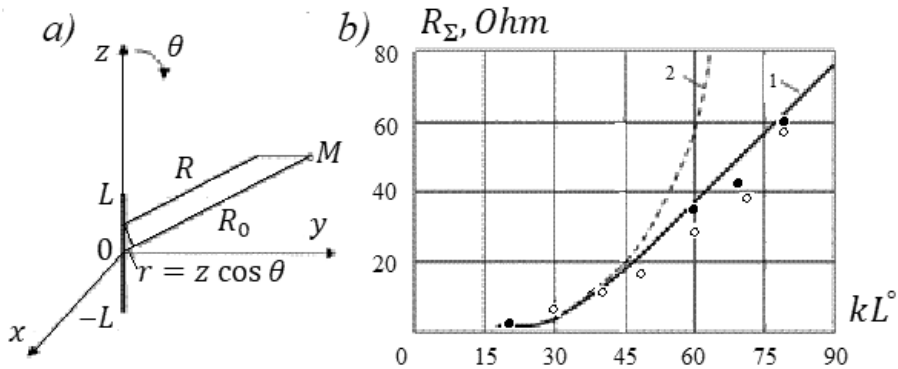


Fig. 2: The pathlength difference of the antenna rays (a) and the radiation's resistance of the antenna (b).

Analytical methods are encountering insurmountable difficulties in integrating squares of electric fields under arbitrary angles  $\theta$ . For a long time, it was believed that the integrals could not be calculated. As shown below, this opinion turned out to be erroneous.

In accordance with the above expressions, we write

$$R_{\Sigma} = \frac{R_0^2}{120\pi J^2(0)} \int_0^{2\pi} d\varphi \int_0^{\pi} \frac{E_{\theta}^2}{R_0^2} \sin\theta d\theta = \frac{1}{30 J^2(0)} \int_0^{\pi/2} E_{\theta}^2 \sin\theta d\theta.$$

As follows from above,  $R_{\Sigma}$  is proportional to the square of the effective antenna length  $L_e$ , calculated with account the different magnitudes of the signals under different angles  $\theta$ . If in this expression for  $R_{\Sigma}$  to replace the integral  $\int_0^{2\pi} d\varphi \int_0^{\pi} E_{\theta}^2 \sin\theta d\theta$  by an approximate expression  $4\pi E_{\theta}^2$ , i.e., to adopt that the field of the dipole with a length  $2L$  is the same under all angles and is equal to the field in the horizontal direction, then

$$R_{\Xi} = 30(kL_e^2),$$

where  $l_e = \frac{2}{k} \tan \frac{kL}{2}$ . This value is clearly overestimated, since the signal rapidly decreases, when the beam deviates from perpendicular to the antenna axis. For example, if  $kL = \pi/2$ , we obtain  $R_{\Xi} = 120$ . A strict calculation in this case gives a value of the order of 80.

Using the rigorous expression for  $E_{\theta}$ , introducing the notation  $\alpha = kL$  and assuming that  $\varepsilon_r = 1$ , we get:

$$R_{\Sigma} = 120 \int_0^{\pi/2} \frac{[\cos(\alpha \cos\theta) - \cos\alpha]^2}{\sin\theta} d\theta.$$

We introduce the new variable  $x = \alpha \cos\theta$ , i.e.,  $d\theta = -dx/(\alpha \sin\theta)$ . If  $\theta = 0$ , then  $x = \alpha$ . If  $\theta = \pi/2$ , then  $x = 0$ . The replacement of a variable leads to an expression

$$R_{\Sigma} = 120 \int_0^{\alpha} \frac{(\cos x - \cos \alpha)^2}{\alpha \sin^2 \theta} dx = 120 \alpha \int_0^{\alpha} \frac{(\cos x - \cos \alpha)^2}{\alpha^2 - x^2} dx.$$

To calculate the resulting expression, we apply integration by parts. Since  $\cos \theta \leq 1$ , then  $x \leq \alpha$ , and in this case  $\int \frac{dx}{a^2 - x^2} = \frac{1}{2\alpha} \ln \frac{\alpha + x}{\alpha - x}$ . The value of the derivative  $\frac{d}{dx} (\cos x - \cos \alpha)^2$  is equal to  $-\sin 2x + 2 \cos \alpha \sin x$ . As a result, we obtain

$$R_{\Sigma} = 60 (\cos x - \cos \alpha)^2 \ln \frac{\alpha + x}{\alpha - x} \Big|_0^{\alpha} + 60 \int_0^{\alpha} \ln \frac{\alpha + x}{\alpha - x} (\sin 2x - 2 \cos \alpha \sin x) dx.$$

It is not difficult to be convinced that the first term of this expression is equal to zero. Indeed, at the upper limit (at  $x = \alpha$ ), the coefficient at the logarithm has the form  $60(\cos \alpha - \cos \alpha)^2 = 0$ . On a lower limit (at  $x = 0$ ) the logarithm  $\ln \frac{\alpha}{\alpha}$ . To the

second term of this expression, one may also apply the integration by parts. The derivative of the first multiplier of the integrand is

$$\frac{d}{dx} \left( \ln \frac{\alpha + x}{\alpha - x} \right) = \frac{1}{\alpha + x} + \frac{1}{\alpha - x}.$$

The integral from the second multiplier has the form  $-\frac{\cos 2x}{2} + 2 \cos \alpha \cos x$ . Accordingly, the second term of an expression for  $R_\Sigma$  takes the form

$$30(-\cos 2x + 4 \cos \alpha \cos x) \ln \frac{\alpha + x}{\alpha - x} \Big|_0^a - 30 \int_0^a (-\cos 2x + 4 \cos \alpha \cos x) \left( \frac{1}{\alpha + x} + \frac{1}{\alpha - x} \right) dx.$$

Here the free member is

$$30(-\cos 2\alpha + 4 \cos^2 \alpha) \ln(2a/\alpha \cdot 0) = (2 + \cos 2\alpha) \ln(2/0),$$

and the integral can be reduced to a set of integral sines and cosines. This method is demonstrated by the example of the integrand summand  $\cos 2x/(\alpha + x)$ :

$$\begin{aligned} \frac{\cos 2x}{\alpha + x} &= \frac{e^{j2(\alpha+x)} e^{-j2\alpha} + e^{-j2(\alpha+x)} e^{j2\alpha}}{2(\alpha + x)} = \\ &= e^{-j2\alpha} [\cos 2(\alpha + x) + j \sin 2(\alpha + x)] + e^{j2\alpha} [\cos 2(\alpha + x) - j \sin 2(\alpha + x)] = \\ &= 2[\cos 2\alpha \cos 2(\alpha + x) + \sin 2\alpha \sin 2(\alpha + x)], \\ \frac{\sin 2x}{\beta + x} &= 2[\cos 2\alpha \operatorname{Si} 2(\alpha + x) - \sin 2\alpha \operatorname{Ci} 2(\alpha + x)]. \end{aligned}$$

The integral is reduced to the sum

$$60 \{ \cos 2\alpha [\operatorname{Ci} 2(\alpha + x) - \operatorname{Ci} 2(\alpha - x)] - 2 \cos \alpha \cos x [\operatorname{Ci}(\alpha + x) - \operatorname{Ci}(\alpha - x)] + \sin 2\alpha [\operatorname{Si} 2(\alpha + x) - \operatorname{Si} 2(\alpha - x)] - \sin 2\alpha [\operatorname{Si}(\alpha + x) - \operatorname{Si}(\alpha - x)] \} \Big|_0^a,$$

whence, substituting the upper and lower limits of integration and considering the free member, we obtain

$$R_\Sigma = 60 \{ (1 + 0.5 \cos 2\alpha) \ln(2/0) + \cos 2\alpha [\operatorname{Ci} 4\alpha - \operatorname{Ci}(2\alpha \cdot 0)] - 2 \cos^2 \alpha [\operatorname{Ci} 2\alpha - \operatorname{Ci}(\alpha \cdot 0)] + \sin 2\alpha [\operatorname{Si} 4\alpha - \operatorname{Si} 2\alpha] \}. \quad (3.13)$$

When using the expression (3.13), one must first determine the functions included in it. To do this, it is need to use the tables of integral sines and cosines, presented, for example, in the book [2]. To obtain the required accuracy, it is necessary to apply the interpolation method. The found values of these functions for several options of the radiator arm length are given in the Table 1. In the calculations, it is necessary

**Table 1:** Magnitudes of Functions Included in Expression for  $R_{\Sigma}$ .

$\alpha$	$\pi/8$	$\pi/6$	$\pi/4$	$\pi/3$	$\pi/2$	$2\pi/3$	$\pi$	$4\pi/3$	$3\pi/2$	$2\pi$	$8\pi/3$
$Si \propto$	0.3894	0.5157	0.7586	0.983	1.369	1.643	1.8506	1.72	1.6095	1.4189	1.6175
$ln \propto$	-0.9347	-0.647	-0.242	0.0459	0.4516	0.739	1.1447	1.432	1.5502	1.8379	2.1256
$Ci \propto$	-0.3931	-0.138	0.1854	0.357	0.4673	0.389	0.0746	-0.166	-0.197	-0.0228	0.1071

to take into account that the integral cosine  $Ci x$  has a singularity at the point  $x = 0$ . If  $x = b\delta$  and the value  $\delta$  tends to zero, then  $Ci x = 0.5(\ln b + \ln \gamma)$ , where  $\ln \gamma = C = 0.577$  is the Euler constant. If one of the terms is equal to  $-\ln(b \cdot 0)$ , then this term allows us to compensate the magnitude  $Ci(b \cdot 0)$ .

In accordance with the foregoing, we start with a symmetric radiator whose arm length at the frequency of the first serial resonance is  $L = \lambda/4$ , i.e.,  $\alpha = \pi/2$ . In accordance with the general expression, we find

$$R_{\Sigma} = 60\{0.5 \ln(2/0) + \cos 2\alpha [Ci 2\pi - Ci(\pi \cdot 0)]\}.$$

We take into account that

$$\ln 2 = 0.693, Ci(\pi \cdot 0) = 0.5(\ln \pi + C), \ln \pi = 1.1447.$$

Substituting magnitudes into the expression for  $R_{\Sigma}$ , we obtain

$$R_{\Sigma} = 60[0.3466 + 0.0228 + 0.5 \cdot 1.1447 + 0.288] = 73.8 \text{ Ohm}.$$

This result is close to magnitudes obtained by different authors when solving the integral equation for the current in a metal radiator. In particular, the equation of Leontovich in the first approximation gives 71.2 Ohm for the resistance of a radiation for the dipole at the point of a first series resonance. The proximity of results confirms the validity of the proposed calculation method, which is based on the Poynting method.

The described procedure gives the following concrete values for the resistance of radiation for the dipole with an arm length equal to  $\lambda/4, \lambda/6, \lambda/8, \lambda/12$  and  $\lambda/16$ : 43.4, 24.6, 12.6, 5.3 и 3.2 Ohm. The calculation results depending on the electric length of the dipole arm are shown in Fig. 2b in the form of a smooth curve 1. For comparison, in the same figure, the values of active components of the input impedance are given by means of the black dots. These magnitudes were obtained using the new method of a solving the Leontovich's equation, described in the fourth chapter. They correspond to the total input current of the antenna, equal to a total sum of the series for the current, and from this point of view they are similar to the result of the solution obtained using the Poynting vector.

Since during the calculations all the upper limits were chosen equal to  $\lambda/2$ , this expression allows to find the resistance of radiation for the antenna with an electrical arm length equal to  $kL = k \frac{\lambda}{2} = \alpha$ .

In order to determine the resistance of radiation for an antenna with a different arm length, one must multiply the radiation's resistance found by the above formula



by  $\tan^2(kL/2)/\tan^2\alpha$ . The possibility of such a simple calculation method is explained primarily by the fact that for the same structure of the radiator a simultaneous change of all its dimensions leads to the same change in the magnitude of the field in all directions. The proposed simple method is valid if only because the radiator field in the horizontal direction is proportional to  $\tan\frac{kL}{2}$ , and the radiation's resistance is proportional to the square of this field. If we take into account that the fields are calculated in the far zone, then the condition for applying the method to radiators with the same structure becomes redundant.

The simple formula yields the following numerical results for an arm length equal to  $\lambda/4.8$ ,  $\lambda/6$ ,  $\lambda/8$ ,  $\lambda/12$  and  $\lambda/16$ : 47.1, 26.7, 13.7, 5.7 и 2.9 Ohm. They are shown in figure by circles. The numerical results obtained in accordance with above general formula coincide in the first approximation with the results of calculations by the simple formula. For relatively short radiators this coincidence is accurate. When the arm length is increased the accuracy is decreased. This simple method is valid since the radiator field in the horizontal direction as the radiator field in an arbitrary direction is proportional to an effective length of the radiator, and the radiation's resistance is proportional to the square of this field.

The results of calculations by the above general formula confirm the applicability of the described simple method. The direct relationship of the simple method with the formula for  $E_\theta$  also evidences this fact: substituting  $\theta = \pi/2$  into this formula, we obtain an expression proportional to the previously calculated effective antenna length  $l_e$ .

The proposed methods can be generalized to the case of linear impedance radiators. The current of a symmetric impedance radiator (dipole), located along  $z$  axis with the center at the origin, is defined by the first expression from the set (2.7). In order to compare with each other the fields of the metal and impedance radiators in the far zone, we use the expression (1.23) for the field  $E_z$ . If the current along the metal radiator is distributed according to a sinusoidal law, then the first multiplier under the sign of the integral, and therefore the first term of this expression, are equal to zero. The second term is also equal to zero, and the expression for  $E_z$  is transformed to (1.25). The calculation of a field of an impedance antenna leads to a similar result. In this case the value  $k$  in the first multiplier of the integrand is replaced by the value  $k_1$ , but this multiplier as before is zero. The expression for the vertical field component of such an antenna differs only by another wave propagation constant along the antenna and by an additional factor  $k_1/k$ .

The difference between the other components of the field is of the same nature. In particular

$$E_\theta = j \frac{60J(0)}{\sin k_1 L} \frac{k_1}{k} \frac{\exp(-jkR)}{\varepsilon_r R} \frac{\cos(k_1 L \cos\theta) - \cos k_1 L}{\sin \theta}.$$

Substituting this magnitude into the expression for  $R_z$ , we will take into account that the current of the impedance radiator is

$$J_1(z) = jJ(0) \frac{ke}{60 k_1 \cos k_1 L} \sin k_1 (L - |z|),$$

i.e., for the same emf of the source, the current amplitude of the impedance radiator is  $k_1/k$  times less than in the metal one. Accordingly, we write for its radiation resistance

$$R_{\Sigma 1} = 120 \left( \frac{k}{k_1} \right)^2 \int_0^{\frac{\pi}{2}} \frac{[\cos(k_1 L \cos \theta) - \cos k_1 L]^2}{\sin \theta} d\theta.$$

Introducing notations  $\alpha = kL$ ,  $\beta = k_1 L$  and the new variable  $x = \beta \cos \theta$ , and considering that  $dx = -\beta \sin \theta d\theta$ ,  $\varepsilon_r = 1$ ,  $\sin \theta$  obtain:

$$R_{\Sigma 1} = 120 \left( \frac{\alpha}{\beta} \right)^2 \int_0^{\beta} \frac{(\cos x - \cos \beta)^2}{\beta \sin^2 \theta} dx = 120 \frac{\alpha^2}{\beta} \int_0^{\beta} \frac{(\cos x - \cos \beta)^2}{\beta - x^2} dx. \quad (3.14)$$

This expression differs from the similar expression for a metal radiator by a factor  $(\alpha/\beta)^2$  and by replacing the magnitude  $\alpha$  by  $\beta$ . Accordingly, for the resistance of radiation for the impedance radiator we will write

$$R_{\Sigma 1} = 60 \frac{\alpha^2}{\beta^2} \left\{ (1 + 0.5 \cos 2\beta) \ln \frac{2}{0} + \cos 2\beta [Ci \ 4\beta - Ci \ (2\beta \cdot 0)] - \right. \\ \left. 2 \cos^2 \beta [Ci \ 2\beta - Ci \ (\beta \cdot 0)] + [Si \ 4\beta - Si \ 2\beta] \sin 2\beta \right\}. \quad (3.15)$$

The analogy of the expressions for the radiation's resistances of metal and impedance antennas allows us to obtain specific results. The values  $R_{\Sigma}$  were previously given for metal radiators with a geometric arm length  $L$ , equal to  $\frac{\lambda}{4}, \frac{\lambda}{4.8}, \frac{\lambda}{6}, \frac{\lambda}{8}, \frac{\lambda}{12}$  и  $\frac{\lambda}{16}$  (at that an electrical arm length is equal to  $kL$ ). With their help, it is possible to determine  $R_{\Sigma 1}$  of the impedance radiators with an electric arm length  $k_1 L$ , i.e., with geometric arm length  $L_1 = kL/k_1$ :

$$R_{\Sigma 1} = R_{\Sigma} (k/k_1)^2. \quad (3.16)$$

If, for example,  $k_1/k = 2$ , then for  $L_1 = \lambda/8, \lambda/9.6, \lambda/12, \lambda/16, \lambda/24, \lambda/32$  the resistances are equal accordingly to 20, 12.3, 6.7, 3.4, 1.4 and 0.8. In Fig. 2b, they are given in the form of a smooth curve 2. They are proportional to the magnitude  $\tan^2(k_1 L/2)$ .

Calculations show that for the same geometric length of the radiator arm the resistance of the radiation for impedance radiator is greater than that of a metal one. For the same electric length, this resistance is significantly less (for the slowing factor 2 it is smaller approximately four times, i.e., inversely proportional to the square of the slowing) – in full accordance with the theory of impedance antennas. For relatively short radiators (with arm length  $L < 0.3\lambda$ ), the radiation's resistance is proportional to the square of the geometric length of the radiator arm. And in accordance with described above simple calculating method one can write for the impedance radiator

$$R_{\Sigma 1} = 80(k/k_1)^2 \tan^2 \left( \frac{k_1 L}{2} \right).$$

If  $L \ll \lambda$ , the effective length of the metal and impedance radiators is same. In this case it is equal to  $L$  for a dipole and to  $L/2$  for a monopole.

Next, we consider an antenna with a surface impedance varying along its length, or rather, its specific version with a stepwise change of the surface impedance along the radiator length. If the radiator is symmetric with respect to the central point, at which the emf is located, then for the current in the segment  $n$ , counting from the free end of each radiator arm, we can write

$$J_n(z) = I_n \sin(k_n z_n + \varphi_n),$$

where  $I_n$  is the amplitude of the sinusoidal current on this segment,  $k_n$  is the propagation constant,  $z_n$  is the coordinate measured from the segment boundary that is farthest from the radiator center,  $\varphi_n$  is the current phase at this point. The continuity conditions of the current and charge (derivatives of current) at the boundaries of the segments

$$I_p \sin \varphi_p = \sin(k_{p-1} l_{p-1} + \varphi_{p-1}), I_p k_p \cos \varphi_p = I_{p-1} k_{p-1} \cos(k_{p-1} l_{p-1} + \varphi_{p-1})$$

allow us to express the amplitude and phase of the current on each segment of length  $l_n$  in terms of the corresponding values of the previous segment:

$$\tan \varphi_p = \frac{k_p}{k_{p-1}} \tan(k_{p-1} l_{p-1} + \varphi_{p-1}),$$

and hence through one of the currents and the parameters of the segments. Let each section of an antenna consists of two segments located on the upper and lower arms of the antenna symmetrically relative to its center. If the number of segments in each arm of an antenna is  $N$ , and two identical segments  $N$  are adjacent to the generator, then the current on the section  $N$  is

$$J(z_N) = I_N \sin(k_N z_N + \varphi_N),$$

and

$$I_n = I_N \prod_{p=n+1}^N \frac{\sin \varphi_p}{\sin(k_{p-1} l_{p-1} + \varphi_{p-1})},$$

$$\varphi_n = \tan^{-1} \left\{ \frac{k_n}{k_{n-1}} \tan \left[ k_{n-1} l_{n-1} + \tan^{-1} \left( \frac{k_{n-1}}{k_{n-2}} \tan \left[ k_{n-2} l_{n-2} + \dots + \tan^{-1} \left( \frac{k_2}{k_1} \tan k_1 l_1 \right) \dots \right] \right) \right] \right\}.$$

Comparing the segments fields with the arms fields of the radiator with a constant impedance, it is easy to be convinced of their analogy, from which it follows that the field of a segment  $n$  of the stepped antenna is

$$E_{\theta n} = j60 \frac{I_n}{\sin \varphi_n} \frac{k_n}{k} \frac{\exp(-jkR_n)}{\varepsilon_r R_n \sin \theta} [\cos((k_n l_n + \varphi_n) \cos \theta - \cos k_n l_n].$$

Here  $R_n$  is the distance from the spherical surface to the end of the segment  $n$  closest to an antenna center. The total field of an antenna is equal to the sum of fields of all segments:

$$E_\theta = \sum_{n=1}^{2N} E_{\theta n},$$

The input current of the antenna is

$$J(0) = I_N \sin(k_N l_N + \varphi_N),$$

Substituting this value into the expression for  $R_{\Sigma 2}$ , we take into account that the wave impedance of the section at the input of the impedance radiator is  $k_N/k$  times greater than the wave impedance of the metal radiator, i.e., for the same emf the amplitude of input current in the impedance radiator is  $k_N/k$  times smaller than in the metal one. Accordingly, for the resistance of antenna radiation we write

$$R_{\Sigma 2} = \frac{P}{J^2(0)} = 120 \left( \frac{k}{k_N} \right)^2 \int_0^{\pi/2} (E_\theta/60)^2 d\theta.$$

Introducing the notations  $\alpha = kL$ ,  $\beta_n = k_n L$  and the new variables  $x_n = \beta_n \cos \theta$ , we find, assuming that  $\varepsilon_r = 1$  and taking into account that  $dx_n = -\beta_n \sin \theta d\theta$ :

$$R_{\Sigma 2} = 120(\alpha/\beta_N)^2 \sum_{n=1}^N \int_0^{\beta_n} \frac{(\cos x_n - \cos \beta_n)^2}{\beta_n \sin^2 \theta} dx_n. \quad (3.17)$$

Each member of the sum in this expression can be replaced by the corresponding expression for the square of effective length of a section.

Suppose, for example, that each arm of radiator consists of two sections with the length  $\lambda/10$ . The first section adjacent to the free end of the antenna is metallic, i.e., the wave propagation constant along it is equal to  $k$ , and the wave propagation constant along the second section, which is adjacent to the generator, is equal to  $2k$ . If in the first approximation to determine the resistance of radiation for the given antenna, we obtain that  $R_{\Sigma 1} = 136$  Ohm. If to change places of the metal and impedance sections, the resistance will change:  $R_{\Sigma 2} = 48$ .

A special case of a surface impedance is a resistive coating. Distributed resistive load leads to a slow change in the amplitude of the sinusoidal current, to its decrease with distance from the generator:

$$J(z) = J(0) e^{-\delta z} \sin k(L - |z|).$$

The decrement  $\delta$  depends on the magnitude of losses in the coating material (see Section 2.5). In this case, for the field of a symmetric radiator at an arbitrary angle  $\theta$  to the antenna, we can write, taking into account the difference of distances from the

central and other points of the antenna to the observation point and generalizing the expression obtained for a metal antenna without losses:

$$E_{\theta} = j \frac{60I_0 \sin \theta}{\exp(j\delta L) \sin kL} \frac{\exp(-jkR)}{\varepsilon_r R} \cos[kL(\cos \theta + \cos kL)] - \cos kL$$

$$= j60J(0) \alpha^2 \sin \theta \frac{(\cos x - \cos \alpha)}{X}.$$

Here  $\varepsilon_r = 1$ , the notations  $\alpha = kL$ ,  $X = \alpha^2 - x^2$  are used, and a new variable  $x = \alpha(\cos \theta + j\delta/k)$  is introduced. Since  $dx = -\alpha \sin \theta d\theta$ , we obtain for the resistance of radiation

$$R_{\Sigma 3} = 120\alpha^3 \int_{j\delta L}^{\alpha+j\delta L} \frac{(\cos x - \cos \alpha)^2 \sin^2 \theta}{(\alpha^2 - x^2)^2} dx,$$

where

$$\frac{\sin^2 \theta}{(\alpha^2 - x^2)^2} = \frac{1 - \cos^2 \theta}{X^2} = \frac{1}{X^2} \left[ 1 - \left( \frac{x}{\alpha} - j \frac{\delta}{x} \right)^2 \right] = \left( 1 + \frac{\delta^2}{k^2} \right) \frac{1}{X^2} + 2j \frac{\delta}{\alpha k} \frac{x}{X^2} - \frac{1}{\alpha^2} \frac{x^2}{X^2}.$$

Applying the integration by parts, we calculate the derivative  $\frac{d}{dx}(\cos x - \cos \alpha)^2$  and integrate the second multiplier using known integrals

$$\int \frac{dx}{X^2} = \frac{x}{2\alpha^2 X} + \frac{1}{2\alpha^3} Y, \int \frac{x dx}{X^2} = + \frac{1}{2X}, \int \frac{x^2 dx}{X^2} = + \frac{x}{2X} - \frac{Y}{2\alpha}.$$

where  $Y = \frac{1}{2} \ln \frac{\alpha + x}{\alpha - x}$ . Further we find the free member and the new integral, and thereafter we need to perform the integration by parts twice more. The last integral can be reduced to a set of integral sines and cosines:

$$60 \left[ -\frac{\delta^2 \alpha}{k^2} \{ [\cos 2\alpha \operatorname{Si} 2(\alpha + x) - \sin 2\alpha \operatorname{Ci} 2(\alpha + x)] \right. \\ \left. - 2 \cos \alpha [\cos \alpha \operatorname{Si} (\alpha + x) - \sin \alpha \operatorname{Ci} (\alpha + x)] \right\} + \\ + \frac{\delta^2 \alpha}{k^2} \{ [\cos 2\alpha \operatorname{Si} 2(\alpha - x) - \sin 2\alpha \operatorname{Ci} 2(\alpha - x)] - 2 \cos \alpha [\cos \alpha \operatorname{Si} (\alpha - x) \\ - \sin \alpha \operatorname{Ci} (\alpha - x)] \} + \\ \left. \left( j \frac{\delta \alpha}{k} + 1 + \frac{\delta^2}{2k^2} \right) \{ (\alpha + x)[\ln(\alpha + x) - 1] + (\alpha - x)[\ln(\alpha - x) - 1] \} \right] \frac{\alpha + j\delta L}{j\delta L}.$$

The sum of free members is

$$60(\cos x - \cos \alpha)^2 \left[ \left( 1 + \frac{\delta^2}{k^2} \right) \frac{x \alpha}{\alpha^2 - x^2} + 2j \frac{\delta \alpha^2}{k(\alpha^2 - x^2)} - \alpha \frac{x}{\alpha^2 - x^2} + \left( 2 + \frac{\delta^2}{k^2} \right) Y \right] +$$

$$120(\sin 2x - 2 \cos \alpha \sin x) \left[ -\frac{\delta^2 \alpha}{2k^2} \ln(\alpha^2 - x^2) + 2j \frac{\delta \alpha}{k(\alpha^2 - x^2)} Y + \right.$$

$$\left. \left( 1 + \frac{\delta^2}{2k^2} \right) \{ (\alpha + x)[\ln(\alpha + x) - 1] - (\alpha - x)[\ln(\alpha - x) - 1] \} \right] dx \Big|_{j\delta L}^{\alpha + j\delta L}.$$

An analysis of metal and impedance antennas with inductive surface impedance has shown that the rigorous method of calculating these antennas can be replaced by simple and easy-to-interpret method, leading to similar results. It is based on calculating the effective length of the radiator, calculated in accordance with the magnitude of the antenna field in the direction of the perpendicular to its axis. A similar approach can be applied to the antenna with the resistive coating. The expression for the field in an arbitrary direction has the form of a fraction whose numerator consists of two terms:  $\cos(kL \cos \theta + j\delta L)$  and  $-\cos kL$ . If in the first summand  $\theta = \frac{\pi}{2}$ , then the numerator is equal to

$$\cos(j\delta L) - \cos kL = \cos(j\delta L) - 1 + 1 - \cos kL = \cos(j\delta L) - 1 + 2\sin^2 \frac{kL}{2}.$$

The denominator taking into account new multipliers has the form

$$\exp(j\delta L) \sin kL [1 - (j\delta/k)^2] = 2 \sin \frac{kL}{2} \cos \frac{kL}{2} (1 + \delta^2/k^2) \exp(j\delta L).$$

For the effective length, we obtain

$$h_e = \frac{2}{k(1 + \delta^2/k^2)} \left[ \tan \frac{kL}{2} + \frac{\cos(\cos \beta_n) - 1}{\sin kL \exp(j\delta L)} \right]. \quad (3.18)$$

Let, for example, the antenna be made of a transparent film CEC005P with a surface resistance  $R_{sq1} = 4.5 \Omega/\text{square}$ , i.e., the exponential decrement  $\delta$  of its current is close to 7.1/m. If the frequency is equal to 5 GHz, then  $\lambda = 0.06 \text{ m}$ ,  $k = 104.7$ ,  $L = \delta/k = 0.0678$ ,  $\cos j\delta L = \cosh 0.1065 = 1.0057$ ,  $\exp(j\delta L) = j1.11$ . Substitution of magnitudes shows that the effective length at an unaltered magnitude of  $k$  practically does not change.

The main disadvantage of antennas with a resistive coating is that the wave propagation constant in such an antenna is many times greater than in a metal one (in this example,  $k$  is 104.7). This is due to the small geometric length of the antenna arm. It is useless to increase this length, since at a distance  $L = 2/\lambda$  from the generator, the current drops to zero. It is known from the theory of impedance antennas that the radiation's resistance of antennas with the same electrical length is inversely proportional to the square of the slowing. Therefore, when  $k$  increases, the magnitude of  $R_x$  sharply drops.

The above results of calculating the resistance of radiation, based on integration by parts, were published in [3]. In all considered cases, they are close to the results obtained by the approximate formulas

$$R_{\Sigma} = 20(kl_e)^2, \quad (3.19)$$

where  $l_e$  is an equivalent length of an antenna. Calculating fields of radiators with different lengths allows to conclude that the results of using this simple formula in the first approximation coincide with the numerical results obtained by means of the general formula (3.12). A similar result follows from the comparison of the fields in arbitrary directions (under different  $\theta$ ). For relatively short radiators (with an arm length  $L < 0.3 \lambda$ ) this is an exact coincidence. Accuracy decreases with increasing arm length. Here is used the fact that the field of the radiator, both in the horizontal and in any other direction, is proportional to  $\tan \frac{kL}{2}$ . Because the resistance of the radiation is proportional to the square of the effective length, the results of calculating the resistance in accordance with the approximate formula are close to accurate results.

The reason of the validity of the approximate formula becomes clear, if to take into account an infinite radius of the surface, on which a power is determined [4]. Since the dimensions of the radiator are finite, one can consider that the distance from any its point to this surface is the same, i.e., the field in the far zone has the character of a spherical wave, the signal magnitude from arbitrary antenna element is the same in any point of the surface, and the projection of Pointing vector on the normal to surface depends only on the angle in a vertical plane between an antenna axis and this normal, i.e., on the angle  $\theta$ :

$$E_{\theta} = E_{\theta 0} \sin \theta. \quad (3.20)$$

In such a situation, during integrating over the radius of the sphere it is expedient to select the angle  $\theta_0$ . This choice permits to simplify the calculation as much as possible. Let  $\theta_0 = \pi/2$ . In this case in expression (3.11) the first term in the numerator of the last cofactor is equal to 1, and the field in the direction perpendicular to the radiator axis is

$$E_{\theta 0} = j60 \frac{J(0)(1 - \cos kL)}{\sin kL} \cdot \frac{e^{-jkR_0}}{R_0} = j30kJ(0) l_e \frac{e^{-jkR_0}}{R_0}. \quad (3.21)$$

Here  $l_e = \frac{2}{k} \tan \frac{kL}{2}$  is the effective length of the linear radiator. According to (3.12) and (3.21)

$$R_{\Sigma} = \frac{1}{30J^2(0)} \int_0^{\pi} |E_{\theta 0}|^2 \sin^3 \theta d\theta = 30(kl_e)^2 \int_0^{\pi} \sin^3 \theta d\theta,$$

i.e.,

$$R_{\Sigma 0} = 20(kl_e)^2. \quad (3.22)$$

The current of an antenna with a distributed surface impedance, constant along the length, is

$$J_1(z) = J_1(0) \frac{\sin k_1(L - |z|)}{\sin k_1 L}. \quad (3.23)$$

This expression differs from expression (1.21) by another propagation constant. The similar difference exists between the fields of symmetric radiators. Instead of (3.11) we get

$$E_{\theta 1} = j60J_1(0) \frac{\exp(-jkR)}{\varepsilon_r R} \frac{\cos(k_1 L \cos \theta) - \cos k_1 L}{\sin k_1 L \sin \theta}.$$

Similarly (3.9) the effective length of a linear impedance radiator is equal to

$$l_{e1} = \frac{2}{k_1} \tan \frac{k_1 L}{2}. \quad (3.24)$$

The resistance of radiation is written in the form

$$R_{\Sigma 01} = 20k^2 l_{e1}^2 = R_{\Sigma 0} \left( \frac{k}{k_1} \right)^2 \left( \tan \frac{k_1 L}{2} / \tan \frac{kL}{2} \right)^2. \quad (3.25)$$

As can be seen from this expression, the resistance of the impedance radiator is greater than the resistance of the metal one with the same geometric length. In the case of the same electrical length, the resistance of the impedance radiator is significantly less—in full accordance with the theory of impedance antennas. If the surface impedance of a symmetrical antenna changes along its length (the antenna has a stepped structure), the expressions for the amplitudes and phases of current in segments are presented in the first part of the Section. The effective length of the segment  $n$  is

$$l_{en} = \frac{2I_n}{k_n I_N} \cos \varphi_n \left[ 2 \sin^2 \frac{k_n l_n}{2} + \tan \varphi_n \sin k_n l_n \right]. \quad (3.26)$$

In the case of an antenna with a resistive coating, the effective length is

$$l_e = \frac{2I_n}{k(1 + \delta^2/k^2)} \left[ \tan \frac{kL}{2} + \frac{\cos(j\delta L) - 1}{\sin kL \exp(j\delta L)} \right]. \quad (3.27)$$

Here  $\delta$  is the damping decrement in the coating material (in a transparent film).

As follows from the said, the Poynting method allows to obtain simple expressions for a radiation's resistance of various antenna options. It is assumed that in all considered antennas the current distribution along the axis of the radiator has sinusoidal character. In the case of in-phase currents distribution the effective length of the radiator depends on the variation law of a current amplitude along its axis. If the current amplitude changes in accordance with linear law, i.e.,  $J(z) = J(0)(1 - \zeta/L)$  the effective length of a symmetric radiator with an arm length  $L$  is equal to

$$R_{\Sigma 0} = 20L^2. \quad (3.28)$$



We consider a more complicated case, when two identical metal radiators are located in parallel without height shift. Let an active radiator  $A_1$  is located in the origin of a coordinates system, and a passive radiator  $A_2$  is located at a distance  $\rho = d$  from it. We determine the mutual impedance between two identical radiators. The field in the horizontal direction, created by the first radiator on the distance  $b$  from its axis, can be written as

$$E_{z1} = -E_{\theta1} = -j30J(0)kl_e \frac{1}{\epsilon_r b}. \quad (3.29)$$

The input impedance of a radiator is

$$Z_A = \frac{P}{J^2(0)} = \frac{1}{30J^2(0)} \int_0^\pi E_\theta^2 \sin\theta d\theta. \quad (3.30)$$

At that  $Z_A = R_A + jX_A$ , where  $R_A$  and  $jX_A$  are accordingly a real and an imaginary component of the input impedance. We will proceed from simple model, according to which

$$R_A = 20 (kl_e)^2 / (\epsilon_r b)^2, X_A = -W \cot kl. \quad (3.31)$$

Here  $l$  is the length of the equivalent long line. For a symmetric radiator with an arm length  $L = \lambda/4$  in accordance with the rigorous results, obtained from the solution of Leontovich's integral equation, these magnitudes are respectively equal to  $R_A = 73.2$  and  $X_A = 42.5$ . Since  $l_e = 2L \cdot \frac{2}{\pi} = 4L/\pi$ ,  $kl_e = 2$ ,  $\epsilon_r = 1$ , then equating the expression for  $R_A$  to the magnitude 73.2, we get:  $b = 1.045$ . If to assume that  $kl = \frac{\pi}{2} + kc$ , then similarly

$$42.5 = -W \cot (\pi/2 + kc) = W \tan kc,$$

whence

$$kc = \tan^{-1} (42.5/W) \cong 42.5/W.$$

The obtained results make it possible to calculate firstly the input impedance of a radiator with any length, if it is known for one length. As follows from the above, at  $L = \lambda/4$  the active component of the input impedance is

$$R_A = 20 (kl_e)^2 / (1.045\epsilon_r)^2.$$

At the same frequency, if the length of the radiator arm is  $L_1$ , then  $kl_e$  is equal to  $\tan \frac{kL_1}{2}$ , i.e.,

$$R_{A1} = R_A \tan^2 \frac{kL_1}{2} = 80 \tan^2 \frac{kL_1}{2} / (1.045\epsilon_r)^2. \quad (3.32)$$

The reactive component of a radiator with  $L = \lambda/4$  is approximately  $X_A = W \cot k(L + c)$ . If the length of the radiator arm is  $L_1$ , and the wave impedance is  $W_1$ , then

$$X_{A1} = -W_1 \cot k(L_1 + c_1) = -W_1 \cot k\left(L_1 + \frac{42.5}{W_1 k}\right). \quad (3.33)$$

Secondly, knowing the distance  $d$  between two identical radiator, one can determine the mutual impedance between them. The field created by the first radiator at a distance  $d$  from it similarly (3.29) is

$$E_{z2}(d) = -j30J(0)kl_e \frac{\exp(-jkd)}{\varepsilon_r (1.045 + d)}. \quad (3.34)$$

Since the field on a metal surface of a second radiator must be equal to zero, an antiphase current will appear in this radiator with the same distribution law along its axis. The field of this current in the direction perpendicular to a radiator axis is  $-E_{z2}(d)$ . The absolute value of this current and its field is  $m = \varepsilon_r (1.045 + d)$  times less than the current and field of the active radiator, and the power created in it is  $m^2$  times less than the power of the first radiator and is opposite to it in phase. This means that the mutual impedance of identical radiators located at a distance  $d$  from each other is equal to  $Z_{12} = Z_A m^2$ , where  $Z_A$  is the self-impedance, which is the identical for both radiators. It should be emphasized that the input impedances of radiators are the same, since the distance between the radiators is small compared to an infinite radius of a sphere, on which the radiated power is determined.

Figure 3 shows the well-known curves for the active ( $R_{12}$ ) and reactive ( $X_{12}$ ) components of the input impedance of a symmetric radiator with an arm length  $L = \lambda/4$ , calculated by the method of induced emf (see, for example, [5]). As can be seen from the figure, the dependence of  $R_{12}$  and  $X_{12}$  on the distance  $d$  is sinusoidal. Expressions (3.32) and (3.33) demonstrate the resembling dependence of these components from the distance between the radiators. If to replace the exponent in the numerator of the expression (3.34) by the sum of sine and cosine, it is easy to make sure, that an active component of a field is proportional to cosine, and a reactive component is proportional to sinus.

Let us compare with these curves our results obtained for the magnitudes  $R_{12}$  and  $X_{12}$  at the points of maximum, where the values of sines and cosines are equal to unity. On the curve for  $R_{12}$  these points are located at  $d/\lambda = 1.25, 2.25, 3.25$ . Here the input resistances  $R_{12} = 80/m^2$  are equal to 15.1, 7.3 and 4.3, i.e., the values  $m$  is respectively 2.3, 3.3 and 4.3. These values are close to shown in the figure. On the curve for  $X_{12}$  the points of maximum are located at  $d/\lambda = 1.0, 2.0, 3.0, 4.0$ , the magnitudes  $m^2$  are equal to 4.2, 9.3, 16.4 and 25.5, i.e.,  $m$  is 2.05, 3.05, 4.05 and 5.05. With their help, it is possible to determine the wave impedance  $W$  of the antenna. As can be seen from the graph, at the second of these points, where  $d = 2$  and  $m^2 = 9.3$ , the value  $X_{12}$  is equal to 9. This means that at  $d = 0$  the amplitude of the curve is equal to  $m^2 X_{12} = 84$ , i.e., in accordance with (3.30)  $W = 84$ . It is easy to verify that dividing  $W$  by  $m^2$  at the other points of the maximum gives magnitudes  $X_{12}$  at these points.

As follows from the above, the Poynting method provides the wide opportunities for calculating not only active, but also reactive impedances, both self and mutual. An equivalent circuit for the two radiators, considering a sphere of infinitely large radius, is shown in Fig. 4. The figure shows the self-resistance of an active radiator  $R_{\Sigma 11}$ , the mutual resistance of both radiators  $R_{\Sigma 12}$  and the self-resistance of a passive radiator  $R_{\Sigma 22}$ . If the decreasing function  $R_{12}$  is replaced by a step function, then there will be jumps of the curve at the boundaries of the segments.

An indisputable advantage of the described approach based on the Poynting method is the simplicity of obtaining results that coincide with the results of

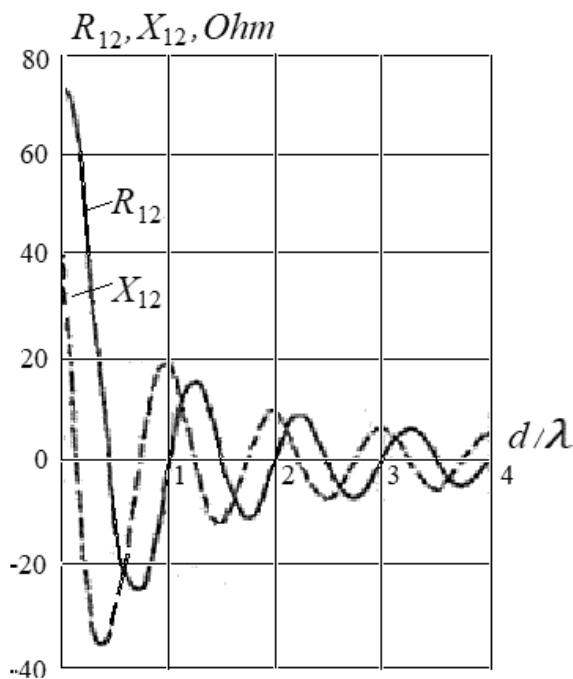


Fig. 3: Mutual resistance of radiation for two identical half-wave radiators.

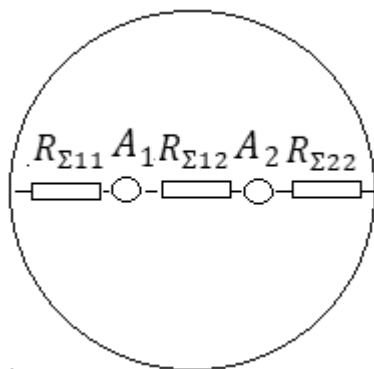


Fig. 4: Equivalent circuit of the system from two radiators.

calculations by the method of induced emf. The described technique for calculating the mutual resistance of two parallel radiators can be generalized to the case of radiators of different lengths and with a shift in height. In the first case (Fig. 5a), the value of the field in the passive radiator, determined by expression (3.34), will change in proportion to its length. In the second case (Fig. 5b), the value  $d$  in this expression should be replaced by the value  $d_1 = d/\sin \theta$ . Suppose, for example, that the active radiator ( $A_1$ ) lies on  $z$  axis, and its center coincides with the coordinates' origin (point O). The second radiator ( $A_2$ ) is in parallel to  $z$ -axis. The distance between the radiators' axes, as in the previous case, is equal  $d$ . The center of the second radiator lies on a straight line passing through the origin at an angle  $\theta$  to  $z$ -axis. The distance from it to  $x$ -axis (shift in height) is  $H$ . In this case, similar points of the radiators are spaced from each other at a distance  $d_1$ , and the field of the first radiator on the surface of the second one is

$$E_{z1}(d) = E_{z1}(0) \frac{\exp(-jkd_1)}{\varepsilon_r (1.045 + d_1)}. \quad (3.35)$$

Calculation of mutual resistances based on the indicated field values gives results that coincide with the graphs presented in [5]. Thus, the check confirms the coincidence of the results of calculations by the described method and the method of induced emf. It should be noted that here both a thin ideally conducting filament and a thin-walled cylinder may be used as models of a metal radiator. There are no fundamental differences between the results of their application.

Various variants of the mutual arrangement of the radiators are considered in [6], where is a systematic description of numerous results obtained by different authors by the method of induced emf for the self and mutual impedances of linear metal radiators. As a rule, they are reduced to the expressions consisting of integral sines, cosines, exponentials, and more complex functions. Therefore, they are rarely used and are replaced by numerical modeling based on the method of moments. As an example of the application of the method described above to the variants described

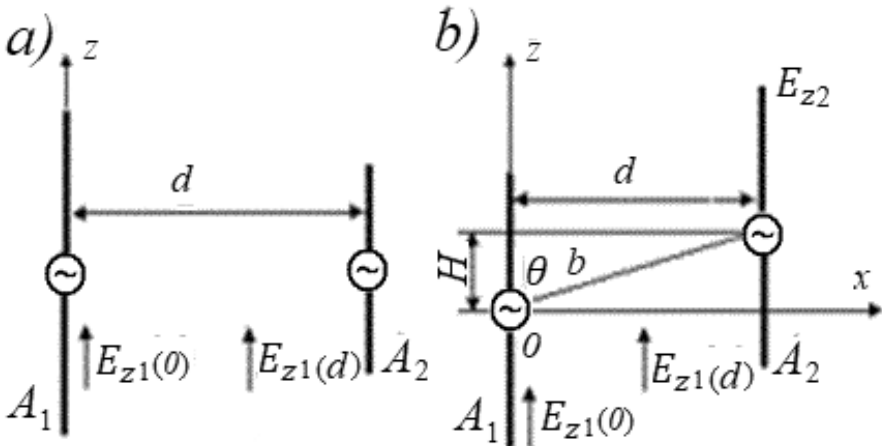


Fig. 5: Radiators of different lengths without a shift (a) and with a shift in height (b).

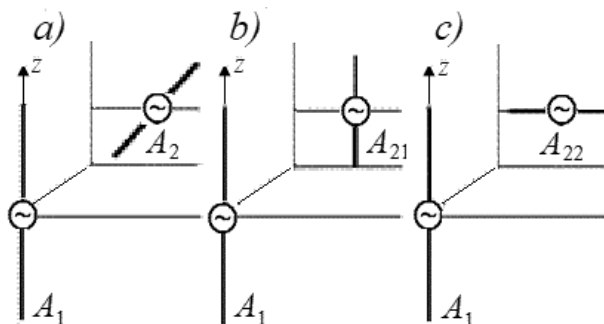


Fig. 6: Radiators of different lengths.

in [6], let us consider the calculation of the mutual impedance of two radiators with different lengths, arbitrarily located in two parallel planes and shifted in height (Fig. 6a). One of them ( $A_1$ ) is vertical, the other ( $A_2$ ) is inclined. Let's split the inclined radiator into two ones: vertical ( $A_{21}$ ) and horizontal ( $A_{22}$ ). Calculating the mutual resistance of radiators  $A_{21}$  and  $A_1$  (Fig. 6b) was described earlier. Radiators  $A_{22}$  and  $A_1$  (Fig. 6c) are located perpendicular to each other, and their mutual resistance is equal to zero.

Calculation of the electrical characteristics of the antenna, based on the use of the Poynting method, is one of the three main methods for analyzing the properties of the antenna along with solving integral equations for the current along the antenna wire and the method of induced emf. Each of these methods is applicable to different types of radiators: metal, slotted, impedance (with constant and stepwise impedance along the length of the antenna). The methods naturally complement each other and give similar results, confirming the rigor of the theoretical approach. Unfortunately, for various reasons the smaller attention to analyze the characteristics of different antenna variants was devoted to the Poynting method. The obtained here results confirm the usefulness and effectiveness of its use.

The next step in the theory of linear radiators was made in the twentieth century. It is known as the method of induced emf. But first, it is necessary to talk about the oscillating power theorem, which significantly changed the results of applying the method of induced emf.

### 3. Measurement of an Antenna Gain in a Fresnel Zone

The results of measuring an antenna directional pattern depend on the dimensions of an antenna proving ground. It is known, that when measuring directivity an observation point should be placed in a far zone of a radiator (in Fraunhofer zone). If the antenna dimensions are great in a comparison with a wavelength, the far zone boundary lies at the distance

$$R_0 = 2a^2/\lambda, \quad (3.36)$$

where  $a$  is the maximum dimension of the antenna, and  $\lambda$  is the wavelength. If the condition (3.36) is met, then the radius-vectors drawn from any antenna point to

an observation point are practically parallel one another, and the fields created by individual antenna elements in an observation point are close on a phase. At  $R < R_0$  the observation points fall within an intermediate zone (Fresnel zone). The limited sizes of a proving ground, and insufficient sensitivity of the measuring equipment frequently result in necessity to place receiving and transmitting antennas in the Fresnel zone (for example, during the gain measurement).

In this zone in difference from a reactive near zone (zone of induction) directly contiguous with an antenna, the active (radiated) power predominates above oscillating. In difference from a Fraunhofer zone the measured directional pattern depends on a distance between the antenna center and the spherical surface, which passes through observation points. The dependence of the directional pattern on a distance entails the directivity alteration and the corresponding gain change. For this reason, it is necessary to determine, how big is the error in a gain measurement for such placement of antennas.

The given problem in relation to linear radiators with different laws of current distribution is considered in [7]. The results were presented as the curves, which can be used as nomograms. In [8] it was described the method of calculating the gain of rectangular aperture in the Fresnel zone, and the calculation results for a uniformly exited antenna are given. This solution has analytical restrictions imposed on the calculation accuracy of fields created by the individual elements of aperture:

- (1) The segments  $R_l$  between these elements to an observation point are parallel to the radius  $R$ , which connects an antenna center with an observation point. It means (see Fig. 7) that the signals are coming in the observation point from the aperture in a form of a straight segment with the length

$$a = 2R \tan \alpha/2.$$

Here  $\alpha$  is the angle, at which the segment  $a$  is seen from the observation point. The signals come to this point from the curvilinear segment having the form of an arc with an aperture  $b = \alpha R$ . As a result, the signal in the observation point is greater than veritable, because  $a > b$ .

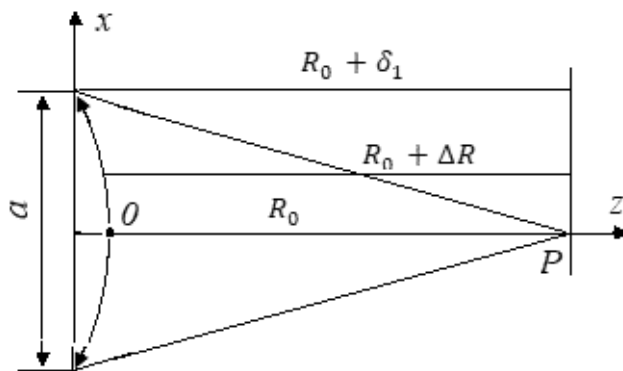


Fig. 7: The field of a broadside array.

- (2) The magnitude  $1/R_1 = 1/(R + \Delta R)$  is replaced by  $1/R$ , i.e., the difference  $\Delta R = R_1 - R$  is not taken into account.

In the method of analysis proposed in [9] in contrast to the method described in [8] a flat antenna is replaced by an equivalent no flat (convex) structure. The distance between any element of this structure and the plane, which passes through the observation point P parallel to the antenna, is equal to the distance between corresponding element of the antenna and the observation point, i.e., one can consider that rays from separate points of antenna to the observation point P are parallel. The suggested method is equivalent to the method of Polk, but it is distinguished from one by greater obviousness, since geometric interpretation of approximate solution is used herein. This permits firstly to select a shape and dimensions of convex structure in such a way as to remove the first analytical restriction and secondly to change the integrand denominator in such a way as to remove the second analytical restriction and to refine results obtained by Polk. In this Section simple expressions are obtained for calculating the error arising when measuring the antenna's gain. The error depends on dimensions of a studied antenna, a wavelength and a distance to receiving antenna, as well as on distribution of a field along an antenna's aperture. Measurement errors induced by repeated many times indirect reflections, reflections from ground and also by nonidentity of antennas are not considered here.

We will assume that antenna presented a broadside array that consists of number of radiating elements with the identical phase (Fig. 8). In the observation point P, located along a normal to the array center, the fields from antenna edges lag in phase from a central element field by  $\varphi = 2\pi\delta/\lambda$ , and, as it is clear from Fig. 7,  $(R_0 + \delta)^2 = R_0^2 + a^2/4$ . For  $\delta, a \ll R_0$

$$R^2 + 2R\delta \cong R^2 + (a/2)^2, \quad (3.37)$$

that is

$$\delta = a^2/(8R).$$

If an allowable path difference from the individual antenna elements is equal to  $\pi/8$ , i.e.,  $\delta = \lambda/16$ , then from this expression follows equality (3.36).

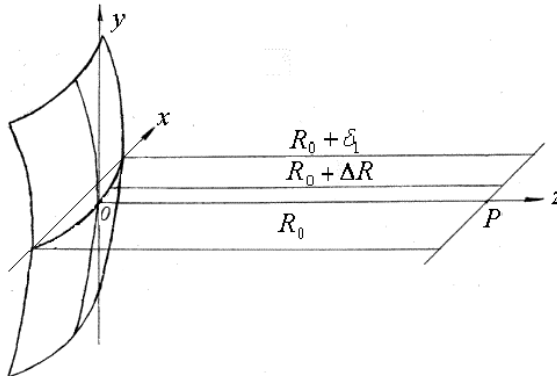


Fig. 8: The equivalent circuit of a broadside array.

If the segments from the antenna points to the observation point are parallel, then in order to consider the delay of fields of different antenna elements, the equivalent circuit of this structure should correspond to Fig. 8, and any radius  $R_1$  must be equal to

$$R_1 = R + \Delta R,$$

where likewise (3.37)

$$\Delta R = x^2/(2R). \quad (3.38)$$

Thus, to a path difference from different antenna elements was identical in the circuits with flat and convex antenna, the line of intersection of the convex antenna depicted in Fig. 8 with a plane  $xOz$  must be a parabola piece (with a length  $b$ ). The end point of a parabola is removed away axis  $x$  by a distance  $\delta_1 = a_1^2/(8R)$ . Let us consider in a first approximation that the parabola length is equal to

$$b_1 = a_1 \left[ 1 + \frac{2}{3} \left( \frac{2\delta_1}{a_1} \right)^2 \right] = a_1 \left( 1 + \frac{\delta_1}{3R} \right),$$

where  $b_1$  is the projection of this segment to axis  $x$ . In that case

$$a_1 = b_1 \left( 1 - \frac{\delta_1}{3R} \right). \quad (3.39)$$

In case of a rectangular arrays with the sides  $a_1$  and  $a_2$

$$R_1 = R + (x^2 + y^2)/(2R).$$

The length of an array projection to axis  $y$  is

$$a_2 = b_2 \left( 1 - \frac{\delta_2}{3R} \right),$$

where  $\delta_2 = a_2^2/(8R)$ .

The replacement of the field of a plane antenna (with the rays, converging to the point  $P$ ), by the field of the convex area (with the parallel rays) allows significantly simplify the field calculations. On the other hand, the field of the uniformly excited area of a convex shape, represented on Fig. 8, differs from a field of a plane area with parallel rays (such a field corresponds to an arrangement of the observation point in the far zone). The bigger are ratios  $b_1/R$  and  $b_2/R$ , the bigger is this difference. The difference between those fields is the magnitude of the error at the measurement in Fresnel zone.

To demonstrate this statement, we will determine the field of an elementary (infinitesimal) dipole of length  $dx$ , whose electrical current  $I_0$  is constant along the dipole length. This field is equal to

$$E_\theta = jZ_0 \frac{kI_0 \exp(-jkR_1)}{4\pi R} \sin \theta \, dx,$$



where  $Z_0 = 120\pi$ ,  $k = 2\pi/\lambda$ . Accordingly, the field of a direct dipole of a length  $a_1$  with current  $I_0$  along a normal to a radiator (for  $\theta = \pi/2$ ) is equal to

$$E_{\theta 0} = jZ_0 \frac{kI_0 \exp(-jkR)}{4\pi R} b_1,$$

The field of the dipole, located along parabola with an arm  $b_1/2$  is

$$E_{\theta 1} = jZ_0 \frac{kI_0 \exp(-jkR_1)}{4\pi R} J,$$

where

$$J = 2 \int_0^{b_1/2} \frac{\exp(-jk\Delta R)}{1 + \Delta R/R} dx = 2 \int_0^{b_1/2} \frac{\exp[-jkx^2/(2R)]}{1 + x^2/(2R)^2} dx.$$

Note that in order to correct the first analytical restriction the top limit  $a_1/2$  of integral  $J$  is replaced by  $b_1/2$ . In order to correct the second analytical restriction, one must add the magnitude  $\Delta R/R$  to the denominator 1 of an integrand.

Within the scope of a used physical model, when values  $kx^2/(2R)$  and  $x^2/(2R^2)$  are small and have the same order of smallness, we shall find:

$$J = 2 \int_0^{b_1/2} [1 - x^2 (1 + jkR)/(2R^2 - k^2 x^4/(8R^2))] dx = \\ b_1 [1 - a_1^2/(24R^2) - k^2 a_1^4/(640R^2) - jka_1^2/(24R)],$$

i.e., in accordance with (3.39)

$$E_{\theta 1} = E_{\theta 0} [1 - a_1^2/(12R^2) - k^2 a_1^4/(640R^2) - jka_1^2/(24R)].$$

For the direct dipole with length  $a_1$  Poynting's vector  $P_{10}$  is equal to

$$P_{10} = \text{Re}(E_{\theta 0} H_{\varphi 0}^*) = |E_{\theta 0}|^2/Z_0.$$

For the curved dipole

$$P_{11} = \text{Re}(E_{\theta} H_{\varphi}^*) = |E_{\theta 0}|^2 \text{Re} \frac{JJ^*}{a_1^2}/Z_0$$

where

$$\text{Re} JJ^*/a_1^2 = 1 - a_1^2/(6R^2) - k^2 a_1^4/(720R^2),$$

i.e.,

$$P_{11} = P_{10} [1 - a_1^2/(6R^2) - a_1^4/(18R^2 \lambda^2)].$$

For the convex uniformly excited area with the sides  $a_1$  and  $a_2$

$$P_1 = P_0 \prod_{i=1}^2 [1 - a_i^2/(6R^2) - a_i^4/(18R^2 \lambda^2)], \quad (3.40)$$

where  $P_0$  is the power created by a flat sector along the normal to it. The expression (3.40) allows to determine a ratio between maximum directivity factors of convex and plane antennas (with uniformly excited areas)

$$D_1/D_0 = \prod_{i=1}^2 [1 - a_i^2/(6R^2) - a_i^4/(18R^2 \lambda^2)].$$

If, for example, the observation point is located at the boundary of the Fresnel and Fraunhofer zones, then for  $a_1 = a_2$

$$a_i^2 = R_0 \lambda/2, a_i^2/(6R^2) = \lambda/(12R), a_i^4/(18R^2 \lambda^2) = 1/72,$$

and

$$D_1/D_0 = [0.9861 - \lambda/(12R)]^2 \approx 0.9724 - \lambda/(6R). \quad (3.41)$$

The formula above takes into account, that  $\lambda/(6R) \ll 1$ . Thus, the error of a directivity measurement in the far zone boundary in a comparison with measurements in the depth of a far zone is about 2.8% (0.12 dB). The result, close to this (0.06 dB), is obtained in [10] for the circular aperture. On a twice-smaller distance the error significantly increases:

$$a_i^2 = R\lambda, a_i^2/(6R^2) = \lambda/(6R), a_i^4/(18R^2 \lambda^2) = 1/18,$$

that is

$$D_1/D_0 = [0.944 - \lambda/(6R)]^2 \approx 0.892 - \lambda/(3R). \quad (3.42)$$

(more than 0.5 dB). The error  $\Delta D$  in decibels in the general case is equal to

$$10 \log_{10} (D_1/D_0) = 4.3 \ln(D_1/D_0) = 4.3 \sum_{i=1}^2 [1 - a_i^2/(6R^2) - a_i^4/(18R^2 \lambda^2)]. \quad (3.43)$$

Since at  $\alpha \ll 1$   $\ln(1 + \alpha) = \alpha$ , then

$$\Delta D_1 = -5.7[(\delta_1 + \delta_2)/R + 2.7(\delta_1^2 + \delta_2^2/\lambda^2)]db. \quad (3.44)$$

In accordance with the presented analysis the second term in parentheses of expression (3.43) is caused by increase of distance from a point of convex area to an observation point, and the third term is caused by a phase's difference of the signals. Both reasons result in total signal attenuation and in a diminution of measured directivity. The calculations demonstrate that the third term is greater than the second, but the second term is not small and affects the magnitude of the gain. If to neglect a first term in (3.44), we will obtain for a linear radiator with length  $a$

$$\Delta D_1 = -15.4\delta_1^2/\lambda^2 = -15.4(a^2/8R\lambda)^2 db.$$

Let  $R = Na^2/\lambda$ . Then  $\Delta D_1 = -0.24/N^2$ , that is at  $N = 0.5; 1; 2; 4$  the magnitude  $\Delta D_1$  is equal to 0.96; 0.24; 0.06; 0.01. This is entirely in agreement with results obtained in [7] by the direct calculation. At that

$$\log_{10} |\Delta D_1| = -(0.624 + 2 \log_{10} N),$$

i.e.,  $\log_{10} |\Delta D_1|$  and  $\log_{10} N$  are related by a linear correlation. This circumstance also is noted in [7].

Let us compare the obtained results with the results, presented in [8]. The proposed method mostly is equivalent to the method of Polk, but is more understandable that saves from occasional mistakes. Besides that,  $\Delta R$  in [8] is considered only in order to calculate a signal phase. In the proposed method an influence of  $\Delta R$  on the signal amplitude is also taken into account. This allows us at the calculation of fields to confine consistently by the magnitudes of the same order of smallness. An accuracy of proposed method of calculation corresponds to accuracy of a distance determination between a convex antenna element and an observation point. Furthermore, the difference between the length  $a_1$  of a straight segment connecting the parabola ends and the length  $b_1$  of a parabola herself is taken into account. This difference allows to consider the structures, where radiuses are not parallel. Integration in [8] that goes in our notation from  $-b_1/2$  to  $b_1/2$  causes increase of the antenna area dimensions and decrease of the calculation accuracy, i.e., resulting ratio  $D_1/D_0$  is higher than veritable.

The values of a ratio  $D_1/D_0$  for the in-phase square aperture, calculated by the proposed method and described in [8] are presented in the Table 2. They confirm previous remarks. It is seen from the table that at the boundary of far zone (more precisely, at the distance, which is considered usually as a boundary of a Fresnel zone and a Fraunhofer zone) the magnitude of gain error, calculated by the proposed method and by the method of Polk is practically the same (it is 3%). Analogous result is obtained in [11].

On the other hand, as easy to prove, at  $R \ll 2 a^2/\lambda$  the proposed method does not give a reasonable result, since a small number of a series terms under the integral sign is used in calculation. But this case corresponds to a gain measurement in a depth of Fresnel zone (far from a boundary with a zone of Fraunhofer), where the measurement accuracy is small, since a radial component of field and an oscillating power are great, and this circumstance increases the error magnitude. Graphs showing a gain error as functions of a magnitude  $\alpha = a/\sqrt{2\lambda R}$  at different values of  $a_2/a_1$  are given in [8]. They are built in accordance with the article of Polk. It is necessary to note that in these Figures a maximal value of  $\alpha$  is 1.5 that corresponds to a magnitude  $R/(2a^2/\lambda) = 0.111$ . At that dot the relative error is close to 100%. The expression (3.40) allows determining the error of the measuring gain in case of uniformly exited radiators. Examples of such radiators are antenna arrays with uniform excitation of rows and uniform excitation of elements in each row.

In some cases, the field along an antenna aperture is distributed in accordance with the cosine law (for example, field along a horn aperture). Let's consider a field of

**Table 2:** Ratio  $D_1/D_0$  for a Square In-phase Aperture.

$R/(2 a^2/\lambda)$	The proposed method	[8]
1	$0.9724 - \lambda/(6R_0)$	0.9726
0.5	$0.884 - \lambda/(3R)$	0.895
0.25	$0.605 - 2\lambda/(3R)$	0.641
0.167	$0.250 - \lambda/R$	0.383

a curved dipole with an arm  $a_1/2$  and a current  $I = I_0 \cos(\pi x/a_1)$ . The field's magnitude is calculated as earlier by the formula (3.1), however

$$J_1 = 2 \int_0^{b_1/2} \frac{\exp(-jkx^2/2R)}{1+x^2/(2R)^2} \cos(\pi x/a_1) dx.$$

If to limit oneself, as was done earlier, by magnitudes of the first order of smallness, we shall find:

$$J_1 = 2 \int_0^{b_1/2} [1 - x^2 (1 + jkR)/(2R^2) - k^2 x^4/(8R^2)] [\exp(j\pi x/a_1) + \exp(-j\pi x/a_1)] dx.$$

Integration of an expression for  $J_1$  gives:

$$J_1 = 2a_1/\pi [1 - a_1^2/(40R^2) - k^2 a_1^4/(160\pi^2 R^2) - jka_1^2/(40R)].$$

The field of a direct dipole with length  $a_1$  and with cosine distribution of a current along a dipole is

$$E_{\theta 2} = 2 E_{\theta 0}/\pi.$$

For the curved dipole at  $\theta = \pi/2$

$$E_{\theta 3}/E_{\theta 2} = J_1 \pi/(2a_1) - a_1^2/(40R^2) - k^2 a_1^4/(160\pi^2 R^2) - jka_1^2/(40R).$$

Accordingly, the power density, created by a planar area, if the field along one of its sides (with length  $a_1$ ) is distributed in accordance with the cosine law, and along other side (with length  $a_2$ ) is fixed, is equal to

$$P_2 = 2P_0/\pi.$$

The power density of no planar area with the same distribution of fields

$$P_3 = P_2 [1 - a_1^2/(20R^2) - a_1^4/(40R^2 \lambda^2)] [1 - a_2^2/(6R^2) - a_2^4/(18R^2 \lambda^2)].$$

i.e., error in the gain's measurement, in decibels is

$$\Delta D_3 = -5.7[(0.3\delta_1 + \delta_2)/R + (1.2\delta_1^2 + 2.7\delta_2^2)/\lambda^2]. \quad (3.45)$$

As it is seen from (3.44) and (3.45), here an error in gain's measurement is smaller than in case of uniformly excited antenna. If the excitation decreases to both edges of an array under the linear law, the magnitude  $\Delta D$  decreases more strongly. It is known, that the field  $E_\theta$  of a direct dipole of length  $a_1$  with linear current distribution along an arm  $I = I_0 (1 - 2x/a_1)$  is equal to half of a field of dipole with a current  $I_0$ , i.e.,

$$E_{\theta 4} = E_{\theta 0}/2.$$

For the curved dipole

$$J_2 = 2 \int_0^{b_1/2} \frac{\exp(-jk\Delta R)}{1 + \Delta R/R} (1 - 2x/a_1) dx = J - \Delta J.$$

where  $J$  was calculated earlier, and  $\Delta J$  is equal to

$$\Delta J = 4/a_1 \int_0^{b_{1/2}} x \frac{\exp(-jkx^2/2R)}{1 + x^2/(2R^2)} dx = 4/a_1 \int_0^{b_{1/2}} x [1 - x^2 (1 + jkR)/(2R^2)] dx,$$

i.e.,

$$\Delta J = a_1/2 [1 - 7a_1^2/(48R^2) - k^2 a_1^4/(384R^2) - jka_1^2/(16R)],$$

whence

$$J_2 = a_1/2 [1 - a_1^2/(48R^2) - a_1^4/(48R^2 \lambda^2) - j\pi a_1^2/(24R\lambda)],$$

and

$$E_{\theta 5}/E_{\theta 4} = 2J_2/a_1 = 1 - a_1^2/(48R^2) - a_1^4/(48R^2 \lambda^2) - j\pi a_1^2/(24R\lambda).$$

If  $P_4$  is the power created by a planar area with currents, falling down to its edges under the linear law, then

$$P_4 = P_0/4.$$

The power of convex antenna with the same distribution is

$$P_5 = P_4 \prod_{i=1}^2 [1 - a_1^2/(24R^2) - a_1^4/(41R^2 \lambda^2)].$$

Accordingly, the error of gain's measurement, in decibels is

$$\Delta D_5 = -4.3[(\delta_1 + \delta_2)/3R + 1.6(\delta_1^2 + \delta_2^2/\lambda^2)].$$

Thus, if the antenna aperture is excited not uniformly and the field falls to array edges, the error of measurements decreases. Figure 9 presents the calculation results of the value  $\Delta D$ , in decibels, for the distance  $R = 5m$  between the antenna and the observation point. The magnitude  $\Delta D$  is given as a function of frequency for different antenna dimensions (in meters), including 0.3 m, 0.4 m and 0.5 m. For square antennas with the side  $a_1$  the magnitude  $\Delta D$  is given as continuous curve, for linear ones with the lengths  $a$  a magnitude  $\Delta D$  is given as dashed line. Figure 9a presents the curves for antennas with uniform excitation and Fig. 9b shows the curves for antennas with not uniform excitation, falling to edges under the linear law.

The results of the measurement of the error magnitude for the square antenna with a side 0.5 m at three frequencies of a range are denoted by circles. Antennas under study are planar co-phased broadside arrays consisting from vertical half-wave micro-strip radiators with operating frequencies 6, 8 and 10.4 GHz. The gain was measured at the distance 5 m and in the far zone. Measurements at the distance 5 m were performed in anechoic chamber of length 7.5 m and at an open test bench of the length about 30 m. The measurements in the far zone also were accomplished at this open test bench. The distance between an antenna under study and a measuring antenna was 25 m. The error of measurement is assumed to be the difference of the mentioned magnitudes. They are pointed in Fig. 9a by circles. Measurements were made by the standard procedure using the device Vector Network Analyzer.

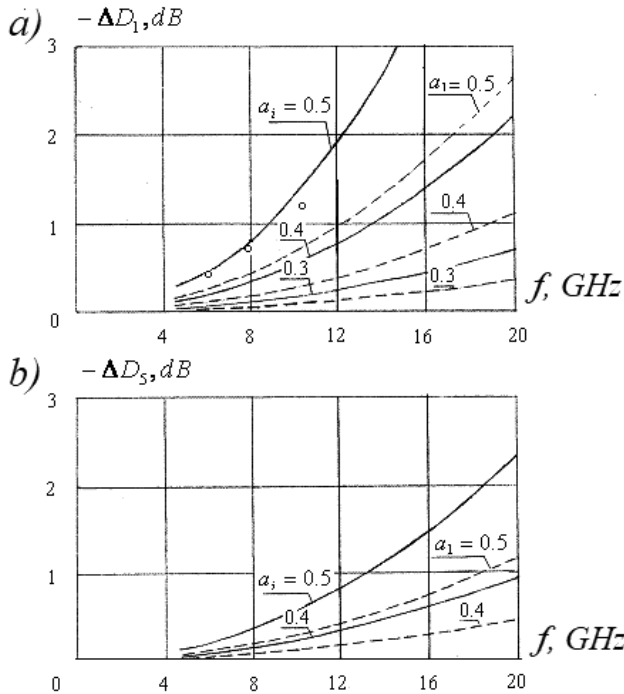


**Fig. 9:** The calculation results for the magnitude  $\Delta D$ : a – for antennas with uniform excitation, b – for antennas with no uniform excitation, falling to edges under the linear law.

The results of calculation and experiments showed that the proposed method of the error calculation at a measurement of directivity of two-dimensional antenna placed in a Fresnel zone is different from the well-known method by greater clarity and allows defining more exactly an error magnitude by means of more rigorous calculating dimensions of radiating surface and by means of taking into consideration an effect of distances between antenna points and observation point on the amplitude of received signal.

If the considered antenna is a broadside antenna with the constant phase and the measuring antenna is in its Fresnel zone, a measured gain always is less than the true, since fields' phases from antenna edges do not coincide with a field phase from its middle. The measurement error is determined by sizes of both antennas. Therefore, the measuring antenna must have small dimensions. With a frequency growth, if antenna's dimensions (geometric dimensions and dimensions in wavelengths) are constant and a distance between them is the same, the error is increasing. In the case of not uniform excitation, which is decreasing to edges, the error is smaller, than in case of uniform excitation.

#### 4. Oscillating Power Theorem

The theorem and its proof for the first time were published in the book [13]. The book was based on lectures delivered by the author for undergraduate and graduate

students and was devoted to electromagnetic waves of ultra-high frequencies. This theorem considers the process of continuous movement of instantaneous power from one element (capacitor, inductor) to another one and from one area of space to another one in accordance with the sinusoidal nature of currents and fields. The reaction of many specialists to the theorem about oscillating power was extremely negative. In their view, this theorem was caused by misunderstanding of the sense of the reactive power. Most experts considered the theorem to be erroneous. This opinion prevailed despite the well-known postulate, which these experts constantly repeated in articles and lectures. The postulate contends that the reactive power has no physical meaning.

Over the years since the first publication, the famous theorem has answered many questions. Let us start with the so-called symbolic method, i.e., with writing equations of the electromagnetic field in a complex form. Widely used electromagnetic fields, time-varying in accordance with sinusoidal law, are called harmonic or monochromatic fields. Both in the theory of alternating currents and in the field theory it is expedient in mathematical researches of harmonic processes, which are described by linear equations, to introduce complex magnitudes. The transition to these designations is performed in the following way. Complex magnitudes, designated as  $E(\omega)$  and  $H(\omega)$ , correspond to magnitudes of electric  $\vec{E}(t)$  and magnetic  $\vec{H}(t)$  fields at a given point. The relation between the physical quantities and their complex values is given by the following expressions:

$$\vec{E}(t) = \text{Re}[E(\omega)\exp(j\omega t)], \quad \vec{H}(t) = \text{Re}[H(\omega)\exp(j\omega t)], \quad (3.46)$$

Here  $\text{Re}A$  is a real part of a complex magnitude, located in the square brackets,  $\omega$  is the circular frequency of the investigated process. Complex magnitudes  $E(\omega)$  and  $H(\omega)$ , related with the instantaneous values by the relations of the type (3.46), correspond to two scalar physical magnitudes  $E(t) = E \cos \omega t$  and  $H(t) = H \cos \omega t$ . If  $E(\omega)$  and  $H(\omega)$  are complex magnitudes:

$$E(\omega) = E \exp(j\alpha), \quad H(\omega) = H \exp(j\beta), \quad (3.47)$$

where  $E$  and  $H$  are the amplitudes, and  $\alpha$  and  $\beta$  are the arguments of the complex magnitudes, then

$$E(t) = E \cos(\omega t + \alpha), \quad H(t) = H \cos(\omega t + \beta).$$

Thus, the amplitudes of the complex magnitudes are the amplitudes of the corresponding instantaneous values of the physical quantities, and the arguments of the complex magnitudes determine the phases of the instantaneous values of these quantities. Similarly, complex magnitudes are introduced for all physical magnitudes, incoming in Maxwell equations. Formal coupling of complex equations with the initial equations is simple: in order to obtain complex equations, one must replace the differentiation operator  $\partial/\partial t$  by the operator of multiplication  $j\omega$ .

As is well known, the energy is determined by product (or by square) of instantaneous values of fields and currents, i.e., by the magnitude

$$a(t)b(t) = \frac{1}{2} AB [\cos(\alpha - \beta) + \cos(2\omega t + \alpha + \beta)]. \quad (3.48)$$

This magnitude, average for the oscillation period  $T$ , is equal to

$$\overline{a(t)b(t)} = \frac{1}{T} \int_0^T a(t)b(t)dt = \frac{1}{2} AB \cos(\alpha - \beta) = \frac{1}{2} \text{Rea}(\omega) b^*(\omega).$$

Similar expression is true also for vector magnitudes. These expressions permit to calculate the average value (constant part) of the energy quantity in accordance with the known complex amplitudes. A similar method can be used for definition of the average value of the variable energy (of an oscillating energy). Indeed, according to (3.48)

$$a(t)b(t) = \overline{a(t)b(t)} + \tilde{\Theta},$$

where it is naturally to assume that the time-dependent second term

$$\tilde{\Theta} = \frac{1}{2} AB \cos(2\omega t + \alpha + \beta) \quad (3.49)$$

is the oscillating fraction of the product  $a(t)b(t)$ . This part oscillates in time with a frequency  $2\omega$ , and its average value is zero. One can rewrite the expression (3.49) as

$$\tilde{\Theta} = \frac{1}{2} \text{Re}[a(\omega)b(\omega)\exp(2j\omega t)].$$

It is seen that half the product of complex amplitudes is the complex amplitude of the oscillating fraction of the product  $a(t)b(t)$ .

As is well known, the energy conservation law for the electromagnetic field is given by expression

$$\frac{dW}{dt} + P + \Sigma = 0. \quad (3.50)$$

Here  $W$  is electromagnetic energy contained in a volume  $V$ ,  $P$  is the source power (it flows out the volume through its boundary surface), and  $\Sigma$  is the radiation power. Passing from the differential formulation to the integral formulation and using the appropriate complex magnitudes, one can write the oscillating power theorem in the form

$$-\tilde{\Sigma} = \tilde{P} + 2j\omega\tilde{W}.$$

Each term of this expression is the sum of the active magnitude (average for the period of oscillation) and the oscillating (variable) fraction. For an instantaneous value of the power flow one can write according to (3.50)

$$p(t) = \bar{P} + \tilde{P}. \quad (3.51)$$

where  $\bar{P} = \text{Re}(EH^*)$ ,  $\tilde{P} = \text{Re}[EH\exp(2j\omega t)]$ .

From here the physical meaning of magnitudes  $EH^*$  and  $EH$  is clear. The first magnitude is the complex amplitude of the active part of the power flow, equal to its average value. The second magnitude is the complex amplitude of the oscillating part of the power flow. In accordance with the law of conservation of energy, if the source of radiation is located inside of a closed surface, then the active (average for



the period of oscillation) power, supplied by the source, is equal to the active power, passing through a closed surface. It is natural to assume that this equality of powers is true for any time, i.e., the oscillating part of the power, supplied by the source, is equal to the oscillating part of the power, passing through a closed surface. Equality (3.51) shows that the instantaneous power consists from the active power and the oscillating power. Reactive power  $\frac{1}{2} \text{Im}(EH^*)$  does not have the physical meaning.

As will be shown in the next Section, the oscillating power theorem has significantly changed the understanding of the method of induced emf. Another example is the losses of asymmetric vertical antenna in earth and a grounding. For a long time, the calculation of losses in a grounding was executed according to the procedure of Brown [14]. This procedure proceeds from an idea of a high ground conductivity, owing to which a magnetic field at the ground surface is virtually identical to a magnetic field of an antenna, located above a perfectly conducting ground, and its strength is equal to the surface current density in the ground. The calculation of a loss resistance is reduced to an integral, which unlimitedly grows, and, consequently, the resistance also unlimitedly grows.

New method of calculating an additional antenna resistance caused by a non-ideal conductivity of the ground (as authors called the resistance of losses in the ground), was proposed and published in 1954 [15]. The magnitude of the loss resistance turned out to be finite. But the calculation method was an intricate procedure, using direct and inverse Fourier-Bessel transformation. A similar result was obtained, using the oscillating power theorem [16]. An analysis showed that the cause of the infinite growth of resistance loss in the Brown procedure was the use of the concept of complex power. Use of an oscillating power allowed not only to simplify calculation, but also to discover the mistake. A detailed comparative description of the different calculation methods and the obtained results is given in [17].

## 5. Method of Induced Emf and an Antenna Reactance

The method of induced emf was proposed in 1922 by Rojansky and Brillouin simultaneously. Klazkin was the first who used it for calculating radiator characteristics. Later on, Pistolkors, Tatarinov, Carter, Brown et al. have contributed to its development. A reference list in the book [6], devoted to the verification and generalization of the available in the literature results, obtained by this method, consists of 96 titles. The method of induced emf allows determining both the active and reactive components of the antenna input impedance. Since the active component can be calculated with a similar accuracy by a simpler method of Poynting (see Section 2), the method of induced emf with time, as emphasized in [18], has for practical purposes become only one of the methods for determining the input reactance of the antenna.

The oscillating power theorem has significantly changed the understanding of the method of induced emf, which for a long time has been the only way to calculate an antenna input reactance. The method of induced emf is formulated as follows.

A cylindrical radiator of height  $2L$  and radius  $a$  is placed inside a closed surface. A complex power, passing through this surface, is equal to a complex power, created by the emf source (by a generator). Assume that the closed surface is a circular cylinder of a height  $2H$  and radius  $b$ , along the axis of which the symmetrical radiator is located (see Fig. 1). A density of power flow, which deserts a volume, bounded by a closed surface, is determined by the Poynting vector, or more precisely by projections of Poynting vector onto the normal to the elements of the surface, i.e., to the sides and end faces of the cylinder. These projections have the following forms

$$P_{\rho} = -E_z H_{\varphi}^*, P_z = E_{\rho} H_{\varphi}^*. \quad (3.52)$$

Here the effective values of  $E$  and  $H$  are used.

Let the cylinder surface coincides with a surface of the radiator, i.e.,  $H = L$ ,  $b = a$ . Then, if the radiator radius is small, the flow of power, passing through the upper and lower covers of the cylinder, will also be small. Therefore, power passing through a closed surface is determined by integrating only over the side surface of the cylinder:

$$P_1 = \int_{-L}^L \int_0^{2\pi} P_{\rho} a d\varphi dz.$$

The power  $P_{\rho}$  is determined from (3.52) and does not depend on the coordinate  $\varphi$ , because the field components do not depend on it. Taking into consideration that  $H_{\varphi}^* = J^*(z)/(2\pi a)$ , we obtain

$$P_1 = - \int_{-L}^L E_z J^*(z) dz.$$

If a current  $J(z)$  is excited by a single generator, located in the middle of a radiator, then a power, created by it, is

$$P_2 = |J(0)|^2 Z_A,$$

where  $Z_A$  is an antenna input impedance. Equating the complex power, created by the source of emf, to the complex power, passing through the closed surface, we obtain

$$Z_{A1} = - \frac{1}{|J(0)|^2} \int_{-L}^L E_z J^*(z) dz. \quad (3.53)$$

The expression (3.53) reveals the essence of the method of induced emf. The other variant of deducing this expression is described in [19].

If to equate two analogous oscillating powers instead of complex powers, namely the power  $P_{K1}$  passing through the closed surface

$$P_{K1} = - \int_{-L}^L E_z J(z) dz, \quad (3.54)$$

and the power  $P_{K2}$  created by a generator,

$$P_{K2} = eJ(0) = J^2(0) Z_A, \quad (3.55)$$

where  $e$  is the emf of a generator, then we will obtain

$$Z_{\text{in}} = -\frac{1}{J^2(0)} \int_{-L}^L E_z J(z) dz. \quad (3.56)$$

As follows from what has been said, the expression for oscillating power differs from the expression for reactive power by the absence of an asterisk denoting complex conjugate values. Therefore, the expression (3.56) for the input impedance of the radiator, derived from the equality of oscillating powers, also differs from the expression (3.53), based on the equality of complex powers, by the absence of an asterisk.

After the appearance of an equality (3.56), equality (3.53) has been called the first formulation of the method of induced emf and the expression (3.53)—the second formulation of this method. The expression (3.53) was first obtained on the basis of the theorem of reciprocity [20–22]. The theorem of reciprocity holds not only for two separate antennas but also for two points on the same antenna. Using that circumstance and applying the theorem to one radiator, one can obtain the expression (3.56). As it is shown here, if to use the concept of oscillating power, then this expression is easily deduced from the energy relations. But even though the expression (3.56) was obtained by means of the oscillating power theorem many years ago [23], most experts kept arguing that it is derived in accordance with the reciprocity theorem in contrast to the expression (3.53), which is obtained by proceeding from an equality of powers. As can be seen from the above, the difference between the first and second formulations is caused by the fact that the first one is based on the equality of complex powers, consisting of the real and reactive component, and the second one—on the equality of the total (summary) powers, consisting of the active and oscillating components. Even here an advantage of the second formulation is obvious, since, as was said above, a reactive power unlike the oscillating power does not have physical meaning.

Indeed, the fact of the presence of oscillating powers is objectively substantiated in the book [13]. The oscillating power is a result of the existence of currents and voltages, the instantaneous values of which vary in time according to a sinusoidal law. By itself, the symbolic method that replaced the sinusoidal dependence of the current on time  $i(t) = I \sin \omega t$  by the exponential one  $i(t) = I \exp(-j\omega t)$  was convenient since it facilitated the calculations. At the same time, there was a temptation to use the second summand of the exponential function as a voltage, and this unreasonable temptation turned into a constantly refuted and simultaneously used reactive power.

Analysis shows that the second formulation is stationary. This fact is its undoubted advantage. To verify this, one must show that, if the antenna current is changed by the value of a first order of smallness, then the input impedance will change by a magnitude of the second order. The input impedance obtained from (3.56) does not change in the first approximation for any distribution of the trial current, which differs from the true current  $J^0(z)$  by a small magnitude  $\delta J(z)$ . This means that if at  $J(z) = J^0(z)$  a self-impedance of the radiator is equal to  $Z_{\text{in}}^0$  then on  $J(z) = J^0(z) + \delta J(z)$  the self-impedance is also equal to  $Z_{\text{in}}^0$ . The corresponding proof was given by J.E. Storer and is described in [24]. As shown in [18], the stationary property of the second formulation is due to the fact that the integral in the expression

(3.56) is a rough functional of the current function, although an integrand is no rough functional of this function.

Let a straight perfectly conducting filament of a small finite radius  $a$ , whose axis coincides with  $z$ -axis, is located in a lossless medium and is used as a model of a vertical symmetrical dipole with arm length  $L$  (see Fig. 1.1a). The current along it is defined by the expression (1.21), i.e., a tangential component of the electric field along a radiator surface is determined by the expression (1.25). In this case both formulations of the method of induced emf give the same result for the components of a dipole input impedance:

$$\begin{aligned} R_A &= \frac{30}{\sin^2 \alpha} [2(C + \ln a - Ci2\alpha) + \sin 2\alpha(Si4\alpha - 2Si2\alpha) + \cos 2\alpha(C + \ln a + Ci4\alpha - 2Ci2\alpha)], \\ X_A &= \frac{30}{\sin^2 \alpha} [\sin 2\alpha(C + \ln a + Ci4\alpha - 2Ci2\alpha - 2\ln L/a) - \cos 2\alpha(Si4\alpha - 2Si2\alpha) + 2Si2\alpha]. \end{aligned} \quad (3.57)$$

Here  $Si x = \int_0^x \frac{\sin u}{u} du$  is an integral sine,  $Ci x = \int_0^x \frac{\cos u}{u} du$  is an integral cosine,  $\alpha = kL$ , and  $C = 0.5772 \dots$  is the Euler's constant.

As can be seen from the expression for antenna reactance,  $X_A$  consists of terms of different order of smallness. The large member inside square brackets does not depend on the frequency. This member gives the summand

$$X_{A0} = -30 \frac{\sin 2\alpha}{\sin^2 \alpha} \cdot 2(\ln L/a - C/2) \approx -120 \ln \frac{L}{1.335a} \cot \alpha.$$

The magnitude  $\chi \approx 1/\Omega$  is called a small parameter of the thin antennas' theory ( $\Omega$  is a parameter, used by Hallen). Let the parameter  $\chi$  is equal to  $\chi = 0.5/(\ln(L/a))$ . Introducing the notation  $W = 60/\chi$ , we obtain an expression for the input reactance of an equivalent long line, open at the end:

$$X_{A0} = -W \cot \alpha.$$

The results of calculations using formulas (3.53) and (3.56) show that the difference between them occurs in the presence of losses in the radiator. Indeed, the current along an ideally conducting metal conductor is determined by the expression (1.21) and is a sine wave. Comparison of expressions (3.53) and (3.56) shows that in the case of a sinusoidal distribution, they are almost the same: in the numerator and denominator of one expression the product of complex conjugate magnitudes is present, and in the numerator and denominator of another expression the product of their real magnitudes is present. The difference was first observed while calculating the losses in antenna conductors (namely while calculation of the losses from the skin effect). In order to determine these losses, one must add a small imaginary magnitude to a purely real propagation constant. In this case the calculation in accordance with the second formulation gave a positive value for losses and the calculation in accordance with the first formulation—a negative one. A similar situation arises when calculating the losses in the magneto-dielectric sheath of impedance antenna.

Calculation of a loss resistance in the ground also confirms the correctness of results received by means of the oscillating power theorem (see Section 6). Thus, the calculation of losses in the medium and in the antenna revealed that application of concept of reactive power is an obvious mistake. The rightness of the second formulation, based on the conception of oscillating power, became a fact. The coincidence of the results of calculations based on using different formulations in the absence of losses in the antennas and the environment shows that in this case the results of the calculations performed in accordance with expression (3.53) are correct. The possibility of their use is beyond question. In the presence of losses, a calculation practically reduces to calculating an input impedance with a real propagation constant  $k$  (its result does not depend on the choice of formulation) and to replacing real value of  $k$  by a complex quantity with the subsequent highlighting and calculating of an additional component of the input resistance.

The second formulation of the method of induced emf was studying, when integral equations of Hallen [25] and Leontovich [26] for the current along a radiator axis were already written and solved. The obtained solutions were given in the form of expansions into a power series. If to use the formulas, presented in [27] and [26], one can show that the solutions of both equations are the same [28]. In this case, the coincidence of the results is not only numerical. The results were obtained in an explicit form (in the form of identical tabulated functions). As already mentioned, solutions, obtained by method of induced emf for the perfectly conducting filament, with using different formulations, gave identical results. They coincide with the solutions of integral equations for radiators with different length, if this length is not close to the parallel resonance (when  $J(0) \approx 0$ ). In the latter case, the input impedance, calculated by the method of induced emf, becomes infinitely large, whereas the integral equations give the finite results.

Summarizing, one can say that both formulations of the method of induced emf are based on the same two theses. The first thesis assumes the sinusoidal character of the current distribution along the radiator. The second thesis signifies the equality of the source power and the power passing through the closed surface. Both formulations are useful only in the case when the current distribution  $J(z)$  along a radiator is known. The selection of the law of the current distribution may be based only on a solution of integral equations for the current, i.e., on a rigorous solution of the problem. Physical basis for the selection of another distribution law does not exist. Hence there is no sense in speaking about the accuracy of the method of induced emf, excluding artificially the error caused by the inexact current definition. The accuracy of this method is the mutual accuracy of expressions (1.21) and (3.53) or (3.56). The calculation experience has shown that (1.21) gives a quite acceptable approximation, until the value of  $\alpha$  is not close to  $\pi/2$ . As to the second thesis, used for derivation of the first formulation, its inapplicability is obvious, since the reactive power has no physical sense, and the input reactance of antenna determined by equating two such quantities also does not have the physical sense. It is difficult to justify the equality of two such quantities. The use of the second formulation significantly improves the results.

The method of induced emf may be used for analyzing more complicated radiators. The expressions (3.53) and (3.56) were obtained without indicating a

concrete coordinate of a feeding point. For this reason, they are applicable to the radiator with  $h \neq 0$ . Really for a radiator with a feed point displaced from the radiator center to point  $z = h$  (Fig. 1.1b) the flow of an oscillating power through the side cylinder surface similarly to an expression (3.54) is

$$P_{K1} = -\int_{-L}^L E_z J(z) dz.$$

The oscillating power created by one generator similarly to an expression of (3.55) is

$$P_{K2} = eJ(h) = J^2(h) Z_A.$$

By equating the right parts of these expressions, we come to

$$Z_A = -\frac{1}{J^2(h)} \int_{-L}^L E_z J(z) dz.$$

Note that in this expression unlike (3.55) not only the denominator other, but also another current distribution  $J(z)$  along the radiator and another field magnitude  $E_z(J)$ .

In the case of a radiator with nonzero surface impedance (Fig. 10) in (3.56) instead of  $E_z(J)$  one must substitute the difference  $E_z(J) - H_\phi Z(z)$ . Here  $Z(z)$  is the surface impedance, i.e., the impedance of the surface section. Actually, in accordance with the boundary condition on the radiator surface, it is necessary to consider that a voltage drop along a radiator makes no contribution to its radiation. Then for an antenna segment with constant surface impedance  $Z$  (Fig. 10a) in a shape of a straight circular cylinder with radius  $a$  we find

$$Z_A = -\frac{1}{J^2(h)} \int_{-L}^L [E_z(J) - ZJ(z)/(2\pi a)] J(z) dz. \quad (3.58)$$

If  $h = 0$  the current distribution  $J(z)$  coincides in the first approximation with the current distribution along an impedance long line, open at the end:

$$J(z) = J(0) \sin k_1 (L - |z|) / \sin k_1 L. \quad (3.59)$$

Here  $k_1 = \sqrt{k^2 - j2k\chi Z/(aZ_0)}$  is the propagation constant of a wave along the impedance line.

The input impedance of a symmetrical radiator with piecewise constant surface impedance (Fig. 10b) is equal to

$$Z_A = -\frac{1}{J_N^2} \sum_{n=1}^{2N} \int_{b_{n+1}}^{b_n} [E_z(J_n) - Z^{(n)} J_n(z)/(2\pi a)] J_n(z) dz. \quad (3.60)$$

where  $n$  is the segment's number,  $2N$  is the total number of segments,  $Z^{(n)}$  is the surface impedance of a segment  $n$ . Current distribution  $J_n(z)$  on each segment  $n$  is sinusoidal. Current distribution  $J(z)$  along the radiator coincides in the first approximation, if  $h = 0$ , with the current distribution along a stepped impedance long line open at the end:

$$J_n(z) = I_n \sin(k_n z_n + \varphi_n), \quad b_{n+1} \leq z \leq b_n, \quad (3.61)$$

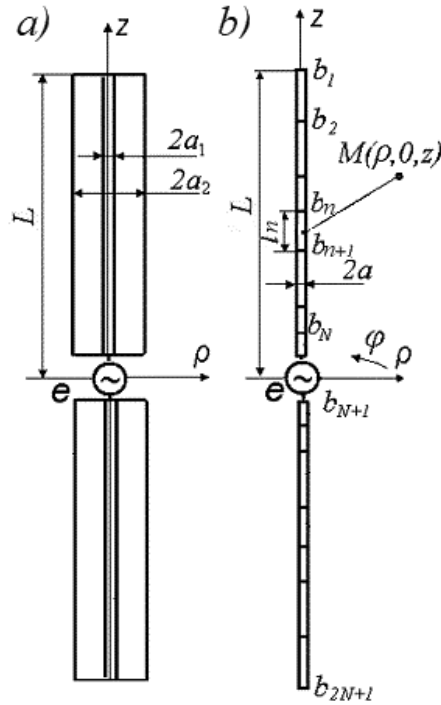


**Fig. 10:** Antennas with constant (a) and piecewise constant (b) surface impedances.

where like to expressions presented in Section 3.2

$$I_n = A_n J(0), \quad A_n = \prod_{p=n+1}^N = \sin \varphi_p / \sin(k_{p-1} l_{p-1} + \varphi_{p-1}),$$

$$\varphi_n = \tan^{-1} \left\{ \frac{k_n}{k_{n-1}} \tan \left[ k_{n-1} l_{n-1} + \tan^{-1} \left( \frac{k_{n-1}}{k_{n-2}} \tan \left[ k_{n-2} l_{n-2} + \dots + \tan^{-1} \left( \frac{k_2}{k_1} \tan k_1 l_1 \right) \dots \right] \right) \right] \right\}.$$

In these expressions  $z_n = bn - z$  is the coordinate along the segment  $n$ ,  $k_n$  is the wave propagation constant along this segment, and  $l_n$  is its length. The expressions are also true for the segment  $N$  too, if to adopt that  $\prod_{p=N+1}^N = 1$ .

In the case of a radiator with one concentrated load  $Z_1$ , located at point  $z = z_1$  (Fig. 11a), the power  $P_{K1}$ , which is radiated by the antenna is :

$$P_{K1} = - \int_{-L}^L E_z(J) J(z) dz,$$

and the power  $P_{K2}$ , which is created by the generator, is  $P_{K2} = J^2(z_1) Z_1$ . The oscillating power produced by the generator is equal to the sum of these powers:

$$P_K = J^2(h) Z_A = P_{K1} + P_{K2},$$

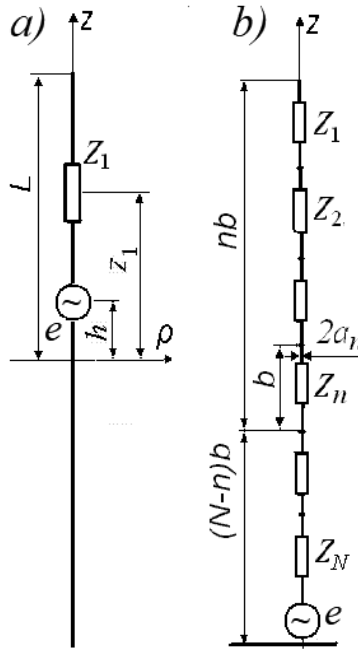


Fig. 11: Antennas with one (a) and several (b) concentrated loads.

that is,

$$Z_A = -\frac{1}{J^2(h)} \left\{ \int_{-L}^L E_z(J)J(z)dz - J^2(z_1)Z_1 \right\}. \quad (3.62)$$

In the case of several loads  $Z_n$  located at points  $z = z_n$  of the asymmetrical radiator (Fig. 11b).

$$Z_A = -\frac{1}{J^2(0)} \left\{ \int_0^L E_z(J)J(z)dz - \sum_{n=1}^N Z_n J^2(z_n) \right\}. \quad (3.63)$$

Free terms in (3.61) and (3.62) are proportional to the square of the current and to the magnitude of a concentrated load. It is necessary to emphasize that the connection of loads changes the current distribution along a radiator and the field of the current.

The method of induced emf may be used for the calculating characteristics of antennas consisting of the several parallel wires and radiators. For a folded radiator (see Fig. 1.13), which is an example of such an antenna, we obtain

$$Z_A = -\frac{1}{J_g^2} \int_{-L}^L E_z(J)J(z)dz. \quad (3.64)$$

Here  $J_g$  is a current of a generator,  $J(z)$  is the total current of an antenna. The current distribution along the antenna wires coincides in a first approximation with



the current distribution along the wires of an equivalent long line and is determined by means of the theory of electrically coupled lines. The properties of the folded radiators were described in Section 1.5. One variant of a multi-radiator antenna is presented in Section 1.4.

As it is noted above, the method of induced emf does not permit to obtain the finite values of the input impedance at the points of parallel resonance, where  $J(h)=0$ , and near these points. The second (integral) variant of solving Leontovich's equation allows us in the case of the symmetrical radiator, if  $J(h) \approx 0$ , to come to the expression

$$Z_A = e/[2J(0) + \frac{1}{e} \int_{-L}^L E_z(J)J(z)dz.] \quad (3.65)$$

One can obtain similar expressions also for more complicated radiators. For example, the input impedance of a radiator with  $N$  concentrated loads and with the displaced feed point is equal to

$$Z_A = e/[2J(h) + \frac{1}{e} \int_{-L}^L E_z(J)J(z)dz - \sum_{n=1}^N Z_n J^2(z_n)]. \quad (3.66)$$

These formulas expand essentially the scope of the method of induced emf. Comparison of the results obtained by numerical methods and with help of these formulas confirms their correctness.

Up to now the subject of discussion was application of the method of induced emf for calculating an input impedance of an antenna. But this method is applied widely also for solving another problem—for estimating the reciprocal influence of radiators by means of calculating their mutual impedances.

The analysis of two-radiator system is based on the fact that a current of one radiator excites the field, which creates a tangential electrical component on the surface of a second radiator. This component creates the field  $E_\zeta(J_1)d\zeta$  on the surface of element  $d\zeta$  of a second radiator. In order to execute the boundary condition  $E_\zeta=0$  on this surface, the own field of a second radiator on its surface must be equal to  $-E_\zeta(J_1)d\zeta$ . The generator of the second radiator must increase the power in an element  $d\zeta$  by  $dP = -E_\zeta(J_1)J_2(\zeta)d\zeta$  and, accordingly, the power in an entire radiator by  $P = \int_{-L_2}^{L_2} E_\zeta(J_1)J_2(\zeta)d\zeta$ . Power  $P$  is equal to the power induced by the first radiator in the second radiator, and the ratio of power  $P$  to the square of the current of the second generator determines the magnitude of additional impedance, which the first radiator induced in the second radiator:

$$Z_{21ind} = -\frac{1}{J_2^2(0)} \int_{-L}^L E_\zeta(J_1)J_2(\zeta)d\zeta. \quad (3.67)$$

The Kirchhoff equation for the second radiator takes the form

$$e_2 = J_2(0)[Z_{22} + Z_{21ind} = J_2(0)Z_{22} + J_1(0)Z_{21}], \quad (3.68)$$

where  $Z_{21} = -\int_{-L_2}^{L_2} E_\zeta(f_1)f_2(\zeta)d\zeta$  is the mutual impedance of the first and the second radiators,  $f_1(z) = J_1(z)/J_1(0)$ ,  $f_2(\zeta) = J_2(\zeta)/J_2(0)$ . One can write a similar expression

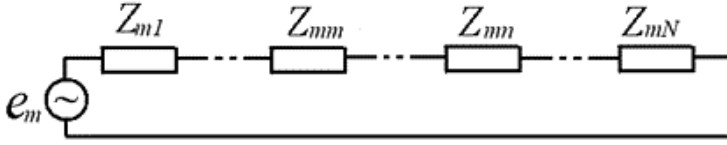


Fig. 12: The equivalent circuit of radiator  $m$ .

for the first radiator. In the case of  $N$  radiators, this expression for the radiator  $m$  has the follow form:

$$e_m = J_1(0) Z_{m1} + \sum_{n=2}^N J_n(0) Z_{mn}. \quad (3.69)$$

The corresponding circuit for the radiator  $m$  is given on Fig. 12.

The expressions presented in this Section are given in the accordance with the second formulation of the method of induced emf. As was said, the formulas, which allow to calculate the mutual impedances of linear radiators for the different variants of their relative placement, are collected in [6].

## 6. Loss Resistance in the Ground

As already mentioned, the theorem about the oscillating power has significantly changed the understanding of the method of induced emf. The losses of asymmetric vertical antenna in an earth and grounding are another example of this change. It is presented in the given Section.

For a long time, the calculation of losses in the grounding was carried out according to the procedure of Brown [14]. This method proceeds from an idea of a high conductivity of the grounding, owing to which a magnetic field  $H_{\varphi}$  at the grounding surface (Fig. 13) is virtually identical to a magnetic field of an antenna, located above a perfectly conducting grounding, and its strength is equal to a density of a surface current in the grounding:

$$J_{\rho}(\rho) = H_{\varphi 0}(\rho). \quad (3.70)$$

The surface current has a radial character.

If a resistance per unit area of the earth's surface is equal to  $R_0$ , then the resistance of an element in the form of a ring with a radius  $\rho$  and a width  $d\rho$  is  $dR_g = (R_0/2\pi\rho)d\rho$ . The power of losses in this ring is  $dP_g = (2\pi\rho|H_{\varphi 0}|)^2 dR_g$ . The resistance of losses, referred to the base of an antenna, can be found from the expression

$$R_g = \frac{1}{|J(0)|^2} \int_a^b dP_g = \frac{2\pi R_0}{|J(0)|^2} \int_a^b |H_{\varphi 0}|^2 \rho d\rho. \quad (3.71)$$

Here  $J(0)$  is the current in the antenna base. Resistance per unit area is equal to

$$R_0 = 1/(s\sigma) = 11\pi/\sqrt{\sigma\lambda},$$

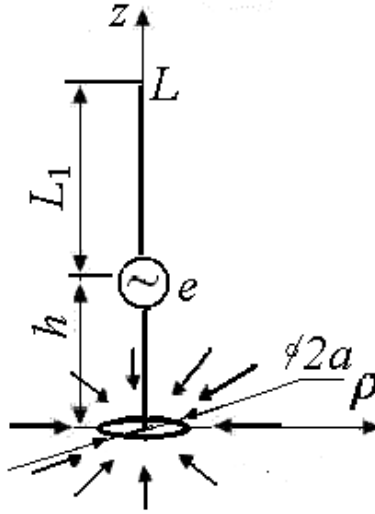


Fig. 13: Magnetic field near a radiator.

where  $s$  is the depth of current penetration into a ground,  $\sigma$  is the conductivity of the ground. A lower limit of integration in (3.71) is an antenna radius or a radius of a grounding, whose conductivity can be considered infinitely great. The upper limit  $b$  must tend to infinity. It is easy to see, however, that in this case the integral diverges. Indeed, the magnetic field of the monopole in the form of a thin conductive filament, mounted vertically on the perfectly conducting ground, can be written as

$$H_{\varphi 0}(\rho) = j \frac{J(0)}{2\pi\rho \sin kL} [\exp(-jk\sqrt{\rho^2 + L^2}) - \cos kL \exp(-jk\rho)]. \quad (3.72)$$

Hence the integrand is

$$|H_{\varphi 0}|^2 \rho = j \frac{J^2(0)}{4\pi^2 \rho \sin^2 kL} [1 + \cos^2 kL - 2 \cos kL \cos k(\sqrt{\rho^2 + L^2} - \rho)].$$

If  $b_2 \gg b_1 \gg L$ , the integral

$$\int_{b_1}^{b_2} |H_{\varphi 0}|^2 \rho d\rho = \frac{J^2(0) (1 - \cos kL)^2}{4\pi^2 \sin^2 kL} \ln \frac{b_2}{b_1}$$

increases unlimitedly with increasing of the upper limit, and consequently the resistance  $R_g$  also increases unlimitedly.

In [29] it was suggested to assume that the upper limit of the integral (3.71) is equal to  $\lambda/2$ . Outside the boundaries of this area the zonal component of a current, which decreases with increasing distance  $\rho$  in accordance with the law  $1/\rho$ , is dominated. This component is considered, when the resistance of radiation is calculated. Inside the indicated area the induction component of zonal current is dominated, it decreases according to the law  $1/\rho^2$ . It is believed that this component causes losses in the ground. These qualitative considerations were a cause for quantitative evaluation, justifying actually arbitrary choice of the upper limit.

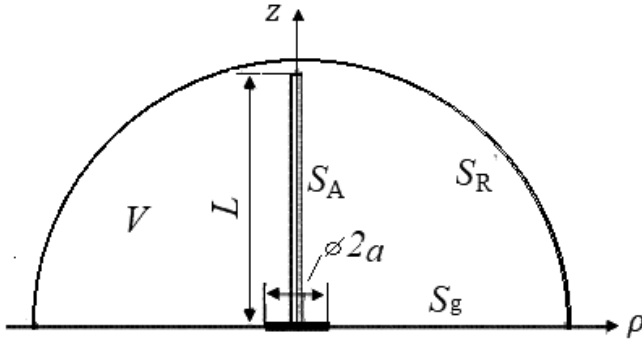


Fig. 14: Closed surface around a radiator.

In 1954 it was derived and published the expression for the additional resistance of the antenna caused by a non-ideal conductivity of the ground [15] (as the resistance of losses in the ground was called by authors):

$$Z_g = \frac{2\pi}{J^2(0)} \int_a^\infty E_\rho H_{\varphi 0} \rho d\rho, \quad (3.73)$$

where  $H_{\varphi 0} = -\frac{1}{2\pi} \frac{\partial}{\partial \rho} \int_0^L J(z) \frac{\exp(-jk\sqrt{\rho^2 + z^2})}{\sqrt{\rho^2 + z^2}} dz$ . Here  $E_\rho$  is a radial component of the electric field on the ground's surface and  $J(z)$  is the current along the antenna. According to the authors' opinion  $H_{\varphi 0}$  is a component of the magnetic field on the surface of the perfectly conducting grounding. Expression (3.73) is derived by means of intricate procedure, using direct and inverse Fourier-Bessel transformation. A similar result can be obtained, using the theorem about the oscillating power. This theorem is applied to a volume  $V$ , bounded by a hemisphere  $S_R$  of a large radius  $R$ , a ground surface  $S_g$  and an antenna surface  $S_A$  (Fig. 14).

Let  $R$  tends to infinity. Since in the steady-state mode the energy within a volume is constant, then

$$\int_{(V)} \vec{E} j dV = \int_{(S=S_R+S_A+S_g)} [\vec{E}, \vec{H}]_n dS + j\omega \int_{(V)} (\mu \vec{H}^2 + \epsilon \vec{E}^2) dV, \quad (3.74)$$

where  $j$  is a density of an extraneous current,  $n$  is an outward normal to the surface  $S$ ,  $\omega$  is a circular frequency,  $\mu$  and  $\epsilon$  are accordingly permeability and permittivity of a free space.

The left part of (3.74) is the total (active and oscillating) power associated with an energy of external source, i.e., with an antenna. This power is equal to

$$P_I = \int_0^L E_z J(z) dz = J^2(0)(Z_{A0} + Z_g).$$

Here  $Z_{A0}$  is the input impedance of an antenna in the case of a perfectly conducting ground. In the absence of losses in the wires the active component of this impedance is equal to the resistance of radiation. Within the limits of solution accuracy, it is supposed that the grounding conductivity is high, and the electromagnetic

field coincides with the field of an antenna mounted on the ground with infinite conductivity, i.e., losses in the ground do not affect the resistance of radiation. The right part of (3.74) is equal to

$$P_{II} = P_1 + P_2 + P_3 + 2j\omega W.$$

Here  $P_1 = \int_{S_R} [\vec{E}, \vec{H}]_n dS_R$  is a total radiated power,  $P_2 = \int_{S_A} [\vec{E}, \vec{H}]_n dS_A$  is a power of the losses in the wires,  $P_3 = \int_{S_g} [\vec{E}, \vec{H}]_n dS_g$  is a power of the losses in the ground,  $W = 0.5 \int_{(V)} (\mu \vec{H}_2 + \varepsilon \vec{E}_2) dV$  is an oscillating energy in the volume V. Since it is considered that electromagnetic fields are the same for the great and infinite ground conductivity, then

$$J^2(0) Z_{A0} = P_1 + P_2 + 2j\omega W, \quad P_3 = J^2(0) Z_g,$$

i.e.,

$$Z_g = \frac{1}{J^2(0)} \int_{S_g} [\vec{E}, \vec{H}]_n dS_g = -\frac{2\pi}{J^2(0)} \int_0^\infty E_\rho H_\varphi \rho d\rho. \quad (3.75)$$

Here,  $E_\rho$  and  $H_\varphi$  are the field components on the surface of a highly conducting ground.

Expression (3.75) differs from (3.73) only by substitution  $H_\varphi$  for  $H_{\varphi 0}$ . As is seen from (3.75), it is necessary to include in the integrand the field of not perfectly conducting, but of the real ground. Since  $J(z)$  is the current of real antenna, which like the input impedance is distinguished from the current along the antenna mounted on a perfectly conducting ground, then  $H_\varphi$  is the magnetic field on the surface of a ground, which has a finite conductivity. In [15] it is written that  $H_\varphi$  is a component of the magnetic field in the case of the perfectly conducting ground. This is a mistake. Erroneous argument was repeated by other authors (see, for example, [30]). Thus, the theorem about the oscillating power allowed not only to obtain simply and clearly the result derived by means of intricate procedure, but enabled to discover the mistake [16].

Impedance boundary conditions on the ground surface have the form

$$Z_0 = -E_\rho / H_\varphi,$$

where  $Z_0$  is the surface impedance. Here, the minus sign is caused by the fact that the current density  $\vec{j} = [\vec{n}, \vec{H}]$  is directed radially toward the origin along the ground. For the ground with high conductivity  $Z_0 = R_0(1+j)$ , i.e.,

$$Z_g = \frac{2\pi R_0(1+j)}{J^2(0)} \int_0^\infty H_\varphi^2 \rho d\rho,$$

where  $H_\varphi = H_{\varphi 1} + j H_{\varphi 2}$ ,  $H_{\varphi 1} = \text{Re} H_\varphi$ ,  $H_{\varphi 2} = \text{Im} H_\varphi$ , i.e., the active component of  $Z_g$  is equal to

$$R_g = \text{Re} Z_g = \frac{2\pi R_0}{J^2(0)} \int_a^b (H_{\varphi 1}^2 - H_{\varphi 2}^2 - 2H_{\varphi 1} H_{\varphi 2}) \rho d\rho. \quad (3.76)$$

The difference between the results of Waite-Pope and Brown is clear from (3.76) and (3.71). If  $H_\varphi = H_{\varphi 0}$ , when  $b_2 \gg b_1 \gg L$ , then

$$\int_{b_1}^{b_2} (H_{\varphi 1}^2 - H_{\varphi 2}^2 - 2H_{\varphi 1} H_{\varphi 2}) \rho d\rho = J^2(0) (1 - \cos kL)^2 F / (2\pi \sin kL)^2,$$

where

$$F = - \int_{b_1}^{b_2} \left( \frac{\cos 2k\rho}{\rho} + \frac{\sin 2k\rho}{\rho} \right) d\rho = -\sqrt{2} \int_{b_1}^{b_2} \frac{\cos 2k\rho}{\rho} d\rho \leq \frac{1}{kb_1 \sqrt{2}}.$$

i.e., integral in (3.76) converges.

Just as expression (3.76) follows from the theorem about the oscillating power, expression (3.71) with an upper limit equal to infinity is obtained in accordance the theorem about the complex power. Both formulas are written in accordance with the law of energy conservation; the additional instantaneous power, given off by the generator because of losses in not-ideally conducting ground at any point of time is equal to the instantaneous power of losses in it. Therefore, both expressions should be true.

Integrands in these expressions are different, because  $Re(E_\rho H_\varphi) \neq Re(E_\rho H_\varphi^*)$ . However, this difference does not exclude equality of integrals. The magnitudes of  $R_g$  must be equal upon substituting into integrals a magnetic component  $H_\varphi$  of field on the surface of a real ground. For this when  $\rho \gg L$  the magnitude of  $H_{\varphi 2}$  must be equal to zero, i.e., the tangential component of the magnetic field on the ground surface in the far zone must be in phase with the current  $J(0)$  in the antenna base.

It is easy to verify that  $H_{\varphi 0}$  satisfies this requirement only in the vicinity of the antenna: if  $\rho \ll L$ ,  $H_{\varphi 0} = J(0)/(2\pi\rho)$ , When  $\rho \gg L$ ,  $H_{\varphi 20}/H_{\varphi 10} = \cot kL$ , i.e.,  $H_{\varphi 0}$  differs substantially from  $H_\varphi$ . The experiment confirms that  $H_\varphi$  coincides with  $H_{\varphi 0}$  only at a short distance from the antennas [31]. Let  $H_{\varphi 0}$  be different from  $H_\varphi$  on some complex value:  $H_{\varphi 0} - H_\varphi = M_1 + jM_2$ . Then one can find the difference of integrands in expressions for  $R_g$  in the cases of perfect and imperfect grounding. Using expressions (3.73) and (3.75), we obtain that this difference in the first case is equal to

$$\Delta_1 = |H_{\varphi 0}|^2 - |H_\varphi|^2 = M_1^2 + M_2^2 + 2H_\varphi M_1,$$

and in the second case is

$$\Delta_2 = (H_{\varphi 10}^2 - H_{\varphi 20}^2 - 2H_{\varphi 10} H_{\varphi 20} - H_\varphi^2 = M_1^2 - M_2^2 + 2H_\varphi (M_1 + jM_2).$$

The magnitude  $\Delta_1$  depends on the sum of the squares of the real and imaginary components of error, and the magnitude  $\Delta_2$  depends on their difference. If  $M_1 + jM_2$  is a value of an order  $\exp(-jk\rho)$  and  $b_2$  grows, an integral  $\int_{b_1}^{b_2} \Delta_1 \rho d\rho$  unlimitedly increases, and integral  $\int_{b_1}^{b_2} \Delta_2 \rho d\rho$  tends to be zero in proportion to  $1/b_1$ . The second version is natural, since the tangential component of the magnetic field on the surface of the real ground far from the antenna cannot have the character of no damped spherical electromagnetic wave, i.e., cannot contain summands of order  $\exp(-jk\rho)/\rho$  incoming in the expression for  $H_{\varphi 0}$ .

The authors of [15] attempted to calculate a change of radiated power, caused by the finite ground conductivity. They considered that it is equal to a difference

between the additional power of the generator determined in accordance with (3.73) and the power of losses in the ground determined by (3.71). This attempt is incorrect, since within the limits of accuracy of the proposed method the radiated power does not depend on the conductivity of the ground, and the power of losses in the ground and the additional power of the generator are identical. For a radiator, whose feed point is shifted from the middle to point  $z = h$  (Fig. 15).

$$J(z) = \begin{cases} J(0) \cos kz / \cosh k, & 0 \leq z \leq h, \\ J(0) \sin k(L - z) / \sin k(L - h), & h \leq z \leq L. \end{cases}$$

The magnetic field on the surface of a real ground

$$H_\phi = j \frac{J(0)}{2\pi\rho \sin k(L - h)} \times \left\{ \exp\left(-jk\sqrt{\rho^2 + L^2}\right) - \exp\left(-jk\sqrt{\rho^2 + h^2}\right) [\cos k(L - h) - \tanh h \sin k(L - h)] \right\}. \quad (3.77)$$

Substituting (3.77) into (3.76), we find

$$Z_g = \frac{R_0}{4\pi \sin^2 \alpha_2} [F_1 + F_2 + j(F_1 - F_2)]. \quad (3.78)$$

where  $\alpha_2 = k(L - h)$ , and  $F_1$  and  $F_2$  for the short radiator with small radius  $a$  of grounding are

$$F_1 = 2\alpha_2^2 [\ln(L + h/2a) - 0.5] + 4\alpha\alpha_0 \ln(\alpha_1^2/4\alpha\alpha_0), F_2 = 0. \quad (3.79)$$

Here  $\alpha = kL$ ,  $\alpha_0 = kH$ ,  $\alpha_1 = k(L - h)$ . As is seen from expression (3.78) for the short radiator, the reactive component  $X_g$  of the loss impedance has inductive character and is equal in magnitude to the active component  $R_g$ . With growth of  $h$  an impedance  $Z_g$  increases, since  $0 \leq h \leq L$ , and a derivative of  $Z_g$  with respect to  $h$  is positive always. In the general case  $F_1$  and  $F_2$  have more complicate character [16].

Results of calculating loss resistance in the ground (water) in *HF* range are presented in Fig. 16. It is assumed that the magnitude is equal to 3 Sm/m. Dimensions are given in meters. Calculations are made in accordance with (3.78): solid lines—in accordance with the general expression, dotted lines—in accordance with (3.79). Results of calculating the loss resistance of impedance antennas excited at the base are shown in Fig. 17. Calculations are made for antennas with a height of 1 and 2 m with a slowdown from 1 to 5 at the same magnitude  $\sigma$ .

The considered examples show that the theorem about the oscillating power changes significantly the understanding of processes related with the transfer of power between the objects. Application of folded and multi-folded radiators largely depends on their losses, particular losses in the ground. Each of the elements of which antenna consists (i.e., monopole and a long line) has losses in the ground. Loss

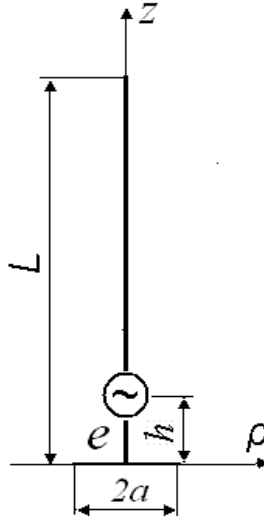


Fig. 15: Radiator with shifted feed point.

resistance  $R_{ge}$  for a monopole is calculated in the usual manner. Regarding the long line, its loss resistance  $R_{gl}$  in the ground is also non-zero. Of course, magnetic fields, created by opposite currents of two closely spaced parallel wires of a line, cancel each other, and the radius of an area, in which the full compensation is absent, is relatively small (the center of this area is located at the middle point between wires). However, it is necessary to consider that, when an observation point is approaching to a conductor with the current, the magnetic field increases. Let  $J_1$  and  $J_2$  be the currents in left and right wire of the line:

$$J_1 = -J_2 = mJ \frac{\sin k(l+z)}{\sin kl}.$$

Here  $mJ$  is the current in the base of the wire and  $l = \lambda/4 - L$  is the wire length (Fig. 18a). If the origin of a rectangular coordinate system coincides with in the middle of an interval between the wires, then the vector potential of the electromagnetic field produced by the current  $J_1$  and its mirror image in the arbitrary points on the ground surface with coordinates  $(\pm x, \pm y, 0)$  located at the distance  $\rho = \sqrt{x^2 + y^2}$  from an axis of the first wire is equal to

$$A_{z1} = \frac{mJ\mu}{2\pi \sin kL} \int_0^L \sin k(l+z) \frac{\exp(-jk\sqrt{\rho^2 + z^2})}{\sqrt{\rho^2 + z^2}} dz.$$

The tangential components of the magnetic field are

$$H_{x1} = \frac{\partial A_{z1}}{\mu \partial y} = \frac{mJ\mu}{2\pi \sin kL} y A_0(L, l, \rho), H_{y1} = \frac{\partial A_{x1}}{\mu \partial x} = \frac{mJ}{2\pi j \sin kL} x A_0(L, l, \rho), \quad (3.80)$$



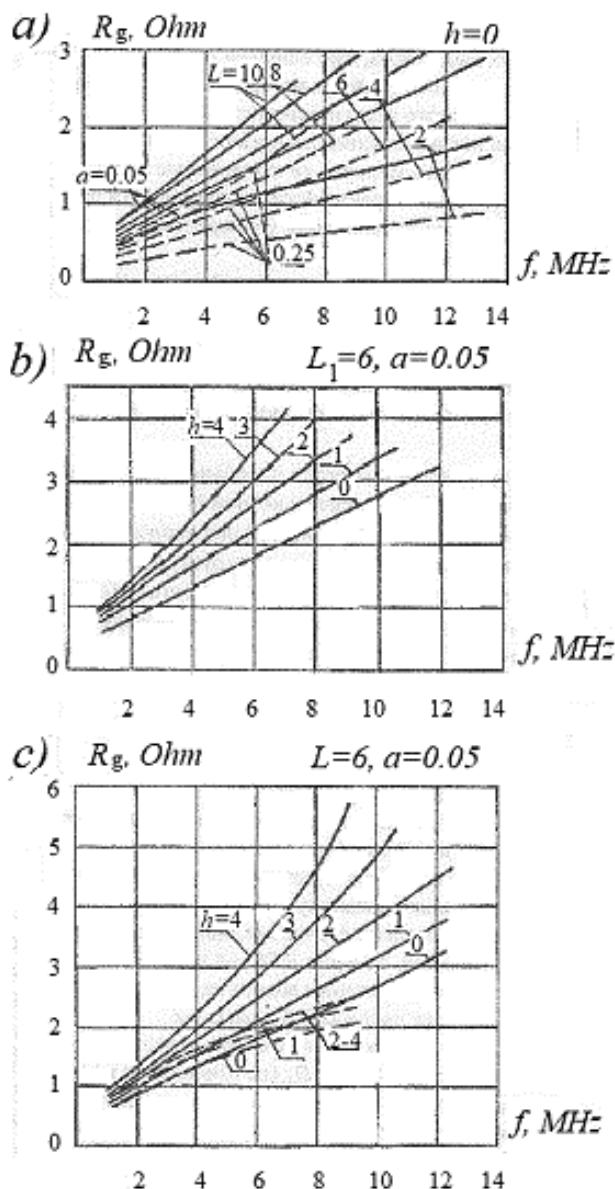


**Fig. 16:** Loss resistances in the water for an asymmetrical metal radiator excited in the base and with shifted feed point.

where

$$A_0(L, l, \rho) = -\frac{\exp(-jkR)}{\rho^2} \left[ \frac{jL}{R} \sin k(l+L) + \cos k(l+L) + \cos kl \right]$$

and  $R = \sqrt{\rho^2 - L^2}$ . In calculating an integral, the substitution  $R = \sqrt{\rho^2 + L^2}$  was used.

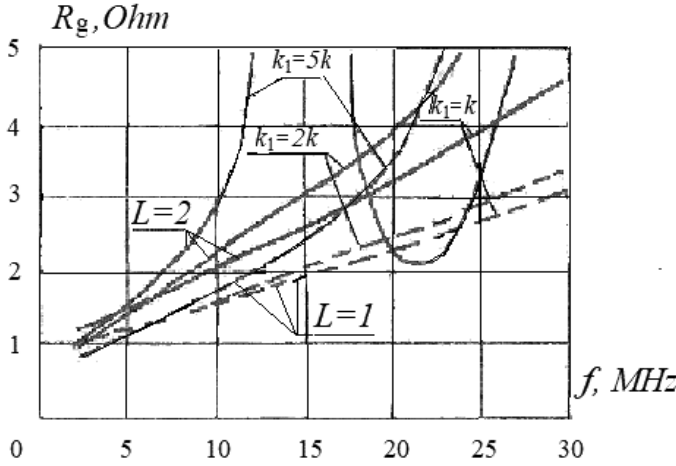


Fig. 17: Loss resistances in the water for an asymmetrical radiator with constant surface impedance excited at the base.

The current density in the ground coincides with the strength of the magnetic field created by wires of the long line. Its components are equal to

$$i_x = -H_y = \frac{mJ}{2\pi \sin kL} [(x + b/2) A_0(L, l, R_1) - (x - b/2) A_0(L, l, R_2)],$$

$$i_y = -H_x = \frac{mJy}{2\pi j \sin kL} [A_0(L, l, R_1) - A_0(L, l, R_2)],$$

where  $R_{1(2)} = \sqrt{(x \pm b/2)^2 + y^2}$ . Introducing a value  $\delta$  satisfying the inequality

$$b/2 \ll \delta \ll L, \lambda/2, \quad (3.81)$$

one can divide the area of losses (Fig. 18b) into two areas, the boundary between which is a circumference of radius  $\delta$ . In the outer area the distance from the long line to the observation point is large in comparison with the distance between the wires. Here the fields produced by the currents  $J_1$  and  $J_2$  cancel each other (Fig. 18c). Thus, for example, when  $x = 0$ ,  $i = -i_1 b/\rho \approx -bH_{x1}/\rho$ , and taking (3.80) into account, we find

$$|i| \leq \frac{1.5mJb}{\pi \sin kL\rho^2}.$$

Power of losses in the outer area

$$P_l = R_0 \int_0^{2\pi} \int_0^\infty |i|^2 \rho d\rho d\varphi \leq \pi R_0 \frac{1.5mJb}{\pi \sin kL\rho^2}$$

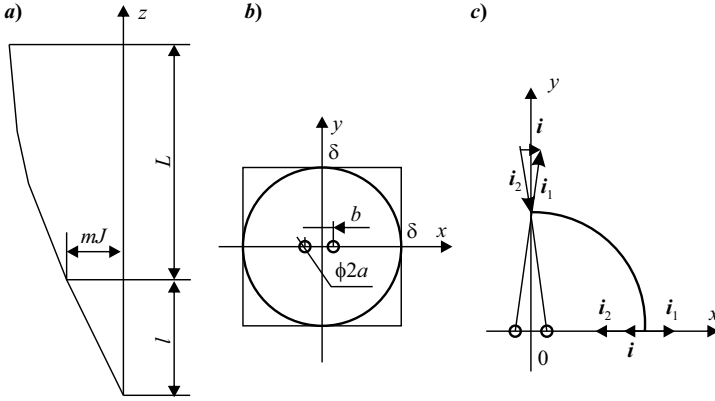


**Fig. 18:** Current distribution along the wire (a), area of losses (b) and currents on a ground surface in the outer area (c).

where  $R_0 = 1/(s\sigma)$  is resistance per unit area of the ground surface. In accordance with (3.81), this value is small and can be neglected. In the inner area  $\rho \ll L, \lambda/2$  expressions for the components of the surface current are greatly simplified:

$$i_x = \frac{mJ}{2\pi} \left[ \frac{x - b/2}{(x - b/2)^2 + y^2} - \frac{x + b/2}{(x + b/2)^2 + y^2} \right],$$

$$i_y = \frac{mJy}{2\pi} \left[ \frac{1}{(x - b/2)^2 + y^2} - \frac{1}{(x + b/2)^2 + y^2} \right]. \quad (3.82)$$

Without wasting adopted accuracy, we calculate the losses not in a circle of radius  $\delta$ , but in the square of side  $2\delta$  (see Fig. 19b). Power of losses in the inner area is

$$P_{II} = 4R_0 \int_0^\delta \int_0^\delta (i_x^2 + i_y^2) dx dy = \frac{R_0 (mJb)^2}{\pi^2} \int_0^\delta \int_0^\delta \frac{dx dy}{[(x - b/2)^2 + y^2][(x + b/2)^2 + y^2]},$$

whence  $R_{gl} = \frac{P_{II}}{(mJ)^2} = \frac{R_0}{\pi} \sum_{i=1}^2 Q_i$ . Here

$$Q_1 = - \int_0^1 [\cot^{-1}(t - b/2\delta) + \cot^{-1}(t + b/2\delta)] \frac{dt}{t},$$

$$Q_2 = \int_0^1 \left[ \frac{\cot^{-1}(t - b/2\delta)}{t - b/2\delta} + \frac{\cot^{-1}(t + b/2\delta)}{t + b/2\delta} \right] dt.$$

One can show that  $\sum_{i=1}^2 Q_i = \pi \ln(b/2a) + 2G$ , where  $G = \int_0^1 \tan^{-1} z \frac{dz}{z} \approx 0.916$  is Catalan's constant. The value  $\delta$ , as would be expected, in this expression is not included. If that  $b/a \gg 1$ , we find

$$R_{gl} = \frac{R_0}{\pi} \ln(b/a) = \frac{11}{\sqrt{\sigma\lambda}} \ln(b/a). \quad (3.83)$$

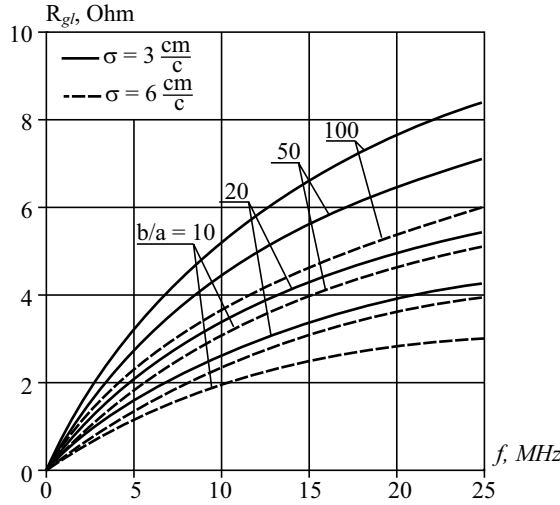


Fig. 19: Loss resistance of the vertical two-wire long line in the water.

This result can also be obtained using known analogy between electric field in a conductive medium and an electrostatic field. The rightness of this approach follows from (3.82): a magnetic field and current density in the ground in the losses area are determined only by the currents in the base of wires and have a quasi-static nature. Similarly, one can obtain for the coaxial line (see Fig. 1.14d)

$$R_{gl} = \frac{R_0}{2\pi} \ln(a_2/a_1) = \frac{5.5}{\sqrt{\sigma l}} \ln(b/a). \quad (3.84)$$

As can be seen from (3.83) and (3.84), the loss resistance in the ground for vertically located long line (both two-wire and coaxial) does not depend on its length  $L$ . This resistance depends only on the ratio of the distance between the wires to the wire radius. Figure 19 shows the dependence of loss resistance  $R_{gl}$  of two-wire line on the frequency at different values  $b/a$  and  $\sigma$  (of sea water). The calculation shows that the distance between the wires cannot be neglected.

One must emphasize that the loss resistance  $R_{gl}$  of the monopole in the ground should be connected in series with the input impedance of the radiator itself, and the loss resistance  $R_{gl}$  of the line in the ground should be connected in series with the input impedance of the line. This is easily seen, proceeding from Fig. 20, where the contour along which the current flows, is shown for both antenna elements. Taking into account losses in the ground, the expression for the input impedances of folded radiator with a gap and the expression for the input admittance of folded radiator with ground connection of the second wire take the form:

$$Z_A = Z_e(a_e) + R_{gl} + jm^2 Wl \tan kL + m^2 R_{gl}, \quad Y_A = \frac{1}{R_{gl} + jWl \tan kL} + \frac{p^2}{R_{gl} Z_e(a_e)}. \quad (3.85)$$

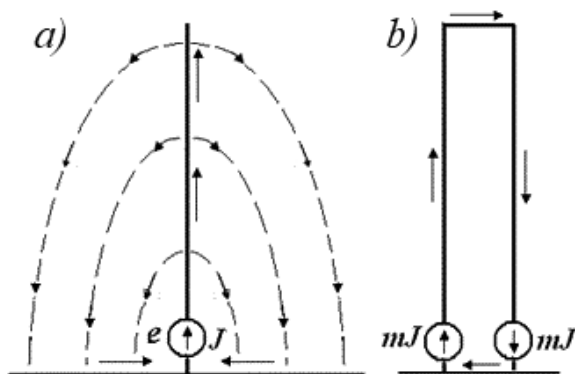


Fig. 20: Direction of currents in monopole and ground (a), in two-wire line and ground (b).

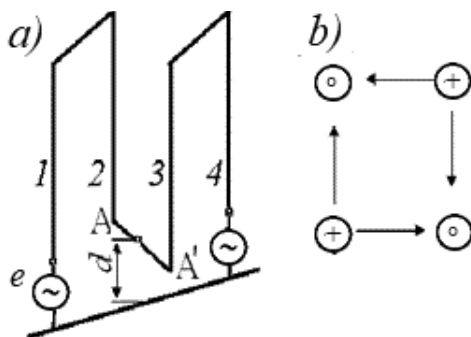


Fig. 21: Losses in the ground for lines of complex shape (a) and with two wires in 'conductor' (b).

In calculating the loss resistance  $R_{gl}$  of multi-folded antennas in the ground it is necessary to determine a loss resistance  $R_{gl}$  for lines of complex shape. Figure 21a shows the two-wire line of length  $2L$ , which in the middle is bent at an angle of  $180^\circ$ . The losses of such line in a ground do not differ from the losses of the line shown in Fig. 20b because the currents in the ground between projections of the wires 2 and 3 are practically absent. The currents between the wires 2 and 3 flow mainly along the connecting bridge  $AA'$ , especially if the distance between these wires is less than the distance  $d$  between this bridge and the ground.

## 7. Loss Resistance in the Wires

In this Section we consider losses in the antenna wires caused by a skin effect. As is known, the surface resistance of a round copper wire with length one meter is  $R_s = \sqrt{f/24a}$ , where  $f$  is a frequency, in MHz,  $a$  is a wire radius, in mm. The resistance of the steel wire is 2.3 times as much.

The surface resistance causes the attenuation of longitudinal electromagnetic waves. Therefore, the propagation constant of a wave along the wire and the wave impedances of the long line and the monopole become complex quantities. Substituting them into the expression for the input impedance, one can find this

**Table 3:** Loss Resistance of Multi-folded Radiators with a Gap.

Type of radiator	Loss resistance in a ground $R_{gA}$	Loss resistance in wires $R_{wA}$
folded	$R_{ge} + 0.25 R_{g0}$	$\frac{R_{\sim} L}{\sin^2 2kL} \left( 1 - \frac{\sin 4kL}{4kL} \right)$
two-folded	$R_{ge} + 0.313 R_{g0}$	$\frac{2R_{\sim} L}{\sin^2 4kL} \left( 1 - \frac{\sin 8kL}{8kL} \right)$
four-folded	$R_{ge} + 0.328 R_{g0}$	$\frac{4R_{\sim} L}{\sin^2 8kL} \left( 1 - \frac{\sin 16kL}{16kL} \right)$
linear	$R_{ge}$	$\frac{R_{\sim} L}{\sin^2 2kL} \left( 1 - \frac{\sin 2kL}{2kL} \right)$

impedance with allowance for the skin effect losses. The imaginary additive to the propagation constant in the first place increases the active component of input impedance  $R_A$ , since the latter is small in comparison with the reactive component  $X_A$ , everywhere except the vicinity of resonances. The loss resistance in the wires  $R_{wA}$  is a sought value of an addition to a given above radiation's resistance  $R_{\Sigma}$ .

In Table 3 the values  $R_{wA}$  are given for several variants of multi-folded radiators with a gap, when attenuation in the wires is weak. It is believed that the radii of wires are small in comparison with the distances between them, i.e., one can neglect by the proximity effect and the corresponding redistribution of current over the wire cross-section. For comparison, the table demonstrates the loss resistance in the wires of a monopole. The table shows that the losses in the wires cause the appearance of additional maxima on the curve for the active impedance when  $kL = (2m + 1)\pi/2$  ( $m$  is a natural number), i.e., near the parallel resonances of the long lines. In these bands of the frequency range, it is impossible to ignore the skin effect losses. At the low frequencies ( $kL \ll 1$ ) the loss resistance increases proportionally to the number and the length of wires.

One can consider that the input admittance of the  $N$ -folded radiator with the ground connection of the unexcited wire with allowance for the losses in the ground and in the wires is equal to

$$Y_A = \frac{1}{j120 \ln(b/a) \tan NkL + R_{gl} + R_{wl}} + \frac{1}{4Z_{N/2}},$$

where  $Z_{N/2}$  is the input impedance of the  $N/2$ -folded antenna with a gap, consisting of two-wire "conductors" (in view of the losses);  $R_{gl}$  is the loss resistance in the ground;

$R_{wl} = \frac{NR_{\sim} L}{\cos^2 NkL}$  is the loss resistance in the wires of the two-wire long line.

Calculation and experimental verification confirmed the rightness of the obtained results. Figure 22 and 23 show the input impedances of two-folded and four-folded radiators with a gap in different frequency bands. The experimental values of the resonant frequencies in the figures are shifted in comparison with the calculated results in the direction of lower frequencies. This small shift is caused by the fact that the calculation did not consider the length of the horizontal connecting bridges between the wires.

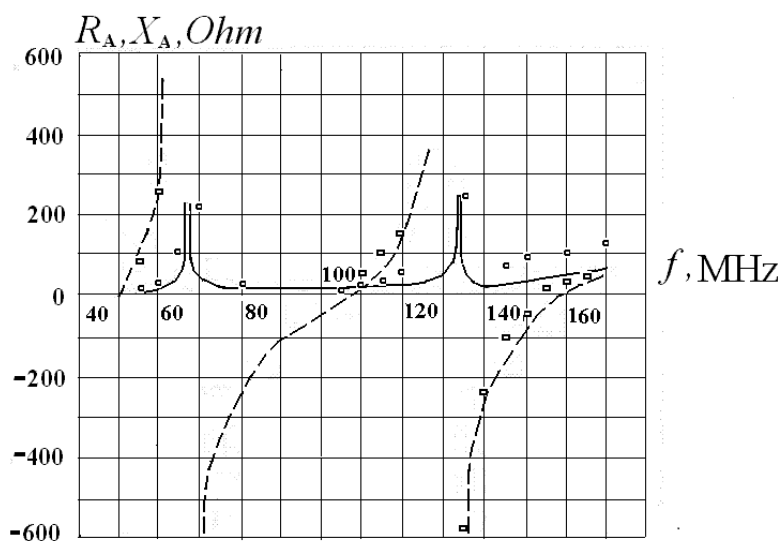


Fig. 22: Input impedance of two-folded radiator with a gap.

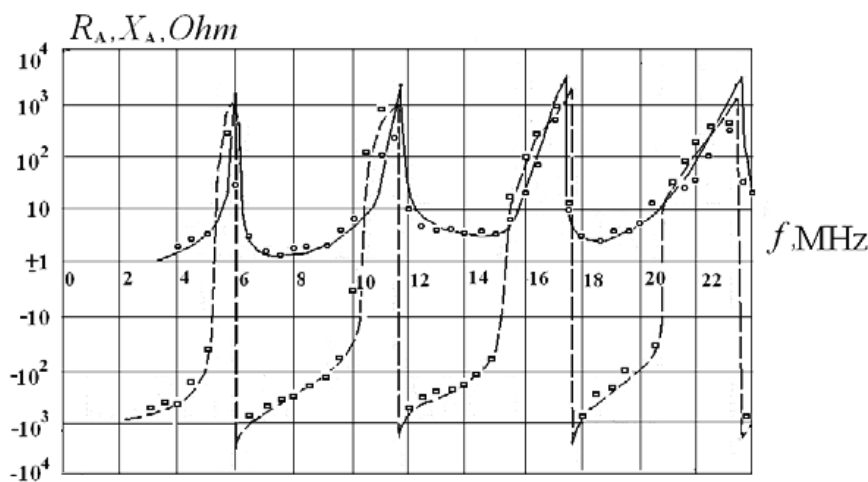


Fig. 23: Input impedance of four-folded radiator with a gap.

Further we pass to Q-factor. Q-factor (quality) is an important electrical characteristic of the antenna. It defines the frequency band, within which one may obtain the given level of matching an antenna with a cable without a change of a tuning. Q-factor characterizes the rate of changing the antenna input impedance as the result of the influence of various external factors and can be used to quantify the sustainability of the antenna tuning, if the sustainability is understood as the preservation of the results of tuning. From this standpoint, the higher the quality factor, the worse the sustainability, and vice versa.

**Table 4:** Expressions for Calculating Electrical Length and Quality of Four-folded and Linear Radiators.

Radiator	Resonance number	Electrical length	Q-factor
four-folded	1	$\frac{1}{4} \tan^{-1} \left( 9.63 \frac{W_m}{W_l} - 0.604 \right)$	$\frac{1}{R_{A1}} \left( -0.94W_m + 0.38W_l + \frac{W_m^2}{W_l} \right)$
“	2	$\frac{1}{2} \tan^{-1} \left( 8 \frac{W_m}{W_l} - 0.05 \right)$	$\frac{1}{R_{A2}} \left( 0.56W_l + 6.3 \frac{W_m^2}{W_l} \right)$
“	3	$\frac{1}{4} \tan^{-1} \left( 1.66 \frac{W_m}{W_l} - 0.1 \right)$	$\frac{1}{R_{A3}} \left( 0.5W_m + 1.4W_l + 1.62 \frac{W_m^2}{W_l} \right)$
“	4	$(\pi - \delta)/2$	$\frac{1}{R_{A4}} \left[ 0.79 \left( 1 + \frac{\Delta^2}{4} \right) W_m + (1.03 + 3.34\Delta^2 + 1.96/\Delta^2) W_l \right]$
quarter-wavelength	1	$\pi/2$	$W_m/93$
short with a matching device	1	$\pi/(2p)$	$\pi W_m / [4pR_A \sin^2 \frac{\pi}{2p}]$

The parameter Q is the magnitude like the quality factor of the resonant circuit. It is calculated at the point of the series resonance of the antenna in accordance with the formula

$$Q_i = \frac{\omega_i}{2R_{Ai}} \frac{dX_A}{d\omega} \bigg|_{\omega=\omega_i} = \frac{(kL)_i}{2R_{Ai}} \frac{dX_A}{d(kL)} \bigg|_{kL=(kL)_i}.$$

Here  $R_{Ai}$  is the active component of the input impedance on the frequency  $f_i$ , in the vicinity of which  $R_{Ai}$  assumed constant.

The expressions for calculating the electrical length  $(kL)_i$  and Q-factor of four-folded radiator with a gap in the first four points of the series resonances are given in Table 4 as an example. The table also indicates for the comparison the electrical length and the quality factor of a quarter-wavelength radiator and of a short linear radiator with a matching device. Table uses the following designations:  $W_m$  is the impedance of the linear radiator, in particular of the equivalent radiator with radius  $a$ ;  $W_l = 120 \ln(b/a)$  is the wave impedance of two-wire long line;  $\Delta = \sqrt{W_l/(4W_m + 5W_l)}$ ,  $p = \lambda/(4L)$ .

## 8. Reciprocity Theorem

The theory of antennas makes it possible to use the solution of radio wave radiation problems when considering radio wave reception issues. This approach is based on the reciprocity theorem. In the general case, the reciprocity theorem considers a linear



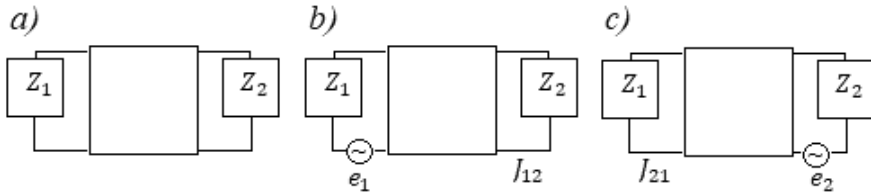


Fig. 24: To the reciprocity theorem.

quadrupole (Fig. 24a), which input poles are shorted by impedance  $Z_1$  and the output poles are shorted by impedance  $Z_2$ . If an emf  $e_1$  is applied to the input poles (Fig. 24b), then in the circuit the currents will be created including the current  $J_{12}$  through impedance  $Z_2$ . If an emf  $e_2$  is applied to the output poles (Fig. 24c), then the currents will also be created in the circuit, including the current  $J_{21}$  through the impedance  $Z_1$ . In accordance with the reciprocity theorem, if emfs are equal ( $e_1 = e_2$ ), the currents excited by them are equal ( $J_{12} = J_{21}$ ). If emfs are not equal, the currents are proportional to them:

$$J_{12}/J_{21} = e_1/e_2.$$

This theorem, when applied to the antennas, is formulated as follows (see, for example, [21]).

If an emf is applied to the terminals of an antenna A and the current is measured at the terminals of another antenna B, then the same current (in both amplitude and phase) will be obtained at the terminals of antenna A, if the same emfs are applied to the terminals of antenna B. It is assumed that the emfs have the same frequency and that the medium is linear, passive and isotropic. An important consequence of this theorem is the fact that under these conditions the transmitting and receiving patterns of an antenna are the same. Also, in the case of matched impedance the power flow is the same either way. As an illustration of the reciprocity theorem for antennas, the book [21] considers two cases presented in Fig. 25. They show that if  $V_b = V_a$ , then in accordance with the reciprocity theorem  $J_a = J_b$ .

J. D. Kraus notes that the ratio of an emf to a current is an impedance. In Case (a) the ratio of  $V_a$  to  $J_b$  may be called the transfer impedance  $Z_{ab}$ , and in Case (b) the ratio  $V_b$  to  $J_a$  may be called the transfer impedance  $Z_{ba}$ . Then from the reciprocity theorem it follows that these impedances are equal. Thus,

$$V_a/J_b = Z_{ab} = Z_{ba} = V_b/J_a.$$

An objective approach to the reciprocity theorem shows that it deals with physical quantities of signals under the same conditions. The power of a transmitted signal  $J^2(0) Z_A = eJ(0)$  also is a real physical quantity. Replacing the value  $eJ(0)$  with the value  $eJ^*(0)$  in the method of induced emf meant the use of a selective and sophisticated approach. This replacement was made, and its stability grew as it used. M.I. Kontorovich showed in [20] the deep erudition and insight and understood that such a replacement contradicts the reciprocity theorem. The oscillating power theorem confirmed the validity of this conclusion.

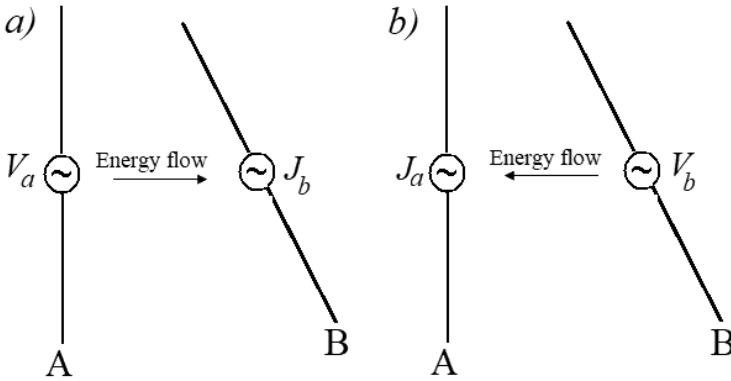


Fig. 25: Illustrations for reciprocity theorem.

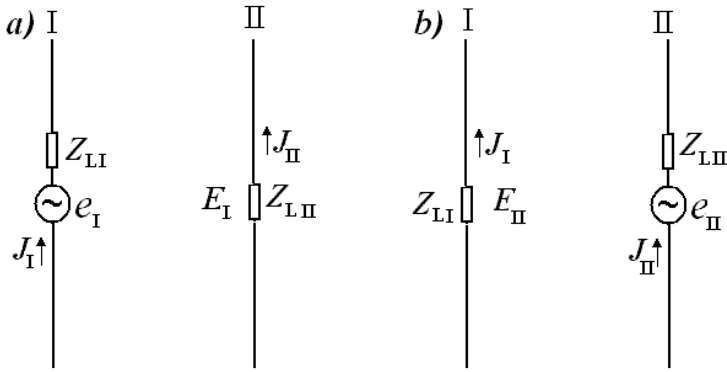


Fig. 26: The reciprocity theorem: a – antenna I radiates, b – antenna II radiates.

As already said, the reciprocity theorem argues that the current in the receiving antenna and all characteristics of the antenna can be found, if the characteristics of the antenna used in transmission mode are known. To prove that, suppose that any two antennas are remote from each other by such a distance that their mutual impedance is zero (Fig. 26a). This condition is accepted for the sake of a proof simplicity and has not principal significance. The load  $Z_L$  is connected in the middle of each antenna. If emf  $e_I$  creates a current  $J_I = \frac{e_I}{Z_{AI} + Z_{LI}}$  at the input of the first antenna, then the field  $E_I = -\frac{30J_I}{\epsilon_r} F_I$  arises near the second antenna and creates in this antenna the current  $J_{II}$  (see Fig. 26a). In similar case, when emf  $e_{II}$  is connected in the second antenna and creates in it the current  $J_{II}$ , the current  $J_I$  arises in the first antenna (see Fig. 26b).

In accordance with the electrodynamic principle of reciprocity,

$$e_I/J_{II} = e_{II}/J_I. \quad (3.86)$$

From these expressions, which are given for the first antenna, it follows that

$$\frac{e_I}{J_{II}} = \frac{J_I(Z_{AI} + Z_{LI})}{J_{II}} = j \frac{\varepsilon_r E_{II}(Z_{AI} + Z_{LI})}{30F_I J_{II}}$$

Similarly, for the second antenna

$$\frac{e_{II}}{J_I} = j \frac{\varepsilon_r E_I(Z_{AII} + Z_{LII})}{30F_{II} J_I},$$

i.e.,

$$\frac{E_{II}(Z_{AI} + Z_{LI})}{F_I J_{II}} = \frac{E_I(Z_{AII} + Z_{LII})}{F_{II} J_I}.$$

If to transfer the magnitudes relating to each antenna into one part of the equation and to assume that each part of the equation is a constant, which does not depend on the properties of the antenna, we get:

$$\frac{J_i(Z_{Ai} + Z_{Li})}{E_i F_i} = \text{const.} \quad (3.87)$$

If to assume that this expression refers to the receiving antenna, then  $J_i$  is the current in the middle of this antenna,  $E_i$  is the field strength near it,  $Z_{Ai}$  and  $Z_{Li}$  are its input impedance and load,  $F_i$  is a function characterizing the effective length and the shape of the directional pattern of antenna in the transmit mode.

The constant of the right side of expression (3.87) can be determined by considering the simple electrical dipole (Hertz dipole) as an antenna. If the axis of receiving dipole lies in the plane of a wave incidence, this constant is equal to 1. In a general case, it is necessary to take into account the polarization of the field and the azimuth, if the horizontal directional pattern of the antenna differs from the circular pattern. As a result, we obtain in accordance with (3.87) that the current in the middle of the receiving antenna is equal to

$$J_i = \frac{E_i F_i(\varphi)}{Z_{Ai} + Z_{Li}} = \frac{e_i}{Z_{Ai} + Z_{Li}} \quad (3.88)$$

The reciprocity theorem shows that the main characteristics of the antenna (input impedance, effective length, directional pattern) coincide for transmit and receive modes. This theorem allows also to analyze a relationship between the field incident onto an array element (onto one radiator) and the field reflected from that element. It is known that when a wave is incident on a flat perfectly conducting metallic surface it is reflected at an angle equal to an angle of incidence. Amplitudes of the incident and reflected fields are identical, and the wave phase changes in a stepwise fashion by  $\pi$ . However, when a metal surface is replaced with a system of radiators, e.g., when it is replaced with a linear array, direction and phase of the reflected field could be essentially changed, because they depend on parameters and electric characteristics of an isolated radiator.

An example of such structure is the in-phase reflector array (Fig. 27a). It is a flat equivalent of a parabolic reflector. The structure consists of primary exciter 1

of antenna array (e.g., a horn) and an array of secondary equally spaced microstrip radiators 2, situated in one plane along surface 3. In order to sum the signals of secondary radiators in the direction, perpendicular to the array plane, their phases should be identical. Since distances  $r_i$  ( $i$  is the radiator number) between the primary exciter and a secondary arbitrary radiator (reradiator) are not identical, this results in a phase difference, which should be compensated with a phase shift in the signal reradiated signal.

The method of calculating the phase step of the reflected field in the signal reradiating can be constructed based on the reciprocity theorem. The reciprocity theorem for two antennas, presented above in the form of (3.86), may be formulated in the following way: if emf  $e_I$  of an antenna I creates current  $J_{II}$  at the input of an antenna II, then the same emf  $e_{II}$  of an antenna II will create at the input of an antenna I the same current  $J_I$  i.e.,

$$J_{II}/e_I = Y_{I,II} = Y_{II,I} = J_I/e_{II} \quad (3.89)$$

where  $Y_{I,II} = |Y_{I,II}| \exp(j\varphi_{I,II})$  and  $Y_{II,I} = |Y_{II,I}| \exp(j\varphi_{II,I})$  are the mutual admittances between antennas. From this it follows that

$$\varphi_{I,II} = \varphi_{II,I} \quad (3.90)$$

i.e., the phase difference between the emf of the exciting antenna and the current of an adjacent antenna does not depend from the source.

In our example the field  $E_I$  acts as a signal source. Let us the source of field is the antenna I, which is excited by the generator  $e_I$  with infinitely high output

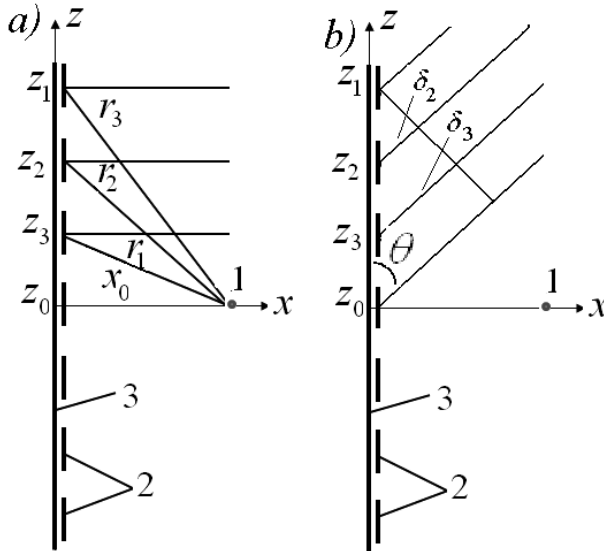


**Fig. 27:** Reflector array, radiating in the perpendicular (a) and in the arbitrary (b) direction, 1 – primary exciter, 2 – secondary micro-strip radiators, 3 – surface for the radiators' placement.

impedance. As usually, we will take into account that the transmitting linear antenna is the aggregate of elementary dipoles with appropriate currents. In this case, because the phase of radiated field outstrips the phase of current by  $\pi/2$ , then the phases difference between the current  $J_{II}$  and emf  $e_I$  is (see Fig. 27a)

$$\varphi_{I,II} = \varphi_{11} + \varphi_{12} + \varphi_{13} + \varphi_{14},$$

where  $\varphi_{11}$  is the phase shift between the current in the antenna I and emf  $e_I$  (in this case it is absent),  $\varphi_{12}$  is the phase shift between the radiated field  $E_I$  and the current of antenna I (it is  $\pi/2$ ),  $\varphi_{13}$  is the phase shift due to the distance between antennas,  $\varphi_{14}$  is the phase difference between current  $J_{II}$  and field  $E_I$ , that is

$$\varphi_{14} = \varphi_{I,II} - \pi/2 - \varphi_{13}.$$

The other source of a signal is the current in antenna II (rather than emf  $e_{II}$ ), which creates the reflected field  $E_{II}$ . The distribution of a current along the receiving antenna differs from distribution along a transmitting antenna. The antenna II is the aggregate of elementary dipoles, each of which is excited by its generator. The currents of the dipoles create in-phase fields. Let the current in the middle dipole (at the antenna center) is excited by the generator  $e_{II}$ . This current is equal to the product of emf  $e_{II}$  and the dipole admittance. Since the dipole impedance is capacitive, the current phase outstrips the emf phase by  $\pi/2$ . That assertion holds true for other dipoles of the antenna II. Accordingly, the phase difference between current  $J_I$  and emf  $e_{II}$  is equal (see Fig. 27b)

$$\varphi_{II,I} = \varphi_{21} + \varphi_{22} + \varphi_{23} + \varphi_{24},$$

where  $\varphi_{21}$  is the phase shift between the current in antenna II and emf  $e_{II}$  (in this case it is  $\pi/2$ ),  $\varphi_{22}$  is the phase difference between field  $E_{II}$  and the current in antenna II,  $\varphi_{23}$  is the phase shift due to the distance between antennas (it is  $\varphi_{13}$ ),  $\varphi_{24}$  is the phase shift between the reflected field  $E_{II}$  and current  $J_I$  (it is zero, since the input impedance of antenna I is infinitely large), that is

$$\varphi_{22} = \varphi_{II,I} - \pi/2 - \varphi_{13}.$$

In accordance with the equation (3.90) this implies that the increment of the phase of the receiving antenna current compared the phase of the incident field and the increment of the phase of the reflected field compared with the phase of the receiving antenna current are the same. As to the amplitude of incident field  $|E_1|$  and the amplitude of reflected field  $|E_2|$ , then at the reflection point

$$|E_2| = |E_1| \cos \gamma \cos \delta,$$

because the total tangential component of both fields on a perfectly conducting metal surface is zero. Here  $\gamma$  is the angle of ray incidence onto an antenna,  $\delta$  is the angle of reflection.

The issue of application of a reciprocity theorem to the reflector array was considered in [32]. The reflector arrays, consisting of microstrip radiators, are described in Chapter 5.

## References

- [1] Poynting, J.H. (1884). On the transfer of energy in the electromagnetic field. *Phil. Trans. Roy. Soc.* 2: 343.
- [2] vKorn, G. and Korn, T. (1961). *Mathematical Handbook for Scientists and Engineers*. New York, Toronto, London: McGraw-Hill.
- [3] Levin, B.M. (2019). Poynting method and antenna radiation resistance. *Proc. of 24th Intern. Seminar DIPED, Tbilisi*, 105–110.
- [4] Levin, B.M. (2021). About using the method of Poynting. *Proc. of 26th Intern.Seminar DIPED, Tbilisi*, 31–36.
- [5] Markov, G.T. and Sazonov, D.M. (1975). *Antennas*. Moscow: Energy (in Russian).
- [6] Lavrov, G.A. (1975). Mutual Influence of Linear Dipole Antennas. Moscow: Sviyaz (in Russian).
- [7] Hacker, P.S. and Schrank, H.E. (1982). Range distance requirements for measuring low and ultralow sidelobe antenna patterns. *IEEE Transactions on Antennas and Propagation*, AP-30(5): 956–966.
- [8] Polk, C. (1956). Optical Fresnel-zone gain of a rectangular aperture. *IEEE Transactions on Antennas and Propagation*, AP-4(1): 65–69.
- [9] Levin, B.M. (2010). About an antenna gain measurement in a Fresnel zone. *IEEE Antennas and Propagation Magazine*, 52(2): 64–700.
- [10] Bleyer, D.J., Wittman, R.C. and Yaghjian, A.D. (1992). On axis fields from a circular uniform surface current. *Proc. of Ultra-wideband Short-Pulse Int. Conf.*, Brooklyn, NY, 285–292.
- [11] Kinber, B.E. and Ceytlin, V.B. (1964). On measurement error of a gain and pattern at short distances. *Radiotechnics and Electronics Engineering*, 9: 1581–1593 (in Russian).
- [12] Fradin, A.Z. and Rizkov, E.V. (1972). *Measurement of Antennas-Feeders Devices Characteristics*. Moscow: Communication (in Russian).
- [13] Vainshtein, L.A. (1988). *Electromagnetic Waves*. Moscow: Sovetskoye Radio (in Russian).
- [14] Brown, G.H., Lewis, R.F. and Epstein, J. (1937). Ground systems as a factor of antenna efficiency. *Proc. IRE*, 753–787.
- [15] Wait, J.R. and Pope, W.A. (1954). The characteristics of a vertical antenna with a radial conductor ground system. *Applied Scientific Research*, 3: 177–195.
- [16] Levin, B.M. and Razumov, V.P. (1979). Loss resistance in the ground. *Antennas*, 27: 125–133 (in Russian).
- [17] Levin, B.M. (2016). *Antenna Engineering: Theory and problems*. London, New York: CRC Press.
- [18] Levin, M.L. (1947). About one new method of finding the thin antenna characteristic reactance, *News of AN USSR, ser. phys.*, 2: 117–133 (in Russian).
- [19] Aizenberg, G.Z. (1962). *Short-Wave Antennas*. Moscow: Communication (in Russian).
- [20] Kontorovich, M.I. (1951). Some remarks in connection with the method of induced emf. *Radiotechnics*, 2: 3–9 (in Russian).
- [21] Kraus, J.D. (1988). *Antennas*. Boston: McGraw-Hill.
- [22] Balanis, C.A. (2005, 2007, 2009, 2012). *Antenna Theory: Analysis and Design*. New York: Wiley & Sons.
- [23] Levin, B.M. (1992). Once again about method of induced emf. *Radio electronics and communications*, 2-3: 17–23 (in Russian).
- [24] Elliott, R.S. (2003). *Antenna Theory and Design*. New York: Wiley-IEEE Press.
- [25] Hallen, E. (1938). Theoretical investigations into the transmitting and receiving qualities of antennae. *Nova Acta Regiae Soc. Sci. Upsaliensis, ser. IV*, 4: 1–44.
- [26] Leontovich, M.A. and Levin, M.L. (1944). On the theory of oscillations excitation in the linear radiators. *Journal of Technical Physics*, 14(9): 481–506 (in Russian).
- [27] Aharoni, J. (1946). *Antennae: An Introduction to Their Theory*. Oxford: The Clarendon Press.
- [28] Levin, B.M. (2013). *The Theory of Thin Antennas and Its Use in Antenna Engineering*. Bentham Science Publishers.

- [29] Nadenenko, S.I. (1946). Selecting dimensions of the antennas grounding system. Radiotechnics, 2: 38–47 (in Russian).
- [30] Maley, S.W. and King, R. J. (1964). Impedance of a monopole antenna with a radial-wire ground system on an imperfectly conducting half space, Part II. Journal of Research NBS/USNC-URSI, 2: 157–163.
- [31] Braude, B.V. and Alexandrova, E.G. (1966). Questions of projecting and methods of calculating parameters of long-wave and superlong-wave antennas, Antennas, 1 (in Russian).
- [32] Levin, B.M. (2008). The reciprocity theorem for a reflect array. Proc. of 19th Intern. Wroclaw Symposium on Electromagnetic Compatibility.

# Integral Equations for Radiators' Currents

---

## 1. Hallen's Equations

Chapter 3 describes the approximate methods of a radiators' calculation. These methods applied on the eve of a broad wave of theoretical works devoted to rigorous methods of calculation. New methods were based on the derivation and solution of integral equations for the antenna currents. It should be recalled that these theoretical works were carried out against the background of a pessimistic attitude towards the possibility of solving the set task. Evidence of this situation is the book [1], where as a rigorous method for analysis of a straight linear radiator it was offered to use the calculation of an elongated ellipsoid (spheroid) with an eccentricity slightly distinguishing from one, i.e., the method based on the calculation of spheroid eigenfunctions. Subsequently, this calculation was brought to the numerical results and forgotten due to the limited possibilities of its use. Such a prospect of an alternative method of analysis was predicted into a commentary on the translation of a book published in the Soviet Union in 1948 (editor S.M. Rytov). True, this translation was published seven years later. The strict method based on the calculation of the eigenfunctions of a spheroid has now basically only of historical interest and lies outside the scope of the present book.

As shown in Chapter 1, knowledge of a current's distribution along a linear radiator allows us to find the electromagnetic field and all electrical characteristics of the radiator. For this reason, calculation of the current's distribution is the important problem of the antenna theory. The important element of this distribution is the absence of current on the radiator's ends:

$$J(\pm L) = 0. \quad (4.1)$$

The electromagnetic field  $E_z(J)$ , created by the radiator current  $J(z)$  must satisfy the boundary condition on the metal surface of an antenna

$$E_z(a, z)|_{-L < z < L} + K(z) = 0. \quad (4.2)$$



Here the cylindrical coordinate system is used,  $a$  and  $L$  are the radius and the arm length of a dipole respectively,  $K(z)$  is an extraneous emf.

Expression (4.2) is the mathematical record of a fact that the total field, which is a sum of the extraneous field and the current's field, is zero on the surface of a perfectly conducting radiator. The extraneous field is specified usually as the product of potentials' difference  $e$  between the gap edges onto  $\delta$ -function. Magnitude  $K_1(z) = e\delta(z)$  corresponds to connecting the generator in the radiator middle, in point  $z = 0$ , and  $K_2(z) = e\delta(z - h)$  to its shift, i.e., to the placement of the generator at point  $z = h$ .

Equality (4.2) contains as in an embryo all integral equations of the theory of the thin antennas. The external appearance of the equations depends mostly on the selection of a radiator model, because this model determines a form of function  $E_z(J)$ . For example, if the radiator model is made in the form of a conductive filament, then using the expression (1.30) for the field, one can obtain Hallen's integral equation for the filament

$$\int_{-L}^L J(\zeta) G_1 d\zeta = -j \frac{1}{Z_0} (C \cos kz + \frac{e}{2} \sin k|z|), \quad (4.3)$$

where

$$G_1 = \exp(-jkR_1)/(4\pi R_1), \quad R_1 = |z - \zeta|.$$

If to use the expression (1.23) for the field of a model in the form a straight thin-wall metal cylinder, we will get Hallen's integral equation with exact kernel

$$\frac{1}{2\pi} \int_{-L}^L J(\zeta) \int_0^{2\pi} G_2 d\varphi d\zeta = -j \frac{1}{Z_0} (C \cos kz + \frac{e}{2} \sin k|z|), \quad (4.4)$$

Here

$$G_2 = \exp(-jkR_2)/(4\pi R_2), \quad R_2 = \sqrt{(z - \zeta)^2 + 4a^2 \sin^2 \varphi/2}.$$

For the current along a filament of a finite radius we may use the expression (1.22) and obtain the often-used integral equation with approximate kernel

$$\int_{-L}^L J(\zeta) G_3 d\zeta = -j \frac{1}{Z_0} (C \cos kz + \frac{e}{2} \sin k|z|), \quad (4.5)$$

where

$$G_3 = \exp(-jkR_3)/(4\pi R_3), \quad R_3 = \sqrt{(z - \zeta)^2 + 4a^2 \sin^2 \varphi/2}.$$

For the current along a filament of a finite radius we also can use the expression (1.22), but with replacement  $R_1$  by  $R_3$ . In this case we obtain Pocklington's integral equation [2]

$$\int_{-L}^L J(\zeta) \left( k^2 + \frac{\partial^2}{\partial z^2} \right) d\zeta = j\omega\epsilon_0 K(z). \quad (4.6)$$

Constant  $C$  in each equation is found from condition (4.1).

The named equations and methods for their solution have much in common with each other. The first solution of the Hallen's equation with an approximate kernel was given by Hallen itself and described in detail in [3]. During the process of the solution, the function of the current  $J(z)$  is presented as a series in the inverse powers of a parameter  $\Omega = 2\ln(2L/a)$ . By means of the method of successive approximations (of the iterative procedure), it was obtained an expression for the current with using integral sines and cosines.

The iterative procedure proposed by King and Middleton [4] gave the more accurate result. In it the common expression for the current is the same, but the parameter of expansion in a series  $\Omega$  is replaced with  $\Psi$ . For example, zero approximation instead of  $J_{0H}(z)/\Omega$  is given by

$$J_{0KM}(z)/\Psi = j \frac{e}{60\Psi \cos kL} \sin k(L - |z|).$$

To find the parameter  $\Psi$ , the function  $\Psi(z)$  is used. This function is defined as

$$\Psi(z) = \int_{-L}^L \frac{J_{0KM}(\zeta)}{J_{0KM}(z)} \frac{\exp(-jkR)}{R} d\zeta.$$

In the capacity of  $\Psi$ , it is taken the value of  $\Psi(z)$  in point  $z = z_m$ , where the current is maximum or close to maximum, i.e.,

$$\Psi = \begin{cases} \Psi(0), & kL \leq \pi/2, \\ \Psi(L - \lambda/4), & kL > \pi/2. \end{cases}$$

Such selection of the expansion parameter is caused by the fact that function  $\Psi(z)$  at point  $z$  on the antenna surface is proportional to the ratio of vector potential  $A_z(z)$  to current  $J(z)$ . For that reason, function  $\Psi(z)$  varies slowly along the antenna, or more precisely it is almost constant except the segments near the wires ends.

The most important common feature of different equations is the complexity of their solution. In the expansion of the function for the current into a series, as a rule, it is not possible to determine more than the first two terms of this series in connection with the existing singularities. The iterative process slowly converges, and it is not obvious that it even converges at all. The search of a numerical solution also does not demonstrate a smooth process. In this regard, the suspicion has arisen that the proposed equations either does not have the solution, or the solution is not the only one.

In connection with the particular importance of this question, it was considered in [5]. The author has comprehensively analyzed the equation

$$\left( \frac{\partial^2}{\partial z^2} + k^2 \right) \int_{-1}^1 J(t) K(z-t) dt = f(z),$$

where

$$K(u) = \frac{1}{2\pi} \int_0^{2\pi} \frac{\exp\{-jk(u^2 + 4a^2 \sin^2 \varphi/2)^{1/2}\}}{(u^2 + 4a^2 \sin^2 \varphi/2)^{1/2}} d\theta.$$

Here  $J(t)$  is the sought current, and  $f(z)$  is the known exciting field. This field is proportional to the tangential component of the electric field and can be considered as continuous function. The integral equation is complemented by the specific property of the current at the wire ends, namely  $J(\pm 1) = 0$ .

The analysis confirmed that the equation has a solution, and this solution is the only.

Further, Leontovich's integral equation [6] and the methods of its solution as applied to various problems are considered in detail, since the severity of this equation and the possibility of its use, in the author's opinion, exceed the similar qualities of other equations (it should be said that the author of the book is not the co-author and/or a relative of the co-author of this article, but he is only his namesake).

Leontovich's equation played an important role in the progress of the theory of thin antennas and rightfully occupies the main place in this book.

## 2. Leontovich's Equation

Let us start with the derivation of the equation. Assume that a source of electromagnetic field are electrical currents parallel to the  $z$ -axis and having a circular symmetry:

$$\vec{j} = j_z e_z, j_z = j_z(z) = \text{const}(\varphi). \quad (4.7)$$

Then a vector potential  $A$  of a field has only component  $A_z$ , which on the surface of the radiator model in a shape of a thin-wall straight metal cylinder with circular cross-section of a radius  $a$  is equal to

$$A_z(\rho, z) = \frac{\mu}{8\pi^2} \int_0^{2\pi} T(z, \varphi) d\varphi, \quad (4.8)$$

where

$$T(z, \varphi) = \int_{-L}^L J(z) \frac{\exp(-jkR)}{R} d\zeta, R = \sqrt{(z - \zeta)^2 + \rho_1^2}, \rho_1 = \sqrt{\rho^2 + a^2 - 2a\rho \cos \varphi}.$$

We integrate  $T(z, \varphi)$  by parts and use successively the circumstance that the radiator radius is small in comparison with its length and the wavelength, i.e., we neglect by the summands of order of  $a/L$  and  $ka$  and keep the summands, which are proportional to the logarithm of these quantities. As a result, we obtain:

$$T(z, \varphi) = -2J(z) \ln p \rho_1 - \int_{-L}^L \exp(-jk|\zeta - z|) \ln 2p |\zeta - z| \left[ \frac{dJ(\zeta)}{d\zeta} - jk J(\zeta) \text{sign}(\zeta - z) \right] d\zeta.$$

Here  $p$  is some constant having the dimensions of inverse length. Since at  $\rho > a$

$$\int_0^{2\pi} \ln p \rho_1 d\varphi \equiv \int_0^{2\pi} \ln(p \sqrt{\rho^2 + a^2 - 2a\rho \cos \varphi}) d\varphi = 2\pi \ln p,$$

then

$$A_z(\rho, z) = (\mu/4\pi) [-2J(z) \ln p + V(J, z)], \quad (4.9)$$

where

$$V(J, z) = \int_{-L}^L \exp(-jk|z - \varsigma|) \ln 2p|\varsigma - z| \left[ jkJ(\varsigma) + \text{sign}(z - \varsigma) \frac{dJ(\varsigma)}{d\varsigma} \right] d\varsigma.$$

The tangential component of the electric field of the antenna is

$$E_{zA}(\rho, z) = -j \frac{\omega}{k^2} \left( k^2 A_z + \frac{\partial^2 A_z}{\partial z^2} \right). \quad (4.10)$$

Substituting (4.9) into (4.10) and setting  $\rho$  equal to  $a$ , we find:

$$E_{zA}(a, z) = -j \frac{1}{4\pi\omega\epsilon_0} \left[ -\chi_1^{-1} \left( \frac{d^2 J}{dz^2} + k^2 J \right) + \frac{d^2 V}{dz^2} + k^2 V \right]. \quad (4.11)$$

Here  $\chi_1 = 1/(2 \ln pa)$  is a small parameter of the thin antennas' theory, used in [6]. As is shown in [7], in the capacity of constant  $1/p$  one should choose the distance to the nearest inhomogeneity, i.e., the smallest of three magnitudes: wavelength  $\lambda$ , antenna length  $2L$  and the radius  $R_c$  of its curvature. In case of a straight radiator, the length of which does not exceed the wavelength, one can consider that  $1/p = 2L$ , i.e.

$$\chi = -\chi_1 = 1/[2 \ln(2L/a)]. \quad (4.12)$$

From (4.10) and (4.11), we obtain with allowance (4.2) the desired equation

$$\frac{d^2 J(z)}{dz^2} + k^2 J(z) = -j4\pi\omega\epsilon_0 \chi K(z) - \chi W(J). \quad (4.13)$$

Here  $K(z) = -E_{zA}(a, z)$  is the field, creating the current in the antenna,  $-j4\pi\omega\epsilon_0 \chi K(z)$  is the extraneous emf, and  $-\chi W(J)$  is emf, created by the antenna currents. As can be seen from (4.13), this equation together with the components, which contain the extraneous emf, the current and the current derivative, also has the element  $W(J) = \frac{d^2 V}{dz^2} + k^2 V$ , incorporating the integral  $V(J, z)$  and its derivative. In Section 1.2 it is shown that one concentrated emf cannot create the sinusoidal current along the dipole. The mentioned element is the additional emf, which depends on the current of the antenna. This emf creates the radiation and distributes it along the antenna.

The meaning of manipulations implemented during derivation of (4.13), first is that a logarithmic singularity was discovered and picked out. The function  $A_z$  in expression 4.9) including integral  $V(J, z)$  is a continuous function everywhere in contrast to the original integral (4.8). Another important advantage of the equation (4.13) is the absence of an argument  $\varphi$ , since the integration with respect to  $\varphi$  already executed. Nevertheless, this equation is derived for the current of a straight thin-wall cylindrical antenna, and so the equation (4.13) is equivalent to Hallen's equation with exact kernel.

To solve the equation (4.13), in [6] the perturbation method is used, i.e., the current is sought in the form of expansion into a series in powers of the small parameter  $\chi$ :

$$J(z) = \chi J_1(z) + \chi^2 J_2(z) + \chi^3 J_3(z) + \dots$$

Further we will use another form for the expansion of the current into a series, which differs little from this form. Another form, as it will become clear later, it is more convenient:

$$J(z) = J_0(z) + \chi J_1(z) + \chi^2 J_2(z) + \chi^3 J_3(z) + \dots = J_0(z) + \sum_{n=1}^{\infty} \chi^n J_n(z). \quad (4.14)$$

Substituting this series into (4.13), equating coefficients for equal powers of  $\chi$ , and considering that  $J(\pm L) = 0$ , we obtain in the case of an untuned radiator the system of equations:

$$\begin{aligned} \frac{d^2 J_0(z)}{dz^2} + k^2 J_0(z) &= -j4\pi\omega\varepsilon_0 \chi K(z), J_0(\pm L) = 0, \\ \frac{d^2 J_1(z)}{dz^2} + k^2 J_1(z) &= -\chi W(J_0), J_1(\pm L) = 0, \\ \frac{d^2 J_n(z)}{dz^2} + k^2 J_n(z) &= -\chi W(J_{n-1}), J_n(\pm L) = 0, n > 1, \end{aligned} \quad (4.15)$$

where  $W(J_{n-1}) = \frac{d^2 V(J_{n-1}, z)}{dz^2} + k^2 V(J_{n-1}, z)$ . Since the solution is sought in the form of a series in powers of a small parameter  $\chi$ , then the functional  $W(J, z)$  included in this equation also must be linear, i.e.,

$$W(J, z) = \sum_{n=0}^{\infty} \chi^n W(J_n).$$

As seen from (4.15), in calculating the terms of the series (4.14), one can think that the current is located on the axis of a radiator. At the same time, the degree of accuracy adopted in deriving the equation is preserved. This circumstance greatly simplifies calculations, including calculations using recurrent formulas. From the first equation, we obtain that in a zero approximation the current is distributed according to a sinusoidal law and at an arbitrary point of the radiator is equal to

$$J_0(z) = J \frac{e\chi}{60 \cos kL} \sin k(L - |z|). \quad (4.16)$$

It is easy to make sure that the input impedance of the antenna in this approximation is

$$Z_{A0} = -j60\chi^{-1} \cot kL.$$

It has only the reactive component, which coincides with the input impedance of the equivalent long line, whose wave impedance is equal to  $60/\chi$ . The active

component appears in the first approximation. As shown in [6], where the tuned and untuned radiators are first considered separately, the expression for the current in the untuned radiator is general in nature and can be used in both cases.

The next member of a series at the feeding point  $z = 0$  is obtained in [6] from the second equation of the system (4.15) in the form

$$J_1(0) = e\chi(B + jC), \quad (4.17)$$

where

$$B = \frac{1}{30\cos^2 \alpha} \{ \cos \alpha (\cos \alpha \text{Di}2\alpha - \sin \alpha \text{Si}2\alpha) - \frac{1}{4} (\cos 2\alpha \text{Di}4\alpha - \sin 2\alpha \text{Si}4\alpha) \},$$

$$C = \frac{1}{30\cos^2 \alpha} \{ \cos \alpha (\sin \alpha \text{Di}2\alpha + \cos \alpha \text{Si}2\alpha) - \frac{1}{4} (\sin 2\alpha \text{Di}4\alpha + \cos 2\alpha \text{Si}4\alpha) - \frac{1}{2} \sin 2\alpha \ln \alpha \}.$$

Here  $\alpha = kL$  is electric length of a symmetric radiator's arm,  $\text{Di}2\alpha = C + \ln 2\alpha - \text{Ci}2\alpha$ ,

$\text{Di}4\alpha = C + \ln 4\alpha - \text{Ci}4\alpha$ , functions  $\text{Si} x$  and  $\text{Ci} x$  are integral sine and integral cosine of the argument  $x$ ,  $C = 0.5772\dots$  is Euler's constant. The obtained result allows us to find the value of the active component  $R_A$  of the radiator input impedance and to determine the additive  $\Delta X$  to the reactive component. To do this, we divide the emf  $e$  by the total input current. The input impedance of an antenna is

$$Z_{A1} = e/[e/Z_{A0} + \chi J_1(0)].$$

The mentioned components are determined by means of expressions  $R_A = (\chi^2 B)/A^2$ ,  $\Delta X = \chi^2 C/A^2$ , where  $A = -j/Z_{A0} = -\chi \frac{\tan \alpha}{60}$ . Hence, in particular, one can find the active and the reactive components of the input impedance for the cylindrical dipole with the arm length  $\lambda/4$ ,  $\lambda/2$ ,  $3\lambda/4$  respectively (if the shape of dipole varies, the magnitude of reactance changes slightly).

Since prior to the development of methods for calculating input impedances based on the use of integral equations, numerical values were obtained only using the method of induced emf., a natural desire was aroused to compare new results with them. Unfortunately, this comparison turned out to be a difficult task. The results, based on the substitution of the values of the known functions, were close to each other in the greater part of the range, except for the parallel resonance's region, when the length of the radiator arm was approaching to the half of wavelength. Near a parallel resonance, the integral equation gives finite values, but the input impedance, calculated by the method of induced emf, increases infinitely, since the denominator of the corresponding expression tended to zero.

New option of solving the system of equations (4.15) was first called by the method of constants' variation. The first attempt of its use was made in [8]. This method is described in Section 3. Its application permits to explain the reason of induced emf in the vicinity of parallel resonance.

### 3. Method of the Constants' Variation

As is known, in accordance with the method of the constants' variation the solution of the inhomogeneous differential equation is sought as follows. First, we are finding the solution of an auxiliary homogeneous equation, whose right-hand side is zero. Then the constant magnitude obtained in this solution is replaced by an unknown magnitude, and the resulting function is substituted into the left side of the equation, which equates with the right side, allowing us to obtain a solution to the inhomogeneous equation. If this equation is of a higher order than the first one, such a technique can meet with insurmountable difficulties. In our case, we are talking about the equation for the current  $J_n$  from the system of equations (4.15). Although this is a second-order equation, the application of the described technique is facilitated by the similarity of the left and right sides of the equation. Each of them contains a function and its second derivative with the same coefficients, i.e., their ratio can be determined using one of the members. This makes it easy to go from solving a known homogeneous equation to solving an inhomogeneous one.

In the capacity of the right side of the inhomogeneous equation for the current  $\chi'' J_n$  we should take the extraneous emf. The variant of the corresponding expression is chosen depending on the symmetry of the radiator. For definiteness, we will consider that the radiator is symmetric. In this case, in accordance with the equations set (4.15) the extraneous emfs are located at the point  $z = 0$ .

As shown in Section 1, the total emf is the sum of the extraneous emf and emfs created by the currents' fields. This means that when calculating the next member of the series for the current, we must consider the additional emf created by the previous member of the series, flowing along the entire length of the antenna. As can be seen from (4.15), the field created by the zero component of the current is equal

$$E_{\zeta}(J_0) = -W(\chi J_0). \quad (4.18)$$

Each next current included in this series is continuous along the radiator, has a sinusoidal distribution and constant amplitude. The field of this current on the surface of the radiator is also continuous. It is obvious, that this field depends not only on the distance from the point of radiation (from an element of a current) to the point of the reception (to the new extraneous emf), but also on the phase of the current. Therefore, the field created by the all elements of the radiator's current at the reception's point is determined by integrating this field along the radiator's length with allowance its phase. Each additional emf is  $\chi$  times larger than the additional emf, created by the previous member of the series. In particular, the negative extraneous emf exciting the zero component of the current is

$$e_1 = -\chi \int_{-L}^L E_{\zeta}(J_0) \sin k(L - |\zeta|) d\zeta. \quad (4.19)$$

Let's write the  $n$ th member of the series (4.14) as

$$J_n = \chi J_{n-1} = (-k\chi)^n J_0. \quad (4.20)$$

Here,  $J_{n-1}$  is the amplitude of the  $(n-1)$ th member of the series for the current. The current  $J_{(n-1)}$  of each segment radiates the field  $-\chi E_\zeta [J_{(n-1)}]$  and creates in the center of a dipole the emf  $e_n$ . This emf is equal to the sum of fields of individual segments, i.e., is calculated as an integral along the entire antenna length:

$$e_n = -\chi \int_{-L}^L [(-\chi)^{n-1} J_1(\zeta) \text{sink}(L-|\zeta|)] d\zeta = -\chi e_{n-1}, \quad (4.21)$$

The expression (4.21) allows us to find and to locate the currents in accordance with the order of smallness, i.e., to write

$$J(z) = J_0(z) + \chi J_1(z) - \chi^2 J_1(z) + \chi^3 J_1(z) - \dots \quad (4.22)$$

The ease, with which these calculations are performed, indicates the advantages of the equation, which suggests that the radiator is located on the axis of the coordinate system. This makes it possible to determine the  $n$ th member of the series (4.14) for the current at an arbitrary point  $z$  of the radiator and, accordingly, the current in the  $n$ th approximation, if previous approximation is known—both in the general case and in the case of symmetric radiator. To find the input current of the antenna, it is need to calculate it at the point  $z = 0$ .

The same result is obtained, if to use the method of the constants' variation and to compare two equations of set (4.15)—for the current  $J_1(z)$  and for the current  $J_n(z)$ :

$$\frac{d^2 J_1(z)}{dz^2} + k^2 J_1(z) = e_1, \quad \frac{d^2 J_n(z)}{dz^2} + k^2 J_n(z) = e_n.$$

The ratio of the currents in the left parts of these equations must correspond to the ratio of the right-hand sides. It is easy to satisfy that considering the change of sign

$$e_n/e_1 = J_n/J_{(1)} = (-\chi)^{n-1}.$$

It is important to note the input impedance  $Z_{A0}$  of a symmetric thin radiator is the same for all currents, since each emf is created in a common point:

$$e_n = \int_{-L}^L E_\zeta(J_n) \text{sink}(L-|\zeta|) d\zeta = J_n(0) Z_A.$$

and the created currents are proportional to emf magnitudes, i.e.,

$$J_n(z) = (-\chi)^{n-1} J_1(z).$$

That allows us to find and to locate the currents in accordance with the order of smallness, i.e., to obtain the expression (4.22).

Oddly enough, expression for  $e_n$  allows us to find the input impedance of the antenna. Multiplying each term of the equality by the value  $J_n(0)$  we obtain the powers



are determined by expression based on the second formulation of the induced emf method. It is easy to verify that the value obtained from the quality of powers

$$-Z_A = \frac{1}{J_n^2(0)} \int_{-L}^L E_{\zeta} (J_n) J_n(\zeta) d\zeta$$

In this formulation differs from the input impedance only in sign. The minus sign indicates that the additional emf, created by the previous member of the series for the current, partially returns power to the generator, providing energy to subsequent members of the series.

The obtained results permit to write a set of equations for the members of the series (4.14) and to find the amplitudes of the currents. The found order of changing the members of the series allows us to conclude that the members of the series (4.14) form a geometric progression. The progression begins with the first term, equal to  $a_1 = J_0(z)$ . The denominator of the progression is constant and equal to

$$q = -\chi. \quad (4.23)$$

This is an important attestation of the usefulness of expression (4.22). If the number  $N$  of members of such a progression grows endlessly, then its sum tends to the limit

$$s = a_1/(1 - q).$$

In our case, the sum of the members of the progression in accordance with (4.22) and (4.23) is equal to

$$\sum_{n=1}^{\infty} \chi^n J_1(z) = \chi J_1(z)/(1 + \chi).$$

Hence the total current of the radiator in accordance with (4.22) is equal to

$$J(z) = \sum_{n=1}^{\infty} \chi^n J_0(z)/(1 + \chi) = J_0(z)/(1 + \chi). \quad (4.24)$$

Here  $e$  is the extraneous emf on the antenna input,  $J_0(z)$  is the current created by this emf,  $J_0(0) = e/Z_A$  is the current on the antenna input. The current  $J_0(z)$  creates the additional emf  $e_1 = -J_0(0) Z_A$ , which causes in the conductor the current  $\chi J_1(z)$ , equal to  $\chi J_1(z) = e_1/Z_A = -J_0(0)$ . Hence the input current of the antenna is

$$J(0) = J_0(0)/(1 + \chi), \quad (4.25)$$

and

$$Z_A = \frac{e}{J(0)} = Z_{A0} (1 + \chi). \quad (4.26)$$

It is necessary to emphasize that the results of calculating the input impedance of a linear symmetric radiator  $Z_{A1}$  in the second approximation, obtained by three methods (by the method of induced emf in the second formulation, by the method described in [6] and by the method presented in the given chapter) are the same. The

expression given in [6] for the input impedance of the untuned radiator, presented as a combination of integral and trigonometric sines and cosines, coincides with the similar expression that the method of induced emf gives as the result of integrating expression (3.56). The difference in the results arises when calculating the input impedance near the parallel resonance, since in this case the method of induced emf. is forced to use the same expression, and the result tends to infinity. In [6], the input impedance at parallel resonance is determined by solving the equation for the tuned radiator, and that allows to obtain the finite result. In fact, these components obtained in a second approximation for the tuned cylindrical dipoles with the circular cross-section and arm length  $\lambda/4$ ,  $\lambda/2$  and  $3\lambda/4$  are equal to

$$R_A = 73.2, 93.5 \text{ and } 105.4; X_A = 42.5, 44.8 \text{ and } 45.5.$$

These values are given for the components of the input impedance  $Z_A$  of the antenna (for the generator load) in the case when the generator is included in the antinodes of the current. If the generator is placed on a distance  $z_0$  from the antinode, then the input impedance of its load changes. For a dipole length, close to  $2L = \lambda/2$ , the input impedance is equal to  $Z_A = (73.2 + j42.5)/\cos(\pi z_0/2L)$ , for the length close to  $\lambda$  the input impedance is equal to  $Z_A = (93.5 + j44.8)/\cos(\pi z_0/2L)$ . Multiplying these magnitudes to the corresponding factor of the Table 1 allows us to find the total components of the input impedance.

One can consider that the active component of the input impedance for the symmetric metal radiator is equal to the active component of the impedance  $Z_{A1}$ . But a simpler and more convenient method of calculating the active component is based on the analogy of a symmetric radiator with a Hertz dipole. In accordance with this analogy

$$R_A(h) = 20k^2 h_e^2, \quad (4.27)$$

where  $h_e = \frac{2}{k} \tan \frac{kL}{2}$  is the effective length of the symmetric metal radiator, equal to a ratio of an area under a current curve to the input current  $J(0)$ . From here

$$R_A(h) = 80 \tan^2 \frac{kL}{2}. \quad (4.28)$$

The result would be more accurate, if we take into account the phase of a dipole current, which is not constant as in the case of the Hertz dipole, but grows in the direction of a generator. This phase at the point located at a distance  $x$  from the free end of the dipole arm is equal in the first approximation to  $\tan^{-1} X_A/R_A$ , where  $X_A$  and  $R_A$  are the reactive and active components of the input impedance for the dipole with the arm length  $x$ .

It should be said that the formula for  $Z_{A1}$  is widely known, and attempts to redetermine it do not give any practically useful result, because do not allow to obtain significantly more precise result compared with elementary calculations, which were ignoring small magnitudes of the order of wire radius. If in the process of calculating it is necessary to determine the integrals of the form

$$Y_m = \int_0^L \frac{\exp(-jkR_m)}{R_m} \sin k(L - \zeta) d\zeta,$$

then the result is almost equal to the result of the calculation, which begins with the neglecting small magnitudes.

The following curves demonstrate active and reactive components of the radiator input impedance in the second approximation and with allowance of the total sum of the series. These figures also allow us to compare the obtained results for different dipole sizes with the results of an application of the method of induced emf. Fig. 1 gives the reactance of dipoles with the ratio  $L/a$  equal to 5 and 50, and Fig. 2 shows the same reactance with the ratio  $L/a$  equal to 500 and 5000, respectively. The total reactance  $X_{A1}$  is given by a solid curve, the reactance in the second approximation  $X_{AII}$ —by a dotted line. In accordance with (4.27) the absolute magnitude of the total reactance is greater than the reactance in the second approximation by  $(1 + \chi)$  times. The magnitudes  $\chi$  and  $1 + \chi$  depending on  $L/a$  are given in Table 1.

From the figures it is seen that the difference between the curves for the total reactance and the reactance in the second approximation is small and decreases with decreasing antenna thickness. For the active components of the input impedance is also valid the similar relation.

The active component  $R_A$  of the input impedance is shown in Fig. 3 and 4. It has a similar character, but the resistance  $R_{A1}$  in the second approximation does not depend from the magnitude  $L/a$ . The total resistance depends on  $L/a$ , it is proportional to  $(1 + \chi)$ . In Fig. 3 there are curves for the active component  $R_{A1}$  in the first approximation, and the total resistance  $R_A$  for  $L/(a = 5)$  and 50 is presented. The total resistance  $R_A$  for  $L/(a = 500)$  is given in Fig. 4. Also, in Fig. 4 it is given the resistance  $R_A(h)$ , which is calculated in accordance with (4.28)

This result can be refined, if to consider that the current is not constant, as in the case of the Hertz dipole, but decreases in approaching to the generator, since the losses cause the current's attenuation in an equivalent long line. As it follows from the presented results and the graphs, illustrating these results, the sum of the series (4.14) is close to the sum of the first two or three terms. L.A. Vainstein, solving the so-called key equation [9] and analyzing the numerical results, came to similar conclusions. He briefly spoke about these results in 1964 in Kharkov, at a conference on diffraction and propagation of radio waves.

Let us summarize.

As shown in Section 1.2, the sinusoidal current of a cylindrical linear radiator located along  $z$  axis creates at the center of the radiator a field  $E_z$ , which has active and reactive components. The scheme of a linear radiator, demonstrating the shape and magnitude of the fields created by the currents of the radiator in its center, is given in Fig. 1.3. This is a copy of the picture presented in [10] to show the difference between the actual electromagnetic field on the surface of a linear radiator excited by a single generator and the idealized representation about it.

A similar result is obtained in Section 1.3 during the solution of the Leontovich's integral equation for the current in a linear radiator. This solution has the form of an expansion in powers of a small parameter  $\chi$ . In the case of a cylindrical radiator, the small parameter is taken equal to  $\chi = -\frac{1}{2 \ln(2l/ae)}$  or to  $\chi = -\frac{1}{2 \ln(L/a)}$ . As the

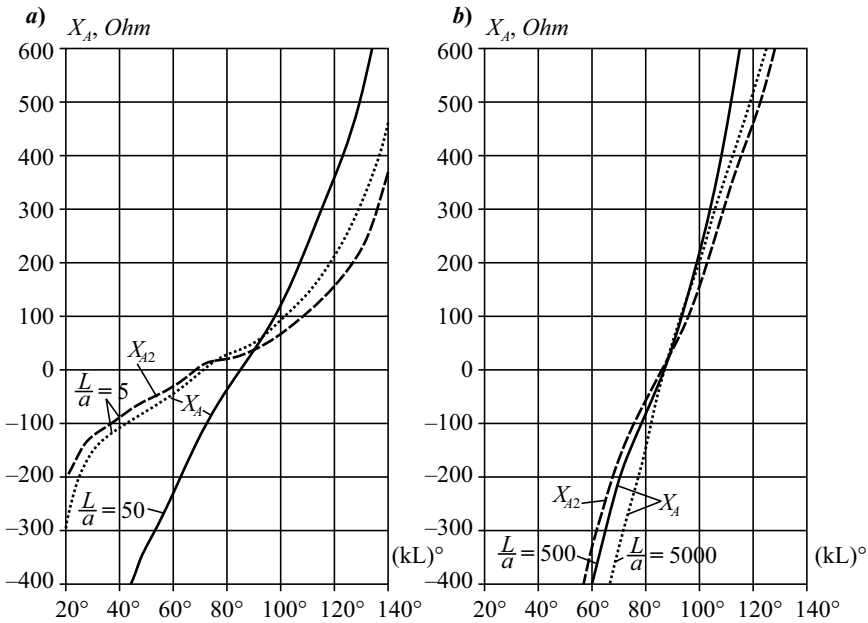


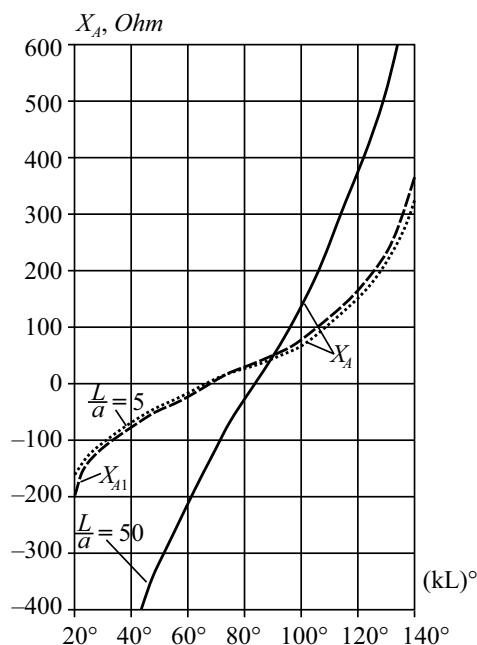
Fig. 1: Reactive component of the input impedance for the dipole with  $L/a = 5$  and  $50$ .

Table 1: Relation of Components.

$L/a$	5	20	50	200	500	2000	5000
$\chi$	0.311	0.167	0.128	0.0944	0.0805	0.0658	0.0587
$1+\chi$	1.311	1.167	1.128	1.0944	1.0805	1.0658	1.0587

first member of the series for the current, a purely imaginary magnitude is used. It is equal to the input current in a homogeneous long line, open at the end. This current is excited by the generator located in the radiator center. Other terms of the series are the additional currents created by new emfs. These emfs are equal to the fields, created in the radiator center by the currents, equal to the previous terms of the series. Section 3 shows that each term of the current's series, which is made in the form of an expansion in powers of a small parameter  $\chi$ , creates in the radiator an additional emf, which is a source of a new current. As was shown above, all terms of the series are determined by the expression (4.22). Each additional current is the sum of real and imaginary components with the same factors  $\chi^n$ .

A comparison of the picture, given in the Fig. 1.3, with the description of an interrelationship between the terms of the series for the current in the Leontovich's equation brightly showed the importance of understanding and using this interrelationship for calculating of the series terms. As follows from the above, the placement of the generator in the center of the radiator consistently leads to the appearance of the sinusoidal currents, additional emfs and created by them new



**Fig. 2:** Reactive component of the input impedance for the dipole with  $L/a = 500$  and  $5000$ .

currents in the antenna wires. The mentioned details allow us to determine the total sum of the series for the current. The additional terms of a series permit to consider them as the members of an infinite geometric progression and to determine their full sum as the sum of this progression. The total current is obtained as result of adding the first term of the series and the sum of the progression. This allows to find the input impedance of the radiator. A similar procedure can be used for solving other integral equations and for the calculations by the method of induced emf. The value of  $\chi$  depends on the shape of the radiator (filament, cylinder, cone, paraboloid, plate) and the ratio of geometric dimensions. The above result allows us to find the input impedance for any of them, if the parameter  $\chi$  is known. In the case of a cylindrical radiator,  $\chi$  is given.

The presented results permit to shift the emphasis during the calculation of the input impedance of a linear radiator. These results open new perspectives for solving problems with the help of integral equations. Unfortunately, for the most part, the solution of such problems was not carried through to the end, but was limited by the calculation of the first terms of the series, the sum of which differs from the total sum of all terms. This has the various reasons. One of them is the need to round off intermediate results, which inevitably leads to errors. The new variant of the solution, which made it possible to calculate the total sum of the series for the current, as shown by an example of its application to the Leontovich's integral equation, significantly increases the probability of bringing the problem to an obvious result. This procedure can be applied to a wide class of equations proposed for currents in various radiators, subject to the transition from the iteration method to the perturbation method.

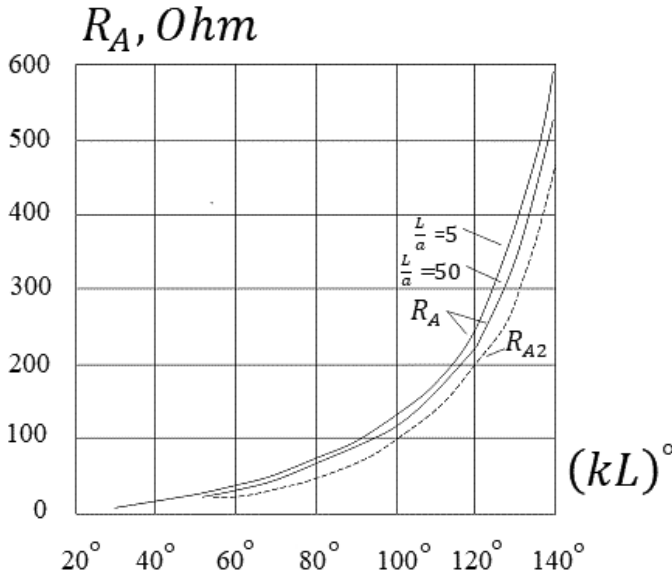


Fig. 3: Active component of the input impedance for the dipole with  $L/a = 5$  and 50.

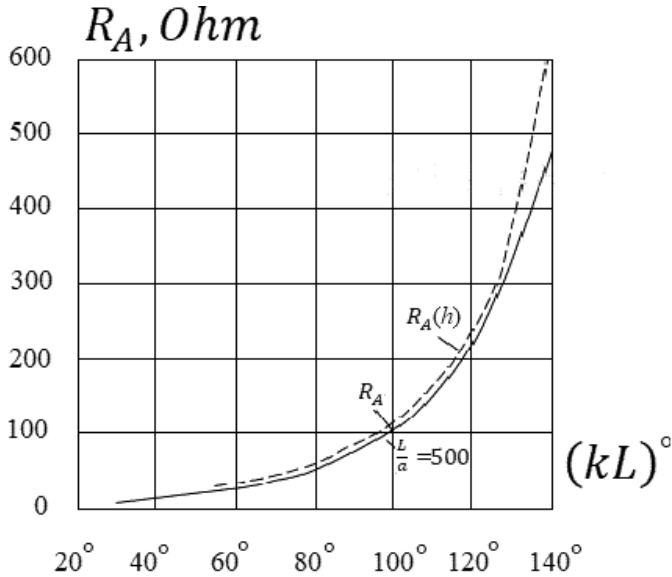


Fig. 4: Active component of the input impedance for the dipole with  $L/a = 500$ .

The calculation shows that the result obtained in [6] (second approximation in terms of current and input impedance) is very close to the exact solution. In this

connection, it must be pointed out that the calculation of the sum of the series (4.14) has mainly the principal interest. Practical results require numerical verification.

#### 4. Integral Equation for Two Metal Radiators

In the analysis of the structures, consisting of several radiators forming the antenna array, we begin with a special case. Let us consider two parallel symmetrical radiators of different length that are axially shifted relative to each other (Fig. 5). According to (1.16), if electric currents  $J_I(\sigma)$  and  $J_{II}(\varsigma)$  with frequency  $\omega$  flow along the radiators, then the field created by these currents is

$$E_z = -j\frac{\omega}{k^2} \left( k^2 A_z + \frac{\partial^2 A_z}{\partial z^2} \right). \quad (4.29)$$

and in accordance with the principle of superposition

$$A_z = A_{1z} + A_{2z}.$$

Using a model of two radiators in the form of two straight thin-walled cylinder with length  $L_1$  and  $L_2$ , with radius  $a_1$  and  $a_2$ , respectively, we write down according to (1.20)

$$\begin{aligned} A_{1z}(\rho, z) &= \frac{\mu}{8\pi^2} \int_{-L_1}^{L_1} J_I(\sigma) \int_0^{2\pi} \frac{e^{-jkR_1}}{R_1} d\varphi d\sigma, \\ A_{2z}(\rho, z) &= \frac{\mu}{8\pi^2} \int_{-L_2}^{L_2} J_{II}(\varsigma) \int_0^{2\pi} \frac{e^{-jkR_2}}{R_2} d\psi d\varsigma. \end{aligned} \quad (4.30)$$

Here  $R_1$  and  $R_2$  are the distances from the observation point with coordinates  $(\rho_1, \varphi_0, z)$  to integration points  $(a_1, \varphi, \sigma)$  and  $(a_2, \psi, \varsigma)$  on the surface of the first and second radiators, respectively, i.e.,

$$\begin{aligned} R_1 &= \sqrt{(z - \sigma)^2 + \rho_1^2 + a_1^2 - 2a_1 \rho_1 \cos(\varphi - \varphi_0)}, \\ R_2 &= \sqrt{(z - \varsigma)^2 + \rho_2^2 + a_2^2 - 2a_2 \rho_2 \cos(\psi - \psi_0)}. \end{aligned}$$

For the current in each radiator one can write an equation like equation (4.13). Let the observation point is located near the surface of the first radiator. Then, if

$$a_1, a_2 \ll d, \quad (4.31)$$

the distance between the axes of two radiators, one can consider that a vector potential  $A_{1z}(\rho, z)$  has a logarithmic singularity near the first radiator, and calculating of it similarly (4.9) gives

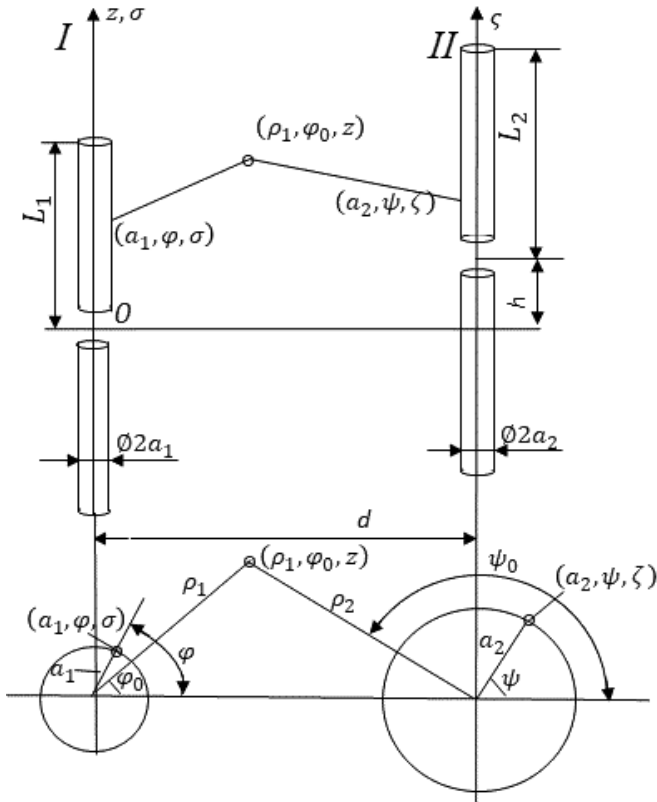


Fig. 5: The structure from two parallel radiators.

$$A_{1z}(a_1, z) = (\mu/4\pi)[-2J(z)\ln pp + V(J, z)].$$

The vector potential  $A_{2z}$  near the first radiator does not have such a feature, since if condition (4.31) is satisfied, the magnitude  $R_2$  is not small for any  $\zeta$  before  $R_2 \geq d - \rho_1 - a_1$ . Accordingly the tangential component of the electric field created by the current  $J_I(z)$  is determined by an expression (4.11), and it has a large magnitude of the order 1. The field  $E_z(J_{II})$ , created by the current  $J_{II}(z)$  of the second radiator on the surface of the first one, does not contain a large summand.

Like (4.2), the boundary condition on the surface of the first radiator has the form

$$E_z(J_I, a_1, z) + E_z(J_{II}, a_1, z) + K_I(z) = 0, \quad -L \leq z \leq L. \quad (4.32)$$

where  $K_I(z)$  is the extraneous field,  $E_z(J_I, a_1, z)$  and  $E_z(J_{II}, a_1, z)$  are the fields of the first and second radiators on the surface of the first radiator. Substituting (4.11) into (4.32), we obtain the integral equation for the current  $J_I(z)$ ,



$$\frac{d^2 J_I(z)}{dz^2} + k^2 J_I(z) = -j4\pi\omega\epsilon_0 \chi [K_I(z) + E_z(J_{II}, a_1, z)] - \chi W(J_I), \quad (4.33)$$

where  $J_I(\pm L_1) = 0$ . Here  $\chi = 1/[2\ln(2L_1/a_1)]$ . Equation (4.33) generalizes equation (4.13) written for the current in a single radiator. The right part of this expression contains three components. The first component is the exciting emf, the second component is emf caused by influence of the second radiator, and the third component is the additional emf, which takes into account the radiation of the first antenna and depends on its current. As is shown in the Section 3, the additional emf is created by the previous member of the current's series  $J_I(z)$ .

While solving the equation (4.33), we represent the currents  $J_I(z)$  and  $J_{II}(\zeta)$  in the form of series in powers of small parameters  $\chi_1$  and  $\chi_2$ , respectively:

$$J_I(z) = \sum_{n=0}^{\infty} \chi_1^n J_{In}(z), \quad J_{II}(\zeta) = \sum_{n=1}^{\infty} \chi_2^n J_{IIn}(\zeta). \quad (4.34)$$

At that  $\chi_2 = 1/[2\ln(2L_2/a_2)]$ . It means that the solution of equation (4.33) is sought as a series in powers of a small parameter, like the series (4.14). Since functionals  $W(J_I, z)$  and  $E_z(J_{II}, a_1, z)$  are linear, they can also be presented in the form of similar series. If  $\chi_1$  and  $\chi_2$  have the same order of smallness:

$$\chi_2 \sim \chi_1, \quad (4.35)$$

then the equation (4.33) for not resonant radiator reduces to the set of equations for  $J_{In}(z)$ , and generalizes the set of equations (4.15), written for a single radiator. In the right side of these equations, a new summand  $(\chi_2/\chi_1)^n E_z(J_{IIn})$  appears next to  $W(J_{In})$ .

From the equation it follows that when one of the radiators is excited by the concentrated emf, the current in it has a sinusoidal character, which is also valid in the presence of a second radiator. Using the method of constants variation, it is easy to be convinced that the second radiator creates the field  $E_\sigma(\chi_2^{n-1} J_{IIn-1})$  involved in excitation of the following current component  $J_{In}(z)$ . The second radiator introduces a new summand into the integrand of the expression (4.21) for the extraneous emf located in the center of the first radiator and excited the  $n$ th component of the current. In the left part of each expression, the first term in a bracket is the extraneous emf for the  $n$ th component of the current produced by a first radiator, and the second term is the extraneous emf for the same component produced by a second radiator.

$$e_n = -\chi^{n-1} \int_{-L}^L E_\zeta [J_{I(n)}(\zeta)] \text{sink}(L - |\zeta|) d\zeta + \int_{-L}^L E_\zeta [J_{IIn}(\zeta)] \text{sink}(L - |\zeta|) d\zeta.$$

From here it is easy to pass to the generalization of expression (4.22):

$$\int_{-L}^L \{E[J_{I(n)}] + E[J_{IIn}]\} J_{I(n)}(\zeta) d\zeta = -J_{I(n)}^2(0) Z_{All}. \quad (4.36)$$

During the analysis of radiators' system of two coupled antennas, it is necessary to consider the conditions (4.31) and (4.35). If these conditions are not met, the calculation may give a significant error. This circumstance must be considered when applying the method of calculation to folded, multi-wire and multi-radiators antennas, whose wires located parallel to each other on the distances, small compared to their length. The parameters  $\chi$  of the coupled radiators, as a rule, have the same order of

smallness. However, one must remember that the possibility of their use requires verification, if they are significantly different from each other.

As it follows from the said here and in Section 3.5, in the case of two radiators the field on the surface of the first radiator is equal to the sum of the fields created by the currents  $J_I$  and  $J_{II}$  of a first and a second radiator

$$E_I = E_I(J_I) + E_I(J_{II}).$$

The oscillating power created by a first radiator is equal to

$$P_I = \int [E_I(J_I) + E_I(J_{II})] J_I(z) dz.$$

Its input impedance is

$$Z_{AI} = \frac{P_I}{J_1^2(0)} = Z_{II} + \frac{J_z(0)}{J_1(0)} Z_{I,II}.$$

Here  $Z_{II}$  is the self-impedance of a first radiator,  $Z_{I,II}$  is the mutual impedance of the radiators. Similarly, in the case of  $N$  parallel radiators, the input impedance of the  $m$ th radiator is

$$Z_{Am} = \sum_{n=1}^N \frac{J_n(0)}{J_m(0)} Z_{mn}. \quad (4.37)$$

where  $Z_{mn}$  is the mutual impedance of the  $m$ th and  $n$ th radiators. The emf at the center of  $m$ th radiator is equal to

$$e_m = \sum_{n=1}^N J_n(0) Z_{mn}. \quad (4.38)$$

Equality (4.37) is the Kirchhoff equation for a circuit. In accordance with this equation, the emf of a circuit is equal to the sum of the voltage drops on its elements. This expression corresponds to the sequential inclusion of circuit elements (Fig. 3.12). Each of them is equal to

$$Z_{Amn} = \frac{J_n(0)}{J_m(0)} Z_{mn}.$$

The sequential circuit, which is shown in Fig. 3.12, is widely used in calculations of radiators systems and is valid for radiators with an arm length  $L \leq 0.4\lambda$ . The Kirchhoff equations (4.38) for several radiators were written for antennas located in parallel to each other. This is a special case. But the equations are valid in the general case of an arbitrary mutual arrangement of radiators. In this case, when calculating the mutual impedance, it is necessary to take the tangential component of the  $n$ th field as the field created by the  $n$ th radiator on the surface of the  $m$ th one. We note a special case that should be remembered. If the current at the input of a nearby radiator is equal to zero (idle), then one must check the possibility of the presence of

current in each of its arms and such a radiator should be considered as two coaxial half-length radiators.

The analysis of structure consisting of several radiators shows that the radiator  $m$  with current  $J_m(z)$  gives the oscillating power to another radiator ( $n$ ), which creates on the surface of the radiator  $m$  the field  $E_n(J_n)$ , where  $J_n(\varsigma) = J_n(0)f_n(\varsigma)$ . This oscillating power is equal to

$$P_{mn} = \int E_n(J_n) J_m(z) dz,$$

at that the integral is taken over the entire length of the radiator  $m$ . From here the additional impedance in its circuit, created by the radiator  $n$ , is equal to

$$Z_{mn} = P_{mn} / J_m^2(0) = \frac{J_n(0)}{J_m(0)} Z'_{mn}, \quad (4.39)$$

where  $Z'_{mn} = \int f_n(z) f_m(z) dz$ . Formula (4.39) allows us to calculate the input impedance of two identical parallel radiators (see Fig. 6) that do not have a vertical shift ( $L_1 = L_2 = L$ ,  $a_1 = a_2 = a$ ,  $h = 0$ ). The current distribution from expression (1.21) and the tangential component of the field from expression (1.25) are substituted into this formula. The value of  $\rho$  in the formulas for  $R_0, R_1, R_2$  must be replaced by the distance  $d$  between the axes of the radiators. The result looks like:

$$\begin{aligned} R_{12} = & \frac{30}{\sin^2 kL} \{ 2[2Cikd - Cik(\sqrt{L^2 + d^2} + L) - Cik(\sqrt{L^2 + d^2} - L)] + \\ & \sin 2kL [Sik(\sqrt{4L^2 + d^2} + 2L) - Sik(\sqrt{4L^2 + d^2} - 2L) - 2Sik(\sqrt{L^2 + d^2} + L) - \\ & 2Sik(\sqrt{L^2 + d^2} - L)] + \\ & \cos 2kL [Cik(\sqrt{4L^2 + d^2} + 2L) + Cik(\sqrt{4L^2 + d^2} - 2L) - 2Cik(\sqrt{L^2 + d^2} + L) - \\ & 2Cik(\sqrt{L^2 + d^2} - L) + 2Cikd] \}; \\ X_{12} = & \frac{30}{\sin^2 kL} \{ 2[Si(\sqrt{L^2 + d^2} + L) + Sik(\sqrt{L^2 + d^2} - L)2Sikd] + \\ & \sin 2kL [Cik(\sqrt{4L^2 + d^2} + 2L) - Cik(\sqrt{4L^2 + d^2} - 2L) - 2Cik(\sqrt{L^2 + d^2} + L) - \\ & 2ik(\sqrt{L^2 + d^2} - L)] - \\ & \cos 2kL [Sik(\sqrt{4L^2 + d^2} + 2L) + Sik(\sqrt{4L^2 + d^2} - 2L) - 2Sik(\sqrt{L^2 + d^2} + L) - \\ & 2Sik(\sqrt{L^2 + d^2} - L) + 2Sikd] \}. \end{aligned} \quad (4.40)$$

When  $d \rightarrow a$ , where  $a$  is the radius of the radiators, these expressions turn into (3.57). Figure 3.3 shows the active and reactive components of the mutual impedance of the radiators with arm length  $L = \lambda/4$  without vertical shift, and in Fig. 7 modulus

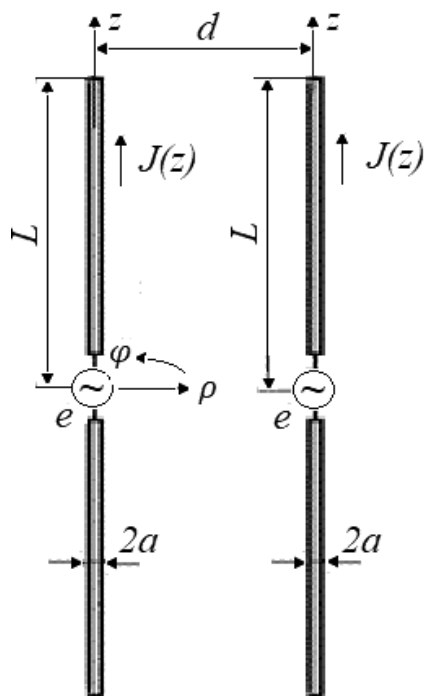


Fig. 6: Two identical radiators.

and phase of it are given. As can be seen from Fig. 3.3, at small  $d$  mutual impedance goes into the self-impedance of the half-wave radiator, equal to  $Z_{12} = Z = 73.1 + j42.5$ . From Fig. 7 it follows that with an increase in the distance  $d$  between the radiators, the modulus of mutual impedance smoothly decreases, and the phase changes according to a law close to linear (when the distance  $d$  increases by the wavelength, the phase changes by a magnitude of the order  $2\pi$ ).

The same results can be obtained by means of Poynting method (see Chapter 3).

## 5. Radiators with Distributed Loads

The next Section is devoted to Leontovich's equation for the current in radiators with distributed surface impedance (or in other words, with distributed loads). The boundary conditions on the surface of the wire with distributed surface impedance, i.e., at segment  $-L \leq z \leq L$ , are given in Section 2.1 in the form of expression (2.1). An example of such a radiator is an antenna in the form of a metal rod covered with a magnetodielectric shell (Fig. 2.3). This antenna has the shape of a circular cylinder, the radius  $a$  of which is small compared to its length  $2L$  and wavelength  $\lambda$ .

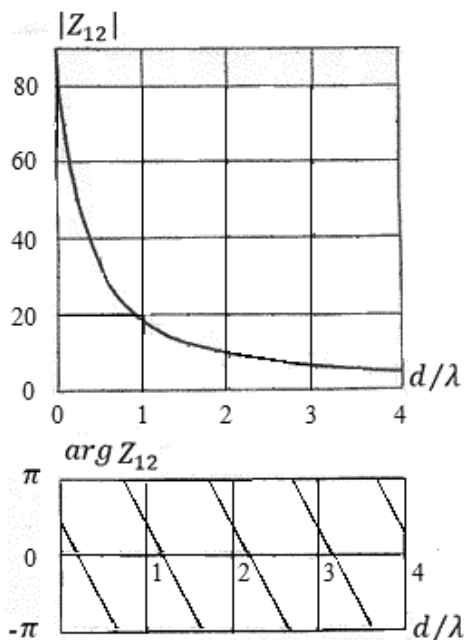


Fig. 7: Modulus and phase of the mutual impedance of parallel half-wave radiators.

Substituting into the boundary condition (2.1) the magnetic field  $H_\varphi(a, z)$  from the expression (2.2) and the tangent component of an electric field  $E_{zA}(a, z)$ , created by the current  $J(z)$ , from the expression (4.11), we obtain the equation for the current in the impedance radiator, analogous to equation (4.13):

$$\frac{d^2 J(z)}{dz^2} + k^2 J(z) = -j4\pi\omega\epsilon_0 \chi [K(z) - J(z)Z(z)/(2\pi a)] - \chi W(J). \quad (4.41)$$

It must satisfy the condition of the current absence at the radiator ends. The right side of the equation consists of three terms. The first term is the exciting emf, the second term is the voltage drop on the distributed load, i.e., on the surface impedance  $Z(z)$ , the third term is the additional emf, which is caused by the fields of previous member of the series and creates the new current  $J_1(z)$ . Assuming that the surface impedance is constant along the length of the radiator, we introduce the designation  $jk\chi Z/60\pi a = U$ .

The equation for the current will take the form

$$\frac{d^2 J(z)}{dz^2} + k_1^2 J = -j4\pi\omega\epsilon_0 \chi K(z) - \chi W(J), \quad (4.42)$$

where the magnitude  $k_1 = \sqrt{k^2 + U}$  is constant in the case of an antenna with a constant surface impedance. If the order of the magnitude  $U$  is close to the order of the magnitude  $k^2$ , then the surface impedance essentially affects the current distribution along the radiator, and the magnitude

$$k_1 = \sqrt{k^2 + U} = \sqrt{k^2 + jk\chi Z / (60\pi a)} \quad (4.43)$$

has a sense of the new propagation constant of a wave along the antenna. The relation  $k_1/k$  is usually called a slowdown.

If for solving the equation (4.42), we apply the expansion of the current into a series, like to the expansion used in [6], then in the first approximation, the current distribution along the radiator has a sinusoidal character:

$$\chi J_1(z) = j \frac{k\chi e}{60 k_1 \cos k_1 L}. \quad (4.44)$$

The input impedance of the radiator in this approximation is purely reactive and is equal to the input impedance of a uniform long line open at the end, in which the wave propagation velocity is  $k_1/k$  times less than in air, and the characteristic impedance is  $k_1/k$  times greater. At that the second equation of the system will allow us to determine the current in the second approximation, to calculate the magnitude of the active component of the input impedance and to make more precise the magnitude of its reactive component. For a variant of an antenna excited by a concentrated emf located in its middle, we get:

$$\chi^2 J_2(z) = j \frac{\chi^2 e}{120 \cos^1 \beta \beta^2} \frac{\alpha^2}{\beta^2} \Theta(\beta, \alpha) \sin k_1 (L - |z|), \quad (4.45)$$

where

$$\begin{aligned} \Theta(\beta, \alpha) = & \frac{1}{2} \left( \frac{\beta}{\alpha} + \frac{\alpha}{\beta} + \frac{2ml}{\alpha} \right) e^{j2\beta} Ei(-j2m) - \frac{1}{2} \left( \frac{\beta}{\alpha} + \frac{\alpha}{\beta} + \frac{2ml}{\alpha} \right) e^{-j2\beta} Ei(j2l) - \\ & \left( \frac{\beta}{\alpha} + \frac{\alpha}{\beta} + j \frac{ml}{\alpha} \right) (1 + e^{j2\beta}) Ei(-jm) + \left( \frac{\beta}{\alpha} + \frac{\alpha}{\beta} + j \frac{ml}{\alpha} \right) (1 + e^{j2\beta}) Ei(jl) + \\ & \left[ \left( 1 + \frac{e^{j2\beta}}{2} \right) \left( \frac{\beta}{\alpha} + \frac{\alpha}{\beta} \right) + j \frac{ml}{\alpha} \right] \ln m - \left[ \left( 1 + \frac{e^{-j2\beta}}{2} \right) \left( \frac{\beta}{\alpha} + \frac{\alpha}{\beta} \right) - \frac{ml}{\alpha} \right] \ln l + \\ & j \left( \left( \frac{\beta}{\alpha} + \frac{\alpha}{\beta} \right) \sin 2\beta + \frac{2ml}{\alpha} \right) \ln \frac{\gamma}{2\alpha} - (1 + e^{-j2\alpha} + 2\cos^2 \beta) + 4e^{-j\alpha} \cos \beta + j \frac{\beta}{\alpha} \sin 2\beta. \end{aligned}$$

Here the notations are used:  $Ei(jx) = Cix + jSix$ ,  $m = \beta + \alpha$ ,  $l = \beta - \alpha$ ,  $\beta = k_1 L$ ,  $\alpha = kL$ . Because the current in the second approximation at the emf application point is equal to

$$J(0) = \chi J_1(0) + \chi^2 J_2(0),$$

then on the frequency far from the parallel resonance

$$Z_{All} = e \left[ \frac{1}{\chi J_1(0)} - \frac{J_2(0)}{J_1^2(0)} \right] = -j \frac{60 \beta}{\chi^\alpha} \cot \beta + \frac{30}{\sin^2 \beta} \Theta(\beta, \alpha),$$

and near the parallel resonance

$$Z_{All} = \frac{e}{\chi^2 J_2(0)} = 120 \beta + \frac{\beta^2}{\alpha^2} \chi^{-2} \Theta^{-1}(\beta, \alpha).$$

The presence of surface impedance significantly changes the characteristics of the antenna. When calculating the field created by the current of the impedance radiator, it must be taken into account that the voltage drop on the antenna itself (on the surface impedance included in the antenna) does not create the radiated field, and therefore in the expression (3.56) for the input impedance, the magnitude  $E_z$  should be replaced by the difference  $E_{z1} = E_z - H_\varphi Z$ . In accordance with the method of induced emf we get instead of (3.56)

$$Z_{All} = \frac{1}{\chi^2 J_2(0)} \int_{-L}^L \left[ E_z(\chi J_1) - \frac{Z \chi J_1(\zeta)}{2\pi a} \right] \chi J_1(\zeta) d\zeta. \quad (4.46)$$

One must remember that the surface impedance not only adds a summand to this expression, but also changes the current distribution along the radiator, since the propagation constant is changed. The field  $E_z(J)$  of an impedance antenna, like the field of a metal radiator, is calculated in accordance with expression like expression (1.23). The first multiplier of an integrand in the right side of the expression (1.23) depends from the propagation constant, which in this case is changed. But despite this fact the mentioned multiplier as before is equal to zero. For the longitudinal component of the electric field of the antenna at an arbitrary point  $M$  with coordinates  $(\rho, 0, z)$  located at a distance  $d$  from the antenna axis (see Fig. 1.2a) we obtain:

$$E_z = -j \frac{30J(0)}{\varepsilon_0} \frac{k_1}{k} \left[ \frac{\exp(-jkR_1)}{R_1} + \frac{\exp(-jkR_2)}{R_2} - 2 \frac{\exp(-jkR_0)}{R_0} \cos k_1 L \right]. \quad (4.47)$$

Here  $R_1 = \sqrt{(z-L)^2 + d^2}$ ,  $R_2 = \sqrt{(z+L)^2 + d^2}$ ,  $R_0 = \sqrt{z^2 + d^2}$  are the distances from the observation point  $M$  to the upper and lower ends of the radiator, as well as its middle (see Fig. 1.2a). Substitution of this expression in (4.46) gives

$$Z_A = j60 \left[ \frac{\exp(-jkR_1)}{R_1} + \frac{\exp(-jkR_2)}{R_2} - 2 \frac{\exp(-jkR_0)}{R_0} \cos k_1 L \right] \sin k_1 (L - z) dz + \frac{Z}{4\pi a} \left( 2L - \frac{\sin 2k_1 L}{k_1} \right). \quad (4.48)$$

This expression differs from the similar expression (3.56) for a metal radiator by a term proportional to the surface impedance  $Z$ . If  $d$  is a distance between two parallel radiators of the same dimensions, then the magnitude  $Z_A$  is a mutual impedance between two radiators. If  $d = a$ , where  $a$  is a radius of the antenna, then  $Z_A$  is the self-impedance of the antenna. It is impossible to reduce expression (4.48) to tabulated functions in the usual way, since the integrand depends on two propagation constants,  $k$  and  $k_1$ . This can only be done for calculating the self-impedance of a thin radiator with the radius  $a \ll L, \lambda$ . To do this, we introduce a magnitude  $\delta$  satisfying the inequality  $a \ll \delta \ll L, \lambda$ . Then if  $|\zeta - z| > \delta$ , then  $R = |\zeta - z|$ , and if  $|\zeta - z| < \delta$ , then  $e^{-jkR} = 1$ . Dividing the integration interval into segments from  $-L$  to  $-\delta$ , from  $-\delta$  to  $0$ , from  $0$  to  $\delta$  and from  $\delta$  to  $L$  and consistently using the specified conditions, we obtain:

$$\begin{aligned} R_A = & \frac{30J(0)}{\sin^2} \left\{ \left( \frac{\beta}{\alpha} + \frac{\alpha}{\beta} \right) \left[ \ln \frac{m}{l} - Cim + Cil + \frac{\cos 2\beta}{2} \left( \ln \frac{m}{l} - 2Cim + 2Cil + Ci2m - Ci2l \right) \right. \right. \\ & \left. \left. + \frac{\sin 2\beta}{2} (Si2m - Si2l - 2Sim + 2Sil) \right] - 2(\cos \beta - \cos \alpha)^2 - \right. \\ & \left. \frac{\beta^2 - \alpha^2}{\alpha} [Sim - Sil + \cos 2\beta(Sim - Sil + Si2l) + \sin 2\beta(Ci2m - Ci2l - Cim + Cil)] \right\}, \\ X_A = & -\frac{60\beta}{\chi\alpha} \cot \beta + \frac{30}{\sin^2 \beta} \left\{ \left( \frac{\beta}{\alpha} + \frac{\alpha}{\beta} \right) \left[ Sim + Sil + \frac{\cos 2\beta}{2} (2Sim + 2Sil - Si2m - Si2l) + \frac{\sin 2\beta}{2} * \right. \right. \\ & \left. \left( \ln \frac{\gamma^2 ml}{4\alpha^2} + Ci2m + Ci2l - 2Cim - 2Cil \right) \right] - 2 \sin \alpha (2 \cos \beta - \cos \alpha) + \frac{\beta}{2} \sin 2\beta - \frac{\beta^2 - \alpha^2}{\alpha} * \right. \\ & \left. [Cim + Cil - \ln \frac{\gamma^2 ml}{4\alpha^2} + \cos 2\beta(Cim + Cil - Ci2m - Ci2l) + \sin 2\beta(Sim + Sil - Si2m - Si2l)] \right\}. \end{aligned} \quad (4.49)$$

Here the notation adopted in (3.57) and (4.45) are used.

The field of the impedance radiator in the far zone and its directional pattern can be calculated by considering the radiator as the sum of the elementary dipoles in accordance with the method described in Section 3.2 and by using the expression



(4.44) for the distribution of a current along the radiator. This calculation for the field of a symmetric radiator with an emf in the center gives

$$E_\theta = j60J(0) \frac{\exp(-jkR_1)}{R} \frac{k_1 k \sin\theta}{k_1^2 - k^2 \cos^2 \theta} [\cos(kL \cos\theta) - \cos k_1 L]. \quad (4.50)$$

Using  $E_\theta$  permits to find by means of expressions of Section 3.2 the radiation power. If we divide this power to the square of the first component of the generator current, we get the antenna's resistance of radiation, which coincides with the magnitude of  $R_A$  presented in (4.49). When the electric length of the radiator is small ( $kL \ll 1$ ), then replacing in expression (4.49) all functions by the first members of the series expansion we arrive at the expression

$$R_A = R_\Sigma = 20k^2 L^2. \quad (4.51)$$

This expression shows that in this case the resistances of radiation for the impedance antenna coincides in magnitude with the resistance of radiation for the metal antenna. In the case of short antennas whose length is comparable to the wavelength ( $L < 0.3 k\lambda/k_1$ ), one can use the formula

$$R_\Sigma = 20k^2 h_e^2. \quad (4.52)$$

In the general case an effective length  $h_e$  of an antenna is equal to the ratio of an area under a current curve to the input current  $J(0)$ . In this case  $h_e = \frac{2}{k_1} \tan \frac{k_1 L}{2}$ , i.e.

$$R_\Sigma = 80 \frac{k^2}{k_1^2} \tan^2 \frac{k_1 L}{2}.$$

The properties of radiators with constant surface impedance, which are considered in this Section, do not depend on the method of impedance creation. Let us for example calculate the surface impedance of an antenna made in the form of a metal rod with radius  $a_1$ , surrounded by a ferrite shell with radius  $a_2$  with absolute magnetic permeability  $\mu$  and dielectric permittivity  $\varepsilon$  (see Fig. 2.6a). In accordance with (4.43)

$$k_1 = k\sqrt{1 + \mu_r \ln(a/a_1)/\ln(2L/a)}.$$

Such an antenna, in addition to ordinary losses, has the losses in the shell. They can be determined by introducing complex magnetic permeability

$$\mu_r = \mu_1 - j\mu_2.$$

Substituting  $\mu_r$  in the expression for  $k_1$ , we obtain the complex propagation constant  $k_1 = k_{11} - jk_{12}$  and the complex magnitudes  $\beta = \beta_0 - j\beta_1$ . Here

$$k_{11} = k\sqrt{1 + \mu_1 A}, k_{12} = kA \frac{\mu_2}{2\sqrt{\mu_1 A}} \ll k_{11}, A = \ln(a/a_1)/\ln(2L/a), \beta_0 = k_{11} L, \beta_1 = k_{12} L \ll 1,$$

$$\ln(\beta + \alpha) = \ln(\beta_0 + \alpha) - j \frac{\beta_1}{\beta_0 + \alpha}, Ci(\beta + \alpha) = Ci(\beta_0 + \alpha) - \frac{\beta_1}{\beta_0 + \alpha} \cos(\beta_0 + \alpha).$$

Substituting these functions into an expression (4.51), we find additional active component in the input impedance, which is created by the second component of  $\beta$  (it is proportional to  $k_{12}$ ). That is an additional resistance of losses in the radiator, caused by the losses in the ferrite. The expression for calculating this resistance in the radiator is given in [12]:

$$\begin{aligned} R_A = R_A|_{\beta_1=0} + \left( \frac{\beta_1}{\beta_0} - \frac{2\beta_1}{\sin 2\beta_0} \right) X_A|_{\beta_1=0} + \\ \frac{30\beta_1}{\sin 2\beta_0} \left\{ \left[ \frac{m_0 l_0}{\alpha \beta_0^2} + \frac{m_0 l_0 (1 - 2\beta_0^2)}{\alpha \beta_0^2} \cos 2\beta_0 - 2 \left( \frac{\beta^2}{\alpha} + \frac{\alpha}{\beta^2} \right) \sin 2\beta_0 \right] (Sim_0 + Si l_0) - \right. \\ - \left[ 2 \left( \frac{\beta^2}{\alpha} + \frac{\alpha}{\beta_0} \right) \cos 2\beta_0 + \frac{m_0 l_0 (1 - 2\beta_0^2)}{\alpha \beta_0^2} \sin 2\beta_0 + \frac{2\beta_2}{\alpha} \right] (Cim_0 + Cil_0) + \\ + \left[ \left( \frac{3\beta^2}{\alpha} + \frac{\alpha}{\beta_0} \right) \sin 2\beta_0 - \frac{m_0 l_0 (1 - 4\beta_0^2)}{2 \alpha \beta_0^2} \cos 2\beta_0 \right] (Si 2 m_0 - Si 2 l_0) + \\ + \left[ \left( \frac{3\beta^2}{\alpha} + \frac{\alpha}{\beta_0} \right) \cos 2\beta_0 + \frac{m_0 l_0 (1 - 4\beta_0^2)}{2 \alpha \beta_0^2} \sin 2\beta_0 \right] (Ci 2 m_0 + Ci 2 l_0) + \\ + \left[ \left( \frac{\beta_0}{\alpha} + \frac{\alpha}{\beta_0} \right) \cos 2\beta_0 + \frac{m_0 l_0}{2 \alpha \beta_0^2} \sin 2\beta_0 + \frac{2\beta_0}{\alpha} \right] \ln \frac{\gamma^2 m_0 l_0}{4 \alpha^2} + \\ + 4 \sin \alpha \sin \beta_0 + \frac{\sin 2\beta_0}{2 \alpha} (\cos 2 \alpha + \cos 2\beta_0 - 2 \cos \beta_0 \cos \alpha + 1) + \\ \left. + \frac{\alpha}{m_0 l_0} \left( \frac{\beta_0}{\alpha} + \frac{\alpha}{\beta_0} \right) (\sin 2 \alpha - 4 \cos \beta_0 \sin \alpha + \frac{\beta_0}{\alpha} \sin 2\beta_0) \right\}. \end{aligned}$$

The described results correspond to the first terms of the series for a current. The new solution method allows us to determine the active and reactive components of the input impedance, corresponding to the total sum of this series, and also to avoid the difficulties of calculating characteristics of impedance antennas. As shown above, the integral equation for the current along the antenna with a constant surface

impedance has the form (4.42). The current is distributed over a sinusoid with a new propagation constant  $k_1$ . If to use the perturbation method and to look for the equation solution in the form of expansion into a series in powers of a small parameter  $\chi$ , for example, to apply the series (4.14), then in the general case of an untuned radiator we get a system of equations, which differs from (4.15) only by replacement  $k$  with  $k_1$ .

As is shown in Section 3, each member of the series for the current radiates the field, which creates the extraneous emf for the following member of this series. This means that, in accordance with (4.18), the extraneous emf created by the first component of the current is equal to

$$E_z(\chi J_1) = -W(\chi J_1).$$

In this case, the magnitude  $\chi J_1(z)$  should be determined from expression (4.44), and the field  $E_z(\chi J_1)$  in accordance with expression (4.47), which in this case should be used instead of (1.25). Replacing in the expression (3.56) the magnitude  $J(z)$  by  $\chi J_1(z)$ , we can find, by a formula like (4.23), the load impedance  $Z_A$  for all current components, starting from the second. For this, it is useful to know the value of  $E_z(\chi J_1)$ . However, as follows from the results of calculating currents and the input impedance of a metal radiator, it is not necessary to calculate this magnitude. The extraneous emf, exciting the  $n$ th component of the current, is determined from (4.21). Introducing the notation of (4.22) and using the formula type (4.23), we come to equality (4.24) for the series. The expression (4.24) allows us to calculate the current of the  $n$ th order of smallness. As was said, the found order of changing the members of the series allows us to conclude that the members of the series (4.14) form a geometric progression. Like the case of a metal antenna without distributed load, this geometric progression is endless, the first term is equal to  $a_1 = \chi J_1(0)$ , the denominator of the progression is constant and equal to  $q = -\chi$ , the sum of its terms tends to the limit  $s = a_1/(1 - q)$ , i.e.,

$$Z_A = \frac{e}{J(0)} = \frac{e [1 + \chi]}{\chi J_1(0)} = -j \frac{60k_1 [1 + \chi]}{k\chi} \cot k_1 L.$$

In this expression, the active component of the input impedance is absent. To determine it, we calculate this component in the first approximation using the formula (4.48). Because an effective length  $h_e$  of an antenna is equal to the ratio of an area under a current curve to the input current  $J(0)$ , then in this case,  $h_e = \frac{2}{k_1} \tan \frac{k_1 L}{2}$ , and

Since  $Z_A = Z_{A1} (1 + \chi)$ , where  $Z_{A1}$  is the input impedance of an antenna in the first approximation, then

$$Z_A = (1 + \chi) \left[ 80 \frac{k^2}{k_1^2} \tan^2 \frac{k_1 L}{2} - j \frac{60k_1}{k\chi} \cot k_1 L \right]. \quad (4.53)$$

The results of calculating the input impedance in accordance with (4.53) are close to the previously obtained results, but the calculation itself is much simpler.

The radiator with a constant surface impedance along its length is a special case of a radiator, whose impedance varies along the antenna. Let, for example, the radiator consists of  $2N$  segments of length  $l_i$ , and on each segment the surface impedance  $Z_i$  is constant (Fig. 2.3). If the radius of the radiator  $a$  is much smaller than the wavelength  $\lambda$  and the length of the radiator  $2L$ , then the current distribution  $J_i$  along each segment has a sinusoidal character in the first approximation. The current is continuous along the antenna and absent at its ends:

$$J_i(b_i) = J_{i-1}(b_i), J_1(b_1) = J_{2N}(b_{2N+1}) = 0.$$

We highlight a logarithmic singularity in the vector-potential of electric field. The total vector-potential is obtained by means of summing up the vector potentials created by the currents of individual segments. Substitute the result in (1.16) and adopt that  $\rho = a$ . Then the integral equation for the current  $J_m(z)$  of each segment of the radiator in accordance with the boundary condition (2.1) can be written in the form:

$$\frac{d^2 J_m(z)}{dz^2} + k^2 J_m(z) = -j4\pi\omega\epsilon_0 \chi [K(z) - J(z)Z_m/(2\pi a)] - \chi \sum_{i=1}^{2N} W(J_i, z), b_{m+1} \leq z \leq b_m.$$

Here  $Z_m$  is the magnitude of the surface impedance at the  $m$ th segment. As before, we consider such an impedance, which significantly affects the distribution of the current. In this case

$$\frac{d^2 J_m(z)}{dz^2} + k_m^2 J_m(z) = -j4\pi\omega\epsilon_0 \chi K(z) - \chi \sum_{i=1}^{2N} W(J_i, z), b_{m+1} \leq z \leq b_m. \quad (4.54)$$

Here  $k_m = \sqrt{k^2 - j k \chi Z_m / (60\pi a)}$  is the wave propagation constant along the  $m$ th segment of the antenna. We search the solution of equation (4.54) in the form of a series in powers of the small parameter  $\chi$ :

$$J_m(z) = \sum_{n=0}^{\infty} \chi^n J_{mn}(z). \quad (4.55)$$

If the values  $J_{m1}(b_m)$  and  $J_{m1}(b_{m+1})$  of currents are given at the ends of the  $m$ th section, and for simplicity it is assumed that the emf is located at the boundary of two segments, then from the equation for  $J_{m1}(z)$  we find

$$\chi J_{m1}(z) = \chi J_{m1}(b_m) \frac{\sin k_m(z - b_{m+1})}{\sin k_m l_m} + \chi J_{m1}(b_{m+1}) \frac{\sin k_m(b_m - z)}{\sin k_m l_m},$$

where

$$I_m = \frac{\chi}{\sin k_m l_m} \sqrt{J_{m1}^2(b_m) + J_{m1}^2(b_{m+1}) - 2J_{m1}(b_m)J_{m1}(b_{m+1})\cos k_m l_m},$$

$$\varphi_m = \tan^{-1} \frac{J_{m1}(b_m) \sin k_m l_m}{J_{m1}(b_{m+1}) - J_{m1}(b_m) \cos k_m l_m}, z_m = b_m - z.$$

In order to find the current distribution along the entire radiator, it is necessary to the boundary conditions for the current to add the conditions of charge continuity at the boundaries of the segments, i.e., put

$$\frac{dJ_i(b_i)}{dz} = \frac{dJ_{i-1}(b_i)}{dz}.$$

This equality is valid for all  $i$ , excluding the point  $z = h$  of generator placement, where

$$\frac{\partial J_{m1}(h+0)}{\partial z} = \frac{\partial J_{m1}(h-0)}{\partial z} = 2 \frac{\partial J_{m1}(h+0)}{\partial z} = -j \frac{ke}{30}.$$

Here  $\frac{\partial J_{m1}(h+0)}{\partial z}$  and  $\frac{\partial J_{m1}(h-0)}{\partial z}$  are the values of the derivatives to the right and left of the point  $z = h$ .

Further, we will consider that the radiator is symmetric, and the emf is included in its center between the  $N$ th and  $(N+1)$ th segments. The found relations make it possible to express the amplitude and phase of the current in any segment through the amplitude and phase of the current of the previous segment, and therefore through the parameters of the segments and one of the currents. These expressions demonstrate the law of current distribution along the radiator and coincide with expressions (2.10) – (2.13), which in the second chapter are given for currents in a stepped impedance long line, which is equivalent to the radiator.

To find the input impedance of the antenna with piecewise constant surface impedance, we first determine the vector potential. To do this, we substitute the current distribution (2.13) into expression (1.19) for the longitudinal tangential component of the vector potential

$$A_z(a, z) = \frac{\mu J(0)}{4\pi} \sum_{i=1}^N A_i \int_{b_{i+1}}^{b_i} \left[ \frac{e^{-jkR_1}}{R_1} + \frac{e^{-jkR_+}}{R_+} \right] \sin[k_i(b_i - \varsigma) + \varphi_i] d\varsigma,$$

where  $A_i = I_i/J(0)$ . From (1.23), using (2.10) and (2.11) for mutual compensation of the summands, we get

$$E_z = -j30J(0) \left\{ \frac{A_1 k_1}{k} \left( \frac{e^{-jkR_1}}{R_1} + \frac{e^{-jkR_2}}{R_2} \right) - \frac{2A_N k_N}{k} \cos(k_N l_N + \varphi_N) \frac{e^{-jkR_0}}{R_0} \right\}. \quad (4.56)$$

This expression generalizes expression (4.47), and it uses the same notation for  $R, R_+, R_1, R_2$  and  $R_0$ .

Substituting (4.56) into (4.46), one can find the input impedance of the antenna:

$$Z_A = j60 \left\{ \frac{A_1 k_1}{k} \left( \frac{e^{-jkR_1}}{R_1} + \frac{e^{-jkR_2}}{R_2} \right) - \frac{2A_N k_N}{k} \cos(k_N l_N + \varphi_N) \frac{e^{-jkR_0}}{R_0} \sin[k_m (b_m - z) + \varphi_m] dz \right\} + \frac{1}{2\pi a} \sum_{m=1}^N A_m^2 Z_m \left[ l_m - \frac{1}{k_m} \sin k_m l_m \cos(k_m l_m + 2\varphi_m) \right]. \quad (4.57)$$

Using the new method for solving the integral equation, we find similarly to (4.53)

$$Z_A = (1 + \chi)(R_A + jX_A), \quad (4.58)$$

where

$$R_A = 20k^2 h_e^2 = 80k^2 (\sum_{m=1}^N h_{em})^2, \quad X_A = -W_N \cot(k_N l_N + \varphi_N).$$

Here  $h_{em}$  is effective length of the segment  $m$ , which is equal to the ratio of the area under the current curve  $J_m(z)$  to the input current  $J(0)$ .  $N$  is the segment number near the generator.

An expression for the radiator's field in the far zone, obtained using (2.13) and (3.13), has the form

$$E_\theta = j \frac{30kJ(0)\exp(-jkR_0)}{\varepsilon_r R_0} F(\theta), \quad (4.59)$$

where

$$F(\theta) = \sin \theta \sum_{m=1}^N A_m \left[ \frac{\cos(\varphi_m - kb_m \cos \theta) - \cos(\varphi_m + k_m l_m - kb_{m+1} \cos \theta)}{k_m + k \cos \theta} + \frac{\cos(\varphi_m + kb_m \cos \theta) - \cos(\varphi_m + k_m l_m - kb_{m+1} \cos \theta)}{k_m - k \cos \theta} \right].$$

The above expressions clearly demonstrate the simplicity of the new method.

## 6. Integral Equations for a System of Radiators

In Section 4 the system consisting of two radiators was analyzed with the help of an integral equation. It was considered that both radiators are excited by the concentrated emf. In this case the current in each radiator has the sinusoidal character, and that is valid also in the presence of the neighboring radiator. The second radiator introduces a new summand into the extraneous emf located in the center of the first radiator. It is shown also that an input impedance of each radiator in the system of two radiators is equal to the sum of a self-impedance of the one radiator and the additional impedance, equal to product of the mutual impedance of the radiators onto the currents ratio at the radiators centers. For example, the input impedance  $Z_I$  of first radiator is equal to

$$Z_I = Z_{I0} + Z_{I,II} \cdot J_2(0)/J_1(0)$$

Here  $Z_{10}$  is the self-impedance of the first radiator,  $Z_{1,II}$  is the mutual impedance of the radiators,  $J_2(0)/J_1(0)$  is the currents ratio at the radiators' centers. Similarly, in the case of  $Q$  radiators, the extraneous emf at the center of radiator  $p$  is

$$E_p = \sum_{q=1}^Q E_p(J_q),$$

where  $E_p(J_q)$  is the field at the center of the radiator  $p$ , created by current  $J_q = J_q(0)f_q(\sigma)$  of the radiator  $q$ ,  $f_q(\sigma)$  is the current distribution in the radiator  $q$ . The oscillating power, created by the radiator  $p$  with current  $J_p = J_p(0)f_p(\sigma)$  in all radiators, is

$$P_p = -\sum_{q=1}^Q \int_{-L_p}^{L_p} E_p(J_q) E_p(J_q) d\sigma,$$

i.e., the input impedance of the radiator  $p$  is

$$Z_p = P_p / J_p^2(0) = \sum_{q=1}^Q J_q(0) Z_{qp} / J_p(0).$$

where  $Z_{qp} = \int_{-L_p}^{L_p} E_p(J_q) f_p(\sigma) d\sigma$  is the mutual impedance of the radiators  $q$  and  $p$ .

In the notation system adopted in Section 4, which is taking into account the order  $n$  of smallness, this expression is given in the form:

$$Z_p^{(n)} = -\frac{1}{J_p^{(n-1)}(0)_+} \sum_{q=1}^Q J_q^{(n-1)}(0) \int_{-L_p}^{L_p} E_p[f_q^{(n-1)}] f_p^{(n-1)}(\sigma) d\sigma.$$

Multiplying the currents of the sources into the input impedances of radiators, we obtain the magnitude of emf, located at the center of radiator  $p$ :

$$e_p = J_p(0) Z_p = \sum_{q=1}^Q J_q(0) Z_{qp}, \quad p = 1, 2, \dots, Q.$$

This is Kirchhoff equation for a close circuit. According to this equation, the emf in the circuit is the sum of voltage drops on the circuit elements. Since the equality is true for each radiator, then in fact the complete system of equations is written by one formula analogous with an expression (3.69), which was presented in accordance with the logic of the method of induced emf. Note that last expression corresponds to the connection of circuit elements with each other in series (see Fig. 3.12). The circuit of connection in series is employed widely in the analysis of radiators system. The input impedance of each radiator is calculated usually in accordance with expression of the type (3.56). For this reason, the connection in series is true for the system of radiators with the arm length smaller than  $0.4 \lambda$ . At higher frequencies near the parallel resonance, it is expedient to use the connection of circuit elements in parallel.

Despite of seeming diversity of described integral equations and methods of their solution, they have a common essential disadvantage. They were developed for specific radiators and possess no flexibility and freedom for the analysis of arbitrarily constructed radiators. The method, which allows analyzing a wire structure consisting of straight segments located arbitrarily and connected partially with each other, offers in this context much greater possibilities (Fig. 8a).

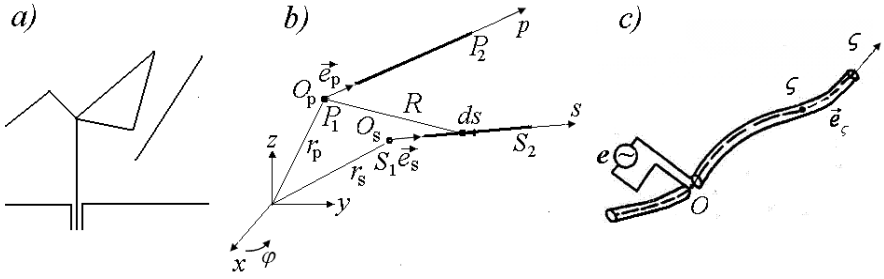


**Fig. 8:** Antenna of straight wire segments (a), from two segments (b), curvilinear antenna (c).

Let as shown in Fig. 8b the current flows along thin perfectly conducting filament, which consists of two wires. The first wire is located along an axis  $p$  between the points  $p_1$  and  $p_2$ , the second wire is located along an axis  $s$  between the points  $s_1$  and  $s_2$ ,  $ds$  is a small element of a second wire. The distance from an element  $ds$  to point  $O_p$  of a first wire is

$$R = \vec{r}_p + p\vec{e}_p - \vec{r}_s - s\vec{e}_s|_{p=0},$$

where  $\vec{r}_p$  and  $\vec{r}_s$  are radii vectors from the coordinates origin to points  $O_p$  and  $O_s$  of the corresponding segments,  $p$  and  $s$  are coordinates measured along the wires and  $\vec{e}_p$  and  $\vec{e}_s$  are the unit vectors, directions of which coincide with wires axes.

To find the electrical characteristics of an antenna we first must determine the vector potential. Let us write for the currents  $\vec{j}_s$  along a second wire:  $\vec{j}_s = j_s(s)\vec{e}_s$ . According to (1.11)

$$\vec{A}_s(\vec{j}_s) = A_s(j_s)\vec{e}_s = \mu\vec{e}_s \int_{s_1}^{s_2} J(s) G ds.$$

If a wire consists of  $N$  segments with different currents, then in order to find the vector potential of the total field one must sum up the vector potentials of fields of all segments:

$$\vec{A} = \sum_{n=1}^N \vec{A}_{sn}(\vec{j}_{sn}) = \sum_{n=1}^N A_{sn}(j_{sn})\vec{e}_{sn},$$

where  $n$  is the segments number and

$$A_{sn}(j_{sn}) = \mu \int_{s_{n1}}^{s_{n2}} J(s_n) G ds_n.$$

In accordance with (1.10) and (1.11), the field of a segment  $s$  in point  $O_p$  is

$$\vec{E}_s(O_p) = \frac{1}{j\omega\epsilon} \int_{s_1}^{s_2} J(s) [k^2 G \vec{e}_s + \text{grad div}(G \vec{e}_s)] ds.$$

The differentiation in the last term is performed with respect to the coordinates of the observation point. Since in the rectangular coordinate system the distance



between an observation point with coordinates  $x_p, y_p, z_p$  and an integration point with coordinates  $x_s, y_s, z_s$  is equal to

$$R = \sqrt{(x_p - x_s)^2 + (y_p - y_s)^2 + (z_p - z_s)^2},$$

then as a result of symmetry  $\text{grad}_p G = -\text{grad}_s G$ , i.e., the differentiation may be performed with respect to coordinates of the point  $s$  instead of coordinates of the point  $p$ . Let us take into consideration that in accordance with the gradient definition  $\vec{e}_s \text{grad}_s G = \frac{\partial G}{\partial s}$ . Using the mathematical identity of expressions  $\text{div}(G\vec{e}_s)$  and  $\vec{e}_s \text{grad}_s G$ , we find

$$\text{div}_p (G\vec{e}_s) = -\frac{\partial G}{\partial s},$$

i.e.,

$$\vec{E}_s(O_p) = \frac{1}{j\omega\epsilon} \int_{s_1}^{s_2} J(s) \left[ k^2 G \vec{e}_s - \text{grad}_p \frac{\partial G}{\partial s} \right] ds.$$

The projection of the field of a segment  $s$  on the axis  $p$  is calculated as a product of  $\vec{E}_s(O_p)$  and  $\vec{e}_p$ :

$$E_{ps} = \vec{E}_s(O_p) \vec{e}_p = \frac{1}{j\omega\epsilon} \int_{s_1}^{s_2} J(s) \left[ k^2 G \vec{e}_s \vec{e}_p - \frac{\partial^2 G}{\partial p \partial s} \right] ds.$$

The projection of the total field of a second wire is the sum of the field's projections of all segments

$$E_p = \sum_{n=1}^N E_{psn} = \frac{1}{j\omega\epsilon} \sum_{n=1}^N \int_{s_{n1}}^{s_{n2}} J_n(s_n) \left[ k^2 G \vec{e}_{sn} \vec{e}_p - \frac{\partial^2 G}{\partial p \partial s_n} \right] ds_n. \quad (4.60)$$

This expression allows us to calculate the directivity pattern of a complex wire structure.

Substituting this field in (4.2), we get the equation generalizing the Pocklington's equation (4.6):

$$\sum_{n=1}^N \int_{s_{n1}}^{s_{n2}} J_n(s_n) \left[ k^2 G \vec{e}_{sn} \vec{e}_p - \frac{\partial^2 G}{\partial p \partial s_n} \right] ds_n = -j\omega\epsilon K_p(p).$$

If  $N = 1$ , this equation converts to (4.6),

$$\int_{-L}^L J(\zeta) \left[ k^2 G \vec{e}_\zeta \vec{e}_z - \frac{\partial^2 G}{\partial p \partial \zeta} \right] d\zeta = -j\omega\epsilon K(z).$$

To this end first the replacement of variables is performed:  $p \rightarrow z, s_n \rightarrow \zeta$ . Furthermore one should consider that the Green's function is symmetrical relative

to the coordinates of the points of observation and integration:  $\partial G/\partial z = -\partial G/\partial \zeta$ . Let the wire antenna have a shape of a polygonal line, along which the coordinate  $\zeta$  is postponed, and the lengths of straight segments tend to be zero. Then we obtain the similar integral equation, which is valid for the current in a curvilinear wire (Fig. 8c). Here,  $\vec{e}_z$  and  $\vec{e}_\zeta$  are unit tangent vectors at the points of observation and integration. If the curvilinear wire is symmetrical relative to some middle point, the form of this equation completely coincides with (4.6).

Another derivation of this equation is given in

## 7. Loop Antenna with Large Dimensions

There are problems that at first sight seem simple, but stubbornly resist decision both a rigorous and approximate. An example of such a problem is a loop antenna, the dimensions of which are comparable to the wavelength. Loop antennas are widely used, primarily as receiving antennas, because they have modest electrical characteristics. They are employed to receive radio communications and broadcasting, as well as for measuring field strength. They are single-turn or multi-turn ones, i.e., they are made in the form of a single flat turn from wire or in the form of several such turns. The shape of the turns is round, rectangular, triangular, rhombic, etc. (Fig. 9).

These antennas are designed to receive a vertically polarized wave. As a rule, they are located vertically and in a horizontal plane have the directional pattern in the form of a figure eight. Their directional pattern has an important and necessary feature, namely the presence of a zero-reception direction. This feature allows us to

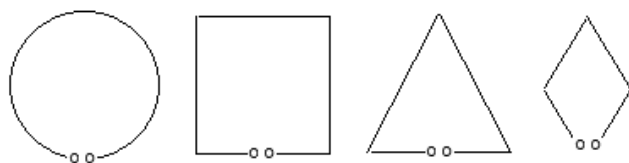


Fig. 9: Options of loop antennas.

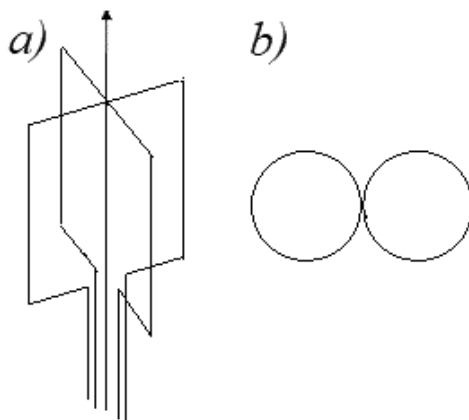


Fig. 10: Loops of a goniometric antenna (a) and its directional pattern (b).

use such an antenna for direction finding and for attenuating interfering signals. The structure of two fixed mutually perpendicular loops (Fig. 10a), attached to a special device (goniometer), ensures the rotation of the directional pattern (Fig. 10b) and changes the direction of zero reception.

The properties of small loops, which length is small compared to the wavelength, are well known (see, for example, [12]). In accordance with the theory of long lines, a small loop, regardless of its shape, can be considered in the first approximation as a segment of a short-circuited long line with the cosine distribution of the current and with a length equal to half perimeter of the loop. If the perimeter is less than  $\lambda(4)$  and the half-perimeter is less than  $\lambda(8)$ , then the cosine argument is less than  $\pi(4)$ , and we can assume that the current amplitude is constant along the entire antenna length.

The current of small loop surrounds the area  $S$ , creating fields  $E_l$ , the sum of which forms the circulation of the vector field. This means that an emf is excited at the loop terminals, and it is equal to

$$e = \oint E_l dl.$$

Such circulation is expressed through the rotor of the field, i.e., in accordance with the Maxwell equations

$$e = \int_S (\text{curl} \vec{E} \cdot d\vec{S}) = -j\omega\mu \int_S (\vec{H} \cdot d\vec{S}).$$

Considering that  $\omega = k/(\sqrt{\mu_0\epsilon_0})$ ,  $\mu = \mu_0\mu_r$ ,  $H = E/\sqrt{\mu_0/\epsilon_0}$ , and taking into attention that the antenna directional pattern, as usual, is  $F(\theta) = \sin\theta$ , we get for the emf at the terminals of small loop in the receiving mode is equal to

$$|e| = kE\mu_r S \sin \theta.$$

Comparing this result for the field of the loop antenna with the field of the elementary dipole in the far zone, we obtain the expression for the effective length of the small loop with area  $S$ :

$$l_e = k\mu_r S.$$

Accordingly, the input impedance of the small loop is

$$Z_A = j\omega\Lambda + 20k^2 l_e^2, \quad (4.61)$$

where  $\Lambda$  is the loop inductance. In the case of a multi-turn loop consisting of  $N$  identical turns,  $S = NS_1$ , where  $S_1$  is the area of a single turn. From here it follows that the effective length of a single-turn loop with length  $Nl$ , the shape of which coincides with the shape of a turn of a multi-turn loop, consisting of  $N$  turns of length  $l$ , is  $N$  times greater than the effective length of this multi-turn loop.

Unfortunately, if the loop dimensions are comparable to the wavelength, the problem becomes much more complicated. In order to determine the characteristics of large loops it is need to know the distribution of current along the loop wire. This

task, as in the case of a linear radiator, requires the solution of an integral equation. Such an equation was proposed only for a circular loop and solved with significant simplifications [12, 13]. Attempts to write and solve an integral equation for the current in contours of different shape have encountered insurmountable difficulties.

Strictly speaking, this problem is reduced to two separate tasks - to the calculation of the active and reactive components of the input impedance. When calculating the reactive component, one can rely on books devoted to the calculation of inductances [14, 15]. They provide information about single-turn and multi-turn coils with various shapes of flat turns, including those with magnetic cores. To calculate the reactive component of the input impedance, you can also use the theory of long lines. It is known that the input impedance of a short-circuited long line is

$$X_A = jW \tan kL, \quad (4.62)$$

where  $L$  is the line length,  $W$  is its wave impedance, equal to  $W = \sqrt{A/C} = \omega L/k = k/\omega C$ , and  $C$  are inductance and capacitance per unit line length.

Of course, the wave impedance changes along the line, since the distance  $d = 2R \sin \theta$  between the two wires changes and, accordingly, the capacitance per unit length between them  $C = \pi\epsilon_0/\ln(d/a)$  also changes. In these expressions  $R$  is the loop radius,  $a$  is the wire radius,  $\epsilon_0 = 10^9/36\pi$  is the permittivity of the free space. In the case of a dipole, the capacitance per unit length of the equivalent line is taken to be half of the capacitance between the wire and the distance to the surface with zero potential. But in the case under consideration, it is desirable to clarify this capacitance. One can divide a short-circuited long line with a piecewise constant wave impedance into segments, calculate the capacitance of each segment and the total capacitance as a sum or integral over the length and then determine the average value of capacitance  $C$  per unit length. If, in this case, the value  $\sin \theta$  is replaced by  $\theta$ , then this integral reduces to the integral logarithm. But the simplest way to determine the average value of  $d$  is to calculate the average value of the sinus: on the line segment from  $\theta = 0$  to  $\theta = \theta_1$  this value is

$$\bar{d} = \frac{2R}{\theta_1} \int_0^{\theta_1} \sin \theta d\theta = \frac{2R}{\theta_1} (1 - \cos \theta_1).$$

In the interval  $\theta$  from 0 to  $\pi/6$  the distance  $\bar{d}$  is equal to  $0.512R$ , in the interval  $\theta$  from 0 to  $\pi/2$  and from 0 to  $\pi$  it is equal to  $1.27R$ . The average value of the logarithm  $\ln(d/a)$  in the range from 0 to  $\pi$  is equal to  $\ln(1.27R/a)$ , the average capacitance per unit length of the line is  $C_2 = \pi\epsilon_0/\ln(1.27R/a)$ , the average wave impedance is equal to  $W = \omega C_2 = 120 \ln(1.27R/a)$ .

To calculate the radiation's resistance of large loop antennas, it is advisable to apply the Poynting method. In this case, we use the version of this method, which is described in Section 3.2 in accordance with [16]. The circuit of the circular loop antenna is shown in Fig. 11. As already mentioned, in accordance with the theory of long lines, we will, in the first approximation, consider the loop antenna as a segment

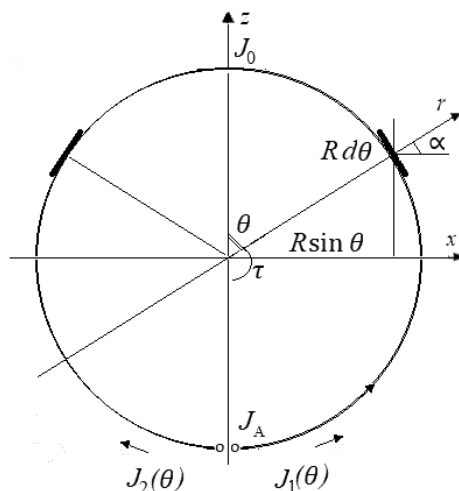


Fig. 11: Circular loop.

of a short-circuited line with a cosine current distribution. The segment length is equal to half the perimeter of the loop.

This approach is like to using the long line method and to choosing a sinusoidal current as a first approximation to the dipole current. We assume that the line length is  $L = R\pi$ , where  $R$  is the loop radius,  $\pi$  is the arc length of each wire (in radians). The length of the segment from the long line end to the arbitrary point  $t$  is equal to  $t = R\theta$ . Since the line is short-circuited, the currents at point  $t$  along the right and left wires are respectively

$$J_1(t) = J_0 \cos kR\theta \text{ and } J_2(t) = -J_0 \cos kR\theta,$$

where  $J_0$  is the current in the antenna top point, i.e., the input antenna current to  $J_A = J_0 \cos kL$ , i.e.,

$$J_1(t) = -J_2(t) = J_A \cos kR\theta / \cos kL. \quad (4.63)$$

Let us calculate the fields created by the wires of the loop antenna in the horizontal direction along the  $x$ -axis (at an angle  $\theta = \pi/2$ ). As is seen from the Fig. 11, the vertical component of the field, radiated by the elementary segment of the right wire with length  $Rd\theta$  centered at point  $t$ , is equal to

$$dE_1\left(\frac{\pi}{2}\right) = j30k \frac{J_A}{\cos kL} \cos kR\theta \sin \alpha \frac{\exp(-jkr + jkR)}{r - R} R d\theta.$$

It is necessary to take into consideration the path-length difference of the rays from arbitrary points of the antenna to the observation point compared to the distance  $r$  from the antenna center. Neglecting the magnitude  $R$  compared to the distance  $r$  in the denominator of this expression and considering that  $\alpha = \frac{\pi}{2} - \theta$ , we obtain for the vertical component of the field of the right wire

$$E_1(\pi/2) = A \int_0^\pi \cos kR\theta \sin \alpha \, d\theta,$$

where  $A = j30kR \frac{J_A}{\cos kL} \frac{\exp(-jkr)}{r}$ . The distance between similar segments of the left and right wires is  $2R\sin\theta$ . Accordingly, the distance between the left segment and the observation point located at an angle  $\theta$  is greater than the distance between the right segment and this point by  $2R\sin^2\theta$ . The vertical projections of both segments are the same, i.e., for the field of the left wire in the same direction one can write

$$E_2(\pi/2) = -A \int_0^\pi \cos kR\theta \sin \alpha \exp(-j2kR \sin^2\theta) d\theta.$$

As can be seen from this expression, the field of the left wire in the direction of the x-axis is significantly less than the field of the right wire. Therefore, as a first approximation, we will assume that

$$E(\pi/2) = E_1(\pi/2)(1 - \Delta),$$

where  $\Delta$  is small constant magnitude.

Each wire of the loop antenna consists of two identical sections of length  $\pi R/2$  (upper and lower). It is easy to verify that in both cases  $\sin \alpha = \cos \theta$  and

$$E(\pi/2) = A(1 - \Delta) \int_0^\pi \cos kR\theta \cos \theta \, d\theta.$$

Let us replace the magnitudes  $\cos kR\theta$  and  $\cos \theta$  with the sums of the exponentials and find the integrals:

$$\begin{aligned} E(\pi/2) &= \frac{A(1 - \Delta)}{4} \int_0^\pi [e^{j\theta(kR+1)} + e^{j(kR-1)\theta} + e^{-j\theta(kR-1)} + e^{-j\theta(kR+1)}] d\theta = \\ &= \frac{A(1 - \Delta)}{4j} \left[ \frac{e^{j\theta(kR+1)}}{kR + 1} + \frac{e^{j\theta(kR-1)}}{kR - 1} - \frac{e^{-j\theta(kR-1)}}{kR + 1} - \frac{e^{-j\theta(kR+1)}}{kR + 1} \right] \Bigg|_0^\pi = \\ &= \frac{A(1 - \Delta)}{2(k^2R^2 - 1)} \{ (kR - 1) \sin(kR + 1)\theta + (kR + 1) \sin(kR - 1)\theta \} \Big|_0^\pi. \end{aligned}$$

Calculation gives

$$E(\pi/2) = \frac{A(1 - \Delta)}{k^2R^2 - 1} [2kR \sin kR\theta \cos \theta - 2 \cos kR\theta \sin \theta] \Big|_0^\pi = d\theta = \frac{4AkR(1 - \Delta)}{1 - k^2R^2} \sin kL,$$

where  $\Delta = \exp(-j2kR\sin^2\theta) \Big|_0^\pi = 0$ , that is

$$E(\pi/2) = j120J_A \tan kL \frac{k^2 R^2}{1 - k^2 R^2} \frac{e^{ik(R-r)}}{r}. \quad (4.64)$$

This expression is actually written for one of the wires of the loop antenna. Therefore, as expected, the value  $h_e$  is mainly determined by the length  $L$  of each wire (by the antenna height) and to a lesser extent depends on its radius  $R$ .

Let us compare this result with the field of an asymmetric vertical linear radiator (monopole) of length  $L$ . This field in the direction perpendicular to the radiator axis is equal to

$$E_M = j30 kh_{eM} J_A(0),$$

where  $h_{eM} = \frac{1}{k} \tan(kL/2)$  is the effective length of a monopole. As can be seen from the comparison of the expressions for the fields, the effective length of the circular loop antenna in the plane of the loop is equal to

$$h_e = \frac{4kR^2}{1 - k^2 R^2} \tan kL. \quad (4.65)$$

If, for example, the semi-perimeter of the loop antenna is  $L = \lambda/6$ , then  $R = L/\pi = 0.053\lambda$ ,  $kR = 0.333$ ,  $k^2 R^2 = 0.11$ ,  $1 - k^2 R^2 = 0.89$ ,  $kL = \pi/3$ ,  $\tan kL = 1.73$ ,  $h_e = 0.862\lambda/2\pi = 0.137\lambda$ . The effective length  $h_{eM}$  of the monopole with height  $L = \lambda/6$  is equal to  $0.092\lambda$ , i.e., 1.5 times less. This inequality is caused by the fact that the current on the loop top is maximum, and at the top point of a monopole is zero. The radiation's resistance of an asymmetric vertical radiator with such an effective length is  $R_{\Sigma} = 40k^2 h_e^2 = 13.3 \text{ Ohm}$ . Its field does not depend on  $\varphi$ , i.e., it has a circular directional pattern in the horizontal plane. If the antenna consists of two vertical wires located at a distance  $d$  with oppositely directed currents, then the total signal is equal to

$$E(\varphi) = \frac{E(J_A, z, \theta)}{r} e^{-jkr} \left[ e^{jk\frac{d}{2} \cos \varphi} - e^{-jk\frac{d}{2} \cos \varphi} \right] = 2j \frac{E(J_A, z, \theta)}{r} e^{-jkr} \sin \left( k \frac{d}{2} \cos \varphi \right). \quad (4.66)$$

In this case, as follows from the above expression, the antenna pattern in the horizontal plane, regardless of its size and angle  $\theta$ , has the shape of a figure-eight, and its area is equal to half the circle area. The directional pattern of a loop antenna in the horizontal plane, regardless of its size and angle  $\theta$ , has the similar shape.

According to the Poynting method, the power radiated by an antenna is defined as the total flow through a spherical surface of infinite radius. This allows us to suppose that the distances from all points of the radiator to this surface are the same, and the fields created by them depend only on the direction of radiation, more precisely, on the angles  $\theta$  and  $\varphi$  [16]. If the vertical directional pattern does not depend on  $\varphi$ , then the power of the radiated signal is proportional to the area bounded by the horizontal pattern. In this case, it is half as much in compare with the circular directional pattern. This means that the radiation's resistance of the loop antenna is half the radiation's resistance of a vertical linear antenna with the same effective height, i.e., for the described loop antenna with the half-perimeter  $L = \lambda/6$  is equal to

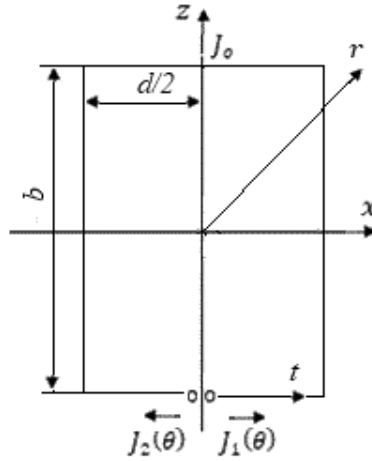


Fig. 12: Rectangular loop.

$$R_z = 20k^2 h_e^2 = 14.8 \text{ Ohm}. \quad (4.67)$$

The presented method allows us to determine the electric characteristics of the of the loop antennas with dimensions comparing with the wave length in the first approximation since it considers changing the distance between the wires. This method does not take into consideration the presence of the surface of zero potential (this surface increases the capacitance between the wires) and the influence of the ground. These factors permit to refine the result, but they have minor importance.

The described method can be applied to loop antennas of various shapes. As an example, consider an antenna in the form of a rectangle with a width  $d$  and a height  $b$  (Fig. 12). In this case, the capacitance per unit length of the line is  $C_2 = \pi\epsilon_0/\ln(d/a)$ , the wave impedance is  $W = \omega C_2 = 120 \ln(d/a)$ , the field of the right wire in the antenna plane in the horizontal direction, as one can easily see, is equal to

$$E(\pi/2) = j30k \frac{J_A(0)}{\cos kL} \frac{e^{jk(d/2-r)}}{r} \int_{d/2}^{L-d/2} \cos ktdt.$$

Here  $L$  is the length of each wire,  $t$  is the distance along the wire from the generator to the given point. It is assumed that the radiation along the horizontal segments of the wires can be neglected. In this case, the effective length of the right wire is

$$h_e = \frac{1}{\cos kL} \int_{d/2}^{L-d/2} \cos k(L-t)dt = \frac{1}{k \cos kL} [\sin k(L-d/2) - \sin kd/2],$$

and the radiation's resistance is equal to

$$R_z = 40 k^2 h_e^2.$$

## 8. Shapes of Small Loop Antenna



It is expedient to consider the issue of a directional pattern in the plane of a loop antenna, depending on the loop shape. As a rule, when describing the properties of loop antennas, it talks about the field, which the circular loop antenna creates in the far zone. However, the field of a square or rectangular loop is very different from the field of a circular loop. Near fields of a circular loop are analyzed only in a limited number of works [17–20]. About a square loop it is known that if its size is small in comparison with the wavelength, then its field in the far zone in the direction perpendicular to the square side coincides with the field of the circular loop (see, for example, [21]). The advantages of square and rectangular loops make them attractive and require calculation of their characteristics in the near zone. For example, it is obvious that if the dimensions of the loops are small, but finite in comparison with the wavelength, then in the near zone the shape of the loop will affect the magnitude of the field.

The following results were published in [22].

The scheme of the rectangular loop is presented in Fig. 13. The loop with dimensions  $a$  and  $b$  lies in a plane  $xOy$ , and its center coincides with the coordinate origin. It is assumed, that the loop sizes are small ( $a, b \ll \lambda$ ), and the amplitude and phase of a current  $J$  along the loop wire does not vary. Let the azimuths of the loop vertexes are accordingly  $\varphi_{01} = \tan^{-1} b/a$ ,  $\varphi_{02} = \pi - \varphi_{01}$ ,  $\varphi_{03} = \pi + \varphi_{01}$ ,  $\varphi_{04} = -\varphi_{01}$ , and the azimuth of an observation point  $P$  is equal to  $\varphi_1$ . The radius-vector  $r$  of each point depends on an angle  $\varphi$  and is equal to

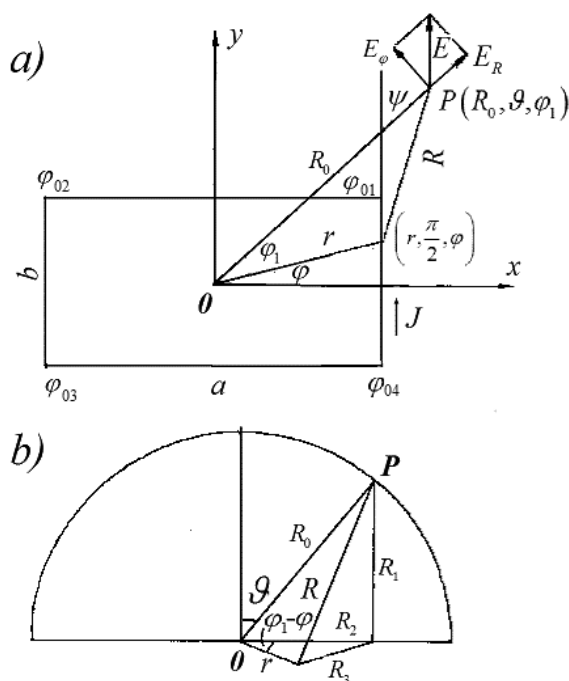


Fig. 13: Geometry of the rectangular loop: a – in the loop plane, b – in axonometry.

$$r = \begin{cases} \frac{a}{2 \cos \varphi}, \varphi_{04} \leq \varphi \leq \varphi_{01} \\ \frac{b}{2 \sin \varphi}, \varphi_{01} \leq \varphi \leq \varphi_{02} \\ -\frac{a}{2 \cos \varphi}, \varphi_{02} \leq \varphi \leq \varphi_{03} \\ -\frac{b}{2 \sin \varphi}, \varphi_{03} \leq \varphi \leq \varphi_{04} \end{cases}. \quad (4.68)$$

The azimuth component  $E_\varphi$  of the electrical field of such an antenna is

$$E_\varphi = -j\omega A_\varphi, \quad (4.69)$$

where  $A_\varphi = \frac{\mu I}{4\mu} \oint_l \frac{\exp(-jkR)}{R} \sin \psi dl$  is an appropriate component of a vector potential,  $\mu$  is the permeability,  $R$  is the distance between the observation point ( $R_0, \theta, \varphi_1$ ) and an integration point ( $r, \pi/2, \varphi$ ),  $\psi$  is an angle between a current vector and a direction from coordinate origin to an observation point,  $k = 2\pi/\lambda$ . Expression (4.69) is written with allowance that a loop current is closed, i.e.,  $\text{div } \vec{A} = 0$ . As is seen from Fig. 13a, the current  $J$  of the arbitrary point ( $r, \pi/2, \varphi$ ) creates in an observation point  $P$  not only azimuth, but also radial component of the electrical field. At that, by contrast to the circular loop, on a rectangular loop wire there is no other point (symmetrical concerning the mentioned direction from the origin to an observation point), which current creates in an observation point the same radial component but with opposite sign. It means, that, in addition to component  $E_\varphi$  the electrical field has also component  $E_R$ . Nevertheless, as well as in the case of a circular loop the field components  $E_\varphi$  and  $H_\theta$  predominate in an antenna far field, and

$$H_\theta = \frac{1}{\mu} \text{curl}_\theta \vec{A} = \frac{1}{j\omega\mu R_0} \frac{\partial}{\partial R_0} (E_\varphi R_0). \quad (4.70)$$

From Fig. 13b it is visible that  $R^2 = R_1^2 + R_2^2$ , where  $R_1 = R_0 \cos \vartheta$ ,  $R_2 = R_0 \sin \vartheta$ ,  $R_3^2 = R_2^2 + r^2 - 2rR_2 \cos(\varphi - \varphi_1)$ , i.e.,  $R^2 = R_0^2 + r^2 - 2rR_0 \sin \vartheta \cos(\varphi - \varphi_1)$ . We write the expression for  $R$  as

$$R = R_0 \sqrt{1+x}, \quad (4.71)$$

at that

$$x = -2r/R_0 \sin \vartheta \cos(\varphi - \varphi_1) + \frac{r^2}{R_0^2} \ll 1.$$

If to represent a function  $\sqrt{1+x}$  as a power series and to restrict ourselves by the first four terms, we obtain

$$\sqrt{1+x} = 1 + \frac{x}{2} - \frac{x^2}{8} + \frac{x^3}{16} - \dots$$

Accordingly

$$R = R_0 - r \sin \theta \cos(\varphi - \varphi_1) + \frac{r^2}{2R_0} [1 - \sin^2 \theta \cos^2(\varphi - \varphi_1)] + \frac{r^3}{2R_0^2} \sin \theta \cos(\varphi - \varphi_1)$$

$$[1 - \sin^2 \theta \cos^2 (\varphi - \varphi_1)]. \quad (4.72)$$

Using the fact that a difference  $R - R_0$  is small, we expand the fraction  $e^{-jkR}/R$  into a series of Taylor. Near the point  $R = R_0$ ,

$$\frac{e^{-jkR}}{R} = \frac{e^{-jkR_0}}{R_0} + \dots + \frac{1}{6} (R - R_0)^3 \frac{\partial^3}{\partial R_0^3} \left( \frac{e^{-jkR_0}}{R_0} \right) + \dots \quad (4.73)$$

The substitution of derivatives in (4.70) and reduction of the similar members gives

$$\begin{aligned} f(\varphi) = & \frac{\exp[-jk(R - R_0)]}{R/R_0} = f_1(\varphi) + jk(1 + \alpha) \sin \theta [f_2(\varphi) \cos \varphi_1 + f_3(\varphi) \sin \varphi_1] + \\ & \frac{k^2}{2} \left[ \alpha(1 + \alpha) \frac{1}{2} (1 + 3\alpha + 3\alpha^2) \sin^2 \theta \right] f_4(\varphi) - \\ & - \frac{k^2}{2} (1 + 3\alpha + 3\alpha^2) \sin^2 \theta [f_5(\varphi) \cos 2\varphi_1 + f_6(\varphi) \sin 2\varphi_1] + \\ & + j \frac{k^3 \alpha}{2} (1 + 3\alpha + 3\alpha^2) \sin \theta [f_7(\varphi) \cos \varphi_1 + f_8(\varphi) \sin \varphi_1] - \\ & - j \frac{k^3}{8} \left( \frac{1}{3} + 2\alpha + 5\alpha^2 + 5\alpha^3 \right) \sin^3 \theta [f_9(\varphi) \cos 3\varphi_1 + f_{10}(\varphi) \sin 3\varphi_1 + 3f_7(\varphi) \cos \varphi_1 + \\ & + 3f_8(\varphi) \sin \varphi_1], \end{aligned} \quad (4.74)$$

where

$f_1(\varphi) = 1, f_2(\varphi) = r \cos \varphi, f_3(\varphi) = r \sin \varphi, f_4(\varphi) = r^2, f_5(\varphi) = r^2 \cos 2\varphi, f_6(\varphi) = r^2 \sin 2\varphi, f_7(\varphi) = r^3 \cos \varphi, f_8(\varphi) = r^3 \sin \varphi, f_9(\varphi) = r^3 (4 \cos^3 \varphi - 3 \cos \varphi), f_{10}(\varphi) = r^3 (3 \sin \varphi - 4 \sin^3 \varphi)$ . In expression (4.74) the symbol  $\alpha$  is equal to  $\alpha = 1/(jkR_0)$ . It is easy also to show, that on the sides of the loop antenna

$$\sin \psi = \begin{cases} \cos \varphi_1 \\ \sin \varphi_1 \\ -\cos \varphi_1 \\ -\sin \varphi_1 \end{cases} dl = \begin{cases} \frac{rd\varphi}{\cos \varphi} = \frac{ad\varphi}{2\cos^2 \varphi} & \varphi_{04} \leq \varphi \leq \varphi_{01} \\ \frac{bd\varphi}{2 \sin^2 \varphi} & \varphi_{01} \leq \varphi \leq \varphi_{02} \\ \frac{ad\varphi}{2 \cos^2 \varphi} & \varphi_{02} \leq \varphi \leq \varphi_{03} \\ \frac{bd\varphi}{2 \sin^2 \varphi} & \varphi_{03} \leq \varphi \leq \varphi_{04} \end{cases} \quad (4.75)$$

Substituting (4.68), (4.74) and (4.75) in expression for  $A_\varphi$ , we get

$$A_\varphi = \frac{\mu I}{4\pi} \frac{e^{-jkR_0}}{R_0} \oint_\varphi f(\varphi) \sin \psi dl = \frac{\mu I}{4\pi} \frac{e^{-jkR_0}}{R_0} jkSF(f) \sin \theta, \quad (4.76)$$

where

$$jkSF(f) \sin \vartheta = \frac{a}{2} \cos \varphi_1 \left( \int_{\varphi_{04}}^{\varphi_{01}} - \int_{\varphi_{02}}^{\varphi_{03}} \right) \frac{f(\varphi) d\varphi}{\cos^2 \varphi_0} + \frac{b}{2} \sin \varphi_1 \left( \int_{\varphi_{01}}^{\varphi_{02}} - \int_{\varphi_{03}}^{\varphi_{04}} \right) \frac{f(\varphi) d\varphi}{\sin^2 \varphi}. \quad (4.77)$$

and  $S = ab$  is the antenna area. Let us introduce the notation

$$F_i = jkSF(f_i) \sin \vartheta. \quad (4.78)$$

Then from (4.74)

$$\begin{aligned} jkSF(f) \sin \vartheta &= F_1 + jk(1 + \alpha) \sin \vartheta (F_2 \cos \varphi_1 + F_3 \sin \varphi_1) \\ &\quad + \frac{k^2}{2} \left[ \alpha(1 + \alpha) - \frac{1}{2} (1 + 3\alpha + 3\alpha^2) \sin^2 \vartheta \right] F_4 - \\ &\quad - \frac{k^2}{2} (1 + 3\alpha + 3\alpha^2) \sin^2 \vartheta (F_5 \cos 2 \varphi_1 + F_6 \sin 2 \varphi_1) \\ &\quad + \frac{k^3 \alpha}{2} (1 + 3\alpha + 3\alpha^2) \sin \vartheta (F_7 \cos \varphi_1 + F_8 \sin \varphi_1) - \\ &\quad - j \frac{k^3}{8} \left[ \frac{1}{3} + 2\alpha + 5\alpha^2 + 5\alpha^3 \right] \sin^3 \vartheta (F_9 \cos 3 \varphi_1 + F_{10} \sin 3 \varphi_1 + 3F_7 \cos \varphi_1 + 3F_8 \sin \varphi_1). \end{aligned}$$

The integration of an expression (4.78) gives

$$\begin{aligned} F_1 = F_4 = F_5 = F_6 = 0, F_2 &= ab \cos \varphi_1, F_3 = ab \sin \varphi_1, F_7 = (a^3 b/4) [1 + b^2/(3a^2)] \cos \varphi_1, \\ F_8 &= (a^3 b/4)[1 + b^2/(3a^2)] \sin \varphi_1, F_9 = (a^3 b/4)(1 - b^2/a^2) \cos \varphi_1, \\ F_{10} &= -(a^3 b/4)(1 - a^2/b^2) \sin \varphi_1, \end{aligned}$$

and accordingly

$$\begin{aligned} F(\varphi) &= 1 + \alpha + k^2/(8[(a^2 + b^2/3) \cos^2 \varphi_1 + (b^2 + a^2/3) \sin^2 \varphi_1]) \propto (1 + 3\alpha + 3\alpha^2) - \\ &\quad - k^2/8(a^2 \cos^2 \varphi_1 + b^2 \sin^2 \varphi_1) (1/3 + 2\alpha + 5\alpha^2 + 5\alpha^3) \sin^2 \varphi_1. \end{aligned} \quad (4.79)$$

The magnitude  $A_\varphi$  is found from (4.76), the magnitude  $E_\varphi$  is equal to

$$E_\varphi = 30k^2 IS \frac{e^{-jkR_0}}{R_0} F(f) \sin \vartheta. \quad (4.80)$$

If the antenna dimensions are infinitesimally in comparison with a wavelength, then

$$E_\varphi = 30k^2 IS (1 + \alpha) \frac{e^{-jkR_0}}{R_0} \sin \vartheta. \quad (4.81)$$

This expression coincides with the known expression for the azimuth component of the field of an elementary circular loop, which radius is small in comparison with

a wavelength (see [23]). In it the area of a circular loop is replaced by the area of a rectangular loop.

Comparing the expressions (4.80) and (4.81), it is easy to see that in expression (4.81) the function  $F(f)$  is replaced by the function  $F_1(f) = 1 + \alpha$ , which is equal to a sum of the first two terms from expressions (4.79) and (4.80). The remaining terms are proportional to the squares of ratios of the loop dimensions to the wavelength and to higher powers of  $\alpha$  (to inverse powers of the distance to the observation point). As is seen from (4.79), the field magnitude in a near field depends on the azimuth of the observation point. The rectangular (noncircular) loop shape is the cause of the appearance of the radial field component

$$E_R = -j\omega A_R, \quad (4.82)$$

where  $A_R = \frac{\mu I}{4\mu} \oint_l \frac{e^{-jkR}}{R} \cos \psi dl$  is the radial component of a vector potential, and

$$\cos \psi = \begin{cases} \sin \varphi_1 & \varphi_{04} \leq \varphi \leq \varphi_{01} \\ -\cos \varphi_1 & \varphi_{01} \leq \varphi \leq \varphi_{02} \\ -\sin \varphi_1 & \varphi_{02} \leq \varphi \leq \varphi_{03} \\ \cos \varphi_1 & \varphi_{03} \leq \varphi \leq \varphi_{04} \end{cases}. \quad (4.83)$$

Subject to (4.83) the expression for  $A_R$  assumes the form

$$A_R = \frac{\mu I}{4\mu} \frac{e^{-jkR_0}}{R_0} jkSG(f) \sin \vartheta, \quad (4.84)$$

where

$$jkSG(f) \sin \vartheta = \frac{a}{2} \sin \varphi_1 \left( \int_{\varphi_{04}}^{\varphi_{01}} - \int_{\varphi_{02}}^{\varphi_{03}} \right) \frac{f(\varphi) d\varphi}{\cos^2 \varphi_0} - \frac{b}{2} \sin \varphi_1 \left( \int_{\varphi_{01}}^{\varphi_{02}} - \int_{\varphi_{03}}^{\varphi_{04}} \right) \frac{f(\varphi) d\varphi}{\sin^2 \varphi}, \quad (4.85)$$

and the function  $f(\varphi)$  is consistent with the formula (4.84). If to introduce the notation

$$G_i = jkSG(f_i) \sin \theta, \quad (4.86)$$

then the expression for  $jkSG(f) \sin \theta$  will be like the expression for  $jkSF(f) \sin \theta$  with change of quantity  $F_i$  to  $G_i$ . The integration of equation (4.86) gives

$$G_1 = G_4 = G_5 = G_6 = 0, G_2 = ab \sin \varphi_1, G_3 = -ab \cos \varphi_1, G_7 = \frac{a^3 b}{4} \left( 1 + \frac{b^2}{3a^2} \right) \sin \varphi_1,$$

$$G_8 = \frac{ab^3}{4} \left( 1 + \frac{a^2}{3a^2} \right) \cos \varphi_1, G_9 = \frac{a^3 b}{4} \left( 1 - \frac{b^2}{a^2} \right) \sin \varphi_1, G_{10} = \frac{a^3 b}{4} \left( 1 - \frac{b^2}{a^2} \right) \cos \varphi_1,$$

and accordingly

$$G(f) = \frac{k^2}{4} \sin 2 \varphi_1 \left[ \alpha \left( \frac{1}{3} + \alpha + \alpha^2 \right) (a^2 + b^2) - \frac{1}{8} \left( \frac{1}{3} + 2\alpha + 5\alpha^2 + 5\alpha^3 \right) (a^2 + 3b^2) \sin^2 \theta \right]. \quad (4.87)$$

The magnitude  $A_R$  is determined from (4.84). The magnitude  $E_R$  is equal to

$$E_R = 30k^2 IS \frac{e^{-jkR_0}}{R_0} G(f) \sin \vartheta. \quad (4.88)$$

As seen from (4.88), the radial component of a field contains only terms, which are proportional to the squares of ratios of loop dimensions to a wavelength, i.e., it is small in comparison with the azimuth component. In addition, the radial component substantially depends on the azimuth. This component vanishes in all directions, perpendicular to each rectangle side, because in this case each two points of a loop, located symmetrically about the its center create in the observation point the fields of the same magnitude and opposite sign. Field  $E_R$  has maximums under angle  $\pi/4$  with respect to the mentioned directions.

In Fig. 14 the calculated results for a field  $E_\varphi$  are indicated. These results depend on a distance  $R_0/\lambda$  (in wavelengths) between the rectangular loop center and an observation point. The loop dimensions were assumed equal to  $a = 2b = \frac{1}{(2k)}$ , an observation point azimuth is  $\varphi_1 = \pi/2$ , and angle  $\theta$  varies from  $\pi/6$  to  $\pi/2$ . The field magnitude is referred to its value for  $\theta = \pi/2$ ,  $R_0/\lambda = 0.1$ .

In Fig. 15 the fields  $E_\varphi$  of the loops, having the same form ( $a = 2b$ ) and different dimensions (in wavelengths) are presented. They are given for  $\theta = \pi/2$ ,  $\varphi_1 = \pi/2$ . These fields in the far zone are the same ( $IS = \text{const}$ ), they are referred to the field of a loop with  $a = 1/(2k)$  and  $R_0/\lambda = 0.1$ . The curve 1 was calculated under the approximate formula for the loop, infinitesimal in comparison with a wavelength. One can see that a loop field in a near zone calculated under the exact formula essentially differs from an approximate one.

In Fig. 16 similar curves are given for various ratios of the sides. The fields of different loops are the same in the far zone ( $IS = \text{const}$ ) and are referred to the loop with  $b = a/2 = 1/(4k)$  and  $R_0/\lambda = 0.1$ .

In Fig. 17 the results are presented for the radial component  $E_R$  of the field. The loop dimensions are  $a = 2b$ , the observation point azimuth is  $\varphi_1 = \pi/4$  and the

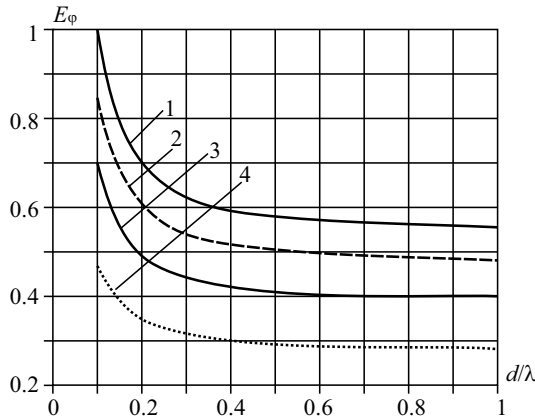
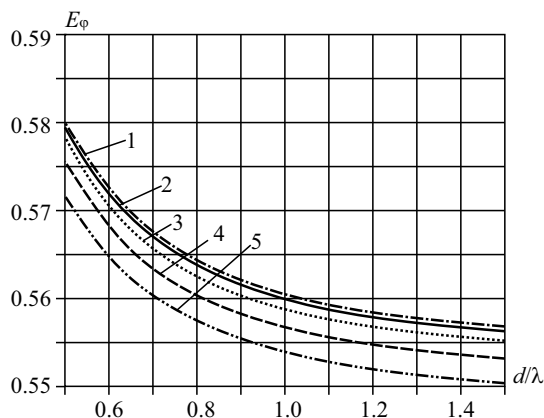
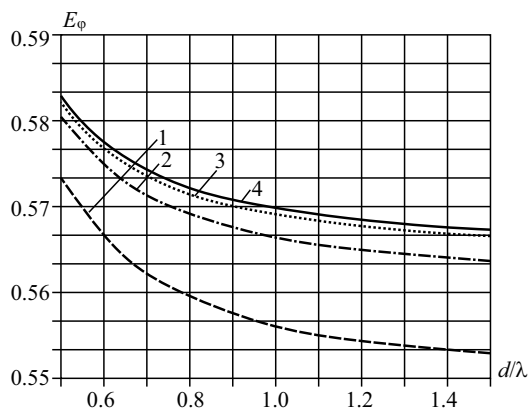


Fig. 14: Components of a field depending on relative distance for various angles  $\vartheta$ .  
Graphs 1–4:  $\vartheta = \pi/2, \pi/3, \pi/4, \pi/6$



**Fig. 15:** Components of a field for the loops with similar form, different sizes and the same far fields.  
Graphs 1–5:  $a = 0, \lambda/8\pi, \lambda/4\pi, 3\lambda/8\pi, \lambda/2\pi$ .



**Fig. 16:** Components of the fields for loop with similar  $a$ , various side ratios and the same far fields.  
Graphs 1–4:  $b = 2a, a, a/2, a/4$ .

angle  $\theta$  is equal to  $\frac{\pi}{2}$ . The magnitudes  $E_R$  of the loops with the same fields  $E_\varphi$  in the far zone ( $IS = \text{const}$ ) refer to the magnitude  $E_\varphi$  of the loop with  $a = 1(2k)$  and  $R_0/\lambda = 0.1$ . As may be seen,  $E_R$  is small in comparison to  $E_\varphi$ , and is equal to zero in case of an elementary loop, whose dimensions are indefinitely small in comparison with a wavelength.

Let us summarize the results of the analysis of rectangular loop.

The azimuthal and radial components of the field of a rectangular loop in the far and near zones are calculated. The results are compared with the field of an elementary circular loop. It is shown that the size and shape of the loop significantly influence the magnitude of its field, especially in the near field.

## 9. Not Linear Structures

Antennas, which today are used, have a wide variety of shapes and dimensions. An antenna located on the surface of a cone, paraboloid, or pyramid, is a wide metal

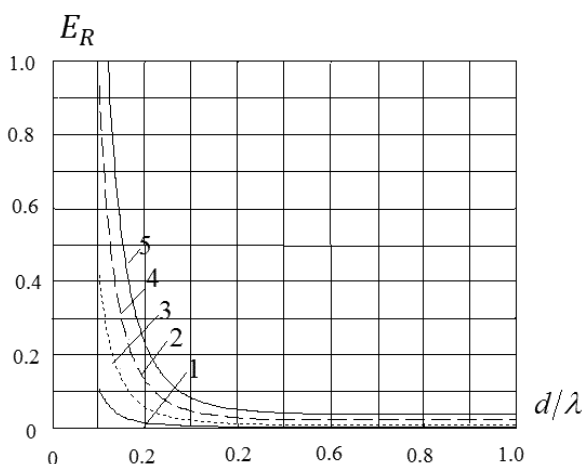


**Fig. 17:** Components of the fields for loops with different sizes and the same far fields.  
Graphs 1-5:  $a = 0, \lambda/8\pi, \lambda/4\pi, 3\lambda/8\pi, \lambda/2\pi$ .

strip, flat or bending along a cross-section. In the axial direction, the antenna can be straight or consist of separate segments of different shape located under different angles to each other. The characteristics of different antennas are calculated with varying degree of accuracy. The equivalent model for flat and three-dimensional antennas consists of intersecting wires. An intricate wire antenna may have a shape of a continuous stepped line. By reducing the lengths of the segments of this antenna, one can in the limit go to smooth curve. Unfortunately, the calculation of such structures as a rule has approximate character.

A rigorous analysis of the antenna characteristics is based on integral equations written and solved for thin direct radiator. As is shown in Section 7, an expression for input impedance of a large loop antenna is based on the long line theory. Integral equation for the current in the circular loop of arbitrary length has not been written up to now. Even the calculation of an inclined asymmetrical antenna from a thin wire (monopole) often is insufficient accurate. The complexity of the concrete calculation is concerned with the complexity of the problem. On the one hand, when distance from the ground increases, the conduction current gradually decreases, turning into a displacement current. On the other hand, the field of the current consists of different components located under different angles.

In Fig. 18a in the capacity of example the  $V$ -radiator structure of thin wires is shown. In Fig. 18b radiator has a similar, but more complex structure. Its arm is made in the form of a circumference arc. For instance, a slot antenna cut in a metal cylinder (tube) of large radius in a plane perpendicular to the cylinder axis has such a shape. Both structures differ from the direct radiator, which is considered by rigorous methods based on solving integral equations for the current. In general case, the antenna arm may consist of several segments of various shape.

In the analysis process it is expedient to replace such an antenna with several auxiliary direct radiators located along the axes of a rectangular coordinate system, to determine the current in each radiator and to solve the equation for an each current. The points of new radiators should coincide with the projections of



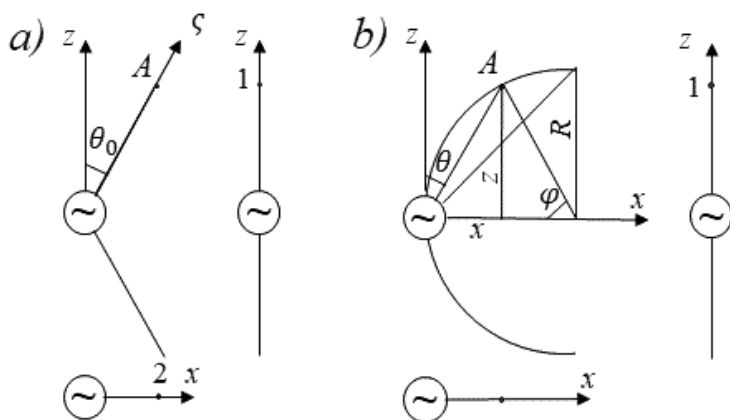


Fig. 18:  $V$ -antenna (a) and antenna with arm in the shape of an arc of a circumference (b).

an original antenna on the new coordinates' axes. This condition allows to reach close coincidence of the currents and fields of new radiators with the currents and fields of an original antenna. The figures show the radiators that replace the original antennas. The numbers 1 and 2 indicate, for example, the points of new radiators corresponding to the starting point A. As can be seen from the figures, the currents of new radiators at points 1 and 2 must be summed in accordance with the rule of the vectors' addition. Their sum must coincide with the current of an original antenna. This equality allows us to determine the magnitudes of currents in the new radiators.

As follows from the said, to determine the horizontal and vertical components of the antenna field, it is necessary to divide the current of the wire into the vertical and horizontal components according to the vector addition rule. Of course, the described method of calculation is not very strict. With increasing antenna size, an error inevitably increases. But the accuracy of the proposed method is quite high. For example, in the case of the  $V$ -antenna (see Fig. 18a) the currents along the vertical and horizontal radiators are equal to  $J_1(z) = J(0) \cos \theta_0 \sin k(L_1 - |z|)$  and  $J_2(x) = J(0) \sin \theta_0 \sin k(L_2 - |x|)$  accordingly, where  $J(0)$  is the current at the antenna input,  $L_1 = L \cos \theta_0$  and  $L_2 = L \sin \theta_0$  are the length of the vertical and horizontal arm of the radiator,  $\theta_0$  is the inclination angle of the  $V$ -antenna arm. In this case, for the first and second derivatives of the vertical radiator current, we get

$$\frac{dJ_1(z)}{dz} = -kJ(0) \cos \theta_0 \cos k(L_1 - |z|), \quad \frac{d^2J_1(z)}{dz^2} = -k^2 J(0) \cos \theta_0 \sin k(L_1 - |z|),$$

i.e., the left side of Leontovich's equation for the vertical radiator is  $\frac{d^2J_1(z)}{dz^2} + k^2J_1(z)$ . Since the left side of equation for the horizontal radiator is similar, then sum of expressions is

$$\frac{d^2J(\zeta)}{d\zeta^2} + k^2J(\zeta), \quad (4.89)$$

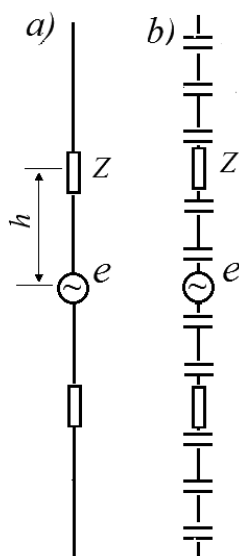


**Fig. 19:** Symmetrical radiators with sinusoidal (a) and in-phase (b) currents with arbitrary complex impedances.

where  $\zeta$  is the coordinate along the original antenna. Expression (4.89) coincides with the left-hand side of Leontovich's equation for an original antenna.

From that it follows that when the integral equation is divided into two, the sum of the left sides in the new integral equations is equal to the left side of the original equation. Similar equality is valid for the right sides of equations. This means that the shape of the curves for the currents of both radiators is the same. Either of the new radiators is direct, that is, the shape of the currents of all radiators coincides with the shape of the current of the direct radiator, and all currents are distributed in accordance with a sinusoidal law. Only the magnitudes of the currents change. They depend on the angle of inclination of the antenna arms.

The case of a symmetric antenna with inclined straight arms of the same length is the simplest. As a second example, let us consider the more complicated case when the antenna has the shape of an arc (Fig. 18b). In this case, the share of current in each of the new radiators is continuously changing. It should be emphasized that this is a fraction of the current, and not its magnitude. The magnitude of the current in the previous case also changes, since in the original antenna it varies in length in accordance with the current distribution. The new antenna has the shape of an arc, and the proportions of the horizontal and vertical currents vary along this arc. The reason for these changes is that the arc continuously turning and its elements are looking in different directions. Therefore, for example, the projections of the segments with identical length on the  $x$ -axis change due to turning from segment to segment.

Let the vertical radiator be located along the  $z$  axis with the center at the origin of coordinates, the horizontal radiator be located along the  $x$  axis with the center at the same point, and the length of each arm is  $L$ . Then the current of the vertical radiator

in the point  $z$  is equal to the total current multiplied by  $\cos \theta$ , and the current of the horizontal radiator in the point  $x$  equal to the total current multiplied by  $\sin \theta$ . As is seen from Fig. 19b,  $\theta = \varphi/2$ . The projections of the arc segment  $OA$  on the axes  $z$  and  $x$  are equal to  $z = R \sin \varphi = R \sin \theta$  and  $x = R(1 - \cos \varphi) = 2R \sin^2 \theta$ . The currents along the new vertical and horizontal radiators in points 1 and 2 are equal respectively to

$$\begin{aligned} J_1(z) &= J(0) \cos \theta_0 \sin k(L_1 - z) = J(0) \cos \theta_0 \sin kR(1 - \sin 2\theta), \\ J_2(x) &= J(0) \sin \theta_0 \sin k(L_2 - x) = J(0) \sin \theta_0 \sin kR(1 - 2\sin^2 \theta). \end{aligned} \quad (4.90)$$

From (4.90) it follows that the currents along the auxiliary radiators must coincide with the projections of the current along the original antenna, i.e., the propagation constants in the auxiliary radiators must differ from  $k$ . In the case of  $V$ -antenna, these magnitudes are constant along both radiators and are equal to  $k_1 = k/\cos \theta_0$  and  $k_2 = k/\sin \theta_0$  in the vertical and horizontal radiators, respectively. In the case of an arc-shaped antenna, the propagation constant must vary along each auxiliary radiator. In a vertical radiator, it should be equal to  $k_1 = k \frac{\sin 2\theta}{\cos \theta_0}$ , in a horizontal radiator  $k_2 = k \frac{2\sin^2 \theta}{\sin \theta_0}$ .

Division of a complex original antenna on two or several straight radiators located along the axes of a rectangular coordinate system allow us to expand the possibilities of using known integral equations for solving new problems.

## 10. Emergency Load

This problem is connected with a possible unexpected change of antenna structure and with an analysis of the consequences of this change (one can name such a change in emergency). In general case, this emergency change can be considered as the appearance of an arbitrary load at an arbitrary point of the antenna. Obviously, the result of this change depends not only on a load magnitude, but also on the antenna structure.

The problem of loads effect on antennas characteristics has a general nature, but it manifests by different variants. Loads can be concentrated and distributed, i.e., their dimensions may be small and comparable with a wavelength. The loads may be non-linear [24]. They include non-linear contacts and pieces of superconducting wires, as well as contacts between wires, damaged for various external reasons. Finally, the elements, specially included in an antenna circuit, both active (resistors) and reactive (capacitors, inductors), also may be considered by the loads. In Fig. 19 two straight symmetrical radiators are shown: a metal radiator with sinusoidal current distribution (*a*) and a radiator with in-phase current (*b*), created by capacitive loads. Arbitrary complex impedances are included in each antenna arm.

An integral equation for the current in an antenna with capacitive loads may be obtained from an integral equation for a current  $J_A(z)$  in a metal radiator. Inclusion of the concentrated complex impedance  $Z$  in a certain point  $z = h$  is equivalent to inclusion at this point of an additional emf  $e_1 = -J_A(h)Z$ . The additional extraneous

emf, created in the wire of radiator, is equal to a product of the current at this point onto the mentioned impedance  $Z$ :

$$K_1(z) = -J_A(h)Z\delta(z-h). \quad (4.91)$$

The boundary condition for an electric field  $E_z(J)$  on a radiator surface with  $n$  loads is written as

$$E_z(J_A)|_{\rho=a, -L \leq z \leq L} + K(z) - \sum_{n=1}^N J_A(h_n) Z_n \delta(z-h_n) = 0. \quad (4.92)$$

Here a cylindrical coordinate system is used;  $a$  is an antenna radius and  $L$  is its arm length. If only one load is included in a radiator, then in accordance with (4.92), Leontovich's integral equation takes a form:

$$\frac{d^2 J_A(z)}{dz^2} + k^2 J_A(z) = -4\pi j \omega \varepsilon \chi [K(z) + W(J_A, z) J_A(z) - J_A(h) Z \delta(z-h)], \quad (4.93)$$

where  $k$  is the wave propagation constant along the antenna,  $\chi = 1/[2 \ln(2L/a)]$  is a small parameter,  $W(J_A, z)$  is a functional. The right side of equation (4.91) contains three summands in square brackets: first summand allows considering the exciting emf  $e$ , second one—the radiation, third one—the load. An equation solution, as usual, is sought in the form of a series in powers of a small parameter  $\chi$ :

$$J_A(z) = \chi J_1(z) + \chi^2 J_2(z) + \dots,$$

that permits to arrive at a system of equations for the terms of series. If  $Z$  is a magnitude of order  $1/\chi$ , i.e., it is comparable with the antenna wave impedance, then the equation for the current  $J(z) = \chi J_1(z)$  of the first order of smallness has the form

$$\frac{d^2 J(z)}{dz^2} + k^2 J(z) = -4\pi j \omega \varepsilon \chi [K(z) - J(h) Z \delta(z-h)], \quad J(\pm L) = 0.$$

If the antenna is excited in the center, and the load is in the point  $z = h$ , the current is equal

$$J(z) = j \frac{\chi e}{15 \cos kL} \sin k(L-|z|) + \frac{\chi^2 e}{900 \sin^2 2kL} \frac{ZZ_1}{z+z_1} \sin kL \sin k(L+\gamma h) \sin k(L-|h|) \sin k(L-\gamma z), \quad (4.94)$$

where  $Z_1 = -j \frac{30 \sin 2kL}{\chi \sin k(L+h) \sin(L-h)}$ ,  $\gamma = \begin{cases} 1, & z \geq h \\ -1, & z \leq h \end{cases}$ . As it was to be expected, the current along the antenna with one concentrated load contains two sinusoidal terms: one of them is created by the generator and the other is caused by the load presence.

The result of affecting a concentrated load on a current distribution in a metal radiator, i.e., in an antenna with a sinusoidal current distribution, confirms that an inclusion of a concentrated complex load  $Z$  in the point  $z = h$  is equivalent to placement of an additional emf  $e_1 = -J_A(h)Z$  in the given point. The distribution of current, created by this emf, depends on the antenna structure, and a magnitude of

generated current at the point of placing load depends on the input impedance in this point. In a straight metal radiator this input impedance in the first approximation is a reactance, equal to

$$jX_M = -jW \text{ctg} k(L-h) - jW \text{ctg} k(L+h),$$

where  $W = 30/\gamma = 60 \ln(2L/a)$  is the wave impedance of each antenna arm;  $L-h$  and  $L+h$  are the arms' lengths. In radiators with in-phase currents created by means of the capacitive loads the input impedance changes substantially. If the capacitances of loads decrease proportionally to the distance from the free end of the antenna, then a current diminishes linearly and the input impedance is

$$jX_{IF} = -j \frac{W_{IF}}{k(L-h)} - j \frac{W_{IF}}{k(L+h)L}.$$

Here  $W_{IF} = \gamma_n W/k$ ,  $\gamma_n$  is the wave propagation constant at the nearest antenna section, and  $W$  is the wave impedance of the antenna with the same dimensions, but without loads.

It is useful to compare the fields created by symmetrical radiators with sinusoidal and in-phase currents. The field of a symmetrical vertical radiator is

$$E_\theta = j30k \sin \theta \frac{e^{-jkR}}{R} \int_{-L}^L J(z) e^{jkz \cos \theta} dz, \quad (4.95)$$

where  $R$  is the distance from the antenna center (from coordinates origin) to the observation point,  $kz \cos \theta$  is the path difference between the antenna center and the point  $z$ . The current's magnitude is symmetrical about the origin. Therefore

$$E_\theta = 2A \sin \theta \int_0^L J(z) \cos(kz \cos \theta) dz, \quad (4.96)$$

where  $A = j30k e^{-jkR}/R$ . In a case of a sinusoidal distribution  $J(z) = J(0) \sin k(L-z)$ . Using a known equality  $2 \sin \alpha \cos \beta = \sin(\alpha - \beta) + \sin(\alpha + \beta)$ , we obtain for the total field of a radiator

$$\begin{aligned} E_\theta &= A \sin \theta \left\{ \frac{\cos k[L - z(1 + \cos \theta)]}{k(1 + \cos \theta)} + \frac{\cos k[L - z(1 - \cos \theta)]}{k(1 - \cos \theta)} \right\} \Big|_0^L \\ &= \frac{2A}{k \sin \theta} [\cos(kL \cos \theta) - \cos kL]. \end{aligned} \quad (4.97)$$

The appearance of identical concentrated loads at points  $h$  and  $-h$ , as already mentioned, is equivalent to inclusion of two generators at these points with emf

$$e_1 = e_2 = -J_A(h)Z,$$

The current  $J_A(h) = J(0) \sin k(L-h)$  is the current in the point of a load inclusion. The output current of each generator is equal to  $J_2(h) = -J_A(h) Z_1/(jX_M)$ , i.e.,

$$J_{1,2}(h) = e_{1,2}/(jX_M) = -J(0) \sin k(L-h)Z/(jX_M).$$

Each generator creates currents in wires, located between it and the antenna ends. Their lengths are equal to  $L - h$  and  $L + h$ . The current in the short wire is equal to

$$J_1(z) = J_1(h) \sin k(L - z) / \sin k(L - h),$$

in the long one

$$J_2(z) = J_2(h) \sin k(L - z) / \sin k(L + h).$$

The field of additional radiators is in accordance with (4.97)

$$E_\theta = \frac{2B}{k \sin \theta \sin k(L - h)} [\cos(kh \cos \theta) - \cos kh + \cos(k(L + h) \cos \theta) - \cos k(L + h)],$$

where  $B = -AZ/[jX_A J(0)]$ .

In an antenna with an in-phase current distribution  $J(z) = J(0)(1 - z/L)$ , i.e., the total field of such a radiator is

$$\begin{aligned} E_\theta &= A \sin \theta \left\{ \frac{\sin(kz \cos \theta)}{k \cos \theta} - \frac{1}{L} \left[ \frac{\cos(kz \cos \theta)}{k^2 \cos^2 \theta} + \frac{z \sin(kz \cos \theta)}{k \cos \theta} \right] \right\}_0^L \\ &= \frac{2A \sin \theta}{k^2 L \cos^2 \theta} [1 - \cos(kL \cos \theta)]. \end{aligned} \quad (4.98)$$

In the presence of loads, the field of additional radiators

$$E_\theta = \frac{2B \sin \theta}{k \cos^2 \theta} \left\{ \frac{1}{kh} [1 - \cos(kh \cos \theta)] + \frac{1}{k(L+h)} [1 - \cos(k(L+h) \cos \theta)] \right\}.$$

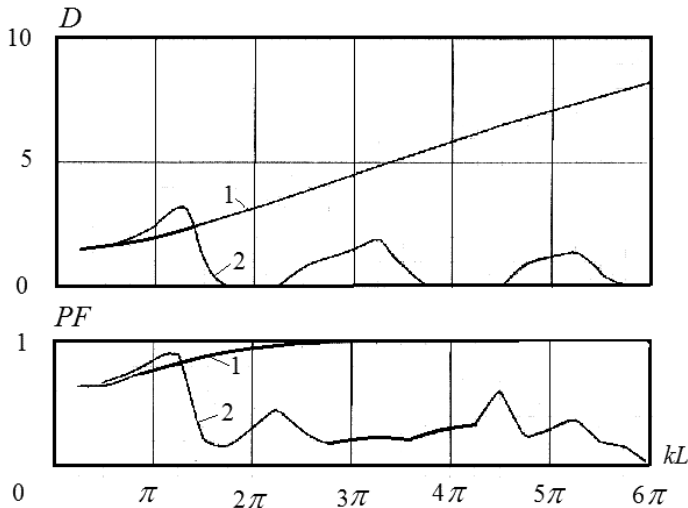


**Fig. 20:** Directivity  $D$  and pattern factor  $PF$  of radiators with in-phase (1) and sinusoidal (2) currents in the absence of arbitrary load.

**Table 2:** Fields of Antennas.

	In-phase currents			Sinusoidal currents		
$h = 0.5L$						
$kL$	$E_\theta$	$\Delta E_\theta$	$(\Delta E_\theta)/E_\theta$	$E_\theta$	$\Delta E_\theta$	$(\Delta E_\theta)/E_\theta$
$0.25\pi$	0.62	0.13	2.1	0.056	1.18	21.1
$0.5\pi$	0.94	1.7	0.8	0.61	$3.1\cdot 10^{11}$	$5\cdot 10^{11}$
$0.75\pi$	4.33	6.2	1.4	1.55	9.8	6.5
$\pi$	12.2	14.4	1.2	1.66	$1.6\cdot 10^{11}$	$10^{11}$
$1.25\pi$	26.4	27.4	1.04	0.89	3.6	4.0
$1.5\pi$	48.3	47	0.97	0.88	$1.4\cdot 10^{10}$	$1.64\cdot 10^{10}$
$1.75\pi$	79.3	74.9	0.94	1.92	17.3	9.0
$2\pi$	121	112	0.93	2.16	$6\cdot 10^{-9}$	$3\cdot 10^{-9}$
$h = 0.3L$						
$0.25\pi$	0.62	0.2	3.2	0.056	1.55	27.7
$0.5\pi$	0.94	2.71	2.88	0.61	$8.4\cdot 10^{11}$	$13.8\cdot 10^{11}$
$0.75\pi$	4.33	10.6	2.45	1.55	0.86	0.55
$\pi$	12.2	25.1	2.06	1.66	$2.1\cdot 10^{11}$	$1.3\cdot 10^{11}$
$1.25\pi$	26.4	47.3	1.79	0.89	7.0	7.86
$1.5\pi$	48.3	79.2	1,64	0.88	$5.6\cdot 10^7$	$6.4\cdot 10^7$
$1.25\pi$	26.4	47.3	1.79	0.89	7.0	7.86
$1.5\pi$	48.3	79.2	1,64	0.88	$5.6\cdot 10^7$	$6.4\cdot 10^7$
$1.75\pi$	79.3	123.4	1.56	1.92	8.4	4.38
$2\pi$	121	182	1.5	2.16	$3.9\cdot 10^{10}$	$1.8\cdot 10^{10}$
$h = 0.5L$						
$0.15\pi$	0.008	0.018	2.2	0.0079	0.051	6.46
$0.3\pi$	0.62	1.18	1.9	0.44	176	400
$0.45\pi$	0.127	0.27	2.13	0.11	3.9	35.5
$0.6\pi$	1.88	3.1	1.68	1.0	15.3	15.3
$0.75\pi$	4.33	6.2	1.43	1.55	9.8	6.3
$0.9\pi$	8.4	10.7	1.27	1.77	110.6	62.5
$1.05\pi$	14.5	16.6	1.14	1.53	319	208.5
$1.2\pi$	23	24.3	1.06	1.04	10.4	10

The described method was used for calculating electrical characteristics of antennas with sinusoidal and in-phase current distribution, as well as characteristics of the same antennas in a case of connecting concentrated loads that substantially change the antennas currents. In Fig. 20 directivity  $D$  and pattern factor  $PF$  of radiators with in-phase (1) and sinusoidal (2) currents, depending on the arm length of the antenna, are presented for the case when arbitrary single loads are absent. As can be seen, the working range of radiators with in-phase currents is much wider.

The results of calculating fields of each antenna without arbitrary loads and in the presence of these single loads (resistors with  $R = 1$  kilo Ohm) are given in Table 2. They allow comparison of the effect of loads on the characteristics of different radiators, depending on their magnitudes. Table 2 uses the following notation:  $E_\theta$  is a total field of antenna without the arbitrary load,  $\Delta E_\theta$  is a total field of antenna with this load,  $(\Delta E_\theta)/E_\theta$  is the ratio of these quantities. A sharp change of the field magnitudes indicates a substantial change of antenna characteristics, the unstable nature of the antenna and a significant effect of arbitrary load on the magnitude and distribution of the current.

The table also shows the electrical length  $kL$  of an antenna arm and the distance  $kh$  from a load to an antenna center. In the first part of Table 2, these values are resonant, and this leads to a very sharp change of fields, especially fields of an antenna with sinusoidal current distribution. In the second part of Table 2 the values  $kh$  change, in the third part similar changes are made in antenna sizes. As a result, the change of the antennas fields became weaker, but the overall result does not change. It shows that the use of radiators with in-phase linear current distribution makes it possible to significantly decrease the effect of loads on the antenna characteristics [25]. This result naturally complements the results of researching antennas with in-phase currents. The analysis confirms the wider frequency range of such antennas, an increase of directivity and the pattern factor, a possible reduction of antennas dimensions, as well as the utility of new methods for comparing antenna characteristics in accordance with current distribution.

## References

- [1] Stratton, J. A. (1941). *Electromagnetic Theory*. New York: McGraw-Hill.
- [2] Pocklington, H.C. (1897). Electrical oscillations in wire. *Proc. Cambridge Philosophical Society*, 324–332.
- [3] Aharoni, J. (1946). *Antennae: An Introduction to Their Theory*. Oxford: The Clarendon Press.
- [4] King, R.W.P. (1956). *Theory of Linear Antennas*. Cambridge: Harvard University Press.
- [5] Jones, D.S. (1981). Note of the integral equation for a straight wire antenna. *Proc. IEEE – H(2)*: 114–116.
- [6] Leontovich, M.A. and Levin, M.L. (1944). On the theory of oscillations excitation in the linear radiators. *Journal of Technical Physics*, 14(9): 481–506 (in Russian).
- [7] Miller, M.A. (1954). Application of homogeneous boundary conditions to the theory of thin antennas. *Journal of Technical Physics*, 24(8): 1483–1495 (in Russian).
- [8] Levin, B.M. (1992). Once again about the method of induced emf. *Radioelectronics and communications*, 2-3: 17–23 (in Russian).
- [9] Vainshtein, L.A. (1959–1961). Waves of a current in a thin cylindrical conductor. *Journal of Technical Physics*, 29(6): 673–699, and 31(1): 29–50 (in Russian).
- [10] Markov, G.T. and Sazonov, D.M. (1975). *Antennas*. Moscow: Energy (in Russian).
- [11] Levin, B.M. (1998). *Monopole and Dipole Antennas for Marine-Vehicle Radio Communication*. St.- Petersburg: Abris (in Russian).
- [12] Fradin, A.Z. (1977). *Antenna-Feeder Devices*. Moscow: Communication (in Russian).
- [13] Bezkakotova, T.B. and Porivaev, B.N. (1971). Input admittance of the thin circular loop antenna. *Radiotechnics and Electronics Engineering*, 16(9): 1712–1715 (in Russian).



- [14] Kalantarov, P.L. and Zeitlin, L.A. (1986). Calculation of Inductances. Leningrad: Energy (in Russian).
- [15] Nemzov, M.V. (1989). Handbook for Calculating the Parameters of Inductors. Moscow: Energyatom (in Russian).
- [16] Levin, B.M. (2021). About using the method of Poynting. Proc. of 25th Intern. Seminar/Workshop DIPED, Tbilisi, 31–36.
- [17] Green, F.M. (1967). The near-zone magnetic field of a small circular-loop antenna. Journal Research. NSB, 71-C(4): 319–326.
- [18] Werner, D.H. (1996). An exact integration procedure for vector potentials of thin circular loop antennas. IEEE Transactions on Antennas and Propagation, AP-44(2): 157–165.
- [19] Overfelt, P.L. (1996). Near fields of the constant current thin circular loop antenna of arbitrary radius. IEEE Transactions on Antennas and Propagation, AP-44(2): 166–171.
- [20] Li, L.W., Leong, M.S., Kooi, P.S. and Yeo, T.S. (1997). Exact solutions of electromagnetic fields in both near and far zones radiated by thin circular-loop antennas: a general representation. IEEE Transactions on Antennas and Propagation, AP-45(12): 1741–1748.
- [21] Kraus, J.D. (1988). Antennas. Boston: McGraw-Hill.
- [22] Levin, B.M. (2004). Field of a rectangular loop. IEEE Transactions on Antennas and Propagation, AP-52(4): 948–952.
- [23] Balanis, C.A. (2005). Antenna Theory: Analysis and Design. New York: Wiley & Sons.
- [24] Shifrin, Ya. S. and Luchaninov, A.I. (2003). Microwave devices with the distributed nonlinearity. Proc. Intern. Conf. on Antenna Theory and Techniques, Sevastopol, 81–86.
- [25] Levin, B.M. (2017). Effect of concentrated loads on characteristics of antennas with different currents distribution. Proc. of 21th Intern. Seminar/Workshop DIPED, Dnipro, 214–216.

# The Problems of Analysis

## 1. Generalized Method of Induced Emf

As is known, the rigorous analysis of antennas characteristics was executed only for a small number of the simplest variants of radiators. As a rule, in the problems under consideration, the characteristics of small radiators located in free space are analyzed. This approach is explained by the complexity of the problems. In this connection, in solving integral equations for the current, numerical methods are widely used. These methods allow us to define the characteristics of complex antennas, whose dimensions are comparable with the wavelength as well as to consider the influence of neighboring antennas and metal bodies. Numerical methods permit to reduce an integral equation to a set of algebraic equations with the help of Moments method. In the general case the integral equation for the current in a wire antenna has the form

$$\int_{(l)} J(\zeta) K(z, \zeta) d\zeta = F(z), \quad (5.1)$$

where  $J(\zeta)$  is the sought function (the current distribution along a wire),  $K(z, \zeta)$  is the kernel of the equation, which depends on coordinate  $z$  of the observation point and on coordinate  $\zeta$  of the integration point.  $F(z)$  is a known function, which is defined by extraneous sources of a field. The terms proportional to the current may enter in these functions, for example in the case of antenna with loads. Here this is of no great importance. The integral is taken over an all length of the wire. It is easy to be convinced that the equations considered earlier are the cases of this equation.

Let us present the unknown current  $J(\zeta)$  as a sum of linearly independent functions  $f_n(\zeta)$ . These functions are called by the basis functions:

$$J(\zeta) = \sum_{n=1}^N I_n f_n(\zeta). \quad (5.2)$$

Here  $I_n$  are unknown coefficients, which in the general case are complex. Substituting (5.2) into (5.1), we obtain:

$$\sum_{n=1}^N I_n \int_{(l)} f_n(\zeta) K(z, \zeta) d\zeta = F(z). \quad (5.3)$$

Often the second system of linearly independent functions  $\varphi_p(z)$  is introduced. They are named by the weight functions. If to multiply both parts of equation (5.3) to  $\varphi_p(z)$  and to integrate over entire wire length and then to repeat the operation at different  $p$ , we shall obtain the set of equations:

$$\sum_{n=1}^N I_n \int_{(l)} \varphi_p(z) f_n(\zeta) K(z, \zeta) d\zeta dz = \int_{(l)} \varphi_p(z) F(z) dz, p = 1, 2 \dots N. \quad (5.4)$$

Obviously, number  $N$  of equations (5.4) must coincide with the number  $N$  of unknown magnitudes. The integration result of each function along the wire length is its moment. The method's name is based on use of calculating the functions' moments.

If the system of weight functions coincides with the system of basis functions, such a variant of the Moments method is known as Galerkin's method. In this case

$$\sum_{n=1}^N I_n \int_{(l)} f_p(z) \int_{(l)} f_n(\zeta) k(z, \zeta) d\zeta dz = \int_{(l)} f_p(z) F(z) dz, p = 1, 2 \dots N.$$

One can rewrite this set of equations in the form

$$\sum_{n=1}^N I_n Z_{np} = U_p, p = 1, 2 \dots N, \quad (5.5)$$

where

$$Z_{np} = \int_{(l)} f_p(z) \int_{(l)} f_n(\zeta) K(z, \zeta) d\zeta dz, U_p = \int_{(l)} f_p(z) F(z) dz.$$

The system of equations (5.4) is also may be written in the form of equations (5.5), if in formulas for  $Z_{np}$  and  $U_p$  to replace  $\varphi_p(z)$  with  $f_p(z)$ .

Expression (5.5) is the set of linearly independent algebraic equations with  $N$  unknown magnitudes  $I_n$ , having the dimensionality of the current. Coefficients  $Z_{np}$  and  $U_p$  have the dimensionalities of the impedance and voltage; they can be calculated, e.g., by means of numerical integration. Accordingly, the expression (5.5) can be interpreted as Kirchhoff equation for the contour  $p$  with current  $I_p$  and emf  $U_p$ . The contour  $p$  enters in a system of  $N$  coupled contours. Here  $Z_{pp}$  is the self-impedance of a contour elements, and  $Z_{np}$  is a mutual impedance of the elements of the contours  $n$  and  $p$ .

The set of equations (5.5) can be solved on the computer with the help of a standard software. If to write down this set in a matrix shape:

$$[I][Z] = [U],$$

where  $[Z]$  is the matrix of impedances,  $[I]$  and  $[U]$  are the current and voltage vectors, then the solution can be obtained by means of a standard matrix inversion:

$$[I] = [Z]^{-1} [U].$$

Substitution of obtained magnitudes  $I_n$  into (5.2) allows us to find a current distribution  $J(\zeta)$ , and later subsequently all electrical characteristics of the radiator.

In practice the calculation of matrix elements  $Z_{np}$  may prove to be extremely difficult, since it is related with the double numerical integration. This difficulty often depends on the equation kernel. To alleviate these difficulties, one can use  $\delta$ -functions in the capacity of weight functions:  $\varphi_p(z) = \delta(z - z_p)$ . Then, the double integral for the calculation of  $Z_{np}$  becomes a common integral, the calculation of  $U_p$  does not require integration, and the expression (5.4) takes the form

$$\sum_{n=1}^N I_n \int_{(l)} f_n(\zeta) k(z_p, \zeta) d\zeta = F(z_p), p = 1, 2 \dots N.$$

One can obtain this equality directly from (5.1) and (5.2), if to equate the left and right parts of the equation (5.1) at the specific points. The number  $N$  of these points corresponds to that of obtained equations. For this reason, the given variant of the Moments method is known as the technique of matching in the points or the collocation method (see, e.g., [1]).

The collocation method ensures an exact equality of the left and right parts of the equation (5.1), at  $N$  points at least. In the intervals between these points, the difference between the left and right parts of the equation may increase sharply. When using the Moments method with another weight functions, the equality may be absent in all points of the interval of  $z$  changing. But equating both moments of function (results of integration with some weight) minimize the difference between the left and right parts at whole interval where  $z$  is changing. This property in the final analysis is almost always more important than the exact equality at the separated points. Therefore, Galerkin's method allows providing, as a rule, an essentially more accurate solution than the collocation method. Yet, sometimes the collocation method is useful, especially if to increase the number of points and to place them correctly.

The choice of basis functions is of a great importance for using the Moments method, since the successful selection of their system permits to decrease the volume and the time of calculations under given accuracy or increases the accuracy under the same calculations' time. For that end, as a rule, the basis functions must correspond to the physical sense of the problem, i.e., must coincide, in the first approximation, with the actual distribution of the current along a radiator and its elements.

Basis functions are customary subdivided into two types: entire-domain functions, which are distinguished from zero on the entire radiator length, and functions of sub-domains, which are distinguished from zero on the radiator segments. Members of Fourier series and polynomials of Tchebyscheff or Legendre can be used in the capacity of basis functions of the first type. Their field of application is limited mainly by solitary radiators of a simple shape. Basis functions of sub-domains are employed typically for an antenna of a complex shape. In particular, such an approach is expedient, if the antenna consists of arbitrarily situated segments of straight wires partially joined with each other. A straight radiator may also consist from physically isolated segments of wire, if concentrated loads are in the radiator at given distances from each other. Piecewise constant (impulse) functions (Fig. 1a), piecewise linear functions (Fig. 1b), and piecewise parabolic functions (Fig. 1c) are shown at Fig. 1 for illustration of sub-domains. These basis functions are special cases of a wider

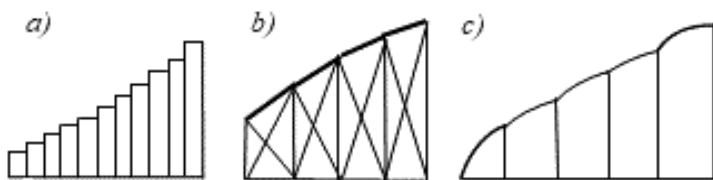


**Fig. 1:** The curve line as the sum of pulsed (a), piecewise linear (b) and piecewise parabolic (c) basis functions of sub-Domains.

class of basis functions—of polynomials. A simplest variant of approximation with the help of a polynomial was proposed in [2]:

$$J(\zeta) = \sum_{m=0}^{M_n} I_{nm} (\zeta - \zeta_n)^m, \quad \sigma_n < \zeta < \zeta_{n+1}.$$

Here,  $M_n$  is the selected degree of the polynomial on the segment  $n$ , and  $I_{nm}$  are unknown coefficients. Comparing this expression with (5.2), we obtain:  $I_n = I_{n0}$ ,  $f_n(\zeta) = \sum_{m=0}^{M_n} \frac{I_{nm}}{I_{n0}} I (\zeta - \zeta_n)^m$  at  $\zeta_n < \zeta < \zeta_{n+1}$  and 0 for other values of  $\zeta$ .

The members of Fourier series similarly can be used as basis functions of sub-domains. A particular case of such functions are piecewise sinusoidal functions:

$$J(\zeta) = \frac{I_p \sin k(\zeta_{p+1} - \zeta) + I_{p+1} \sin k(\zeta - \zeta_p)}{\sin k(\zeta_{p+1} - \zeta_p)}, \quad \zeta_{p-1} \leq \zeta \leq \zeta_p.$$

Comparing this expression with (5.2) and choosing a simplest variant, one can write:

$$f_p(\zeta) = \begin{cases} \sin k(\zeta - \zeta_{p-1}) / \sin k(\zeta_p - \zeta_{p-1}), & \zeta_{p-1} \leq \zeta \leq \zeta_p, \\ \sin k(\zeta_{p+1} - \zeta_p) / \sin k(\zeta_{p+1} - \zeta_p), & \zeta_p \leq \zeta \leq \zeta_{p+1}, \\ 0 & \text{elsewhere.} \end{cases} \quad (5.6)$$

Application of expression (5.2) with the basis functions in the form (5.6) is equivalent to dividing of wire onto the short dipoles with overlapped arms and with centers at points  $\zeta_p$ , wherein  $I_p$  is the current in the center of the dipole  $p$ . Such a look at the resulting structure allows us to say that expressions (5.2) and (5.5) generalize the expression (1.21). When lengths of short dipoles are decreased, piecewise sinusoidal basis functions are converted to piecewise linear functions. Figure 1b permits to visualize how the basis functions of sub-domains form the aggregate curved line corresponding to distribution of the current along an antenna.

In [3] the use of functions in the form (5.6) was proposed as the basis and weight functions. Such variant of the Moments method has two advantages. First, a rapid convergence of results is ensured, i.e., dimension of the matrix  $[Z]$  is small in comparison with dimensions of the matrixes, when using other basis and weight functions. This means that application of piecewise sinusoidal functions as the basis and weight functions corresponds to the physical content of the problem. Second, closed expressions containing integral sines and cosines can be used to calculate many matrix elements.

The advantages of this variant of the Moments method are especially significant when calculating complex antennas. The integral equation for the current in the metal antenna is based on the fulfillment of the boundary condition on its surface. In accordance with (4.60), the boundary condition for a metal antenna of complicate shape has the form

$$\sum_{n=1}^N \int_{S_{n1}}^{S_{n2}} J_n(S_n) \left[ k^2 G \vec{e}_{s_n} \vec{e}_p - \frac{\partial^2 G}{\partial_p \partial s_n} \right] ds_n = -j\omega \varepsilon K_p(p). \quad (5.7)$$

Let us substitute the current distribution (5.2) with weight functions (5.6) into the equation (5.7) for a complicated wire radiator and multiply both parts of the equation to the weight function  $f_p(z)$  in accordance with Galerkin's method. Integrating the result along the entire wire length, we obtain, repeating this operation for different  $p$ , a set of  $N$  equations of type (5.5) with  $N$  unknown magnitudes  $I_n$ . The coefficients in these equations are equal to

$$Z_{ps} = -\frac{1}{j\omega \varepsilon} \int_{Z_{s-1}}^{Z_{s+1}} f_s(z) \int_{\zeta_{p-1}}^{\zeta_{p+1}} f_p(\zeta) \left[ k^2 G_3 \vec{e}_\zeta \vec{e}_z - \frac{\partial^2 G_3}{\partial z \partial \zeta} \right] d\zeta dz, \quad U_s = \int_{Z_{s-1}}^{Z_{s+1}} f_s(z) K_s(z) dz. \quad (5.8)$$

Comparing (5.8) with expression (3.56), where the magnitude  $E_{ps}$  is substituted from Section 4.6, it is easy to be convinced that the expression for  $Z_{ps}$  corresponds to the mutual impedance between dipoles  $p$  and  $n$ , determined by the method of induced emf. As seen from (5.8), the dipoles are considered as isolated, i.e., the current of each dipole is distributed in accordance with the sinusoidal law. Substituting extraneous field  $K_s(z)$  into (5.8), we see that magnitude  $U_s$  is the emf of the generator connected at the center of the dipole  $s$ . Therefore, the set of equations (5.5) with coefficients  $Z_{np}$  and  $U_p$  is the set of Kirchhoff equations for the dipoles constituting the wire antenna.

Thus, the Galerkin's method that was proposed by Richmond for calculating the current's distribution in a complicated antenna, is equivalent to dividing of the radiator onto isolated dipoles. Their own and mutual impedances are calculated by the method of induced emf. For calculating the antenna with concentrated loads, it is expedient to divide this antenna onto short dipoles and to place each load in the center of each dipole. It is useful to generalize the set of equations (5.5) and to write it in the form:

$$\sum_{p=1}^P I_p Z_{ps} = U_s - I_s Z_{ss}, \quad s = 1, 2 \dots N,$$

or in the matrix form

$$[I][Z] = [U - IZ].$$

The accuracy of the method of induced emf for calculating a dipole as is known decreases when the dipole length increases. The high accuracy of calculation is obtained at dipole arm length  $L \leq 0.4\lambda$ . The advantage of the generalized method of induced emf consists in the fact that one can divide the long dipole onto several short dipoles, e.g., with the arm length no greater than  $0.2\lambda$ . That allows ensuring the required exactness.

Calculation of the coefficients  $Z_{ps}$  requires the double numerical integration. But the problem is simplified essentially, if the method described in [4] is used for calculating the mutual impedance of two arbitrarily situated dipoles. Here, the double integrals are reduced to the common integrals, and each integral is a sum of series, consisting of the members with successively changing signs. The components of series are calculated by means of recurrence formulas, almost as quickly as the components of the power series. This manner of calculating  $Z_{ps}$  is useful in general-purpose software.

In substance the generalized method of induced emf makes it possible to ensure the accuracy of calculating complex antennas close to the accuracy of calculating the simplest radiators. Therefore, it is the basis for all calculation programs used in modern computers. This allows us to complete the story of a rigorous theory of thin linear radiators.

## 2. Effect of Volume Metal Designs on Antenna Characteristics

The generalized method of induced emf made it possible to consider the influence of metal structures on the directivity characteristics of antennas. The dependence of the antennas characteristics from nearby metal bodies takes place for any antennas located on any objects. But, as a rule, this influence is especially great and the task to reduce this effect is especially difficult when placing antennas on moving objects, for examples, on ships. One of the most important and most difficult tasks of analyzing the antennas characteristics is to consider the influence of three-dimensional metal structures. A feature of the ship's antenna field is, as already mentioned, the limited space for placing antennas, in connection with which antennas are installed near various metal structures—masts, superstructures, chimney, rooms, etc. These structures and a ship hull participate in the formation of electromagnetic radiation, and their influence on the characteristics of the antenna is often decisive. Such designs surround any antenna and are included in the structure of the antennas themselves. Knowledge of the laws of this influence is extremely important for predicting the actual characteristics of ship's antennas.

The analysis of the influence of these objects is complicated even in the simplest cases when, for example, only one superstructure is considered—in the form of a circular or elliptical cylinder of infinite length. In principle one can consider the influence of the superstructure, assuming that a superstructure is an additional passive antenna, like a thin linear radiator. But this approach yields too rough approximation. The influence of a ship's hull and superstructures on the characteristics of antennas for a long time studied experimentally. But the practical possibilities of a comprehensive analysis with the subsequent selection of optimal solutions in this case are small. An analysis method based on replacing a metal body with a system of intersecting thin wires is more effective [3, 5]. In such a formulation, the problem is reduced to calculating the current distribution in a wire structure consisting of randomly oriented wire segments. The wires diameters are considered small in comparison with the lengths of the segments and the wavelength. Knowing the currents of wires, we can calculate all electrical characteristics of a radiator.

A widespread use of a calculation program based on the above replacement and the Moments method substantially changed the situation. As a rule, the used algorithm includes one of the integral equations, Galerkin's method and a system of piecewise sinusoidal basis functions. In general, the new method of analysis has become part of a generalized method of induced emf. One of the first problems considered using a new method was the problem of an influence of a cylindrical superstructure on the parameters of an antenna and antenna array [5]. The content of a problem is clear from Fig. 2. This figure shows a wire structure equivalent to a thick superstructure in the shape of a circular cylinder of finite height, near which a whip antenna is placed. As it follows from the figure, the metal cylinder is replaced by a wire structure from equally spaced wires located along its generatrices and radii of a butt-end. The origin of coordinates system for the convenience of calculations is combined with the center of the cylinder base. The wires diameter for simplicity is taken equal to the diameter of a whip antenna. The surface of the earth is considered as perfectly conductive, and the structure under consideration is symmetrical with respect to this surface. The mirror image of a superstructure is given in the figure by dotted lines.

Table 1 presents input impedance  $Z_A$  and maximal directivity  $D_{max}$  for the whip antenna of height 6 m located near a superstructure of a diameter 5 m and a height 6 and 20 m on the three HF frequencies.  $D_{max}$  is given with respect to maximal directivity of the quarter-wave monopole. These characteristics also are presented for the case when the superstructure is absent ( $L_s = 0$ ). Calculating amplitudes and phases of the currents in the base of each wire of the superstructure shows that their values are symmetrical with respect to axis y. At the same time currents in the superstructure wires on the side of an antenna and on the opposite side differ substantially both in amplitude and in phase.

The calculated directional patterns of a whip antenna 6 m high and 0.016 m in diameter near superstructures of different heights  $L_0$  are shown by curves on Figs. 3 and 4 at three frequencies of the HF range in the horizontal and vertical planes. The experimental values are represented by points of various shapes. The coincidence of the calculated and experimental data is good.

The calculations show that antenna characteristics to a high degree depend on a superstructure presence and on its height. The resistance of radiation decreases at all sections of a frequency range excepting the region of a parallel resonance. The radiation in the direction of a superstructure decreases sharply. The superstructure height significantly affects the radiator properties in an entire frequency range. The good agreement of calculation with experiment confirms indirectly the choice rightness of the wire structure. As is seen from Fig. 2, in this structure the circular wires are absent, i.e., calculation does not take into consideration cross-currents induced on the cylinder surface. Calculating electrical characteristics of the whip antenna located near the superstructure with height 6 m, whose equivalent structure is supplemented by horizontal wires, was performed to verify the rightness of a model.

The mentioned wires were placed in parallel planes at 2 m from each other and each wire had the shape of a regular polygon inscribed in a circumference with a radius equal to the radius of a cylinder. The directional pattern of the antenna located near the structure with additional horizontal wires was almost identical the



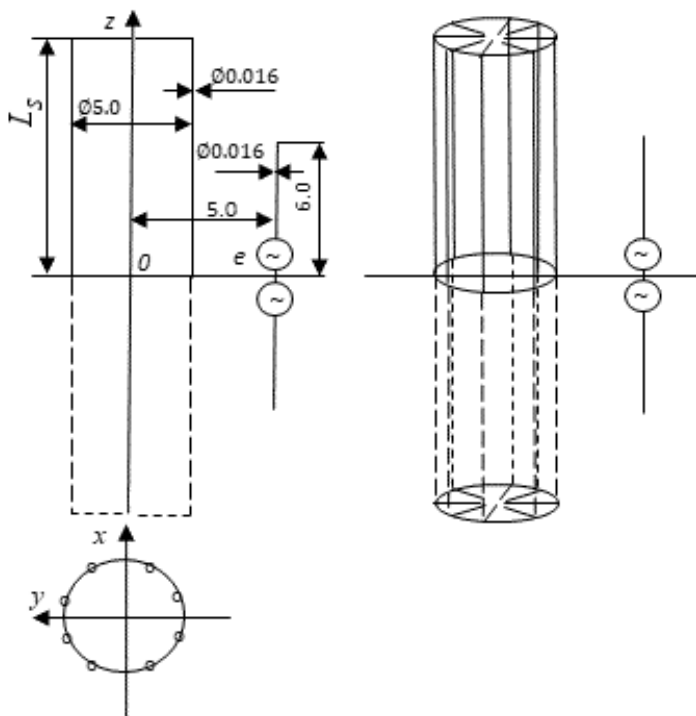


**Fig. 2:** Whip antenna near the metal superstructure.

**Table 1:** Characteristics of the Whip Antenna, Located near the Superstructure.

<i>f</i> , MHz	<i>Z<sub>A</sub></i> , Ohm			<i>D<sub>max</sub></i>		
	<i>L<sub>s</sub></i> = 0	6	20	0	6	20
6.0	6.0 – j353	3.7 – j351	1.8 – j350	1.86	2.46	4.32
12.5	39.7 + j20.9	24.7 + j38	17.0 + j28.2	2.00	5.39	5.32
19.0	289 + j424	356 + j505	185 + i448	2.35	4.76	6.80

directional pattern without these wires (the directivity differs by 1–2%), the input impedance changes in an interval of 5–10%. The currents in the horizontal wires are substantially smaller than currents in the vertical conductors, for example, at a frequency of 6 MHz they are smaller by a factor of 10<sup>5</sup>. Calculations showed also that the lengths of the segments into which the conductors are divided should not exceed 0.2λ. The wires number of a selected structure in such problem must be chosen based on the condition that the distance between the parallel wires is of the order of (0.6 – 0.8)λ. When these conditions are met, the shape of the directional pattern becomes stable.

Calculations allow us to find the minimum height of a cylindrical superstructure, at which the characteristics of an antenna located close to it coincide with the characteristics of the same antenna located next to the infinitely long cylinder. From the calculations it follows that the height of such a superstructure should be greater

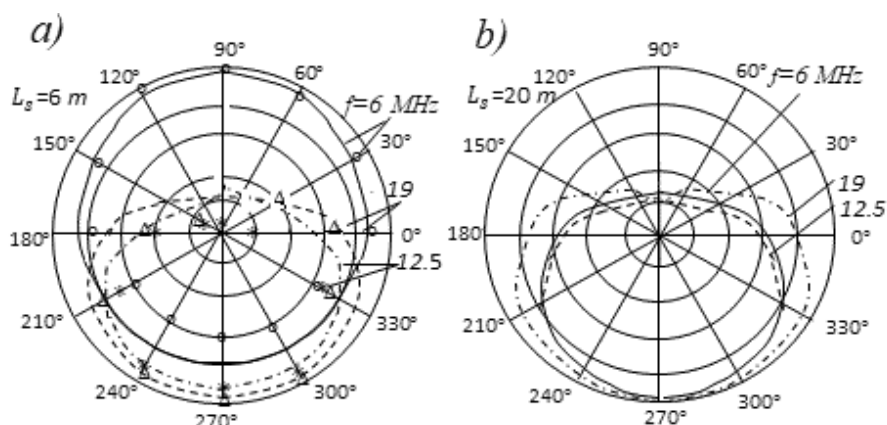


Fig. 3: Horizontal directional patterns of a whip antenna near a superstructure.

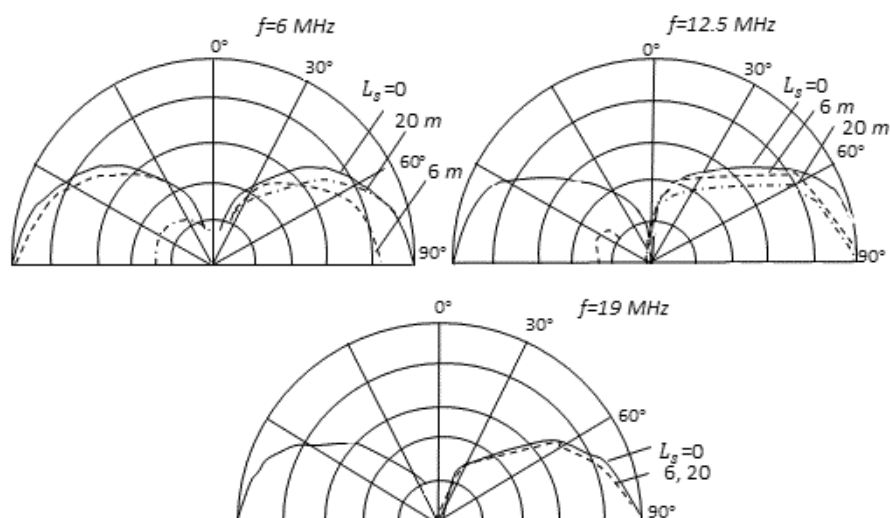


Fig. 4: Vertical directional patterns of a whip antenna near a superstructure.

than the height of an antenna by about a quarter of the wavelength. At the next stage of work, similar results were obtained for antennas located near superstructures of a complex shape. Comparing the influence of similarly sized superstructures on the properties of antennas equally distant from the axes of differently-shaped superstructures showed that the results of this influence is basically the same.

Different authors called different magnitudes for the minimal number of conductors, which ensure the equivalence of electrodynamic properties of a metal body and its model. These differences are caused by such circumstances as solving different problems and using different basis functions. It is advisable to arrange the conductors of the structure along the most probable directions of the currents' spreading. In this case, the number of conductors and the amount of computation will be minimal.

The discussion results of this issue were later summarized in [5]. In this paper, three different types of problems are considered: calculation of directional patterns, calculation of mutual coupling, and calculation of input impedances. The directional pattern is not affected by minor changes in the distribution of a current, and accurate results are obtained, when a few of basis functions is small. Calculation of the mutual coupling and the input impedances requires the more accurate representation of the current. To obtain specifically accurate results one must to take much basis functions. The presented table describes the various options of structures. For a single wire, when calculating the directional pattern, it is required to use from 6 to 10 basis functions per a wavelength. Thick wires require more functions than thin wires—up to 15 per a wavelength. For wire meshes and surfaces the number of basis functions is given per square with a side equal to the wavelength and depends on the surface shape: for a flat one—about 40, for a three-dimensional one, it is more. For bodies of revolution, the number of functions per wavelength along the generatrix should be of the order of 20 and depends on the maximum circumference length. Active elements require more functions than passive ones.

An excessive increase in the number of functions can worsen the result, since rounding off the calculated magnitudes will lead to a significant error.

The loads included in the antenna allow us to obtain the concrete electrical characteristics by means of an antenna length's selection. If it is possible to manufacture and install antennas of the required length, then the freedom to choose this length permits to weaken the influence of closely located metal structures, for example, of superstructures, on the directional pattern of antenna and antenna array [6]. Figure 5 demonstrates the results of calculating the directional patterns of a monopole situated near a metal superstructure in the shape of a circular metal cylinder of finite length. The directional patterns in the horizontal plane are presented at two frequencies of *HF* range.

Two variants of antennas are examined: first, the monopole without loads of a height 6 m and a diameter 0.016 m, secondly, the radiator of a height 12 m and a diameter 0.06 m with nine capacitive loads, ensuring optimal electrical characteristics on the frequencies from 8 to 22 MHz. The relative arrangement of the superstructure and the antennas as well as the superstructure dimensions are given in Fig. 5a. The calculations were performed with help of a program based on the Moments method. The circular cylinder during calculation was replaced with a structure consisting of equidistant wires, located along generatrices of the cylinder and radii of its upper surface (butt-end). Figure 5b shows results of calculating directional patterns of both radiators in a horizontal plane on two frequencies of *HF* range (12.5 and 19 MHz). As is seen from Fig. 5b, the radiation of an ordinary monopole (curve 1) in the direction of superstructure decreases sharply, and the use of an antenna with loads (curve 2) allows to weaken this effect.

Figure 6 demonstrates similar results for a uniform linear antenna array located near the superstructure. The same two variants of antennas are adopted as the array elements. The mutual arrangement of the superstructure and the antennas as well as the superstructure dimensions are given in the figure and the phase shift between antenna currents is adopted as zero. The calculation results show that in an upper part of a frequency range the superstructure influence on the directional pattern of

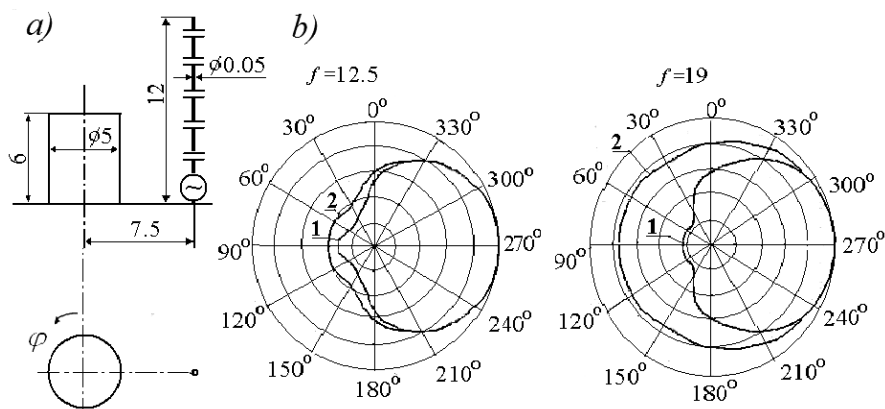


Fig. 5: An antenna near the superstructure (a) and its horizontal directional pattern (b).

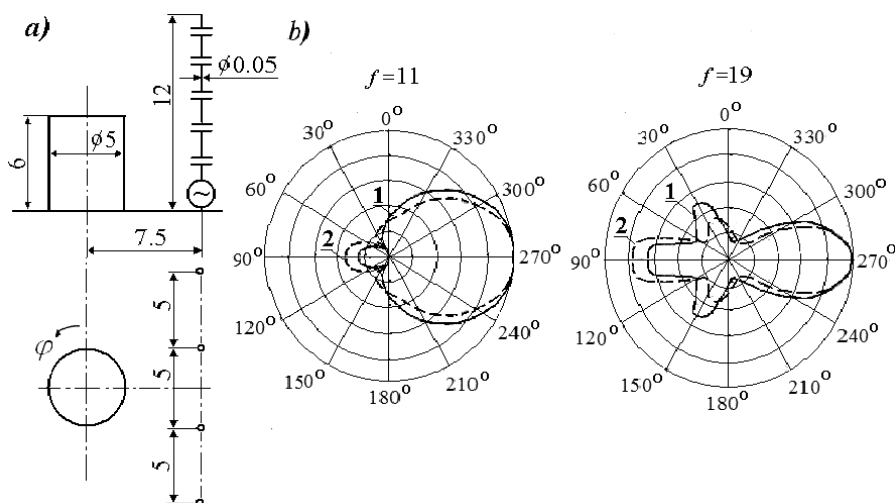


Fig. 6: A linear antenna array near a superstructure (a) and its horizontal directional pattern (b).

array, consisting of monopoles without loads, is slighter than its influence on the directional pattern of the sole monopole. This is apparently concerned with the fact that the superstructure does not hinder the propagation of electromagnetic waves from the side antennas. Nevertheless, the use of radiators with loads in this case also allows to reduce the superstructure influence and to increase the signal in its direction.

From the described examples it follows that modern calculation programs not only reveals regularity of the harmful effect of closely-spaced metal structures on the characteristics of ship's antennas, but also allow to propose methods that would substantially weaken this effect or even eliminate it. The variety of existing on ships conditions for the antenna installation makes it advisable to analyze typical installation options, in particular typical arrangements for the relative positions of antennas near secondary radiators (masts, antennas, chimney, superstructures), which

have a substantial influence on their characteristics. As a rule, the characteristics of antennas are substantially distorted, if they are located near two superstructures, for example, near a chimney and a mast or a ship mast and a free-standing antenna-mast.

Examples of two options of antenna placement and results of calculating their characteristics are given in Fig. 7 and 8. Figure 7a is a layout chart of a whip antenna on the upper bridge of one of ships, while Fig. 8a demonstrates the arrangement of a whip antenna on the upper bridge of a tanker. In both cases, the antennas are located near a chimney and a mast, the dimensions and location of which are visible from the figures. The dimensions are given in meters, the numbers marked: 1—antenna, 2—mast, 3—chimney. During the calculation the chimney was replaced by a structure of eight wires located along the generatrices of a circular cylinder and the radii of its butt-end, and the mast was replaced with two parallel wires of different diameters.

As a rule, the characteristics of antennas are substantially distorted, if they are located near two superstructures, for example, near a chimney and a mast or a ship mast and a free-standing antenna-mast.

The results of calculations and experimental verification of the directional patterns of the whip antennas in the horizontal plane are given in Figs. 7b and 8b at frequencies 6 and 12 MHz. It can be seen from the figures that the superstructures significantly change the characteristics of the whip antennas, and experiments confirm the calculations. The Table 2 shows the input impedance and the gain of a half-wave asymmetric radiator located in free space (at the same frequencies).

In connection with these results, to avoid misunderstandings, it is necessary to recall that, as it is said above and is shown in [7] and [8], the use of concentrated loads provides freedom of choice of the antenna length, if the design capabilities are had and allows us to obtain the required characteristics in the desired operating range.

The goal of another task was to analyze the characteristics of the antenna depending on the construction, on which it is installed. The main ship's antenna is an antenna operating in the range of medium frequencies. With allowance for peculiarity of their propagation, these electromagnetic waves should be directed along the earth's surface and have a vertical polarization. In the horizontal plane, the directional pattern of the antenna should be close to circular. The efficiency of the main antenna should be sufficient to create an electric field with an intensity  $50 \cdot 10^{-9}$  V/m at a distance 150 miles from the ship when the main radio transmitter of the ship is connected to the antenna.

The effective antenna height increases with increasing length and width of the horizontal load. It is possible to increase the load efficiency without changing its

**Table 2:** Characteristics of a Whip Antennas.

Variant of placement	$Z_A, \text{Ohm}$		$G$	
	$f_A = 6.5 \text{ MHz}$	$f_A = 12.5 \text{ MHz}$	$f_A = 6.5 \text{ MHz}$	$f_A = 12.5 \text{ MHz}$
in free space	$6 - j353$	$39.7 + j20.9$	1.9	2.0
in accordance with Fig. 7	$0.9 - j350$	$22 + j37.5$	5.9	5.9
in accordance with Fig. 8	$5.7 - j349$	$40 + j13$	5.0	3.7

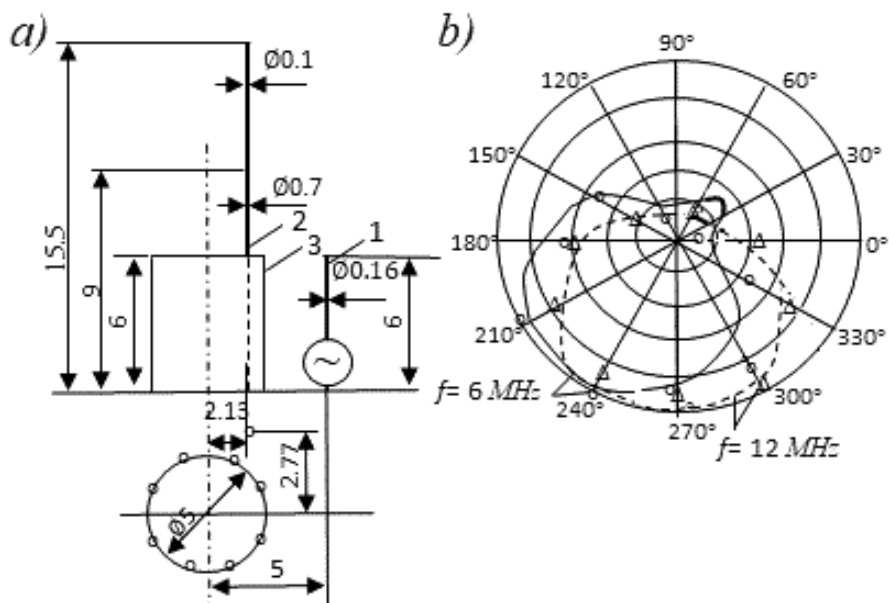


Fig. 7: Layout of the whip antenna on the upper bridge of the ship (a) and horizontal directional pattern of this antenna (b). 1 – whip antenna, 2 – mast, 3 – chimney.

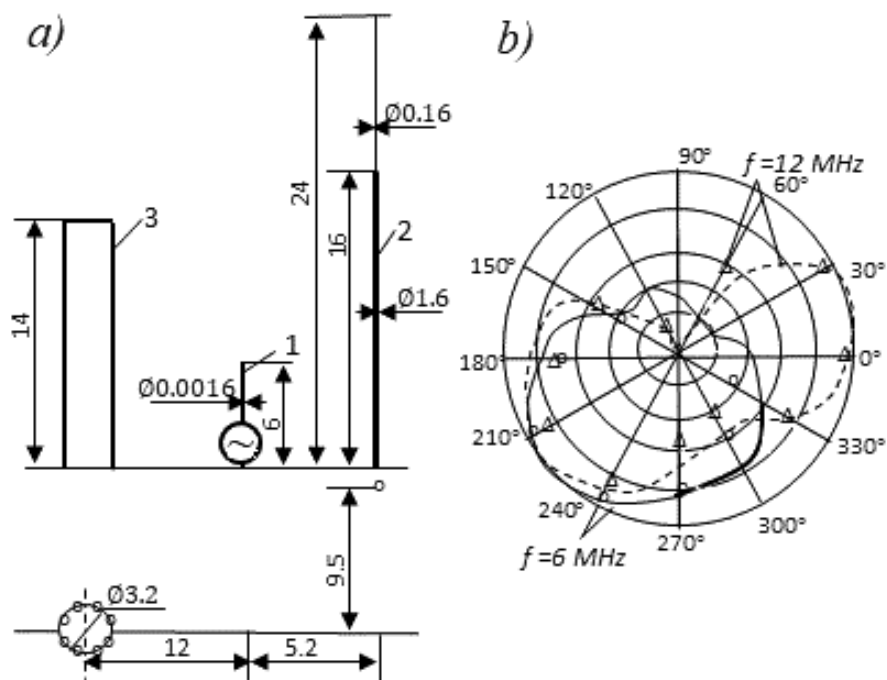


Fig. 8: Layout of a whip antenna on the upper bridge of a tanker (a) and horizontal directional pattern of this antenna (b). 1 – whip antenna, 2 – mast, 3 – chimney.

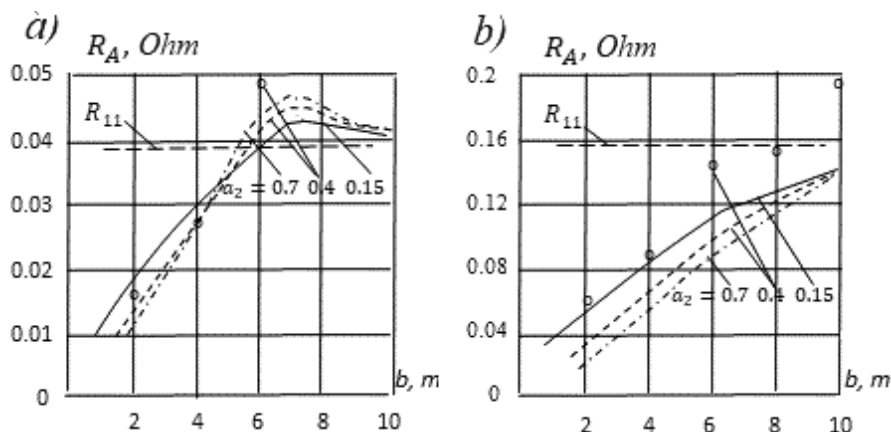


Fig. 9: Dependence of the radiation resistance of the wire antenna on the distance to a mast.

length by replacing the usual structure of the parallel wires with the meandering load described in Section 1.8. Disadvantages of wire antennas are obvious: they require a second mast, which hinders cargo operations, they are torn in stormy conditions. In addition, the mast, near which the vertical antenna wire is suspended, not only plays a role of a support but also creates an additional parasitic capacitance between the antenna and the ground, reducing the resistance of a radiation.

The calculating procedure of a radiation's resistance for an antenna with excitation in the base, the wire of which is parallel to the mast, is described in [9]. It is based on a theory of a folded radiator. Figure 9 shows the results of calculating the radiation's resistance for antennas 6.5 and 13 m high at a frequency 0.46 MHz depending on the distance  $b$  between an antenna and a mast for different radii  $a_2$  of the mast (all dimensions are indicated in meters). The radius of the antenna wire is equal to  $a_1 = 3.7 \cdot 10^{-3}$  m. The points in the figure give the results of an experimental check, when the mast radius is equal to  $a_2 = 0.4$  m. For comparison the graphs show the radiation's resistance  $R_{11}$  of an antenna located away from the mast.

It is seen from the figure that active component  $R_A$  of the antenna input impedance drops sharply as the distance between the antenna and the mast is small. Horizontal wire loads weaken the influence of the mast. But in this case also it is necessary to move the antenna away from a mast as far as possible (from 4 to 8 m, depending from the mast height).

### 3. Influence of Installation Site

The ship's short-wave antennas in real conditions are installed on various objects and elevations—pillars, masts, chimneys, brackets, etc. The characteristics of such antennas differ significantly from the characteristics of antennas mounted on an infinite ideally conducting plane. When placing antennas on an object, much attention needs to be paid to a shape of their directional patterns in a vertical plane. The input impedance, and consequently the operation mode of a cable and the load impedance of a radio transmitter also depend on dimensions of a rod or mast, on which an antenna is placed (see Fig. 10).

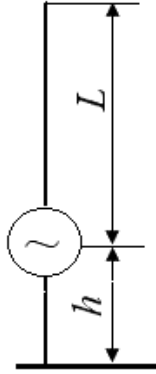


Fig. 10: Whip antenna on the pillar (rod).

The antenna mounted on the pillar can be considered as a radiator with an excitation point shifted from the base. For generality, we assume that the propagation constants  $k_1$  along the antenna and  $k_2$  along the pillar have different magnitudes and differ from the wave propagation constant  $k$  in air. In this case, the result can be used both for a metal antenna and for an antenna with impedance boundary conditions. In addition, different values of the propagation constants make it possible to consider the decrease in wave velocity along a thick structure.

We define the electric field in a far zone, considering the radiator of finite length as the sum of elementary electric radiators. In accordance with (3.10) we write:

$$E_\theta = j \frac{30k \exp(-jkR) \sin \theta}{\varepsilon_r R} \int_{-L}^L J(z) \exp(jkz \cos \theta) dz = j30kJ(h) \frac{\exp(-jkR)}{\varepsilon_r R} h(\theta). \quad (5.9)$$

where

$$h(\theta) = \frac{\sin \theta}{J(h)} \int_{-L}^L J(z) \exp(jkz \cos \theta) dz. \quad (5.10)$$

Here  $J(h)$  is a generator's current,  $R$  is a distance from the origin (from a pillar base) to an observation point,  $J(z)$  is a current along the radiator. The integral is calculated both along a radiator (along an antenna and a pillar), and along its mirror image. The current distribution along an antenna is like the current distribution along a long line open at the end:

$$J(z) = J(h) \frac{\sin k_1 (L - |z|)}{\sin k_1 (L - |h|)}, \quad h \leq |z| \leq L.$$

The distribution of current along a pillar is like the distribution at a short circuit (to a ground):

$$J(z) = J(h) \frac{\cos k_2 z}{\cos k_2 h}, \quad 0 \leq |z| \leq h.$$



From here

$$h(\theta) = h_1(\theta) + h_2(\theta), \quad (5.11)$$

where

$$h_1(\theta) = \frac{2k_1 \sin \theta}{\sin k_1 L_1 (k_1^2 - k^2 \cos^2 \theta)}.$$

$$[\cos(kL \cos \theta) - \cos k_1 L_1 \cos(kh \cos \theta) + k \cos \theta \sin k_1 L_1 \sin(kh \cos \theta)].$$

$$h_2(\theta) = \frac{2 \sin \theta}{\cos k_2 h (k_2^2 - k^2 \cos^2 \theta)} [k_2 \sin k_2 h \cos(kh \cos \theta) - k \cos \theta \cos k_2 h \sin(kh \cos \theta)].$$

The quantity  $h(\theta)$  is sometimes called a generalized effective height of an antenna. It connects the electric field in an arbitrary direction with a generator' current:

$$h(\theta) = h_e F(\theta, \varphi),$$

where  $h_e$  is the effective height of a symmetric radiator, and  $F(\theta, \varphi)$  is the directional pattern. Equalities (5.9), (5.10) and (5.11) allow us to determine the field in a far zone and the directional pattern of an antenna mounted on a pillar. When  $k_1 = k_2 = k$ , the formulas are significantly simplifying:

$$E_\theta = j60J(h) \frac{\cos kh \cos(kL \cos \theta) - \cos kL \cos(kh \cos \theta)}{\sin k_1 L \cos kh \sin \theta} \frac{\exp(-jkR_0)}{R_0}.$$

Putting  $h = 0$ , we obtain an expression for the directional pattern of an impedance radiator:

$$E_\theta = j60J(h) \frac{k_1 k \sin \theta [\cos(kL \cos \theta) - \cos k_1 L]}{(k_1^2 - k^2 \cos^2 \theta) \sin k_1 L} \frac{\exp(-jkR_0)}{R_0}.$$

The effective height  $h_e$  of an antenna on a pillar is determined from (5.11) by substitution  $\theta = \pi/2$ :

$$h_e = h(\pi/2) = h_{e1} + h_{e2},$$

$$\text{where } h_{e1} = \frac{1}{k_1} \tan \frac{k_1 L_1}{2}, h_{e2} = \frac{1}{k_2} \tan k_2 h.$$

The radiation's resistance of an asymmetric radiator with a shifted excitation point is

$$R_\Sigma = 40k^2 h_e^2 = 40 \left( \frac{1}{k_1} \tan \frac{k_1 L_1}{2} + \frac{1}{k_2} \tan k_2 h \right)^2.$$

The reactive component of an input impedance of this radiator is

$$X_A = X_{A1} + X_{A2},$$

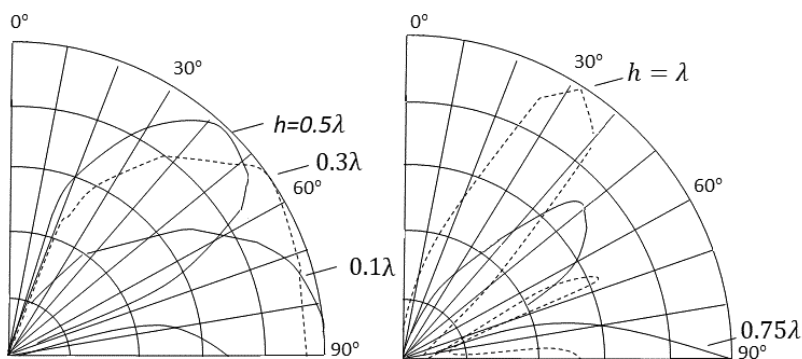


Fig. 11: Vertical directional patterns of an antenna with length  $L = \lambda/4$  on a pillar of different height

where  $X_{A1} = -60 \ln \frac{2L_1}{a_1} \cot k_1 L_1$  is the reactive component of an antenna input impedance, and  $X_{A2} = -60 \ln \frac{2h}{a_2} \tan k_2 h$  is the reactive component of a pillar.

The directional patterns of antennas with a length  $L = \lambda/4$ , mounted on pillars of different heights are presented in Fig. 11. The figure shows that a change in the pillar height leads to a significant change of the directional pattern of this radiator.

Using the based on the Moments method program for calculating electrical characteristics of antennas, it is easy to verify that placing an antenna on a pillar significantly changes its input characteristics as compared with placement on a metal plane: resonances are shifted toward low frequencies, the main lobe of a directional pattern in the vertical plane deviates from the ground at lower frequencies.

The above expressions and calculations are given for the perfectly conductive earth. If the conductivity of an underlying surface is not infinite (for example, the conductivity of a sea surface), then this surface does not create a system of currents equivalent to a mirror image. But during calculating the fields at a large distance from an antenna, we can assume that the surface creates a distorted mirror image equivalent to the field of a current that in contrast to  $-1$  is multiplied by some reflection coefficient. Since this coefficient depends on the angle of a beam incidence, the equivalent current of a distorted mirror image depends on the point, at which the beam was reflected, and consequently on the observation point. In this case, the current distribution along a mirror image of an antenna and a pillar is determined by the equalities

$$J(z) = \begin{cases} J(h)R \frac{\sin k_1 (L - |z|)}{k \cos \theta}, & h \leq |z| \leq L, \\ J(h)R \frac{\cos k_2 z}{\cos k_2 h}, & 0 \leq |z| \leq h. \end{cases}$$

Here  $R$  is reflection coefficient

$$R = |R| \exp(j\Phi) = \frac{\varepsilon'_r \cos \theta - \sqrt{\varepsilon'_r - \sin^2 \theta}}{\varepsilon'_r \cos \theta + \sqrt{\varepsilon'_r - \sin^2 \theta}},$$

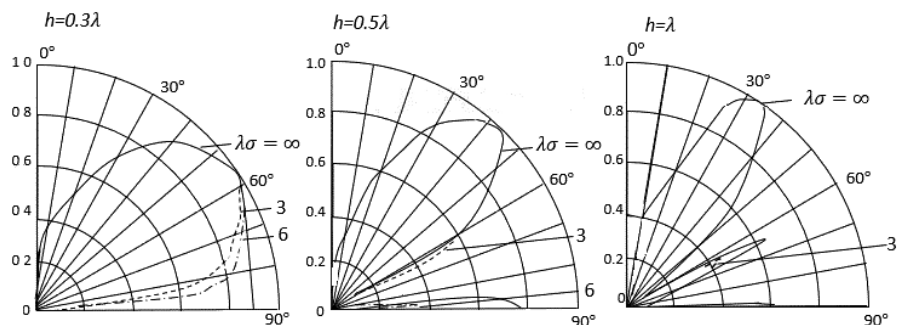


**Fig. 12:** Vertical directional patterns of the antenna with length  $L = \lambda/4$ , on the pillars of different heights depending on surface conductivity.

$\varepsilon'_r$  is relative complex permeability of the medium equal to  $\varepsilon'_r = \varepsilon'/\varepsilon_0 = \varepsilon_r - j60\lambda\sigma$ ,  $\varepsilon_0$  is the absolute permeability of the air,  $\lambda$  is the wave length,  $\sigma$  is conductivity of the medium.

In Fig. 12 directional patterns of antennas with a length  $L = \lambda/4$ , mounted on pillars of different heights are given for three values of the product  $\lambda\sigma$ : 3 cm, 6 cm and  $\infty$ . The relative dielectric constant is  $\varepsilon_r = 80$ . It can be seen from the figures that a decreasing the conductivity of the underlying surface leads to a weakening of radiation under small angles to the horizon. Moreover, in the case of a short pillar, the directional pattern has one lobe. If the conductivity of the medium is high, then the lobe is pressed to the surface. When the medium conductivity decreases, in the directional pattern (in the horizontal direction) a dip is formed.

In the case of a long pillar, the vertical directional pattern consists of several lobes. Decreasing in the medium conductivity leads to a sharp decrease in the lower lobe of the directional pattern, i.e., to reduce radiation under angles optimal for radio communications. Thus, the parameters of underlying surface significantly affect the characteristics of the antennas and should be consider when developing and installing them. The methodology and results of calculating the loss resistance of a metal antenna with a shifted excitation point in the decameter wavelength range depending on conductivity of the underlying surface are described in [9].

Along with other installation options, ship's antennas of the HF range often mounted on a bracket that is installed on one of the ship's decks (Fig. 13). At that 6-meter whip antennas are usually placed on brackets 0.5 m long, and 10-meter and other close to them in height whip antennas are placed on brackets 1 m long.

The characteristics of antennas mounted on the brackets are substantially differ from the characteristics of antennas located on the infinite perfectly conducting plane. Previously, an influence' study of the ship's hull and other metal structures on these characteristics was carried out, as a rule, experimentally. But measurements of this kind both on the objects and on the models are very time-consuming and do not allow to identify the basic laws of this influence. The analysis method, based on replacing metal surfaces with a system of thin wires, turned out to be more effective [10].

In Fig. 14 the wires' structure, using for solving such problems, is shown. A whip antenna with a height  $L = 6$  m an average radius  $a_1 = 0.008$  m is mounted on a

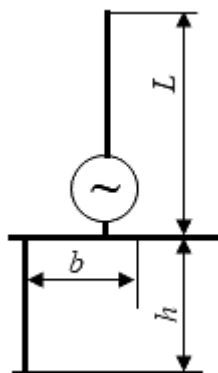


Fig. 13: Antenna on a bracket.

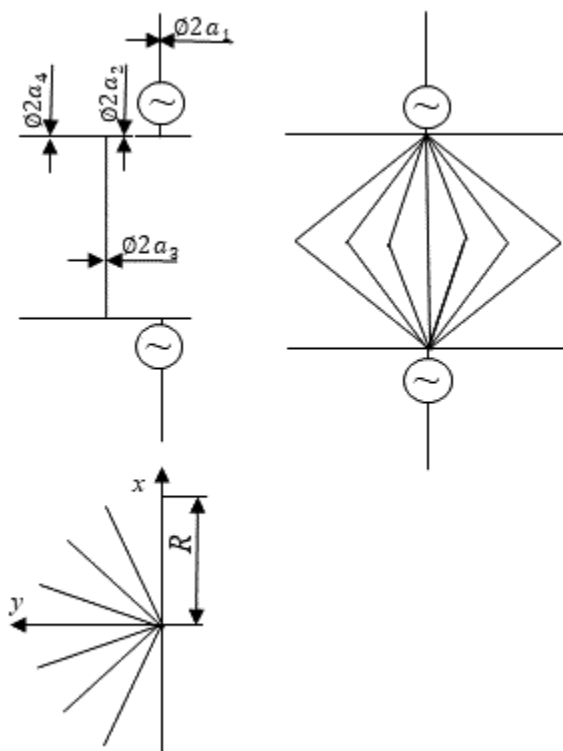


Fig. 14: Equivalent wires structure for the whip antenna mounted on the bracket.

bracket of a length  $b = 0.5$  m with an equivalent radius  $a_2 = 0.1$  m. The bracket height above a lower deck is  $h = 8$  m. A horizontal surface of the deck near the antenna is replaced by structure of nine radial wires with length  $R$  located at identical angles. The vertical (side) surface of the ship is replaced by a system of seven wires also located at the equal angles. The mirror image is made like the main structure.

The results of calculating the electrical characteristics of an antenna mounted on a bracket depend on the choice of a length  $R$  of radial wires. Calculations, performed

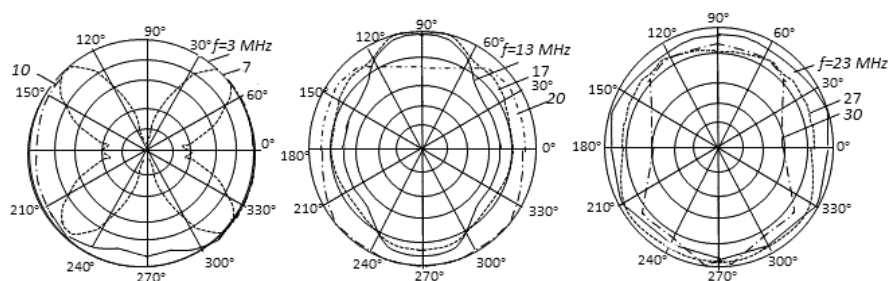


Fig. 15: Directional pattern of antenna on a bracket in a horizontal plane.

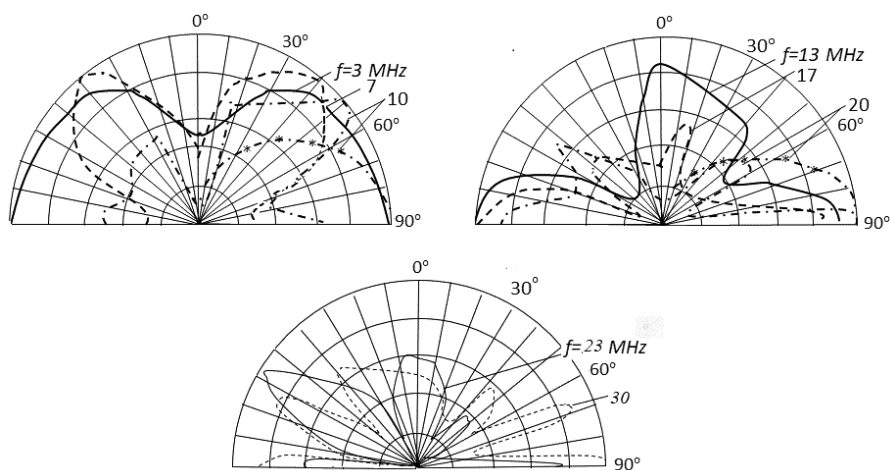


Fig. 16: Directional pattern of antenna on a bracket in a vertical plane.

at a frequency 5 MHz shown that directional patterns of a whip antenna with a height  $L = 6$  m mounted on the bracket substantially change with increasing  $R$ , if  $R$  is less than  $R_0$ , where  $R_0 = L + \frac{\lambda}{4} = 21$  m. During further increase of  $R$  directional patterns cease to change. Therefore, in the calculations, the lengths of the radial wires were taken equal to  $R_0$ , depending on the wavelength and antenna height. To exclude the additional calculation error associated with sharply differing dimensions of wires, its expedient to put that the wires have the same length.

In Figs. 15 and 16 the directional patterns of the described construction in the horizontal and vertical planes are given at different frequencies. The calculation results showed that the antenna directional patterns on the bracket in the vertical plane have a complex form, and at high frequencies they have a multi-lobe character. The corresponding curves for the antenna mounted on the plane (they are indicated by asterisks \*) have a simpler shape in the form of a single lobe. A small side lobe appears only at a frequency 30 MHz.

The calculation of an input impedance of an antenna shows also that its installation on a bracket significantly changes both the active and reactive components of its impedance. In particular, the frequency of a first series resonance decreases (similarly the radiator mounted on a pillar), and the frequency of a first parallel resonance (in contrast to a mentioned radiator) increases.

The method described above uses two innovations. First, the large dimensions of the ship's hull are taken into consideration with the help of radial wires of limited length. The mutual impedances between short radiators located at a large distance from each other are small, and taking them into account does not refine a result, but leads to gross errors related with rounding of the results. To get rid of gross errors length  $R_0$  is used in the capacity of such a magnitude. Second, the radial wires are located along the assumed directions of the currents.

Comparison of the described method for calculating characteristics of an antenna mounted on a bracket with other methods, for example, with the combined method based on the Moments method and geometric diffraction theory [11], corroborates an advantage of the described method, since it considered the structure's details and demonstrates a high accuracy of obtained results.

The combined method also was applied to the radiator mounted on a bracket. In this case the structure was considered as the radiator located on a wedge. But this calculation method did not permit to consider the presence of a bracket and its dimensions. With the help of a combined method, it was impossible to calculate the input impedance of an antenna located near the end of a wedge. The presence of a bracket and its dimensions were not use during calculation in principle.

The procedure, which was used in [11] is based, as already said, on the joint use of two methods. One of them, the Moments method, provides high accuracy of the results. Another method, based on the geometric theory of diffraction, is purely approximate. In connection with these circumstances, the question arises of the applicability of this approach to a problem requiring an exact solution. The need for an exact solution follows from the fact that using the approximate method does not allow us to bring the solution to a useful result. The relevance of the issue raised is associated with the frequent use of the described approach. A negative answer cannot be considered unambiguous; a positive answer requires careful analysis.

In Fig. 17 the short-wave antenna installed on a cross-beam (in other words, on a horizontal rod, mounted on a ship's mast) is presented. This installation of a whip antenna was used in a practice of ships' designing along with an installation of antennas on pillars and brackets. During the calculating characteristics of such antennas, one must consider the wire structures of various complexity (Fig. 18). The first of these structures (Fig. 18a) can be used for a relatively thin mast, the other two structures are suitable for thicker masts, including superstructures. During a study, various options were considered. In the first structure, the number of wires in different elements of a mast varied, but the result depended weakly on these changes. Therefore, when calculating the following options, in addition to the horizontal rod only two wires were used: one wire for the upper and lower sections of a mast, respectively.

The study showed that the directional pattern of these antennas in the horizontal plane is primarily determined by the elements of the surrounding structure, located at the same level with an antenna. In the option, presented in Fig. 18a the horizontal directional pattern is close to circular one (see Fig. 19). In the options, presented in Fig. 18b and 18c it resembles the directional pattern of an active radiator located next to a passive one. The directional pattern of the antenna in the vertical plane changes significantly when moving it from the ship's deck to the beam-cross and resembles

the directional pattern of an antenna mounted on a pillar, whose height is close to a mast height. In this case, the radiation into the side of the mast is usually greater than to the opposite one. The second lobe of the vertical directional pattern becomes dominant already at a frequency 20 MHz. The currents excited in a horizontal beam-cross create the radiation to zenith' direction. The input characteristics of such an antenna are very different from the input characteristics of an antenna located on a perfectly conducting plane. The *TWR* level decreases, the first series resonance shifts toward low frequencies. Generally, the characteristics of antenna mounted on the beam-cross are significantly worse than the characteristics of antenna located on the deck.

Experimental verification was carried out on models. The results are given in Fig. 19. The coincidence of the calculated data with the experiment confirms the effectiveness of the used analysis method. Details of the calculations were published in [9] and transferred to the designers for use in further work.

The developed programs saved performers from the need to idealize the shape of a superstructure replacing it with an ellipsoid or an infinitely long cylinder, and neglecting segments and radii, which were small compared with the wavelength, antenna length and the superstructure height. Analysis of the characteristics of HF antenna located on the pillar, bracket and beam-cross allowed to determine the degree of distortion of the antenna's characteristics depending on the geometric dimensions of these structures. In particular, the inadmissibility of installing antennas on the beam-cross was demonstrated.

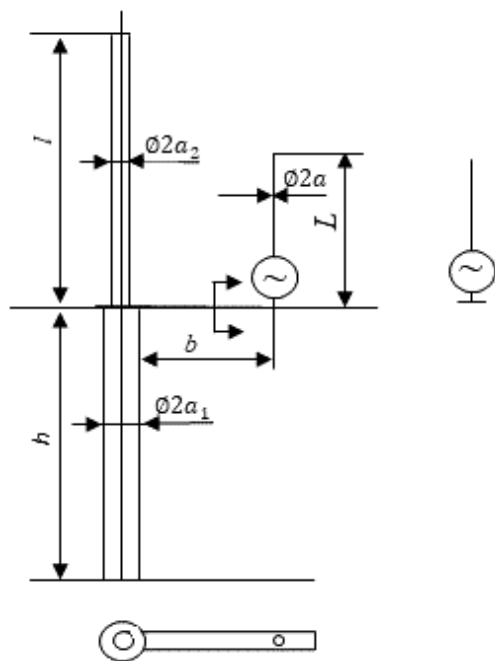


Fig. 17: Whip antenna on a cross-beam.

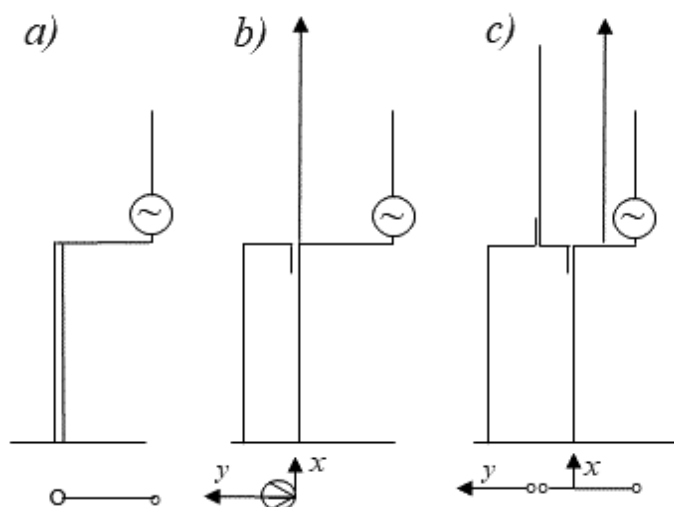


Fig. 18: Wire structures for calculating characteristics of antennas mounted on a cross-beam.

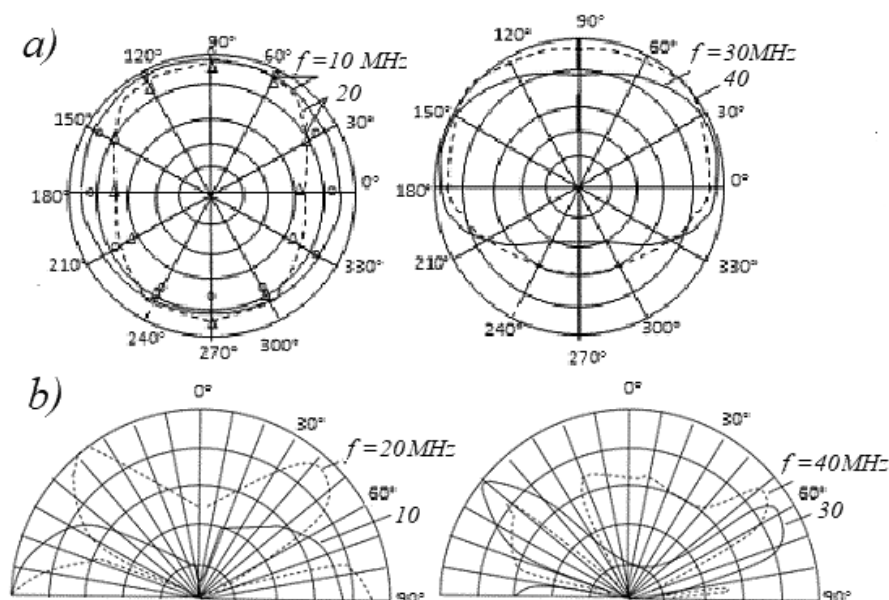
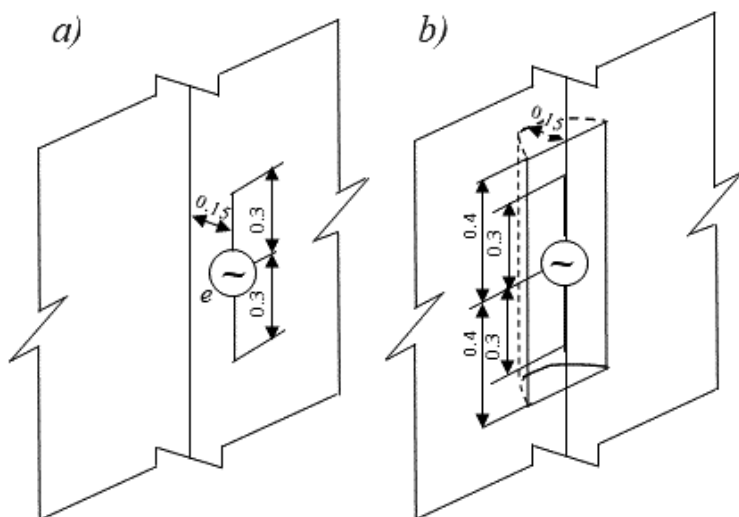


Fig. 19: Directional pattern of antenna located on a beam-cross in a horizontal plane.

To conclude this section, we present the results of the characteristics analysis of one more antenna—a symmetric radiator placed in a metal trough, which is located on a flat metal surface [12]. The task of calculating the electrical characteristics of a symmetric radiator near such a surface (Fig. 20a) is solved quite simply. But this task becomes much more complicated if the radiator is in a metal trough of finite length flush with a metal body (Fig. 20b) on the surface of a ship or an aircraft. We assume





**Fig. 20:** Symmetric radiator near a flat metal surface (a) and near this surface with a trough (b).

that the trough has the shape of a half cylinder with flat metal butt-ends. The axis of a radiator coincides with the axis of a trough. Another variant of the same problem is the problem of a radiator placed in a dielectric capsule floating along a sea surface.

When solving the problem of a radiator near a perfectly conducting surface this surface in accordance with the method of mirror images commonly is replaced by a second radiator located behind it at the same distance and having the same geometrical dimensions, but with an oppositely directed exciting emf (Fig. 21a). For the radiator in a trough near the flat surface this method is not very productive.

In this case, an analysis method, in which the metal surface is replaced by a system of thin wires [3, 5] is useful. In such a formulation, as already said, the problem is reduced to calculating the current distribution in a wire structure consisting of randomly oriented wire segments. Knowing the currents along the wires, we can calculate all electrical characteristics of the radiator.

While replacing a metal surface with a wire structure, as shown earlier, the correct choice of the number of wires and their location is of great importance. Increasing the number of wires and their lengths leads to increase in the calculation time (approximately proportional to a square of the number of short radiators, into which the wires are divided). An excessive increase in the number of these radiators as already said can worsen the result. An insufficient number of wires and short radiators also give a large error. The wires of a structure should be placed along the probable directions of currents propagation. This allows us to reduce a wires number and to minimize the amount of computation.

For example, calculations show that the directional pattern of a whip antenna near a wire structure equivalent to a cylindrical superstructure practically does not change in real variants of a mutual location of an antenna and a superstructure, if the wire structure is supplemented with horizontal wires. Other antenna characteristics: input impedance, directivity—also change slightly. All these characteristics with an

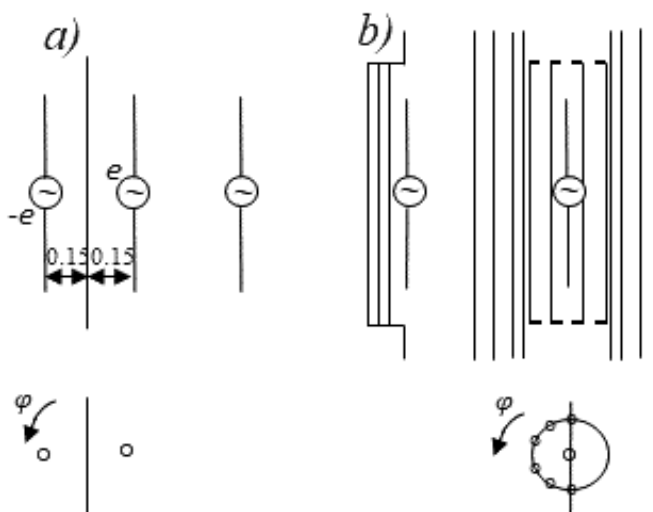


**Fig. 21:** Equivalent wire structure for a radiator near a flat metal surface (a) and near this surface with a trough (b).

addition of horizontal wires change only, if a distance between an antenna and a superstructure is small. But in practice, these options do not use, since in this case the antenna loses the properties of the radiator.

To analyze the electrical characteristics of the vertical radiator located along an axis of the cylindrical trough, it is expedient to use the wires' system shown in Fig. 21b. As can be seen from the figure, the trough is replaced by the wires located along the cylinder generatrices and the radii of its ends. These wires are continued in a vertical direction up and down at a distance equal to a quarter of a wavelength. The lengths of arcs between adjacent wires forming a cylindrical surface are taken equal to  $0.04\lambda$ . Outside a trough, the gaps between wires are also the same. Each half-plane on both sides of a trough is replaced by a structure of three vertical wires spaced from a trough edge by  $0.08\lambda$ ,  $0.16\lambda$  and  $0.24\lambda$ . These wires are also extended beyond the upper and lower ends of trough by  $0.25\lambda$ . Specific elements of a structure were taken in accordance with the assumption confirmed by calculations that the elements closest to the radiator have the greatest influence on its characteristics. These areas must be carefully modeled.

The described structure was used to calculating the electrical characteristics of a symmetrical vertical radiator with an arm length 0.3 m, located along an axis of a cylindrical trough with a length 0.8 m and a radius 0.15 m. The calculations were performed at frequencies from 150 to 600 MHz, which corresponds to a radiator with an arm length from  $0.15\lambda$  to  $0.6\lambda$ . The radius of a radiator is 0.005 m. The radii of other wires of structure for the simplicity are taken of the same magnitude.

The horizontal directional patterns, calculated by the described method for a radiator located along an axis of a trough, are presented in Fig. 22a-c. For comparison, in Fig. 22d similar directional patterns are given for the same radiator located near a flat metal surface at a distance, equal to the trough depth (at a distance  $0.15\lambda$  from it). According to the calculations, the backward radiation (in the directions to

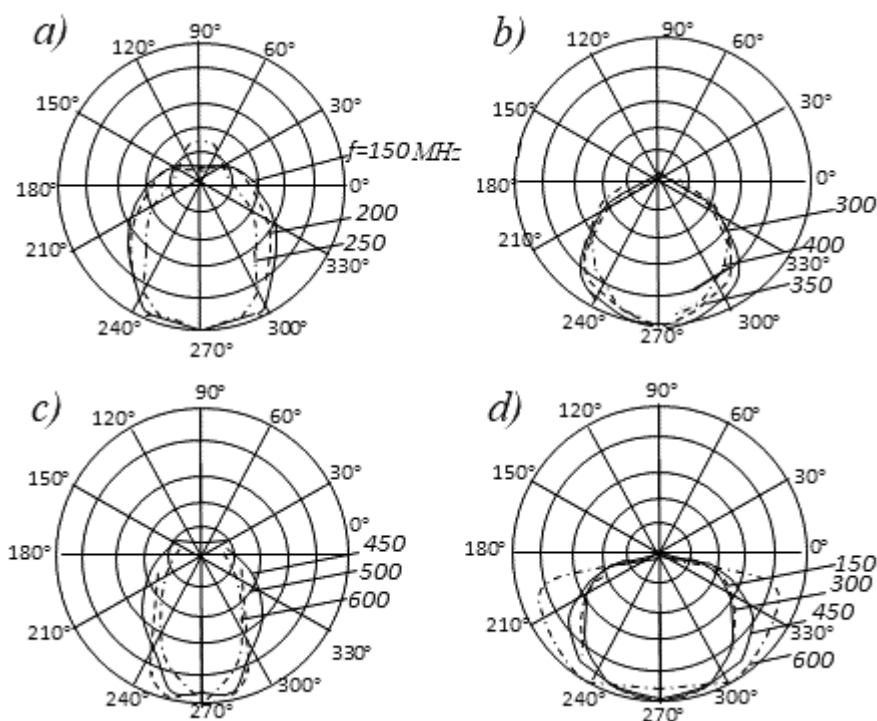


**Fig. 22:** Horizontal directional patterns of a symmetrical vertical radiator near the surface with a trough (a – c) and the flat surface (d).

a trough) is small, indicating a good approximation of a metal surface by means of a wire structure.

At the same time, the difference between the directional patterns of the radiators located near the flat surface and the surface with a trough is clearly visible from the figure. In the case of the trough the horizontal directional pattern has a narrower lobe.

The directional patterns of both radiators in a vertical plane perpendicular to a metal surface are shown in Fig. 23. From theirs it follows that the presence of a trough reduces the electric length of the radiator, because the second lobe appears at a higher frequency. At the same time, the difference between the influence of a flat surface and a surface with a trough is clearly visible from the figure. In the case of the trough the vertical directional pattern also has a narrower lobe.

This conclusion is confirmed by the results of calculating the directivity of both radiators given in Table 3. The directivity of a radiator near a flat surface varies slightly in the frequency range. The directivity of a radiator placed near a surface with a trough increases with increasing frequency. At frequencies from 300 MHz and higher (with an arm length greater than  $0.25\lambda$ ) its directivity significantly exceeds the directivity of another radiator.

A similar conclusion can be made by comparing the input impedances of the radiators (Fig. 24). Curves 1 correspond to a radiator located at the surface with a trough, curves 2—to a radiator near a plane. It is seen that the second resonance of

**Table 3:** Directivity of Radiator.

$f$ , MHz	150	200	250	300	350	400	450	500	550	600
Radiator in metal trough	6.3	6.9	5.8	8.9	10.4	11.4	12.4	13.4	14.8	17.4
Radiator near metal plane	7.4	7.3	7.3	7.4	7.5	7.6	7.9	8.1	8.3	8.4

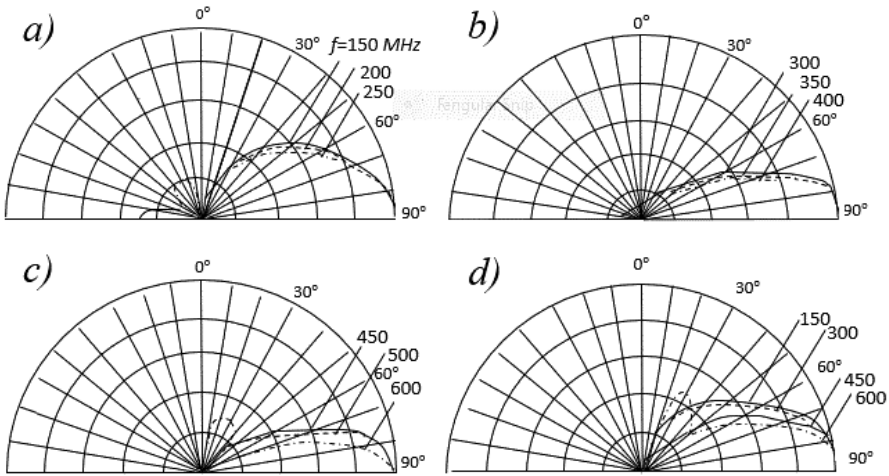


**Fig. 23:** Vertical directional patterns of a symmetrical vertical radiator near the surface with a trough (a-c) and the flat surface (d).

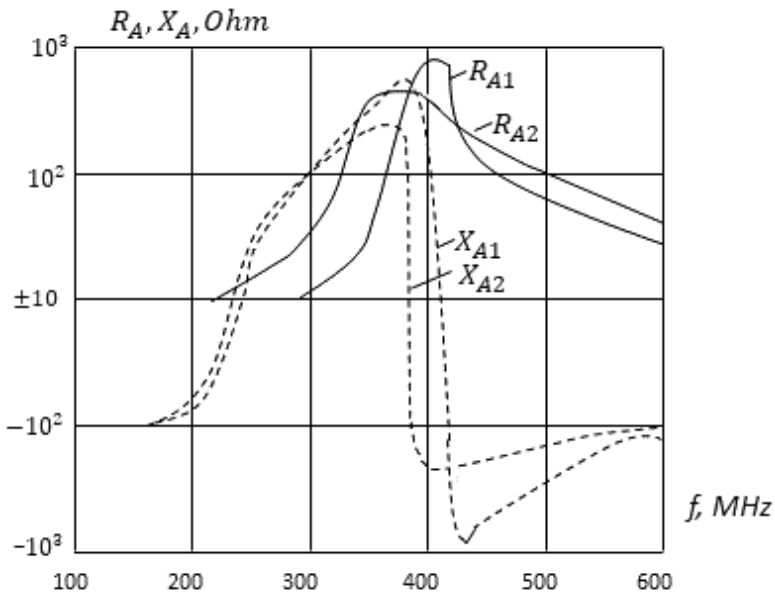


**Fig. 24:** Input impedances of a symmetrical vertical radiator near the surface with a trough (1) and the flat surface (2).

the radiator in a trough is located at a higher frequency. The resistance of this radiator is significantly reduced except for the area of a parallel resonance.

#### 4. Method of Complex Potential

The generalized method of induced emf has played an important role in solving problems of an antenna technology. The use of the complex potential method for solving electrostatic problems was not less important.

The problem of calculating an electrostatic field is reduced to a determination of a field strength at all points in accordance with electric charges of conducting bodies. This problem is completely solved, if to find the potential as a function of coordinates. When the potentials in the points are known, in the case of two conducting bodies one can find a capacity between them (as the ratio of the charge of each body to difference of their potentials). In a system of few conducting bodies one can determine self and mutual potential coefficients and after that the partial capacitances.

If any problem of calculating an electrostatic field of charged conducting bodies located in homogeneous and isotropic dielectric is solved, this solution can be used for a solution of other problems. For example, the method of an electrostatic analogy allows to find constant electric fields and currents in a homogeneous weakly conducting medium, if a shape and geometrical dimensions of bodies with a high conductivity, placed in this medium, coincide with a shape and dimensions of bodies, located in a dielectric. The principle of correspondence allows building a picture of magnetic field created by constant linear currents on the base of a picture of electric field created by linear charges, if currents and charges are identically distributed in a space. The only difference between these structures consists in a fact that lines of equal magnetic potential are located on a place of electric field lines and magnetic field lines are located on a place of lines of equal electric potential [13].

Electrostatic problem considers usually a system of charged conducting bodies surrounded with a dielectric, in which volumetric charges are absent. There is only the information about the potential  $U_n$  of each body  $n$  or the information about the total charges  $q_n$  of all bodies. A potential distribution in a space is unknown. A charge distribution along surface of each body is also unknown. This is the main difficulty of a problem, especially in the case of inhomogeneous medium. It is presented either as potential  $U_n$  of each body  $n$  or as total charges  $q_n$  of all bodies. A potential distribution in a space is unknown. A charge distribution along surface of each body is also unknown. It is the main difficulty of a problem, especially in the case of inhomogeneous medium.

The electrostatic field is a stationary force field, i.e., it does not change over time. The sources of the field are electric charges, the location of which in space does not change. The free charge is distributed over the conductor surface. The electric field is created between two charges located in a homogeneous isotropic medium, and as a result an interaction force arises (in accordance with Coulomb's law). The electric field is characterized by the vector of field intensity  $\vec{E}$ . If the field is defined at all points, then a family of curve lines can be drawn in such a way that the direction of the tangent to the curve line at each point coincides with the direction

of the vector  $\vec{E}$ . These lines are called the field lines or the lines of the field intensity. In accordance with what has been said, the vector of field line element is equal to  $d\vec{l} = \lambda \vec{E}$ , where  $\lambda$  is a scalar factor. The rectangular components of the element  $d\vec{l}$  are equal to  $dx = \lambda E_x$ ,  $dy = \lambda E_y$ ,  $dz = \lambda E_z$ . From here we get the equation of the field line

$$dx/E_x = dy/E_y = dz/E_z.$$

The circulation of the vector  $\vec{E}$  of the electrostatic field along an arbitrary closed path  $C$  is equal to zero:

$$\oint_C \vec{E} \cdot d\vec{l} = 0.$$

This means that in an electrostatic field the work of an electric force along a closed path is zero, i.e., the integral  $U(A) = \oint_A^P \vec{E} \cdot d\vec{l}$  does not depend on the integration path. The function  $U(A)$  is called by the potential of the electric field at point  $A$  relative to point  $P$ , the potential of which is equal to zero. The point at infinity is usually chosen as the zero potential point.

The potential of the electric field in the point  $A$  relative to a point  $P$  is numerically equal to the work that must be expended to remove a negative electric charge, which is equal to unit, from point  $A$  into infinity. If the distance from some initial point  $O$  to points  $A$  and  $P$  is denoted by  $l$  and  $l_p$ , then for the potential of point  $A$  we can write

$$U(x, y, z) = \int_l^{l_p} \vec{E} \cdot d\vec{l} = \int_l^{l_p} E \cos \alpha \, dl.$$

Differentiating this potential with respect to the lower limit, we obtain

$$\partial U / \partial l = -E \cos \alpha.$$

Choosing the movement direction in accordance with one of the coordinate axes and considering that  $\alpha$  is the angle between the direction of the vector  $\vec{E}$  and the direction of movement, we find

$$\partial U / \partial x = -E_x, \quad \partial U / \partial y = -E_y, \quad \partial U / \partial z = -E_z,$$

where  $E_x$ ,  $E_y$ ,  $E_z$  are the projections of the vector  $\vec{E}$  onto the coordinate axes. If to choose  $\alpha = \pi/2$ , assuming that the direction of movement is perpendicular to the lines of force, then  $\frac{\partial U}{\partial l} = 0$  and  $U = \text{const}$ . Thus, when moving over a surface, to which the field lines are orthogonal, the potential remains constant. Such a surface is called a surface of equal potential (equipotential one). For  $\alpha = 0$ , i.e., when movement coincides with the direction of the field lines, the potential changes to the maximum extent:  $\frac{\partial U}{\partial l} = -E$ . Its change is characterized by the vector *rad*  $U$ , whose projections are equal to  $\partial U / \partial x$ ,  $\partial U / \partial y$ ,  $\partial U / \partial z$ .

The pages that you read from the beginning of Section 4 were necessary to explain the basic idea behind the complex potential method. These pages based on the first pages of the book [13] and partly uses its text.

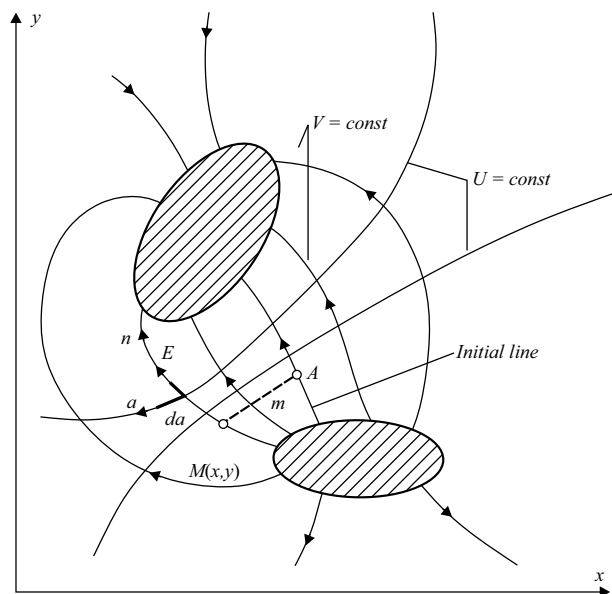


**Fig. 25:** Plane-parallel field of two wires.

The problem of calculating an electric field of charged bodies gets simplified, if the all magnitudes characterizing the field depend only on two coordinates. The field of several infinitely long and parallel to each other cylindrical wires with the charges uniformly distributed along their length (the plane-parallel field) conforms to such condition. In this case the all lines of a field and lines of an equal potential lie in the planes of wires cross-sections, and the field picture is the same in all such planes. If the axis  $z$  of a rectangular coordinates system is parallel to wires axes, the potential  $U$  of a plane-parallel field is a function of only two coordinates,  $x$  and  $y$ .

The cross-sections of two wires and the picture of a field around them, including lines of an equal potential and lines of a field, are represented in Fig. 25. The surfaces of an equal potential are the cylindrical surfaces with generatrix, parallel to an axis  $z$ . The lines of an equal potential in a plane  $xOy$  are defined by equations of the type

$$U(x, y) = \text{const.} \quad (5.12)$$

Let some field line is regarded in the capacity of initial line. If we shall connect an arbitrary point  $M(x, y)$  with any point  $A$  of an initial line, we obtain the curvilinear segment  $MmA$ . Let this segment move parallel to itself in the direction of axis  $z$  and pass the distance  $l$ . At that the function

$$V(x, y) = \Psi_E / l$$

represents the flow of an electrical field  $\vec{E}$  per unit length of wires through the sector traversed by this segment. That function is named by flow function. The magnitude

$V(x,y)$  has the same magnitude for all points located along the same line of field. And so, the equation

$$V(x, y) = \text{const}, \quad (5.13)$$

which defines aggregate of such points, is named by the equation of the field strength line.

Mark that those equations (5.12) and (5.13) define two families of curves intersecting at the right angle. Let  $dn$  is an element of the field line and  $da$  is an element of a line of equal potential, i.e., they are mutually perpendicular. We assume that coordinates  $n$  and  $a$  grow in directions shown in Fig. 25. The potential  $U$  increases in direction opposite to the vector  $\vec{E}$ , i.e., in the direction of decreasing the coordinate  $n$ . It is considered customary that the flow function increases in the same direction, in which  $a$  increases. Under these conditions the electric field strength may be expressed in terms of  $U$  and  $V$  in the form

$$E = -\frac{\partial U}{\partial n} = \frac{\partial V}{\partial a},$$

or, in cartesian coordinates,

$$E_x = -\frac{\partial U}{\partial x} = \frac{\partial V}{\partial y}, E_y = -\frac{\partial U}{\partial y} = -\frac{\partial V}{\partial x}, \quad (5.14)$$

from whence after repeat differentiation, it is easy to be convinced that both functions  $U$  and  $V$  satisfy the Laplace's equation

$$\frac{\partial^2 U}{\partial x^2} + \frac{\partial^2 U}{\partial y^2} + \frac{\partial^2 U}{\partial z^2} = 0. \quad (5.15)$$

If a distribution of charges is known, then in a homogeneous medium with permittivity  $\varepsilon$  one can find the potential  $U$ , which is defined by all charges located in a finite volume  $v$  of a space from the expression

$$U = \frac{1}{4\pi\varepsilon} \int_{(v)}^{\square} \frac{\rho_v}{r} dv$$

where  $\rho_v$  is a volume density of a charge,  $r$  is a distance from an observation point to an integration point (point of charge location). This integral is solution of Poisson equation.

If a distribution of charges is unknown, then one must ascertain the necessary and sufficient requirements, under execution of which a field is determined by only one way (uniqueness theorem). It is the following requirements. Firstly, in the case of a homogeneous medium, since charges in it are absent, a field must satisfy the Laplace's equation, i.e., in a rectangular coordinates system  $(x, y, z)$  the expression (5.15) must be valid. Secondly, the surfaces of conducting bodies must be by surfaces



of equal potential, i.e., on each surface  $U = Um = \text{const}$ . Thirdly, if total charges  $q_m$  of bodies are given, then for each body the condition must be fulfilled

$$q_m = - \int_{(S_m)}^{\square} \varepsilon \frac{\partial V}{\partial n} dS,$$

where  $S_m$  is the surface of body  $m$ ,  $n$  is the normal to that surface.

We shall regard a cross-section's plane of a plane-parallel electrostatic field as a plane of the complex variable  $z = x + jy$ . Regular analytic function  $\zeta(z) = \zeta(x, y) + j\eta(x, y)$  of complex variable  $z$  in accordance with the Cauchy-Riemann conditions satisfies the following relations

$$\partial\eta/\partial x = -\partial\zeta/\partial y, \quad \partial\eta/\partial y = \partial\zeta/\partial x. \quad (5.16)$$

It is easy to verify that conditions (5.14) coincide with conditions (5.16), i.e., the function

$$\zeta(z) = V(x, y) + jU(x, y), \quad (5.17)$$

the active and reactive components of which are equal to the values  $V(x, y)$  and  $jU(x, y)$  respectively, is a regular analytical function of the complex variable  $z$  in some area. This function is called the complex potential of a plane-parallel field and, in accordance with what has been said, satisfies Laplace's equation and the first requirement of the uniqueness theorem. This means that the problem of a field calculation is solved, if the function  $\zeta(z)$ , satisfying the boundary conditions at the wires surface, is found. Laplace's equation is valid in different systems of coordinates.

The complex potential method has become a reliable assistant for engineers in calculating capacitances of complex shapes. As is said, the detailed description of this method and examples of its application to problems of parallel cylindrical wires located in a homogeneous medium are given in [13]. There it is shown that the complex potential of a solitary wire with a circular cross-section and with the charge  $\tau$  per unit length located in the homogeneous medium with permittivity  $\varepsilon$  has the form

$$\zeta(z) = -j \frac{\tau}{2\pi\varepsilon} \ln z + C, \quad (5.18)$$

where  $C = C_1 + jC_2$  is the constant magnitude, whose coefficients  $C_1$  and  $C_2$  depend on the selecting an initial field line and a line of zero potential.

The complex potential of the line consisting of two wires, which are located at the distance  $2b$  from each other and have the linear charge densities accordingly  $\tau$  and  $-\tau$ , is equal to

$$\zeta(z) = -j \frac{\tau}{2\pi\varepsilon} \ln \frac{z+b}{z-b} + C. \quad (5.19)$$

In the following sections of a Chapter the method of complex potential is generalized, firstly, to piecewise homogeneous media and, secondly, to three-dimensional structures.

## 5. Piecewise Homogeneous Media

The problem of a field calculation becomes complicated in the case of the heterogeneous (in particular, piecewise-homogeneous) medium adjacent to a wire [14]. Such a problem arises, if the solitary wire is located at the boundary of two media, for example, air and dielectric, and the relative permittivity  $\varepsilon_r$  of dielectric is different from 1 (Fig. 26). The wire cross-section is considered a circle.

It should be noted first of all that the potential at a wire surface is constant. The potential of infinitely distant point may not be equal to zero, since in that case the potential of infinitely long wires at a finite distance will be infinitely great. Nevertheless, it is obvious that at a great enough distance from charged wire, the potential in the all directions is the same. And therefore, supposition that the lines of equal potential are circumferences with the center in the origin of coordinates and that the surfaces of equal potential are the surfaces of the circular cylinders are natural.

The wire surface may be replaced by a system of  $N$  equidistant filaments with charge linear densities  $\tau_n$  ( $n$  is a filament number), the sum of which is equal to  $\tau$  (to the linear density of wire charge). The potential of each filament at the distance  $r$  from its axis is

$$U_n = -(\tau_n / (2\pi\varepsilon_n)) \ln (r/r_p).$$

Here  $\varepsilon_n$  is the permittivity of a medium around a filament,  $r_p$  is the distance to a surface of zero potential. To the potentials of all filaments may be identical on a surface of circular cylinder with a radius  $\rho = r + a$ , where  $a$  is a wire radius, the ratio  $\tau_n/\varepsilon_n$  must be the same for each  $n$ :

$$\tau_n/\varepsilon_n = \text{const}(n), \quad (5.20)$$

i.e., the surface density of wire charge must be proportional to the permittivity of a medium adjacent to a given part of this surface. Here the word 'adjacent' signifies

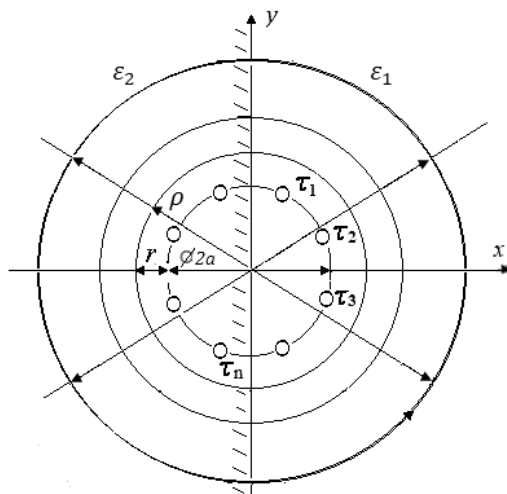


Fig. 26: Field of a wire located on the boundary of two media.

that the medium occupies volume from a wire surface to infinity within an angle equal to the arc length along the surface, adjacent to this medium.

Expression (5.18) for a field structure of the solitary wire with the circular cross-section, located in homogeneous medium, may be written in a shape of more general expression:

$$\zeta(z) = jA \ln z + C, \quad (5.21)$$

where  $A$  is a constant magnitude. Using designation  $z = \rho e^{j\varphi}$ , we obtain:

$$\zeta(z) = V(z) + jU(z), \quad V(z) = -A\varphi + C_1, \quad U(z) = A \ln \rho + C_2, \quad (5.22)$$

from whence the equations for the field lines and for the lines of equal potential accordingly take the view:

$$\varphi = \text{const}, \quad \rho = \text{const}.$$

The field structure of a wire located at a boundary of two media has a similar character. As it was indicated earlier, here the lines of equal potential are circumferences with  $\rho = \text{const}$ . Therefore, for the complex potential of such field we shall use an expression (5.21). The constant  $A$  in this expression is determined in accordance with the fact that in going around a wire cross-section along the closed contour the angle  $\varphi$  increases by  $2\pi$ , and the function  $V$  increases by  $\Psi_E/l$ , where  $\Psi_E$  is the flow of the vector  $\vec{E}$  through the cylindrical surface covering the wire segment of length  $l$ . In the case of the heterogeneous media, it is expedient to replace  $\Psi_E$  by  $\Psi_D$ , i.e., to replace the flow of vector  $\vec{E}$  by the flow of vector  $\vec{D}$ , where  $\vec{D}$  is the vector of electrical displacement. Besides, one must consider that the density of this flow in the different media may be diverse, i.e.,

$$\Delta V = \frac{1}{l} \sum_i \Psi_{D_i} / \epsilon_i, \quad (5.23)$$

where  $i$  is the number of a medium. If  $\rho_v$  is a volume density of a wire charge, then integration of Maxwell equation

$$\text{div} \vec{D} = \rho_v \quad (5.24)$$

with respect to wire volume  $v$  gives for left part of equation

$$\int_{(V)} \text{div} \vec{D} dv = \oint_{(S)} \vec{D} d\vec{S} = \sum_i \oint_{S_i} \vec{D} dS_i,$$

for the right part

$$\int_{(V)} \rho_v dv = \sum_i \int_{S_i} \sigma_i dS.$$

Here  $S$  is the wire surface,  $S_i$  is the area of this surface adjacent to  $i$ -medium,  $\sigma_i$  is a density of a surface charge on this area. Equating both sides of the equation, we find

$$\sum_i \Psi_{Di} = \sum_i q_i, \quad (5.25)$$

i.e., the flow  $\Psi_{Di}$  of the displacement vector through the wire surface into  $i$ -medium is equal to the charge  $q_i$  per unit length of the surface area adjacent to this medium. In accordance with (5.23)

$$\Delta V = \frac{1}{l} \sum_i q_i / \varepsilon_i, \quad (5.26)$$

If to introduce such a quantity  $\varepsilon_i$

$$\sum_i q_i / \varepsilon_i = q / \varepsilon_e, \quad (5.27)$$

where  $q$  is the total wire charge per unit of its length, then as seen from (5.25), the quantity  $\varepsilon_e$  has meaning of the equivalent permittivity for the heterogeneous medium. In accordance with (5.19), if  $\Delta\varphi_i$  is the arc length of the wire circumference, which is adjacent to  $i$ -medium, then the equality

$$q_i / (\varepsilon_i \Delta\varphi_i) = \text{const}(i) \quad (5.28)$$

is correct. It is obvious also that

$$\sum_i q_i = q. \quad (5.29)$$

It is easy to show by using (5.26) and (5.27) that

$$q_i = q \varepsilon_i \Delta\varphi_i / (\sum_i \varepsilon_i \Delta\varphi_i), \quad (5.30)$$

whence

$$\varepsilon_e = \frac{q}{\sum_i q_i / \varepsilon_i} = \frac{1}{2\pi} \sum_i \varepsilon_i \Delta\varphi_i. \quad (5.31)$$

If  $N$  media with the same angle width are adjacent to the wire, then

$$\varepsilon_e = \frac{1}{N} \sum_{i=1}^N \varepsilon_i. \quad (5.32)$$

For variant, depicted in Fig. 26,  $N=2$ , and the equivalent permittivity is equal to the half sum of magnitudes  $\varepsilon_1$  and  $\varepsilon_2$ :

$$\varepsilon_e = (\varepsilon_1 + \varepsilon_2) / 2. \quad (5.33)$$

Substituting (5.25) into (5.24) and using that according to (5.21) in going around the cross-section of wire the function  $V$  increases by  $\Delta V = -2\pi A$ , we obtain

$$A = -\tau / (2\pi \varepsilon_e), \quad (5.34)$$

and consequently

$$V = \tau\varphi/(2\pi\epsilon_e) + C_1, \quad U = -\tau \ln \rho/(2\pi\epsilon_e) + C_2. \quad (5.35)$$

It is necessary to note that only the magnitude  $\epsilon_e$  is included in the expressions (5.35). This means that in this case, as in the case of homogeneous medium, the angles between field lines are equal (irrespective of the medium, in which they are located), if an increase of a flow of a vector  $\vec{E}$  at the transition from one line of a field intensity to other line is identical. If increase of potential between neighbors' lines of the equal potential also is the same, the radii of the circumferences of an equal potential change according to geometric progression. It should also be noted that the method used for calculating the equivalent permittivity of an inhomogeneous medium adjacent to a wire is based on Maxwell's equations, i.e., is strict, in contrast to the method described in the known book, which is based on arbitrarily used concept of fringing.

Consider, using the obtained results, the important practical case of two-wire line (Fig. 27). In the beginning we shall assume that the wires are infinitely thin. The expression (5.19) for the complex potential of the field of such a line located in a homogenous medium may be written in the form

$$\zeta(z) = jA \ln \frac{z+b}{z-b} + C. \quad (5.36)$$

Introducing the notations  $z+b = \rho_1 \exp(j\varphi_1)$ ,  $z-b = \rho_2 \exp(j\varphi_2)$ , where  $\rho_1$  and  $\rho_2$  are the lengths of segments connecting the observation point M to the wires axes, and  $\varphi_1$  and  $\varphi_2$  are the angles between these segments and  $x$ -axis, we obtain

$$V = A(\varphi_2 - \varphi_1), \quad U = A \ln(\rho_1/\rho_2). \quad (5.37)$$

Here it is accepted that  $C=0$ . In this case the line of zero potential coincides with the ordinate axis, and the initial line of a field intensity consists from the segments of abscissa axis located from the wires of two-wire long line to infinity. The lines of equal potential are the circumferences with the centers coinciding with the axes of the long line's wires. The field lines are the circumferences, which passes through the wires' axes; the centers of these circumferences coincide with the coordinates' origin.

Let a circular dielectric cylinder of radius  $b$  is placed between the wires of a line, and its axis is parallel to the wires and is located at the same distances from both wires. The boundary of a dielectric cylinder (the circumference) is shown by a thick line, it coincides with the line of field. The lines of equal potential intersect it at the right angle. It means that the dielectric cylinder does not change the field structure. As in the case of the solitary wire, to the potential near the wire may be the same in the air and in the dielectric medium, the surface density of charge must be proportional to the permittivity of the medium, adjacent to a given part of wire. So, the magnitude  $A$  in the expressions (5.36) – (5.37) is defined by the equality (5.34), and the equivalent permittivity is defined by the expression (5.33).

If the wires of the real transmission line are not infinitely thin, but have the circular cross-sections of finite radius, then always one can place the axes of wires so



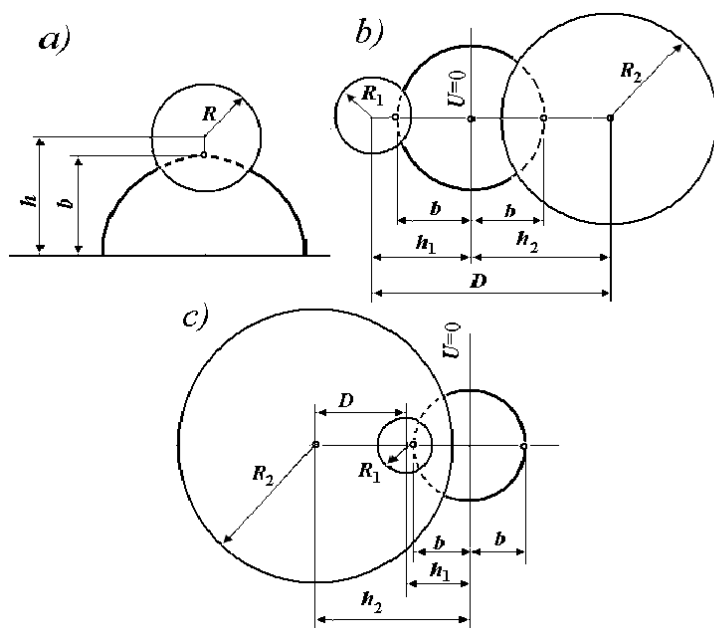


**Fig. 28:** The two-wire lines in the shape of a cylinder over the metal plane (a) and of two cylinders with different axes, which do not encompass (b) and encompass (c) one another.

where  $R_1$  and  $R_2$  are the cylinders radii, and  $D$  is the distance between their axes. At last, for the variant depicted in Fig. 28c

$$h_1 = \frac{1}{2D} (R_2^2 - D^2 - R_1^2), \quad b = \sqrt{h_1^2 - R_1^2}.$$

The capacitances of the solitary wire and of the two-wire transmission line are proportional to the permittivity of medium. In the case of the heterogeneous medium consisting of homogeneous layers the magnitude must be replaced by an equivalent permittivity—in accordance with above-presented expressions. In particular, if the solitary wire is located at a boundary of two media (see Fig. 26), the equivalent permittivity is equal to arithmetic average of the magnitudes  $\varepsilon_1$  and  $\varepsilon_2$ . This conclusion conforms completely to the known thesis, in accordance with which the capacitance between two conductors located symmetrically relative to a plane boundary of two media with the permittivity  $\varepsilon_1$  and  $\varepsilon_2$  is equal to half-sum of the capacitance values between the same conductors in homogeneous media with permittivity  $\varepsilon_1$  and  $\varepsilon_2$  accordingly [15]. If the wire is solitary, the metal cylinder of infinite radius, axis of which coincides with the wire axis, may be accepted as the second conductor.

If the boundary of two media goes along a broken line, whose point of sharp bend coincides with the wire center (this boundary is shown by dotted line in Fig. 26), then in accordance with (5.31)

$$\varepsilon_e = \frac{1}{2\pi} (\varepsilon_1 \Delta\varphi_1 + \varepsilon_2 \Delta\varphi_2).$$

If a few media, the boundaries of which coincide with radial surfaces, are adjacent to the solitary wire, then in the case of equal arc length of surface sections, which are adjacent to these media, the equivalent permittivity is determined by the expression (5.44), and at the different arc length it is determined by the expression (5.31). This conclusion coincides with results obtained in [16, 17]. In [16] it is shown that electrostatic field of the wires system of an arbitrary shape located in a piecewise-homogenous medium coincides with a field in a homogenous medium, if the media boundaries coincide with the surfaces of wires and the surfaces of the equal fields in the homogenous medium (this condition is called the condition of invariance). Accordingly, in [17] the following expression for a capacitance between the wires located in a piecewise-homogenous medium was obtained:

$$C = \sum_{i=1}^N \frac{\varepsilon_i}{\varepsilon_0} C_{i0}.$$

Here  $C_{i0}$  is the capacitance between the wire segments adjacent to medium  $i$ , if the wires are in a homogeneous medium with permittivity  $\varepsilon_0$ .

It is obvious that the condition of invariance is performed in the case when the boundaries of a media adjacent to the solitary wire coincide with radial surfaces. From this expression for  $C$ , it is easy to obtain (5.31) and (5.32), if to use as the second wire the metal cylinder of infinite radius, coaxial with the solitary wire. For the line of two infinitely thin wires located along generatrices of the circular dielectric cylinder the condition of invariance is performed also. Since the angular width of both media adjacent to each wire is equal to  $\Delta\varphi_1 = \Delta\varphi_2 = \pi$ , then  $C_{10} = C_{20}$ , i.e., the magnitude  $\varepsilon_e$  is also determined by the equality (5.33). This proposition stays true, if the thin wires are located along arbitrary selected generatrices, the length of arc between which is not equal to  $\pi$ .

If between the wires a thin dielectric insert bounded by two arcs of two circumferences is located, and the centers of arcs lie on the axis  $y$  in the points  $y = \pm d$  (in Fig. 27 the insert boundaries are shown by the dotted lines), then in accordance with (5.31)

$$\varepsilon_e = \varepsilon_1 + (\varepsilon_2 - \varepsilon_1)\alpha/\pi,$$

Here  $\varepsilon_1$  is the air permittivity,  $\varepsilon_2$  is the dielectric permittivity of an insert,  $2\alpha$  is an angle between arcs.

The capacitance between the metal cylinders per unit length (see Fig. 28) is

$$C = \frac{2\pi\varepsilon_e}{\ln \left\{ \left[ \frac{h_1}{R_1} + \sqrt{\left( \frac{h_1}{R_1} \right)^2 - 1} \right] \left[ \frac{h_2}{R_2} \pm \sqrt{\left( \frac{h_2}{R_2} \right)^2 - 1} \right] \right\}},$$

where sign plus in the second square bracket is taken, when one must calculate the capacitance between cylinders depicted in Fig. 28b, and sign minus corresponds to Fig. 28c. For two cylinders of the same radius ( $R_1 = R_2 = R$ )

$$C = \pi\varepsilon/\ln [h/R + \sqrt{(h/R)^2 - 1}] = \pi(\varepsilon_1 + \varepsilon_2)/2 \cosh^{-1}h/R.$$



This result coincides with the expression, which one may obtain from presented in [15] expression (8-7) for the linear capacitance of two-wire long line located in the dielectric near the cylindrical interface of two media, if the distance between the axis of each wire and the interface is a small magnitude of the order of the wire radius. One must note that these expressions are true at the arbitrary location of the charged filaments (of the equivalent linear wires) along the cylindrical interface of two media, i.e., at any arc length between filaments (not only at arc length  $\pi$ ). For the circular cylinder located over a metal plane (see Fig. 28a)

$$C = 2\pi\epsilon_e / \ln [h/R + \sqrt{(h/R)^2 - 1}].$$

At that, if  $h/R \gg 1$ ,

$$C = 2\pi\epsilon_e / \ln 2(h/R),$$

that coincides with the expression, which one may obtain from presented in [15] expression (8-8) for the two-wire line with isolation of the belt type.

The issues of applying the complex potential's method to the calculation of capacitances, for example in heterogeneous environments, are considered in the Chapter 6.

## 6. Characteristics of Directivity of Antennas Arrays

As shown in Section 1.1, if the sources of electromagnetic field are distributed continuously in some volume  $V$ , and a medium surrounding volume  $V$  is a homogeneous isotropic dielectric, the solution of equation (1.9) for the vector potential  $A$  of a harmonic field is given by the expression (1.12), where  $G = \exp(-jkR)/(4\pi R)$  is the Green's function and  $R$  is the distance from an integration point to an observation point located in a far region. If all radiators inside a volume have the same direction, then

$$A_p = \frac{A_p(0)}{j_p(0)} \iiint_{(V)} j_p \exp(jkz \cos \theta) dV,$$

where  $A_p(0)dV$  is the vector-potential of a field, created by an elementary volume with current density  $j_p(0)$  located at the coordinate origin. If  $E_p(0)dV$  is a field of this volume, then the total field is

$$E_p = \frac{E_p(0)}{j_p(0)} \iiint_{(V)} j_p \exp(jkz \cos \theta) dV. \quad (5.38)$$

As an example, we shall consider an elementary linear radiator (Hertz dipole) located along  $z$ -axis. It is a filament with length  $b$  with current amplitude  $I$ , constant along a filament. In a far region, the filament's field is defined by expression

$$E_{\theta 0} = j(30kIb/R)\exp(-jkR) \sin \theta.$$

Substituting it in (5.38), we obtain expression for the field of a symmetrical radiator (dipole) located along  $z$ -axis with the center at the coordinate origin. Another

example is a linear antenna array situated along  $x$ -axis (Fig. 29a). In this case, one must replace (5.38) with a sum

$$E = \frac{E_1}{J_1(0)} \sum_{n=1}^N J_n(0) \exp[jk(n-1)d_1], \quad (5.39)$$

where  $E_1$  is the field of a first radiator,  $d_1 = d \cos \varphi \sin \theta$  is path difference of beams from the adjacent radiators to an observation point with arbitrary coordinates  $\varphi$  and  $\theta$ ,  $n$  is the radiator number. The radiators of an antenna array are excited by currents with equal amplitudes and linearly increasing phase displacement:

$$J_n(0) = J_1(0) \exp[-j(n-1)\psi]. \quad (5.40)$$

Here,  $\psi$  is the phase shift between currents of adjacent radiators. Using the formula for a sum of  $N$  terms of a geometric progression with the denominator  $\exp[j(kd \cos \varphi \sin \theta - \psi)]$ , omitting factor  $\exp[j(N-1)(kd \cos \varphi \sin \theta - \psi)/2]$ , which defines a phase characteristic of an array, and normalizing the result to 1, we obtain expression for an amplitude characteristic of an array

$$F_N(\theta, \varphi) = \frac{\sin[N(kd \cos \varphi \sin \theta - \psi)/2]}{N \sin[(kd \cos \varphi \sin \theta - \psi)/2]}. \quad (5.41)$$

As seen from (5.39), the directional pattern of a system of identical and equally oriented directional radiators is the product

$$F(\theta, \varphi) = F_1(\theta, \varphi) F_N(\theta, \varphi), \quad (5.42)$$

where  $F_1(\theta, \varphi)$  is the directional pattern of a solitary radiator. Equality (5.42) is called by the theorem of multiplication of directional patterns, and  $F_N(\theta, \varphi)$  is an array factor. If a system of radiators consists of no directional in horizontal plane antennas, e.g., of vertical monopoles, its horizontal pattern coincides with the array factor, and the vertical one depends on the corresponding directional pattern of a solitary radiator. One should emphasize that the array factor also depends on angle  $\theta$ .

A rectangular array (Fig. 29b) can be considered as a linear structure consisting of  $M$  linear arrays. Therefore, the array factor of the rectangular array is

$$F_{MN} = F_M F_N, \quad (5.43)$$

where  $F_M$  is the array factor of a linear array of  $M$  radiators situated along the  $y$ -axis:

$$F_M(\theta, \varphi) = \frac{\sin[M(kd \cos \varphi \sin \theta - \xi)/2]}{M \sin[(kd \cos \varphi \sin \theta - \xi)/2]}.$$

The electrical characteristics of a radiators system at given frequency are conditioned by its phasing mode, i.e., by choice of a phase shift between the currents of radiators. Antenna array can have two modes of phasing: the maximal radiation forward and a minimal radiation backward. In the first mode, the phases of radiators'

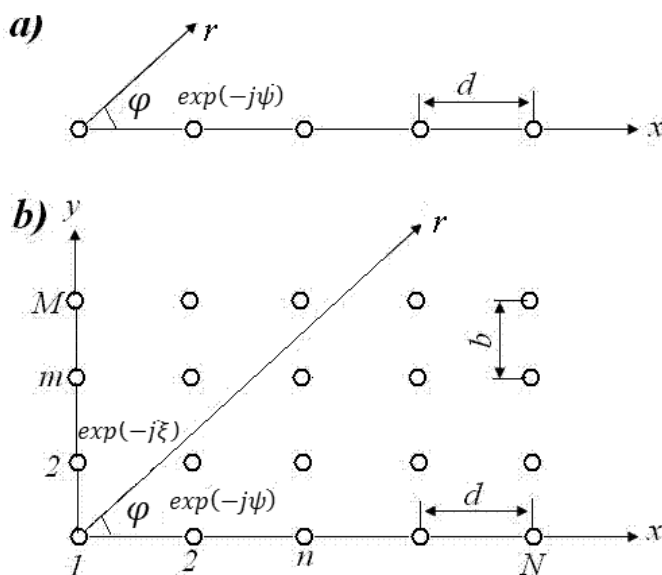


Fig. 29: Uniform antenna array: a – linear, b – rectangular.

fields are identical at the observation point with a given azimuth; in the second mode, the field is minimal or zero in the direction opposite the direction towards the correspondent. The first mode can be created in any array, while the second one is feasible not always. For example, it is unfeasible in a linear array.

The phases difference of signals coming from the adjacent radiators of one row of the rectangular array to an observation point, located in the same horizontal plane as an array is equal to the value  $\Phi_{12} - \Phi_{11} = kd \cos \varphi - \psi$ , and the difference of signals phases from radiators of adjacent rows is  $\Phi_{21} - \Phi_{11} = kb \sin \varphi - \xi$ . Here,  $\Phi_{mn}$  is the phase of signal, coming from the radiator  $m$  of the row  $n$ . At the observation point with azimuth  $\varphi_m$ , phases of all signals will be the same, if

$$\psi_m = kd \cos \varphi_m, \quad \xi_m = kb \sin \varphi_m = (b\psi_m/d) \tan \varphi_m. \quad (5.44)$$

These conditions are necessary and sufficient for implementation of the first phasing mode. The second mode can be applied, e.g., in a two-row array, where the fields of radiators of each row are summed together in phase, and then the fields of different rows are summed together in anti-phase. The condition of no signal in direction  $\varphi_0$  has the form

$$\psi_0 = kd \cos \varphi_0, \quad \xi_0 = kb \sin \varphi_0 + \pi = \frac{b\psi_0}{d} \tan \varphi_0 + \pi. \quad (5.45)$$

Calculation of the phase shifts in accordance with equalities (5.44) and (5.45) for different angles  $\varphi$  of the maximal radiation (in the first case  $\varphi = \varphi_m$ , in the second case  $\varphi = \varphi_0 + \pi$ ) clearly demonstrates the difference between the modes (Fig. 30).

Apart from a rectangular array, on object, e.g., on a ship, the other variant can be implemented. This variant uses the existing set of ship antennas. As a result, an array

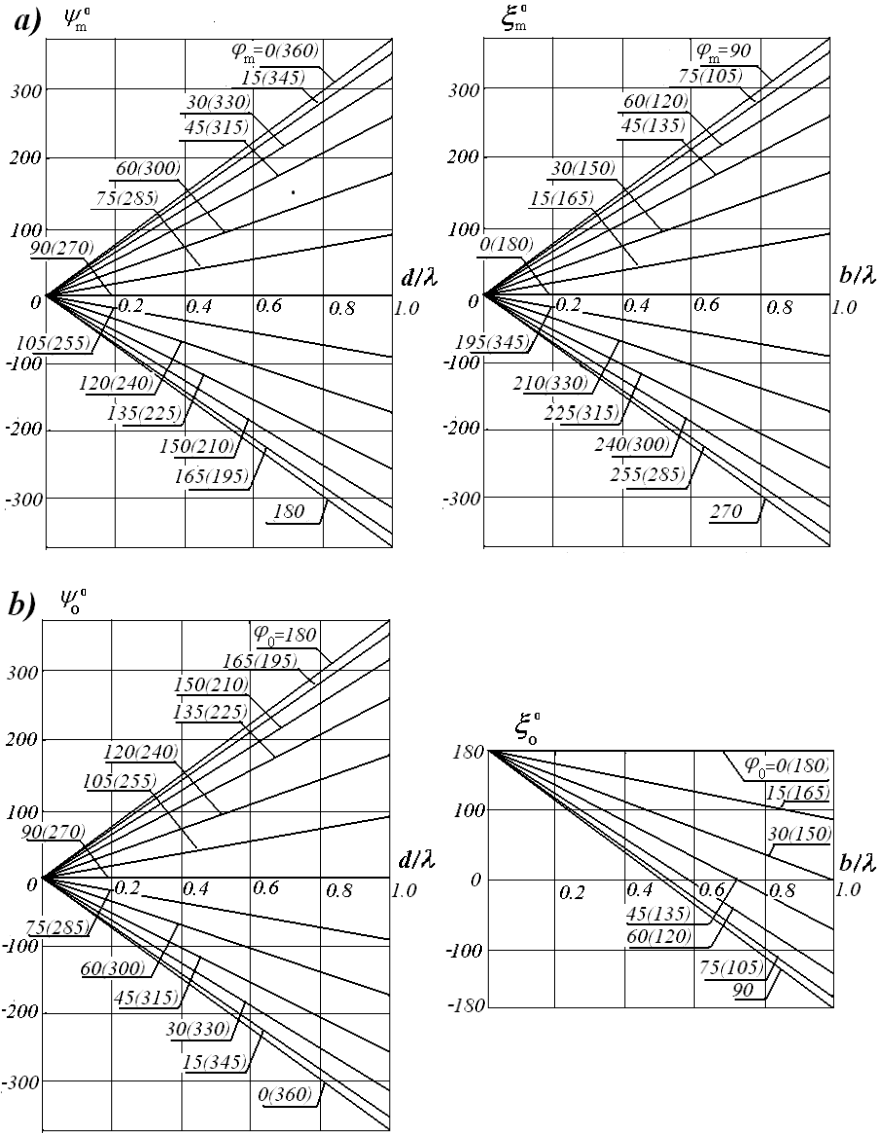


Fig. 30: Phase shifts in the modes of maximum radiation forward (a) and zero radiation backward (b).

of arbitrarily located radiators is formed. Let the current in the base of the radiator  $n$  be  $J_n(0) = |J_n| \exp(-j\psi_n)$ . Figure 31a presents phase shift  $\varphi_m$ , ensuring coinciding the field phase of a radiator  $n$  in the far region with the field phase of the radiator located at the coordinate origin. If this condition is met for all radiators, their fields are summed together in the observation point (in the mode of radiation forward). The phase of the field of radiator  $n$  in the far region is

$$\Phi_n = -kr_n - \psi_n,$$

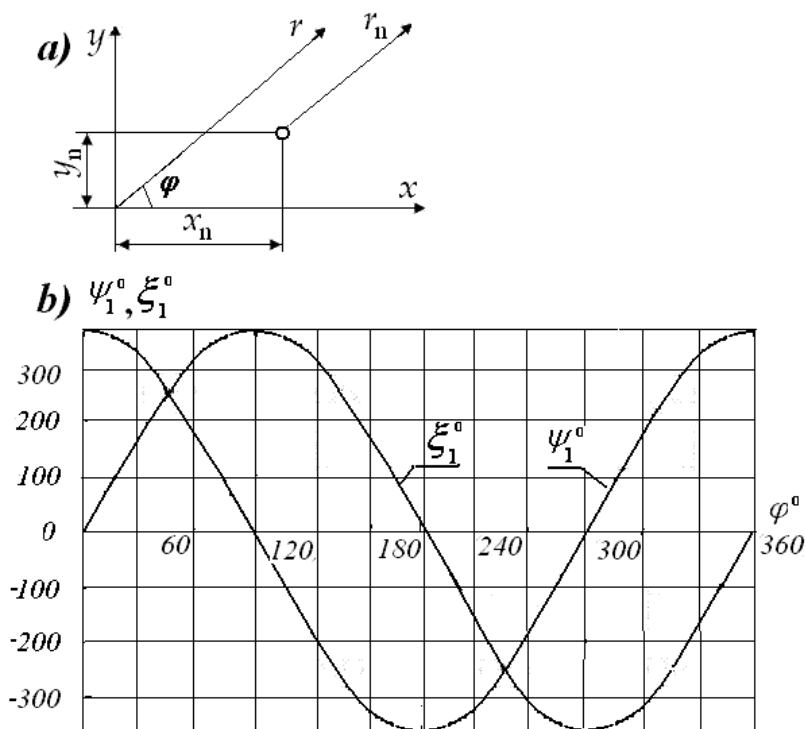


Fig. 31: Circuit of the placement of radiator  $n$  (a) and dependence of  $\psi_1$  and  $\xi_1$  on  $\varphi$  (b).

where  $r_n = r - x_n \cos \varphi - y_n \sin \varphi$  is the distance from the radiator to the observation point. If  $\Phi_n = \text{const}(n) = -kr$ , then  $\psi_n = k(x_n \cos \varphi + y_n \sin \varphi)$ . Let  $x_n/\lambda = D + d/\lambda$ ,  $y_n/\lambda = B + b/\lambda$ , where  $D$  and  $B$  are integers,  $d/\lambda$  and  $b/\lambda$  are proper fractions. Then

$$\psi_n = D\psi_1 + B\xi_1 + \psi_m + \xi_m. \quad (5.46)$$

Here,  $\psi_1 = 2\pi \cos \varphi$  and  $\xi_1 = 2\pi \sin \varphi$  are found from Fig. 29b (depending on  $\varphi$ ),  $\psi_m$  and  $\xi_m$ —from Fig. 30a or expression (5.44).

As is well known, the directional characteristics of a radiator are defined by the magnitude of directivity, which is given to the ratio of the maximal intensity of radiation to its average intensity in the surrounding space. This parameter represents the factor, into which one must increase the power in going from a directional antenna to isotropic antenna under the condition of field preservation at the receiving point. Since the field strength of a directional antenna is  $E = E_m F(\theta, \varphi)$ , where  $E_m$  is the field in the direction of maximum radiation, then the power of such antenna is equal to an integral from the Poynting vector over the sphere surface of the great radius  $r$ :

$$P_\Sigma = \int_{(S)} \frac{E_m^2 F^2(\theta, \varphi)}{Z_0} dS.$$

Here the surface element is equal to  $dS = r^2 \sin \theta d\theta d\varphi$ . The radiation power for isotropic antenna is

$$P_{\Sigma 1} = \int_{(s)} \frac{E_1^2}{Z_0} dS = \frac{4\pi r^2 E_1^2}{Z_0},$$

where  $E_1$  is the field of no directional antenna, which in accordance with condition of the fields equality at the observation point must be equal to  $E_1 = E_m(\theta_1, \varphi)$ . Therefore, we obtain for directivity factor in an arbitrary direction

$$D_1 = \frac{P_{\Sigma 1}}{P_{\Sigma}} = \frac{4\pi F^2 - (\theta_1/\theta_1)}{\int_0^{2\pi} d\varphi \int_0^{\pi} F^2(\theta, \varphi) \sin \theta d\theta}. \quad (5.47)$$

In direction of the maximal radiation, when  $F(\theta_1, \varphi_1) = 1$ , the directivity is

$$D_m = \frac{4\pi}{\int_0^{2\pi} d\varphi \int_0^{\pi} F^2(\theta, \varphi) \sin \theta d\theta}. \quad (5.48)$$

As one can see from (5.47) and (5.48), the magnitude  $D_1$  is determined easily, if  $D_m$  and  $F(\theta_1, \varphi_1)$  are known:

$$D_1 = D_m F^2(\theta_1, \varphi_1).$$

Figures 32–34 present the maximum directivity of linear and two-row antenna arrays consisting of isotropic radiators. Directivity factor is calculated in accordance with (5.48). For the two-row array  $F(\theta, \varphi)$  in conformity with (5.43) is replaced by  $F_{MN}(\theta, \varphi)$ . The calculated directivity of several arrays at three frequencies and at different azimuths of a main lobe is given in Table 4 in the mode of a maximal radiation forward. Processing calculation results allows us to build other characteristics of directivity for a system of radiators: a width of main lobe, a level of side lobes, and a level of radiation in the opposite direction. In particular, the half-power width of

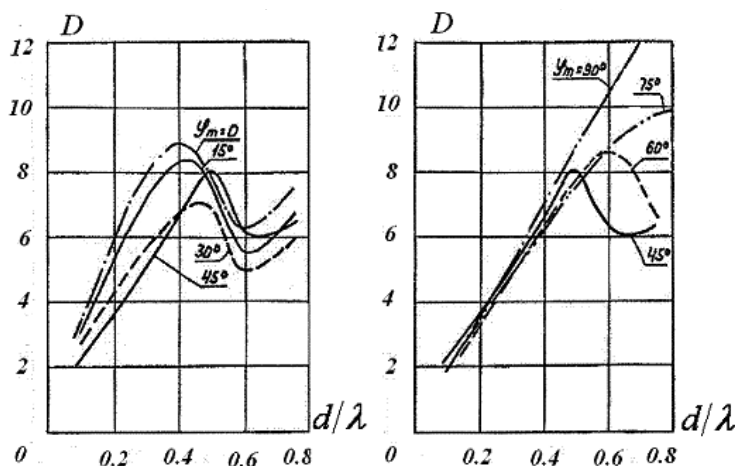
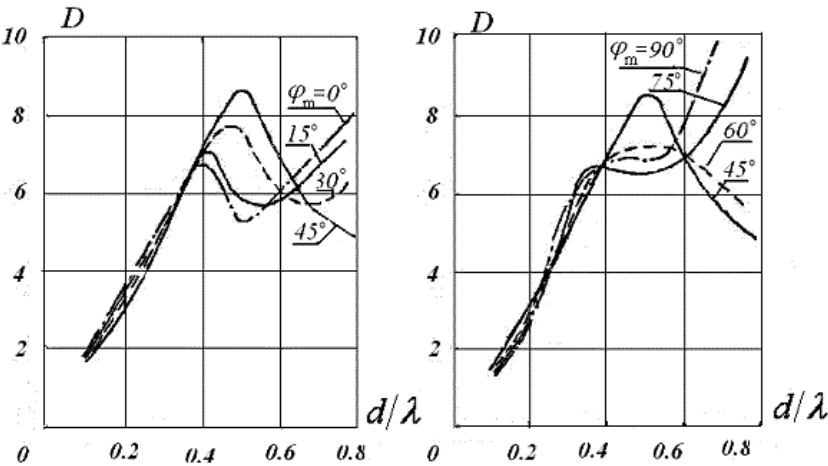


Fig. 32: Directivity of a linear array from 8 radiators.

**Table 4:** Directivity of Antenna Arrays in the Mode of Maximal Radiation Forward.

Array type	$d/\lambda = 0/2$	0.4	0.6	0.2	0.4	0.6
	in units			in decibels		
Linear, 4 radiators	1.8–3.2	3.1–5.5	2.9–4.9	2.5–5.0	4.9–7.4	4.6–6.9
Linear, 8 radiators	3.3–6.0	6.2–8.9	5.0–10.3	5.2–7.8	7.9–9.5	7.0–10.1
Square, 4 radiators	1.8	3.5–4.0	3.5–3.8	2.5	5.4–6.0	5.0–5.8
Two-row, 8 radiators	2.5–3.5	6.7–7.2	5.7–7.9	4.0–5.4	8.2–8.6	7.–9.0



**Fig. 33:** Directivity of a two-row array from 8 radiators in a mode of a maximal radiation forward.

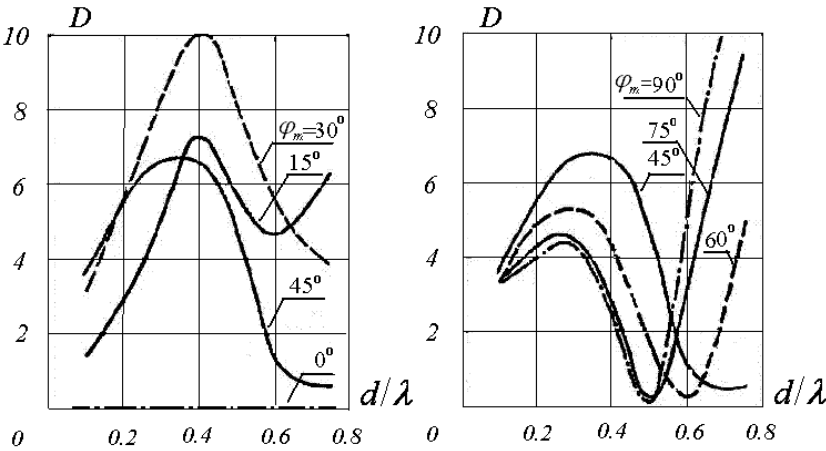


**Fig. 34:** Directivity of a two-row array from 8 radiators in a mode of a zero radiation backward.

a main lobe is presented in Fig. 35. Since the directional pattern has several main lobes, two curves correspond to it in Fig. 35: the lower one is for one lobe, the upper one is for a total width of the lobes.

Analysis of the above drawings allows us to determine the width of a frequency range for different options of antennas arrays, depending on the number of radiators.

On Fig. 36 in accordance with [18] the optimal angles of radiation and reception of radio waves depending on a frequency are presented. They were obtained by means of calculating different lines of radio communications under various propagation conditions by means of statistical processing of these calculations. The shaded area of a picture shows the region of the angles that provide radio communication in eighty percent of cases, i.e., the used antenna must have a high radiation level in this area. In practice, the elevation angle of the main lobe of a vertical directional pattern of a real antenna often falls into the area below the shaded area. In this regard, when developing antennas and placing them on the object (designing), it is necessary to pay great attention to a quality of their vertical pattern. For this purpose, it was suggested to introduce a special parameter—the pattern factor (PF), which is equal to the average level of radiation under predetermined angles:

$$PF = \frac{1}{K} \sum_{k=1}^K F(\theta_k), \quad (5.49)$$

where  $K$  is an angle's number  $\theta_k$  within the limits of angular sector from  $\theta_1$  to  $\theta_K$  (e.g., from  $90^\circ$  to  $60^\circ$ ) and  $F(\theta_k)$  is a magnitude of normalized directional pattern in the vertical plane for the angle  $\theta_k$ .

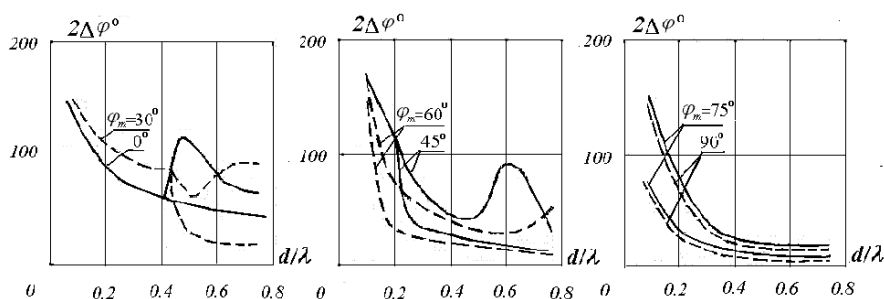


Fig. 35: Width of one main lobe (—) and total width of lobes (---) in a linear array from 8 radiators.

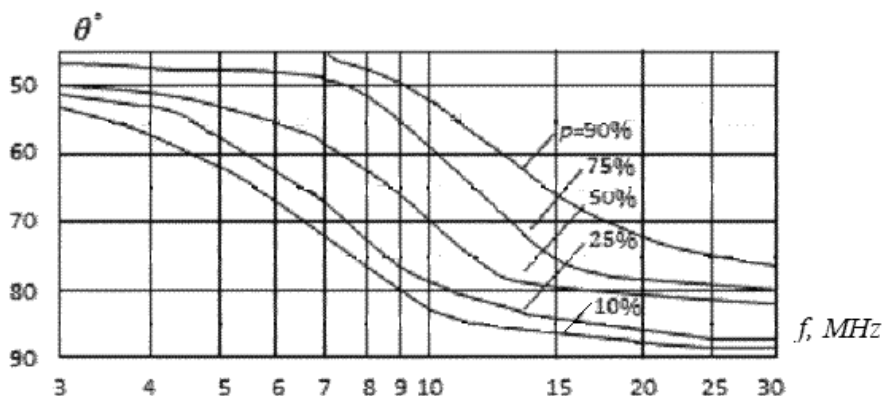


Fig. 36: Optimal angles of radiation and reception.



## 7. Calculating Directivity Factor with Help of Main Directional Patterns

In this Section a simple method of calculating the directivity of antennas and antenna arrays is considered. The method is based on a measurement of main directional patterns. In the case of intricate directional pattern these calculations often cause serious difficulties.

As is well known, directivity  $D$  is one from basic electrical performances of any antenna. An antenna gain  $G$  depends on a directivity and is equal to

$$G = D\eta, \quad (5.50)$$

where  $\eta$  is an efficiency. A knowledge of these magnitudes allows planning an improvement of antenna characteristics. The value of  $G$  can be defined by direct measurements. As regards magnitudes of  $D$  and  $\eta$ , it is very difficult to measure them or to interpret the measurements' results. For example, for evaluating  $D$  it is necessary to know the three-dimensional directional patterns of an antenna. But as a rule, they are measured only in two main planes: horizontal and vertical. The calculation difficulties are increased with a decreasing cross-section of the main lobe, i.e., with increasing directivity, caused for example by increased numbers of radiators in the antenna array.

Method of the directivity calculation of the narrow-beam antenna is described in [19]. It is based on a method proposed in [20] for calculating intermediate values in the measured directional pattern.

Usually, it is regarded that the magnitude of a directional antenna pattern in an arbitrary direction is equal to

$$F(\theta, \varphi) = F_1(\theta) F_2(\varphi), \quad (5.51)$$

where  $F_1(\theta)$  is a directional pattern in a vertical plane  $xOz$ ,  $F_2(\varphi)$  is a directional pattern in a horizontal plane  $xOy$ ,  $\theta$  and  $\varphi$  are angles in a spherical coordinates system, and  $x$ ,  $y$  and  $z$  form a rectangular system of coordinates (Fig. 37). The calculations show, that the expression (5.51) is true only in a small area, limited by a main lobe of a directional pattern. The proposed in [20] method proceeds from the revealing a curve, which is an aggregate of points with an identical signal magnitude. In this article the angle  $\delta = \pi/2 - \theta$  is used instead of the angle  $\theta$ . It means that the magnitude of the directional pattern is equal to

$$f(\delta, \varphi) = f(\delta_1, 0) = f(0, \varphi_1), \quad (5.52)$$

where  $\delta_1$  and  $\varphi_1$  are values of coordinates  $\delta$  and  $\varphi$  at the points of intersections of the mentioned curve with planes  $xOz$  ( $\varphi = 0$ ) and  $xOy$  ( $\delta = 0$ ) respectively (see Fig. 37).

Assume that the direction of a maximum radiation coincides with the  $x$ -axis, and the directional pattern is symmetric about the planes  $xOz$  and  $xOy$  (Fig. 38). For example, in-phase array, located in a plane  $yOz$ , has such a directional pattern. In this

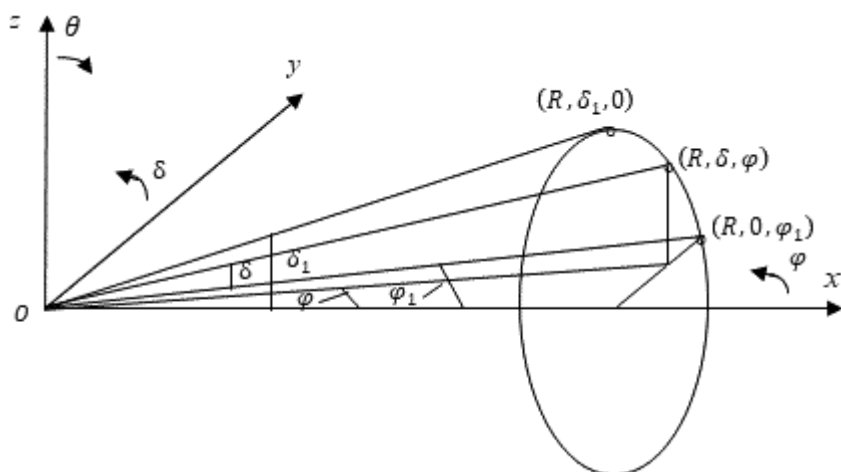


Fig. 37: The coordinate system and the directional pattern.

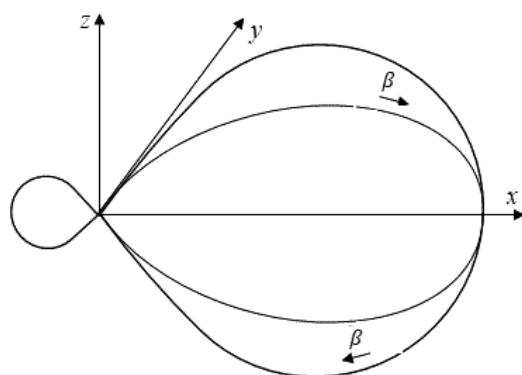


Fig. 38: Symmetric directional pattern.

case curves with identical directivity in the first approximation will be have the form of circumferences or ellipses:

$$f(\delta_1, 0) = f_1(\delta_1), f(0, \varphi_1) = f_2(\varphi_1). \quad (5.53)$$

If for convenience we introduce a new angular coordinate  $\beta$ , measured from axis  $x$  (see Fig. 38), then, as it is easy to show, the new and the old coordinates will be connected among themselves by the relation:

$$\beta = \cos^{-1}(\cos \delta \cos \varphi). \quad (5.54)$$

Let us the curves with identical signal magnitude have a form of circumference, i.e., the main lobe of a three-dimensional directional pattern has circular symmetry. Then we obtain

$$\delta_1 = \varphi_1 = \beta = \cos^{-1}(\cos \delta \cos \varphi), \quad (5.55)$$

More often this curve is an ellipse. Let  $a_1$  be the length of its vertical axis, i.e., the length of the segment between the upper and lower points of the directional pattern corresponding to the same signal magnitude (to the given magnitude of the directional pattern). In the same way  $a_2$  is the length of its horizontal axis, i.e., the length of segment between left and right points of the directional pattern with the same magnitude of a signal. Denote relation of lengths  $a_1$  and  $a_2$  by  $a = a_1/a_2$ . Then at  $a < 1$

$$\delta_1 = \cos^{-1}(\cos \delta \cos a\varphi), \varphi_1 = \frac{1}{a} \cos^{-1}(\cos \delta \cos a\varphi), \quad (5.56)$$

and at  $a > 1$

$$\delta_1 = a \cos^{-1}\left(\cos \frac{\delta}{a} \cos \varphi\right), \varphi_1 = \cos^{-1}\left(\cos \frac{\delta}{a} \cos \varphi\right). \quad (5.57)$$

As is known, maximal directivity factor of an antenna with the pattern, symmetrical about planes  $xOz$  and  $xOy$ , is equal to

$$D = \pi / \int_0^\pi \int_0^{\pi/2} f(\delta, \varphi) \cos \delta \, d\delta d\varphi, \quad (5.58)$$

whence

$$D = \pi / \left[ \int_0^{\pi/2} \int_0^{\pi/2} f(\delta, \varphi) \cos \delta \, d\delta d\varphi + \int_0^{\pi/2} \int_0^{\pi/2} f(\delta, \psi) \cos \delta \, d\delta d\psi \right]. \quad (5.59)$$

The first summand of the denominator corresponds to a forward half-space, the second summand - to a back half-space. Here in the second integral the change of variable  $\varphi = \pi - \psi$  is performed. At  $a < 1$  in accordance with (5.52), (5.53) and (5.56) we obtain

$$f(\delta, \varphi) = f_1(\delta_1) = f_1[\cos^{-1}(\cos \delta \cos a\varphi)]. \quad (5.60)$$

At  $a > 1$  according to (5.52), (5.53) and (5.57) one can obtain the similar expression. The expression (4.59) in view of (4.60) allows calculating antenna directivity, if its directional patterns are given in main planes.

In Fig. 39 the experimental directional pattern of a planar uniform antenna array with in-phase excitation is shown at a frequency 3.4 MHz depending from angles  $\varphi$  and  $\delta$ . As one can see from the figure, the factor  $a$  is equal to 1 in intervals  $160^\circ$ – $180^\circ$  and  $135^\circ$ – $145^\circ$ , to 0,63 in an interval  $145^\circ$ – $160^\circ$  and to 0,69 in an interval from  $90^\circ$  to  $120^\circ$  along an azimuthal angle. It means that a main lobe of the three-dimensional pattern has circular symmetry, i.e., the points located on the main lobe have a signal of identical magnitude, and the locus of these points is a circumference. Such circular symmetry on some side lobes is absent, and the account of these circumstances increases calculation accuracy. In an interval  $120^\circ$ – $135^\circ$  the factor  $a$  is greater than 1.

Calculation in accordance with the described procedure gives the magnitude of directivity, equal to 18,6 dB, if to consider intervals with  $a = 1$ . If we also consider the interval  $120^\circ$ – $135^\circ$  with  $a > 1$ , we obtain an outcome 18.2 db. The measured antenna gain is equal to 18 db. Thus, one must admit a good conformity of calculated and experimental results.

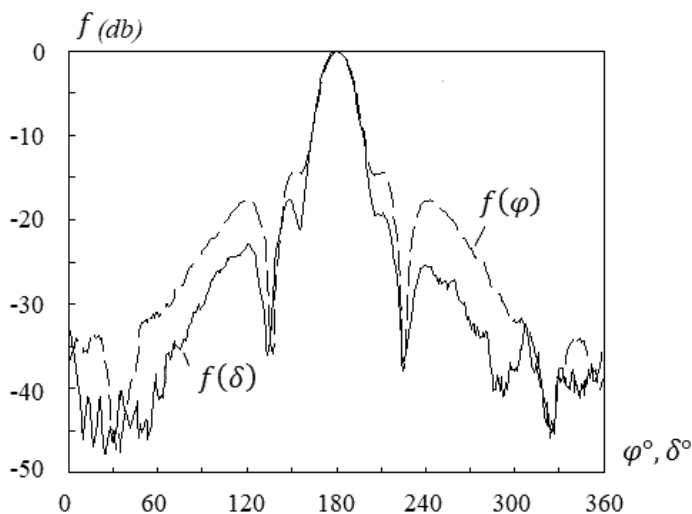


Fig. 39: Experimental directional patterns of antenna.

For antennas with one narrow major lobe and small minor lobes the theory [21] recommends expression

$$D = 41253/(\theta_1 \theta_2),$$

where  $\theta_1$  and  $\theta_2$  are half-power beam widths of the directional pattern (in degrees) in two mutually perpendicular planes. For planar arrays a better approximation is

$$D = 32400/(\theta_1 \theta_2).$$

The calculation in accordance with these formulas for the directional patterns, presented on Fig. 39, gives accordingly 20.2 and 19.2 dB, i.e., the error is much greater.

The program of directivity calculation uses two procedures: the procedure of antenna pattern estimation between the important angles and the procedure of integrals calculation by summation of numerical magnitudes. These methods can be used too for the solution of other problems.

Let's, for example, one can decrease side lobes of the directional pattern of the antenna, and it is necessary to define how as result the directivity factor will change. First one must determine the initial value of a directivity in accordance with (5.60) and next reduce the side lobes to a given level  $f_0$  and calculate the new directivity. For example, one can reduce the side lobes in a vertical plane in the range of angles from  $\varphi_{11}$  to  $\varphi_{12}$  and in a horizontal plane in the range of angles from  $\delta_{11}$  to  $\delta_{12}$ . At  $a < 1$  the new directivity is

$$D_1 = \pi \left\{ \int_0^{\pi/2} \int_0^{\pi/2} f_1(\delta_1) \cos \delta d\delta + \int_{\varphi_{11}}^{\varphi_{12}} \int_{\delta_{11}}^{\delta_{12}} [f_0 - f_1(\delta_1)] \cos \delta d\delta d\varphi \right\}^{-1},$$

i.e.,

$$\frac{D}{D_1} = 1 + \left\{ \int_{\varphi_{11}}^{\varphi_{12}} \int_{\delta_{11}}^{\delta_{12}} [f_0 - f_1(\delta_1)] \cos \delta d\delta d\varphi \right\} / \left[ \int_0^\pi \int_0^{\pi/2} f_1(\delta_1) \cos \delta d\delta d\varphi \right] =$$

$$1 + \left[ \frac{f_0}{\pi} (\varphi_{12} - \varphi_{11}) (\sin \delta_{12} - \sin \delta_{11}) - \frac{1}{\pi} \int_{\varphi_{11}}^{\varphi_{12}} \int_{\delta_{11}}^{\delta_{12}} f_1(\delta_1) \cos \delta d\delta d\varphi \right].$$

The program of the magnitude  $D$  calculation was written in MATLAB and presented in [20].

## 8. Anechoic Chambers

An anechoic chamber is a closed room for measurements of the directional patterns and the gain of an antenna. The room is shielded, i.e., walls, floor and ceiling are covered by a metal screen and a material absorbing electromagnetic waves. That allows us to eliminate external electromagnetic fields and an own field of the antenna, which is reflected from the metal objects. The elements of an absorber, placed on a metal screen, are equivalent to the two-wire long lines, which are shortly circuited on the end and have the input impedances close to a wave impedance of the free space. This ensures a decrease of a reflection from a room walls, floor and ceiling (see, for example, [11]).

The absorber is executed from a dielectric material impregnated by carbon (for example, from urethane foam). To secure a small reflection factor in a wide frequencies range, the wave impedance of the coating should vary along a covering thickness. Therefore, each absorber piece consists of pyramids or wedges established on a flat metal sheet. A typical example of such a product is the pyramidal absorber VHP-NRL, produced by the firm Eccosorb and designed for operation at frequencies from 120 MHz to 50 GHz. The absorber VHP-12 of total thickness (a sheet plus a pyramid) 0.305 m provides a reflection factor from  $-35$  to  $-50$  dB at normal incidence of an electromagnetic wave in a range from 1 to 24 GHz. At inclined incidence of an electromagnetic wave a reflection factor grows. Because an anechoic chamber has finite dimensions, the presence of reflections causes the appearance of parasitic signals in a receiving point, which create measurements errors. At that there is a question, as far as the error value is great at measurements of patterns and gains for antennas with the different sizes on various radiofrequencies.

In Fig. 40 the placement of transmitting and receiving antennas in the anechoic chamber (top view) and the ray trajectory between antennas at single wave reflection from a wall are shown. The angle of a wave incidence in a reflection point depends on distance between two antennas, and between antennas and walls. Because the reflection factor grows with growth of the angle of incidence, to decrease this factor, the antennas should be located on a room axis, equally spaced from both side walls, and equally spaced from the floor and the ceiling.

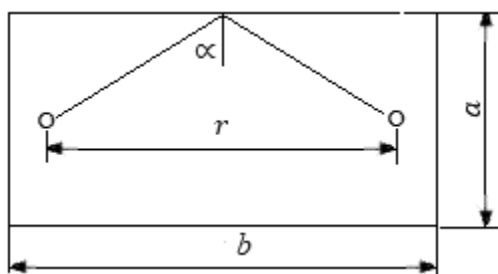


Fig. 40: Placement of antennas in an anechoic chamber.

At the antennas' placement, indicated in the figure, the angle of ray incidence on a side wall is equal to  $\alpha = \tan^{-1} \left( \frac{r/a}{2/a} \right) = \tan^{-1} (r/a)$ , and an angle of ray incidence on a ceiling (floor) is  $\beta = \tan^{-1} (r/h)$ , where  $a$  and  $h$  are the room width and height accordingly,  $r$  is the distance between antennas. Let, for example,  $r = 7$  m,  $a = 4.3$  m,  $h = 2.5$  m. Then  $\alpha = 58.4^\circ$ ,  $\beta = 70.4^\circ$ . At the incidence angle  $58.4^\circ$  a reflection factor is increased on 10–13 dB in comparison with normal incidence [23], i.e., for a material VHP-12 the value of the reflection factor  $\Gamma_1$  changes from –22 dB at 1 GHz to –40 dB at 5–24 GHz. At the incidence angle  $70.4^\circ$  the reflection factor is increased on 20 dB, i.e., for a material VHP-12 the value of the reflection factor changes from –12 dB at 1 GHz to –30 dB at 5–24 GHz.

The incidence angles  $58.4^\circ$  (to the side wall) and  $70.4^\circ$  (to the ceiling) correspond to a ray deviation from an axis 'the transmitting antenna—the receiving antenna' on  $31.6^\circ$  in horizontal plane and on  $19.6^\circ$  in a vertical one. At the patterns and gains measurement they are the most dangerous angles causing measuring errors. If during the transmitting antenna rotation on an azimuth (in a horizontal plane) the main pattern lobe coincides with a dangerous angle, the normalized (referred to a maximum) signal, reflected from a wall, is equal to  $\Gamma_1$ , i.e., a signal magnitude in a receiving point even at a signal absence on the given azimuth is  $\Gamma_1$ . The smaller pattern values on a given azimuth  $31.6^\circ$  in principle are not measurable. That is fair too for the angle  $19.6^\circ$  in a vertical plane. If a room width is more than its height, to escape from reflected signals, it is expedient at measurement of a vertical pattern to rotate an antenna in a horizontal plane (around of a vertical axis). At the same time, it is necessary to remember that the presence of reflected signals in a vertical plane on the angle about  $19.6^\circ$  to an axial line will result to the minima filling in horizontal pattern.

We will consider the antenna with a high directivity and narrow main lobe, which a half-width does not exceed the value of a dangerous angle in both planes. Let  $U_m$  is the magnitude of a signal in a direction of a maximum, and  $U_s$  is the magnitude of a signal (we shall name it a spurious one) under the dangerous angle  $\varphi = \pi/2 - \alpha$ . Then the value of a parasite signal, in decibels, in absence of the reflected signal is equal to

$$B = 20 \log(U_s/U_m),$$

and  $U_s = U_m 10^{B/20}$ . Length of a path of a reflected signal is equal to a path length of a direct signal multiplied by a factor  $1/\sin \alpha$ , i.e., at ideal mirror reflection of the signal from a wall we shall receive in a receiving point

$$U_{r1} = U_m \sin \alpha.$$

Actual reflection factor is

$$\Gamma_1 = 20 \log(U_{r2}/U_{r1}),$$

Here  $U_{r2}$  is the reflected signal in a receiving point, and  $U_{r2} = U_m 10^{\Gamma_1/20} \sin \alpha$ . The measured value of this signal is

$$U_r = U_{r2} F = U_m 10^{\Gamma_1/20} F \sin \alpha.$$

where  $F$  is the directional pattern of a receiving antenna. The phases of the reflected and direct signals are close to each other. If they coincide, the accepted signal is

$$B_1 = 20 \log[(U_s + U_r)/U_m] = 20 \log(10^{B/20} + 10^{\Gamma_1/20} F \sin \alpha),$$

i.e.

$$B_1 = B + 20 \log(1 + 10^{\Gamma_1 - B/20} F \sin \alpha).$$

The magnitude  $\Delta = B_1 - B = 20 \log(1 + 10^{\Gamma_1 - B/20} F \sin \alpha)$  is a measurements error, in decibels, caused by reflection from a wall. At  $U_r/U_s \ll 1$ , it is equal to

$$\Delta = 20 \log(1 + U_r/U_s) = 8.6 U_r/U_s.$$

Let us examine as an example the horizontal directional pattern with side lobes  $-15$  and  $-20$  dB with respect to the main one. We will consider that the signal maximum is radiated in a horizontal plane (reflection from a floor and ceiling may be neglected), and the side lobe direction coincides with a dangerous angle, i.e., at measurement of a side lobe the spurious signal reflected from a wall, is maximal one, because it is created by the main lobe. In Table 5 for a few frequencies  $f$  (in gigahertz) the calculation results are given: the electrical thickness  $d/\lambda$  of a material VHP-12 (in wave lengths), the reflection factor  $\Gamma_1$  for the incidence angle  $58,4^\circ$  (in decibels) and maximal measurements errors  $\Delta_1$  and  $\Delta_2$  (in decibels) for side lobes values  $-15$  and  $-20$  dB accordingly. At that the magnitude  $F$  is taken equal to 1.

The influence of a reflected signal created by side lobes on a radiation level in the main direction is much weaker. As in the previous case, the measured magnitude of the reflected signal in a receiving point is

$$U_r = U_s 10^{\Gamma_1/20} F \sin \alpha = U_m 10^{(B+\Gamma_1)/20} F \sin \alpha,$$

i.e., at a phase coincidence of the reflected and direct signals in a receiving point instead of value  $20 \log(U_m/U)$ , where  $U$  is a level of isotropic signal, we shall receive

$$D_1 = 20 \log[(U_m + U_r)/U] = D + 20 \log[1 + 10^{(B+\Gamma_1)/20} F \sin \alpha].$$

**Table 5:** Measurements Errors of Antennas with a High Directivity.

$f, \text{GHz}$	0.9	2.5	3.5	5.7	10.5
$d\lambda$	0.91	2.54	3.56	5.79	10.67
$-\Gamma_1, \text{dB}$	22	28	29	40	40
$\Delta_1, \text{dB}$	2.4	1.3	1.2	0.3	0.3
$\Delta_2, \text{dB}$	3.9	2.2	2.0	0.8	0.8
$2\delta_1, \text{dB}$	0.18	0.08	0.08	0.02	0.02
$2\delta_2, \text{dB}$	0.1	0.04	0.04	0.012	0.012

At  $U_r/U_m \ll 1$ , the measurements error caused by reflection from one of walls, is equal

$$\delta = D_1 - D = 8.6 \cdot 10^{(B+\Gamma_1)/20} \text{Fsin } \alpha.$$

If the antenna is located along the axis of a symmetric room and its directional pattern is symmetric in a horizontal plane, i.e., the signals created by the side lobes and reflected from both walls are identical, the measurements error will be doubled (as distinct from the previous case). The double magnitudes of errors  $2\delta_1$  and  $2\delta_2$  are given in Table 5 (at  $F = 1$ ) for side lobe  $-15\text{dB}$  and  $-20\text{ dB}$  accordingly. The values  $\delta_1$  and  $\delta_2$  do not depend from value  $D$ . The calculations show that the error value, which at a gain measurement is introduced by reflected signals of the side lobes, does not exceed  $0,2\text{ dB}$ , and it can be neglected. At measurement of the side lobes, the error caused by reflections can have an essential effect on obtained results, and one needs to take it into account.

The distortions caused by radiation on other angles are smaller than considered ones. At small angles of a deviation from the chamber axis the signal of the transmitting antenna is incident on a face wall (behind the receiving antenna) with an incidence angle close to normal one and with high absorption. At greater angles of a deviation from an axis an incidence angle and the reflection factor decrease. Besides, to get in the receiving antenna, the given signal should be reflected from walls at least twice.

Previously the matter concerned antennas with a high directivity and narrow main lobe, which a half-width does not exceed a dangerous angle in both planes. If a half-width of a main lobe is greater than a dangerous angle, it causes essential errors at a gain measurement. In this case we shall receive in a direction of a maximum

$$D_2 = 20 \log \frac{U_m + U_r}{U} = D + 20 \log [1 + 10^{(B+\Gamma_1)/20} \text{Fsin } \alpha],$$

where

$$B_1 = 20 \log (U_1/U_m),$$

and  $U_1$  is the magnitude of a signal on the angle  $\varphi$  to a maximum. If  $U_r/U_m \ll 1$ , the gain measurement error caused by a signal reflection from one of surfaces is equal to

$$\Delta = 8.6 U_r/U_m = 8.6 \cdot 10^{(B+\Gamma_1)/20} \text{Fsin } \alpha.$$



**Table 6:** Measurements Errors of Antennas with a Broad Main Lobe.

$f, \text{GHz}$	0.9	2.5	3.5	5.7	10.5
$d\lambda$	0.91	2.54	3.56	5.79	10.67
$-\Gamma_2, \text{dB}$	12	22	25	30	36
$\Delta_3, \text{dB}$	1.07	0.34	0.24	0.14	0.07
$\Delta_4, \text{dB}$	0.19	0.1	0.07	0.03	0.02
$2(\Delta_3 + \Delta_4), \text{dB}$	2.52	0.88	2.62	0.34	0.18
$-\Gamma_3, \text{dB}$	8	18	21	25	32
$-\Gamma_4, \text{dB}$	14	25	28	34	41
$\Delta_5, \text{dB}$	2.7	0.86	2.61	0.38	0.17
$\Delta_6, \text{dB}$	0.34	0.09	0.07	0.03	0.02
$2\Delta_4 + \Delta_5 + \Delta_6, \text{dB}$	3.4	1.15	0.82	0.047	0.23

The maximal error is equal to the sum of errors caused by reflections from both walls, floor and ceiling. If the main lobe of a directional pattern has cross-section close to circular, a signal under the dangerous angle in a vertical plane has a greater magnitude. For this signal the reflection factor in the formula for  $\Delta$  is equal to  $\Gamma_2$ —to the reflection factor for an incidence angle  $70.4^\circ$  (see Table 6). Let, for example,  $U_1/U_m = 0.5$ , i.e.,  $B_1 = -6$ . The appropriate value  $\Delta_3$  at  $F = 1$  is given in Table 6. In the same place it is shown the error  $\Delta_4$  caused by the reflection from each wall (it is adopted that the ratio of a signal under the angle  $\varphi$  away from a maximum is equal to  $U_2/U_m = 0.3$ ) and the total error  $2(\Delta_3 + \Delta_4)$ .

Let us consider variant of antennas placement on different distances from a floor and a ceiling. Let, for example, the antennas are placed at height 1,6 m, i.e., the ray incidence angle on the ceiling is  $\beta_1 = 75.6^\circ$  and on the floor  $\beta_2 = 65.6^\circ$ . At that the signal magnitude in a direction of a reflection point located at the ceiling is  $U_1 = 0.8U_m$  ( $B_1 = -2$ ), and in a direction of a floor  $U_1 = -0.2U_m$  ( $B_1 = -14$ ).

Table 6 shows the reflection factors  $\Gamma_3$  and  $\Gamma_4$  for the incidence angles  $\beta_1$  and  $\beta_2$  and the measurements errors caused by reflection from the ceiling ( $\Delta_3$ ) and the floor ( $\Delta_6$ ). Also, it is given the total error ( $2\Delta_4 + \Delta_5 + \Delta_6$ ) from a ceiling, floor and both walls. From the Table 6 it is visible that the antennas placement out of a room axis results in essential increase of errors. At the gain measurement in directions near to the main maximum the error grows, since the values  $U_1$  and  $U_m$  in the expression for  $B_1$  trade places, and the magnitude  $B_1$  becomes positive. However, this error is not so critical, because at antennas tests the magnitude of a maximal gain has a greater importance than the form of a main lobe. Somehow or other it follows from this that at designing of the anechoic chamber, which height is usually smaller than width, the special attention should be given to antennas placement on equal distances from a floor and a ceiling.

Natural manner of an error reduction is an increase of an anechoic chamber dimensions and application of an absorbing material of higher quality (with smaller reflection factor). If the absorber of different quality is used at creation of an anechoic chamber, then the more high-quality absorber must be used to cover the surfaces sections in the middle of the chamber.

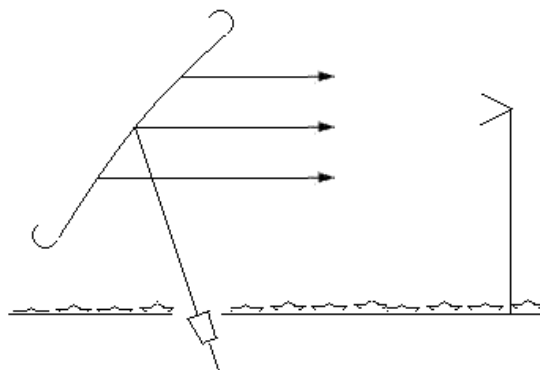


**Fig. 41:** A spherical-to-plane wave transformation.

The perspective method of a gain and pattern measurement is developed by the Lithuanian company “Geo” [24]. The method is based on transmission and reception of electromagnetic pulses with the time length in a few picoseconds (gating). In this case signals reflected from the chamber walls simply fail to hit the recording device. A positioner and a personal computer are used in the automated measuring system.

Other manner consists in reduction of an electromagnetic field incident upon walls. For this purpose, a parabolic reflector with a feed displaced to a floor is established at a room end-wall (see Fig. 41). The reflector transforms a spherical wave created by the feed to a plane one. The antenna under study is used as receiving one. Important advantage of this manner is the creation indoors of homogeneous field (of the plane wave with constant amplitude and phase along its wave front). It is equivalent to approach of a far zone to the experimental antenna, i.e., allows reducing distance between transmitting and receiving antennas (to shorten the chamber length).

## 9. Turn of the Directional Pattern

Improving the quality of measurements in an anechoic chamber is an important practical task. Another practical task is creation of an antenna array with a guided directional pattern. For example, one of the ways to improve the quality of service for cellular communication users, as well as its profitability, is creation of a base station antennas with such directional pattern. In this case, the simplest and most essential requirement to this pattern is an ability to turn its main lobe in horizontal and vertical planes. These turns permit to provide high-quality communication for the maximum number of users depending on a time of day, in the case of popular events, etc. Important conditions of a successful execution of a stated task are, firstly, electrical, and not mechanical turn of a beam and, secondly, the preservation, if possible, of the available equipment of base stations.

The antenna of the base station is as a rule a uniform linear phased array located along a vertical axis. The width of a directional pattern in the vertical plane is equal from  $5^\circ$  to  $15^\circ$ , in the horizontal plane it is equal to and more. The direction of a maximum radiation coincides with a perpendicular to an array axis (at zero phase

shift between the elements) or differs somewhat from it in accordance with the required angle of inclination.

In most cases to perform turning the directional pattern in a vertical plane is easier than in a horizontal plane. For this, a phase shift between the array elements should be provided by introducing phase-shifting circuits into the distribution scheme. Changing a phase shift during operation (for example, using the switches), one can change an inclination angle of a main lobe of a directional pattern. However, this requires a partial replacement of a base station equipment, primarily the antennas.

To avoid this and not to change an existing antenna array, one can install along its vertical axis an additional radiator and to excite it with a given phase shift. In fact, this is an increase of an antenna array by one element. Depending on a magnitude of a phase shift, one or another inclination angle of a general directional pattern can be obtained. The power supplied to this element may be close to the excitation power of each element of an existing antenna. In order to change during operation an angle of a main lobe inclination, one can either switch on or switch off the additional radiator or use it in phase-shifting circuits.

The possibility of implementing such an antenna system is confirmed by the following example. Let the existing antenna be a vertical array of  $N$  identical in-phase radiators located at a distance  $b$  from each other. The array factor is

$$f_1(\theta) = \sin \frac{Nkb \cos \theta}{2} \left| \left( N \sin \frac{kb \cos \theta}{2} \right) \right|,$$

where  $\theta$  is the angle between the array axis and the radiation direction (Fig. 42),  $k$  is the wave propagation constant in the air.

If the directional pattern of an additional radiator coincides with the directional pattern of an element of the antenna array, then, considering a new antenna system as a combination of two radiators: an array of  $N$  elements with an input current  $I_1$  and an additional radiator  $A_{(2)}$  with the input current  $I_2$ , we obtain an overall array factor, equal to

$$f(\theta) = f_1(\theta) + a \exp[j(kd \cos \theta + \psi)], \quad (5.61)$$

where  $a = I_2/I_1$ ,  $d$  is the distance between the centers of two radiators,  $\psi$  is the phase shift in the second radiator. From here

$$f(\theta) = \sqrt{[f_1(\theta) + a \cos(kd \cos \theta + \psi)]^2 + a^2 \sin^2(kd \cos \theta + \psi)}.$$

For the maximum of directional pattern, we can write

$$\begin{aligned} \frac{d|f(\theta)|}{d\theta} = \frac{1}{|f(\theta)|} \left\{ [f_1(\theta) + a \cos(kd \cos \theta + \psi)] \left[ \frac{df_1(\theta)}{d\theta} + akd \sin(kd \cos \theta + \psi) \sin \theta \right] - \right. \\ \left. - \frac{a^2 kd}{2} \sin 2(kd \cos \theta + \psi) \right\} = 0. \end{aligned} \quad (5.62)$$

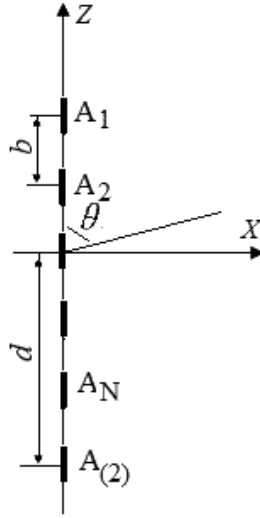


Fig. 42: Array of  $N$  radiators with additional antenna  $A_{(2)}$ .

Let  $\theta = \frac{\pi}{2} - \delta$ . We will assume that a deviation angle of maximum radiation from the horizontal is small, i.e.,  $\delta \ll 1$ . Then, in a first approximation,  $\sin \theta = 1$ ,  $\cos \theta = \delta$ ,  $f_1(\theta) = 1$ , i.e.

$$[1 + a \cos(kd\delta + \psi)] \left[ \frac{df_1}{d\theta} + akd \sin(kd\delta + \psi) \right] = \frac{a^2 kd}{2} \sin 2(kd\delta + \psi).$$

We introduce the notation  $\alpha = \frac{kb \cos \theta}{2}$ , i.e.,  $f_1(\theta) = \frac{\sin Na}{N \sin \alpha}$ . Respectively

$$\frac{df_1}{d\theta} = \frac{df_1}{d\alpha} \frac{d\alpha}{d\theta} = -\frac{kb \sin \theta}{2N^2 \sin^2 \alpha} [N^2 \sin \alpha \cos Na - N \sin Na \cos \alpha],$$

and  $\alpha = kb\delta/2 \ll 1$ . Replacing the trigonometric functions of a small argument by the first members of a series, we find:

$$\sin \alpha = \alpha \left( 1 - \frac{\alpha^2}{6} \right), \sin Na = Na \left[ 1 - \frac{(Na)^2}{6} \right], \cos \alpha = 1 - \frac{\alpha^2}{2}, \cos Na = 1 - \frac{(Na)^2}{2},$$

i.e.

$$\frac{df_1}{d\theta} = \frac{k^2 b^2 (N^2 - 1) \delta}{12}.$$

whence  $\frac{df_1}{d\theta} = [a^2 kd \sin 2(kd\delta + \psi)/2] / [1 + a \cos(kd\delta + \psi)] - akd \sin(kd\delta + \psi)$ . If the current  $I_2$  of the additional radiator is small, then  $a$  also is small, and respectively  $\frac{df_1}{d\theta} = -akd \sin(kd\delta + \psi)$ , we obtain

$$I_2 \sin(kd\delta + \psi) = -(N^2 - 1)kb^2 \delta / 12ad. \quad (5.63)$$

Let, for example,  $N = 6$ ,  $d = 4b$ ,  $a = 0,2$ ,  $b = 0,8 \lambda$ . Then  $\sin(20\delta + \psi) = -17,5\delta$ , i.e., at  $\delta = 0,05$  (at that  $\sin^{-1} \delta = 3^\circ$ ),  $\psi = -118^\circ$ . The given example shows that a phase shift between the currents in a secondary radiator and a main array should be sufficiently large. This shift will be the more, if the more will be a difference between the powers in these two parts of the total array. Nevertheless, a vertical turn of the directional pattern is possible.

In contrast to the turning in a vertical plane, the ability to turn a directional pattern in a horizontal plane is problematic. Installing a single additional radiator in the array plane along the horizontal axis does not solve a problem, not only because an additional antenna does not have a narrow directional pattern in a vertical plane, and therefore a system gain drops sharply. A significant drawback of such a device is the fact that to turn a general directional pattern, the power in an additional radiator must be  $G$  times greater than a power in existing radiators to the signals of both antennas at a receiving point were equal ( $G$  is an array gain). A competent technical solution is an installation of a second antenna array parallel to the first one, with a given phase shift between the currents of both arrays. However, the implementation of this solution significantly increases a complexity and a cost of an equipment.

As is known, an additional radiator with characteristics like the characteristics of the main radiator can be created, using mirroring of the main radiator in a perfectly conducting metal plane. In this case, the signal of an additional radiator differs from the signal of the main radiator by a fixed phase. The total directional pattern of a system of two such radiators is

$$F(\theta, \varphi) = f_1(\theta, \varphi)f(\varphi),$$

where  $f_1(\theta, \varphi)$  is the directional pattern of a single radiator,  $f(\varphi) = \sin \frac{kd \cos \varphi}{2}$  is the factor of an antenna array from two radiators,  $d = 2d_1$  is a distance between the axes of these radiators. It is equal to twice distance between the main radiator and a metal plane. As can be seen from this expression, even the turn of a metal plane does not lead to the turn of a directional pattern, if the direction of a maximum radiation of a main antenna does not change (the signal simply decreases in the direction of the minimum of the array factor). Mechanical (or electromechanical) turn of the main antenna around a vertical axis allows to turn the directional pattern around this axis and makes the metal plane unnecessary. But such an adjustment of a beam by means of mechanical turn is expensive and impractical.

The analysis shows that the turn of the directional pattern in the vertical plane is real and may be accomplished by simple means. The turn in the horizontal plane by the simple means is impossible.

## 10. Method of Compensation and a Cell Phone

Development of radio engineering and the widespread use of the radio devices in the national economy and in everyday people life led to a problem of protecting living organisms and sensitive instruments from strong electromagnetic fields in a near zone of each transmitting antenna. The protection of devices is necessary, since a radiation of nearby devices can disrupt their normal operation, causes spontaneous

switching on and switching off in the device, changes operating regimes etc. The protection of living organisms is required first in the vicinity of powerful transmitting centers, where the electrical field strength is great, and, secondly, if next to the user it is located the mobile equipment, which operates in the transmitting mode. A cellular phone is such a device.

The undoubted advantage of mobile communication consists in the freedom of its use to everyone, regardless of age, health, and location. If the radio liberates personal human contacts from fetters of wire systems, a cellular phone allows replacing the radio station, mounted on a truck or another vehicle, by a small device that may fit in a child palm. As a result, the advent of cellular communication looks like a big bang due to the rapid increase in the number of handsets, the widespread proliferation of phone contacts, and due to the rapid growth of concern about the potential harm of these devices for human health, in particular due to carcinogenicity.

Together with proliferation of mobile communication systems, there has been an increasing concern about possible hazards for the user, especially for the user's head, which is irradiated by a handset antenna. During a phone conversation, a personal cellular phone is placed next to user's head, and its transmitting antenna irradiates sensitive human organs (brain, eyes, etc.). The absorbed power in the first cell phones was close to half on a radiated power. To minimize any possible health risk, it is necessary to reduce the amount of that power.

A correlation between irradiation and parotid tumor for a long time was a subject to scientific debate, mostly due to the inherent difficulties of empirical research. Rumors and the truth about the potential harm of irradiation required reducing the Specific Absorption Rate (SAR) in the user's head. This is an extremely complex problem, since one must reduce the near field of the transmitting antenna without decreasing the far field and at that not spoil the directional pattern of the antenna. In addition, the problem is not limited by the cellular phones, since a person often works with a low-power transmitter or uses it. This transmitter can be located nearby in a production area or in a vehicle.

The rather obvious idea of head protection by means of screening, i.e., by shading effect, is unrealizable. The near field has no ray structure, and hence the shadow behind a metallic screen can cover only an area approximately equal to the screen size. For example, to protect the users head of the cellular phone user, the screen must be much larger than the cross-section of the handset housing. For similar reasons, one should discard the idea of using an absorber, i.e., a dielectric shield that absorbs some part of energy. The distortion of the antenna directional pattern is still another obvious disadvantage of using screens and absorbers.

The protective action of the compensation method [25] is based on a different principle—on the mutual suppression of fields, created by various radiating elements in a certain volume. The diverse variants of using this principle provides an opportunity to reduce irradiation of user's organism, especially his head, without distorting the antenna pattern in the horizontal plane. In accordance with the key variant of the compensation method, as shown in Fig. 43, the main radiator 1 is supplemented with second (auxiliary) radiator 2, situated in the plane, passing through the center of a human head and the excitation point of the main radiator. The second radiator is placed between the head and the main radiator and is excited approximately in anti-

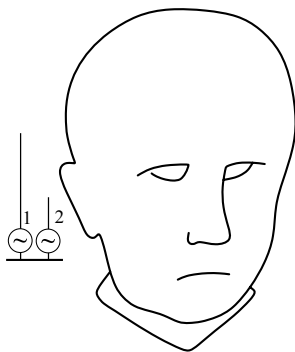


**Fig. 43:** Two radiators next to a head.

phase with it (not exactly in anti-phase, because the field phase is changed on the interval between the radiators). So, the fields of two radiators compensate each other at a certain point inside the head, and this point is surrounded by a dark spot, i.e., by a zone of a weak field.

The dipole moment of the auxiliary radiator must be smaller than that of the main radiator, since the field of an electrical radiator, decreases quickly. To get the same magnitude of field at the compensation point, if the currents of radiators differ substantially, it is enough to place the radiators at a distance a few centimeters from each other (1–2 cm at frequency 1 GHz). Therefore, the common field in the far zone is little different from the main radiator field, and the directional pattern stays close to the circular directional pattern, existing in the absence of compensation.

Fields of linear radiators near the human head are shown in Fig. 44. As seen from the figure, the feed point  $A_1$  of a main radiator, which coincides with the origin of cylindrical coordinate system, and a compensation point  $C$  are located along the horizontal straight line, passing through a head center. This line is defined as the structure axis. The feed point  $A_2$  of an auxiliary radiator is placed on this line at a distance  $b$  from the main radiator. Assume that both radiators are vertical and have equal lengths. Inside the human head at compensation point  $C$  (at distance  $\rho_0$  from point  $A_2$ ) the fields of both radiators must be equal in magnitude and opposite in sign:

$$E_{z2}(\rho_0) = -E_{z1}(b + \rho_0). \quad (5.64)$$

In the capacity of linear radiators with finite lengths, one can employ monopoles with a feed point in their base. A linear radiator creates two electric field components:  $E_z$  and  $E_\rho$ . If a straight perfectly conducting filament of finite length is used as model of a vertical linear radiator, the electric field components with allowance of a mirror image in a cylindrical coordinate system  $(\rho, \varphi, z)$  are given by expressions (1.25) and (1.29). Similar expressions also hold for the auxiliary radiator. As can be seen from them, the simultaneous compensation of both  $E_z$  and  $E_\rho$  field components by adjustment of the current  $J_{A2}$  of the auxiliary radiator is impossible. Since  $E_z$  is greater than  $E_\rho$ , and  $E_\rho$  along the  $\rho$ -axis (at  $z = 0$ ) is zero, it is expedient to prefer compensation of  $E_z$  components.

Since feed points  $A_1$  and  $A_2$  and compensation  $C$  lie on the structure axis, components  $E_z$  of both radiators in a homogeneous medium with relative permittivity

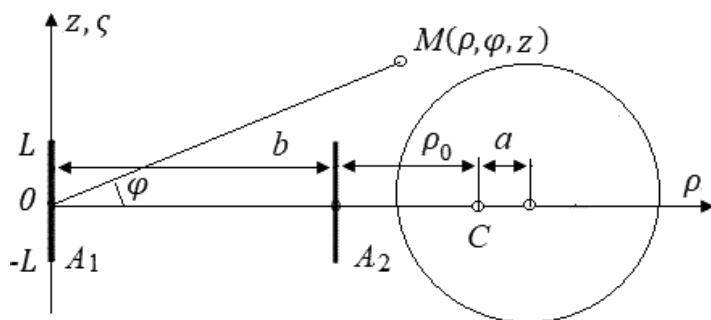


Fig. 44: Fields of phone radiators close to a human head.

$\varepsilon_r$  are determined by expression (1.25), but for the main radiator  $\rho_1 = \rho$ , and for the auxiliary radiator  $\rho_2 = \sqrt{(\rho - b)^2 + \rho^2 \sin^2 \varphi}$  (Fig. 45).

If the emf is connected in the input of the first radiator, the circuit looks, as shown in Fig. 46. The radiators are accomplished as the monopoles of finite lengths,  $R_{A1}$  and  $R_{A2}$  are the output impedances of a first and second generators accordingly. Generally,  $R_1 = R_2 = R$ .

The analysis of a circuit from two linear radiators is based on the method of calculating the folded antenna and on the superposition principle. We divide the main generator  $e_1$  into two generators  $e_{1/2}$ , the same in magnitude and in direction, and include in a foundation of an auxiliary radiator two generators, equal in magnitude to  $e_1/2$  and opposite in direction. According to a superposition principle, the field at each point is the sum of the fields, created by currents of all generators. Therefore, as shown in Fig. 47 one can divide the original circuit onto two circuits with two generators in each one and then calculate and sum the currents at points  $B$  and  $D$ , created in each of the circuits. This procedure allows analyzing the antenna system as a superposition of two subsystems with in-phase and anti-phase currents.

The currents along the wires of a first circuit are anti-phase. They are equal in magnitude and opposite in direction. The two parallel wires form a long line with the load  $2R$  in the input. The line is open on the end. Let the currents along the wires of a second circuit will be in-phase, i.e., the potentials of points, situated in both wires at the same height (including lower points of wires) are identical. For this the emf's in the wires basis of a second circuit must be equal, if the radii of wires are the same. In this case, the parallel wires form a monopole with the input resistance  $R/2$ . For the two-wire line, we can write

$$e_1 = J_1 (Z_1 + 2R), \quad (5.65)$$

where  $J_1$  is the input current and  $Z_1 = -jW_l \cot kL$  is the input impedance of the line with length  $L$ ,  $W_l = 120 \ln(b/a)$  is the wave impedance of a line,  $b$  is a distance between two wires, and  $2a$  is a diameter of each wire. The current at point  $B$  is  $J_{BII} = e_1 Y_1$ , and the current at point  $D$  is  $J_{DII} = -e_1 Y_1$ , where  $Y_1 = 1/(-jW_l \cot kL + 2R)$ . For the monopole, we write

$$e_1/2 = J_r (Z_r + R/2), \quad (5.66)$$



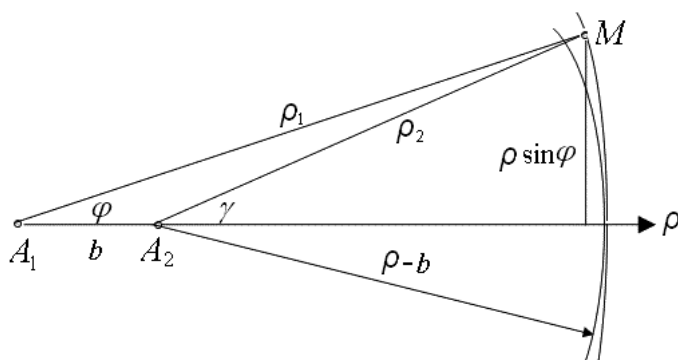


Fig. 45: Two linear radiators in cylindrical coordinate system (top view).

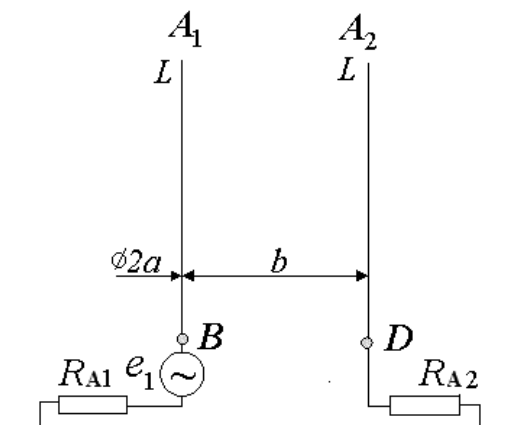


Fig. 46: Two radiators in the near region of each other.

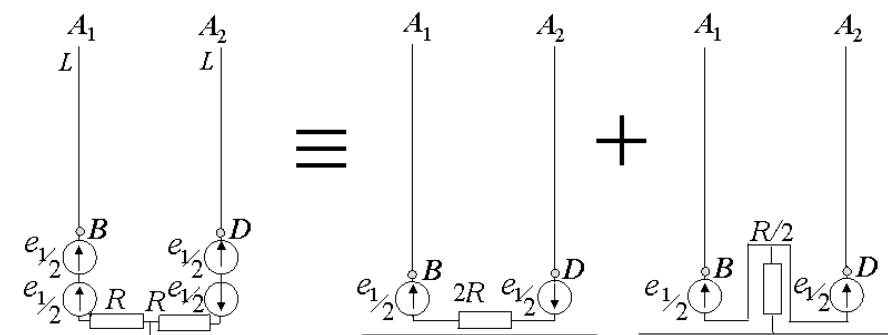


Fig. 47: Division of a considered circuit into two circuits.

where  $J_r$  is the input current of the monopole, and  $Z_r = Z_m(L, a_e)$  is the input impedance of a monopole with length  $L$  and equivalent radius  $a_e$ , equal to  $\sqrt{ab}$ . The currents at points  $B$  and  $D$  are the same and equal to

$$J_{B1r} = J_{D1r} = e_1 / (4Z_r + 2R) = e_1 Y_2, \quad (5.67)$$

where

$$Y_2 = 1/[4Z_m(L, a_e) + 2R].$$

So, if emf  $e_1$  is connected to the input of the first radiator, the currents in a first and a second radiator basis are

$$J_{11} = e_1 (Y_1 + Y_2), J_{21} = e_1 (-Y_1 + Y_2). \quad (5.68)$$

If emf  $e_2$  is connected to the input of the second radiator, then, similarly to (5.68), the currents in the foundations of a first and a second radiator are

$$J_{12} = e_2 (-Y_1 + Y_2), J_{22} = e_2 (Y_1 + Y_2). \quad (5.69)$$

According to the superposition principle, the terminal currents of the radiators are

$$J_{A1} = J_{11} + J_{12} = (e_1 - e_2) Y_1 + (e_1 + e_2) Y_2, J_{A2} = (e_2 - e_1) Y_1 + (e_1 + e_2) Y_2. \quad (5.70)$$

The input admittances of the radiators are

$$Y_{A1} = J_{A1}/e_1 = Y_1 + Y_2 + e_2(Y_2 - Y_1)/e_1, Y_{A2} = J_{A2}/e_2 = Y_1 + Y_2 + e_1(Y_2 - Y_1)/e_2. \quad (5.71)$$

As is known, the current and the input impedance of a radiator depend significantly on the neighboring radiator current. For a system of two radiators one can write

$$e_1 = J_{A1} Z_{11} + J_{A2} Z_{12}, e_2 = J_{A1} Z_{21} + J_{A2} Z_{22}. \quad (5.72)$$

Here,  $e_1$  and  $e_2$  are the driving emf's, connected respectively to the terminals of a first and a second radiators,  $Z_{11}$  and  $Z_{22}$  are their self-impedances,  $Z_{12}$  and  $Z_{21}$  are their mutual impedances. Each expression in (5.72) is a Kirchhoff equation for a series connection of circuit elements.

The expressions (5.72) can be rewritten as

$$J_{A1} = \frac{e_1 Z_{22} - e_2 Z_{12}}{Z_{11} Z_{22} - Z_{12} Z_{21}}, J_{A2} = \frac{e_2 Z_{11} - e_1 Z_{21}}{Z_{11} Z_{22} - Z_{12} Z_{21}}, \quad (5.73)$$

i.e., the current in each radiator is the sum of the currents, produced by its self-generator and the generator of the neighboring radiator (because of the mutual coupling between radiators). The ratio of the currents depends on the level of mutual coupling between the radiators, which is determined by their dimensions and position. Comparing (5.68) – (5.69) with (5.73), one can determine the self- and the mutual impedances of the radiators (for wires of equal radii). Considering that

$$J_{11} = \frac{e_1 Z_{22}}{Z_{11} Z_{22}} = e_1 (Y_1 + Y_2), J_{12} = \frac{-e_2 Z_{12}}{Z_{11} Z_{22} - Z_{12}^2} = e_2 (Y_2 - Y_1),$$

$$J_{21} = \frac{-e_1 Z_{12}}{Z_{11} Z_{22} - Z_{12}^2} = e_1 (Y_2 - Y_1),$$

we obtain:

$$Z_{11} = Z_{22}, \quad Y_1 + Y_2 = \frac{Z_{11}}{Z_{11}^2 - Z_{12}^2}, \quad Y_1 - Y_2 = \frac{Z_{12}}{Z_{11}^2 - Z_{12}^2}. \quad (5.74)$$

Summing and subtracting the left-hand and right-hand parts of last two expressions, we find:  $2Y_1 = 1/(Z_{11} - Z_{12})$ ,  $2Y_2 = 1/(Z_{11} + Z_{12})$ , that is,  $Z_{11} + Z_{12} = 1/(2Y_2)$ ,  $Z_{11} - Z_{12} = 1/(2Y_1)$ , and consequently

$$\begin{aligned} Z_{11} = Z_{22} &= 0.25(1/Y_1 + 1/Y_2) = Z_m(L, a_e) - j0.25W_l \cot kL + R, \\ Z_{12} &= 0.25(1/Y_2 - 1/Y_1) = Z_m(L, a_e) + j0.25W_l \cot kL. \end{aligned} \quad (5.75)$$

One can see from (5.75) that the result of proximity of the radiators is the additional terms of self and mutual impedance of each radiator. The mutual coupling between the radiators affects the current distribution along each radiator and causes the anti-phase currents in addition to the in-phase components. For equal radii of the wires, the in-phase, and the anti-phase currents of the first radiator are

$$J_{A1}^{(i)}(z) = (e_1 + e_2) Y_2 \frac{\sin k(L - |z|)}{\sin kL}, \quad J_{A1}^{(a)}(z) = (e_1 + e_2) Y_1 \frac{\sin k(L - |z|)}{\sin kL}. \quad (5.76)$$

In accordance with (1.31), the total fields of the radiators in plane  $\varphi = 0$  are given by

$$\begin{aligned} E_{z1}(z) &= -j 30F_1/\varepsilon_r [(e_1 + e_2) Y_2 + (e_1 - e_2) Y_1], \\ E_{z2}(z) &= -j 30F_2/\varepsilon_r [(e_1 + e_2) Y_2 + (e_2 - e_1) Y_1]. \end{aligned} \quad (5.77)$$

Here,  $F_m = \frac{1}{\sin kL} [\exp(-jkR_{m1})/R_{m1} + \exp(-jkR_{m2})/(R_{m2} - 2 \cos kL \exp(-jkR_{m0}/R_{m0}))]$ , where  $m$  is the radiator number,  $R_{m1} = \sqrt{(z-L)^2 + \rho_m^2}$ ,  $R_{m2} = \sqrt{(z+L)^2 + \rho_m^2}$ ,  $R_{m0} = \sqrt{z^2 + \rho_m^2}$ . To the total field  $E_z = E_{z1} + E_{z2}$  will be equal to zero at the compensation point, the ratio of emf's, driving the radiators, must be

$$\frac{e_2}{e_1} = - \frac{\sin k(L - |z|)}{\sin kL}. \quad (5.78)$$

Here,  $F_{m0}$  is the value of function  $F_m$  at the compensation point. Equation (5.78) allows finding the voltage amplitude and phase at the input of the second radiator, if those amplitude and phase of the first radiator are known. Using (5.72), we find:

$$J_{A1}/e_1 = Y_1 + Y_2 + e_2(Y_2 - Y_1)/e_1, \quad J_{A2}/e_1 = Y_2 - Y_1 + e_2(Y_1 + Y_2)/e_1.$$

Substituting (5.78) in these expressions, we obtain for the ratio of currents

$$J_{A2}/J_{A1} = -F_{10}/F_{20}. \quad (5.79)$$

It coincides with the currents' ratio in the absence of mutual coupling between the radiators. This occurs, when the radiators have the same length. For  $L = \lambda/4$ , we obtain in the first approximation

$$F_{10} = \exp(-jkR_{20})/R_{20},$$

i.e.

$$J_{A2}/J_{A1} = -R_{20} \exp[-jk(R_{10} - R_{20})]/R_{10}, \quad (5.80)$$

where  $R_{20} = \sqrt{L^2 + \rho_0^2}$ ,  $R_{10} = \sqrt{L^2 + (\rho_0 + b)^2}$ . As it follows from the above expressions, the dipole moments of linear radiators must be in inverse proportion to the distances between the radiators and the compensation point.

Application of the compensation method requires analyzing its efficiency. To this end, one needs to calculate the field in the space, surrounding radiator, and to determine the irradiation reduction factor. The problem is complicated due to the heterogeneous nature of the medium. For example, antenna of cellular phone is near the user's head, hand and body, consisting of many tissues with different permittivity, which is much higher than permittivity of free space. Since the field strength and hence the dissipated power is maximal near the antenna, the capability to calculate correctly the near field of the antenna with due account of a presence of a user's body is crucial for results accuracy.

Consider a linear antenna tangent to the user's head, which is modeled by a vertical prolate ellipsoid (Fig. 48a). One may interpret the structure in the capacity of a linear radiator situated along the flat boundary between two half-spaces—between an air with  $\epsilon_r = 1$  and a head with  $\epsilon_r \neq 1$ , as shown in Fig. 48b. It is a crude approximation, because the head dimensions are magnitudes of the order of a wavelength.

The problem of finding the electromagnetic field of a linear radiator, located along the boundary between two media, reduces to calculation of the electrostatic field in a heterogeneous (or more exactly, piecewise-homogenous) medium [14]. Such problem arises if an isolated wire is located at the interface of two media, e.g., air and a dielectric medium with  $\epsilon_r \neq 1$ , as shown in Fig. 48c.

As already mentioned, a structure of the quasi-stationary electrical field of alternating linear currents is like to a structure of the magnetic field, created by constant linear currents. The magnetic field structure coincides with the structure of the electrostatic field of the line charges (principle of correspondence). As is shown in Section 5, an application of a method of complex potential to piecewise homogeneous medium allow us to reduce the electrostatic problem for a heterogeneous medium to a problem for homogeneous medium. This analogy is true in the approximation of the first order of smallness.

The solution for the electrostatic field in a heterogeneous medium is demonstrated by Fig. 48c, where an isolated charged straight wire is located at the interface of two homogeneous media. The field in a two-homogenous medium coincides with the field in a homogenous medium, if to assume that equivalent permittivity can be calculated with help of (5.33).

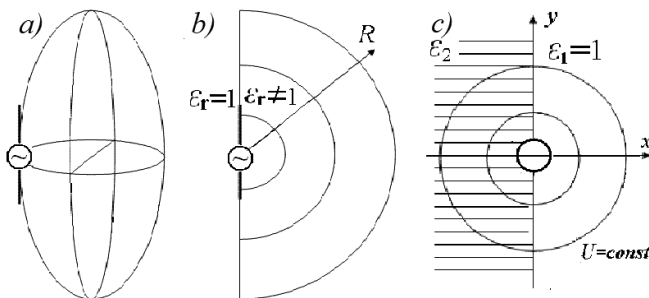


**Fig. 48:** The environment: head and antenna (a), antenna and interface (b), charge and heterogeneous medium (c).

Thus, the field of a linear radiator located at the boundary of two media differs only by a magnitude of relative permittivity. Analysis of a heterogeneous environment that uses a homogeneous medium as an equivalent replacement substantially simplifies calculation of an irradiation power and a factor of loss reduction. The obtained results are verified with the program CST, based on the Moment Method, which allows to consider detailed characteristics, including heterogeneity of a medium.

The relative permittivity of the brain, muscles and skin has similar values and on the average is about 40–50. Only the permittivity of bones differs substantially from this value. Accordingly, equivalent permittivity  $\epsilon_{er}$  of the human tissues and the air is close to 20–25, and the field magnitudes in the vicinity of an antenna, located near the head, can be calculated in a homogenous medium with  $\epsilon_{er}$ . The dark spot dimensions for dipoles of finite length can be determined, using equations (5.77), written for the field of such radiators in the cylindrical coordinates. The dark spot boundary is determined by radius  $\rho_n$ , at which  $n = |E_z/E_{z10}|$  is equal to a given value, where  $E_z$  is the common field and  $E_{z10}$  is the field of the main radiator.

In order to simplify calculation of the factor of loss reduction, assume that the field strength increases linearly from compensation point with the coordinate  $t = 0$  to dark spot boundary, where  $t = t_0$ , so that  $|E_z/E_{z10}| = nt/t_0$ , where  $n = \text{const}$ , and hence the loss power grows in proportion with the square of a distance. If  $s = t/t_0$ , the total power of losses inside the dark spot is given by

$$P = P_0 \int_0^1 (ns)^2 ds = P_0 n^2/3$$

where  $P_0$  is the loss power within the boundaries of dark spot caused by the main radiator in the absence of the auxiliary one. For  $n_0 = 0.2$ , the loss power is smaller by a factor of  $3/(0.2)^2 = 75$  (or 18.8 dB). For  $n_0 = 0.1$  the factor of loss reduction is 300 (24.8 dB), and for  $n_0 = 0.04$  the factor is 1875 (32.7 dB). In practice this factor is equal to roughly a half of the calculated value, since the field within the dark spot has a more complicated structure, i.e., the factor of reduction is approximately equal to

$$P_0/P = 1.5/n_0^2.$$

To find the boundary of the dark spot, one must determine the radius  $\rho_n$  as a function of  $z$  and  $\varphi$ . In Fig. 49 ratio  $n = |E_z/E_{z10}|$  is plotted as a function of  $\rho$  for  $\lambda = 30$ ,  $L = 7.5$ ,  $\rho_0 = 1$  and different values of  $b$  (all dimensions are in centimeters).

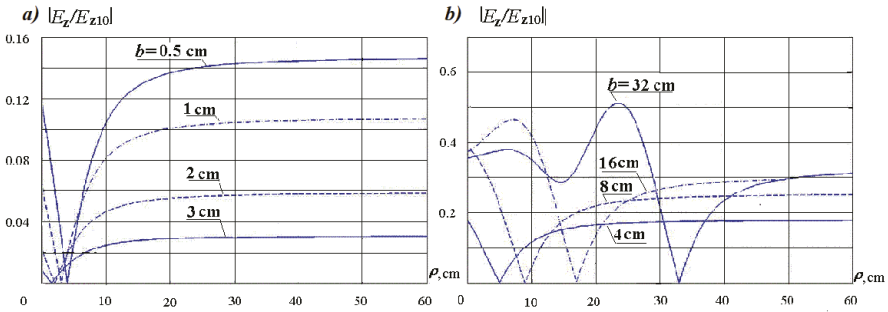


Fig. 49: Change of  $n = |E_z/E_{z10}|$  along the  $\rho$ -axis.

Table 7: The Length of Dark Spot for Different  $b$  and  $n_0$ .

$b$	$n_0 = 0.01$	0.02	0.04	0.07
0.5	3.53	6.80		
1	1.89	3.89	7.67	
2	1.00	2.00	4.17	8.12
3	0.71	1.42	2.91	5.43
$b$	$n_0 = 0.07$	0.10	0.14	0.25
4	4.28	6.58	11.38	
8	2.89	4.29	6.43	49.60
16	2.44	3.56	5.24	23.63
32	2.29	3.35	4.88	11.73

The magnitudes of fields  $E_{z10}$  and  $E_z$  are calculated at  $z = 0$ ,  $\varphi = 0$  by the above formulas. The boundaries of the dark spot in the  $\rho$ -direction, denoted as points  $\rho_1$  and  $\rho_2$ , are found as the intersection points of curve  $n$  with given level  $n_0$ . Along the segment  $\rho_1\rho_2$  (between the points  $\rho_1$  and  $\rho_2$ ),  $n$  is smaller than the required value of  $n_0$ . Length  $\Delta\rho = \rho_2 - \rho_1$  of the segment, i.e., the dark spot length, is presented in Table 7 for different values of  $b$  and  $n_0$ , i.e., for different levels of field reduction at the boundary of the dark spot. One can see from Table 7 that the length of dark spot for given level decreases, when distance  $b$  between radiators increases. But at large distances, when at the boundary of dark spot increases, the length of dark spot increases also. Therefore, for small values of  $b$ , the dip (downfall) of a curve  $n$  becomes narrower and deeper. For great values of  $b$ , the dip of a curve  $n$  is wider.

Figure 50 shows a few examples of the dark spot boundaries in the horizontal plane ( $z = 0$ ) for  $f = 1$  GHz,  $\rho_0 = 1$  cm and different values of  $b$  and  $n_0$ . In the figure, fields  $E_{z10}$  and  $E_z$  are calculated, using equations (1.25) at  $z = 0$  and given angles  $\varphi$ , in the manner like the preceding case. The difference between coordinates  $\rho_1$  and  $\rho_2$ , denoting the start and end of the corresponding segment with  $n \leq n_0$ , determines the length of dark spot in the given direction. From Fig. 50 it is seen that the dark spot width is, as a rule, greater than its length. The spot height is close to its length. This result is particularly important, as it shows, in which direction movements of the head are more dangerous in terms of the growth of the absorbed power.

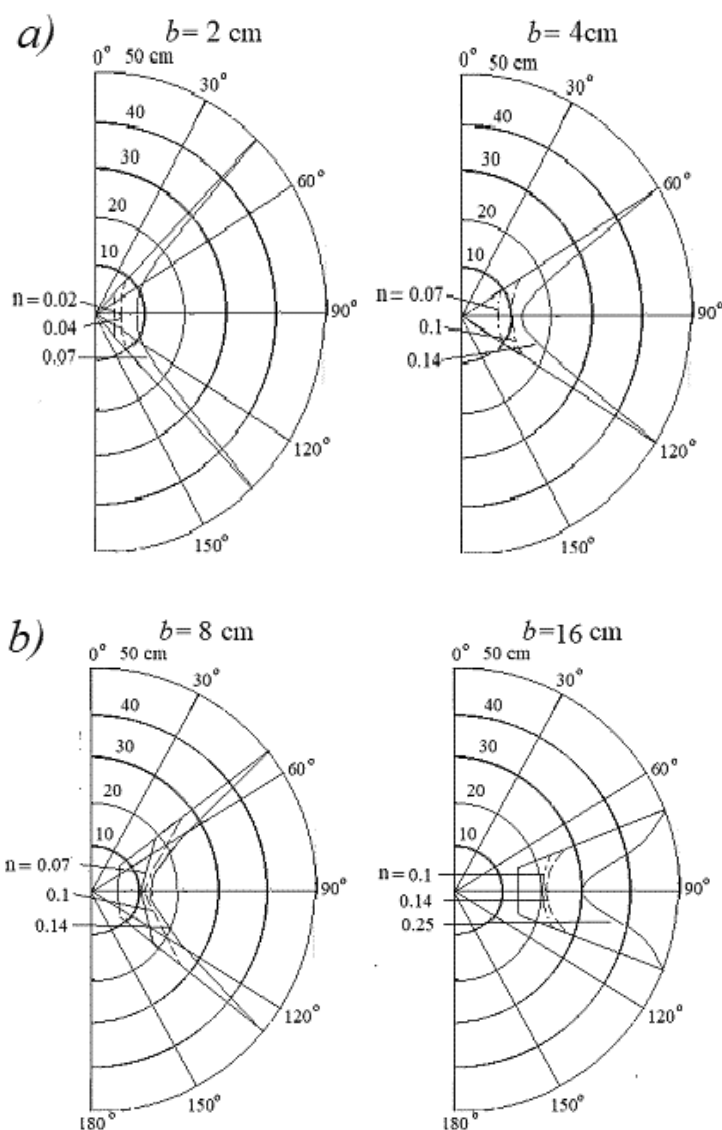


Fig. 50: Boundaries of the dark spot in a horizontal plane.

The calculations also show that at the optimal selection of the relative positions of the radiators and a compensation point, the dark spot volume increases, and the field inside it substantially decreases. One can choose the structure parameters so that the spot dimensions would coincide with the human head dimensions. That will allow to diminish sharply loss power in all of head, and increases a freedom of the user's head movements.

Employing several auxiliary radiators allows increasing the dark spot volume further.

The use of an auxiliary radiator in the compensation method on the one hand allows to reduce the field in the near region and on the other hand must not distort a circular directional pattern in a horizontal plane. Retention of a far field strength and directional pattern is a crucial issue for any method of SAR reduction. To retain the shape of directional pattern and to avoid a deep dip in it along a structure axis, the phases of fields created by the two radiators should not differ by more than a few degrees. The small distance between the antennas and the small difference between the phases of currents created by the generator ensure the preservation of the circular shape of the directional pattern. But to reduce to zero the common field at the compensation point, the fields of radiators at this point must have opposite phases.

If a main radiator current is  $J_{A1}$ , the current of an auxiliary radiator can be equal to  $J_{A2} = J_{A1} D e^{-j\psi}$ , where  $D$  is a ratio of the dipole moments of the radiators, and  $\psi$  is a phase difference between the currents. In this case, the field of an auxiliary radiator is  $E_{z2} = E_{z1} D e^{ju}$ , where  $E_{z1}$  is the main radiator field, and  $u = kl - \psi$ . Here  $l$  is the path difference between rays from the radiators to a point located at angle  $\varphi$  (see Fig. 45). The common directional pattern in a horizontal plane can be written as

$$|F| = |1 + D \exp(ju)| / \sqrt{(1 + D \cos U_m)^2 + D^2 \sin^2 u_m}, \quad (5.81)$$

where  $u_m$  is a magnitude of  $u$  for a maximum denominator. Since  $D$  and  $u_m$  are constant, a denominator of (5.81) is independent of  $\varphi$ . If the directional pattern of main radiator is circular, the ratio of a pattern maximum to its minimum, which is a measure of the pattern distortion is equal to

$$F_{\max}/F_{\min} = |1 + D \exp(iu)|_{\max} / |1 + D \exp(iu)|_{\min} = (1 \pm D)/(1 \mp D), \quad (5.82)$$

where the upper sign applies when  $D$  is positive, and the lower sign applies if  $D$  is negative. It is easy to show that when the maximum of directional pattern differs from the minimum by 6 dB (deviation of 3 dB from the average level), we obtain  $|D| = 0.33$ , and when the difference between the maximum and the minimum is 3 dB, we have  $|D| = 0.17$ .

It is necessary here to explain that cellular communication is not the only area of application where one must create a weak field region near the transmitting antenna. The task is vital, if, for example, a mobile transmitter is in a vehicle close to users and other passengers. Creating a weak field region in such cases is an efficient technique of protecting against irradiation. A problem is often complicated because of the transmitter operation in a broad frequency band. The analysis of directional pattern is essential for this problem, since there is commonly some degree of freedom to choose the antenna location. This helps to keep the undistorted directional pattern.

From (5.80), taking into consideration that  $R_1 = \rho_0 + b$ ,  $R_2 = \rho_0$  (see Fig. 44), we obtain the space  $D = R_2/R_1 = \rho_0/(\rho_0 + b)$ , which reduces to  $\rho_0 = b/\beta$ , where  $\beta = 1/D - 1$ . Let the main radiator be situated on the structure axis, at a distance 3 cm from the head, i.e.,  $\rho_0 + b = 3$ , and the compensation point is placed on the head surface. In this case, if  $D = 0.33$ , then  $\beta = 2$ ,  $\rho_0 = b/2 = 1$ ,  $b = 2$ . If  $D = 0.17$ , we have  $\beta = 4.88$ ,  $\rho_0 = 0.5$ ,  $b = 2.5$ . The results point out the necessity for a tradeoff between the level of irradiation reduction and a directional pattern of a two-antenna structure,



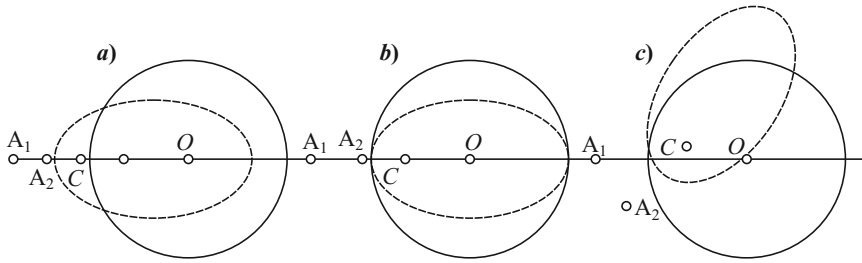


**Fig. 51:** The dark spot: compensation point is located outside (a) and inside (b) the head and outside the symmetry axis (c).

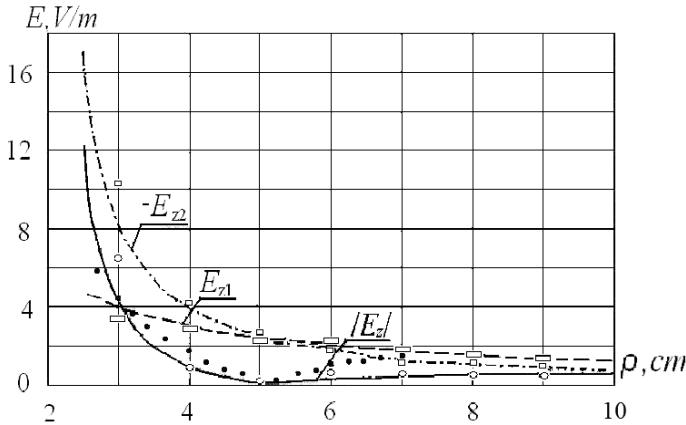


**Fig. 52:** Field strength in the dark spot: comparison of calculation, simulation, and measurements.

especially in cases when the antenna platform is subject to spatial restrictions. However, the changes of directional pattern are predictable and small.

Figure 51 shows three variants of the dark spot position relative to the head (here the dark spot boundaries are given by a dotted line and the head boundary are given by the solid curve). Feed points  $A_1$  and  $A_2$  of main and auxiliary radiators and compensation point  $C$  in Figs. 51a and 51b lie on the structure axis, and so the dark spot is symmetric relative to the axis. Figure 51a has the compensation point placed outside the head, and Fig. 51b has it inside the head, close to its surface. In the latter case, the all-dark spot lies inside a head result in a significant reduction of loss inside the head. Figure 51c corresponds to a case, where an auxiliary radiator is located out of the axis, and the axis of dark spot does not coincide with the structure axis. Such a displacement of a dark spot from the head center may result in the increase of a loss power in it.

Calculation of the dimensions of dark spot were accomplished by the MATLAB program and verified both experimentally and by means of CST program. The simulations were carried out with allowance for the user's head and without that. The results of calculations, simulations, and measurements with allowance for the user's head are given in Fig. 52. The main and auxiliary radiators were located at point  $\rho = 0$  and  $\rho = 2$  cm. The head was placed at a distance 4 cm from the main radiator. The point  $C$  was located at  $\rho = 5$  cm.

Table 8: Level of SAR.

Number of radiators	Figure	Total SAR	Maximal local SAR (in 1g)
1		0,00793	0,166
2	5.51a	0,00257	0,0235
2	5.51b	0,00225	0,0162

As it was said, the calculations were performed in accordance with the MATLAB program. The calculation results are presented in the form of the dashed, dash-dotted, and solid curves plotted for absolute magnitudes of fields  $Ez1$ ,  $Ez2$  and  $Ez = Ez1 + Ez2$  (here  $Ez1$  and  $Ez2$  are the fields of the main and auxiliary radiators,  $Ez$  is the total field). The presence of the head was considered by replacing with  $\varepsilon\varepsilon$ . It is easy to be convinced that in the interval from  $\rho = 4$  to  $\rho = 10$  cm the field  $Ez$  is substantially less than the field  $Ez1$ .

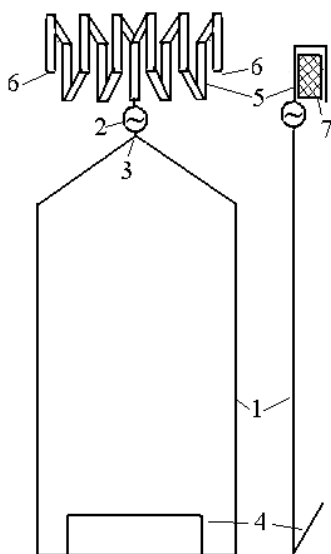
The simulation was performed by means of the CST program. The rectangles, squares and empty circles are the simulation results (model of the head is included in the CST program). The measurements of the common field  $Ez$  were carried out in laboratory conditions; they are presented with dark circles. The presence of the user's head was considered. If the user's head is absent, the results of calculations, simulations and measurements are in good agreement. However, as one might expect from the approximate estimation of  $\varepsilon\varepsilon$ , the coincidence between the results with allowance for the head is not too good, but a qualitative agreement exists.

Table 8 shows the total and maximum local SAR (in W/kg) with the auxiliary radiator and without it. The compensation points are in accordance with Figs. 51a and 51b. The maximal absorbed power and the maximal local SAR exist near the main radiator and the maximal reduction of the loss power occurs here, too. The obtained results show that under realistic conditions the compensation method allows to reduce the power absorbed by the head three to four times as well as to reduce the maximal local power five to ten times. The distortion of directional pattern due to the auxiliary antenna is relatively small provided that this antenna is properly located.

## 11. New Antenna for a Personal Cellular Phone

Cellular communication imposes high requirement for antenna of personal phone and at the same time limits the possibility of its installation. An increase in the number of subscribers requires using several high frequency bands, and accordingly installation of separate antennas (one for each band). One can use a single antenna, but it must be very wideband and that complicates greatly the task. In addition, cell phones support the diversity of applications, which require placing many components and devices into the phone housing. These circumstances lead to space constraints and leave a small area for the antennas. Extensive use of mobile phones may lead to potential health risk as a result of the impact of irradiation on human organism.

A new antenna, which is presented in this section, offers a possible solution to the described problems. The structure of the offered antenna is shown in Fig. 53. It is an asymmetrical dipole, which is excited by a generator 1 at a feed point 2.



**Fig. 53:** The equivalent circuit of the antenna.

The lower arm of the dipole is a metal plate 3, to bottom edge of which a small plate 4 is attached at an acute angle. The upper arm is a multi-folded structure 5, open at the ends (at points 6). It is excited at its mid-point. A dielectric plate 7 is located inside this structure.

The first distinction of the offered antenna from the known antennas is the use of the phone's ground (chassis) as a radiator. This suggestion was made in [26]. The phone's ground is a rectangular metal plate, whose length is close to a quarter of a wavelength at the main operating frequency. The offered design permits to unite an antenna with the ground, removing the need for installation of a separate antenna and a special metal counterpoise. Components of radio transmitter and receiver can be mounted at the metal antenna, which replaces the ground for these elements. Filters, placed on the plate, may provide a short circuit for direct currents and insulation (the gap) of circuit at high frequency.

The second distinction of the offered antenna is implementation of the top arm in the shape of a multi-folded radiator (meander). This arm has a small height. Its contribution to the antenna's radiation is small, but it allows to match the antenna to a cable or a generator. The reactive component of its impedance compensates the reactive component of the lower arm, providing serial resonances at operating frequencies. Its complex structure provides many degrees of freedom, including number of sections, their dimensions, the width and thickness of the wires, types, and magnitudes of concentrated loads. This permits to change the input reactance of the antenna in wide limits and provide operation at few bands of frequencies.

The third distinction of the offered antenna is the use of special measures for decreasing the field in its near region and corresponding reduction in the irradiation of the user's head (reducing SAR). These special measures are firstly the multifolded radiator 5 with the dielectric insert 7 and secondly, a small metal plate 4. The multi-folded radiator is fabricated in the shape of a three-dimensional structure

that protrudes in the direction of the user's head. The dielectric plate is inserted between the wires of this structure. The short metal plate is attached to the bottom edge of the lower arm. These structures create anti-phase currents in the antenna and hence small auxiliary fields, which compensate for the main field at a certain point (compensation point) and form around this point an area of a weak field (a dark spot).

The multi-folded structure 5 is more sensitive to external objects and actions than plate 3. To reduce the impact of the user's hand, it is expedient to apply the plate as the lower arm of the antenna, and the multi-folded structure as the top arm. The user's hand in this case will lie on the handset housing not far from the plate, but further from the meander. It is the fourth distinction of the offered antenna.

The input impedance of an asymmetrical dipole, consisting of two different arms, in the first approximation, is equal to half the sum of input impedances of two symmetrical radiators: one with arms identical to the lower arm of the asymmetrical dipole, and the other radiator with arms identical to its top arm [5]. This relation is exact for the reactive component  $X_A$  of the antenna input impedance and approximate for the active component  $R_A$ . At that

$$X_A = X_{A_1} + X_{A_2}, R_A \approx R_{A_1} + R_{A_2}, \quad (5.83)$$

where  $X_{A_1}$  and  $R_{A_1}$  are respectively the reactive and resistive components of the input impedance of the lower arm (Fig. 54a), and  $X_{A_2}$  and  $R_{A_2}$  are corresponding components of the input impedance of the top arm (Fig. 54b).

The lower arm of the offered antenna is a monopole realized as a wide metal plate with a length  $L_1$  and a width  $d$ . Such an antenna is named a strip monopole. Its characteristics are like those of a linear cylindrical radiator with a circular cross-section of a radius  $a_e$ . As is shown in [21] this radius  $a_e$  in the first approximation is equal to  $d/4$ . As said in Section 2.7 cylindrical radiator with a circular cross-section of radius  $a_e$ . As is shown in [27] this radius  $a_e$  in the first approximation is equal to  $d/4$ . It is also considered that its magnitude is a trade-off and may be used during calculation of the input impedance and the scattering characteristics of the radiator [21]. The input impedance of the monopole in the first approximation is equal to

$$Z_{A1} \cong R_{A1} - jW_1 \cot k L_1. \quad (5.84)$$

Here  $W_1 = 30\Omega$  is the wave impedance of the monopole,  $\Omega = 2 \ln (2L_1/a_{e1})$  is the parameter of a theory of linear antennas,  $R_{A1}$  at frequencies near a first series resonance is close to 40 Ohm. When  $d \cong L_1/2$ , then  $a_{e1} = L_1/(2\pi)$ , and  $\Omega = 2 \ln(4\pi) \approx 5$ .

For good matching, it is expedient to realize a region of monopole's excitation in the shape of a flat triangle (see Fig. 54a). It is the transition from the wide plate of antenna to the inner conductor of a coaxial cable. Calculations show that the wave impedance of a tapered line is close to the standard cable's wave impedance, when the angle at the vertex of the tapered plate is close to  $80^\circ$ .

The upper arm of an antenna in the first approximation may be considered as a multi-folded radiator, mounted on a metal plate (see Section 1.7 of Chapter 1). The current in each wire can be divided into in-phase and anti-phase components. This system is reduced to an aggregate of a radiating linear antenna (monopole) and few non-radiating long lines. The multi-folded radiator can be executed either with shorting to the ground or with a gap (see Fig. 54b). In the latter case the input

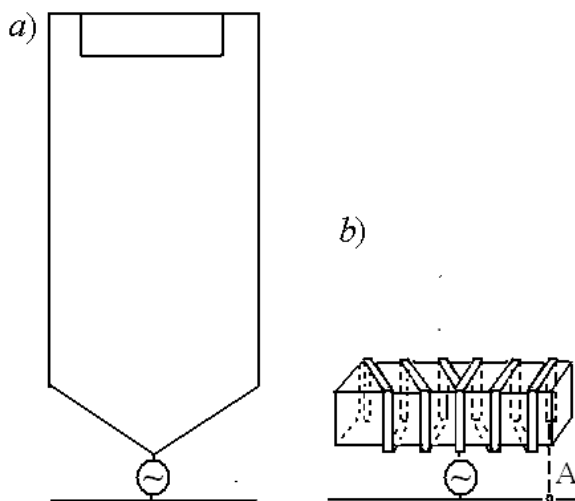


Fig. 54: The lower (a) and the top (b) arms of the asymmetrical dipole.

impedance of the multi-folded radiator is a series connection of a monopole and the two-wire long lines, shorted at their ends. The expressions for the input impedances  $Z_{A2}^{(n)}$  of these antennas with a different number  $n$  of wires are presented in Section 1.7.

As can be seen from these expressions, the radiation's resistance of the given antenna is equal to the radiation's resistance of a monopole with the same height. The reactive component of its input impedance has additional resonances, and the first parallel resonance is defined by a line of length  $SL/2$ , i.e., its frequency is smaller approximately by a factor  $S/2$  in comparison with the frequency of the first series resonance of an ordinary monopole with the same height. The frequency of the first series resonance of a multi-folded antenna is still smaller, approximately twice. Such a type of an input impedance simplifies selecting dimensions of a structure, whose series resonances coincide with the given operating frequencies. Thus, in this case the monopole's effective length is

$$h_e = \left( \frac{1}{k} \right) \tan \left( \frac{kL_1}{2} \right) + L_2/2, \quad (5.85)$$

where  $L_2$  is length of an upper arm. If, for example,  $kL_1 = \frac{\pi}{2}$ ,  $L_2 = L_1/4$ , then  $h_e = \frac{1}{k} + L_1/8$ .

Accordingly, the radiation resistance of the antenna is

$$R_\Sigma = 20k^2 h_e^2 = 20(1 + \pi/16)^2 \approx 29. \quad (5.86)$$

From that the radiation's resistance of the monopole (of the metal plate) mainly determines the antenna's resistance overall, i.e., this resistance is close to 30 Ohm, if the operating frequency is close to the frequency of a first series resonance. Contribution of the upper arm to a resistance is small as compared with contribution of the lower arm. But the reactance of a monopole is close to zero, if the plate length is equal to a resonant length, i.e., if it is close to  $\lambda/4$ . Therefore, to ensure matching with a cable or generator, an upper arm should have a series resonance at a first

operation frequency. Accordingly, the reactance of the upper arm of a multiband antenna should compensate the monopole reactance at other operation frequencies.

The directional pattern of an antenna in the horizontal and vertical planes does not differ from a typical directional pattern of monopole, since the radiation of the long lines can be neglected, provided the distances between the wires are small. The analysis of the considered antenna demonstrates that its structure firstly allows to obtain the series resonances at required frequencies. Secondly, the considered antenna contains a radiating element of large length, close to  $\lambda/4$ , and that permits to provide an effective radiation and reception of signals.

If the multi-folded antenna is shorted to ground at points A, its input admittance is equal to

$$Y_{A2}^{(S)} = 1/[4Z_{A2}^{(S/2)} + 1/[j120 \ln(b/a) \tan(SkL/2)]]], \quad (5.87)$$

where  $Z_{A2}^{(S/2)}$  is the input impedance of an antenna with a gap, whose conductors consist of two wires. Therefore, in this case, the input impedance is a parallel connection of two impedances: the impedance of  $S/2$ -folded radiator with a gap and the impedance of a close-end line of length  $SL/2$ . Such type of input impedance complicates selecting dimensions of a structure.

To produce a small auxiliary field with the aim to compensate a main field in the user's head without changing the distant field, it is expedient to use the multi-folded structure, which protrudes toward the user's head. This structure allows to create an anti-phase field in the near region of an antenna and to nullify the total field at a compensation point, located not far from the neighboring edge of the user's head. Around the mentioned point an area of a weak field (a dark spot) is created. We shall demonstrate this effect by means of the folded radiator with a gap in a point A.

This point is located along a plane passing through the compensation point and placed on the side of the phone housing near to the head.

The folded radiator consists of two parallel wires. If to connect two current's generators of equal magnitude  $J/2$  and opposite directions to the bottom of a the right wire in parallel with each other and to divide the main generator into two parallel generators, equal in magnitude (to  $J/2$ ) and coinciding in direction, then, as a result, voltages and currents of this circuit do not change. According to the superposition principle, the voltage and the currents at each point are equal to the sum of the voltages and the currents, produced by all generators. Therefore, as shown in Fig. 55, one can divide the considered circuit on to two circuits with two generators in each and then calculate and sum of the currents in any wire of each circuit. The left circuit is a linear radiator (monopole), the right circuit is a two-wire long line.

The current in each wire consists of an anti-phase current of the line and the component of the in-phase current in the linear radiator. In Fig. 56 the currents' distribution along the wires is presented: the distribution of the in-phase currents  $J_1^{(in)} = pJ$  and  $J_2^{(in)} = mJ$  along wires 1 and 2 of the monopole (a), the distribution of the anti-phase current  $J_1^{(an)} = mJ$  and  $J_2^{(an)} = mJ$  along the wires of close-end line (b) and the total currents' distribution (c).

The in-phase currents in both wires are distributed by sinusoidal law; the ratio of their magnitudes depends on the wire capacitances, for identical wires

the magnitudes are equal. The anti-phase currents are the same in magnitude, but opposite in sign and are distributed by cosine law. In the first wire the currents are added, since they have the same sign. In the second wire they are opposite in sign, and under these conditions the dipole moment of negative current is greater due to cosine distribution. This gives a possibility for compensation of the fields, created by the wires' currents. The total current of the second wire is less than the total current of the first wire. But since the second wire is located nearer to the compensation point, then, although the wires' currents are different, their fields at the compensation point are the same in magnitude.

This effect is better pronounced if, firstly, the folded radiator is replaced by a multi-folded structure, and, secondly, if a dielectric plate is placed between the wires. In this case the field of the first wire is attenuated quicker with the wires spacing. As a result, firstly, one can decrease this distance, i.e., decrease the thickness of phone housing. Secondly, the electric lengths of the long lines increase, i.e., one can decrease geometric lengths of lines, for example, to excite the multi-folded structure in the middle of its width and not at a side point.

The additional anti-phase current is produced by the small plate 4 (see Fig. 53).

It should be emphasized that the structure without a connecting bridge between the upper ends of the wires consists from a monopole and an open-end two-wire line. In this case, the total current of the second wire is zero, and hence the compensation of the field of a first wire is not possible.

It is useful to compare the characteristics of the proposed antenna with the characteristics of a symmetrical dipole. As previously indicated, if the lengths  $L_1$  and

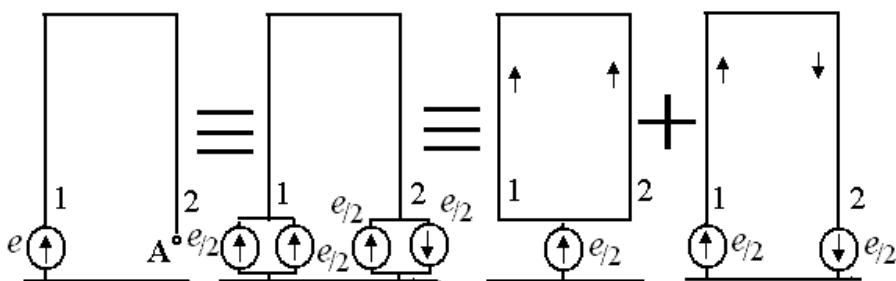


Fig. 55: Division of the folded radiator into two circuits.

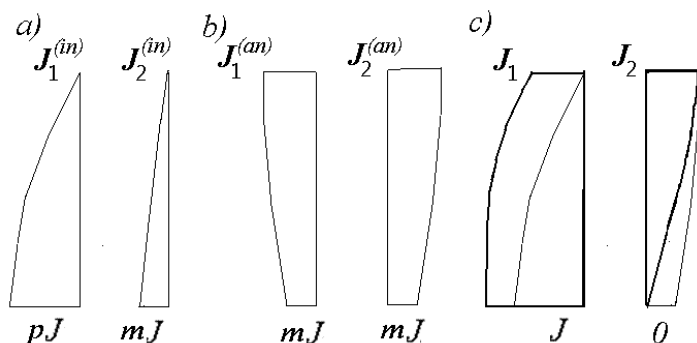


Fig. 56: The distribution of in-phase (a), anti-phase (b) and total (c) currents.

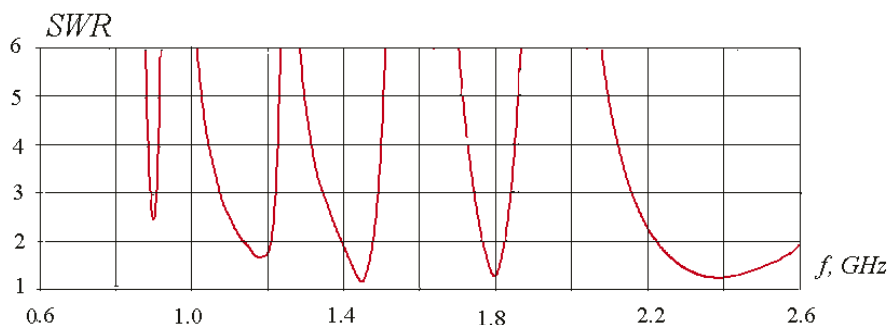


Fig. 57: Standing wave ratio of the proposed antenna.

$L_2$  of the lower and upper arm of the described antenna are equal, respectively, to  $\lambda/4$  and  $\lambda/16$ , the active component of an input impedance is close to 30 Ohm, and the reactive component is close to zero. The phone housing with such a length allows us place a symmetrical dipole with arm length  $\lambda/8$ , which is smaller twice. Its resistance is equal to

$$R_{\Sigma} = R_{\Sigma 0}/n^2, \quad (5.88)$$

where  $R_{\Sigma 0} \approx 80$  Ohm is the active component of the resonant dipole's input impedance, and  $n = 2$ . From (5.88) it follows that in this case  $R_{\Sigma} \approx 20$  Ohm.

It is more substantial that the dipole impedance has a reactive component, which increases the losses in a cable much stronger than the low value of  $R_{\Sigma}$ . If the length of a dipole arm is  $\lambda/8$ , its input reactance is equal to a wave impedance. Let us take a relatively small wave impedance of 100 Ohm. It is easy to be convinced that in this case travelling wave ratio (TWR) in the cable with  $W = 50$  Ohm is equal to 0.08, while TWR for a monopole with resistance 30 Ohm and zero reactance in the same cable is 0.6, i.e., 7.5 times greater. This example shows the obvious advantage of the proposed antenna, resonant dimensions of which fit into the dimensions of the phone chassis.

Simulation of the proposed antenna was executed using the CST program, and the results were compared with the results of the planar inverted F antenna (PIFA). The results of tuning are given in Fig. 57, where the standing wave ratio (SWR) of the proposed antenna is shown. The calculated results of reducing field in a near zone in the given direction by means of the proposed antenna are presented at Fig. 58. Here the fields of an antenna are shown at frequencies 0.9 and 1.8 GHz depending on the distance  $S$  from its plane are shown along a line perpendicular to this plane in two directions: a solid curve—in the direction of decreasing field (towards the dark spot), a dotted curve—in the opposite direction. Figure 58a demonstrates the calculation results for the antenna located in the air. The results obtained with allowance of the model of a head are given in Fig. 58b. The calculation uses the model of a head as part of the program CST. As is seen from figures, the fields in the required direction essentially decreases.

A full-scale model of the new antenna was fabricated in accordance with results of the calculation. In Fig. 59 the calculated and experimental values of an antenna



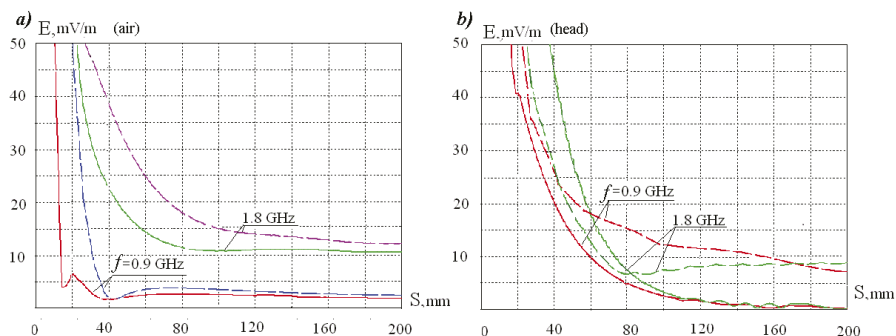


**Fig. 58:** Field in the near region of antenna in the presence of user's head as a function of distance  $S$  from the antenna plane.

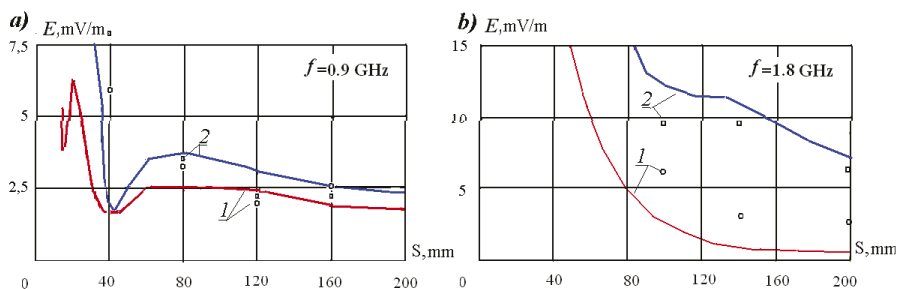


**Fig. 59:** Near field at a frequency 0.9 (a) and 1.8 GHz (b) in direction of a head (1) and in the opposite direction (2).

near field in the direction of a head (this curve is denoted by the number 1) and in the opposite direction (curve 2) at the frequency 0.9 and 1.8 GHz are compared. As can be seen from the Figure, the field of the antenna in the direction of the head is substantially smaller. The experimental values were determined by means of measurement in the phantom model.

The directivity of the offered antenna is presented in Table 9. In Table 10 the level of SAR in the user's head is shown for the proposed antenna and antenna *PIFA* at a frequency 0.9 GHz.

The proposed asymmetrical antenna with the long arm and zero reactance on the operating frequencies has high electrical characteristics and creates in the far region the electromagnetic field, which exceeds significantly the field of the other antennas of the same dimensions. In particular, the field of the new antenna at the same transmitter power is much greater than the field of antenna *PIFA*. The results of researching the new antenna, including simulations and experimental tests, corroborate that this antenna is promising for use in modern cellular phones. In contrast to known antennas this antenna is multi-frequency, i.e., it can operate on multiple frequencies simultaneously and has high electrical characteristics, since it provides without switching frequency, good match with the cable and correspondingly high efficiency.

**Table 9:** Directivity of the Proposed Antenna.

Frequency, GHz	Directivity, dB
0.9	2.59
1.8	4.48

**Table 10:** SAR of Antennas.

Antenna	$f$ , GHz	Total	Max local in 10 g	Max local in 1 g	Max point
<i>PIFA</i>	0.9	0.061	3.62	5.8	345.8
Proposed	0.9	0.013	0.762	1.41	21.6

Additional advantage of this antenna is reducing the user's head irradiation, since this antenna uses the new method for its reducing. It should be emphasized that this method may be used for reducing the irradiation produced by other antennas.

## 12. Struggle with Environmental Influences

Application of the compensation method, described above, under realistic conditions often meets with difficulties, since the operation of a complicated radiating structure is disrupted by various external influences, caused by changes in the environment. At times, approaching of the metallic objects to the antenna or insignificant displacement of the antenna elements as consequence of user's movement results in a tuning disturbance. In such cases, the compensation point may be displaced and the field inside the dark spot can grow significantly. The disturbances are to be counteracted. As an example of the external action, we consider the impact of metallic objects approaching to an antenna.

To eliminate the consequences of the influence, one can try to retain the amplitudes and phases of the driving voltages and currents (the first method) or prevent the change of the radiator fields (the second method). But it should be noted, first, that the appearance of a metal body near a radiator changes the current at all points along the radiator, whereas the feedback circuits can adjust the current only in a single point in each radiator, e.g., at its input. And, second, one must say that a metal body causes different changes of the radiator fields in the entire space, whereas the feedback circuits can adjust the field only in one or two points. Therefore, the efficiency of both methods, especially of the first one, is inherently limited. This section is devoted to the comparative analysis of efficiency of both methods. It should be emphasized that the analysis considers cases of severe distortion in antenna systems.

The circuit of the regarded antenna system is given in Fig. 60. The system consists of two monopoles (A is the main radiator; B is the auxiliary radiator), which are mounted on a metal plate near the model of a human head. The compensation point is located inside the head, near its front boundary. Dimensions in the figure are indicated in centimeters. Figure 61 shows the same circuit for the case, when a vertical metal sheet in the shape of a square is placed not far from the antenna system (at the distance 0.5 m from the radiators). The metal sheet in the proximity to a

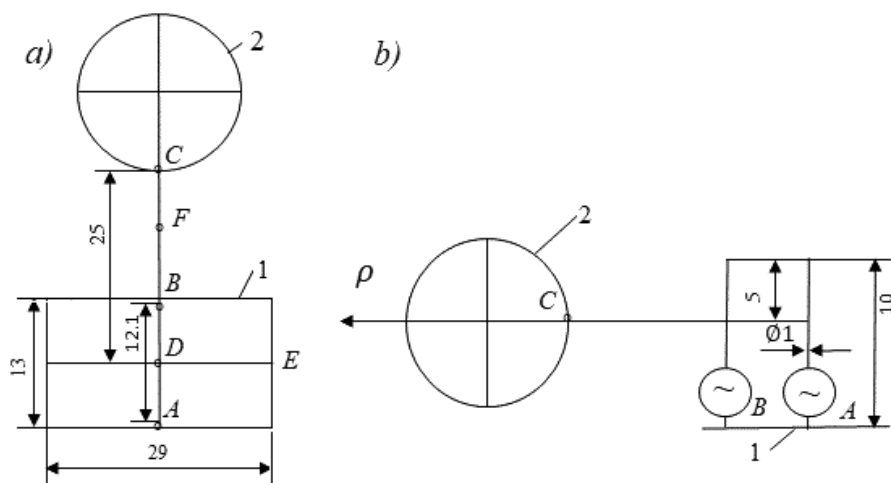


Fig. 60: Circuit of antenna system near the model of a human head: top view (a) and side view (b).

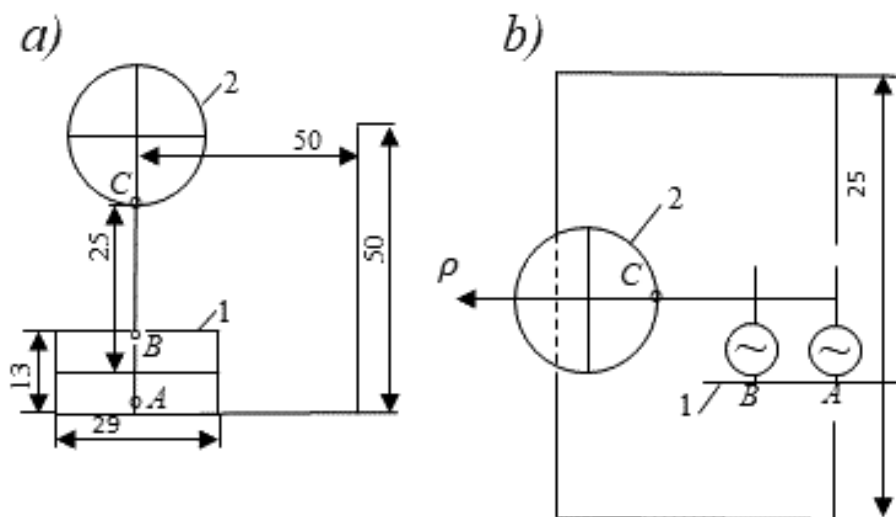
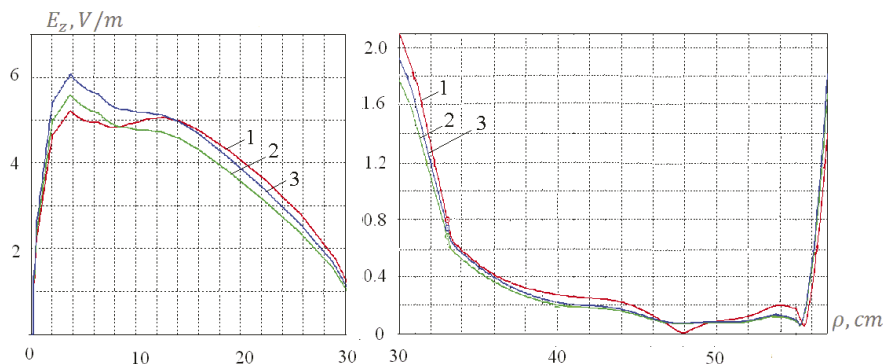


Fig. 61: A metal sheet, placed not far from the antenna: top view (a) and side view (b).

cellular phone may appear, e.g., when a phone's user enters an elevator or a car. The metal sheet affects the antenna system and causes the growth of fields in the zone of a weak field.

Let us start with the relatively simple system with a single radiator. The input current of a single radiator in the absence of the metal sheet is  $J_{A1} = e_A / Z_A$ , where  $e_A$  is the electromotive force, and  $Z_A$  is the input impedance of the radiator. The metal sheet changes an input impedance of the radiator and makes it equal to  $Z'_A$ . To avoid the current change in the radiator base, one must change the emf at its input to the magnitude

$$e'_A = J_{A1} Z'_A = e_A Z'_A / Z_A. \quad (5.89)$$



**Fig. 62:** The field of the single radiator  $A$  in the absence of (1) and the presence of (2) the metal sheet and after regulation of the emf (3).

For a single radiator of height 10 cm and diameter 1 cm we have:  $e_A = 1$ ,  $Z_A = 38.6 + j12.8$ ,  $Z'_A = 41.7 + j14.3$ ,  $e'_A = 1.09 \exp(j0.0145)$ . Figure 62 shows the field of single radiator  $A$  along the horizontal line, passing through the radiator and the center of the head in the absence (1) and presence (2) of a metal sheet and after regulation of the emf (3). Figure 62 and following figures were divided into two parts in order to use the different scales.

In the case of two radiators, one must first calculate the amplitude and the phase of the emf of the second radiator, which ensures the field compensation at a given point. For this purpose, one must excite both radiators by emf  $e_1$ , calculate the fields  $E_1$  and  $E_2$  of each radiator at the compensation point and use emf  $e_2 = -e_1 E_1/E_2$  as emf for the second radiator. It should be noted that the field and the input impedance of each radiator are calculated in the presence of another radiator, whose input is grounded.

Calculations were performed with the CST program, which permits to simulate the total circuit of both generators and to find the self-impedances  $Z_{11}$  and  $Z_{22}$  of each radiator and their mutual impedance  $Z_{12}$ . The solution of the set of two equations  $e_1 = J_1 Z_{11} + J_2 Z_{12}$  and  $e_2 = J_2 Z_{22} + J_1 Z_{12}$  allows to find currents  $J_1$  and  $J_2$ . The metal sheet changes the self- and mutual impedances of the radiators. To avoid the change of the currents at radiators bases, the emfs must be changed to

$$e'_1 = J_1 Z'_{11} + J_2 Z'_{12}, \quad e'_2 = J_2 Z'_{22} + J_1 Z'_{12}, \quad (5.90)$$

where the new impedances are marked by primes. Calculating the new emfs, we may find the new fields and ascertain the regulation results.

For two radiators of the same dimensions, we at first obtain  $e_1 = 1$ ,  $E_1 = 0.48 \exp(j1.11)$ ,  $E_2 = 1.09 \exp(j2.54)$ , i.e.,  $e_2 = 0.44 \exp(j1.71)$ . Accordingly in the compensation mode we obtain for impedances:  $Z_{11} = 37.3 + j16.2$ ,  $Z_{22} = 39.5 + j16.8$ ,  $Z_{12} = 0.67 - j28.9$ , and for currents:  $J_1 = 0.013 - j0.0008$ ,  $J_2 = 0.0064 + j0.018$ . The results of impedances regulation are followed:  $Z'_{11} = 40.6 + j17.1$ ,  $Z'_{22} = 42.0 + j18.9$ ,  $Z'_{12} = 2.04 - j28.02$ , and for emfs:  $e'_1 = 1.04 \exp(j0.04)$ ,  $e'_2 = 0.51 \exp(j1.7)$ . The calculated curves for the fields of the two-radiator structure are presented in Fig. 63.

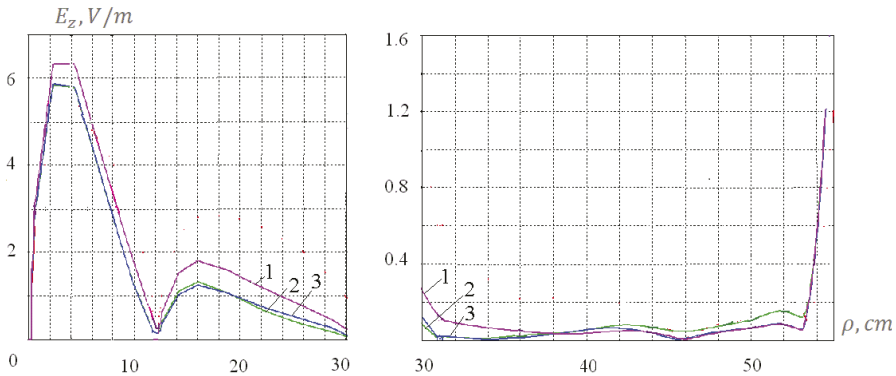


**Fig. 63:** The field of two radiators in the absence of (1) and the presence of (2) the metal sheet and after regulation of the emf (3).

The verification of regulation results involves computation of fields along the horizontal line, passing through the radiators and the center of the user's head, as well as calculation of the total SAR and the local SAR (in 1 g). The results, obtained for the single radiator and for the structure from two radiators when the metal sheet is absent or present and after regulation of the emfs in accordance with expressions (5.89) and (5.90) are compared to each other.

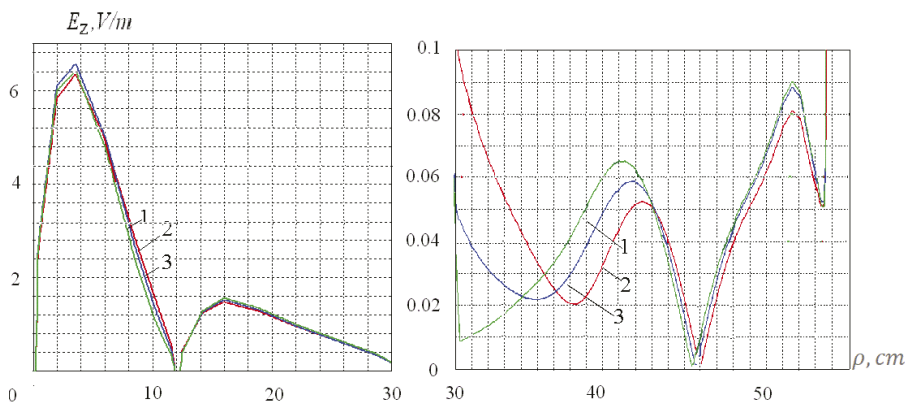
The total SAR and the maximal local SAR for the corresponding cases are given in Table 11. The calculated amplitudes of field at the compensation point are also given in Table 11. The maximal level of SAR and the fields are presented in W/kg and in V/m, respectively. As one can see from the table and figures, the results indicate the rather low efficiency of the correction method, based on retaining the exciting currents in the bases of radiators.

The implementation of the second method calls for use one radiator as a measuring antenna and the second radiator as a local transmitting antenna (i.e., as a field source), or using in turn both radiators as a measuring and a transmitting antenna, or using the third radiator as a measuring antenna. The third radiator may be mounted at any suitable and convenient place. The regulation is performed in the following way. The field at the receiving point is measured in the presence of a metal sheet and is compared with its magnitude in the absence of the metal sheet (i.e., in the compensation mode), and afterwards the emf of transmitting antenna is changed with the aim to get the initial value of the field.

The results of such regulation are given in Fig. 64 and Table 12 for the following variants: (1) the main antenna is used as the transmitting and the auxiliary antenna is used as the receiving one, (2) the opposite case: the main antenna is used as the receiving, whereas the auxiliary antenna is used as the transmitting one, (3) both emfs are replaced. Figure 65 and Table 12 present the results of field regulation, using the third antenna located in the center of a metal plate, i.e., at point D (see Fig. 61) for the following variants: (4) the emf and the field of the main antenna is changed so that its field at point D becomes equal to its original field (before distortion), (5) the field of the auxiliary antenna is changed for this purpose, (6) the fields of both antennas are changed.

**Table 11:** SAR and Field at Regulation of emf in Accordance with Currents.

Characteristic	Total SAR	Local SAR	Field	Total SAR	Local SAR	Field
	one radiator			two radiators		
Sheet is absent	$4.5 \cdot 10^{-5}$	$1.54 \cdot 10^{-3}$	0.79	$1.4 \cdot 10^{-5}$	$0.3 \cdot 10^{-3}$	0.0029
Sheet is present	$2.8 \cdot 10^{-5}$	$0.29 \cdot 10^{-3}$	0.68	$1.7 \cdot 10^{-5}$	$0.11 \cdot 10^{-3}$	0.0044
With regulation	$3.4 \cdot 10^{-5}$	$0.34 \cdot 10^{-3}$	0.74	$2.1 \cdot 10^{-5}$	$0.18 \cdot 10^{-3}$	0.1214

**Fig. 64:** The fields of the structure from two radiators after emf regulation based on the fields, received from by these radiators.

As one can see from Table 12 and Fig. 64 and 65, the method, based on the measurement of the fields, demonstrates a higher efficiency. But acceptable results are obtained only at application of variant 6. Other variants, including placement of the third antenna at points *E* and *F* (see Fig. 61), do not give satisfactory results. And the monitoring signal is a weak signal that serves as the signal of feedback for both the main and auxiliary radiators. Therefore, proper regulation by both methods requires that no signal from the transmitter impinges on the measuring antenna during the measurements of field.

To prevent the changes of field under external actions (e.g., at the approach of a metallic object), one may use a manual or an automatic regulation. Figure 66 gives the block diagram of an automatic regulation. It contains transmitter 1, main radiator  $A_1$  and auxiliary radiator  $A_2$ , connected to the transmitter through the power divider 2, the amplitude controller 3 and the phase shifter 4. The amplitude controller and the phase shifter provide the initial tuning and the field compensation at a given point. The amplitude controller is usually implemented by means the potentiometer, and the phase shifter is implemented by means the delay line, the low-pass filter, or the high-pass filter. Two circuits, consisting of the amplitude controllers 13 and 15 and the phase shifters 14 and 16, provide two reference signals for the radiators  $A_2$  and  $A_1$ , respectively.

The external action (e.g., an approach of a metal body) changes the phases of the signals of the both radiators, received by antenna. The phase detector 7 compares in

**Table 12:** SAR and Field at Regulation of emf in Accordance with Fields.

Variant	Total SAR	Max. Local SAR	Field
1	$1.99 \cdot 10^{-5}$	$0.137 \cdot 10^{-3}$	0.035
2	$1.83 \cdot 10^{-5}$	$0.151 \cdot 10^{-3}$	0.070
3	$2.02 \cdot 10^{-5}$	$0.152 \cdot 10^{-3}$	0.052
4	$1.57 \cdot 10^{-5}$	$0.102 \cdot 10^{-3}$	0.070
5	$1.45 \cdot 10^{-5}$	$0.125 \cdot 10^{-3}$	0.130
6	$1.18 \cdot 10^{-5}$	$0.090 \cdot 10^{-3}$	0.047

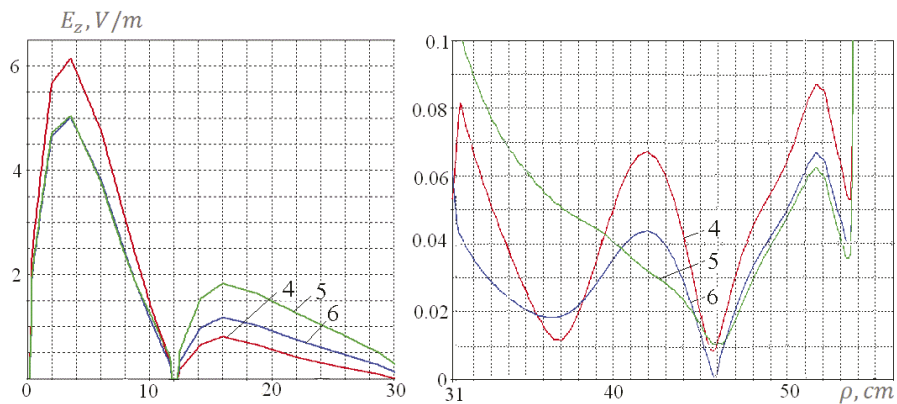


**Fig. 65:** The fields of the structure from two radiators after emf regulation, based on the fields, received by a third radiator.

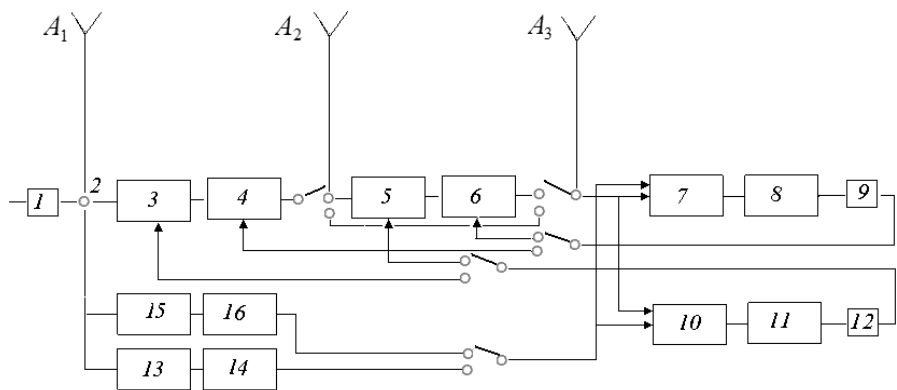


**Fig. 66:** Block diagram of the automatic regulation, based on the constancy of fields.

turn these phases with phases of the reference signals and produces an error signal, proportional to the difference of the said phases. Low-pass filter 8 removes short-term fluctuations of the error signal. The error signal passes through amplifier 9, controls the phase shifters 4 and 6 and brings up the optimal phase differences. As it can be seen from Fig. 66, a feedback circuit is constructed, and it provides a phase self-tuning action, like action of a phase locked loop (PLL).

The second feedback circuit is used for predicting the optimal signal amplitudes. It is like an automatic gain control (AGC) circuit. The input signal of radiator  $A_2$  is compared in amplitude by comparator 10 (operational amplifier) with the reference signal. Low-pass filter 11 removes short-term fluctuations of the signal at the comparator output. The error signal passes through the amplifier 12, controls the amplitude controller 3 and brings up the amplitudes' relationship to the optimal ratio.

As a result, two feedback circuits allow optimizing the amplitude relationship and the phases of the emf, feeding main radiator  $A_1$  and auxiliary radiator  $A_2$ . In contrast to the conventional automatic gain control circuits, the amplitude difference, and the phase difference of the two different radiator signals are not zero in this case.

The obtained results show that it is possible to automatically adjust a complicated antenna system under conditions of intensive disturbances. The proposed method, based on measurement of the fields, demonstrates a higher efficiency. It allows to obtain acceptable practical results under severe disturbance of the antenna system operation even in cases, when (as in our example) the zero field is not achievable.

## References

- [1] Popovic, B.D. (1973). Theory of cylindrical antennas with lumped impedance loadings. *The Radio and Electronic Engineer*, 3: 243–248.
- [2] Djordjevic, A.R., Popovic, B.D. and Dragovic, M.B. (1979). A method for rapid analysis of wire antenna structures. *Archive fur Electrotechnik* (W. Berlin), 01: 17–23.
- [3] Richmond, J.H. (1966). A wire-grid model for scattering by conducting bodies. *IEEE Transactions on Antennas and Propagation*, AP-14(6): 782–786.
- [4] Lavrov, G.A. (1975). *Mutual Effect of Linear Radiators*. Moscow: Communication (in Russian).
- [5] Perini, J. and Buchanan, D.J. (1982). Assessment of MOM techniques for shipboard applications. *IEEE Transactions Electromagnetic Compatibility*, 1: 32–39.
- [6] Levin, B.M. and Fominzev, S.S. (1984). Influence of cylindrical re-radiator on parameters of an antenna and antenna array, *Radiotechnics and Electronics Engineering*, 29(11): 2140–2147 (in Russian).
- [7] Levin, B.M., Fradin, A.Z. and Yakovlev, A.D. (1993). Using loads in wire antennas to obtain given characteristics. *Proc. of Intern. Symposium on Electromagnetic Compatibility*. St.-Petersburg (USSR), 1: 319–322.
- [8] Levin, B.M. (2019). *Wide-range and Multi-frequency Antennas*. London, New York: CRC Press.
- [9] Levin, B.M. (1998). *Monopole and Dipole Antennas for Marine-Vehicle Radio Communications*. S.-Petersburg: Абрис (in Russian).
- [10] Levin, B.M. (1995). Asymmetric radiator at the edge of the wedge (of the ship deck). *Proc. Intern. Symposium on Electromagn. Compatibility and Electromagn. Ecology* (S.-Petersburg): 35–36 (in Russian).
- [11] Thiele, G.E. and Newhouse, T.H. (1975). A hybrid technique for combining moment methods with the geometrical theory of diffraction. *IEEE Transactions on Antennas and Propagation*, AP-23(1): 62–69.
- [12] Levin, B.M. (1995). Symmetrical dipole on the axis of a trough with finite length. *Radiotechnics and Electronics Engineering*, 40(5): 689–694 (in Russian).
- [13] Mirolubov, N.N., Kostenko, M.V., Levinstein, M.L. and Tichodeev, N.N. (1963). *Methods of Electrostatic Field Calculation*. Leningrad: Visshaya Shkola (in Russian).
- [14] Levin, B.M. (1997). Calculation of electrostatic field in heterogeneous media. *Radiotechnics and Electronics Engineering*, 42(8): 916–920 (in Russian).
- [15] Iossel, Yu. Ya., Kochanov, E.S. and Strunsky, M.G. (1981). *Calculation of Electrical Capacitance*. Leningrad: Energoisdat (in Russian).



- [16] Bachvalov, Yu. A. and Panukov, L.A. (1982). Condition of static fields intensity invariance in the piecewise-homogenous media. *Izvestiya vuzov of USSR – Electromechanica*, 4: 408–410 (in Russian).
- [17] Bachvalov, Yu. A. and Panukov, L.A. (1983). Condition of static fields intensity invariance in the piecewise-homogenous media. *Izvestiya vuzov of USSR – Electromechanica*, 926–31 (in Russian).
- [18] Stark, A. (1980). Optimum pattern shape of a short-wave antennas from radio link computations, *Proc. Intern. Symposium on Antenna and Propagation, Quebec*, 1: 306–307.
- [19] Levin, B.M. (2006). An antenna directivity calculation on the basis of main patterns. *Proc. of 18 Intern. Wroclaw Symposium. on Electromagn. Compatibility*, 64–67.
- [20] Vered, U. (2000). Estimation of intercardinal antenna pattern based on cardinal data. *Proc. 21 IEEE Convention of the Electrical and Electronic Engineers in Israel*, 37–41.
- [21] Balanis, C.A. (2005). *Antenna Theory: Analysis and Design*. New York: Wiley & Sons.
- [22] Kraus, J.D. (1988). *Antennas*. Boston: McGraw-Hill.
- [23] Emerson and Cuming. *Microwave Products: Microwave absorbers and low loss dielectrics*.
- [24] Gupta, O.P. (2002). Electronically steerable multi-beam antenna for mobile wireless base stations. *Paratek. Circle reader service*, 12: 19–20.
- [25] Bank, M. and Levin, B. (2007). The development of the cellular phone antenna with a small radiation of human organism tissues. *IEEE Antennas Propagation Magazine*, 49(4): 65–73.
- [26] Levin, B., Bank, M., Haridim, M. and Tsingauz, V. (2010). Dimensions of a dark spot produced by the compensation method. *Proc. of 20th Intern. Wroclaw Symposium on Electromagn. Compatibility*, 317–322.
- [27] Bank, M. and Haridim, M. (2009). A printed monopole antenna for cellular handset. *Intern. Journal of Communication*, 2: 54–61.

# Application of Method of Complex Potential

---

## 1. Symmetrical Cable of Delay and Coaxial Chamber for Calibrating Measuring Devices

Symmetrical cable of delay is an example of a specific device, for calculating electrical characteristics of which it is necessary to consider the medium heterogeneity. An ordinary coaxial delay cable has an interior wire in the shape of a spiral and an exterior wire in the shape of a circular metallic cylinder. In contrast to it the symmetrical delay cable has two interior spiral wires.

In principle the spiral wires may be reeled on two parallel dielectric cores or on common core. An inductance in both cases is approximately the same, but the capacitance between wires in the case of two parallel cores is many times less, so a linear delay

$$T = \sqrt{AC} \quad (6.1)$$

is small, and a wave impedance of a cable

$$W = \sqrt{AC} \quad (6.2)$$

is big (in the presented expressions  $A$  is a cable inductance per unit length, and  $C$  is a cable capacitance per unit length). To increase capacitance, in symmetrical cables of delay two isolated wires are reeled up on common core. The wires are wound in opposite directions: otherwise, they will form a bifilar spiral with low inductance.

It is necessary to remind that a capacitance per unit length of the symmetrical cable is equal to

$$C = C_{12} + C_{11}/2, \quad (6.3)$$

where  $C_{12}$  is the partial capacitance between spiral wires, and  $C_{11}$  is the partial capacitance between each wire and external screen. Thus, for defining the delay

time and the wave impedance of the cable one needs to calculate the capacitance between two coaxial cylindrical spirals of the equal radius reeled towards each other and the capacitance between each spiral and external screen. The capacitance  $C_{11}$  is calculated enough simply. When winding is dense,  $C_{11}$  is the capacitance per unit length between two coaxial circular cylinders. Radius of one cylinder is equal to the screen radius, and radius of the second one is equal to the winding radius. When winding is rare, it is the capacitance between the straight wire and the metal plate, located at a distance, which is equal to the screen radius.

The calculation of the capacitance  $C_{12}$  is result of solving two problems. The first problem is the calculation of the capacitance between the wires located in the homogeneous medium (air). It is considered in Section 2. The second problem is an account of influence of the medium heterogeneity, since in fact the dielectric cylinder (polyethylene core) with the permittivity differing from the air permittivity is placed inside the spirals. About this problem one can express the next considerations based on the results of Section 5.5.

As it was shown in Section 5.5, the capacitance of the transmission line, the wires of which are located along generatrices of the circular dielectric cylinder, is proportional to the equivalent permittivity, which is equal to arithmetic average of the permittivity's magnitudes of cylinder material and surrounding medium (of air). This proposition stays true, if the thin wires are located along arbitrary selected generatrices, the length of arc between which is not equal to  $\pi$ . From here with the high degree of reliability one can draw a conclusion that at placing polyethylene or any different core inside the spirals the capacitance between them increases in proportion to the same equivalent permittivity.

The coaxial chamber for calibrating instruments for measuring strength of the electromagnetic field is another example of analogous device (of the same kind). The coaxial chamber is the section of coaxial line with increased dimensions, in which electromagnetic wave is excited. This chamber secures the high degree of screening of measuring instruments. The electromagnetic field in it is uniform. The problem of reflected waves does not arise.

The chamber for calibrating instruments for measuring the strength of electromagnetic field in the air is shown in Fig. 1. Its central conductor 2 is made in the shape of a cylindrical spiral. The conical junctions 1 at the chamber ends provide outputs onto the standard coaxial connectors, one of which (input 9) is joined to a generator 10, and another (output 7) is joined to a matched load 8. The coaxial line and the conical junctions are constructed so that the wave impedance is constant. The measuring instrument 6 to be calibrated as a rule is manufactured in the shape of multi-turn loop of a finite radius. It is introduced into a chamber and placed inside the volume confined by the spiral. Signal from the instrument through the preliminary amplifier 5 and the coupling line 4 feeds the recording device 3.

The described circuit of the measurement gives an error caused by the fact that the strength of the magnetic field inside the volume, confined by the spiral, has not only longitudinal ( $H_z$ ), but also parasitic radial component ( $H_\rho$ ). This component distorts the measurement results, since emf, created at the ends of multi-turn loops, contains terms proportional both components.

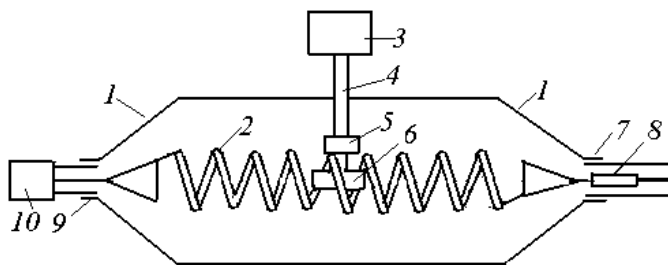


**Fig. 1:** Coaxial chamber with one spiral conductor for calibrating instruments, permitting to measure the magnetic field in the air.

To eliminate the radial component of a magnetic field, the central conductor of the coaxial chamber must be executed as is shown in Fig. 2 from the two spiral conductors 12 and 13 with opposite direction of winding, and at that one conductor connects with the generator through phase inverter 14, which changes the phase of the current by  $\pi$ . As a result of a summing fields created by the currents of both conductors, the components  $H_r$  cancel one another and the components  $H_z$  are added together and form the practically uniform magnetic field.

In the last years the development of methods and facilities for the measurements of the electromagnetic field strength in conductive liquids (sea-water, soil, etc.) acquired the important significance. The measurements results depend on the medium conductivity, which may change within wide limits. Because of this, the preliminary calibration of instruments is here especially necessary. The coaxial chambers for such calibration in the conductive liquid were described in [1]. For calibrating the meter of an electric field, the central part of a coaxial chamber is made in the shape of a cylindrical tank with dielectric walls. The tank is filled by the conductive liquid, and the measuring antenna is placed inside the tank along its axis.

When calibrating instruments for measurement of the magnetic field strength it is expedient to place the tank 11 with the conductive liquid inside volume confined by the cylindrical spirals (see Fig. 2). The tank diameter must be less than thickness of the skin-layer to exclude the error, which is caused by attenuation of the electromagnetic field in the radial direction. The equivalent circuit of the coaxial chamber with two spiral conductors excited in anti-phase is presented in Fig. 3. The equivalent circuit of the symmetrical delay cable has analogous view. In both cases it is the asymmetrical line of two wires located over ground (external screen). But in the case of the coaxial chamber the additional reactance  $jQ$  per unit length caused by the surface impedance is connected in each a wire of the line:

$$jQ = Z_1 Z_2 / [2\pi a_1 (Z_1 + Z_2)].$$

Here  $Z_1$  is the surface impedance of the spiral wire,  $Z_2$  is the surface impedance of the conductive liquid, and  $a_1$  is the spiral radius.

The impedance  $Z_1$  is introduced in the following way. The outward spiral surface mentally metallizes (replaced by metal coating), i.e., the spiral is replaced by a metal cylinder with a radius  $a_1$ . Wave slowing along this wire is considered by means of including in the obtained conductor the surface impedance. If to regard

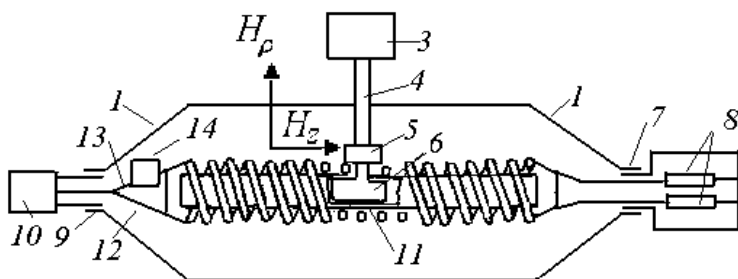


**Fig. 2:** Coaxial chamber with two spiral conductors for calibrating instruments, permitting to measure the magnetic field in a conductive liquid.

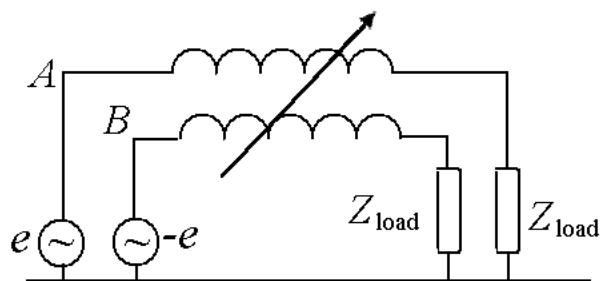


**Fig. 3:** Equivalent circuit of the line with two spiral conductors.

that impedance is purely reactive (there are no losses in the spiral wire), then at low frequencies it has inductive character. The surface impedance of the spiral wire is equal to

$$Z_1 = j2\pi a_1 \omega A,$$

where  $\omega$  is the circular frequency,  $A = \pi\mu_0 w^2 a_1^2 K_a/L^2$  is the spiral inductance per unit length,  $\mu_0$  is the permeability of the free space,  $w$  is the number of winds,  $L$  is the length of winding,  $K_a$  is the coefficient, which is equal to 1, if  $a_1 \ll L$ , and decreases smoothly, when  $a_1/L$  increases [2]. When the frequency increases, the self-capacitance of the spiral changes the surface impedance  $Z_1$ , i.e., the spiral behaves as a parallel circuit with the resonant circular frequency  $\omega_0$ :

$$Z_1 = j \frac{2\pi a_1 \omega}{1 - (\omega/\omega_0)^2} A.$$

If the vessel with the conductive liquid is placed inside the volume confined by the cylindrical spiral, then that is equivalent to connection in the wire of the additional surface impedance  $Z_2$ , which is parallel to the impedance  $Z_1$  and is equal to

$$Z_2 = \frac{k_1 J_0(k_1 a_1)}{\sigma_1 j_1(k_1 a_1)}.$$

Here  $k_1$  is the propagation constant of the wave in the conductive liquid,  $\sigma_1$  is the specific liquid conductivity. It is considered that the radius of a vessel coincides with the spiral radius.

The structure of two wires with different surface impedances, which are located over ground, has two different propagation constants (see Section 2.2). In the partial case, when the wires are the same and have equal surface impedance, then regardless of the boundary conditions (loads at the ends of the line) the components of the currents and voltages with the propagation constant  $k_i$  are same in both wires (in-phase wave), and the components with the propagation constant  $k_a$  are equal in magnitude and opposite in sign (anti-phased wave), i.e.,

$$k_i = \sqrt{k_2^2 + \omega Q(\beta_{11} + \beta_{12})}, k_a = \sqrt{k_2^2 + \omega Q(\beta_{11} - \beta_{12})},$$

where  $k_2$  is the propagation constant of wave in the medium between the spiral wires and the external screen;  $\beta_{11}$  and  $\beta_{12}$  are accordingly the self (for each wire) and the mutual (between the wires) coefficients of electrostatic inductions.

In the circuit depicted in Fig. 3 two equal in magnitude and opposite in sign voltages excite two spiral wires, i.e., create only anti-phase wave, and the impedance between points  $A$  and  $B$  is the input impedance of the two-wire line with the propagation constant  $k_a$  and the wave impedance

$$W_a = 2k_a / [\omega(\beta_{11} - \beta_{12})].$$

If to turn from the coefficients of electrostatic inductions to the partial capacitances  $C_{ik}$ , we shall obtain:

$$k_a = \sqrt{k_2^2 + \omega Q(C_{11} + 2C_{12})}, W_a = k_a / [\omega(C_{11}/2 + C_{12})]. \quad (6.4)$$

Here, as in expression (6.3),  $C_{12}$  is the mutual capacitance between wires per unit length and  $C_{11}$  is the analogous capacitance between each wire and the ground (between a wire and an external screen). To the regime of a traveling-wave may exist in the two-wire line, its loading impedance  $2Z_{load}$  must be equal to the wave impedance  $W_a$ .

As it was indicated already, the equivalent circuits of the coaxial cable of delay and the chamber for calibrating instruments for measuring strength of electromagnetic field are the same. In both cases there are two coaxial cylindrical spirals of equal radius reeled in opposite directions and located in the metal screen. In the equalities (6.1) – (6.2) the spiral inductance is taken into consideration by means of the cable inductance  $\Lambda$ , in the equality (6.4) by means of the surface impedance  $Z_1$  included in the impedance  $jQ$ . Additionally, in (6.4) the properties of the dielectric cylinder (of the vessel with the conductive liquid) located inside the volume confined by the cylindrical spirals (the losses in this cylinder) are taken into account.

For calculation of the wave impedance and the propagation constant of the equivalent long line one must know the partial capacitances  $C_{11}$  and  $C_{12}$ . The problem of the capacitances' calculation, as already it was said during consideration of symmetrical cable of delay, breaks down into two problems. The first problem is the calculation of the capacitances between wires located in a homogeneous medium. This problem has independent importance, since its solution is necessary

for calibrating instruments for measuring the magnetic field strength in the air and producing suitable basic standards. It is considered in the follow section. The second problem is the account of heterogeneous medium influence. The capacitance between spiral wires owing to a presence of a dielectric core (the polyethylene cylinder with the conductive liquid) inside spirals increases in proportion to an equivalent permittivity. At that the permittivity is regarded as the real magnitude, since the imaginary component of  $\varepsilon$  (losses in the conductive medium) is considered by means of introducing the surface impedance  $Z_2$ .

## 2. Calculation of Capacitances

In this section the problem of calculating capacitance between two coaxial cylindrical spirals of the same radius reeled in opposite directions (Fig. 4a) are examined. It is considered that the wire diameter  $2a$  is small in comparison with a lateral and longitudinal dimension of a spiral.

It is known [3] that, if a system consists of two identical wires and a sum of their charges is equals zero (i.e., the system is electro neutral), the capacitance between wires coincides with the mutual partial capacitance and is equal to

$$C_l = \frac{1}{2(\alpha_{11} - \alpha_{12})}, \quad (6.5)$$

where  $\alpha_{11}$  and  $\alpha_{12}$  are the self and mutual potential coefficients of the wires. We use the cylindrical system of coordinate  $(\rho, \varphi, z)$  with axis  $z$  along a spiral axis and the point  $O$  in the plane going through initial points of the wires. The letter  $x$  designates the coordinate, which is counted along the wire. In the arbitrary point of a spiral wire

$$x = \sqrt{z^2 + \rho_0^2 \varphi^2},$$

where  $\rho_0$  is the radius of the cylindrical surface, on which a spiral is reeled, and  $\varphi$  is the total rotation angle from the initial point of the wire to the point with coordinate  $z$ . In Fig. 4b the scan of the first spiral turn is given. As seen from the figure,

$$z/x = s/b, \quad \rho_0 \varphi/x = 2\pi\rho_0/b,$$

where  $s$  is a spiral pitch, and  $b = \sqrt{s^2 + (2\pi\rho_0)^2}$ . From here

$$x = zb/s, \quad \varphi = 2\pi x/b. \quad (6.6)$$

If  $L$  is a spiral length, then the length of each spiral wire is

$$l = Lb/s.$$

In accordance with the method of Howe we consider that the linear charge density  $\tau$  is the same along the wire length:

$$\tau = q/l,$$

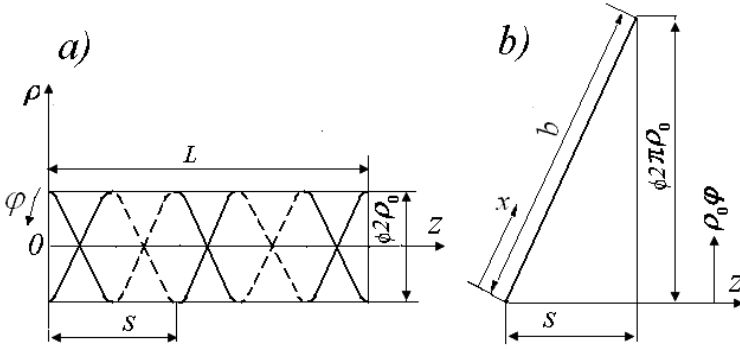


**Fig. 4:** Two-thread cylindrical spiral with the opposite winding (a) and a drawing of the developed spiral turn (b).

where  $q$  is the total charge of a wire. Then the charge  $\tau dx$  of the wire element  $dx$  located in the point with coordinates  $(\rho_0, \varphi, z)$  creates in the point  $M$  with coordinates  $(\rho_0, \varphi', z')$  the potential, which is equal to

$$dU_M = \tau dx / (4\pi\epsilon_0 R_1). \quad (6.7)$$

Here  $\epsilon_0$  is the permittivity of the free space,  $R_1$  is the distance from the point  $M$  to the element  $dx$ . For simplicity we regard that a potential is determined by the filament charge located on the wire axis, i.e.,

$$R_1 = \sqrt{(z - z')^2 + 4\rho_0^2 \sin^2 \frac{\varphi - \varphi'}{2} + a^2} = \frac{S}{b} \cdot \sqrt{(x - x')^2 + \left[ \frac{2\rho_0 b}{s} \sin \frac{\pi(x - x')}{b} \right]^2 + \frac{a^2 b^2}{s^2}} \quad (6.8)$$

The total potential of all charge  $q$  in the point  $M$  is

$$U_M(x') = \frac{q}{4\pi\epsilon_0 l} \int_0^l \frac{dx}{R_1}. \quad (6.9)$$

If to average this magnitude over the wire length and to divide it into  $q$ , we obtain the potential coefficient  $\alpha_{11}$ :

$$\alpha_{11} = U_{11}/q = \frac{1}{4\pi\epsilon_0 l} \int_0^l dx' \int_0^l \frac{dx}{\sqrt{(x - x')^2 + \left[ \frac{2\rho_0 b}{s} \sin \frac{\pi(x - x')}{b} \right]^2 + \frac{a^2 b^2}{s^2}}}. \quad (6.10)$$

When calculating  $\alpha_{12}$  we must consider that two spiral wires are reeled in the opposite directions. Besides, the input points in the initial cross-section are shifted along the perimeter of the cross-section by  $\pi$  relatively one another. Therefore, if relationships (6.6) are true for one wire, then for the second wire in the observation point  $M$  we get

$$x' = z'b/s, \quad \varphi' = \pi - 2\pi x'/b.$$



Accordingly for the distance  $R_2$  from the point  $M$  to the element  $dx$  we obtain instead of (6.8)

$$R_2 = \frac{s}{b} \sqrt{(x-x')^2 + \left[ \frac{2\rho_0 b}{s} \sin \frac{\pi(x-x')}{b} \right]^2 + \frac{a^2 b^2}{s^2}}. \quad (6.11)$$

Calculating the total potential of the charge  $q$  of the adjacent wire in the point  $M$  and averaging this magnitude over the considering wire, we find:

$$\alpha_{12} = \frac{1}{4\pi\epsilon_0 l} \int_0^l x' \int_0^l \frac{dx}{\sqrt{(x-x')^2 + \left[ \frac{2\rho_0 b}{s} \cos \frac{\pi(x+x')}{b} \right]^2 + \frac{a^2 b^2}{s^2}}}. \quad (6.12)$$

Integrals (6.10) and (6.12) cannot be expressed in terms of elementary functions, since their integrands besides  $(x-x')^2$  contain the squares of trigonometric functions, arguments of which also depend on  $x$  and  $x'$ . And so, one may determine them only numerically. At that the double integral (6.10) may be reduced to the ordinary one. Let us introduce the notations:

$$A = \frac{1}{4\pi\epsilon_0 l l}, \quad t = x - x', \quad f(t) = 1/.,$$

Then  $\alpha_{11}$  is equal to

$$\alpha_{11} = A \int_0^l dx' \int_0^l f(x-x') dx.$$

Since the function  $f(t)$  is an even function relative to argument  $t$ , and an integration domain is the square with a side  $l$ , then  $\alpha_{11} = 2A \int_0^l dx' \int_0^{x'} f(t) dt$ . Changing the order of integration, we find:

$$\alpha_{11} = 2A \int_0^l f(t) dt \int_t^l dx' = 2A \int_0^l (l-t) f(t) dx. \quad (6.13)$$

If the wire radius  $a$  is small, then when  $t$  tends to zero ( $x$  tends to  $x'$ ) the integrand in the expression (6.10) rises sharply and troubles numerical integration. Reducing the double integral to the ordinary one substantially facilitates the calculation.

For calculating capacitance between two coaxial cylindrical spirals one can propose an approximate method as the alternative to a numerical method. The approximate method allows us to determine the capacitance, caused by multiple crossing of the wires with each other. In order to calculate this capacitance, one must sum the capacitances of nodes of crossing. Let us present the node of crossing in the shape of four united in pairs wire segments with lengths  $l_1$  and  $l_2$  (Fig. 5), at that

$$l_1 + l_2 = l_0 = \frac{l}{2w}, \quad (6.14)$$

where  $w$  is the number of spiral turns. For the simplicity we consider that the wire segments are straight. Then we obtain

$$C_l = \sum_{n=1}^N C_{l_0}^n = 2 w C_{l_0}^{(n)}. \quad (6.15)$$

Here  $n$  is the node number,  $N$  is the number of the nodes (it is equal to  $2w$ ), and  $C_{j0}^{(n)}$  is the capacitance between two intersecting wires of a node  $n$ . Similarly (6.5)

$$C_{l_0}^{(n)} = 0.5/[\alpha_{11}^{(n)} - \alpha_{12}^{(n)}], \quad (6.16)$$

where  $\alpha_{11}^{(n)}$  and  $\alpha_{12}^{(n)}$  are the self and mutual potential coefficients of wires of a node  $n$ . If the radii  $a$  of the wires is small in comparison with its lengths  $l_0$ , then

$$\alpha_{11}^{(n)} = \frac{1}{2\pi\epsilon_0 l_0} [\ln(2l_0/a) - 1]. \quad (6.17)$$

To find the value of  $\alpha_{12}^{(n)}$ , one must calculate potentials  $U_M(u)$  and  $U_N(u)$  in the points of left and right segments of one wire and average these potentials over the wire length. In the common case, if the segments lengths are different, we obtain (see Fig. 5):

$$\begin{aligned} U_M(u_1) &= q/(4\pi\epsilon_0 l_0) \left\{ \int_0^{l_2+u_1 \cos \gamma} dv/\sqrt{v^2+u_1^2 \sin^2 \gamma} + \int_0^{l_1-u_1 \cos \gamma} dv/\sqrt{v^2+u_1^2 \sin^2 \gamma} \right\} = \\ &= \frac{q}{4\pi\epsilon_0 l_0} \left[ \sinh^{-1} \frac{l_2+u_1 \cos \gamma}{u_1 \sin \gamma} + \sinh^{-1} \frac{l_1+u_1 \cos \gamma}{u_1 \sin \gamma} \right]. \end{aligned}$$

Here  $\gamma$  is the angle between the wires. Similarly

$$U_N(u_2) = \frac{q}{4\pi\epsilon_0 l_0} \left[ \sinh^{-1} \frac{l_1+u_2 \cos \gamma}{u_2 \sin \gamma} + \sinh^{-1} \frac{l_2-u_2 \cos \gamma}{u_2 \sin \gamma} \right],$$

i.e.,

$$\begin{aligned} U_{12} &= 1/l_0 \left[ \int_0^{l_1} U_M(u_1) du_1 + \int_0^{l_2} U_N(u_2) du_2 \right] = \\ &= \frac{q}{2\pi\epsilon_0 l_0} \left[ \sinh^{-1} \left( \tan \frac{\gamma}{2} \right) + \frac{l_1}{l_0} \sinh^{-1} \frac{l_2/l_1 + \cos \gamma}{\sin \gamma} + \frac{l_2}{l_0} \sinh^{-1} \frac{l_1/l_2 + \cos \gamma}{\sin \gamma} \right]. \end{aligned}$$

and accordingly

$$\alpha_{12}^{(n)} = \frac{U_{12}}{q} = \frac{1}{2\pi\epsilon_0 l_0} \left[ \sinh^{-1} \left( \tan \frac{\gamma}{2} \right) + \frac{l_1}{l_0} \sinh^{-1} \frac{l_2/l_1 + \cos \gamma}{\sin \gamma} + \frac{l_2}{l_0} \sinh^{-1} \frac{l_1/l_2 + \cos \gamma}{\sin \gamma} \right]. \quad (6.18)$$

From (6.16) – (6.18)

$$C_{l_0}^{(n)} = \pi\epsilon_0 l_0 \left[ \ln \frac{2l_0}{a} - 1 - \sinh^{-1} \left( \tan \frac{\gamma}{2} \right) - \frac{l_1}{l_0} \sinh^{-1} \frac{l_2/l_1 + \cos \gamma}{\sin \gamma} - \frac{l_2}{l_0} \sinh^{-1} \frac{l_1/l_2 + \cos \gamma}{\sin \gamma} \right]^{-1}.$$

If  $l_1 = l_2$ , then taking (6.14) – (6.16) into account we obtain:

$$C_l = \pi\epsilon_0 l_0 \left[ \ln \frac{l_0}{aw} - 1 - \sinh^{-1} \left( \tan \frac{\gamma}{2} \right) - \sinh^{-1} \left( \cot \frac{\gamma}{2} \right) \right]^{-1}. \quad (6.19)$$

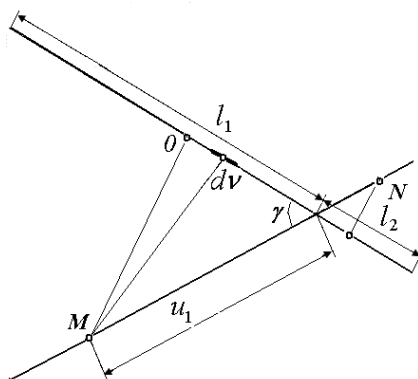


Fig. 5: The node of crossing of the straight wires.

Here it is easy to make sure,

$$w = l/s, \tan(\gamma/2) = 2\pi\rho_0/s.$$

Figure 6 demonstrates the calculations' and measurements' results of a capacitance between the wires of two-thread spiral with dimensions (in meters):  $L = 0.32$ ,  $2a = 1.5 \cdot 10^{-3}$ ,  $\rho_0 = 0.045$ . The capacitance is given for the different number  $w$  of the spiral turns. The curve 1 is obtained by the numerical method in accordance with the expressions (6.5), (6.12) and (6.13), the curve 2 is obtained by the approximate method, in accordance with the expression (6.19). The measured values are marked by the circles. As one can see from figure, both calculation methods give the similar results (the difference is from 2 to 4%), which coincide well with the experiment. That indicates the applicability of the approximate method for the calculation of the capacitance between the spiral wires. When the wire diameter rises, the accuracy of the approximate method decreases.

The obtained results show the applicability of the approximate method not only for the calculation of a capacitance between two coaxial cylindrical spirals, but also for the calculation of capacitances of itself nodes of crossing. The expression (6.18) permits to calculate the capacitance between two crossed wires located both in a free space and in a homogeneous medium with permittivity or next door to the interface of two media, whose equivalent permittivity equals  $\varepsilon_e$  (with help of replacement  $\varepsilon_0$  to  $\varepsilon$  or  $\varepsilon_e$ ). One can also generalize the approximate method to the case of wires covered with a sheath (Fig. 7a). If a sheath radius is small in comparison with the cross and longitudinal spiral dimensions, i.e., if a sheath thickness is close to a wire radius, then one can consider that a wire surface and an external sheath surface are equipotential surfaces, and the capacitance  $C_l$  between wires consists of three capacitances connected in series:

$$\frac{1}{C_l} = \frac{1}{C_{1l}} + \frac{1}{C_{2l}} + \frac{1}{C_{3l}},$$

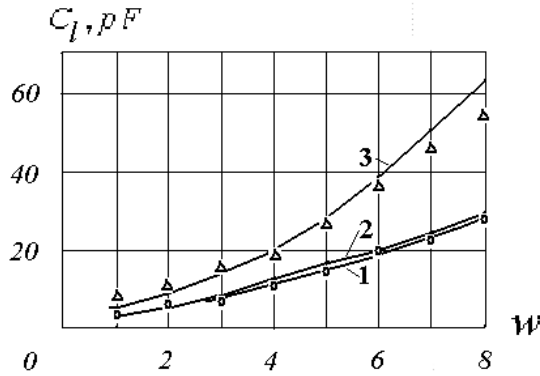


Fig. 6: Dependence of a spiral capacitance from the turns' number.

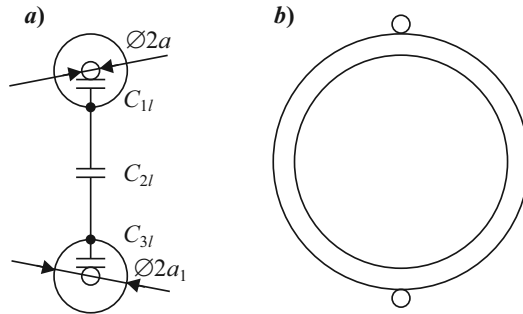


Fig. 7: The cylindrical spiral of the wires coated by a sheath (a) or reeled around a dielectric framework (b).

where  $C_{1l}$  and  $C_{3l}$  are the capacitances between the external and internal surfaces of each sheath, and  $C_{2l}$  is the capacitance between spiral wires, whose radius is equal to the external radius  $a_1$  of the sheath, i.e.,

$$C_{1l} = C_{3l} = 2\pi\epsilon_1 l / \ln(a_1/a).$$

Here  $\epsilon_1$  is an absolute permittivity of a sheath), and  $C_{2l}$  is calculated according to expression (6.19)—with substitution  $a_1$  for  $a$ .

If the spiral consisting from two filaments is reeled around a thin dielectric framework of a cylindrical shape (Fig. 7b), then in the first approximation the capacitance between wires is equal to the capacitance between the spiral wires in the sheath, whose thickness close to the framework thickness.

The calculation result of a capacitance between the wires of such a spiral, which is reeled around a cylindrical framework of a thickness  $a_1 - a = 0.005$  m with the relative permittivity  $\epsilon_{r1} = 2.6$ , is presented in Fig. 6 as the curve 3. The measured values are marked by the triangles. Coincidence of the calculation with the experiments is sufficiently good.

### 3. Intersecting Wires on the Boundary of Two Mediums

In Chapter 5 it is shown that when a wire is placed at the boundary between two media the equivalent dielectric constant should be used for calculating capacitances. In practice, in placing wires at an interface the coincidence of the wire axis with this boundary is not always possible. Along with other reasons, one must remember about the finite diameter of the wire. As a result, the mutual capacitance of the wires changes significantly. The equivalent dielectric constant also changes. As said in the previous Section, in an electrically neutral system of two identical wires, the capacitance between the wires is equal to

$$C = 0.5/[\alpha_{11} - \alpha_{12}],$$

where  $\alpha_{11}$  and  $\alpha_{12}$  are the own and mutual potential coefficients of the wires, respectively. If the radii  $a$  of the wires is small compared to their lengths  $l$ , then

$$\alpha_{11} = \frac{1}{2\pi\epsilon l} (\ln 2l/a - 1).$$

As shown in Section 5.5, in the case of placing wires along the interface between two media, when calculating potential coefficients and capacitances, one should instead of  $\epsilon$  substitute the equivalent value  $\epsilon_e$ , which is equal to the average value of the dielectric constants:

$$\epsilon_e = (\epsilon_1 + \epsilon_2)/2.$$

However, if the wires are raised above the interface, then the value of  $\epsilon_e$  depends not only on  $\epsilon_1$  and  $\epsilon_2$ , but also on the geometric dimensions of the structure, in particular on the distance between the wires. When calculating the own potential coefficient  $\alpha_{11}$ , one must use the expression given in [3] (page 233) for the capacitance of a straight wire, parallel to the interface between two media. In accordance with this expression, if the distance  $h$  between the axis of the wire and the interface is small compared to its length, i.e.,  $h, a \ll l$ , then

$$\alpha_{11} = \frac{1}{2\pi\epsilon_1 l} \{ \ln(2L/a) - 1 + m[\ln(l/h) - 1] \}.$$

Here  $m = (\epsilon_1 - \epsilon_2)/(\epsilon_1 + \epsilon_2)$ ,  $\epsilon_1$  and  $\epsilon_2$  are the values of dielectric constant in a medium containing and not containing a conductor, respectively. Comparing two expressions for  $\alpha_{11}$ , we obtain for the equivalent permeability

$$\epsilon_e = \epsilon_1 \left[ 1 + m \frac{\ln\left(\frac{l}{h}\right) - 1}{\ln(2l/a) - 1} \right].$$

When calculating the mutual potential coefficient  $\alpha_{12}$ , we use the expression for the capacitance of a two-wire long line with a distance  $d$  between the axes of the wires next to a flat interface between two dissimilar media. The expression is given in [3] (page 258). At  $h, a \ll d, l$

$$C = \frac{\pi \varepsilon_1 l}{\ln(d/a) + k \ln(d/2h)}.$$

In this case, the equivalent dielectric permittivity is

$$\varepsilon_e = \varepsilon_1 \left[ 1 + m \frac{\ln(d/2h)}{\ln(d/a)} \right]^{-1}.$$

As can be seen from this expression, if the wires are raised above the interface, then the value of  $\varepsilon_e$  depends not only on  $\varepsilon_1$  and  $\varepsilon_2$ , but also on the geometric dimensions of the structure, for example, on the distance between the wires of the line.

Special interest is caused by spirals consisting of two intersecting wires wound on a dielectric cylinder (Fig. 8a). If the spiral wires lie on the surface of the cylinder, then as the equivalent dielectric constant we can take a value equal to the arithmetic mean of the permeabilities of the boundary media. However, if the spiral wires are located above the surface of the cylinder (Fig. 8b), this method is not applicable.

Let us use the known expression for the capacitance per unit length of a line from two spiral filament located not far from a cylindrical interface of two media ([3], page 259)

$$C_l = \pi \varepsilon_1 \left[ \cosh^{-1} \frac{2b \sin \theta/2}{a} + \frac{m}{2} \ln \frac{b^4 - 2b^2 \rho^2 \cos \theta + \rho^4}{(\rho_0^2 - \rho^2)^2} \right].$$

The meaning of designations is understandable from Fig. 8b. It is considered that in this expression the wire radius  $a$  is small in comparison with another dimensions.

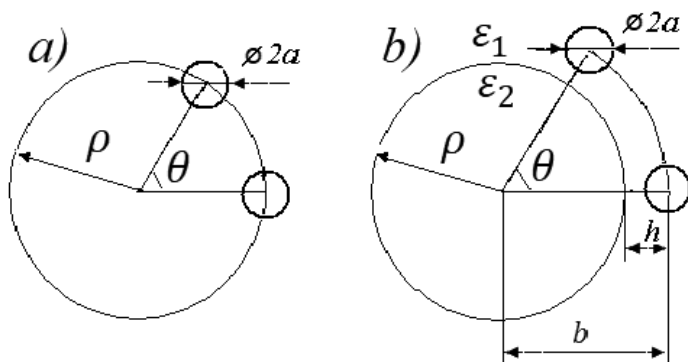


**Fig. 8:** The cylindrical spiral from two wires reeled round a dielectric cylinder (a) and located over a cylinder surface (b).

If a distance  $h = b - \rho$  between the interface and an axis of each wire is the magnitude of the order  $a$ , then the second addend of a denominator is equal to

$$\frac{m}{2} \ln \left[ 1 + \frac{b^2 \rho^2 \sin^2 \theta + 2}{h^2 (b - h/2)^2} \right] \cong m \ln \left( \frac{\rho}{h} \sin \theta/2 \right). \quad (6.20)$$

Here it is considering that  $h/2b \ll 1$  and  $\rho/b \gg 1$ .

In this case, we are dealing with an inhomogeneous medium consisting of two homogeneous media with different dielectric permittivity: the air medium with a dielectric permittivity  $\varepsilon_1$  and the dielectric cylinder with a permittivity  $\varepsilon_2$ , above which at a height  $h$  a two-start spiral is located. Let us replace the inhomogeneous medium by the homogeneous medium with equivalent permittivity  $\varepsilon_e$ . In order to with such a replacement, the capacitance  $C$  between the wires of the spiral by unit of its length did not change, the equality must be satisfied

$$C_l = \pi \varepsilon_e / \cosh^{-1} \left( \frac{2b}{a} \sin \theta/2 \right). \quad (6.21)$$

Hence

$$\varepsilon_e = \frac{C_l}{\pi} \cosh^{-1} \frac{2b \sin \theta/2}{a} = \varepsilon_e \left[ 1 + m \ln \left( \frac{\rho}{h} \sin \theta/2 \right) / \cosh^{-1} \left( \frac{2b}{a} \sin \theta/2 \right) \right]^{-1}. \quad (6.22)$$

As one can see from (6.22), if the wires of the spiral are located over the media interface, then the magnitude  $\varepsilon_e$  depends not only on  $\varepsilon_1$  and  $\varepsilon_2$ , but also on geometrical dimensions of structure, i.e., on a distance  $R \approx 2b \sin(\theta/2)$  between the wires. If the wires' segments are shifted along a cylinder axis, it is necessary to determine this shift. Substitution of the magnitude  $\varepsilon_e$  in (6.7) permits to obtain the expressions for the potential  $dU_M$ , created by the charge  $\tau dx$  of wire element  $dx$  in the point  $M$ , and for the potential coefficients  $\alpha_{11}$  and  $\alpha_{12}$ .

The calculation results for the capacitance  $C_l$  between the wires of double-start spirals with parameters (in meters):  $L = 0.3$ ,  $2a = 1.8 \cdot 10^{-3}$ ,  $\rho = 0.03$  for the different number  $w$  of the spiral turns are presented in Fig. 9. Solid curves are determined in accordance with expressions (6.5), (6.21) and (6.22). The curve 1 is plotted for the spiral located in the free space, the curve 2—for the spiral reeled around the cylinder with relative permittivity  $\varepsilon_2 = 2.8$  (the wires axes coincide with the media interface), the curves 3 and 4 for wires, which are located above the interface at the height of  $h = 0.3$  and  $h = 0.6$  m.

In Section 2 the approximate calculation method for the capacitance between the coaxial cylindrical spirals located in the air is described. This method assumes that the capacitance is equal to the sum of capacitances of nodes of crossing. For the approximate estimation of the capacitance between the spirals located over the cylindrical interface it is necessary to increase the mentioned capacitance by a factor  $\varepsilon_1/(1 + Bm)$ , where  $B = 1 - \ln(4h/a)/\ln(4b/a)$ . Dimensions  $h$  and  $b$  are shown in Fig. 8b. The results of this estimation are presented in Fig. 9 for the variants 1 and 2 by dotted lines.

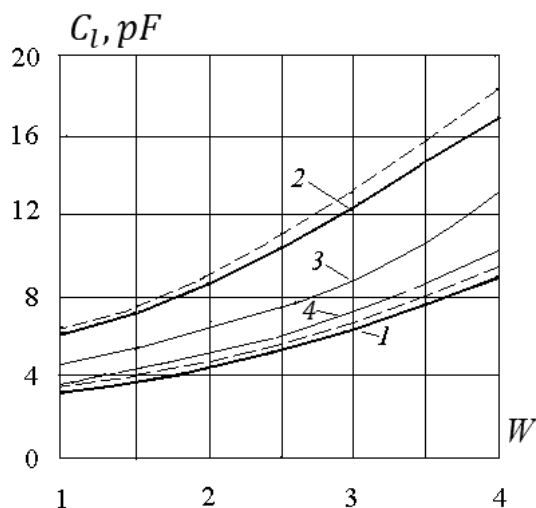


Fig. 9: Capacitance of a spiral reeled on a dielectric cylinder depending on the turns' number.

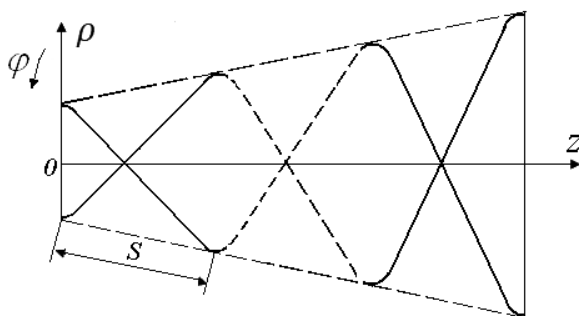


Fig. 10: The conical spiral.

In the case of conical spirals with constant winding angle (Fig. 10) the angle  $\gamma$  between wires at the crossing point does not change along the spirals, and the radius  $\rho(z)$  and pitch  $s(z)$  of each spiral increases in proportion to  $z$ :

$$s(z)/s(0) = \rho(z)/\rho(0) = 1 + z/z_0,$$

Here  $z_0$  is the distance from the spiral start to the cone vertex. The lengths  $l_0^{(n)}$  of wires in crossing nodes increase in the same fashion. If with increasing  $z$  the wire radius increased according to this law, then the potential coefficients  $\alpha_{11}^{(n)}$  and  $\alpha_{12}^{(n)}$  would be inversely proportional to the length  $l_0^{(n)}$ , and when calculating the capacitance  $C_l$  would need to be replaced the magnitude  $\ln(l/aw)$  by the identical for all segments magnitude  $\ln[2l_0^{(n)}/a^{(n)}]$ . However, the radii of the wires in conical spirals as a rule do not change along the line, and that introduces an additional error into the calculation when using. This error is relatively small, since it has logarithmic character of dependence on a wire radius.



#### 4. Capacitances in a System of a Few Conductors

Generalization of the concept ‘capacitance between the two conductors’ in the case of a system with an arbitrary but finite number of conductors is the concepts of self and mutual partial capacitances. A ratio of conductor charge to its potential, if all conductors of a system, including conductor under study, have the same potential, is called the partial capacitance of the conductor in a many-body system. The ratio of one conductor charge to a potential of other conductor, if all conductors of a system, except the latter one, have zero potential, is called the mutual partial capacitance between the conductors. The relationship between the charges and potentials in the system of  $N$  conductors in accordance with these concepts is expressed by a system of equations:

$$Q_i = \sum_{n=1}^N C_{in} (U_i - U_n), \quad i = 1, 2 \dots N, \quad (6.23)$$

Here  $Q_i$  and  $U_i$  are a charge and a potential of conductor  $i$ ,  $C_{ii}$  is its self-capacitance,  $C_{in}$  is the mutual partial capacitance between conductors  $i$  and  $n$  ( $i \neq n$ ). Here  $C_{in} = C_{ni}$ .

To the system of  $N$  conductors, occupying a finite volume, it is need to add the conductor  $(N + 1)$  in the form of a sphere of infinite radius. Let this conductor has zero potential. In the resulting system the self-capacitance of any conductor, except conductor  $(N + 1)$ , may be interpreted as a mutual partial capacitance between this conductor and the sphere.

The system of equations (6.23) can be transformed by means of uniting terms with the factor  $U_i$  and obtaining expressions relating charges and potentials of conductors:

$$Q_i = \sum_{n=1}^N \beta_{in} U_n, \quad i = 1, 2 \dots N,$$

where  $\beta_{in}$  is named by coefficient of electrostatic induction. Another form of writing these relations is

$$U_i = \sum_{n=1}^N \alpha_{in} Q_n, \quad i = 1, 2 \dots N.$$

The values  $\alpha_{in}$  are called potential coefficients. The coefficients  $\beta_{in}$  and  $\alpha_{in}$  are related as follows:

$$\beta_{in} = \Delta_{in} / \Delta_N, \quad (6.24)$$

where  $\Delta_N = |\alpha_{in}|$  is the  $N \times N$  determinant, and  $\Delta_{in}$  is the cofactor of a determinant  $\Delta_N$ . The coefficients  $\beta_{in}$  and  $C_{in}$  are also related:

$$C_{in|_{i \neq n}} = -\beta_{in}, \quad C_{in|_{i=n}} = \sum_{n=1}^N \beta_{in}. \quad (6.25)$$

In a specific case when a system consists of a single conductor, the concept of the self-capacitance coincides with the concept of an isolated conductor capacitance. When such conductor consists of several ( $N$ ) connected conductors, its capacitance is equal to

$$C_0 = \sum_{n=1}^N C_{nn}.$$

If  $N = 2$ , then

$$C_0 = C_{11} + C_{22}, \quad C_{11} = \beta_{11} + \beta_{12}, \quad C_{22} = \beta_{21} + \beta_{22},$$

where  $\beta_{11} = \alpha_{22}/(\alpha_{11}\alpha_{22} - \alpha_{12}^2)$ ,  $\beta_{12} = \beta_{21} = -\alpha_{12}/(\alpha_{11}\alpha_{22} - \alpha_{12}^2)$ ,  $\beta_{22} = \alpha_{11}/(\alpha_{11}\alpha_{22} - \alpha_{12}^2)$ , i.e.,

$$C_0 = \frac{\alpha_{11} + \alpha_{22} - 2\alpha_{12}}{\alpha_{11}\alpha_{22} - \alpha_{12}^2}.$$

If the algebraic sum of all conductors' charges in the system is zero, the system is called electrically neutral. For an electrically neutral system consisting of two conductors, the concept of mutual partial capacitance coincides with the concept of capacitance between two conductors. Thus, as shown in [3], it is necessary to take into account the capacitance between each conductor  $n$  and the sphere of infinite radius, i.e., the self-capacitance  $C_{nn}$ . Accordingly, a capacitance between the two conductors (Fig. 11) is equal to

$$C = C_{12} + \frac{c_{11}c_{22}}{c_{11} + c_{22}} = \frac{c_{11}c_{12} + c_{22}c_{12} + c_{11}c_{22}}{c_{11} + c_{12}}.$$

Using (6.24) and (6.25), we find for  $N = 2$ :

$$C = \frac{\beta_{11}\beta_{22} - \beta_{12}^2}{\beta_{11} + \beta_{22} + 2\beta_{12}} = \frac{1}{\alpha_{11} + \alpha_{22} - 2\alpha_{12}}.$$

As an example, we consider the open-end two-wire transmission line from the wires of different lengths ( $l_1$  and  $l_2 = l_1 - l$ ) and with the same radius  $a$ . This line was described in Section 1.6 (see Fig. 1.20). As seen from the Fig. 1.20b, the considering structure consists of three conductors denoted in the figure by Roman numerals: I is the short wire, II is the parallel to it segment of the long wire with the same length, and III is the additional segment of the long wire (with the length  $l$ ). The load of the line (1) is the capacitance  $C$  between the conductors I and III. It cannot be calculated directly like the capacitance between the conductors I and III, located in free space, at least because that presence of the conductor II significantly changes it. It is necessary firstly to find the capacitance  $C_s$  between the conductor I and the totality

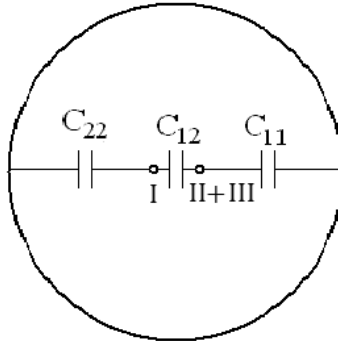


Fig. 11: Partial capacitances in a system of two wires.

of conductors *II* and *III*, after that to find the capacitance  $C_0$  between the conductors *I* and *II* and to subtract it from the first one:  $C = C_s - C_0$ . The self-capacitances of conductors must be calculated in accordance with expression (1.63).

At that, calculating capacitance between parallel conductors of equal length means that not only the mutual partial capacitance between mentioned conductors, but the parallel to it capacitance of a series connected partial capacitances between each conductor and the sphere of infinite radius are considered. If under the calculation to consider only the capacitance between the conductors, then the calculated value of  $l_0$  for  $l = 0$  will not be different from zero. This result is caused by the approximate nature of the theory of two-wire transmission line, which is based on the postulate about the extremely small distance between the wires axes. If this distance tends to zero, the partial capacitance between the conductors becomes infinitely great, and the parallel to it self-capacitance between each conductor and the sphere of infinite radius can be neglected.

A widespread mistake that the field of a long line is concentrated mainly between the wires is also caused by the approximate theory. In fact, only half energy flow is concentrated inside the imaginary cylinder passing through the equivalent thin filaments (see Section 7).

## 5. A long Line from Converging Straight Wires and a Slotted Antenna on a Cone

As pointed above, the problem of calculating electric field of charged bodies is substantially simplified, if the all magnitudes and dimensions depend only on two coordinates (such a field is called the plane-parallel field). A three-dimensional problem is solved only in a few particular cases, whereas a two-dimensional problem is considered more widely—for the different number of wires and for various shape of their cross-section. In this connection an attempt to use the solution results of two-dimensional problems for electrostatic fields' calculations in three-dimensional problems, when a mutual location of metal bodies reminds the two-dimensional variant, is of interest.

The fields calculation of two infinitely long charged filaments converging to one point—to a generator is an example of such a problem (Fig. 12a). The linear charge densities of both filaments are same in magnitudes and opposite in sign:

$$\tau_1 = -\tau_2 = \tau.$$

Analogue of this three-dimensional problem is two-dimensional problem of two parallel charged filaments (Fig. 12b). The scalar potential of two such filaments in accordance with (5.37) is equal to

$$U(x, y) = \frac{\tau}{2\pi\epsilon} \ln \rho_1 / \rho_2, \quad (6.26)$$

where  $\epsilon$  is the dielectric permittivity of the medium,  $\rho_1$  and  $\rho_2$  are the distances from the observation point  $M$  to the filament axes. At that

$$\rho_2^2 = (b - x)^2 + y^2, \quad \rho_1^2 = (b + x)^2 + y^2.$$

Here  $b$  is the half of a distance between the filaments' axes.

As has been said earlier, lines of equal potential  $U = \text{const}$  in the plane field of two charged filaments are the circumferences with the centers on the axis of abscissas. From here in particular it follows that the field of two parallel no coaxial metallic cylinders has similar character, since one can always locate the axes of the equivalent filaments so that in their field two surfaces of equal potential coincide with the surfaces of the metallic cylinders (Fig. 13a). Lines of force  $V = \text{const}$  are the circumferences with the centers on the axis of ordinates.

One must remind that in accordance with the uniqueness theorem the solution of an electrostatic problem must satisfy Laplace's equation, and that surfaces of conductive bodies must coincide with the surfaces of equal potential. The three-

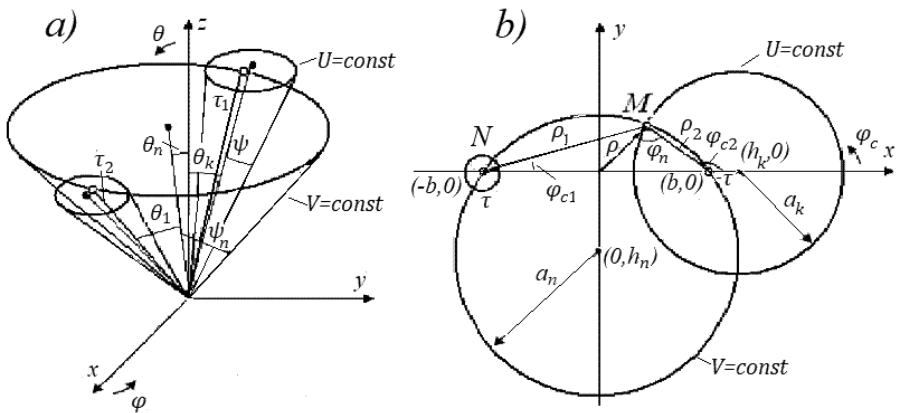


Fig. 12: Three-dimensional (a) and two-dimensional (b) problems for two infinitely long charged filaments.

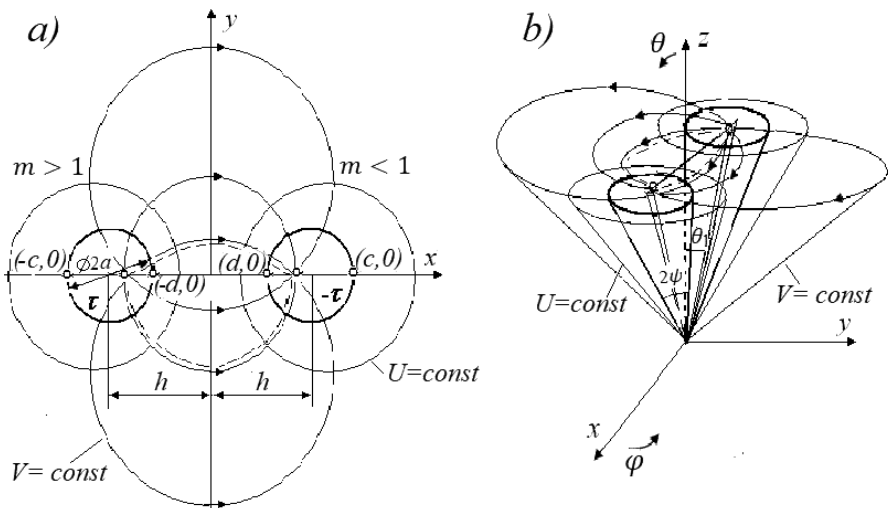


Fig. 13: The two-dimensional problem for two metal cylinders (a), and the three-dimensional problem for cones (b).

dimensional problem about two convergent charged lines (see Fig. 12a) is a particular case of a conical problem, in which conductive bodies have a shape of a cone with the top in the coordinates' origin (Fig. 13b). The conical and cylindrical problems are compared with each other in [4], where it is shown that Laplace's equation remains correct in going from one problem to another problem, if the replaceable variables are related by equalities:

$$\rho = \tan(\theta/2), \varphi_c = \varphi. \quad (6.27)$$

Here  $\rho$  and  $\varphi_c$  are cylindrical coordinates, and  $\theta$  and  $\varphi$  are spherical coordinates.

The result of such transformation of coordinates is mapping of spherical surface of an arbitrary radius  $R$  in the plane  $(\rho, \varphi_c)$ . Here the line of that surface intersection with any circular cone (with a vertex in the coordinates' origin) transforms into the circumference. Therefore, the three-dimensional conical problem may be reduced to a two-dimensional one, in which the coordinates of the conductive bodies are related with the coordinates in the bodies of an initial problem by equalities (6.27).

In accordance with an analogy between the conical and the cylindrical problems the case of the two convergent charged filaments located at an angle  $2\theta_0$  to each other in the plane  $xOz$  (see Fig. 12a) corresponds to two parallel filaments spaced at the distance  $2b = 2z \tan(\theta_1/2)$  from each other (see Fig. 12b). The case of the two metal cones with the angle  $2\psi$  at the vertex of each cone and with the angle  $2\theta_1$  between the cones' axes (see Fig. 13b) corresponds to two metallic cylinders of the radius  $a = (c - d)/2$ , the distance between axes of which (see Fig. 13a) is equal to  $2h = c + d$ . Since according to (6.27)

$$c = \tan[(\theta_1 + \psi)/2], d = \tan[(\theta_1 - \psi)/2],$$

it is not difficult to make sure that

$$a = \frac{\sin \psi}{\cos \theta_1 + \cos \psi}, h = \frac{\sin \theta_1}{\cos \theta_1 + \cos \psi}.$$

In particularly

$$\begin{aligned} \theta_1 &= \tan^{-1} c + \tan^{-1} d = \tan^{-1} \frac{2h}{1 - (h^2 - a^2)}, \\ \psi &= \tan^{-1} c - \tan^{-1} d = \tan^{-1} \frac{2a}{1 - (h^2 - a^2)}. \end{aligned} \quad (6.28)$$

It is necessary to emphasize that upon the transition from the cone to the cylinder the cone axis does not coincide with the cylinder axis.

The scalar potential of the electric field created by the two convergent charged filaments by analogy with (6.26) is equal to

$$U(\theta, \psi) = \frac{\tau}{2\pi\epsilon} \ln(\rho_1/\rho_2),$$

where

$$\begin{aligned}\rho_2^2 &= [\tan(\theta_0/2) - \cos\varphi \tan(\theta/2)]^2 + \sin^2\varphi \tan^2(\theta/2), \\ \rho_1^2 &= [\tan(\theta_0/2) + \cos\varphi \tan(\theta/2)]^2 + \sin^2\varphi \tan^2(\theta/2).\end{aligned}$$

In the given case the surfaces of equal potential  $U = \text{const}$  are the circular cones, the axial lines of which lie in the plane  $xOz$ . Each surface satisfies an equation:

$$\rho_2/\rho_1 = m = \text{const}.$$

For the plane problem the line of equal potential is the circumference with the center in the point  $h_m = (1 + m^2)b/(1 - m^2)$  and with the radius  $a_m = 2mb/|1 - m^2|$ . Using these magnitudes and equalities (6.28), we find the angle  $\theta_m$  between the axis  $z$  and the axis of an equipotential circular cone in the conical problem

$$\theta_m = \tan^{-1} \frac{2h_m}{1 - (h_m^2 - a_m^2)} = \tan^{-1} \left( \frac{1+m^2}{1-m^2} \tan\theta_0 \right),$$

and also, the angle  $\psi_m$  between the cone generatrix and its axis

$$\psi_m = \tan^{-1} \frac{2a_m}{1 - (h_m^2 - a_m^2)} = \tan^{-1} \frac{2m \tan\theta_0}{|1 - m^2|}.$$

The surfaces of field strength  $V = \text{const}$ , in which field lines are located, are also circular cones. Actually, in the plane problem the flow function appears in accordance with (5.37) as

$$V = -\frac{\tau}{2\pi\epsilon} (\varphi_{c2} - \varphi_{c1}).$$

The sense of the angles  $\varphi_{c2}$  and  $\varphi_{c1}$  is clear from Fig. 12b. The equation of the field line

$$\varphi_{c2} - \varphi_{c1} = \varphi_n = \text{const}$$

is the equation of a circumference, the radius of which is equal to  $a_n = b/\sin\varphi_n$ . The axis of this circumference is located at a distance  $h_n = b \cot\varphi_n$  from axis  $z$ .

In the conical problem the axial lines of the circular cones  $V = \text{const}$  also lie in the plane  $yOz$  forming with axis  $z$  the angle

$$\theta_n = \tan^{-1}(\cot\varphi_n \tan\theta_0),$$

and the angle  $\psi_n$  between the cone axis and generatrix is equal to

$$\psi_n = \tan^{-1}(\tan\theta_0/\sin\varphi_n).$$

If to reduce a conical problem to a cylindrical, it permits to calculate the capacitance per unit length and the wave impedance of the long line consisting of two convergent filament or cones. It is known, for example, that the capacitance per

unit length of the line consisting of two wires with radius  $a$  located at the distance  $2h$  from each other is equal to

$$C_l = \frac{\pi\epsilon}{\ln [h/a + \sqrt{(h/a)^2 - 1}]} = \frac{\pi\epsilon}{ch(h/a)}, \quad (6.29)$$

and the wave impedance is

$$W = 1/(cC_l) = 120ch^{-1}(h/a).$$

Here  $c$  is the light velocity.

For two convergent cones we obtain in accordance with (6.29)

$$C_1 = \frac{\pi\epsilon}{ch^{-1}(\sin \theta_1 / \sin \psi)}, \quad W_1 = 120ch^{-1} \frac{\sin \theta_1}{\sin \psi}.$$

For a dipole with an angle  $2\alpha$  between axes of conic arms (see Fig. 14)  $\sin \psi = a/L$ ,  $\theta_1 = \alpha$ , i.e.,

$$W_2 = 120ch^{-1}(L \sin \alpha/a).$$

The case of two convergent charged shells, located along a surface of a circular cone with the angle  $2\theta_0$  at vertex (Fig. 15a) is of specific interest. Let the arc length in a cross-section of each charged shell be equal to  $2a$ . The structure from two coaxial cylindrical shells of radius  $a = \tan(\theta_0/2)$  with similar arc length in a cross-section (see Fig. 15b) corresponds to this three-dimensional problem.

In order to obtain a visualization about the character of an electrostatic field of two cylindrical shells, one must sum up the fields of pairs consisting of symmetrically located parallel filaments 1-1', 2-2', 3-3' and so on. Their charges are equal in magnitude and opposite in sign (see Fig. 15b). The lines of equal potential for each pair are the circumferences with the centers on the curve passing through the filaments. The common (summary) curve consisting of these circumferences with the same constant  $m$  is the line of equal potential, which envelopes a shell cross-section. It is a curve of a complicated shape, extended along both sides of each shell and smoothly bent around its ends. The symmetry axis of structure, i.e.,  $y$ -axis, is also one of the lines of equal potential.

In accordance with the principle of duality, the radiator of two converging straight metal wires has an analogue in the form of two slot antennas, cut in a metal cone and converging to its vertex (to a generator). As is seen from Fig. 15a, two charged shells, located along a surface of a circular cone with the angle  $2\theta_0$  at vertex and converged to the generator, also correspond to this case. Let the arc length in a cross-section of a charged shell is equal to  $2a$ .

The field lines for each pair of the filaments are circumferences with centers on the symmetry axis  $y$ , which pass through the filaments. Two lines coincide with the circumference, on which the shells are situated, i.e., these lines close two gaps between the shells. Field lines inside this circumference connect the symmetrically placed filaments with each other and cross the lines of equal potential at right angles. The field structure in the case of two uniting (convergent) shells (see Fig. 15a) is of a similar nature, the only difference being that the surfaces of equal potentials

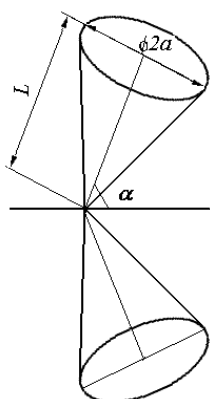


Fig. 14: An inclined dipole.

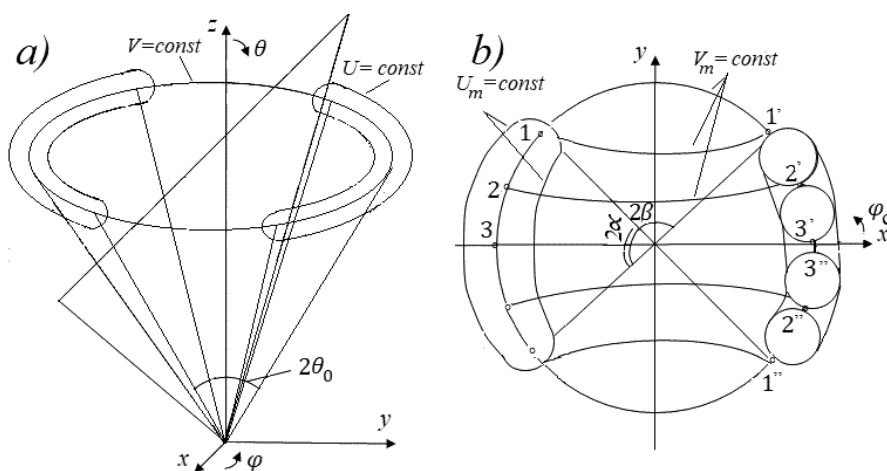


Fig. 15: Three-dimensional (a) and two-dimensional (b) problems for non-closed coaxial shells.

$U = \text{const}$  and the surfaces of field strength  $V = \text{const}$  coincide with conic surfaces rather than with cylindrical ones.

The capacitance  $C_l$  per unit length and the wave impedance  $W$  of the transmission line formed by two cylindrical shells [3, 5] are equal to

$$C_l = \varepsilon K(\sqrt{1-k^2})/K(k), \quad W = 120\pi K(k)/K(\sqrt{1-k^2}), \quad (6.30)$$

where  $K(k)$  is the complete elliptic integral of a first kind with an argument

$$k = \tan^2(\beta/2). \quad (6.31)$$

Here  $2\beta$  is the angular width of the slot,  $2\alpha = \pi - 2\beta$  is the angular width of the metal shell, i.e.,  $C_l$  and  $W$  depend only on angular slot width  $2\beta$  and hence on angular width  $2\alpha$  of the metal shell cross-section. Magnitudes  $C_l$  and  $W$ , as it follows from (6.72),



are independent of cylinder radius  $a$ . This means that both expressions are true for a conical structure with invariable cross-section.

Magnitudes  $C_l$  and  $W$  are constant along the conic line, i.e., two-wire line from the convergent shells is a uniform line. As it is known, an input impedance of a uniform two-wire line, when its length infinitely increases, tends to its wave impedance. Therefore, the input impedance of an infinitely long line excited by a generator situated near the cone vertex is

$$Z_l(k) = 120\pi K(k)/K(\sqrt{1-k^2}), \quad (6.32)$$

i.e., such long line has the high level of matching with the generator in an unlimited frequency range.

The structure under study can be treated on the one hand as a two-wire line and on the other hand as an antenna. The antenna is a symmetrical  $V$ -radiator, with the arms shaped as two convergent metal shells located along the surface of the circular cone. Finally, we can consider this structure as a slot antenna in a conic screen [5].

If  $Z_E(2\alpha)$  is the input impedance of a metallic (electric) radiator with angular arm width  $2\alpha$ , and  $Z_S(2\beta)$  is the impedance of a slot antenna with width  $2\beta$ , then, if the structure length is great, we find

$$Z_E(\alpha) = Z_S(\beta) = Z_l(k) = 120\pi K(k)/K(\sqrt{1-k^2}). \quad (6.33)$$

In Fig. 16 it is shown two metal cones with different variants of the slots. In the first variant (see Fig. 16a) the slot edge coincides with the cone generatrix. This variant was considered earlier. In the second variant (see Fig. 16b) the slot edge is a spiral, and the metallic cone with the slot in it forms double-start spiral, which is excited near the vertex. It is considered that the angular slot width is constant. Strictly speaking, expressions (6.30) – (6.33) are true only for the variant of the slot antenna shown in Fig. 16a. But, if the angular width of the metal shell in both variants is the same, one can believe with a high probability that the capacitances per unit length, the wave impedances, and consequently the input impedances of radiators are the same in both cases.

It is useful to compare the input impedances of metallic and slot radiators with the same width. If, for example, the metal shell width is  $2\alpha = 2\pi/3$ , then  $\beta/2 = \pi/12$ ,  $k^2 = 0.00515$  and  $K(\sqrt{1-k^2})/K(k) = 2.56$ , i.e.,  $Z_E(2\pi/3) = 120\pi/2.56$ . If the slot width is  $2\beta = 2\pi/3$ , then  $\beta/2 = \pi/6$ ,  $k^2 = 0.111$ ,  $K(\sqrt{1-k^2})/K(k) = 1.56$ . Accordingly  $Z_S(2\pi/3) = 120\pi/1.56$ . Therefore, the impedances of metallic and slot radiators of the same width  $2\pi/3$  are related to each other by the expression  $Z_E(2\pi/3) \cdot Z_S(2\pi/3) = \frac{(120\pi)^2}{(2.56 \cdot 1.56)}$ , from whence it follows that

$$Z_S(2\pi/3) = (60\pi)^2/Z_E(2\pi/3).$$

In the general case, if the structure length is great, it is easily verified that

$$Z_S(2\alpha) = (60\pi)^2/Z_E(2\alpha), \quad (6.34)$$

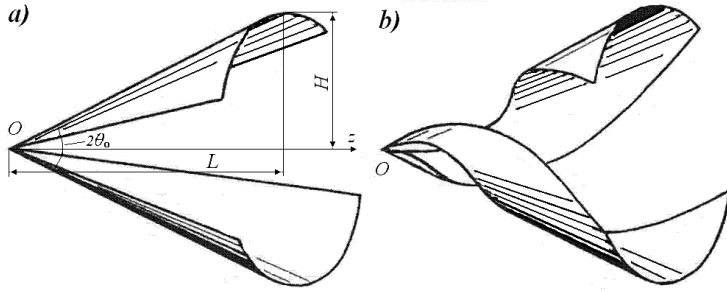


Fig. 16: The slot antennas at the cone with straight (a) and spiral (b) edges.

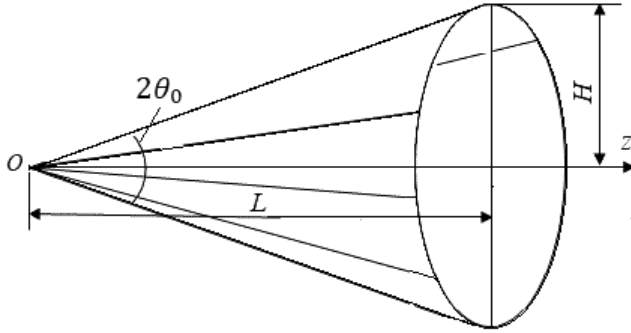


Fig. 17: The slot antenna with the straight-line edges at the cone.

when  $Z_E(2\alpha)$  is the input impedance of a metallic (electric) radiator with angular arm width  $2\alpha$ , and  $Z_S(2\alpha)$  is the input impedance of a slot antenna with width  $2\alpha$ .

Radiators with the same width of the metal shell and the slot are of particular interest. If to set that  $2\alpha = 2\beta = \pi/2$ , we obtain:  $k^2 = 0.0294$ ,  $K(\sqrt{1-k^2})/K(k) = 2.0$ , i.e.,

$$Z_E(\pi/2) = Z_S(\pi/2) = 60\pi. \quad (6.35)$$

As can be seen from (6.35), the slot radiator of infinite length with angular arm width  $2\alpha = \pi/2$  mounted on a cone has a constant and purely resistive input impedance, and hence it has a high level of matching with a source (with cable or generator) in an unlimited frequency range. If the radiator has finite dimensions, the frequency range is limited, but remains sufficiently wide. The such slot in a metal cone is shown in Fig. 17. In this option the edges of a slot coincide with the cone generatrices.

These results do not answer the question why, when the width of metallic and slot radiators is changes, the product of their wave impedances does not change, i.e., expression (6.34) remains true. In accordance with (6.35), if  $\alpha = \beta = \pi/4$ , then  $k = \tan^2(\pi/8)$ ,  $K(\sqrt{1-k^2})/K(k) = 2.0$ , and  $Z_E(\pi/4) = Z_S(\pi/4) = 60\pi$ . The function  $K(k)$  is the complete elliptic integral of the first kind of the argument  $k$ . It is calculated by the formula

$$K(k) = \int_0^1 \frac{dt}{\sqrt{(1-t^2)(1-k^2 t^2)}}. \quad (6.36)$$

Let us change the angular width of the radiators. Let  $\alpha/2 = \pi/8 + \delta$  and  $\beta/2 = \pi/8 - \delta$ , where  $\delta \ll \pi/8$ . Then the magnitude  $k_m$  for the metallic radiator is equal to

$$k_m = \tan^2(\pi/8 + \delta).$$

Introducing the notation  $T = \tan(\pi/8)$ , it is easy to show that  $\tan(\pi/(8 + \delta)) \approx T + \delta(1 + T^2)$  and

$$k_m^2 = \tan^4(\pi/(8 + \delta)) \approx T^4 + 4\delta T^3 (1 + T^2),$$

i.e.,

$$\sqrt{1 - k_m^2 t^2} = \sqrt{1 - T^4 t^2 - 4\delta T^3 (1 + T^2) t^2} = \sqrt{1 - T^2 t^2} \left[ 1 - \frac{2\delta T^3 (1 + T^2) t^2}{1 - T^4 t^2} \right]$$

and

$$\sqrt{1 - (1 - k_m^2) t^2} = \sqrt{1 - t^2 + T^4 t^2 + 4\delta T^3 (1 + T^2) t^2} = \sqrt{1 - t^2 + T^4 t^2} \left[ 1 - \frac{2\delta T^3 (1 + T^2) t^2}{1 - t^2 + T^4 t^2} \right].$$

Then

$$K(k_m) = \int_0^1 \frac{dt}{\sqrt{(1 - t^2)(1 - k_m^2 t^2)}} = K(T) + 2\delta T^3 (1 + T^2) \int_0^1 \frac{dt}{(1 - T^4 t^2) \sqrt{1 - t^2} \sqrt{1 - T^4 t^2}},$$

and

$$\begin{aligned} K(\sqrt{1 - k_m^2}) &= \int_0^1 \frac{dt}{\sqrt{(1 - t^2)[1 - (1 - k_m^2) t^2]}} \\ &= K(\sqrt{1 - T^2}) + 2\delta T^3 (1 + T^2) \int_0^1 \frac{dt}{(1 - t^2 + T^4 t^2) \sqrt{1 - t^2} \sqrt{1 - t^2 + T^4 t^2}}. \end{aligned}$$

Similar expressions for the slot radiator, more precisely for located next to it the metallic radiator with an angular width  $\beta$ , are obtained by replacing  $\delta$  with  $-\delta$ . This means that

$$K(k_m)K(k_s) = K^2(T) - 4\delta^2 T^6 (1 + T^2)^2 \left[ \int_0^1 \frac{t^2 dt}{(1 - T^4 t^2) \sqrt{1 - t^2} \sqrt{1 - T^4 t^2}} \right]^2,$$

$$\begin{aligned} &K(\sqrt{1 - k_m^2}) K(\sqrt{1 - k_s^2}) \\ &= K^2(\sqrt{1 - T^2}) - 4\delta^2 T^6 (1 + T^2)^2 \left[ \int_0^1 \frac{t^2 dt}{(1 - t^2 + T^4 t^2) \sqrt{1 - t^2} \sqrt{1 - t^2 + T^4 t^2}} \right]^2 \end{aligned}$$

Therefore, in the first approximation

$$\frac{K(k_m)}{K(\sqrt{1 - k_m^2})} \frac{K(k_s)}{K(\sqrt{1 - k_s^2})} = \frac{K^2(T)}{K^2(\sqrt{1 - T^2})}, \quad (6.37)$$

i.e., in accordance with (6.34), when the angular width of the metallic and slot radiators is different,

$$Z_E Z_S = Z_A^2,$$

where  $Z_A$  is the input impedance of the self-complementary radiator. Thus, if  $\alpha/2$  is distinguished from the required magnitude  $\pi/8$  by a small magnitude  $\delta$ , the product  $Z_E Z_S$  distinguishes from  $(60\pi)^2$  on  $\delta^2$ , that confirms the stationary property of the ratio (6.35).

It is necessary to emphasize that the last expression and the expression (6.37) have a higher degree of accuracy than a first approximation, since the neglected terms are not only proportional to  $\delta^2$ . Actually, the magnitude, which is multiplied to  $\delta^2$ , is equal to the product of the same function  $f(T) = -4T^6(1 + T^2)^2$  onto the integral, where the ratio of the values located in the numerator [this magnitude is equal to  $k(T)$ ] in and in the denominator [this magnitude is equal to  $\sqrt{1 - k^2}$ ] is the same as in expression (6.37). Therefore, it should expect that the substitution of functions with precision up to  $\delta^2$  will show that difference between the left and right sides of an expression (6.26) is equal to the magnitude of the third order of smallness.

The method of calculating the wave and input impedances of the metallic and slot radiators located along a surface of a circular cone by means of using the wave impedance of infinitely long uniform line may be applied also in other cases, for example to the radiators located along the pyramid sides. Let the pyramid has two metal sides (in the shape of the flat triangles), two sides-slots, and the rectangular cross-section (Fig. 18). The wave impedance of the line formed by two triangular plates depends on the constant along the line relation of magnitudes  $b$  and  $d$  ( $b$  is the plate width in the given cross-section,  $d$  is the distance between plates). But the wave impedance does not depend on absolute values of these magnitudes. That means that the two-wire line is also uniform, and that its input impedance with increasing line length tends to the wave impedance  $W$ .

Angles  $\alpha$  and  $\beta$  are related by the expression  $\tan \alpha / \sin \beta = b/d$ . As one can see from a given formula,  $W$  is the function of two arguments: the ratio  $b/d$  and the

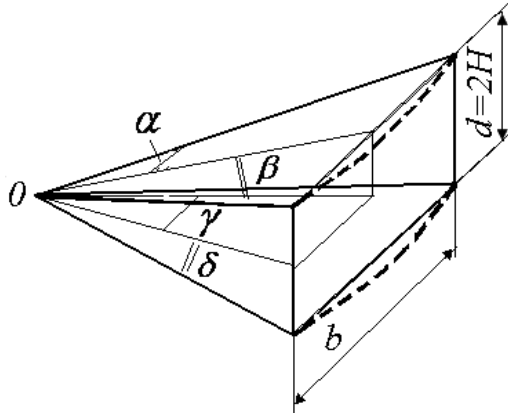


Fig. 18: Antenna, located along the pyramid sides.

angle  $\alpha$ . If, for example,  $b/d = 1$ , the change of from  $15^\circ$  to  $30^\circ$  (and accordingly  $\beta$  from  $15.5^\circ$  to  $35.3^\circ$ ) results in the change of the wave impedance from  $42.3 \pi$  to  $45 \pi$ , i.e.,

$$Z_E = Z_S = (42.3 - 45)\pi.$$

$Z_S$  is equal to input impedance of the metal radiator located next to the slot. If  $b/d = 2$ ,  $\beta = 30^\circ$ , then  $Z_S = 28.2\pi$ .  $Z_E$  is the input impedance of the metal radiator, which is identical to the slot in the shape and dimensions. One can show that in this case,  $\sin \delta = \sin \beta \cos \alpha = 1/(2\sqrt{2})$ ,  $\gamma = \tan^{-1}(b \tan \beta/d) = 63.4^\circ$ , i.e.,  $Z_E = 54.2\pi$ , and  $Z_E Z_S = (39.1\pi)^2$ . If  $b/d = 5$ ,  $\beta = 15^\circ$ , then  $Z_E = 12.7\pi$ . As for  $Z_S$ , it is equal to input impedance of located next to the slot metal radiator, which has the ratio  $b/d$ , equal to  $1/5$ , and the angle  $\beta$  is calculated in accordance with equality  $\tan \beta / \tan \gamma = d/b$ , where  $\gamma = 15^\circ$  (with mutual replacing  $b$  by  $d$  the angles  $\beta$  and  $\gamma$  are interchanged). It is easy to be convinced that  $\beta = 53.3^\circ$ , i.e.,  $Z_S = 105\pi$ , and

$$Z_E Z_S = (36.6\pi)^2.$$

As the calculations show, the product  $Z_E Z_S$  depends on the ratio  $b/d$ , but always it is smaller than  $(60\pi)^2$ . The smaller angle  $\alpha$  the closer wave impedance of the radiator located along the pyramid sides to the wave impedance of the conical radiator with the same angular width.

On the example of a conical radiator, we shall consider in detail using results of solving two-dimensional problems in the analogous three-dimensional problem. It is known that located at the cone infinitely long radiators with the same angular width of the metal shell and the slot have the constant and purely resistive input impedance. It permits to secure a high level of the matching in unlimited frequency range. If the radiator has the finite dimensions, then the frequency range is limited, but remains rather wide. The Section 5.4 describes the requirements for the task, under which the field is uniquely determined. In particular, the shape and size of conductive bodies in both problems should be the same.

In going to the two-dimensional problem in accordance with the conditions (6.27), the radiator length remains finite, if the radiator before transition had a finite length and therefore differs from the system of infinitely long cylindrical wires. Limitation on the length of wires changes the nature of the problem. Line of infinite length can be considered uniform. If the line length is finite, then in calculating its total capacity it is necessary to consider the partial capacitance between the wire of each line and the surface of zero potential (see Fig. 11). Since the lateral dimensions of the line are small in comparison with its length, it is expedient to consider that the distance to the surface of zero potential is equal to double generatrix length ( $2l = 2H/\sin \theta_0$ ). Assuming that the maximal lateral dimension of the metal shell is  $2aa$ , we estimate the additional capacitance per unit length of the cylinder as

$$C_1 = \frac{2\pi\epsilon}{\ln(4l/aa)},$$

where  $a$  is the cross-section radius.

The partial mutual capacitance between the metal shells depends on an arc length  $2\alpha$ . If  $2\alpha = \pi/2$ , this capacitance in accordance with (6.30) is equal to  $C_0(\pi/2) = 2\varepsilon$ . When arc length is changed, the capacitances  $C_0$  and  $C_1$  are changed too. The wave impedance of a transmission line formed by the metal shell and its reflection in the ground is equal to

$$W(2\alpha) = \frac{k}{\omega[C_0(2\alpha) + (C_1(2\alpha)/2)]} = \frac{120\pi\varepsilon}{C_0(2\alpha) + C_1(2\alpha)/2}. \quad (6.38)$$

Here  $C_0(2\alpha)$  is the partial mutual capacitance per unit length, when the value  $2\alpha$  is arbitrary.

The input impedance of the slot antenna, which shape and dimensions coincide with shape and dimensions of the metal radiator, is equal to the input impedance of the metal radiator located near the slot, whose width is  $2\beta = \pi - 2\alpha$ . Its wave impedance is equal to

$$W(2\beta) = \frac{120\pi\varepsilon}{C_0(2\beta) + C_1(2\beta)}. \quad (6.39)$$

Here  $C_0(2\beta)$  is the partial mutual capacitance per unit length, when the length of the metal shell cross-section is  $2\beta$ . The difference between  $\alpha$  and  $\beta$  leads to different wave impedances of the metal and slot radiators. In the general case we are talking about the difference between the structures answering to expressions (6.38) and (6.39). This difference exists between the metal and slot antenna. Both antennas are located on the same cone structure, but have the different width. Similar difference exists between the antennas located along the sides of a regular pyramid (with square cross-section and a value  $b/d$ , equal to 1) and along the sides of an irregular pyramid (with rectangular cross-section and a value  $b/d$ , not equal to 1).

In accordance with (6.36) one can suppose that the reactive components change slowly in beginning and after that began to oscillate synchronously in opposite phase. In this case the second summand in the right part of expression (6.38) is positive and compensates the decrease of the first item caused by  $R_{A2}$  decrease. In the common case the input impedance of the metal radiator with the finite length  $L$  and the angular width  $2\alpha$  is approximately equal to  $Z_{A1} = R_{A1} - jW(2\alpha)f_1(kl)$ . Here  $l = L/\cos\theta_0$  is the generatrix length. The input impedance of the metal radiator situated next to the slot is approximately equal to  $Z_{A2} = R_{A2} - jW(2\beta)f_2(kl)$ . The different width of these radiators despite the same length causes a small difference of their impedances, which is shown schematically as distinction first between  $R_{A1}$  and  $R_{A2}$ , and second as distinction between  $f_1(kl)$  and  $f_2(kl)$ . If  $\alpha = \beta$ , the product  $Z_{A1}Z_{A2}$  is equal to

$$Z_{A1}Z_{A2} = [R_{A1} - jW(2\alpha)f_1(kl)]^2. \quad (6.40)$$

If  $\alpha \neq \beta$ , then

$$Z_{A1}Z_{A2} = R_{A1}R_{A2} - W(2\alpha)W(2\beta)f_1(kl)f_2(kl) - jR_{A1}W(2\beta)f_2(kl) - jR_{A2}W(2\alpha)f_1(kl). \quad (6.41)$$

In this case, if  $\alpha > \beta$ , an equivalent radius of the first radiator is greater than that of the second one, i.e., its partial mutual capacitance between the arms per unit length is greater, and its wave impedance is smaller. The partial capacitance between each arm and the surface of zero potential (see Fig. 11) also decreases the wave impedance of the radiator. The function  $f_1(kl)$  changed faster than  $f_2(kl)$ .

If  $\alpha = \beta$ , then in the case of increasing the cone length the reactive components of both radiators change fast and together and asymptotically approach to zero. As a result, the input impedance of each infinite radiator is purely active and does not depend on the frequency. This result is consistent with (6.35). If,  $\alpha \neq \beta$ , then in accordance with (6.36), one can suppose that the reactive components change slowly in the beginning and after that, oscillate synchronously in opposite phase. In this case the second item in the right part of expression (6.41) is positive and compensates for the decrease of the first item caused by  $R_{12}$  decrease.

One must emphasize that the performance of self-complementary radiators is not always preferable in comparison with that of radiators close thereto in shape. That would be, if the wave impedance of the cable was equal to  $60\pi$  Ohm. When using a standard cable with a wave impedance 100 Ohm, the matching level in each frequency range may be higher, if, for example, to use the pyramid with a rectangular cross-section and the diminished input impedance closed to the cable wave impedance.

## 6. Field of a Long Line from Converging Parabolic Wires

The infinite long, identical in shape and dimensions metal and slot radiators, which fill the all plane, are called self-complementary. In [6] it was shown first that the structure consisting of electric and magnetic radiators of the same shape and dimensions may not be flat. The volumetric self-complementary structure has the properties like the properties of the plane structure. It has the constant and purely resistive input impedance, which ensures a high level of matching with a cable in the wide frequency range. Equal power is radiated into the inner and outer corner of the cone, regardless of the angle at the apex of a cone and the width of the metal and slot radiators.

Reducing conical three-dimensional problem to two-dimensional (to plane problem) plays a big role in the development of electromagnetic theory and its use in antenna engineering. The analysis shows that a choice of surface for placement of the self-complementary radiating structure is not accidental. It is the surface of rotation.

As was said earlier, use of the expressions (6.27), allows us to reduce the conical three-dimensional problem to the two-dimensional one. These expressions relate with each other the variables of spherical and cylindrical systems of coordinates, and this replacement permits to transfer from one self-complementary structure to another one. This result plays a big role in the development of electromagnetic theory and its use in the antenna engineering. A similar result can be obtained, if we reduce the parabolic problem to the plane problem. The generatrix of a circular cone is a straight line. The curve line also may be used as a generatrix. If such a generatrix has a parabolic shape, the metallic surface assumes the shape of a paraboloid of rotation. Calculating the field of two infinitely long charged filaments of curvilinear

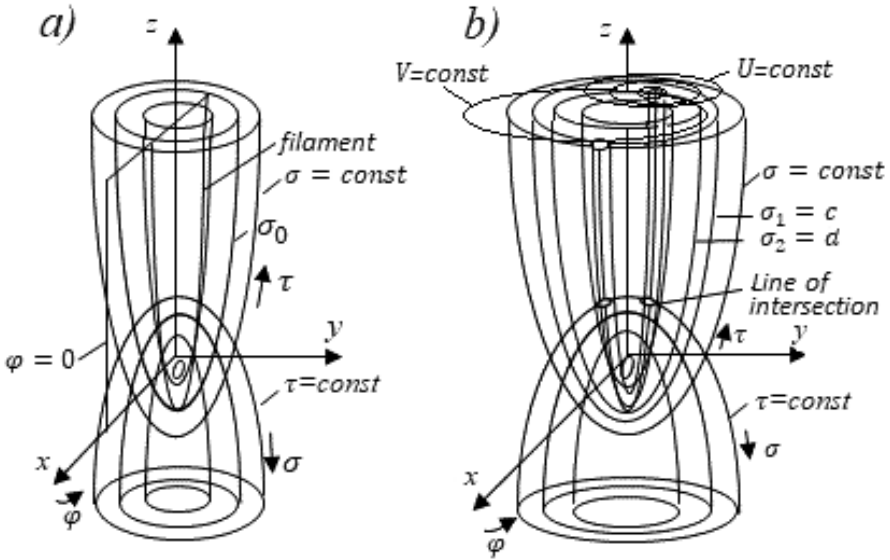


**Fig. 19:** Three-dimensional problem for two infinitely long parabolic filaments (a), and solid geometrical figures (b).

shape located on the paraboloid surface and converging to its vertex (Fig. 19) is a matter of unconditional interest.

Use of parabolic coordinates  $(\sigma, \tau, \varphi)$  facilitates an analysis of such a structure. This is a system of orthogonal curvilinear coordinates [7]. The coordinate surfaces of such a system are, first, the confocal paraboloids of rotation ( $\sigma = \text{const}$ ,  $\tau = \text{const}$ ), whose focal point coincides with the origin of coordinates system, and, second, the half-planes ( $\varphi = \text{const}$ ), passing through the axis of rotation (see Fig. 19). Rectangular coordinates are related to parabolic coordinates by the equalities:

$$x = \sigma\tau \cos \varphi, \quad y = \sigma\tau \sin \varphi, \quad z = (\tau^2 - \sigma^2)/2. \quad (6.42)$$

Parabolic lines are located along the surface of a paraboloid, or more exactly they are lines of intersection of this surface with the half-planes, passing through the axis of rotation. As in the case of convergent straight wires, it is expedient to reduce the calculation problem of an electrostatic field of two charged parabolic filaments to the calculation of the field of two parallel filaments (see Fig. 12b). To this end the Laplace's equation in accordance with the uniqueness theorem must remain true at the transition from one problem to another, and the surfaces of conductive bodies must coincide with the surfaces of equal potential.

In the cylindrical coordinates system  $(\rho, \varphi, z)$ , the Laplace's equation for a potential  $U$  has the form

$$\frac{\partial}{\partial \rho} \left( \rho \frac{\partial U}{\partial \rho} \right) + \frac{1}{\rho} \frac{\partial^2 U}{\partial \varphi^2} = 0. \quad (6.43)$$



Here, it is taken into account that  $\partial U/\partial z = 0$ , i.e., the lines parallel to  $z$ -axis have a constant potential (the field is plane-parallel). In the system of parabolic coordinates Laplace's equation has the form

$$\frac{1}{\sigma^2 + \tau^2} \left[ \frac{1}{\sigma} \frac{\partial}{\partial \sigma} \left( \sigma \frac{\partial U}{\partial \sigma} \right) + \frac{1}{\tau} \frac{\partial}{\partial \tau} \left( \tau \frac{\partial U}{\partial \tau} \right) + \left( \frac{1}{\sigma^2} + \frac{1}{\tau^2} \right) \frac{\partial^2 U}{\partial \varphi^2} \right] = 0. \quad (6.44)$$

As seen from (6.44), the equation is symmetrical with respect to  $\sigma$  and  $\tau$ , that is, the equation for each unknown quantity is valid irrespective of an equation for another quantity. In particular, for  $\sigma$  we obtain

$$\frac{1}{\sigma^2} \left[ \frac{1}{\sigma} \frac{\partial}{\partial \sigma} \left( \sigma \frac{\partial U}{\partial \sigma} \right) + \frac{1}{\sigma^2} \frac{\partial^2 U}{\partial \varphi^2} \right] = 0. \quad (6.45)$$

Here  $U(\sigma) = U(\tau)$ , if other coordinates are the same. If, for example,  $\partial U/\partial z = 0$ , then in accordance with (6.42)  $\sigma = \sqrt{\tau^2 - 2z}$ ,  $\tau = \sqrt{\sigma^2 + 2z}$ , i.e.,

$$\partial \sigma / \partial z = -1/\sigma, \quad \partial \tau / \partial z = 1/\tau, \quad \text{and} \quad \frac{\partial U}{\partial z} = \frac{\partial U}{\partial \sigma} \frac{\partial \sigma}{\partial z} + \frac{\partial U}{\partial \tau} \frac{\partial \tau}{\partial z} = 0,$$

whence

$$(1/\tau) \partial U / \partial \tau = (1/\sigma) \partial U / \partial \sigma.$$

Comparison of (6.43) and (6.45) shows that these equations coincide, if the replaceable variables are related by equalities:

$$\rho = \sigma, \quad \varphi_c = \varphi. \quad (6.46)$$

Here  $\rho$  and  $\varphi_c$  are the cylindrical coordinates,  $\sigma$  and  $\varphi$  are the parabolic coordinates. Hence, the Laplace's equation holds true in the transition from the parabolic problem to the cylindrical, if expressions (6.46) are true. These expressions were first obtained in [7].

The substitution of variables in accordance with (6.46) results in the transforming (mapping) of parabolic surface  $\tau = \text{const}$  onto the plane  $(\rho, \varphi_c)$  for an arbitrary  $\tau$ . The line of this surface intersection with any paraboloid  $\sigma = \text{const}$  is transformed into a circumference. Two parabolic filaments situated along surface  $\sigma = \sigma_0$  in the plane  $xOz$  (see Fig. 19a) are transformed into two parallel wires spaced at distance  $2b = 2\sigma_0$  in the cylindrical coordinates system (see Fig. 12b). Two geometrical figures located between parabolic surfaces  $\sigma_1 = c$  and  $\sigma_2 = d$  (see Fig. 19b) are transformed into two solid cylinders of radius  $a = (c - d)/2$ , whose axes located at the distance  $2h = c + d$  (see Fig. 13a).

The scalar potential of the electric field for two parabolic charged filaments situated along surface  $\sigma = \sigma_0$  (with linear charge density equal to  $\pm q_0$ ) similarly to (6.26) is equal to

$$U(\sigma, \varphi) = \frac{q_0}{2\pi\epsilon} \ln(\rho_2/\rho_1),$$

where

$$\rho_2^2 = (\sigma_0 - \sigma \cos \varphi)^2 + \sigma^2 \sin^2 \varphi, \rho_1^2 = (\sigma_0 + \sigma \cos \varphi)^2 + \sigma^2 \sin^2 \varphi.$$

The designation  $q_0$  is used here instead of  $\tau$  in order to avoid confusion.

The surfaces of equal potential  $U = \text{const}$  in the given case are the volumetric geometrical figures, and their planes of symmetry coincide with the plane  $xOz$ . Each surface satisfies an equation

$$\rho_2/\rho_1 = m = \text{const}.$$

For the plane problem the line of equal potential is the circumference with the center in the point

$$h_m = b(1 + m^2)/(1 - m^2)$$

and with the radius

$$a_m = 2bm/|1 - m^2|.$$

Using these magnitudes, we find the coordinate  $\sigma$  of the parabolic surface, on which the axis of volumetric figure is located:

$$\sigma_m = h_m = \sigma_0 (1 + m^2)/|1 - m^2|,$$

and also, we determine the semi-axis length of the closed curve formed by the intersection of this volumetric figures with the surface  $\tau = \text{const}$ :

$$a_m = (\sigma_{1m} - \sigma_{2m})/2 = 2m\sigma_0/|1 - m^2|.$$

The angle  $\psi_m$  between the paraboloid generatrix and axis is equal to

$$\psi_m = \tan^{-1} \{2a_m/[1 - (h_m^2 - a_m^2)]\} = \tan^{-1} (2m/|1 - m^2|) \tan \theta_0.$$

The surfaces of field strength  $V = \text{const}$ , in which force lines are located, are also circular paraboloids. Their axial lines lie in the plane  $yOz$  on the parabolic surfaces

$$\sigma_n = h_n = \sigma_0 \cot \varphi_n,$$

and the semi-axis lengths of the closed curves on the surface  $\tau = \text{const}$  are equal to

$$a_n = (\sigma_{1n} - \sigma_{2n})/2 = \sigma_0/\sin \varphi_{cn}.$$

The sense of the angle  $\varphi_{cn}$  is clear from Fig. 12b, where it is designated by  $\varphi_n$ . Indeed, in the plane problem the flow function appears as

$$V = -q_0 (\varphi_{c2} - \varphi_{c1})/(2\pi\varepsilon).$$

The equation of the field line

$$\varphi_{c2} - \varphi_{c1} = \varphi_{cn} = \text{const}$$

is the equation of a circumference, the radius of which is equal to  $a_n = b/\sin \varphi_{cn}$ , and the axis is remote from axis  $z$  to the distance  $h_n = b \cot \varphi_{cn}$ . In the parabolical problem the axial lines of the circular paraboloids  $V = \text{const}$  also lie in the plane  $yOz$  and form with axis  $z$  the angle

$$\theta_n = \tan^{-1} (\cot \varphi_{cn} \tan \theta_0),$$

and the angle  $\varphi_n$  between paraboloid axis and generatrix is equal to

$$\varphi_n = \tan^{-1} (\tan \theta_0 / \sin \varphi_{cn}).$$

From this it is clear that one of the surfaces of the equal field strength created by the parabolic  $V$ -radiator coincides with the parabolic metallic surface passing through the axes of this radiator. Lines of magnetic field lie in this surface, and therefore the radiator field in consequence of insertion of the metallic surface does not change.

Use of the equalities (6.46) allows us to reduce the parabolic problem to the cylindrical problem and to calculate capacitance  $C_l$  per unit length and the wave impedance  $W$  of a long line consisting of two volumetric figures with the parabolic axes. By analogy with (6.29), we find:

$$C_l = \frac{\pi \varepsilon}{ch^{-1} [(\sigma_1 + \sigma_2)/(\sigma_1 - \sigma_2)]} \quad W = 120ch^{-1} [(\sigma_1 + \sigma_2)/(\sigma_1 - \sigma_2)].$$

The input impedance of a uniform two-wire line, when the line length increases, tends to its wave impedance

$$Z_{AB} = 120ch^{-1} \frac{\sigma_1 + \sigma_2}{\sigma_1 - \sigma_2}.$$

The case of two charged converging shells located along the paraboloid surface (Fig. 20) is of a specific interest. This structure is a variant of placing metallic and slotted antennas of finite length on surface of rotation. If the arc lengths of converging shells are equal to  $2\alpha$ , then this parabolic problem is like the problem for the long line from two coaxial cylindrical shells. The electrostatic field of such line is shown in Fig. 15b. The field structure in the case of two shells located on the paraboloid surface is of a similar nature, but surfaces of equal potential  $U = \text{const}$  and surfaces of field strength  $V = \text{const}$  coincide with parabolic surfaces rather than with the cylindrical surface.

As seen from (6.30), capacitance  $C_l$  per unit length and wave impedance  $W$  of an equivalent line are dependent only on arc length  $2\beta$  of the slot antenna in the cross-section and, accordingly on arc length  $2\alpha = \pi - 2\beta$  of the metallic shell. For this reason, expressions (6.30) are true for both the parabolic and conical shells. Magnitudes  $C_l$  and  $W$  are constant along the long line, i.e., the two-wires long line is uniform. The wave impedance and the input impedance of an infinitely long line excited by a generator situated near the paraboloid vertex are equal to

$$W = Z_{AB}(\alpha) = 120\pi K(k)/K(\sqrt{1-k^2}),$$

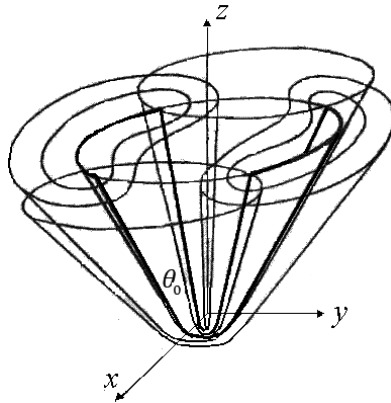


Fig. 20: Three-dimensional problem for non-closed coaxial shells located on the paraboloid.

where in the case of two metal plates (one dipole)  $k = \tan^2(\beta/2)$ . If  $\alpha = \beta$ , the radiator is self-complementary, and  $Z_{AB}(\pi/4) = 60\pi$ .

The results of a calculation show that decreasing an inclination angle of the antenna arm with respect to ground (and corresponding increase of the arm length without height increase) improves the electrical characteristics of the antenna. If the inclination angle of the radiator located on the surface of a cone and a paraboloid is the same, then the radiator on the paraboloid surface has the greater gain particularly in the lower part of the frequency range. The directional patterns of the radiators in a vertical plane (pattern factor) are approximately the same. The directivity of both antennas is greater than the directivity of the flat vertical antenna.

Coordinate systems, considered earlier, have a circular structure (a circular cross-section). In order to analyze electric fields of charged bodies elongated in the horizontal direction, we need to use corresponding structures with a horizontal section, for example, in the shape of an ellipse. Vertical generatrix of such a structure can have the shape of a parabola (Fig. 21) or the shape of a broken line.

In the first case the structure has the form of elliptical paraboloid. In the second case a vertical cross-section has a shape of triangle, rectangle or trapezoid. In both the cases the possibilities of calculating electric fields created by charged three-dimensional structures are significantly expanded. For example, one can use these structures to calculate the field in a phantom, to determine the fields of flat radiators, and so on.

As a coordinate system for calculating the fields of an elliptical paraboloid, one can use a system of orthogonal curvilinear coordinates  $(\tau, \psi, \sigma)$  [7, 9]. Coordinate surfaces of this system are created by two mutually orthogonal families of horizontal ellipses and vertical parabolas. The coordinate  $\tau$  in this system is the radius of the ellipse,  $\psi$  is the angle between this radius and the axis  $x$  (see Fig. 21). In a rectangular coordinate system, the elliptic equation has the form  $x^2/a^2 + y^2/b^2 = 1$  (here  $a$  and  $b$  are the major and minor semi-axis of the ellipse). Correspondingly, the rectangular and curvilinear coordinates are related by relations  $x = \tau \cos \psi$ ,  $y = \tau \sin \psi$ . The vertical coordinate  $\sigma$  is equal to  $cz^2$  or  $cz$ .

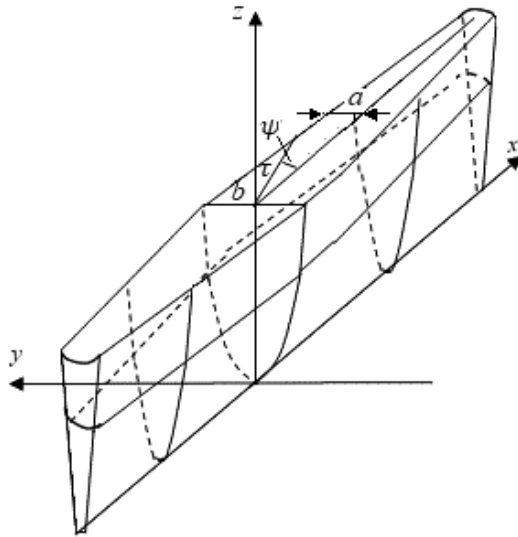


**Fig. 21:** Three-dimensional body, elongated in the horizontal direction.

Since it was not possible to find detailed information about the proposed coordinate system, the problem is considered in a general form [9]. The Laplace's equation for a curvilinear orthogonal coordinate system in the general case has the form

$$\Delta V = \frac{1}{e_1 e_2 e_3} \left[ \frac{\partial}{\partial u} \left( \frac{e_2 e_3}{e_1} \frac{\partial V}{\partial u} \right) + \frac{\partial}{\partial v} \left( \frac{e_3 e_1}{e_2} \frac{\partial V}{\partial v} \right) + \frac{\partial}{\partial w} \left( \frac{e_1 e_2}{e_3} \frac{\partial V}{\partial w} \right) \right] = 0. \quad (6.47)$$

Here  $u = \tau$ ,  $v = \psi$ ,  $w = \sigma$ ,  $e_1^2 = \left( \frac{\partial x}{\partial u} \right)^2 + \left( \frac{\partial y}{\partial u} \right)^2 + \left( \frac{\partial z}{\partial u} \right)^2$ ,  $e_2^2 = \left( \frac{\partial x}{\partial v} \right)^2 + \left( \frac{\partial y}{\partial v} \right)^2 + \left( \frac{\partial z}{\partial v} \right)^2$ ,  $e_3^2 = \left( \frac{\partial x}{\partial w} \right)^2 + \left( \frac{\partial y}{\partial w} \right)^2 + \left( \frac{\partial z}{\partial w} \right)^2$ , i.e.,  $e_1 = 1$ ,  $e_2 = \tau$ ,  $e_3 = 1/(2\sqrt{c\sigma})$ , or  $1/c$ ,  $e_1 e_2 e_3 = \tau e_3$ .

The substitution of the said magnitudes in (6.47) yields

$$\Delta V = \frac{1}{\tau} \left[ \frac{\partial}{\partial \tau} \left( \tau \frac{\partial V}{\partial \tau} \right) + \frac{1}{\tau} \frac{\partial^2 V}{\partial \psi^2} + \frac{\tau}{e_3^2} \frac{\partial^2 V}{\partial \sigma^2} \right] = 0. \quad (6.48)$$

As was mentioned, in accordance with the uniqueness theorem, when the three-dimensional problem is reduced to a plane task, the Laplace's equation (6.43) must remain valid and the metallic surfaces must coincide with lines of equal potential. Let us compare the resulting equation (6.48) with the Laplace's equation (6.43) in a cylindrical coordinate system. In (6.43) it is taken into account that  $(\partial U)/\partial z = 0$ , i.e., the potential does not depend on  $z$ . If we will assume that

$$\tau = \rho, \quad \psi = \varphi, \quad (6.49)$$

then equation (6.48) coincides with (6.43). The essential difference between expressions (6.43) and (6.48) is that the value  $\rho$  in (6.43) does not depend on the

angle  $\varphi_c$ , and the value  $\tau$  in (6.48) depends on  $\psi$ . That fact drastically changes the field's structure.

We will consider a particular case of such a structure with a cross-section that does not depend on the coordinate  $z$ . As was said in the Chapter 5 in accordance with [6], if the solitary wire of a circular cross-section with the charge  $q$  per unit length is in a homogeneous medium with dielectric permittivity  $\varepsilon$ , then its complex potential is equal to

$$\zeta(z) = V(x, y) + jU(x, y) = -\frac{q}{2\pi\varepsilon} j \ln z + C, \quad (6.50)$$

where  $V(x, y)$  is the flow of the electric field strength (of the vector  $\vec{E}$ ),  $U(x, y)$  is the potential of the total sum of charges. Equation  $V(x, y) = \text{const}$  is the equation of the field strength line, and  $U(x, y) = \text{const}$  is the equation of the equal potential line in the plane of the cross-section,  $x$  and  $y$  are rectangular coordinates in this plane. Introducing the notation  $z = \rho e^{j\varphi_c}$ , where  $\rho$  and  $\varphi_c$  are polar coordinates in the indicated plane, we obtain expression (5.22) and equations for the line of field strength and the line of equal potential in the shape

$$\varphi_c = \text{const}, \rho = \text{const}.$$

Go over to the complex potential of a solitary wire with elliptic cross-section, we arrive in accordance with (5.22) for curve of the field strength at equation  $V(x, y) = -A\psi + C_1$  and for the curve of equal potential at equation  $U(x, y) = A \ln \tau + C_2$ . The corresponding field is presented in Fig. 22a.

The complex potential of a structure consisting of two conductors with a circular cross-section, which are located at a distance  $2b$  from each other, is equal to  $\zeta(z) = Aj \ln \frac{\partial^2 V}{\partial \sigma^2} + C$ . Let's introduce the notations:  $z + b = \rho_1 e^{j\varphi_1}$ ,  $z - b = \rho_2 e^{j\varphi_2}$ , where  $\rho_1$  and  $\rho_2$  are the lengths of the segments between the axes of the conductors and the observation point  $M$ ;  $\varphi_1$  and  $\varphi_2$  are the angles between these segments and the axis  $x$ . If to assume that  $C = 0$  we find:

$$V = A(\varphi_2 - \varphi_1), U = A \ln \rho_1/\rho_2. \quad (6.51)$$

In this field the line of zero potential coincides with the ordinate axis, the initial line of the field strength is the abscissa axis between the line conductors and infinity. Lines of equal potential are the ellipses with focal points on the axis  $x$ , lines of field strength are the ellipses with focal points on the axis  $y$  passing through the wires' axes. The capacitance per unit height of two identical conductors with an elliptical cross-section, if the small axes of the ellipses are located on the same straight line (Fig. 23a), is equal to (see [3])

$$C_l \approx \frac{\pi\varepsilon}{sh^{-1} d/\sqrt{a^2 - b^2} - sh^{-1} b/\sqrt{a^2 - b^2}}.$$

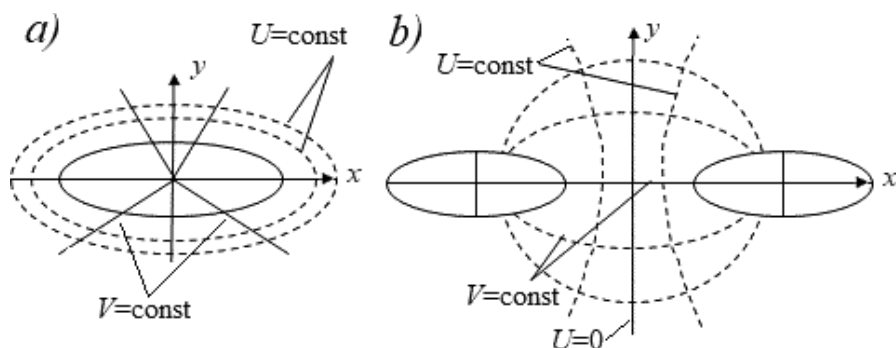


Fig. 22: Field of one (a) and two (b) three-dimensional bodies, elongated in the horizontal direction.

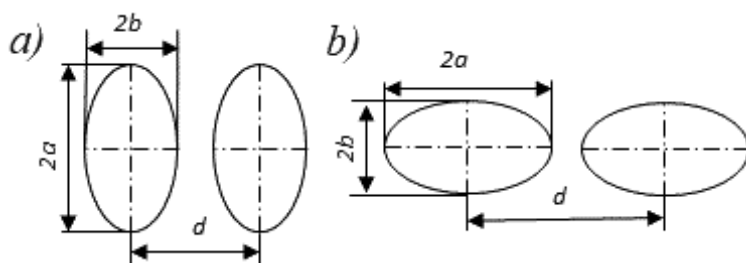


Fig. 23: Two identical wires with an elliptical cross-section.

If the great axes of ellipses are located on the same straight line (Fig. 23b), this capacitance is equal to

$$C_l \approx \frac{\pi \varepsilon}{sh^{-1} d / \sqrt{a^2 - b^2} - sh^{-1} a / \sqrt{a^2 - b^2}}.$$

The new coordinate systems in particular coordinates of elliptic paraboloid allow to substantially simplify the solution of separate tasks. One of these tasks is a problem of phantoms.

The so-called phantoms were developed to determine the energy that a human body receives during an irradiation. Designers tried to create the devices of such shape, which coincides with the shape of the human body. As a result, different devices essentially differ from each other by shape and dimensions. But the people have not identical dimensions, i.e., excessive accuracy does not make sense. Since the developed phantoms have a complex shape and unknown characteristics, measurements on different phantoms give different results and users when they compare these results with each other doubt these measurements.

An attempt to compare the measurement results in different phantoms depending on their shape and dimensions was previously made using a system of parabolic rotation coordinates [11]. The coordinate system for an elliptical paraboloid permits significantly simplify the solution of this problem. The human body in the phantom

is modeled by a vessel with a liquid. The dielectric constant and conductivity of a liquid must be equal to the average values of these magnitudes for the human tissues at operating frequencies. A probe immersed in the liquid records the field values at the points inside a phantom. The field is created by the transmitting antenna (by a horizontal dipole) located under the vessel with the liquid. The field magnitude at the measurement point depends on the medium between the radiating antenna and the point of observation, more precisely on the capacitance of the indicated interval. This interval consists of three parts: a free space between the transmitting antenna and the vessel, the dielectric shell of the vessel and the space between the shell and the probe. The shell serves as a boundary between different media, so its surface is the surface of an equal potential, and other such surfaces pass inside the vessel in parallel to its shell.

The dielectric constant of the fiberglass shell is equal to  $\varepsilon_1 = 2.7$ , the permeability of a liquid is  $\varepsilon_2 = 41.5$ . The shell capacitance is equal to  $C_1 = \varepsilon_1 S_1/d_1$ , where  $S_1 = Ll$  is the area of the vessel side surface from the lower boundary to the level of the vessel's liquid (see Fig. 21),  $d_1$  is the shell thickness,  $l$  is the length of parabola between the lower boundary and the liquid level, and  $L$  is the vessel's perimeter (the ellipse length) along the midline between these boundaries. A similar formula permits to calculate the capacitance of the liquid's layer between the envelope and the probe. The air with permeability 1 practically does not affect the capacitance value.

Calculating capacitances of the side phantom used by Holon Technological Institute gave the following results: the capacitance of the dielectric shell is equal to  $C_1 = 0.027 \mu\Phi$ , the capacitance of the liquid's layer with the thick of 2 cm is  $C_2 = 0.021 \mu\Phi$ , the total capacitance is  $C_1 = 0.012 \mu\Phi$ . The previous results presented in [11] ( $0.0086 \mu\Phi$ ;  $0.010 \mu F$ ;  $0.0047 \mu F$ ) were substantially corrected. The field created by the external antenna is successively reduced after passing each layer.

The effective method of solving three-dimensional electromagnetic problems by means of using results of solving two-dimensional problems is based on such a replacement of variables, at which the Laplace's equation remains valid. The beginning of this method development was the work of Carroll, which allowed solving spherical problems in accordance with results obtained for the cylindrical structures. Later, the region of the method employment was significantly expanded by means of using different systems of orthogonal curvilinear coordinates. New works in this direction permit to get new useful results.

## 7. Distribution of Energy Flow between the Wires of the Long Line and Antenna

The energy transmitted along the wires of two-wire and multi-wire long lines propagates in the space surrounding the wires, i.e., passes through the cross sections of the corresponding structures. In this case the geometrical dimensions of the structure depend only on two coordinates (the field is plane-parallel), i.e., the problem of calculating electric fields of charged bodies is substantially simplified. Nevertheless, this problem does not arouse interest to its strict solution, because the result is considered known. This result was obtained long ago and is shrouded in outdated prejudice.



The method of complex potentials allows us to determine how the energy flow is distributed in the space, in which the wires of the long lines are located. As shown in Sections 5.4 and 5.5, in the case of plane-parallel electrostatic field, flow function  $V(x,y)$  allows us to define the energy flow (the flow of vector  $\vec{E}$ ) through the cylindrical surface of unit length located between the given and zero surface of the field strength. For two parallel infinitely long charged filaments the flow function is defined by the first expression (5.37) and is equal to,  $V = \frac{\tau}{2\pi\epsilon}(\varphi_1 - \varphi_2)$ , i.e., it is proportional to the difference of angles  $\varphi_1 - \varphi_2$  between two directions, whose are limiting the flow on the sides. As seen from Fig. 12b, the flow from a left charged filament  $N$  goes to a right charged filament  $M$  through the cylindrical volume, whose cross-section has the form of a circle with a center at the coordinates' origin. At that the flow goes through an arc, i.e., crosses an arc, which length is equal to a half of the circumference, surrounding the filament  $N$ . It means that the flow goes inside the angle, which is equal to  $\pi$ , that is, the part of the flow, which goes into this volume, is equal to a half of the total flow.

That is valid in both cases of two parallel and two convergent charged filaments: in both cases a half of the flow is directed inside a circular cross-section located between the filaments. This result is based on the equality of the angles at the transition from the cylindrical problem to conical: in accordance with (6.27)  $\varphi_c = \varphi$ . It is true also for two parabolic charged filaments. In accordance with the electrostatic analogy method, the fraction of the constant current in two wires with high conductivity located in a homogeneous weakly conductive medium inside the volume bounded by a circular cylinder (or cone, or paraboloid) too will be the same, if a constant voltage is applied to the wires.

In accordance with the conformity principle the magnetic field of constant linear currents coincides with the electric field of linear charges, if the currents and the charges are identically distributed in space. This means, that a half of the energy flow propagating along a long line, consisting of two parallel (divergent) wires, is concentrated inside the circular cylinder (cone, paraboloid) passing through these wires. Similar postulates are true for the system of two wires with finite radius (see Fig. 13), if we consider the energy flow inside the cylindrical (conical, parabolical) surface, and this surface passes through the filaments, which create the field, whose equipotential surfaces coincide with the outer surfaces of the wires.

If the slotted antenna is located on the circular cone (or the circular paraboloid), then the line of two coaxial shells (see Fig. 6.15a) may be imagine as the sum of pairs of the filaments 1-1'', 2-2'', 3-3'' and so on, which are placed diametrically opposite and have opposite in sign charges (see Fig. 15b). The flow of each pair inside the structure also is equal to a half of the total flow. That means that if symmetrical slotted antennas are located on the circular metal cone (or paraboloid), then the same power is radiated into input and output space independently on the angle at the cone vertex. The field symmetry inside the cylinder, cone and paraboloid is the reason of such equality of powers. One must also remind that expression (6.33) is true for infinite long line. The input impedance of finite line is closed to  $60 \pi$ , but is not equal to it. This fact is confirmed by calculation results.

From said above it follows that in a direction along the any long line consisting of two round wires (Fig. 24a) only the half of the energy flow goes within the cylinder, whose generatrices coincide with the wires. The second half of the energy despite of wide-spread opinion goes through the surrounding space. The same is obtained in the asymmetrical option when the wire 1 located over ground 2 (Fig. 24b): only half of an energy flow goes between the wire 1 and a ground within the cross-section 3. Also, the magnitude  $m$  in the expression (2.58) for the cone and paraboloid of finite length is closed to 0.5. But, if a cross-section of a cylinder (or cone, or paraboloid) has unclosed form, and for example consists of two arcs 4 (Fig. 24c) of different radii, then the flow fraction passing through the structure is not equal to half. Unfortunately, the all these results are approximate, because they do not consider the infinitely distant surface with zero potential.

For a long time, it was believed that most of the energy flow along a symmetric and asymmetric long line is concentrated in the volume, which in Fig. 24 is bounded by a dotted line. The analysis shows that for the identical permittivity on both sides of the dotted line about half of the energy flow passes outside this volume. If volume 3 is filled by the matter with an increased dielectric constant  $\varepsilon_1$ , then the power flux  $P_1$ , passing through this volume is  $\varepsilon_1$  times greater than the flux in the surrounding space, i.e., equal to  $P_1 \approx P(1 - 1/\varepsilon_1)$ , where  $P$ —the total flow.

Account of an infinitely distant surface with zero potential allows us to refine an obtained result. The cross-section of a line in the form the wire 1 located over ground 2 with allowance of the surface 3 of zero potential is presented in Fig. 25a, and if there is a mirror image, in Fig. 25b. This structure is more complex than the structure of a common long line from one wire, which is shown in Fig. 24b. Here in the vicinity of a wire 1 there are two surfaces with the same (zero) potential: the metal surface 2 (grounding) and the metal surface 3. The wire forms with these surfaces the two-wire long lines of a length  $L$ .

At that both lines are in the air, and the propagation constant of the wave along the both lines is equal to the wave propagation constant in the air. The wave impedance of a long line between a wire and a ground is equal to  $W_1 = k/(\omega C_1) = 60 \ln \frac{2b}{a}$ , where  $b$  is the distance between a wire axis and a surface 2,  $a$  is a wire radius. The wave impedance of a long line between a wire and a surface 3 is equal to  $W_2 = k/(\omega C_2) = 60 \ln \frac{l}{a}$ , where the magnitude  $l$  is a distance, greatest of three magnitudes: wavelength  $\lambda$ , wire length  $L$  and radius  $R_c$  of wire curvature (see Section 4.2). In the given case it is equal to  $L$ , i.e.,  $W_2 = 60 \ln L/a$ , and the total wave impedance of the antenna shown in Fig. 25a is  $W = W_1 W_2 / (W_1 + W_2)$ . If  $W_1 = W_2$ , then emf  $e_1$  on the input of the long line between a wire and a ground is equal to a half of emf  $e$  of the generator. But in this case  $W_1 \ll W_2$ .

Since, as is shown in Section 6, the input impedance  $Z$  of a uniform two-wire line tends to its wave impedance  $W$ , then it should be assumed that the input impedance  $Z_1$  of a long line between a wire and a ground is proportional to  $W_1$ , and the input impedance  $Z_2$  of a structure between a wire and a surface 3 is proportional to  $W_2$ , i.e., the fraction of the current and energy flow along the line between a wire and ground is equal approximately to  $0.5 \frac{1}{W_1} / \frac{1}{W} = \frac{W_2}{(W_1 + W_2)} \approx 1 - \frac{W_1}{W_2}$ .

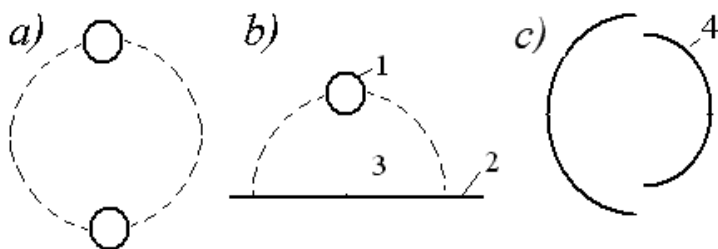


**Fig. 24:** Cross-section of the line from two round wires (a), one wire located over ground (b) and unclosed tube (c).

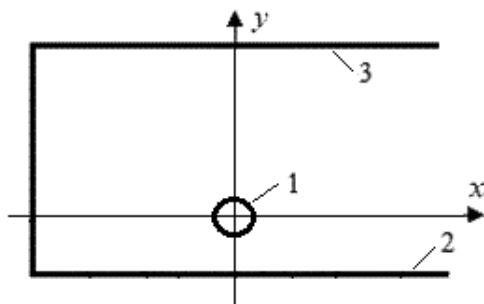


**Fig. 25:** Equivalent structure of the wire located over ground.

By means of the method of complex potentials one can solve the problem of the energy distribution in a structure of a microstrip antenna. The designs and electrical characteristics of microstrip antennas, as well as examples of their application, are described in [12–14].

The microstrip antenna (Fig. 26) presents a thin metal strip 1 (with thickness  $t$ ) located at a small height  $h$  above the ground plate 2, at that  $t, h \ll \lambda$ , where  $\lambda$  is the wavelength. The strip and ground plate are separated by dielectric plate 3 (substrate) as shown in the figure. The radiating elements and the feed lines are usually photoetched on the dielectric substrate. The metallic strip may be having any configuration, but square, rectangular, and circular are the most common because simpler fabrication and analysis. The feed line is made or as a conducting strip 4, as a rule, of smaller width (Fig. 26a) or as coaxial line 5 (Fig. 26b). In the last case the inner conductor of the coax is attached to the metal strip 1, and the external conductor—to the ground plate 2.

With help of microstrip antennas one can create linear and circular polarization. Arrays of microstrip antennas allow to provide the high directivity.

It may seem surprising, but the closest relatives of microstrip antennas should be considered the volume antennas located on a cone, a paraboloid, and a pyramid. All listed antennas consist of two symmetrical radiators: metal and slotted, located under a right angle to each other. They are excited at the point located on the top of a cone, a paraboloid, and a pyramid.

Antennas located on a cone and a paraboloid are usually called complementary or self-complementary, but it would be more correct to call them self-complementary

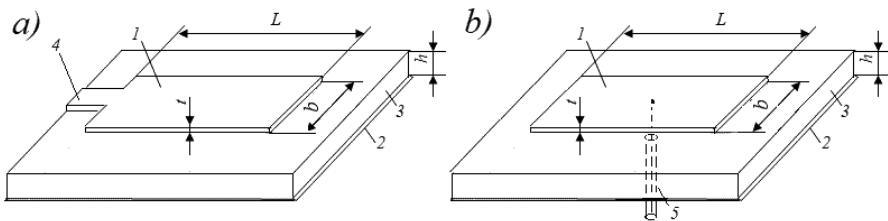


Fig. 26: Microstrip antennas with feed lines made as a conducting strip (a) and as coaxial line (b).

antennas of limited dimensions, in contrast to flat self-complementary antennas that occupy the entire infinite plane. The surface of an antenna on the pyramid is not a smooth surface of rotation with axial symmetry and strictly speaking such an antenna cannot be called complementary. But its characteristics are like those of complementary antennas. The upper and lower faces of the pyramid are made metallic and they form an electric dipole; the two side faces are slots and they form a magnetic dipole. The pyramid cross-section has a rectangular shape. Such structure is easier to realize, than for example conical, and on medium waves the lower arm of the antenna is created as a reflection of the upper arm in the ground.

As can be seen from Fig. 18, the pyramid structure is closest to the structure of the microstrip antenna. In the case of the microstrip antenna the upper and lower trapezoid faces of the pyramid are replaced by rectangular strips, and the metal strips of the antenna and the feed line are joined with each other. The slot radiator is also rectangular, although its width is substantially less than the width of the metal radiator. Basically, microstrip antenna is no different from the structure of the antenna located on the pyramid. The differences are minor.

From said, it follows that in the microstrip antenna the all elements of the so-called transmission-line located along the length  $L$ , do not simply transfer energy from an excitation point to an aperture at an opposite end of the antenna, but radiate the signal, i.e., each antenna element is a source of a field—just as the elements of a two-wire long line radiate weak signals, if the distance between the wires is not zero. Ignoring this radiation is the main disadvantage of the so-called transmission-line model. Wave attenuation in the antenna substrate cannot serve as the justification for such an approach.

Let us compare the microstrip antenna with the antenna on the pyramid, not considering the permittivity of the substrate. A cross-section of the microstrip antenna is given in Fig. 27. The dotted line in the figure shows a mirror image in the grounding (metal plate). The capacitance of the symmetric structure between a microstrip antenna and its mirror image is two times less than the capacitance of the asymmetric structure. Considering the microstrip antenna as a combination of two longitudinal radiators: metal and a slot, we determine an input impedance of each one. The capacitance of a metal radiator per unit length can be calculated as the capacitance between two identical plates with a common plane of symmetry.

A strict expression for its calculation contains complete and incomplete elliptic integrals of the first and second kind and requires the solution of an equation consisting of such functions. We will use for calculations the approximate functions. Here and below, we extensively employ the formulas given in [3]. If the width of the

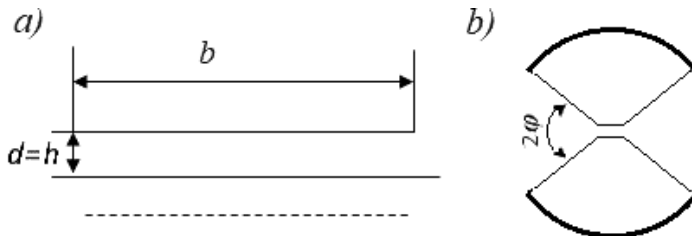


Fig. 27: Cross-section of a microstrip (a) and a cylindrical (b) antenna.

metal plate is equal to  $b$ , and the distance between the plates is  $d$ , then at  $b/d > 27$  the capacitance between the plates per unit length is  $C_l \approx \varepsilon b/d$ . When  $1 < b/d \leq 27$ ,

$$C_l \approx \varepsilon \frac{b}{d} \left\{ 1 + \frac{d}{\pi b} [1 + \ln(2\pi b/d)] \right\}.$$

If, for example,  $d = h = 0.7874$  mm,  $b = 33.15$  mm, then for the capacitance between the metal plates (according to the approximate first formula and the more accurate second one) we obtain

$$C_{l1} = 42.1\varepsilon, \quad C_{l2} = 44.2\varepsilon.$$

The wave impedance of a long line formed by two metal strips of width  $b$  located in a free space at a distance  $d$  from each other, is  $W = k/(\omega C)$ , where  $k = 2\pi/\lambda$  is propagation constant of the wave in air,  $\omega = 2\pi f$  is circular frequency,  $\lambda$  is wave length,  $f$  is frequency,  $\lambda f = c = 3 \cdot 10^8$  is speed of light. Since  $1/c = 120\pi \varepsilon_0$ , where  $\varepsilon_0 = 10^{-9}/(36\pi)$  is the absolute permittivity of the free space, we get that  $W = 120\pi \varepsilon_0 / C_{l2} \cong 2.7\pi$ . This magnitude is equal to the wave impedance  $W_M$  of the metal radiator included in the structure of the complementary antenna.

To calculate the wave impedance  $W_s$  of a metal radiator identical to a slot in shape and size, it is need to determine the capacitance between the metal strips having dimensions of slots and located on the slots' places. Capacitance between plates with width  $d$ , located at a distance  $b$  from each other, if  $d/b \leq 1$ , is equal to  $C_1 \approx \pi \varepsilon_0 / \ln(4b/d)$ , i.e.,  $C_1 = 0.613\varepsilon_0$ , and  $W_s = 195.8\pi$ . For the asymmetric antenna the product of wave impedances is  $W_E W_s \cong (23\pi)^2$ . For the symmetrical antenna this product is 4 times larger, i.e., it is equal to  $(46\pi)^2$ . As is known, the product of the wave impedances of self-complementary antennas is  $(60\pi)^2$ . In the given case, this magnitude is significantly smaller, since the surface on which they are located, cannot be called smooth.

The symmetrical structure consisting of a microstrip antenna and its mirror image is like the structure of a complementary antenna consisting of two unclosed shells (Fig. 27b) separated by angles  $2\varphi$ . The capacitance between them per unit length of shells is equal to (see [3])

$$C_l = \varepsilon K(\sqrt{1-k^2})/K(k),$$

where  $K(k)$  is the complete elliptic integral of the first kind from the argument  $k = \tan^2 \varphi/2$ . Let's compare this structure with the structure of the microstrip antenna.

For the given dimensions of this antenna, assuming that the structure radius is equal to  $R = b/2$ , and the angle  $\varphi$  is equal to  $\varphi = h/R$ , we find  $\varphi/2 = h/b = 0.024$ . In accordance with expression for  $C_l$  we get  $k = 0.00056$ ,  $\sqrt{1-k^2} = 0.9999998$ ,  $K(k) = 1.5708$ ,  $K(\sqrt{1-k^2}) = 8.87$ , that is  $C_{l1} = 5.7\epsilon$ .

If replace the angle width  $2\varphi$  of the slot with the angular width of the shell (it is equal to  $2\alpha = \pi - 2\varphi$ ), we get  $\alpha/2 = 0.7616$ ,  $k = 0.909$ ,  $K(k) = 2.3217$ ,  $\sqrt{1-k^2} = 0.416$ ,  $K(\sqrt{1-k^2}) = 1.6464$ , that is the capacitance between the slots is  $C_{12} = 0.71\epsilon$ . Wave impedances are respectively  $W_E = 21.05\pi$ , and  $W_s = 169\pi$ . The product of the wave impedances is  $W_E W_s = (60\pi)^2$ —full agreement with the properties of the self-complementary structures. The difference between the results for the structures shown in Fig. 27a and 27b is, of course, caused with the difference in the distances between the arms of the metal radiators.

As mentioned above, each of the radiators presented in Fig. 26 can be simultaneously viewed as a long line and as an antenna. This approach does not differ from the usual comparison of a linear antenna with an equivalent long line. That greatly simplifies calculating the wave impedance and other characteristics of an antenna. The structure of the microstrip antenna and the dimensions of its cross-section are constant along its length  $L$ , i.e., the equivalent long line is uniform, and its wave impedance is constant.

However, it is necessary to note a significant difference between a microstrip antenna and a long line (and antennas associated with it). Known antennas are often divided into symmetrical (e.g., the dipole) and asymmetric (e.g., the monopole). In this case, a structure is called asymmetric, if it consists of a real antenna and its mirror image in the ground or grounding. Asymmetry essentially means a change in the sign or direction of the current. The asymmetry of a microstrip antenna is caused by the difference in the media adjacent to it from above and below and the large width of the plate compared to the thickness of the substrate. This results in a different magnitude of currents along the top and bottom surfaces of the plate. In this case, the emf on both surfaces at the point of connection of the generator is the same. The voltages are also the same on both sides of the plate along its entire length.

Thus, the structure of a microstrip antenna is more complex than the structure of a common long line. To simplify this structure, we will use the method of analysis analogous to a method, which was applied to the wire located over ground. Let us replace the metal plate with width  $b$  by a metal cylinder 1 with a radius  $a = b/\pi$  (with the same surface area). The cross-section of such a structure is shown in Fig. 28. As can be seen from this figure, in the vicinity of the radiator there are two surfaces with the same (zero) potential. This is, firstly, the metal surface 3, on which the antenna is located (grounding). This is, secondly, the surface of zero potential 4, which is located at a distance from the radiator equal to the total length  $2L$  of an antenna. The substrate is noted by the number 2. The mirror image in the ground is not shown in order not to complicate the figure.

The substrate is one of the main elements of a microstrip antenna. It changes all its electric characteristics: capacitance per unit length, propagation constant, electric field—and complicates antenna calculation. In accordance with the theory of a long line the propagation constant of the wave along the metal wire 1 is equal to

$k_1 = k \sqrt{\mu_r \varepsilon_r}$ . An increase of the propagation constant leads to a corresponding increase of the wave impedance and the reactive component of the input impedance.

As shown in Chapter 5, if the solitary wire or metal plate are located at the boundary of two media, for example, the air space with  $\varepsilon = 1$  and dielectric with the relative permittivity  $\varepsilon_s$  (Fig. 26), the equivalent permittivity of the environment is equal to  $\varepsilon_e = 0.5 + \varepsilon_s/2$ , It means that for  $\mu_r = 1$

$$k_1 = k \sqrt{0.5 + \varepsilon_s/2} = \omega \sqrt{\varepsilon_0 \mu_0} \sqrt{0.5 + \varepsilon_s/2}. \quad (6.53)$$

Here  $\varepsilon_0$  an absolute permittivity of the air. In this case the wave impedance of a long line located between the metal plate and the ground is equal to  $W_1 = k_1/(\omega C_1)$ , where  $C_1 = \varepsilon_0 \varepsilon_e \frac{b}{h}$  is the capacitance per unit length of the line, i.e.,

$$W_1 = 120\pi \frac{h}{\varepsilon_e b} \sqrt{0.5 + \varepsilon_s/2}. \quad (6.54)$$

The capacitance per unit length between a single wire and an infinitely distant surface of zero potential is twice as large as the capacitance of the symmetrical linear radiator from two arms (two wires). The wave impedance  $W_2$  of a long line between a single wire and this surface is half as much as the wave impedance of such a radiator. Therefore, the wave impedance of a long line located between the metal plate of an antenna and this surface is

$$W_2 = 60 \frac{k_1}{k} (\ln 2L/a - 1) = 60 \sqrt{0.5 + \varepsilon_s/2} (\ln 2L/a - 1), \quad (6.55)$$

where  $L$  is the length of an antenna arm,  $a \cong b/\pi$  is its equivalent radius.

Respectively the reactive and active components of the input impedance of described the microstrip antenna are equal to

$$X_A = -\frac{W_1 W_2}{W_1 + W_2} \cot k_1 L, R_A = 80 \left( \frac{k}{k_1} \tan \frac{k_1 L}{2} \right)^2. \quad (6.56)$$

The structure shown in Fig. 28 is obtained by means of replacing the metal plate with width  $b$  by a metal cylinder with a radius  $a = b/\pi$  (with the same surface area). That gives some error. But the new structure permits to define the influence of the zero potential surface 4. This surface is usually not considered, and that leads to a significant error. Moreover, it is necessary to remember and take into consideration that the mentioned replacement, which leads to an approximate choice of the value  $a$  in the expression for the wave impedance, is a standard substitution used in the derivation and solution of integral equations for current, and the error caused by this substitution it is minimal.

As can be seen from Fig. 26, microstrip antennas are made in two versions: asymmetric and symmetrical. In the first version, the equivalent of an antenna is a segment of a long line, excited at one end and open at the other end (analogous to a monopole). Wave impedance  $W_1$  was obtained for this option. The symmetrical

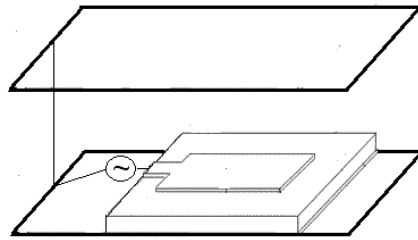


**Fig. 28:** Simplified equivalent structure of the microstrip antenna: 1 – radiator, 2 – substrate, 3 – grounding, 4 – surface of zero potential.

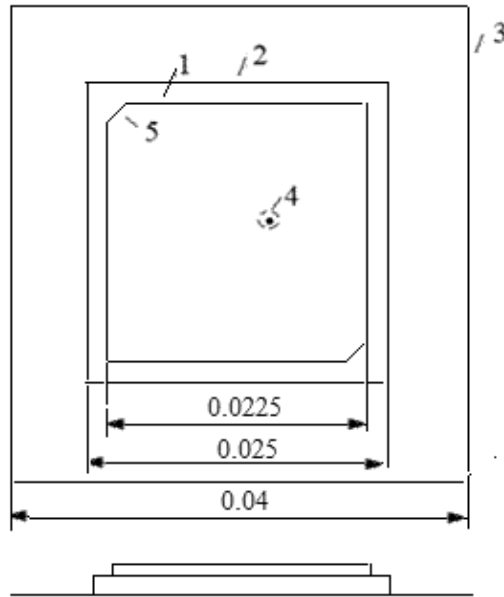


**Fig. 29:** General view of the microstrip antenna with circular polarization. 1 – metal plate, 2 – substrate, 3 – grounding, 4 – cable, 5 – cut corners.

radiator (dipole) is the equivalent of the second option. It consists of two identical arms remote from each other. If the dimensions of these arms coincide with the dimensions of the asymmetric option, then the wave impedance  $W_2$  of the symmetric option is twice as large.

The described method for calculating the characteristics of a microstrip antennas was developed on a significant revision of the previously proposed method [8] and is described in [15].

The rightness of the proposed method was verified by means of using the experimental results obtained on the development of a microstrip antenna with circular polarization [16]. As known, a circular polarization compared to linear polarization has a few advantages in the transmission and reception of radio signals. In the paper [16] it was considered a square microstrip antenna excited by a coaxial cable (Fig. 29). This work has become significant step forward in expanding the employment of microstrip antennas.



The main option of an antenna was designed to operate at the frequency 2.49 GHz. The dimensions of the antenna model (in meters) are given in the figure. The thickness of the metal plate (strip) is approximately 0.01 mm. Two corners of the conductive strip were cut off in order to obtain circular polarization. The circular polarization is created by the rotating current and depends on the depth of the cut off. This depth is selected experimentally and is equal to 0.0028 m. The thickness of the substrate is 3.48 mm, its relative permittivity is  $\epsilon_r = 6.8$ . To optimize the model performance at the specified frequency, the cable connection point is shifted from the center and located at 0.0242 and 0.2095 m from the left and bottom edges of the grounding. The cable radius is 1.6 mm. The paper confirms the possibility of creating a circularly polarized antenna with sufficiently high electrical characteristics: the antenna SWR at the fundamental frequency is 1.5, the bandwidth under the level 6 dB is equal to 0.13 GHz, and the axial ratio is 1.27 db.

Let us apply to this antenna the described method of calculating characteristics. The equivalent permittivity of the antenna substrate is equal to  $\epsilon_e = (6.8+1)/2 = 3.9$ . Since frequency is equal to  $f = 2,49 \cdot 10^9$ , the wave length is  $\lambda = c/f = 0.12$  m, and slowing is  $k_1/k = \sqrt{\epsilon_e} = 1.97$ , then the resonant length of the symmetrical antenna is  $L = \lambda/(2\sqrt{\epsilon_e}) = 0.03$  m. The antenna length, which is equal to the diagonal of the square, with allowance for the cuts, is somewhat less: it is equal to 0.026 m. Therefore, it had to slightly increase this length by shifting the excitation point. This result serves as a clear confirmation of the validity of the described technique and shows that the substrate even of a small thickness significantly increases the equivalent permittivity of the environment.

The obtained results allow us to return to two topics, which already were discussed. The first theme is the traditional approach that makes it difficult to accept new results. The second topic concerns the necessity to analyze the energy flows in the space surrounding an antenna. An analysis of the characteristics of a microstrip antenna based on such the approach showed that its field has a plane-parallel structure, which significantly changes the properties of the radiator.

These results show that the theory of a long lines can essentially help when the considered task is insoluble by the simple methods and causes mathematical difficulties during the use of integral equations.

## 8. Reflector Arrays from Microstrip Antennas

An explosive wave of theoretical work on antennas in the middle of the last century led to the creation of rigorous methods for analyzing and the synthesizing antennas. The widespread use of new antenna options was a side effect of this wave. One of these options was microstrip antenna, considered in a previous Section. The reason for a widespread use of microstrip antennas was the fact that on aircraft, ships, and other moving objects, where size, weight, price, and ease of installation are especially important, low-profile antennas of the appropriate shape and design are needed. Such antennas can be mounted flush on metal surfaces, and it needs only feed lines, which are usually placed under the grounding. As said above, the designs and electrical characteristics of microstrip antennas, as well as examples of their application, are given in [12–14]. Typical structures of microstrip antennas are shown in Fig. 26.

Major operational disadvantages of this antenna are its small efficiency and very narrow frequency bandwidth, which is typically only a fraction of a percent or a few percent. The reason for this lower efficiency is that the antenna thickness is usually very small, and the waves generated within the dielectric substrate undergo considerable reflections when they go along the edge of the strip.

In order to analyze the electrical characteristics of microstrip antenna (patch), several models have been proposed. Greatest attention was paid to model in the form of a two-wire long line [10]. This model treats the antenna as a segment of a transmission line with length  $L$  terminated at both ends by a radiation elements with the admittance  $Y_r$ . It is considered that the transmission line does not radiate because of reflections and acts as a transformer. Each radiating element is made in the form of a slot (with length  $b$  and width  $h$ ), which is perpendicular to the feed line. If the length of the transmission line is approximately  $\lambda/2$ , where  $\lambda$  is the wavelength of the line, then the fields at the aperture of two slots have the same directions, and the slots form a two-element array with a distance  $\lambda/2$  between the elements. The field components parallel to the antenna axis add up in phase and create a maximum radiation along the perpendicular to the ground plane.

As is convincingly stated in [18] the transmission-line model 'has the advantage of yielding very simple expressions for both the real and imaginary part of  $Y_r$ , but it has three important shortcomings: (a) the expressions used for  $Y_r$  are inaccurate for narrow patches (i.e., for  $b \leq \lambda_0$ , where  $\lambda_0$  is free-space wavelength), (b) the mutual coupling between the main radiating slots is neglected, (c) the influence of the side slots on the radiation conductance is neglected.' Here the slots with length  $b$  are called the main radiating slots, and the slots with length  $L$  are called the side slots. Let us give the author the right to such terminology, but it is necessary to change the order of the listed deficiencies, since the main deficiency is the weak interest to the side slots.

In Section 7 the structure of a microstrip antenna was compared with the structure of an antenna located on a pyramid and it was shown that the two-wire long lines radiated along all its length may serve as an equivalent of a microstrip antenna. The method of a complex potential was used for an analysis of the substrate influence on the properties of this antenna. Also, it was said about the importance of expanding a frequency range and improving the characteristics of microstrip antennas. The solution of these problems primarily depends on the nature of a current distribution along a particular antenna. These problems are considered in Chapter 7.

The microstrip antennas are widely used as re-radiators in a reflector array. Reflector arrays became widespread in the capacity of a flat equivalent of a parabolic reflector. Microstrip antennas can be used in such an array as re-radiators. A simplified model of a microstrip antenna in the receive mode is shown in Fig. 30a, the equivalent circuits of the antenna are given in Fig. 30b, c, d.

An input impedance of a flat electric radiator excited at its center is equal to

$$Z_A = R_\Sigma - jW \cos \frac{k_1 L}{2}, \quad (6.57)$$

where  $R_\Sigma$  is the resistance of radiation,  $W$  is the wave impedance of the flat radiator.  $Z_L$  on Fig. 30 is the load impedance. The reflect array, in which microstrip antennas

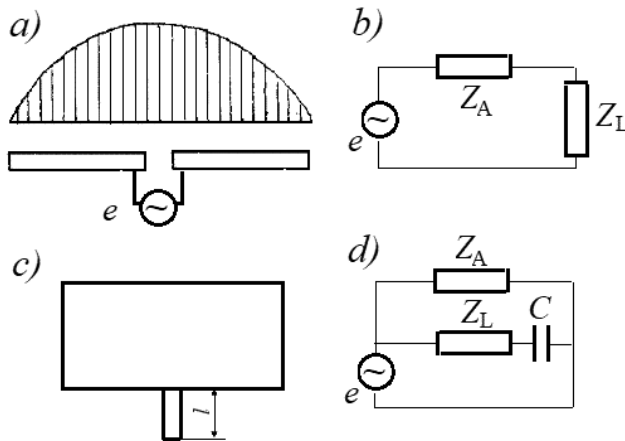


**Fig. 30:** Microstrip antenna in the receive mode (a) and her equivalent circuits for different loads (b, c, d).

are used as re-radiators, creates reflected field with phase depending on the electrical circuit of reradiating antenna. The phase increment of the reflected field relative to the phase of the incident field is determined in accordance with the reciprocity theorem. This theorem argues that the current in the receiving antenna and all the characteristics of the antenna can be found, if the characteristics of the antenna used in transmission mode are known. Applicability of this theorem for the reflect arrays was substantiated in [19].

The amplitude and phase of the current created in a re-radiator depend on the impedance of load. When the load is absent, the current in the antenna is equal to

$$I_A = e/Z_A = e/|Z_A| \exp \{j \cot^{-1}[(W/R_\Sigma) \cot(kL_1/2)]\}. \quad (6.58)$$

Magnitude  $\cot^{-1}[(W/R_\Sigma) \cot(kL_1/2)]$  is the phase increment of the current in the antenna relative to the phase of the incident field. In accordance with the reciprocity theorem, this increment is equal to the phase increment of the reflected field relative to the phase of the antenna current. Hence, the phase step at reradiation is

$$\varphi_1 = 2 \tan^{-1} [(W/R_\Sigma) \cot(kL_1/2)].$$

The value of the step is zero for a tuned antenna, is negative for an elongated antenna, and is positive for a shortened antenna. Increasing of a dipole radius  $a$  reduces its wave impedance  $W$  and decreases the phase step (Fig. 31a).

The approximate method for calculating the phase step of the reradiated field based on the reciprocity theorem, is simple and efficient. After only slight sophistication, this method can be used to analyze antenna with a load. For the capacitive load  $C$ ,

$$I_A = \frac{e}{Z_A - (j/\omega C)} = e/\sqrt{|Z_A|^2 + (1/\omega C)^2} \exp \left\{ j \tan^{-1} \left[ \frac{1}{R_\Sigma} \left( \frac{1}{\omega C} + W \cot \frac{kL_1}{2} \right) \right] \right\},$$

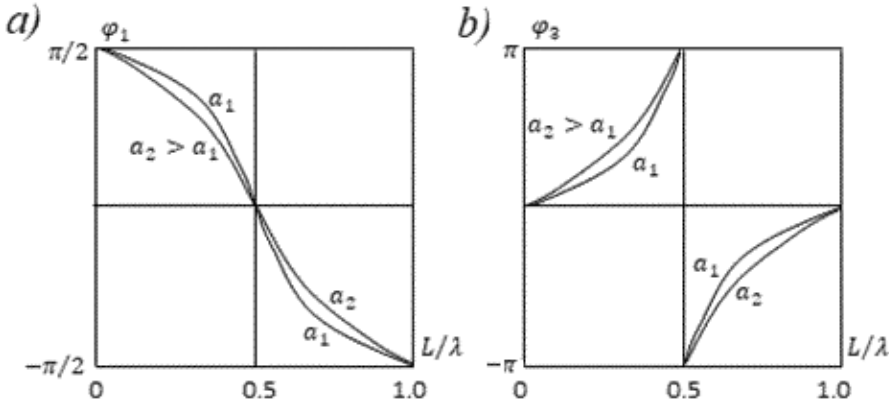


Fig. 31: The step of a field phase at reradiating depending on the antenna length.

i.e., the phase step at reradiating is

$$\varphi_2 = 2 \tan^{-1} \left[ \frac{1}{R_{\Sigma}} \left( \frac{1}{\omega C} + W \cot \frac{kL_1}{2} \right) \right]. \quad (6.59)$$

Here  $\omega$  is the circular frequency of the signal. In the tuned antenna, if the load is fabricated in the form of a dissipative stub (Fig. 30c),

$$I_A = e (Z_A + Z_1)/Z_A Z_1 = e \sqrt{|Z_1|^2 + R_{\Sigma}^2} / (R_{\Sigma} |Z_1|) \exp \{ j \tan^{-1} [R_{\Sigma}/W \tan k_1 L] \},$$

the phase step at reradiating is

$$\varphi_3 = 2 \tan^{-1} [R_{\Sigma}/W \tan k_1 L]$$

(see Fig. 31b). Similarly, for Fig. 30d

$$\varphi_4 = 2 \tan^{-1} \left[ R_{\Sigma}/W \left( \frac{1}{\omega C} + W \cot k_1 L \right) \right].$$

One can apply the above results to calculation of the necessary phase increment of a microstrip antenna at the reradiating. If the signals' phases of secondary radiators are equal, then the signals are added in the direction perpendicular to the array plane.

Let the coordinates of the primary source are  $x_0, y_0$  and  $z_0$  (see Fig. 3.27a). Then the phase increment in the re-radiator  $i$ , needed to compensate the phase difference in the direction of the  $x$ -axis, must be equal to  $\zeta_i = k[\sqrt{x_0^2 + (y_i - y_0)^2 + (z_i - z_0)^2} - x_0]$ . The choice of geometric dimensions of the re-radiator  $i$  allows to obtain phase step  $\varphi_{li} = \zeta_i$ .

In Fig. 32 it is given the field phase increment  $\varphi_1$  created at 60 GHz by a microstrip antenna situated on a substrate with a thickness 0.254 mm with a relative permittivity of 2.22 as a function of the antenna length. The results were obtained by means of the proposed technique. Curves 1 and 2 correspond to antenna widths of 0.3 and 2.3 mm. The rigorous method for calculating the step magnitude was

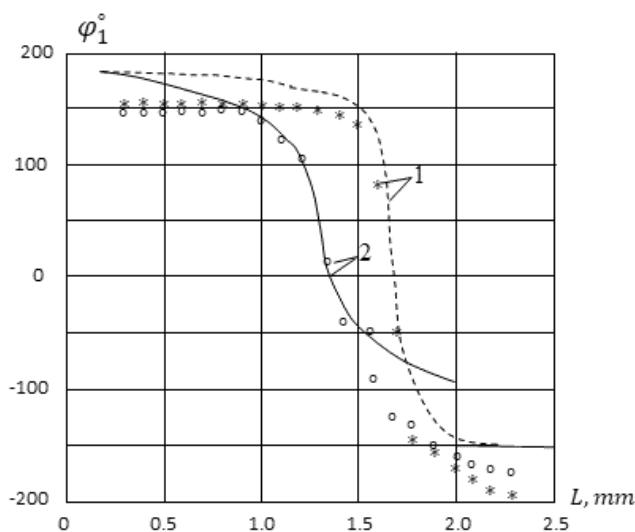


**Fig. 32:** Phase increment  $\varphi_1$  of microstrip antennas with lengths of 0.3 mm (curve 1) and 2.3 mm (curve 2).

described in [20]. It relies on the analysis of a plane wave incidence to an infinite periodic array from identical elements, i.e., on solution of the analysis problem in the spectral domain and on the Floquet's theorem. The open and closed circles in Fig. 32 correspond to the results presented in [20]. As seen from the figure, the correspondence is satisfactory.

Along with simple microstrip antennas, in reflection arrays multilayer (multiple-story) microstrip antennas can be used. The field phase increment in a simple antenna at reradiating is less than  $360^\circ$  (the smooth phase increment in the case of a sufficiently thick substrate at changing strip length in a dependence from a frequency does not exceed  $300^\circ$ ). The maximal phase step, attainable, e.g., in a two-story antenna, is  $540^\circ$ . In a two-story microstrip antenna (Fig. 33) two rectangular metal plates are separated from each other and from the metal plane by a dielectric substrate. The upper plate is smaller than the lower one.

Characteristics of a multiple-story antenna can be calculated by the method described above. The phase increment of the field created at 12.5 GHz by a two-story microstrip antenna containing substrates of a thickness of 3 mm with a relative permittivity of 1.03 is shown in Fig. 34 as a function of antenna length. The antenna is a square. The calculating curves were obtained with the use of the proposed technique. The open and closed circles in the figure demonstrate the results presented in [21].

To get the maximal signal of an antenna array in the prescribed direction, in this direction the phases of the radiators' fields must be equal. Therefore, if this angle varies in the plane  $xOz$ , the phases must vary linearly in dependence of coordinate  $z_i$ :  $\psi_i = k(z_i - z_j) \cos \theta$  (see Fig. 3.27b). To simplify the control procedure, the field phases should be controlled by an electric signal.

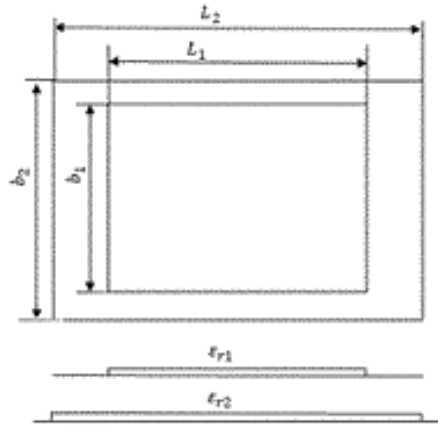
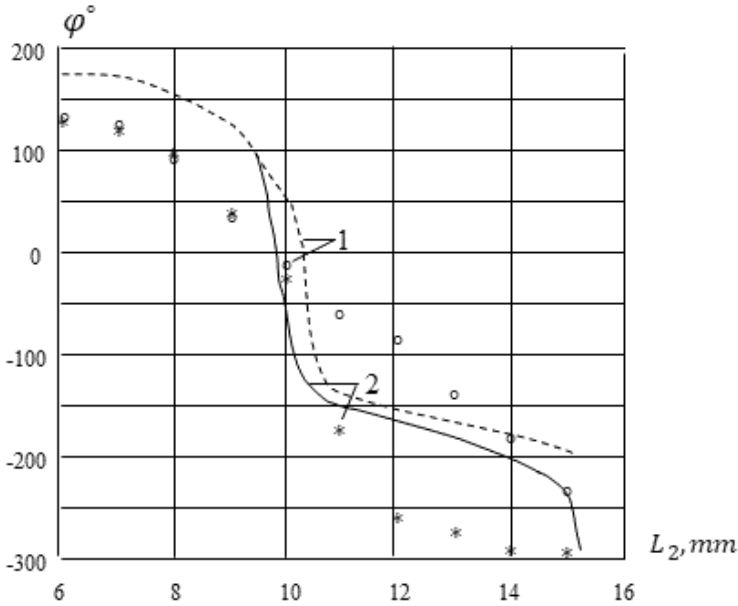


Fig. 33: Two-story microstrip antenna.


 Fig. 34: Phase increment  $\varphi$  of a two-story microstrip antennas with  $L_1/L_2 = 0.6$  (curve and points, dependence 1) and 0.8 (curve and points, dependence 2).

The circuits of microstrip antennas with loads are best suitable for continuous control of a phase of a reradiated field. To include the load in series into the circuit of a receiving antenna, a slot can be cut in the central part of the plane radiator across its axis. Such a slot filled with a dielectric creates the simplest load in the form of a capacitor with a capacitance  $C$ . This capacitance can be easily controlled via varying the permittivity of a special material placed between the capacitor plates by means of the electric voltage. In this case the phase increment at reradiation is determined by expression (6.59).

The tangent of angle  $\varphi_2$  depends on two summands. The first summand,  $\alpha = 1/(R_\Sigma \omega C)$  is caused by the presence of the capacitor in the radiator center. The second summand  $\beta = (W/R_\Sigma) \cot(k_1 L/2)$  is obtained because of the different distances between the separate radiators and the point of observation. The second term must be used to compensate the phase difference caused by the difference in distances between primary radiator 1 and re-radiators 2 of the array (see Fig. 3.27a), while the first term can be used for turning the directional pattern. The total phase increment in the re-radiator  $i$  must be equal to  $\varphi_{2i} = \xi_i + \psi_i$ . Here, if reactance  $1/(j\omega C_i)$  of capacitors  $C_i$ , corresponding to  $\varepsilon_r = 1$ , varies linearly with coordinate  $z_i$ , then, applying equal voltages to the capacitors filled with the same dielectric, we find that the reactance of these capacitors retains a linear dependence on this coordinate. This statement is equally true for the first term established the angle of turning.

Note, however, that the second term takes different values for different re-radiators because they depend on distance  $r_i$ . Therefore, phase  $\varphi_2$  will vary nonlinearly if to applicate the same voltage to all capacitors. If the second term is absent, then for the angular turning the directional pattern requires a linear dependence of phase  $\psi_i$  on the coordinate  $z_i$  is required. The value  $\tan \psi_i = 1/(R_\Sigma \omega C_i)$  and, accordingly, capacitance  $C_i$  do not possess this property. This means that in the general case the angular displacement of the directional pattern requires application of an individual voltage to each capacitor.

If the angle  $\theta$  of the maximum array's radiation is close to  $\pi/2$ , i.e.,  $\alpha \ll \beta$ , a special analysis is required. In this case, by expanding the function  $\varphi_2 = \tan^{-1}(\alpha + \beta)$  into the Taylor series, we obtain

$$\varphi_2(\alpha + \beta) = \tan^{-1} \beta + \alpha/(1 + \beta^2).$$

Here, the member  $\frac{\alpha}{1 + \beta^2} = \left[ R_\Sigma \omega C \left( 1 + \frac{1}{R_\Sigma} W^2 \cot^2 \frac{k_1 L}{2} \right) \right]^{-1}$  is proportional to reactance  $1/(j\omega C)$  of the capacitor  $C$ . Hence, phases of the fields created by secondary radiators will vary linearly with the coordinate upon application of equal voltages to the capacitors filled with the same dielectric. If the direction of the maximum radiation differs substantially from the perpendicular to the array plane, different voltages can be applied to several groups of antennas in order to bring the law of variation of phase  $\varphi_2$  long the antenna closer to a linear. The number of these voltages can be substantially less than the total number of radiators.

At calculation of the capacitance formed by a slot cut in the plate of a microstrip antenna, it should be taken into consideration that this capacitance consists of two terms: capacitance between thin plane plates and capacitance of the plane capacitor between the plate edges.

From the above it follows that the use of capacitive loads in microstrip antennas can play an important role in the control of flat reflected arrays. No less important role, as shown in Section 4.2, can be played by capacitive loads located across the axis of the microstrip antenna in order to expand its frequency range.

## References

- [1] Levin, B.M. and Markov, V.G. (1997). Calculation of fields in coaxial chamber with two helical conductors. Proc. of 14th Intern. Wroclaw Symposium on Electromagnetic Compatibility (Wroclaw), 215–219.
- [2] Kalantarov, P.L. and Zeitlin, L.A. (1986). Calculation of Inductances. Leningrad: Energoisdat, (in Russian).
- [3] Iossel, Yu. Ya., Kochanov, E.S. and Strunsky, M.G. (1981). Calculation of Electrical Capacitance. Leningrad: Energoisdat (in Russian).
- [4] Carrel, R.L. (1958). The characteristic impedance of two infinite cones of arbitrary cross-section, IEEE Transactions on Antennas and Propagation, AP-6(2): 197–201.
- [5] Buchholz, H. (1957). Elektrische und Magnetische Potentialfelder. Berlin (in German).
- [6] Levin, B.M. and Markov, V.G. (1997). Method of Complex Potential and Antennas. St.-Petersburg: Ship Electrical Engineering and Communication (in Russian).
- [7] Korn, G.A. and Korn, T.M. (1961). Mathematical Handbook for Scientists and Engineers. New York, Toronto, London: McGraw-Hill.
- [8] Levin, B.M. (1993). Slot antenna on the cone and pyramid, Radiotechnics and Electronics Engineering, 38(12): (in Russian).
- [9] Angot, A. (1957). Complements de Mathematiques. Paris (in French).
- [10] Mirolubov, N.N., Kostenko, M.V., Levinstein, M.L. and Tichodeev, N.N. (1963). Methods of Electrostatic Field Calculation. Leningrad: Visshaya Shkola, 1963 (in Russian).
- [11] Levin, B.M. (2014). Reduction of a parabolic problem to a 2D problem and a phantom, Radiotechnics and Electronics Engineering, 59(7): 697–703 (in Russian).
- [12] Balanis C.A. (2005). Antenna Theory: Analysis and Design. New York: Wiley & Sons.
- [13] Johnson, R.C. (1993). Antenna Engineering Handbook. New York: McGraw-Hill.
- [14] Microstrip Antennas, edited by Pozar D.M. and Schaubert D.H. (1995). New York: IEEE Press.
- [15] Levin, B.M. (2022). About microstrip antennas, Applied Science, and Innovative Research, 6(3): 1–20.
- [16] Barbakadze, V., Tabatadze, V., Petoev, I. and Zaridze, R. (2021). Directed circular polarized antenna. Proc. 28th Seminar DIPED, Tbilisi, 177–180.
- [17] Munson, R.E. (1974). Conformal microstrip antennas and microstrip phased arrays. IEEE Transactions on Antennas and Propagation, AP-22(1): 74–78.
- [18] Pues, H. and Van de Capelle, A. (1984). Accurate transmission line model for the rectangular microstrip antenna. Proc. IEE-H, 6, 384–340.
- [19] Levin, B.M. (2013). The Theory of Thin Antennas and Its Use in Antenna Engineering. Bentham Science Publishers.
- [20] Menzel, W., Pilz, D. and Al-Tikriti, M. (2002). Millimeter-wave folded reflector antennas with high gain, low loss and low profile. IEEE Antennas and Propagation Magazine, 44(3): 24–29.
- [21] Tsai, F.-C.E. and Bialkowski, M.E. (2003). Designing a 161-element Ku-band microstrip reflect array of variable size patches using an equivalent unit cell waveguide approach. IEEE Transactions on Antennas and Propagation, AP-51(10): 2953–2962.



# Synthesis Problems

## 1. In-phase Current Distribution

The inverse problem of the antennas' theory, or the problem of synthesis, is the problem of creating antennas with the required electrical characteristics. A particular case of such a task is the creation of a wide-range radiator, i.e., creation of an antenna providing in a wide frequency range a high level of matching with a transmitter or a cable and a maximal radiation in a plane, perpendicular to the antenna axis. This task is of great practical importance. A promising method for its solving is the use of concentrated loads.

A typical linear radiator (thin, without loads) fails to meet mentioned requirements. The reactive component of its input impedance is great everywhere, except an area of the series resonance. That leads to a low level of antenna matching with cable. If the radiator arm is larger than  $0.7 \lambda$ , the radiation in the plane, perpendicular to antenna axis, decreases, since the current distribution along a thin linear radiator without loads (Fig. 1a) is close to the sinusoidal, and at high frequencies anti-phase segments are formed on the current curve (Fig. 1b, curve 1).

The electrical characteristics of a linear radiator, i.e., its input impedance, directional pattern, etc., depend on current distribution along its axis. In order to change this distribution, one can use extraneous fields (exciters) or loads—both distributed and concentrated. Even only one load can significantly change the current distribution, and hence the electrical characteristics of the antenna. If a great number of loads are placed along the antenna at small electrical distances from each other, we can consider that they are included continuously along the entire antenna length, and that means a transition from the radiator with a finite number of loads to the radiator with distributed load, i.e., to the radiator with surface impedance. The boundary condition on the surface of this radiator, i.e., along  $z$  axis of the cylindrical system of coordinates between the points  $z = -L$  and  $z = L$ , are given by (2.1). The boundary conditions of such kind are valid, if the structure of the field inside one medium (e.g., inside an antenna cover) is independent of the field structure in another medium (e.g., in ambient space).

By including concentrated loads across the radiator length, one can, depending on their magnitudes and points of connection, obtain the current distribution other

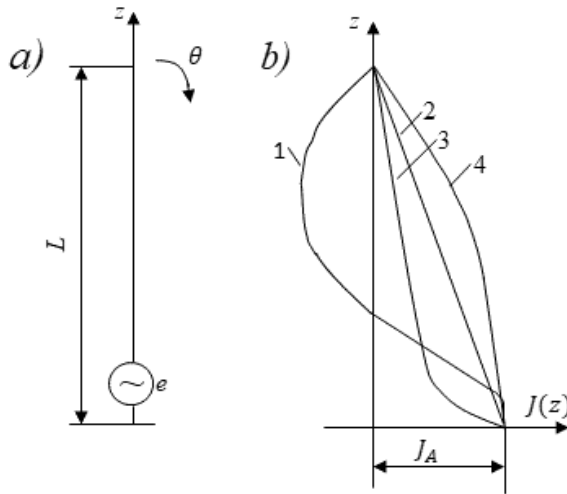


Fig. 1: A linear monopole (a) and the laws of current distribution along it (b).

than the sinusoidal. The experimental results show that a radiator with linear or exponential in-phase current distribution allows us to ensure good performance (high matching level, required shape of the vertical directivity pattern) in a wide frequency range. In particular, such distribution may be created with help of capacitive loads [1, 2]. These results confirm the known fact that the radiation maximum in the direction, perpendicular to the dipole axis, is attained, if the current is in-phase along the entire length of the antenna. Moreover, a long radiator with an in-phase current has high resistance of radiation, which allows to rise the matching level.

As said earlier, an ordinary two-wire long line is an equivalent of a metal radiator. An impedance two-wire long line is an analogous equivalent of an impedance radiator. Unlike the metallic radiator a tangential component of an electric field on a surface of an impedance radiator is not equal to zero, and that causes an additional voltage drop on each element of wire length. The impedance long line, equivalent to the impedance radiator with a constant surface impedance, is shown in Fig. 2.1, and the long line, which is equivalent the radiator with a piecewise constant impedance, is shown in Fig. 2.2. Characteristics of these long lines are given in Section 2.2. Using the expression (2.6) for the square of the propagation constant for current  $J(z)$  in the radiator with constant surface impedance we will write the expression for the generalized wave propagation constant  $\gamma_m$  at the segment  $m$  of a radiator with a piecewise constant impedance in the shape

$$-\gamma_m^2 = k^2 - j2k\chi Z^{(m)}/(a_m Z_0). \quad (7.1)$$

Here  $\chi$  is a small parameter,  $a_m$  is a middle radius. In the general case  $\gamma_m$  is a complex magnitude. In a particular case, when this magnitude is purely imaginary ( $\gamma_m = jk_m$ ), the current distribution at the segment  $m$  of the line has sinusoidal character.

If the law of changing the propagation constant, which allows ensuring the required current distribution, is found, then the expression (7.1) can be used for calculating the surface impedance  $Z^{(m)}$ . The required values of the surface impedance

and the law of its change along the radiator can be realized by means of concentrated loads, connected in an antenna wire (see Fig. 2.4). As is said in Section 2.1, if in accordance with (2.14) the concentrated loads  $Z_m$  are located uniformly along an antenna segment  $m$  at small ( $kb \ll 1$ ) distance  $b$  from each other, this is equivalent to creating a surface impedance  $Z_m = bZ^{(m)}/(2\pi a_m)$  on this segment, i.e., at arbitrary  $\gamma_m$  the current on the segment  $m$  of a stepped line is

$$J(z_m) = I_m \sin h(\gamma_m z_m + \varphi_m), 0 \leq z_m \leq b, \quad (7.2)$$

where  $I_m$  and  $\varphi_m$  are the amplitude and phase of the current along the segment  $m$ , respectively, and  $z_m$  is the coordinate, measured from the segment end, i.e.,  $z_m = (N - m + 1)b - z$ .

Suppose we want to obtain in the long line the given distribution of the current

$$J(z) = J_A f(z), \quad 0 \leq z \leq L, \quad (7.3)$$

where  $J_A$  is the input current of the line (the current of generator),  $f(z)$  is a real and positive distribution function, which corresponds to the in-phase current. If to equate currents  $J(z)$  and  $J(z_m)$  at the beginning and the end of  $m$ th segment, then in the case of a small segment length the current distribution along the line is close to the required one. In accordance with (7.2) and (7.3), at  $z_m = b$  and  $z_m = 0$

$$I_m \sin h(\gamma_m b + \varphi_m) = J_A f[(N - m)b], \quad I_m \sin h\varphi_m = J_A f[(N - m + 1)b].$$

If to divide the left- and right-hand parts of the first equation onto the respective parts of the second equation and, considering that  $b$  is a small magnitude, to be confined by the first terms of expansion of hyperbolic functions with small arguments into series, we will get

$$\tanh \varphi_m = \gamma_m b / \left\{ \frac{f[(N - m)b]}{f[(N - m + 1)b]} - 1 \right\}. \quad (7.4)$$

For the segment  $(m + 1)$ , similarly to (7.4),

$$\tanh \varphi_{m+1} = \gamma_{m+1} b / \left\{ \frac{f[(N - m - 1)b]}{f[(N - m)b]} - 1 \right\}. \quad (7.5)$$

The voltage and current are continuous along a stepped line, hence

$$\tanh \varphi_{m+1} = (\gamma_{m+1}/\gamma_m) \tanh(\gamma_m b + \varphi_m). \quad (7.6)$$

Equations (7.4) and (7.5) present a system of equations that allow us to relate  $\gamma_m$  and  $\gamma_{m+1}$  with each other. The solution of this system shows that magnitude  $\gamma_m$  is independent of  $\gamma_{m+1}$ :

$$\gamma_m = \frac{1}{b} \sqrt{1 - \frac{2f[(N - m)b] - f[(N - m - 1)b]}{f[(N - m + 1)b]}}. \quad (7.7)$$

As is clear from (7.3), function  $f(z)$  defines the law, in accordance with which the amplitude of the current changes along the radiator. In the case of in-phase current distribution along the antenna, its directional pattern in the vertical plane has a form

$$F(\theta) = \sin \theta \int_{-L}^L f(z) \exp(jkz \cos \theta) dz.$$

Calculations show that in this case in contrast to sinusoidal distribution, the radiation maximum with growing frequency does not deviate from the perpendicular to the radiator axis. Increasing  $L/\lambda$  makes the main lobe narrower and increases the maximal directivity.

At linear distribution of the in-phase current amplitude (see Fig. 1b, curve 2),

$$J_2(z) = J_A (1 - z/L), \quad (7.8)$$

where  $z = (N - m + 1)b - z_m$ , i.e.,

$$f_2(z) = (L - z)/L = [(m - 1)b + z_m]/(Nb),$$

The linear distribution is a particular case of the exponential one (see Fig. 1b, curves 3 and 4):

$$J_{3,4}(z) = J_A \frac{\exp(-\alpha z) - \exp(-\alpha L)}{1 - \exp(-\alpha L)},$$

that is

$$f_{3,4}(z) = \frac{\exp(-\alpha z) - \exp(-\alpha L)}{1 - \exp(-\alpha L)} = \frac{\sin h \left\{ \frac{\alpha}{b} [(m - 1)b + z_m] \right\}}{\sin h \frac{\alpha Nb}{b}}, \quad (7.9)$$

where  $\alpha$  is the logarithmic decrement. If  $\alpha$  is positive, the curve of a current is concave, i.e., the current quickly decreases from the maximum value near the generator to zero near the free end of the antenna. If  $\alpha$  is negative, the curve of a current is convex, i.e., the current is more uniformly distributed along the dipole. The steepness of a curve depends on the value of  $\alpha$ . It is easy to show that if  $\alpha$  tends to zero, the expression for  $J_{3,4}(z)$  turns into  $J_2(z)$ .

In the general case of an in-phase current distribution along the antenna, its field  $E_\theta$  at an arbitrary angle to its axis in accordance with expression (3.10) has the form

$$E_\theta = j \frac{30k \exp(-jkR) \sin \theta}{\varepsilon_r R} \int_{-L}^L J(z) \exp(jkz \cos \theta) dz.$$

For an exponential distribution, calculation of the integral gives the expression

$$E_\theta = J \frac{60k J(0) \exp(-jkR)}{\varepsilon_r R} \frac{\cos \theta}{k^2 \cos^2 \theta + \alpha^2} \cdot \{k \cos \theta - e^{-\alpha L} [k \cos \theta \cos(kL \cos \theta) + \alpha \sin(kL \cos \theta)]\}.$$

For a linear distribution we get

$$E_\theta = J \frac{60J(0)}{\varepsilon_r} \frac{\exp(-jkR)}{R} \frac{1 - \cos(kL \cos \theta)}{\sin \theta}.$$

The antenna input impedance in the first approximation is equal to the input impedance of a stepped long line:

$$Z_i = -jW_N \coth(\gamma_N b + \varphi_N).$$

Here, as is seen from (2.7),  $W_N = \gamma_N W/k$ , where  $W$  is the wave impedance of a metal monopole of the same dimensions without loads. If  $m = N$  and  $f(0) = 1$ , then using equalities (7.5) and (7.6) we obtain for the linear current distribution that

$$Z_i = -j(W/kb)[f_2(-b) - 1]. \quad (7.10)$$

As seen from this expression, reducing the reactive component of the input impedance requires a slow variation of function  $f(z)$  near the antenna base, so that the difference in square brackets should be a small magnitude—of the order of  $kb$ . Otherwise, the reactive component of input impedance will be great.

For the exponential distribution, replacing  $f_2(-b)$  with  $f_3(-b)$ , we obtain from (7.10)

$$Z_{A3} = -j(W/kL)f_x(aL/2), \quad (7.11)$$

where  $f_x(x) = x(1 + \coth x)$ . The graph of function  $f_x(x)$  is given in Fig. 2a. In particular for the linear distribution

$$Z_{A2} = -j \frac{W}{kb} \left( \frac{N+1}{N} - 1 \right) = -j W/(kL).$$

Accordingly, for the effective length of the radiator in this case we obtain

$$h_e = \int_{-L}^L \left( 1 - \frac{|z|}{L} \right) dz = L,$$

The radiation's resistance in the first approximation is equal to

$$20k^2 h_e^2 = 20k^2 L^2$$

Based on the results obtained in Chapter 4, the input impedance of the antenna is

$$Z_{A2} = (-jW/kL + 20k^2 L^2) (1 + \chi).$$

Figure 2b compares the input impedance  $X_{A1}$  of a uniform long line with sinusoidal current distribution and the input impedance  $X_{A3}$  of a non-uniform line with exponential in-phase current distribution depending on frequency. Here, the magnitude  $\alpha$  is counts as constant. In the first case the input impedance has a shape

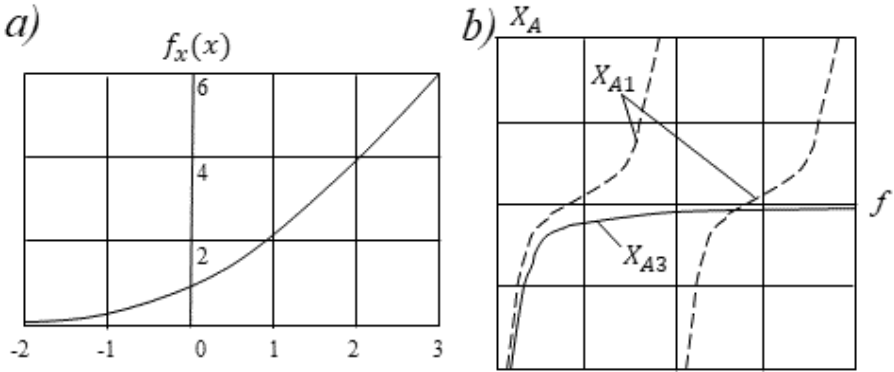


Fig. 2: Function  $f_x(x)$  (a), and the input impedances of uniform and non-uniform line (b).

of a cotangent, in the second case the curve smoothly approaches to the axis with frequency growth and that allows ensuring good matching in a wide range. As seen from Fig. 2a and expression (7.11) for  $Z_{A3}$ , if  $\alpha$  decreases, the input impedance of a long line at a given frequency diminishes. It means that a decrease of  $\alpha$  results in a decrease of the reactive component of the antenna input impedance. Simultaneously the effective height grows, since the area, bounded by the curve of the current, increases; hence, the radiation's resistance grows too. Thus, at exponential distribution, it is expedient to decrease  $\alpha$ , for example, to use the negative magnitudes of  $\alpha$ . According to (2.14) and (7.1),

$$-\gamma_m^2 = k^2 - jk\chi Z_m / (30b). \quad (7.12)$$

In order to create the in-phase current distribution, magnitude  $\gamma_m$  should be purely real or purely imaginary along the entire antenna, and magnitude  $\gamma_m^2$ , correspondingly, only positive or only negative:

$$\text{sign } \gamma_m^2 = \text{const } (m).$$

In order to the in-phase distribution has been realized in a wide frequency range, magnitude  $\gamma_m$  should be real:

$$\gamma_m^2 > 0. \quad (7.13)$$

Indeed, if the values of  $\gamma_m$  (and also  $\varphi_m$ ) will purely imaginary, the hyperbolic sine in the formula (7.2) would become the trigonometric sine. With frequency growth, an argument of a sine will increase and become more than  $\pi$ , and the sine will change sign. If  $\gamma_m$  is real, then, as seen from (7.4), if function  $f(z)$  changes monotonically (decreases with growth of  $m$ ), the sign of  $\varphi_m$  coincides with sign of  $\gamma_m$ . As it follows from (7.7), in order that  $\gamma_m$  will be real, following condition must be carried out

$$f[(N-m)b] \leq \frac{1}{2} \{f[(N-m+1)b] + f[(N-m-1)b]\}. \quad (7.14)$$

i.e., function  $f(z)$  cannot be convex.

Two variants of carrying-out of condition (7.14) in a wide frequency range follow from (7.12). The first variant takes place if

$$k^2 \ll jk\chi Z_m/(30b). \quad (7.15)$$

i.e.

$$\gamma_m^2 = jk\chi Z_m/(30b). \quad (7.16)$$

If one takes into account that parameter  $\chi$  is, strictly speaking, a complex magnitude ( $\chi = \chi_1 - j\chi_2$ ), then the admittance of load is equal to

$$Y_m = 1/Z_m = j\omega C_m + 1/R_m, \quad (7.17)$$

where

$$C_m = 4\pi\epsilon\chi_1/(b\gamma_m^2), \quad R_m = b\gamma_m^2/(4\pi\epsilon\omega\chi_2).$$

From (7.17) it follows, that if the magnitude  $\gamma_m^2$  is positive, each load should be executed as a parallel connection of a resistor and a capacitor (Fig. 3a). The resistance of the resistor should vary in inverse proportion to frequency, and the capacitance of the capacitor should remain constant. When creating an actual antenna, it is expedient to choose the value of  $R_m$  for the middle frequency of the range.

To obtain required current distribution  $f(z)$  along the antenna, the magnitude  $\gamma_m$  should correspond to equality (7.7). Substitution of (7.7) into (7.17) gives

$$C_m = 4\pi\epsilon\chi_1 b \left\{ 1 - \frac{2f[(N-m-1)b] - f[(N-m-1)b]}{f[(N-m+1)b]} \right\}, \quad R_m = \frac{\chi_1}{\chi_2 \omega C_m}. \quad (7.18)$$

By comparing (7.14) and (7.18), one can easily be convinced that, if inequality (7.14) holds, the values of  $C_m$  are not negative. For exponential and linear distribution,

$$C_{m3} = \frac{8\pi\epsilon\chi_1}{\alpha^2 b \{1 + \coth [\alpha(m-1)b/2]\}}, \quad C_{m2} = \frac{4\pi\epsilon}{\alpha} \chi_1 (m-1), \quad R_m = \frac{\chi_1}{\chi_2 \omega C_m}. \quad (7.19)$$

One can see from (7.19) that in the particular case, if one must obtain a law of current distribution, close to the linear, capacitances of loads should decrease towards to the free end of the antenna in proportion to the distance from it:

$$C_{m2} = C_{N2} (m-1)/(N-1).$$

where  $C_{N2}$  is the capacitance of the capacitor near the antenna base. The resistances of resistors should grow towards to the free end of the antenna:

$$R_{m2} = R_{N2} (N-1)/(m-1).$$

Thus, to obtain an in-phase current distribution that ensures high electrical characteristics of an antenna in a wide frequency range, each load should represent

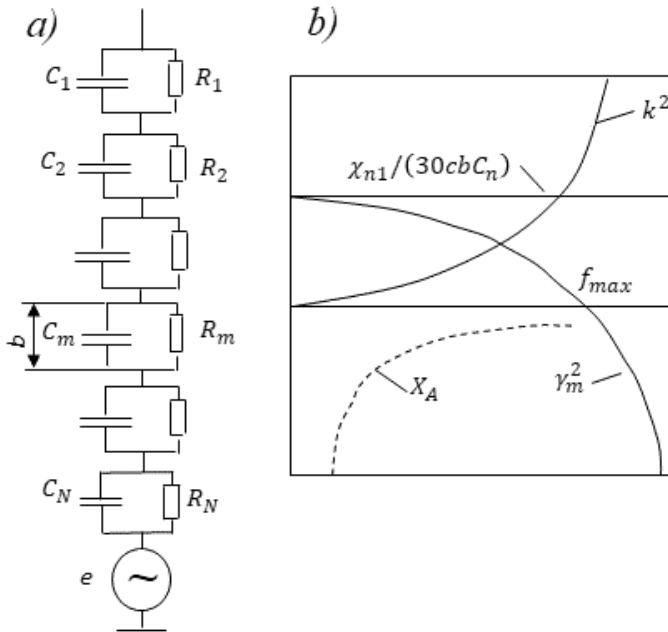


**Fig. 3:** An antenna circuit with capacitors and resistors (a), and the dependence of a propagation constant from the frequency (b).

a parallel connection of a resistor and a capacitor. For the first time the expediency of using a complex load for creation a linear current distribution was demonstrated in [3]. Later on, a main attention was given to antennas with capacitive loads. As it follows from the given analysis and the calculation results, if resistors are included in parallel with the capacitors, then the linear law of current distribution along the radiator is observed more precisely, and the operating frequency range increases. However, use of resistors leads to efficiency reduction, so the question of their application should be decided in each particular case.

Figure 3b shows a plot for  $\gamma_m^2$  versus frequency for an antenna with capacitive loads:

$$\gamma_m^2 = -k^2 + \chi_1 4\pi\epsilon/(bC_m). \quad (7.20)$$

For the propagation constant to be real at a given frequency  $f$ , capacitances of capacitors should not exceed the magnitude

$$C_m \leq \frac{X_1}{30k^2 bc} = \frac{2.54 \cdot 10^5 X_1}{f^2 b}. \quad (7.21)$$

Here,  $c$  is the light speed (in m/s), capacitance  $C$  is measured in farads, if frequency  $f$  is measured in Hertz's. In the case of linear distribution, capacitance  $C_{N2}$  near the antenna base is greater than others capacitances and should be chosen in accordance with (7.21). Similarly, under other distributions, this expression determines the maximum capacitance.



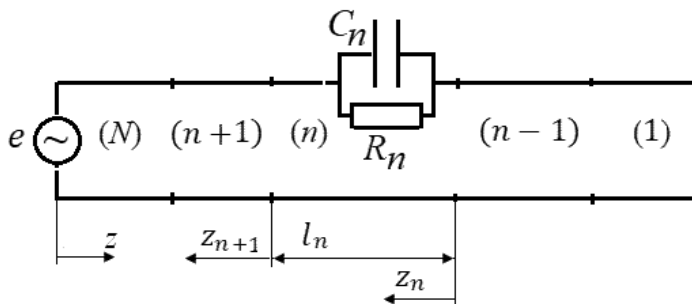


Fig. 4: The long line, equivalent to a metal radiator with resistors and capacitors.

From (7.20) it follows, that at low frequencies the propagation constant is real along the entire antenna. As the frequency increases, the magnitudes  $\gamma_m$  become purely imaginary (first of all, on segments, adjoining to the generator), i.e., the current distribution along these segments of the radiator becomes sinusoidal, and the main lobe of the directional pattern deviates from the perpendicular to the dipole axis. This effect limits the antenna frequency range from above. From below, the range is limited by frequencies, where the reactive component of input impedance is still great. In order that the magnitude  $\gamma_m$  does not become purely imaginary when frequency is increasing, the capacitances of capacitors should decrease with growth of frequency (e.g., vary in inverse proportion to square of the frequency).

The circuit of long line equivalent to a metal radiator with concentrated loads in the form of a parallel connection of a resistor and a capacitor is given in Fig. 4.

With help of the second option of realization of condition (7.21) one can make similar conclusions.

This option is feasible, if the second summand of the right-hand part of (7.12) is proportional to  $k^2$ :

$$-\gamma_m^2 = k^2 [1 - j\chi Z_m / (30kb)],$$

and the magnitude of concentrated load  $Z_m$  is equal to the sum of two summands, whose signs are the same when the frequency changes. In this case the load  $Z_m$  is

$$Z_m = -J \frac{30kb}{\chi} \left( 1 + \frac{\gamma_m^2}{k^2} \right) = -j\omega |\Lambda_m|,$$

i.e., it is a negative inductance  $-|\Lambda_m| = -\frac{30b(1 + \gamma_m^2/k^2)}{(\chi c)}$ . At small ratio  $\gamma_m/k$  the inductance weakly depends on the frequency  $f$ . In this case, the value  $\gamma_m^2 = k^2 [\chi |\Lambda_m| c / (30b - 1)]$  is positive, if

$$|\Lambda_m| > 30b / (\chi c).$$

Negative inductance is a circuit element with negative purely reactive impedance, proportional to frequency. This element is equivalent to frequency-dependent capacitance:

$$-j\omega |\Lambda_m| = 1 / (j\omega C_m),$$

where

$$C_m = 1/(\omega^2 |\Lambda_m|) = C_{m0} f_0^2 / f^2. \quad (7.22)$$

Here  $C_{m0}$  is the magnitude of an equivalent capacitance  $C_m$  at frequency  $f = f_0$ . The magnitude  $C_{m0}$  does not depend on  $f$ .

As follows from that, in order to maintain the in-phase current distribution in a wide frequency range, the capacitances of concentrated loads must change in inverse proportion to the square of the frequency. If it were possible, its capacitance could be satisfying the condition (7.13) and eliminate the constraint (7.15). But, strictly speaking, purely reactive impedances can only grow, and negative inductances do not exist in nature. Therefore, the use of constant capacitors allows creating in-phase current distribution only in limited frequency bands.

The executed analysis allows making a number of practical conclusions. In order that the concentrated loads may efficiently influence the current distribution, the distance between them must be small in comparison with the wavelength. For creating a wide-range radiator, only capacitors should be used as reactive elements, since inclusion of reactive two-terminal elements of a more complex type, whose structure includes inductance coils, results in narrowing of the operating range. Capacitors enable creation along a radiator in a wide frequency range an electromagnetic wave with real propagation constant that is realized in the form of an in-phase current with an exponentially decreasing amplitude (i.e., the current amplitude has the form of the concave curve). Obtaining a convex curve of the current with the help of simple concentrated elements (resistors, capacitors, inductance coils) is impossible.

Method of the impedance long line was proposed in [4], results of its application for creating wide-range linear radiator were first described in [5]. This approximate method, according to which one can build an antenna with in-phase current distribution, allows us to provide high electrical characteristics of the antenna in a wide frequency range. The method is based on the analysis of properties of the impedance long line and on the calculation of loads magnitudes that provide the specified current distribution.

Together with the method of impedance long line another approximate method for calculating magnitudes of loads, which provide the required current distribution, is developed [6]. This method is based on the calculation of the characteristics of an ordinary long line from two metal wires. The method allows in accordance with the required current distribution to find the law of changing the equivalent line length and to determine loads, which must be included in each antenna segment to implement this law. Use of this method and the method of impedance long line gives analogous results.

Figure 5 shows an asymmetrical radiator of height  $L$  with  $N$  loads, which are uniformly spaced along it at a distance  $b$  from each other. A current distribution along the radiator in a first approximation is like the current distribution along an open at the end long line, with the loads  $Z_m$  included in series. The current distribution along each line segment, located between adjacent loads, has sinusoidal character:

$$J(z_m) = J_m \sin k(z_m + l_{e,m-1}), 0 \leq z_m \leq b. \quad (7.23)$$

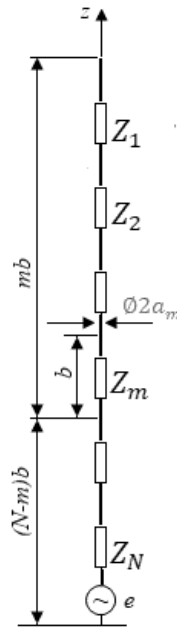


Fig. 5: Antenna with a several concentrated loads.

Here  $z_m = (N - m + 1)b - z$  is the coordinate, measured from the end of the segment  $m$ ,  $J_m$  is the amplitude of a current on the segment  $m$ ,  $l_{e,m-1}$  is the equivalent length of all preceding segments with  $(m - 1)$  loads, whose total length is equal to  $(m - 1)b$ . The magnitudes  $l_{em}$  and  $l_{e,m-1}$  are mutually related by the expression:

$$-jW \cot kl_{em} = Z_m - jW \cot k(b + l_{e,m-1}).$$

where  $W$  is the wave impedance of the line. Note that the length  $l_{em}$ , if  $m = N$ , is equal to the equivalent length  $L_e$  of the radiator. This expression permits to find the magnitude  $Z_m$  of  $m$ th load:

$$Z_m = -jW [\cot kl_{em} - \cot k(b + l_{e,m-1})].$$

If the distance between loads is small ( $kb \ll 1$ ), then

$$Z_m = -jW \frac{\sin k(b + l_{e,m-1} - l_{em})}{\sin kl_{em} \sin k(b + l_{e,m-1})} \approx -jW \frac{k(b + l_{e,m-1} - l_{em})}{\sin^2 kl_{em}}.$$

By means of the last two expressions one can calculate the magnitudes of loads. For this it is necessary to determine the law, in accordance with which the equivalent length grows along the line. The choice of this law depends on the required current distribution along the radiator. In the general case similarly (7.3)

$$J(z_m) = J_A f(z), \quad 0 \leq z_m \leq b, \quad (N - m)b \leq z \leq (N - m + 1)b, \quad (7.24)$$

where  $J_A$  is the current amplitude in the antenna base, and  $f(z)$  is the law of current distribution. Henceforth we shall assume that the function  $f(z)$  is real and positive, i.e., we shall consider only in-phase distributions. Suppose, we want to obtain a given current distribution  $J(z)$  along the antenna. For this we set assume that the current  $J(z_m)$  at the beginning and the end of each segment coincides with the current  $J(z)$ . If the segments' lengths are small, the distribution of the current along the line is close to the required one. In a general case we have in accordance with (7.23) and (7.24)

$$J_{m+1} \sin k(b + l_{em}) = J_A f[(N - m - 1)b] \text{ at } z_{m+1} = b,$$

$$J_{m+1} \sin kl_{em} = J_A f[(N - m)b] \text{ at } z_{m+1} = 0.$$

If to divide the left and right parts of the first equality onto the corresponding parts of the second equality and to retain only the first terms of the expansion of trigonometric functions into a series, then considering that the magnitude  $b$  is small, we will obtain

$$1 + kb \cot \sin kl_{em} = f[(N - m - 1)b]/f[(N - m)b],$$

i.e.

$$l_{em} = \frac{1}{k} \tan^{-1} \frac{kb}{f[(N - m - 1)b]/f[(N - m)b] - 1}. \quad (7.25)$$

As is seen from (7.25), the equivalent length  $l_{em}$  is frequency dependent. Knowing  $l_{em}$  and  $l_{e,m-1}$ , one may in accordance with the expression for  $Z_m$  find the loads magnitudes. They also have a frequency-dependent nature:

$$Z_m = -j \frac{W}{kb} \left\{ \frac{f[(N - m - 1)b]}{f[(N - m)b]} - 2 + (1 + k^2 b^2) \frac{f[(N - m + 1)b]}{f[(N - m)b]} \right\}. \quad (7.26)$$

An input impedance of the long line open at the end is a first approximation to a reactive component of antenna input impedance. In a general case it is equal to

$$Z_A = -jW \cot kL_e = -j \frac{W}{kb} [f(-b) - 1].$$

This expression shows that the function  $f(z)$  should change slowly near the antenna base and the difference  $f(-b) - 1$  should be small, of the order of  $kb$ . Otherwise, the reactive component of the antenna input impedance will be great.

We define, for example, the loads' magnitudes providing the exponential distribution (7.9) of the current amplitude along the radiator. The linear distribution (7.8) is its particular case. The equivalent lengths of the long lines for the exponential and linear distribution in accordance with (7.25), (7.9) and (7.8) are equal to

$$l_{em3,4} = \frac{1}{k} \tan^{-1} \frac{kb[1 - \exp(-mab)]}{\exp(ab) - 1}, l_{em2} = \tan^{-1} (mkb).$$

As is seen from these expressions, if  $\alpha > 0$ , the equivalent length of the antenna arm does not may exceed quarter of the wave length. The input impedance of a long line with the exponential and linear current distribution may be written in the form

$$Z_{A3,4} = -j \frac{W[\exp(-ab) - 1]}{kb[1 - \exp(-\alpha L)]}, Z_{A2} = -j W/(kL).$$

Using expressions (7.26) and (7.11), we find the magnitudes of the loads, which provide the exponential law of the current amplitude distribution along the radiator:

$$Z_m = -j \frac{W}{kb} \frac{2(\cosh ab - 1) + k^2 b^2 \exp(-ab)}{1 - \exp(-mab)} \{1 - \exp[-(m-1)ab]\}. \quad (7.27)$$

If the product  $ab$  is not small, then, neglecting by second term of the numerator, we obtain

$$Z_m = 1/(j\omega C_m),$$

where

$$C_m = \frac{b[-1 \exp(-mab)]}{2Wc(\cosh ab - 1)}.$$

As is seen from this formula, the sign of  $C_m$  coincides with the sign of  $\alpha$ .

Thus, in order to obtain an exponential distribution of current amplitude with a great decrement, one must use capacitive loads. Capacitors allow us to create only a concave current distribution (with  $\alpha > 0$ ). In order to obtain a convex distribution (with  $\alpha < 0$ ), the capacitances must be negative. If  $ab \ll 1$ , then, confining by the first terms of the functions' expansion into a series, we find from (7.27)

$$Z_m = 1/(j\omega C_m) + j\omega \Lambda_m, \quad (7.28)$$

where

$$C_m = \frac{m}{cW\alpha}, \quad \Lambda_m = -\frac{wb(m-1)}{cm}.$$

In order to obtain the exponential distribution with a small decrement  $\alpha$ , using capacitors, the negative inductances  $\Lambda_m$  should be included. They can be neglected, if the first term of (7.28) is much larger than the second one, i.e.,  $\alpha \gg k^2 b(m-1)$ . If  $\alpha = 0$ ,

$$Z_m = j\omega \Lambda_m = -jkbW(m-1)/m,$$

i.e., in the case, when the loads are fabricated in the form of negative inductances, proportional to  $(m-1)/m$ , we obtain a purely linear distribution.

As it follows from the executed analysis, the method of the long line with loads and method of the impedance long line leads to similar results. Comparison of these

results allows to apply both these methods to specific problems, using specific details of the current distribution along the radiators. As already mentioned, one of important tasks of antenna technics is creating a radiator, which ensures a maximum field in the plane perpendicular to the radiator axis in a wide frequency range. An ordinary linear radiator fails to meet this requirement: if the radiator arm is larger than  $0.7\lambda$ , the radiation in the plane, perpendicular to antenna axis, decreases. In this case one can use V-antenna formed by two converging inclined wires. If arm length  $L$  is greater than  $0.7\lambda$ , an ordinary V-antenna has preferential radiation along the bisector of the angular aperture. However, with growing frequency side lobes of the directional pattern increase, and the main lobe of this pattern in the antenna plane diminishes. If the arm length is greater than about  $1.25\lambda$ , the main lobe splits, and the radiation along the bisector sharply decreases.

Including capacitive loads in the antenna wire allows to expand the frequency range, in which there are the directed radiation along the bisector of the angle of aperture, and to increase the useful signal in this direction. Consider a symmetric V-dipole with arm length  $L$  and arbitrary angular aperture  $\alpha = \pi - 2\theta$  (Fig. 6). The far field along the bisector of the angular aperture, created by an elementary segment  $d\zeta$  of the upper antenna arm located near the origin of coordinates system is equal to

$$E_{\theta}(\zeta)d\zeta = E_{\theta}(0)[J(\zeta)/J(0)] \exp(jk\zeta \sin \theta_0)d\zeta,$$

where  $\zeta$  is the coordinate measured along the radiator axis,  $J(z)$  is the current along the upper arm,  $J(0)$  is the current near point 0, and  $k\zeta \sin \theta_0$  is the path-length difference between the points 0 and  $\zeta$ . To ensure that all the far fields of different points coincide in phase, the current distribution along this arm must correspond to the expression

$$J(\zeta) = J(0)f(\zeta)\exp(-jk\zeta \sin \theta_0). \quad (7.29)$$

Here  $f(\zeta)$  is a real and positive function.

Let  $N$  loads  $Z_n$  be located uniformly along a wire of each antenna arm at a distance  $b$  from each other. If the load spacing is small ( $kb \ll 1$ ), then, as in the case of the linear dipole, as well, the replacement of concentrated loads by distributed surface impedance  $Z(\zeta)$  practically does not change the current distribution along the antenna. We assume that the surface impedance of each antenna segment with load  $Z_n$  is constant and equal to  $Z^{(n)}$  in accordance with (2.14).

As is said in Section 2.1, the current distribution along the antenna with piecewise constant surface impedance coincides in the first approximation with current distribution along an equivalent impedance line, i.e., along the line with a stepped variation of the propagation constant. Here, the wave propagation constant  $\gamma_n$  along the segment  $n$  is related to surface impedance  $Z^{(n)}$  in accordance with (7.1). If the law of changing propagation constant is known, one can use magnitude  $\gamma_n$  for calculating concentrated loads  $Z_n$ , which are needed for the embodiment of this law. The current along the segment  $n$  of a stepped line is

$$J(\zeta_n) = I_n \sinh(\gamma_n \zeta_n + \varphi_n), \quad 0 \leq \zeta_n \leq b, \quad (7.30)$$



equations that allows us to relate  $\gamma_n$  and  $\gamma_{n+1}$ . From solution of this set of equations it follows that magnitude  $\gamma_n$  is independent of  $\gamma_{n+1}$ :

$$\gamma_n = \frac{1}{b} \left\{ 1 - \frac{2f[(N-n)b] - f[(N-n-1)b]}{f[(N-n+1)b]} - 2jkb \sin \theta_0 \frac{f[(N-n)b] - f[(N-n-1)b]}{f[(N-n+1)b]} \right\}^{\frac{1}{2}}. \quad (7.31)$$

This expression generalizes expression (7.7) for a linear dipole and transforms into it at  $\theta_0 = 0$ .

The possibility of implementation of propagation constant  $\gamma_n$  is determined by the possibility of implementation of concentrated loads. According to (7.12), at low frequencies, when inequality (7.15) and correspondingly equality (7.16) are true, the load value is

$$Z_n = -j30(\gamma_n^2 b^2)/(k b \chi). \quad (7.32)$$

By substituting (7.31) into (7.32), we get

$$Z_n = R_n + 1/j\omega C_n, \quad (7.33)$$

where

$$R_n = \frac{60}{\chi} \sin \theta_0 \frac{f[(N-n-1)b] - f[(N-n)b]}{f[(N-n+1)b]},$$

$$C_n = 4\pi\epsilon_0 b \chi / \left\{ 1 - \frac{2f[(N-n)b] - f[(N-n-1)b]}{f[(N-n+1)b]} \right\}.$$

As seen from (7.33), each load should be a series connection of a resistor and a capacitor, where the resistance of the resistor is positive, if function  $f(\zeta)$  decreases monotonically with growing  $\zeta$ , and the capacitance of the capacitor is positive, if function  $f(\zeta)$  is concave. The resistance depends on the angular aperture of the antenna and the form of function  $f(\zeta)$ , whereas the capacitance depends only on the latter. For a linear radiator with loads ensuring the maximal radiation in the plane, perpendicular to its axis, each load should, when condition (7.12) holds, represent a capacitor. Capacitors ensure real wave propagation constant  $\gamma_n$  and an in-phase distribution of the current along an antenna. In V-antenna with capacitors, the resistor must be included in series with the capacitor, and that leads to a phase lag of a current wave along an antenna wire. Such phase delay is necessary for a V-dipole, since it compensates the path-length difference from individual segments to an observation point and ensures coincidence of phases of fields, created by segments in the far zone along the bisector of the angular aperture.

The use of resistors in a transmitting antenna is inexpedient. This means that the loads of a V-dipole should not differ from the loads of a linear radiator, which ensure an in-phase current distribution along an antenna wire.



At high frequencies, when condition (7.12) does not perform, to create the in-phase current distribution along a linear radiator, the load must represent a negative inductance (a capacitance, which is inversely proportional to square of frequency). Similarly, the load for a V-dipole should be a series connection of a capacitor with a frequency-dependent capacitance and a resistor. In order for the propagation constant to be real and the current along an antenna to be in-phase, the capacitances should not exceed the value determined by inequality (7.21).

## 2. Method of Mathematical Programming

Use of the mathematical programming methods [7] plays a major role in solving the inverse problems of creating antennas. These methods allow determination of optimal parameters of an antenna, in particular its geometric dimensions and magnitudes of concentrated and distributed loads for creating antennas with specified characteristics, or more precisely, with characteristics that are as close as possible to the given ones.

The last remark is caused by the fact that the range of changes in the parameters of the radiator is limited, i.e., not every value of the electrical characteristic of the antenna can be practically realized. Different characteristics are optimal when different parameters. Moreover, an antenna should have certain properties not at a single fixed frequency, but in the entire operation range. Therefore, the selected parameters are a result of a compromise, reached with the help of the mathematical programming method.

The problem of mathematical programming in the general case is stated as follows: it is necessary to find vector  $\vec{x}$  of parameters that minimizes some objective function  $\Phi(\vec{x})$  under imposed constraints  $\Phi_i(\vec{x}) \geq 0$ . Depending on the type of functions  $\Phi(\vec{x})$  and  $\Phi_i(\vec{x})$ , mathematical programming is divided into linear, convex and non-linear one. In the case at hand, the problem is solved by non-linear programming methods since the type of function  $\Phi(\vec{x})$  is unknown.

The objective function  $\Phi(\vec{x})$  (or general functional) is a sum of several partial functionals  $\Phi_j(\vec{x})$  with weighting coefficients  $p_j$  and penalty function  $\Phi_{ij}$ :

$$\Phi(\vec{x}) = \sum_{(j)} p_j \Phi_j(\vec{x}) + \sum_{(i)} \Phi_{ij}.$$

The partial functional is an error function for one or the antenna characteristics. The weighting function allows taking into account an importance of this characteristic and the sensitivity of corresponding functional to change of vector  $\vec{x}$ . A penalty function is zero, if the parameters lie within a given interval, and has great magnitude, even if only one of the parameters falls outside the interval limits.

For an antenna with concentrated loads the controlled parameters  $x$  are magnitudes of loads, coordinates  $z_n$  of their connection points and the wave impedance  $W$  of the cable. Under loads understood simple elements: capacitors with capacitances  $C_n$ , coils with inductance  $\Lambda_n$  and resistors with resistance  $R_n$ . Values  $z_n$ ,  $W$ ,  $C_n$ ,  $\Lambda_n$  and  $R_n$  should be real, positive and frequency-independent, and  $z_n$  smaller than antenna length  $L$ . These requirements naturally limit the variation interval of parameters.

Different ways of an error function formation are known. Good results are produced by means of quasi-Tchebyscheff criterion:

$$\Phi_j(\vec{x}) = \frac{1}{N_f} \left[ \frac{f_{j0}}{f_{j\min}(\vec{x})} - 1 \right] \left\{ \sum_{(n_f)} \left[ \frac{(f_{j0}f_j(\vec{x}) - 1)}{(f_{j0}f_{j\min}(\vec{x}))} \right]^s \right\}^{1/s}. \quad (7.34)$$

Here  $N_f$  is a number of points of the independent argument (e.g., a number of frequencies in given range),  $n_f$  is frequency number,  $f_j(\vec{x})$  is one of electrical characteristics of an antenna,  $f_{j\min}(\vec{x})$  is its minimal magnitude in the considered interval,  $f_{j0}$  is a hypothetical value of the characteristic, which must be reached,  $S$  is the power, allowing to control the method sensitivity.

Another criterion is called a root-mean-square criterion. It uses another error function:

$$\Phi_j(\vec{x}) = \frac{1}{N_f N_l} \sum_{n_f=1}^{N_f} \sum_{n_l=1}^{N_l} [f_j(\vec{x}) - f_{j0}]^2.$$

Here  $N_f$  and  $N_l$  are numbers of independent arguments points (e.g., the number of frequencies in a given range and a number of division points on the wire),  $n_f$  is the point number,  $f_j(\vec{x})$  is one the electrical characteristic of the antenna (e.g., a current or a voltage),  $f_{j0}$  is a hypothetical value of the characteristic, which must be reached.

The choice of optimizable characteristics depends on a stated problem. For creation of a wide-range radiator one must use in the capacity of characteristics  $f_j(\vec{x})$  a travelling wave ratio ( $TWR$ ) in a cable and a pattern factor ( $PF$ ), which is equal to the average level of radiation at predetermined angles range. If resistors with resistances  $R_n$  are used as loads, it is necessary to supplement the set of  $f_j(\vec{x})$  by the characteristic of antenna efficiency ( $\eta_A$ ):

$$TWR = \frac{2a}{a^2 + b^2 + 1 + \sqrt{(a^2 + b^2 + 1)^2 - 4a^2}} PF = \frac{1}{K} \sum_{k=1}^K F(\theta_k),$$

$$\eta_A = 1 - \frac{1}{J_A^2 R_A} \sum_{n=1}^N |J_n|^2 R_n. \quad (7.35)$$

Here the following designations are used:  $a = R_A/W$ ,  $b = X_A/W$  are ratios of active and reactive components of antenna impedance to the wave impedance of a cable, respectively,  $K$  is number of angles  $\theta_k$  in a vertical plane within the limits of an angular sector from  $\theta_1$  to  $\theta_K$  (for example, from  $60^\circ$  to  $90^\circ$ ),  $k$  is the angle number within this sector,  $F(\theta_k)$  is a magnitude of normalized directional pattern in the vertical plane for  $\theta = \theta_k$ ,  $N$  is the number of loads,  $J_n$  and  $J_A$  are the current in the  $n$ th load and in the antenna base, respectively.

If the method of mathematical programming is used to create a given current distribution  $J(z)$ , it is expedient to use as characteristics  $f_j(\vec{x})$  both real and imaginary current components:

$$f_1 = \text{Re } J(z, f), \quad f_2 = \text{Im } J(z, f),$$

or amplitude and phase of the current:

$$f_3 = |J(z, f)|, f_4 = \tan^{-1} \left[ \operatorname{Im} \frac{J(z, f)}{\operatorname{Re}} J(z, f) \right].$$

In cases, when an analytical expression for objective function  $\Phi(\vec{x})$  is absent, the minimum of function must be found by a numerical method, based on gradient search. Gradient search is an iterative procedure, in which we move step by step from one set of parameters  $\vec{x}_m$  to another set  $\vec{x}_{m+1}$  in a direction of maximal decrease of the objective function. Therefore, this method is called the method of steepest descent:

$$\vec{x}_{m+1} = \vec{x}_m - \alpha_m \operatorname{grad} \Phi(\vec{x}_m).$$

Here  $m$  is the iteration number,  $\alpha_m$  is the scale parameter. Each iteration in essence is the search of a functional's minimum (of an objective function) in the direction of anti-gradient. The result of this search is the determination of the coefficient  $\alpha_m$ , at which the objective function  $\Phi(\vec{x}_m)$  becomes minimal. At that the values of parameters  $\vec{x}$ , which correspond to this minimum, are determined.

A modification of the steepest descent method is the method of conjugate gradients. In this case the iteration 1,  $(Q - 1)$ ,  $(2Q + 1)$  and so on are calculated according to the anti-gradient (here  $Q$  is number of parameters) and the rest of the steps correspond to the expression

$$\vec{x}_{M+1} = \vec{x}_M - \alpha_M \vec{G}_M,$$

where

$$\vec{G}_M = \operatorname{grad} \Phi(\vec{x}_M) + \left| \frac{\operatorname{grad} \Phi(\vec{x}_M)}{\operatorname{grad} \Phi(\vec{x}_{M-1})} \right|^2 \vec{G}_{M-1}.$$

As said already, the minimum of an objective function  $\Phi(\vec{x}_M)$  and the values of parameters, which correspond to this minimum, are determined in each iteration. In essence, each iteration searches a parameter  $\alpha_m$ . The calculation ends when the decrease of the objective function from iteration to iteration becomes smaller than a preset value, or the number  $M$  of iterations exceeds certain limit  $M_0$ .

The most rational method consists in a sequential increase (for example, doubling) of magnitude  $\alpha$  and further interpolating the function  $\Phi(\vec{x}_M)$  in a considered interval by a polynomial of a given power. It is convenient to use cubic interpolation, since the number of interpolation nodes (four) is large enough, and the root of the derivative (the value  $a$ , that turns the derivative into zero) is found analytically. If the first step results in an increase, rather than decrease of the objective function, the step should be reduced by a factor of  $10^p$ , where  $p = 1, 2, \dots$ , whereupon the linear search goes on again with doubling a step.

The mathematical programming method (synthesis) presupposes multiple computations of the antenna's electrical characteristics at different initial parameters (analysis). Performing such calculations requires incorporation of a special program into the synthesis software. This program allows determining of all electrical

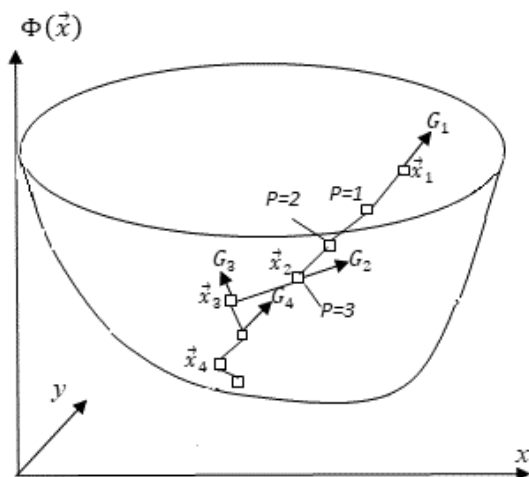


Fig. 7: Iterative procedure as the motion along the surface  $\Phi(\vec{x}_M)$  to an optimum.

characteristics of an antenna, i.e., calculating the functions  $f_j(\vec{x})$  for vector  $\vec{x}$  of initial parameters at given emfs and loads. The most laborious of these calculations is computation of self and mutual impedances between antenna segments (between so-called short dipoles). Therefore, in order to speed up the calculations, it is expedient to fixate, for example, points of placing concentrated loads, in order that the coordinates of short dipoles and their mutual impedances do not change from iteration to iteration. If there are many loads, i.e., the distances between them are small in comparison with the wave length, this restriction will have no effect on the synthesis results.

As regards initial magnitudes of concentrated loads, these magnitudes must be found by the approximate physical method, described in Section 1. The results of the calculations show that the computational process in this case speeds up. But the most important result of using these magnitudes consists in reducing the error probability since an arbitrary choice of the initial parameters may cause an optimization process, which will lead to a local, rather than true, minimum of the objective function.

The described iterative procedure is essentially the motion in the vector space  $\vec{x}_m$  along the surface  $\Phi(\vec{x}_M)$  in the direction of a minimum of a general functional. A particular case of such motion, when the vector  $\vec{x}_m$  consists of two parameters ( $x$  and  $y$ ) is shown in Fig. 7. The algorithm of the iterative procedure is presented in Fig. 8.

It is necessary to emphasize that the method of mathematical programming makes it possible to realize the synthesis of a wide-range radiator, i.e., this method chooses the optimum capacitive loads that provide the highest possible level of  $TWR$ ,  $PF$  and efficiency in a given frequency range. The synthesis program, using the mathematical programming method, allows to lead the problem solution to the desired goal.

Other methods of solving often stop halfway and do not reach the goal. For example, earlier it was proposed to split the synthesis's process of antennas with the given electrical characteristics into two stages and at the first stage to limit

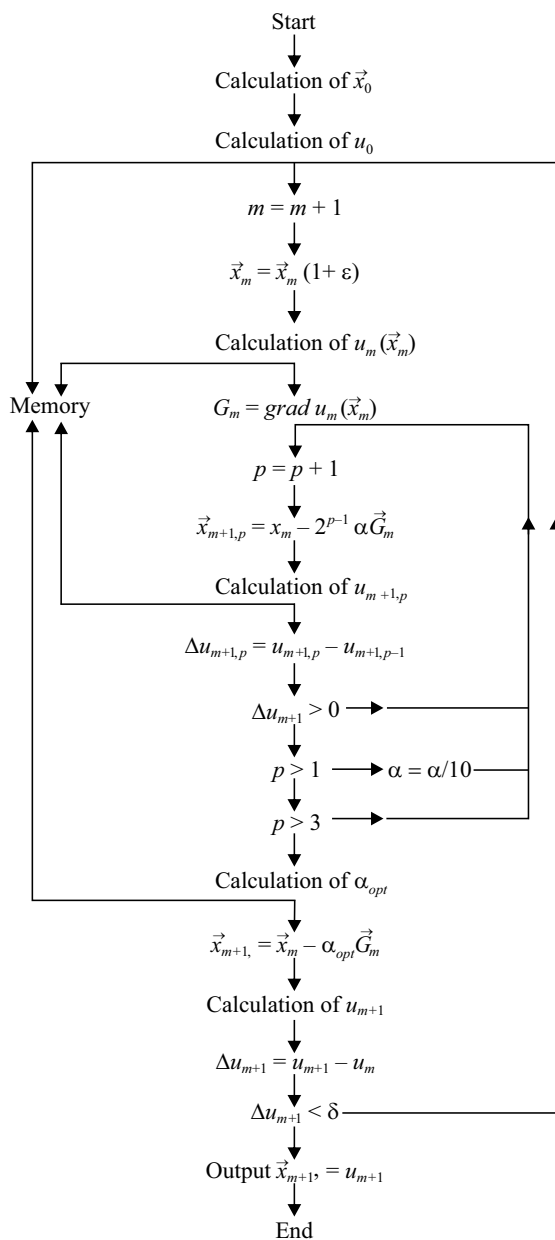


**Fig. 8:** Algorithm of optimization program.

ourselves by calculating the current distribution. The parameters of the antenna, providing such distribution, should have been determined at the second stage. The first stage was investigated sufficiently. It covers a wide class of the tasks (one of the possible options is the task of creating a broadband antenna). Much less attention was paid to the second stage of the synthesis. In principle, if the required current

distribution along a wire antenna is known, one can split the wires of an antenna onto short dipoles and define currents at the centers of these dipoles. The amplitudes of piecewise sinusoidal basis functions are equal to the currents at the corresponding antenna segments. It is easy to calculate the magnitudes of loads, which one must connect at these points to obtain the desired currents.

But the impedances of loads, calculated by this method, consist of active and reactive components, which are changed with frequency. The calculated active component of load impedance may be negative, and this is evidence of impossibility to create such distribution with the help of passive elements. As to the reactive component, it is necessary to solve still the problem of its implementation in the given frequency range with the help of a set of simple elements. Therefore, it is necessary to solve the task of creating an antenna with the chosen type of loads. This is the new problem, which as the problem of creating a wide-range radiator, may be solved only by the mathematical programming method.

The method of mathematical programming offers a wide scope for solution of various problems of synthesis. During its application the results of calculation of antennas with concentrated capacitive and capacitive-resistive loads were analyzed and considered. Practical conclusions made as a result of their analysis is given in Section 1. The results of applying the described technique to specific tasks are described in the following Sections. They allow us to make a general conclusion that the linear antenna with concentrated capacitances decreasing in proportion to the distances from its free ends, allow the creation of in-phase current with a linear amplitude distribution and obtain high electrical characteristics in the wide frequency range.

### 3. Application of Results to Concrete Tasks

Figure 9 gives  $TWR$  in cable with wave impedance  $75 \Omega$ , which is produced by three asymmetrical antennas. The calculations are performed for an antenna of height 12 m and radius 0.03 m, with ten capacitors located at distance 1.2 m from each other (the upper and lower capacitors are placed at the distance 0.6 m from the antenna ends).

Curve 1 in Fig. 9 corresponds to a radiator without loads, i.e., to a whip antenna, curve 2—to a radiator with loads, whose capacitances are frequency independent. Here, the capacitance  $C_{n_0}$  of the bottom capacitor was chosen equal to 177 pF. In this case the propagation constant is real along the entire antenna up to frequency 10 MHz. Capacitances  $C_{n_0}$  of others capacitors decrease in the direction of the free end of the antenna in proportion to the distance from it. That allows to obtain the current distribution along the radiator, which is close to the linear law. Curve 3 is given for a radiator with frequency-dependent capacitive loads. Their capacitances are changed in accordance with (7.22), where  $f_0 = 20$  MHz.

Table 1 shows lower  $f_1$  and upper  $f_2$  frequencies of the operating range of each antenna. At the frequency  $f_1$   $TWR$  becomes greater than 0.2, at the frequency  $f_2$  a field strength along a perpendicular to an antenna axis becomes less than 0.7 of the maximum field strength (as a rule,  $f_2$  corresponds to the second maximum on curve of  $TWR$ ).  $TWR$  of a whip antenna with growth of frequency quickly decreases below level of 0.2, and the frequency, corresponding to this point, is taken as  $f_2$ . Moreover,

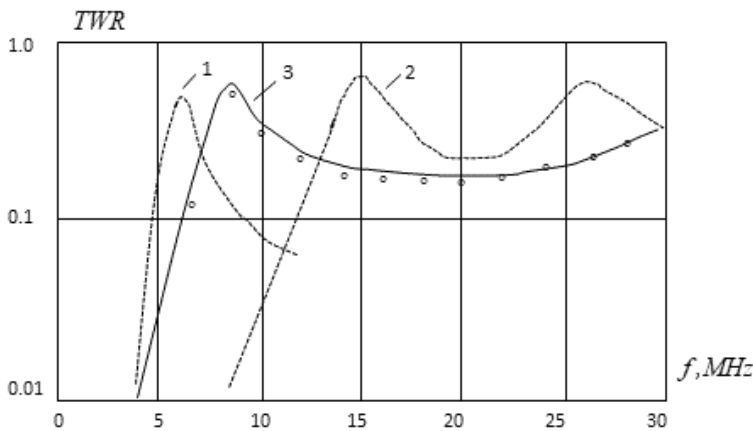


**Fig. 9:** Input characteristics of radiators without loads (1), with constant (2) and frequency-dependent (3) capacitive loads.

**Table 1:** Frequency Ratio of Radiators.

Version of antenna	Frequency, MHz		Range width $\Delta f$ , MHz	Frequency ratio $k_f$
	$f_1$	$f_2$		
1	5.2	7.7	2.5	1.5
2	12.3	26.0	13.7	2.1
3	6.3	34.0	27.7	5.4

Table 1 for each antenna reports a range width  $\Delta f = f_2 - f_1$  and frequency overlap ratio  $k_f = f_2/f_1$ .

Figure 9 also presents the results of experimental verification of  $TWR$  for the variant 3. The measurements were performed by means of an antenna model in a scale 1:10. The frequency range was split into short intervals, and the capacitances of loads used in each interval were equal to capacitances calculated for the middle of the interval. The calculated and experimental results are reasonably well consistent with each other. The most practical and accessible realization of antennas with frequency-dependent capacitances is the use of tunable capacitors, for example, switched ones in accordance with the signal from the console (control panel).

The methods of impedance long line and metallic long line with loads allows to define potential capabilities of antennas with loads. The results, obtained by means of these methods, can be used for solving the optimization problem of an antenna with loads by the mathematical programming method.

Application of synthesis program for selection of the optimal capacitive loads permits to obtain maximal  $TWR$  and PF in the predetermined range of frequencies  $f_1 - f_2$ . During this work all weighting coefficients  $p_j$  as a rule were taken to be the same. The calculations show that four-five iterations allow us to synthesize a simple antenna. The number of optimized electrical characteristics in this case has little effect on the synthesis time. For example, the time of optimizing  $TWR$  and PF is almost equal to the time of optimizing only  $TWR$ . The choice of criterion has practically no

effect on the results of synthesis of wide-range radiators and the calculation time. In particular, the root-mean-square criterion had no advantage as compared with the quasi-Tchebyscheff criterion and was rarely used. As a hypothetical value of the characteristic  $f_{j0}$  it is advisable to choose a maximum magnitude, since its decrease leads to a worsening of the result in the synthesized antenna. An increase of index  $S$  in expression (7.34) accelerates the process convergence. In the calculations it was assumed that  $S = 6$ .

Figure 10 gives the basic dimensions of the developed antenna with loads. It is the monopole of height  $L = 12$  m with nine capacitors spaced equidistantly. The capacitance  $C_0$ , equal to capacitance of a typical ceramic insulator (15 pF), is located at the base of the antenna in parallel with its input.

The results of the antenna synthesis are presented in Table 2, where the basic characteristics of the radiators are given. In Table 2 the following designations are used:  $a$  is antenna radius,  $N$  is the number of used capacitors,  $N_f$  is number of frequencies,  $M$  is a required number of iterations. Frequency overlap ratio for the antenna variants with numbers 1–6 was adopted equal to two. As seen from table, the increase of antenna radius from 0.03 m to 0.15 m at frequencies up to 30 MHz results in growing minimal  $TWR$  approximately by a factor 1.5. The variation of radius has a weaker influence on minimum of PF. Optimal capacitive loads are given in Table 3.

Figure 11 shows the electrical characteristics of variants 1–3 (antenna radius is 0.03m) and of a whip antenna, which has the same geometrical dimensions and the same capacitance  $C_0$  of the insulator. The characteristics of the antenna with a radius 0.15 m (variants 4–6) are similar. As seen from the calculations, the curve of  $TWR$  can have two maximums at high frequencies. The curves of  $PF$  do not decrease monotonically with frequency, but have maximums too. In addition to calculated curves, the pictures demonstrate (by dots and other symbols) the results of experimental verification, carried out on the model in the scale 1:5. The calculation and experiment coincide well.

As it follows from Table 2 (variants 1–6), if the frequency overlap ratio for various ranges is identical, the level of antenna matching with a cable is different in the different ranges. This level substantially rises, if the frequency growth. In order to obtain more uniform and, on the whole, better characteristics over the entire frequency range (at unchanged number of sub ranges), it is expedient to split the total range into parts such that the overlap ratio in different sub ranges increases with increase of frequencies. The results of solving this problem are presented in Table 2 as variants 7–12.

The electrical characteristics of variants 10–12 with radius 0.15 m as well as of a monopole without loads with the same radius and with capacitance  $C_0$  at the base are given in Fig. 12. Data of Table 2 confirm a general increase of  $TWR$  level in comparison with variants 1–6. In all the sub ranges, increase of the antenna radius causes a rise of minimum  $TWR$  (approximately by a factor 1.5), together with a rise of minimal pattern factor at high frequencies.

The optimization's result of 12-meter antennas with capacitances  $C_0 = 15$  pF in the base are presented in Fig. 13 in the form of curves for the minimal  $TWR$  depending on relative antenna length  $L/\lambda_{max}$  ( $\lambda_{max}$  is the maximum wavelength) at various overlap ratios  $k_f$  and different antenna radii  $a$ . These curves determine the



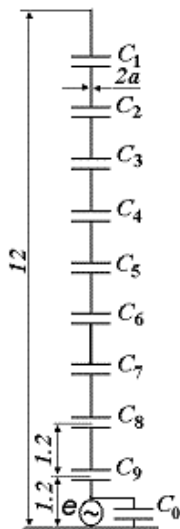


Fig. 10: Synthesized antenna with nine capacitors.

Table 2: Main Characteristics of Antennas.

Version	$L, m$	$a, m$	$N$	$f_1 - f_2, \text{MHz}$	$N_f$	$M$	$TWR \text{ min}$	$PF \text{ min}$
1	12	0.03	9	7.5–15	16	4	0.123	0.819
2	“	“	“	15–30	“	“	0.273	0.610
3	“	“	“	30–60	“	5	0.360	0.562
4	“	0.15	“	7.5–15	“	4	0.205	0.813
5	“	“	“	15–30	“	5	0.414	0.680
6	“	“	“	30–60	“	4	0.380	0.605
7	“	0.03	“	8.5–13	10	3	0.217	0.870
8	“	“	“	13–22	“	5	0.216	0.0,790
9	“	“	“	22–60	20	8	0.204	0.0,437
10	“	0.15	“	8.5–13	10	5	0.314	0.829
11	“	“	“	13–22	“	4	0.278	0.0,859
12	“	“	“	22–60	20	5	0.322	0.565

maximum attainable characteristics, which can be obtained by means of antennas with constant capacitive loads.

Results of calculations and experiments presented in this Section show that the described procedure based on the using of capacitive loads is an effective way to optimize the characteristics of antennas. Application of this procedure confirms its validity and usefulness. The calculation results also show that if it is necessary, the antenna frequency range can be expanded in the direction of high frequencies at a sufficiently high  $TWR$ ; for example, one can obtain  $TWR \geq 0.2$  in the range with a frequency ratio about 10. But the directional patterns in the additional (high-frequency) part of the range turned out worse, reducing the frequency ratio to three.

Table 3: Optimal Capacitive Loads, pF.

Version	$C_1$	$C_2$	$C_3$	$C_4$	$C_5$	$C_6$	$C_7$	$C_8$	$C_9$
1	44.3	33.2	91.2	432	-	-	-	-	-
2	84	164	143	182	-	-	-	-	-
3	37.3	81.1	127	181	2 58	369	516	6 91	883
4	8.7	20.6	36.5	51.1	58.7	53.3	50.6	88.1	156
5	2.0	3.9	5.4	6.1	9.5	12.2	15.7	21.1	18.3
6	51.2	134	219	340	477	633	804	981	1150
7	10.7	28.4	57.0	76.7	86.4	86.8	53.5	216	409
8	4.5	19.0	11.4	15.8	26.4	29.8	32.4	23.0	35.7
9	33.9	72.8	115	164	223	296	385	492	608
10	8.4	18.4	30.3	40.4	47.1	53.3	82.8	151	248
11	1.7	5.6	12.2	11.7	17.6	41.0	30.5	56.4	240
12	21.1	0.2	39.2	231	519	909	1380	1900	2450
13	20.3	76.3	122	78.5	0.1	107	351	761	1340
14	2.9	26.9	0.3	42.1	22.6	59.1	35.8	55.0	73.1

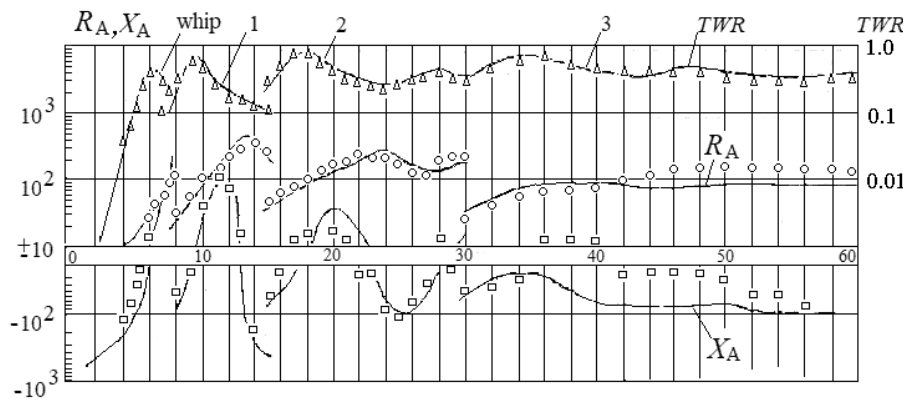


Fig. 11: Input characteristics of 12-meter antennas with radius 0.03 m.

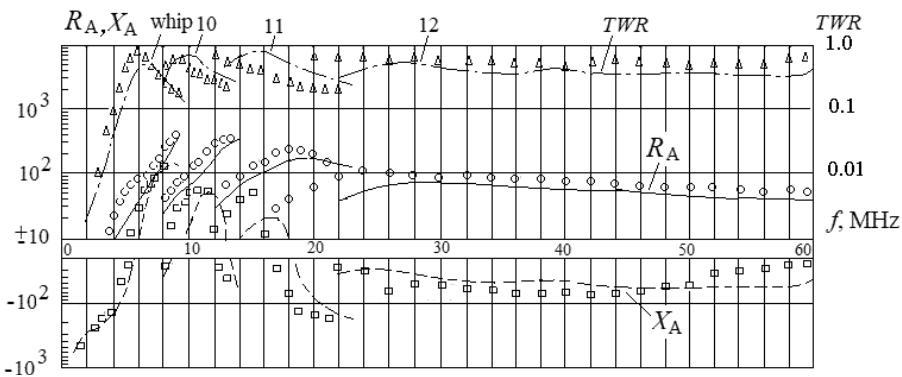


Fig. 12: Input characteristics of 12-meter antennas with radius 0.15 m.

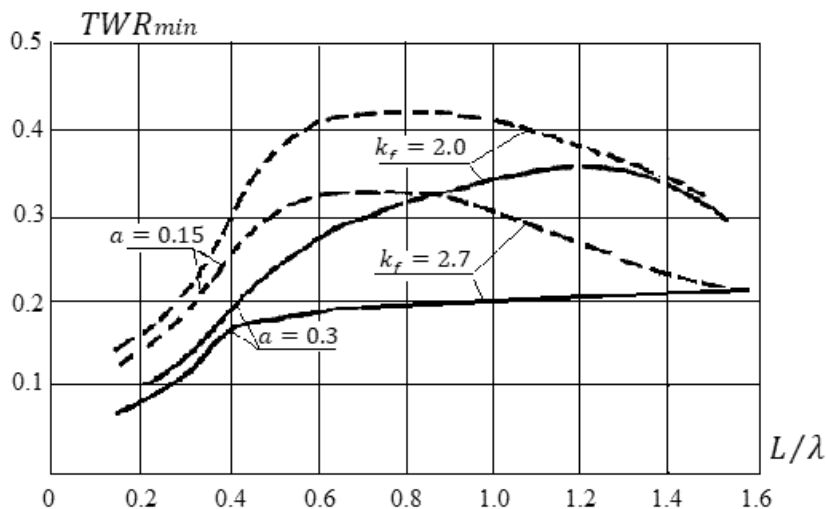


Fig. 13: The maximum level of matching for the antenna with constant capacitances.

As it became clear later, this circumstance was caused by the fact that under calculations of the objective function in accordance with (7.34) the used weighting coefficients  $p_j$  were adopted equal in magnitude. The different sensitivity of partial functionals to the vector  $\vec{x}$  did not considered. Using a multi-tiered structure (see Chapter 8) allows to ensure desired directional pattern in the over wide range. Joint application of both principles, i.e., using a multi-tiered structure and capacitive loads in the wires of each tier allows to ensure high level of matching and required directional pattern.

Thus, the method of mathematical programming is an efficient method of optimization of antennas with capacitive loads. Its software may be used for optimization of antennas with loads of other kinds. The procedure developed for solving the described problem can be effectively used to solve other problems. We will begin to talk about that from creating the desired current distribution in a certain frequency range. It should be emphasized that the creation of a specific current distribution does not mean a strict coincidence of the given and the obtained distribution at all frequencies. This requirement means only obtaining a distribution, which is close to the required as far as possible. In [6] as an example synthesis of antenna with a given current distribution in a certain frequency range is considered. The calculation is performed for the monopole of height 6 m and radius 0.0065 m with ten capacitive loads, which are located along it at distance 0.6 m from each other. The distance from the upper load to the antenna end and from the bottom load to its base is half as much. The capacitance of the bottom load is taken equal to 18 pF, in which case the propagation constant  $\gamma_n$  is real along the entire antenna up to frequency 40 MHz.

Initial calculation of loads magnitudes was executed in accordance with an approximate theory of a long line with loads. Figure 14a shows the equivalent lengths  $l_{en}$  of this long line measured from its free end to the points  $n$  of capacitors location. The capacitances  $C_n$  of these loads are given in Fig. 14b. The corresponding curves

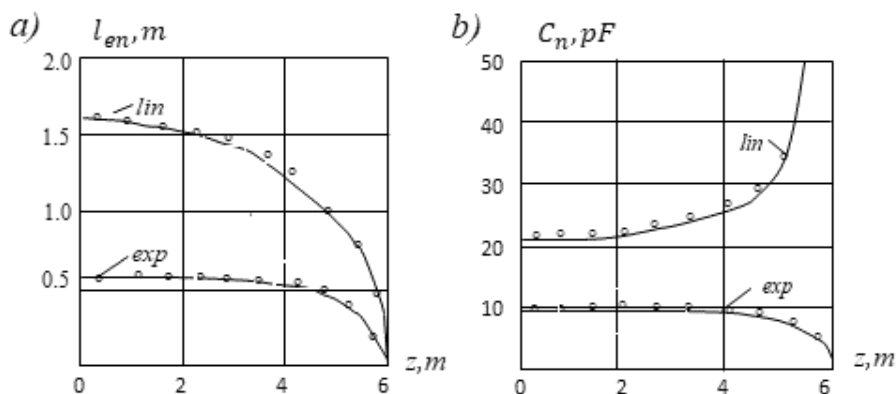


Fig. 14: Results of approximate calculation of equivalent lengths (a) and the capacitances (b).

for the antennas with linear and exponential distribution of the current amplitude are indicated by labels 'lin' and 'exp'. Equivalent lengths and capacitances were calculated at the frequency  $f=40$  MHz.

This data was used to design two antennas with in-phase currents: it was necessary to obtain in one antenna at the frequency  $f=40$  MHz a linear distribution of the current amplitude, and in the second antenna at the same frequency an exponential distribution of the current amplitude (with a logarithmic decrement  $\alpha=2$ ). The capacitive loads of the antennas were calculated by approximate methods. The design results allowed us to accomplish a rigorous calculation of the amplitude and phase of the current in both options. They are given in Fig. 15a for a linear distribution and in Fig. 15b for an exponential distribution. As can be seen from the figures, at  $f=40$  MHz the amplitude distribution is close to the required and the phase curves have a slight slope. When the frequency changes, that is, at  $f=30$  and  $f=50$  MHz, the distribution of current amplitude and phase is not preserved.

In order to provide the required current distribution in a range from 40 to 80 MHz, the synthesis of the antenna was performed by the method of mathematical programming. These results are shown in Fig. 16 for the linear (a) and exponential (b) distributions respectively. The currents amplitude and phase were obtained by means of optimizing antennas' electrical characteristics. The objective function was formed, using the root-mean-square criterion. Parameters calculated by the method of a long line with loads at the middle frequency  $f=60$  MHz, were taken as an initial approximation. The number  $N_f$  of used frequencies in a given range is equal to nine and the number  $N_l$  of points on a wire is equal to 11.

The results were improved significantly. In each figure, four curves for current amplitude are given: the curve, labeled by  $f_0$ , corresponds to the required distribution, and curves labeled by  $f=40, 60$  and  $80$ , corresponds to the synthesis result at frequencies 40, 60 and 80 MHz. As is seen from the figures, overall, the obtained distribution is close to the required distribution, but is not identical to it. However, the reason for this difference is limited opportunities of antennas rather than inexact methodology. Thus, in addition to the successful solution of a problem, the used method permits to determinate the potential opportunities of antennas.

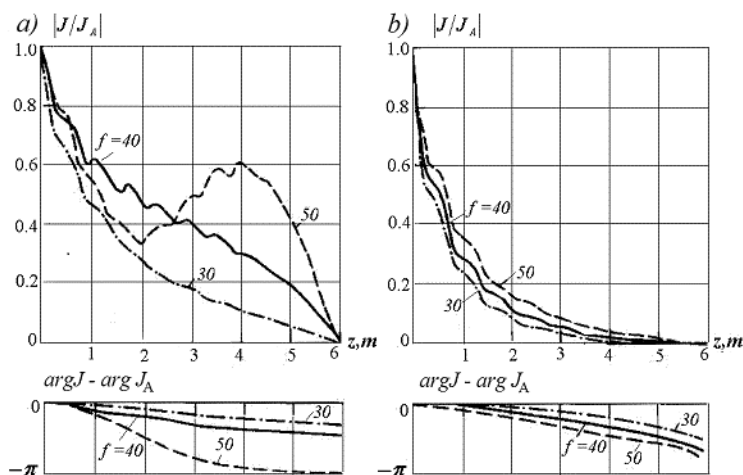


Fig. 15: Amplitudes and phases of the currents in antennas with loads, calculated by approximated method at  $f=40$  MHz.

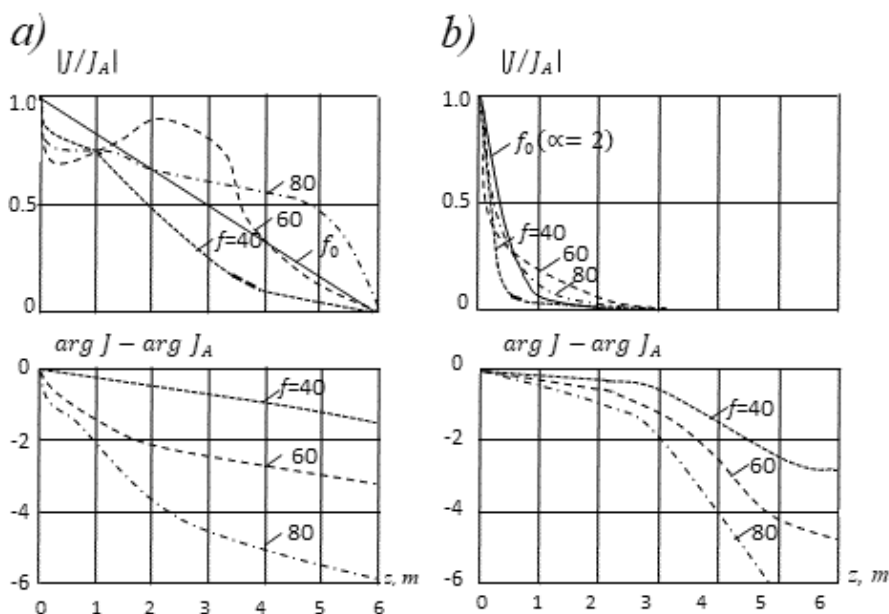


Fig. 16: Results of synthesis of linear (a) and exponential (b) current distribution in a range from 40 to 80 MHz.

The procedure of creating antennas with the required electrical characteristics makes it possible to solve the different tasks. For example, it allows us to solve the problem of reducing the influence of closely spaced metal superstructures.

As shown in Section 1, capacitive loads can be used to improve electrical characteristics of a directional V-antenna. As an example of a V-dipole we shall consider the antenna with arm length  $L = 1.5$  m and radius 0.025 m. Fifteen capacitors are included in each arm with spacing 0.1 m between loads (the first and last loads

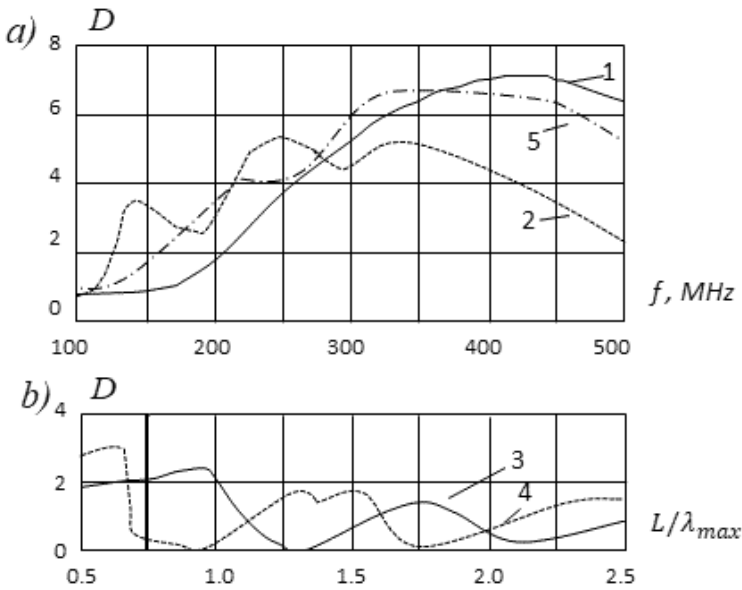


Fig. 17: Directivity of V-dipole (a) and of straight vertical dipole (b).

are placed at a distant 0.05 m from the antenna end and center). To the propagation constant remains real at frequencies up to 100 MHz, the capacitor closest to the generator was taken with the capacitance 33.5 pF. The capacitances of other loads decrease along the antenna according to the linear law. As shown in Section 1.5, using capacitors, one can ensure the current distribution along an antenna close to linear and the high level of matching with a cable.

Figure 17a shows the directivity of V-dipole with capacitive loads (curve 1) and without loads (curve 2) along the bisector of angular aperture with width  $90^\circ$ . For the sake of comparison, Fig. 17b shows similar curves for a linear dipole (curve 3 with loads, curve 4 without loads). The loads magnitudes and the antenna arm length are the same. The calculations were executed in a frequency range from 100 to 500 MHz.

As seen from the figures, the directivity of a straight vertical dipole without loads in the direction, perpendicular to the dipole axis, quickly decreases at  $L \approx (0.6-0.7)\lambda$ . For a straight dipole with loads, this threshold value is found at  $L \approx (1-1.2)\lambda$ . The directivity of V-dipole along the angular aperture bisector is much higher and retains in a substantially wider frequency range—from 350 ( $L = 1.75\lambda$ ) to 500 MHz ( $L = 2.5\lambda$ ). The loads increase the directivity of V-dipole by a factor between 1.4 and 2.8.

The presented results show that antennas with in-phase current have higher electrical characteristics than ordinary antennas produced of metal wires with sinusoidal currents. In-phase current is a current whose phase is close to constant or at least does not change sign along the antenna wire. In this case, the amplitude of the current falls along the wire towards the free end of the antenna, according to a linear or exponential law. To obtain in-phase currents, one can include concentrated capacitive loads along the antenna wire. Their capacitances should not exceed certain magnitudes depending on the signal frequency.

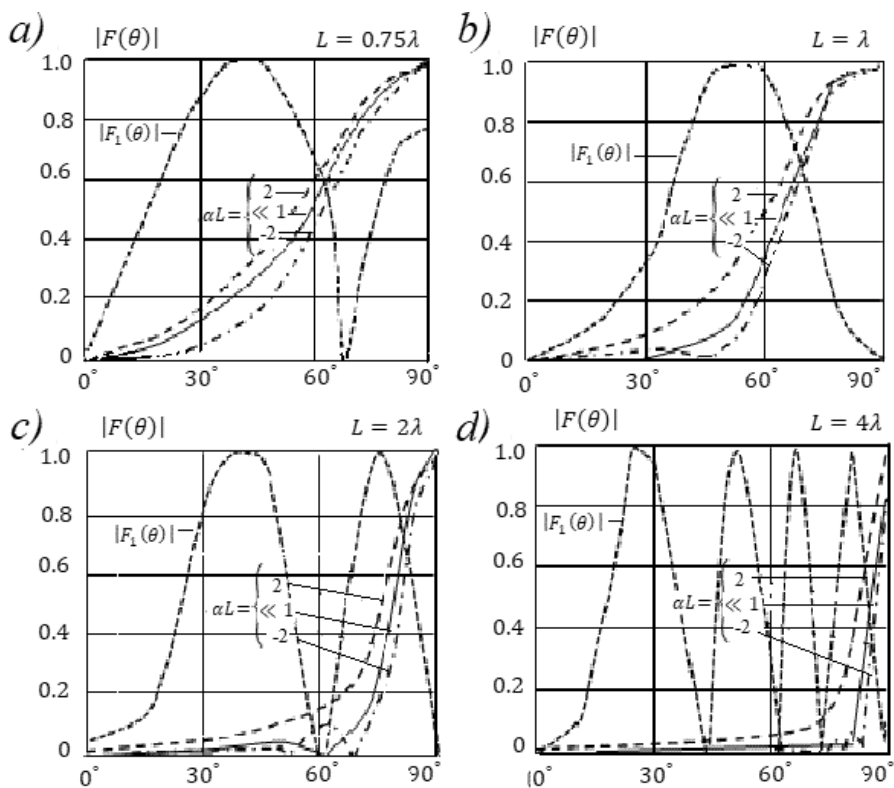


**Fig. 18:** Directional patterns of radiators with the arm length  $L$ , equal to  $\frac{3}{4}\lambda$ (a),  $\lambda$ (b),  $2\lambda$ (c),  $4\lambda$ (d), and different distribution laws of the current.

The in-phase current distribution not only allows to provide a high level of antenna matching with a cable or a generator, but also leads to a significant change in an antenna pattern. Figure 18 demonstrates the normalized directional patterns in a vertical plane, created by vertical symmetrical metal radiators with in-phase currents distributed in accordance with exponential (with different damping decrement  $\alpha$ ) and linear ( $\alpha = 0$ ) law. The length of the radiator arm  $L$  changes from  $3/4\lambda$  up to  $4\lambda$ . For the sake of clarity, the curves are plotted in a rectangular coordinate system. Here, for comparison, the directional patterns  $F_1(\theta)$  of a radiator with a sinusoidal current distribution are presented also. As is seen from Fig. 18, in the case of a linear and exponential in-phase distribution, unlike a sinusoidal one, the radiation maximum with increasing frequency does not deviate immediately from the perpendicular to the radiator axis. The increase of  $L/\lambda$  tapers the main lobe and increases the directivity. The width of the main lobe decreases with decreasing  $\alpha$ , including the transition to negative values of  $\alpha$ .

The antenna input impedance in the first approximation is equal, as it is shown in Section 3.1, to the input impedance of the stepped long line.

## 4. Method of Electrostatic Analogy

Increasing the number of linear elements in the antenna complicates the problem of its analysis and synthesis. These are, for example, the director, log-periodic and self-complementary antennas. Solving problems concerned with these antennas requires new approaches and new mathematical methods.

As is known, when solving mathematical problems, an analogous form of equation often lends essential assistance. For example, the first two Maxwell's equations that became a basis for classical electromagnetic theory, allowed to substantiate the principle of similarity and duality (see Section 2.2). In accordance with the principle of duality by replacing variables and conditional introducing a magnetic current, one can obtain expression for currents, fields, and characteristics of a magnetic radiator, like expressions for an electric radiator.

A similar method of solving problems is used in many other cases. For example, there is the known analogy between a picture of electrostatic field of charged conducting bodies located in a homogeneous and isotropic dielectric and a picture of constant currents in a homogeneous, weakly-conducting medium. In this case, bodies placed in the medium must have high conductivity and their shape and geometric dimensions must coincide with the shape and dimensions of the conducting bodies located in a dielectric.

If a picture of an electric field of linear charges is known, then, using the correspondence principle, one can construct a picture of a magnetic field of constant linear currents, provided the currents and charges are distributed in space identically. The difference between these pictures is only that lines of equal magnetic potential are located at places of lines of electric field strength, and lines of magnetic field strength are located at places of lines of equal electric potential [8].

Generalizing the principle of correspondence, it is advisable to compare electromagnetic fields created by high-frequency currents of linear radiators with electrostatic fields of charges, which are placed on linear conductors. The charge and the current uniformly distributed along each conductor. Both fields are directly proportional to the magnitudes of the current or the magnitudes of the charge, and in the far zone, they are inversely proportional to the distance from the source. In accordance with Maxwell equation for a harmonic field

$$\operatorname{div} \vec{E} = \rho$$

an electrostatic field  $\vec{E}$  in a free space is proportional to a magnitude of stationary charge  $\rho$ . In accordance with another equation

$$\operatorname{curl} \vec{H} - j\omega\epsilon_0 \vec{E} = \vec{j}$$

an electromagnetic field  $\vec{E}$  depends on a current  $\vec{j}$ —a moving flow of charges. In a far zone an electromagnetic field created by a current is a plane wave, i.e.,  $E$  and  $H$ , have identical phase, and one can consider that an electromagnetic field  $E$  is proportional to a magnitude of a current, and the structures of electrostatic and electromagnetic fields are the same.



The offered method of electrostatic analogy is based on a similarity between two structures consisting of high-frequency currents and constant charges. It is assumed that shapes and dimensions of radiators coincide with shapes and dimensions of conductors. In the case of several radiators a ratio of emf in their centers is equal to a ratio of charges placed on the conductors. The positive charge, equal to  $Q_0$ , is located on the conductor 0, which corresponds to the active radiator. The negative charges (their number is equal to  $N$ ) are located on the conductors  $i$ , corresponding to passive radiators. They are equal to  $-Q_i$  and their sum is  $\sum_{i=1}^N (-Q_i) = -Q_0$ , i.e., the sum of all charges is zero, and the conductors form an electrically neutral system. In this system

$$Q_i/Q_0 = C_{0i}/\sum_{(i)} C_{0i},$$

where  $C_{0i}$  is the partial capacitance between conductors 0 and  $i$ . Thus, the charges of the conductors  $i$  are directly proportional to the partial capacitances between these conductors and the conductor 0 (see, for example, [9]). Equivalent replacement of a complex structure of high-frequency radiators by a structure from constant charges placed on conductors sharply simplifies the problem, reducing it to the electrostatic problem. In accordance with the said, it is natural to call the proposed method by 'the method of electrostatic analogy.'

The considered method allows analyzing the problem in a general view, for example, to study and to compare different laws of current distribution along the individual radiators. This is an undoubted advantage of this method. Characteristics of complex antennas are usually calculated by using complex programs based on the Moments method. For discussed problems, such a method is in essence a trial-and-error method. The Moments method does not permit comparison of antennas with different distribution of currents in a general form. Therefore, this method is not applicable here. The approximate method does not give exact results. But if this method is correct, i.e., corresponds to the physical essence of the problem, its accuracy is the same for different distributions of the current and the method allows us to choose the best option.

The Preface emphasizes the usefulness of the methods, which are based on an understanding of the physical content of electrodynamic problem and permits to simplify it and obtain an approximate solution, the result of which may be used as initial value for the numerical solution by the method of mathematical programming. The method of electrostatic analogy is an approximated method of this type.

It is expedient to consider the procedure of applying the electrostatic method as a concrete example. As an example, the director-type antenna (Yagi-Uda antenna) described in [10] was adopted. It should be recalled that the problem of optimizing the antenna characteristics by choosing dimensions of its elements and using mathematical programming methods was first solved with respect to the director-type antenna, and this decision confirmed the correctness of the chosen approach. Work [10] was one of the first and most profound works devoted to optimization of the director-type antenna.

The antenna circuit is given in Fig. 19. The antenna consists of four metal radiators (active radiator, reflector and two directors). On Fig. 19, the antenna dimensions are

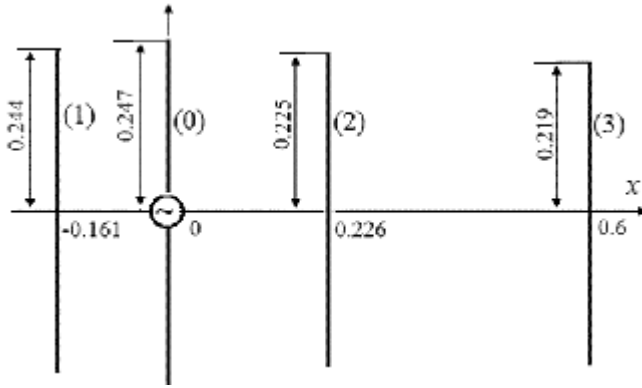


Fig. 19: Dimensions of the optimized director antenna from metal radiators.

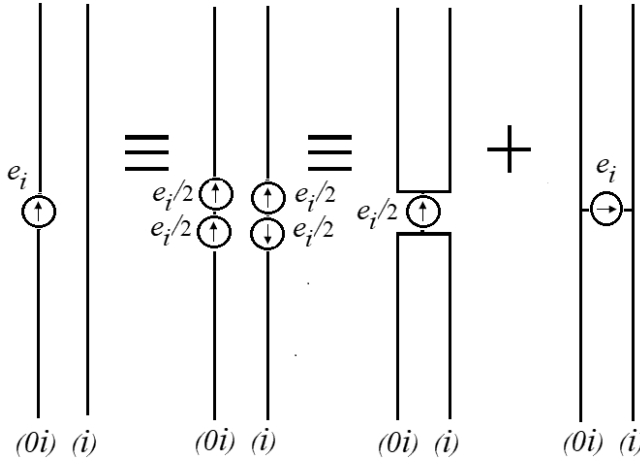


Fig. 20: Circuit from two parallel vertical wires.

shown in meters. They were determined by solving the optimization problem in a strict formulation. Let's start with the capacitance between the conductors. If the radii of the conductors  $i$  and  $0$  are the same, equal to  $a = 0.001$  m and the lengths  $l_0$  and  $l_i$  of these wires are slightly different from each other, then the partial capacitance  $C_{0i}$  between these wires in the first approximation is equal to

$$C_{0i} = \pi \varepsilon_0 l_i / \ln(b_i/a),$$

where  $\varepsilon_0$  is the medium permittivity, and  $b_i$  is the distance between the wires.

If to divide the wire  $0$  of the antenna into three wires and to denote these wires by indices  $0i$ , then the antenna circuit is divided into three circuits. Each circuit consists of two conductors: of wire  $i$  and wire  $0i$  (Fig. 20). The generator is also divided into three generators located in the centers of the wires  $0i$ . The values of their emfs are defined as (7.36)

$$e_i = e Q_i / Q_0, \quad (7.36)$$

where  $e$  is the emf of the active radiator  $\theta$ .

As shown in the theory of folded antennas, the circuit of two parallel vertical wires located at a distance  $b_i$  can be divided into a dipole and a long line, open at both ends. The current at the center of each dipole is equal to

$$J_{id} = e_i / (4Z_{id}).$$

The reactive component of its input impedance is  $X_{id} = -120 \ln(2L_0/a_{ei}) \cot kL_0$ , where  $L_0 = l_0/2$  is the arm length of the active radiator,  $a_{ei} = \sqrt{ab_i}$  is its equivalent radius,  $k$  is the propagation constant. The current at the center of each wire of the long line is equal to

$$J_{il} = e_i / (2jX_{il}),$$

where  $jX_{il} = -j120 \ln(b_i/a) \cot kL_i$  is the reactive input impedance of the long line with length  $L_i = l_i/2$ . The currents of the active and passive radiators are equal to the sum and difference of the dipole wire current  $J_{id}$  and the current  $J_{il}$  of the long line, i.e., total current  $J_0$  of the active radiator and the total current  $J_i$  of each passive radiator are equal to

$$J_0 = \sum_{i=1}^3 (J_{id} + J_{il}), J_i = J_{id} - J_{il}.$$

The amplitude and phase of the fields created by each radiator depend on its structure. The radiator structure determines the law of current distribution along it. If the radiator arm is a straight metallic conductor, its current is distributed according to the sinusoidal law  $J(z) = J(0) \sin k(L - |z|)$ . In this case, as is shown in Section 1.6, the far field of the radiator is equal to

$$E_\theta = \frac{AJ(0)}{\sin \theta} \cdot \frac{\exp(-jkR)}{R} [\cos(kL \cos \theta) - \cos kL],$$

where  $A = j60$ ,  $R$  is the distance to the observation point. If the concentrated capacitive loads realize the in-phase current, distributed along the radiator axis in accordance with a linear law  $J(z) = J(0)(L - |z|)$ , then the far field of the radiator, as is shown in Section 1, is equal to

$$E_\theta = \frac{AJ(0) \sin \theta}{\cos^2 \theta} \cdot \frac{\exp(-jkR)}{R} [1 - \cos(kL \cos \theta)].$$

From Fig. 19 it is clear that the maximum radiation of the considered antenna is directed to the right, that is, towards the radiator 3. Since the radiator 1 is located on the left of the active radiator  $\theta$  at a distance  $b_1$  from it, its field lags behind the field of the active radiator, first, per phase corresponding to a time of signal propagation from radiator  $\theta$  to the radiator 1, and secondly, per phase corresponding to the propagation time of the signal in the opposite direction—from the radiator 1 to the radiator  $\theta$  (the signal of radiator 1 must come to the radiator  $\theta$  an angle  $\theta$ , i.e., the path length between the wires is  $b_1/\sin \theta$ ). The total phase difference is equal to  $\psi_1 = -kb_1(1 + \sin \theta)/\sin \theta$ . Similarly, in the case of radiators 2 and 3, this phase difference is equal to  $\psi_2 = kb_2(\sin \theta - 1)/\sin \theta$  and to  $\psi_3 = kb_3(\sin \theta - 1)/\sin \theta$ , respectively.

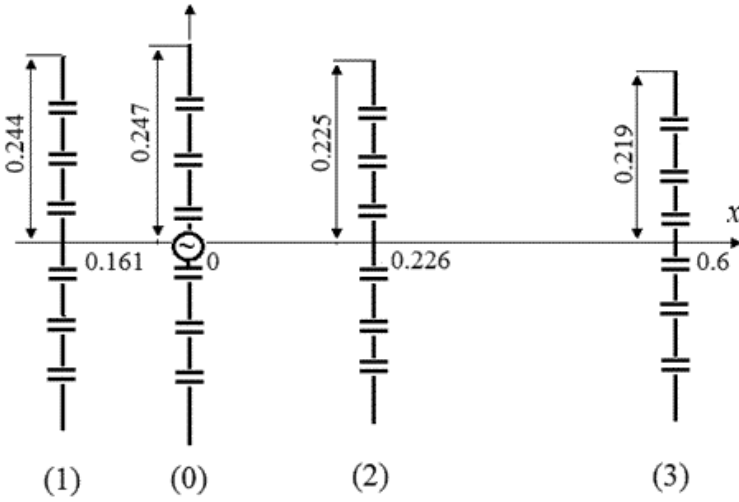


Fig. 21: Director antenna with straight in-phase radiators.

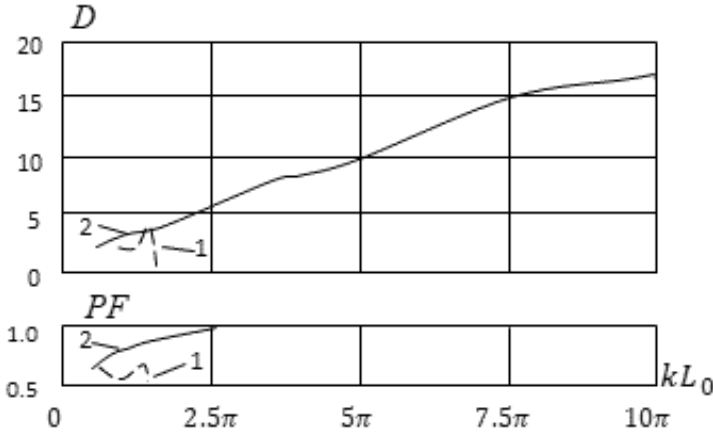


Fig. 22: Directional characteristics of director-type antennas with sinusoidal (1) and in-phase (2) currents.

The described procedure permits to determine the total field of the director-type antenna shown in Fig. 21. In accordance with (7.36), emfs of the different radiators are equal to  $e_1 = 0.388e$ ,  $e_2 = 0.335e$ ,  $e_3 = 0.277e$ . The total field of this antenna with radiators in the form of straight metal wires is

$$E = \frac{AJ(0)}{\sin \theta} \sum_{i=1}^3 e_i \cdot \frac{\exp(-jkR)}{R} \left\{ \left( \frac{1}{4Z_{id}} + \frac{1}{2Z_{il}} \right) [\cos(kL \cos \theta) - \cos kL] \right. \\ \left. + \left( \frac{1}{4Z_{id}} - \frac{1}{2Z_{il}} \right) \exp(j\psi_i) [\cos(kL_i \cos \theta) - \cos kL_i] \right\}.$$

The emfs of the radiators do not change.

The inclusion of concentrated capacitive loads along the linear radiators, whose magnitudes of which vary in accordance with the linear or exponential law, permits

to create radiators with in-phase current. While retaining the dimensions of the radiators and the distances between them, we get the director-type antenna shown in Fig. 21. The total field of such an antenna is calculated by the formula

$$E = \frac{AJ(0)}{\sin \theta} \sum_{i=1}^3 e_i \cdot \frac{\exp(-jkR)}{R} \left\{ \left( \frac{1}{4Z_{id}} + \frac{1}{2Z_{il}} \right) [1 - \cos(kL_0 \cos \theta)] \right. \\ \left. + \left( \frac{1}{4Z_{id}} - \frac{1}{2Z_{il}} \right) \exp(j\psi_i) [1 - \cos(kL_i \cos \theta)] \right\}.$$

The results of calculating the directivity and the pattern factor of a director-type antenna with straight metal wires are given in Fig. 22 (curves 1). These results are not identical to the results presented in [10], since here an approximate calculation procedure was used, but these results are like them. The basic working frequencies of both antennas are practically the same. The results of calculating these characteristics for the antenna with in-phase currents are given in Fig. 22 by curves 2. They speak for themselves. The antenna with in-phase currents operates over a wide frequency range, and its directivity steadily and smoothly increases with increasing frequency, that is, the quality factor of this antenna is small. Of course, we must bear in mind that these characteristics are valid only, if the current is in-phase. But the frequency overlap ratio of antennas with capacitive loads with a high level of matching is a magnitude of the order 10.

As has already been said, the method of electrostatic analogy is based on the resemblance of a structure with high-frequency currents and a structure with constant charges. Comparison of electromagnetic fields created by high-frequency alternating currents of linear radiators with electrostatic fields of charges placed on linear conductors of electrically neutral system shows similarity of the mathematical structures of both fields.

This method allows us to propose a simple and effective procedure for calculating the directional characteristics of the director-type antennas consisting from linear radiators. The procedure uses information about the basic antenna dimensions and current distributions along the radiators. The detailed information on the types and magnitudes of concentrated loads does not require. As calculations show, the director-type antennas consisting from the linear radiators with in-phase currents provide a high directivity and smooth variation of characteristics in a wide frequency range. The results obtained with the help of this method can be used to solve the problem of optimizing various director-type antennas by mathematical programming methods.

Similar results can be obtained for V-radiators. In this case, the operating range decreases, but *TWR* increases at concrete frequencies. The circuit of such director-type antenna with V-radiators is given in Fig. 23. Calculations were performed for antennas with the same lengths of radiators and the same distances between them as in the antenna shown in Fig. 21. The angles in radiators between the arms and the vertical in each antenna are the same and in different antennas are equal to 10°, 20°, and 30°, respectively. In this case, the total antenna field is equal to

$$E = \frac{AJ(0)}{\sin \theta} \sum_{i=1}^3 e_i \cdot \frac{\exp(-jkR)}{R} \left\{ \left( \frac{1}{4Z_{id}} + \frac{1}{2Z_{il}} \right) [1 - \cos(kL_0 \cos(\theta - \theta_0))] \right\}$$

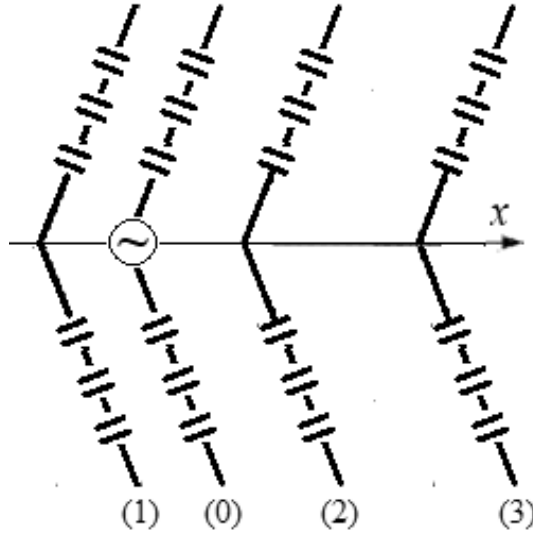


Fig. 23: Director-type antenna from V-radiators with in-phase currents.

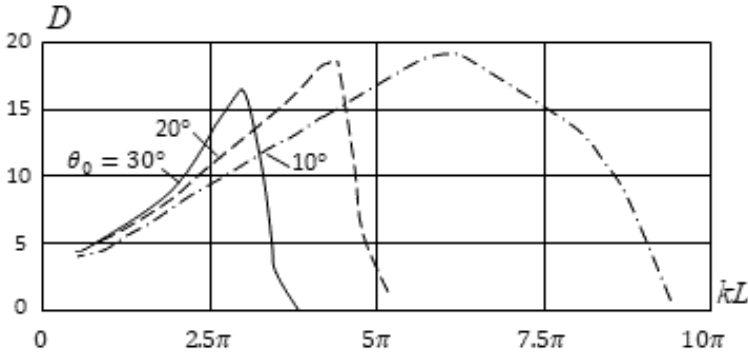


Fig. 24: Directivity of director-type antennas, consisting from V-radiators with in-phase currents.

$$+ \left( \frac{1}{4Z_{id}} - \frac{1}{2Z_{il}} \right) \exp(j\psi_l) [1 - \cos(kL_0 \cos \langle \theta - \theta_0 \rangle)] \Big\}.$$

The directional characteristics of the director-type antennas with V-radiators are shown in Fig. 24. The magnitude of pattern factor does not drop below 0.85. The results show that these antennas, in comparison with the antennas consisting from straight in-phase radiators allow increasing directivity but in a narrower frequency range. In this case the directivity and frequency range depend on the inclination of the antenna arm: if this angle increases, the directivity at low frequencies also increases, but the frequency range becomes narrower.

The electrostatic analogy method was proposed in 2017 [11]. But the need for such a method was understood long ago. A.F. Chaplin with his pupils stubbornly paved the way to it. On the other hand, A.F. Yakovlev persistently tried to improve the electrical characteristics of a log-periodic antenna. His results are discussed in the next Section.

## 5. New Options of Log-periodic Antennas

As is known, log-periodic antennas belong to the class of frequency-independent antennas. Their design is based on the principle of complementarity and automatic ‘cut-off’ of the currents outside the active region. In accordance with the principle of electrodynamic similarity any radiator has the same electrical characteristics at different frequencies, if its geometric dimensions vary with frequency in proportion to the wavelength (in the first approximation the requirement about corresponding change of the conductivity may be neglected). Not only the tunable antennas, but also the antennas, whose shape is completely determined by the angular dimensions, conform to the principle of electrodynamic similarity. In this case the change of a scale does not change the radiator, i.e., the radiator shape and dimensions in wavelengths at different frequencies are the same.

The property of the automatic ‘cut-off’ of currents means that the field at each frequency is radiated by a current of a small antenna segment, which is named by the active area, and that the electric current outside the boundaries of this area is quickly attenuated. Here, coordinates and dimensions of radiated segment are rigidly related with the wavelength. If the frequency changes, the antenna segment radiating the field shifts along the antenna. Both longitudinal and cross electrical dimensions of this radiating area remain constant and ensure the invariability of the characteristics. Thus, the log-periodic antenna has a constant input impedance and invariable directivity characteristics in a wide band.

If the antenna has finite dimensions, its frequency range is finite, but in this finite range the antenna has the properties of an infinite antenna. The maximal wavelength depends on the maximal cross dimension of the antenna (on its width), and the minimal wavelength depends mainly on the accuracy of the observing required dimensions near the excitation point.

Log-periodic dipole antenna (LPDA) shown in Fig. 25, is a collection of dipoles, with dimensions forming a geometric progression with denominator  $1/\tau$ ,

$$R_{n+1}/R_n = l_{n+1}/l_n = 1/\tau.$$

Here  $R_n$  is the distance from the vertex of the angle  $\alpha$  to dipole  $n$ ,  $l_n$  is the arm length of dipole  $n$ ,  $\alpha$  is the angle between the antenna axis and the line passing through the dipoles ends. Accordingly, the antenna electrical characteristics are repeated at frequencies forming the geometric progression with the same denominator. It means that directivity characteristics and input impedance of the antenna are periodic functions of  $\ln f$  (logarithm of frequency). If the electrical characteristics are functions of  $\ln f$ , their values are repeated with period equal to  $\ln \tau$ . This peculiarity defined the antenna name.

Weak variation of antennas characteristics within the periodic interval is an indispensable condition for their weak dependence on frequency. In order to meet this condition, the interval must be small. But this is insufficient condition.

LPDA shown in Fig. 25 consists of two structures situated in one plane. Each structure is shaped as a straight wire, with linear conductors attached to it at right angles alternately from the left and from the right. Their lengths increase with the

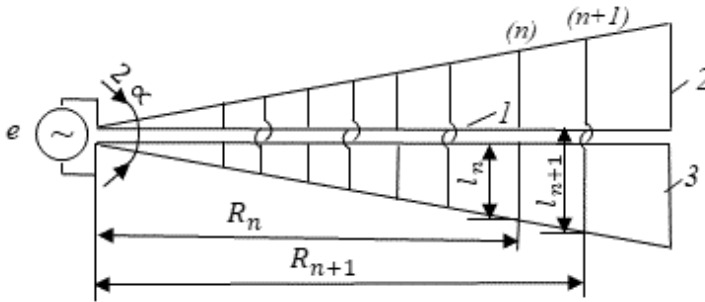


Fig. 25: Log-periodic dipole antenna  
1 – longitudinal wire, 2 – cross wire, 3 – interval between the cross wires.

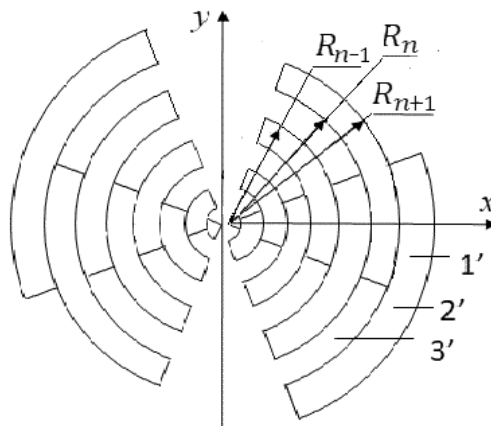


Fig. 26: Flat self-complementary log-periodic antenna.  
1' – metal sector, 2' – metal strip, 3' – slot.

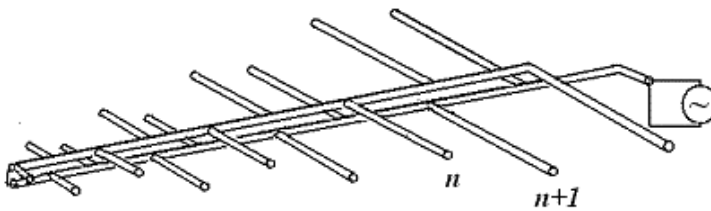


Fig. 27: Design of antenna LPDA.

growing distance from the excitation point in accordance with the law of geometric progression. Such antenna is a simplified and modified variant of a flat log-periodic structure shown in Fig. 26, which is a self-complementary structure. This structure consists from metal plates and slots coinciding with each other in shape and dimensions. The input impedance of a flat infinite self-complementary structure is purely active, independent of the frequency, and is equal to  $60\pi$  Ohm. Designing log-periodic antenna in the form of a self-complementary structure ensures a weak variation of antenna' electrical characteristics within each interval.

Each of the two structures, forming LPDA, differs from the structure, forming an arm of a flat log-periodic antenna. The angular metal sector 1' is replaced with



a longitudinal wire 1. The metal strip 2', situated along the arc of a circumference, is replaced with a lateral wire 2, tangent to the arc. The slot 3' is replaced with an interval 3 between the lateral wires. Such a construction is essentially simpler for implementation and, at the same time, is close to the original one in the electrical properties.

The turn of one metal structure (of one antenna arm) around the y-axis (see Fig. 26) through the angle  $\pi$  and placing both structures in one plane allow providing unidirectional radiation. The unidirectional log-periodic antenna shown in Fig. 25 may be interpreted as a linear array of symmetrical radiators. These radiators have monotonically changed lengths and are excited by a two-wire transmission line. A generator is connected to the line from the side of shorter radiators.

A reasonable implementation of an antenna design, which requires no special balun, is shown in Fig. 27. The cable is placed inside one of two tubes forming a two-wire distribution line. The cable sheath and the tube of distribution line form a single unit, and an inner conductor of the cable is connected to the second tube at the antenna vertex. This design provides connection of the distribution line' wires, which is implemented at the distance  $\lambda_{max}/8$  from the base of first dipole. Here  $\lambda_{max}$  is the maximal wavelength.

The active area of LPDA consists of dipoles with the arm length close to  $\lambda/4$ . In their input impedance an active component is predominant, and the reactive component is small. In actual practice the number of dipoles, forming the active area, usually is equal to five. For the sake of simplicity, we will assume that the active area consists from only three dipoles, and the arm length of central dipole is equal to  $\lambda/4$ .

As is seen from Fig. 25, the arms of dipoles connected alternately to one or another conductor of the distribution line. This structure is equivalent to a mutual crossing of conductors on the segments between the dipoles. With allowance for this crossing the phase of electrical current in the longer dipole exceeds the phase of the current in the resonance radiator, and the phase of the current in the shorter dipole is less than the phase of current in the resonance radiator, i.e., the longer dipole acts as a reflector, and the shorter dipole acts as a director. As a result, the fields of individual radiators are summed in the direction toward the excitation point (to the shorter dipoles) and cancel each other in the opposite direction.

The waves in the distribution line reflected from dipoles of the active area cancel each other to a large degree, since the reactive components of the input impedances of short and long dipoles are opposite in sign. This explains a high level of matching of the antenna' active area and the distribution line. In addition, the electrical length of the line from the excitation point to the active area remains unchanged when the frequency changes. Therefore, an impedance of active area transformed to the antenna input is the same at different frequencies.

The dipoles located outside the active area are excited weakly due to the great reactive impedance. The short dipoles at the beginning of the structure practically fail to radiate, since the fields created by them are summed up almost in anti-phase because of crossing wires and the proximity of dipoles to each other (as compared with the wavelength). As a result, the EM wave along this segment of the line does not weaken, i.e., the structure of currents and voltages at the line segment between the excitation point and the active area is close to the traveling wave. The short dipoles

act as capacitances shunting the distribution line and thereby decreasing slightly its wave impedance. The long dipoles situated behind the active area radiate weakly too, since, first, their input impedances are great and, second, the power of the EM wave at that segment of line drops substantially as a result of attenuation in the active area.

The method of LPDA calculation [12] is based on antenna presentation in the form of a parallel connection of two multipoles (Fig. 28). The first multipole consists of dipoles and is defined by matrix  $Z_A$  of mutual impedances. The second multipole is a distribution line, which is defined by matrix  $Y_l$  of admittances. For each cross-section  $n$  of the structure, consisting from two multipoles, the following equalities are true:

$$J_{nA} Z_{nA} = J_{nl} / Y_{nl}, \quad J = J_{nA} + J_{nl}, \quad (7.37)$$

i.e.,  $J_{nl} = J_{nA} Z_{nA} Y_{nl}$ . Here  $J_{nA}$  is the current at the dipole input,  $Z_{nA}$  is the input impedance of the dipole (with allowance for coupling with neighboring dipoles),  $J_{nl}$  is the current of the distribution line,  $Y_{nl}$  is the admittance of the line in the cross-section  $n$ , and  $J$  is the extraneous current at given point. It should be noted that in calculating  $J_{nA}$  the mutual coupling with neighboring dipoles is accounted, and in calculating  $Y_{nl}$  it is considered that the distribution line is shorted at the terminals of neighboring dipoles (during calculating the current created by the given source it is considered in accordance with Kirchhoff's law that the other sources are shorted).

A first equation of (7.37) is written for a voltage along a closed circuit, and a second equation is written for a current at the input point. From here,

$$J = (1 + Z_{nA} Y_{nl}) J_{nA}.$$

Accordingly, a matrix equation for the column-vector  $[J_A]$  of the dipole input currents is written in the form

$$[J] = ([E] + [Z_A][Y_l])[J_A], \quad (7.38)$$

where  $[E]$  is an identity matrix,  $[J]$  is the column-vector of currents exciting the lines connecting the multipoles with each other. Since the source of excitation is only the generator located at the input of distribution line, we put that the current

of this generator is equal to  $|J_0|$ , then  $[J] = \begin{bmatrix} J_0 \\ 0 \\ \dots \\ 0 \end{bmatrix}$ . Solving equation (7.38), we find

the column-vector  $[J_A]$ , and then matrix  $[V_A] = [Z_A][J_A]$  of the voltages at the dipoles' inputs. The first element of the matrix at the input of the shortest dipole is the input voltage. If the exciting current  $J_0$  is equal to 1, this first element is equal to the input impedance of the antenna.

When designing LPDA, it is important to choose the geometric dimensions in such a way that the electrical characteristics changed weakly in a range from  $f$  to  $\tau f$ . The magnitude  $\tau$  and all antenna characteristics depend essentially on the parameter  $\sigma$ , which is equal to the distance between the half-wave dipole and the neighbor shorter dipole (in wavelengths):

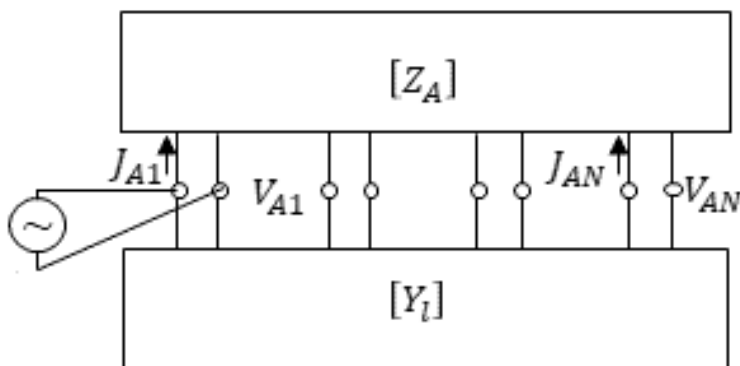


Fig. 28: Equivalent circuit of LPDA.

$$\sigma = 0.25(1 - \tau)\lambda \cot \alpha. \quad (7.39)$$

In substance, this expression is dependence on the angle  $\alpha$  in view of  $\tau$ . As it is shown in [12, 13], the characteristics change weakly, if  $\tau > 0.8$  and  $0.05 \leq \sigma/\lambda \leq 0.22$ . Under these conditions, the currents of the dipoles, located near the resonant (half-wave) radiator, reach a maximum and the wave along the distribution line is so attenuated in the active area that the follow dipoles practically do not radiate.

In [14] by means of generalization of data available in the literature the optimum relationship of the basic parameters is defined in the form:

$$\sigma/\tau = 0.191.$$

This ratio does not depend on the values of  $\alpha$ ,  $l_n/a_n$  and  $Z_0$ ). Here  $a_n$  is the radius of dipole  $n$ ,  $Z_0 = 60 \cosh^{-1} [(D^2 - 2a^2)/(2a^2)]$  is the wave impedance of the distribution line,  $a$  is the radius of the distribution line's wires, and  $D$  is the distance between axes of these wires. Substitution of the ratio  $\sigma/\tau$  into (7.39) permits to obtain simple expressions connecting the optimal parameters  $\tau$  and  $\sigma$  with the antenna dimensions:

$$\tau = 1/(1 + 0.765 \tan \alpha) = L/[L + 0.765(l_1 - l_N)], \sigma = 1/(4 \tan \alpha + 5.23). \quad (7.40)$$

The value  $L$  in these expressions is the distance between the first and the last ( $N$ th) dipole.

The antenna with  $\sigma/\tau = 0.191$  has a narrow directional pattern and high front-to-back ratio. *SWR* of this antenna in a properly designed LPDA is typically smaller than 1.5. But since log-periodic antennas have rather large overall dimensions, then the task of reducing the dimensions of a log-periodic antenna has always been the main task of the developers. In order to decrease transverse dimensions, it is expedient to shorten the longest dipoles using loads of different kind or structures with the slowing-down properties, i.e., by means of mechanisms used usually for reducing the monopole's and dipole's length. The options of slowed-down structures are numerous. It should be noted that the slowing factor is always greater than the factor of the wire length reduction.

Slowing-down allows to reduce the length of the monopole in  $m$  times for the given frequency of the first resonance or to decrease the resonance frequency in  $m$  times for the given length of the monopole. But the resistance of radiation at the resonance frequency in consequence of the length reduction decreases in  $m^2$  times and the antenna wave impedance is increased in  $m$  times. And both results impair matching of each element of LPDA and an antenna overall with a cable. Attempts to decrease longitudinal dimensions of an antenna by using slowing-down in the distribution line or at the expense of additional dipoles connection failed, since violation of relationships of geometric progression and increasing the dipoles number causes, as a rule, sharp deterioration of electrical characteristics and gives insignificant decrease of overall dimensions.

In [14] it is described the variant of log-periodic antenna, which operates in two adjacent frequency bands and allows making the antenna shorter than an antenna designed for operation in the total range. Basically, the authors' proposal reduces to the use of linear-spiral dipoles, i.e., radiators, each of which consists of straight and spiral dipole. They arranged coaxially and have the common excitation point. The dipoles length is the same, but the spiral wire length is twice as much as the straight rod's length. Linear-spiral dipole in contrast to straight and spiral dipole has two series resonances, and the ratio of the resonant frequencies in the case of the same length of both dipoles is equal to the slowing factor of the spiral dipole.

As said before, resonant dipole and its nearest neighbors create an active area, passing through which the electromagnetic wave actively radiates energy. LPDA with linear-spiral dipoles has two active areas, and they provide a signal radiation in two bands of the frequency range. The experimental check of log-periodic antenna with linear-spiral dipoles confirm that this proposal is promising. With comparable electrical characteristics the length of log-periodic antenna, in which only straight dipoles are used, is in 1.8 times as large as the length of the antenna with linear-spiral dipoles. If only spiral dipoles are used, the length of an antenna with these dipoles 1.3 times less than the length of an antenna with linear dipoles.

The length of log-periodic antenna can be reduced by increasing the angle  $\alpha$  between the antenna axis and the line passing through the dipoles ends. This option seems the most simple and natural. But, as it is seen from (7.39), an increase in  $\alpha$ , if  $\tau$  is constant, leads to a decrease in the distance between the dipoles and to an increase in their mutual influence, and consequently to decreasing both the directivity and the active component of input impedance. As the result, the frequency characteristics of the antenna are deteriorated.

One can increase the angle  $\alpha$  by another manner. LPDA consists (see Fig. 25) of two asymmetric structures located in the same plane and excited in opposite phases. If these structures are located at an angle  $\psi > \alpha$  to each other, the resulting three-dimensional structure will incorporate two planar structures, distant from each other. The monopoles are attached to the conductor of the distribution line alternately from the left and right. The distance between the monopoles, situated on the one side of the conductor, is almost twice as large as in a planar LPDA. This reduces their mutual influence and allows for increasing the angle  $\alpha$ . However, this antenna occupies a great volume, and that makes its installation difficult and changes its characteristics,

for example, it increases input resistance and creates additional problems in the utilization of the antenna.

Asymmetrical coaxial log-periodic antennas, described in [14], do not have these disadvantages. The two-wire distribution line in this antenna is replaced by a coaxial line, and dipoles are replaced by monopoles. The assembled antenna is presented in Fig. 29. The antenna consists of two structures (internal and external), which are shown in Fig. 30. The first structure (Fig. 30a) is a straight conductor (the central wire of the coaxial distribution line), to defined points of which at the right angle the wires' segments of required length are connected alternately from left and from right. These segments are monopoles, located in one plane and excited by means of this conductor.

The second structure (Fig. 30b) is designed as a long cylindrical metal tube. The long tube is the outer envelope of a coaxial distribution line. The monopoles are connected with the center conductor and the outer envelope of the coaxial line. They are the radiators, whose excitation points shifted from the base. As can be seen from Fig. 29, these monopoles are located inside the short tubes (coaxial shells). The short tubes are inserted in the long tube, they are open on the both ends (inside and out).

In accordance with the usual practice of designing log-periodic antenna, its dimensions must correspond to the geometric progression with denominator  $1/\tau$ :

$$R_{n+1}/R_n = l_{n+1}/l_n = h_{n+1}/h_n = 1/\tau. \quad (7.41)$$

Here  $h_n$  is the distance from the axis of the distribution line to an excitation point of radiator  $n$ . Other dimensions were designated previously. It is necessary to provide the coincidence of wave impedance of each short tube with the resistance of located in this tube monopole on the frequency of the first series resonance. This requirement determines the choice of the ratio of a tube diameter to a radiator diameter.

From above it follows that the two-wire distribution line is replaced in the proposed antenna by a coaxial distribution cable, and the dipoles are replaced by monopoles connected to the internal conductor of this cable. The outer envelope of the cable is used as a ground. This envelope in turn serves as a ground for monopoles, which are excited in anti-phase with it, and that substantially distinguishes the given ground from large metal sheet. This means that the proposed structure realizes an asymmetrical version of the usual log-periodic antenna (symmetrical version of such antenna is implemented as the antenna LPDA). Accordingly, it is possible to increase significantly the angle  $\alpha$  and to shorten the antenna without fearing decrease of directivity and increase of losses, i.e., deterioration of frequency-independent characteristics. Since the monopoles are the radiating elements of the antenna, then by analogy with the LPDA, it is expedient to name this antenna by LPMA.

The operating principle of a symmetrical antenna was reviewed earlier by means of the analysis of processes in its active area. The processes in the active area of an asymmetrical antenna are practically do not differ from the processes in a symmetrical antenna, since the waves in a coaxial distribution line are like the waves in the two-wire line and are depended on the monopoles as the waves in a symmetrical structure are depended from the dipoles. In the surrounding space the equally excited dipoles and monopoles produce the same fields.

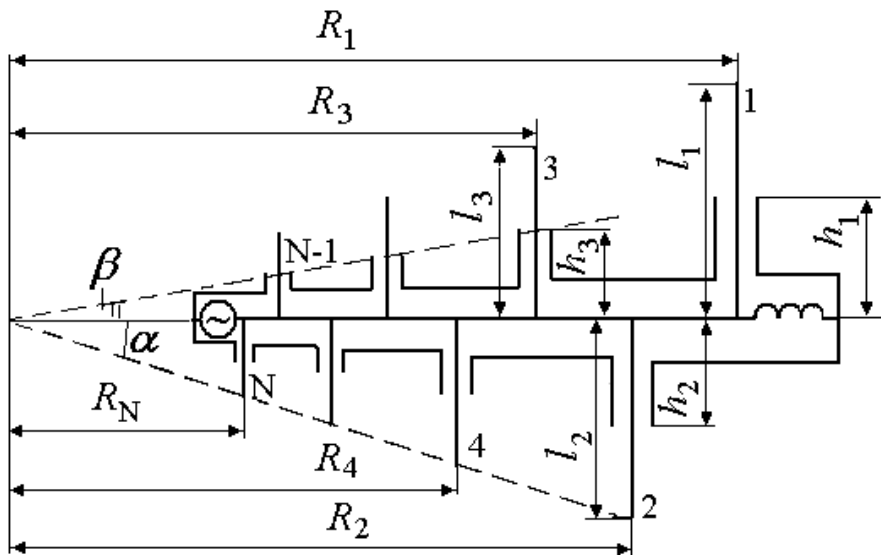


Fig. 29: The structure of asymmetrical coaxial log-periodic antenna.

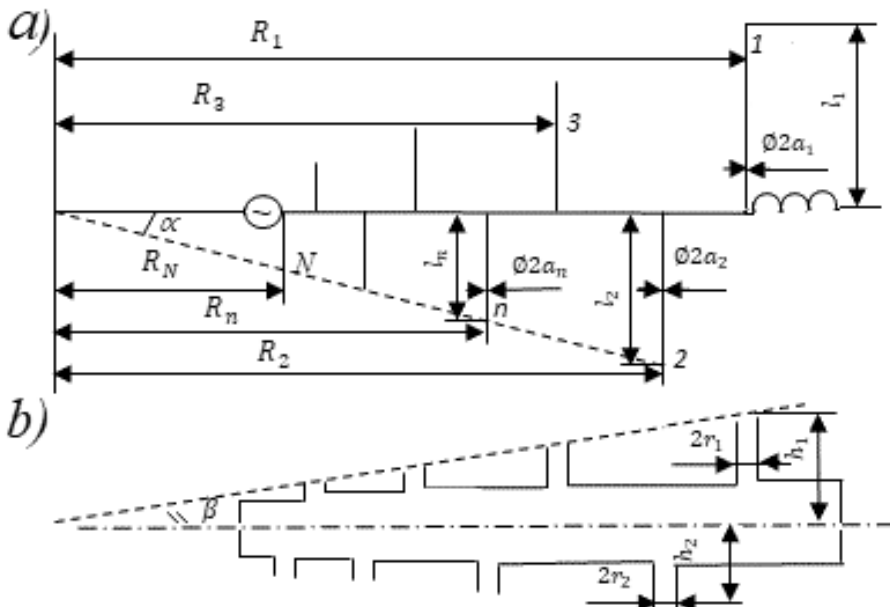


Fig. 30: Internal (a) and external (b) structures, from which asymmetrical coaxial log-periodic antenna consists.

The mock-up of an antenna has been manufactured and tested by authors. It was designed for use in the range of 200–800 MHz. Antenna characteristics were measured for the two variants of its mounting on the metal mast: (1) installation with help of a cantilever, the radiators are mounted vertically, (2) installation on the mast top, the radiators are mounted horizontally, and the gravity center coincides

with a mast axis. The distribution line was manufactured in the shape of a truncated pyramid with a square cross-section and the internal conductor was made in the shape of a horizontal plate of variable width.

The history of the creation of LPMA, described in detail, makes it possible to get acquainted with the difficulties that arise when trying to reduce the dimensions and to achieve a minimal improvement in the properties of log-periodic antennas. These difficulties are caused by the complex structure of the antenna itself. As said above, this structure does not withstand rough intervention.

In this chapter it was shown that connection of concentrated capacitive loads along a linear radiator and application of in-phase currents distribution in the director-type antennas provides the higher directivity in a wide frequency range. In this case, it is expedient to use the method of electrostatic analogy as an approximate method of analysis, the results of which one can later apply as initial values for solving the problem by the method of mathematical programming. As was shown in Section 4, this method is based on an analogy between two structures consisting of high-frequency currents and constant charges. This method allows us to use a new approach to solving the problem of reducing antenna dimensions.

In accordance with a well-known method of calculating log-periodic antenna [12], we consider an active region of this antenna consisting of three radiators (Fig. 31) and determine fields of these radiators when emf  $e$  is in the middle radiator, in the center of this region. We will regard that the arm length of the middle radiator of the active area is equal to  $L_0 = \lambda/4$  ( $\lambda$  is the wavelength), the arm length of the left (longer) radiator is  $L_1 = \lambda/(4\tau)$ , and the arm length of the right (shorter) radiator is  $L_2 = \lambda\tau/4$ . Here  $\tau$  is a denominator of a geometric progression, according to which the radiators' dimensions are changed. The magnitude of another parameter ( $\sigma$ ) is given in (7.39). As said in [14], generalization of information in the engineering literature leads to the conclusion that the minimum changes in the electrical characteristics of the log-periodic antenna within the frequency interval from  $f$  to  $f\tau$  occurs when  $\sigma/\tau = 0.19$ . We will assume that this relation is valid for the considered antenna. Let  $\tau$  be equal

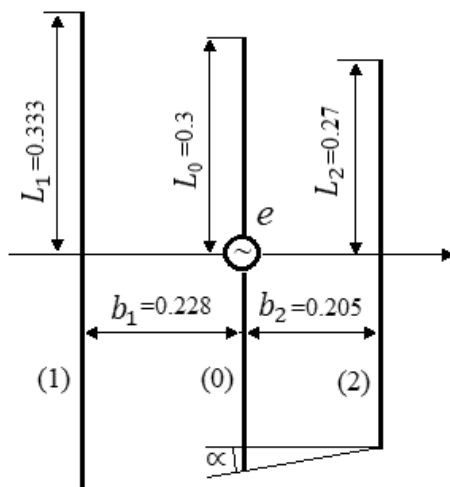


Fig. 31: The antenna of three radiators.

to 0.9. Then  $L_1 = L_0/0.9 = 0.278\lambda$ ,  $L_2 = L_0 \cdot 0.9 = 0.225\lambda$ ,  $\alpha = 0.146$ ,  $b_1 = 0.19\lambda$ ,  $b_2 = 0.171\lambda$ .

To use farther the theory of folded antennas we divide the active radiator (conductor 0) into two conductors (with numbers 01 and 02) and the obtained group of the four conductors into two circuits: the first circuit with conductors 01 and 1 and the second circuit with conductors 02 and 2. In accordance with the method of the electrostatic analogy we assume that the ratio of the emf in the wires 01 and 02 is equal to the ratio of the partial capacitances  $C_{01}$  and  $C_{02}$ , i.e.,  $e_1 = 0.52e$ ,  $e_2 = 0.48e$ .

As shown in the theory of folded antennas, the circuit of two parallel vertical wires located at the distance  $b_i$  from each other can be divided into a dipole and a long line, opened on both ends. The current in the center of each dipole is equal to  $J_{id} = e_i/(4Z_{id})$ . The current in the center of each conductor of a long line is equal to  $J_{il} = e_i/(2X_{il})$ . Accordingly, the current in the center of the active radiator is the sum of the currents of the dipole and the long line, and the current in the center of the passive radiator is the difference between these values, i.e.,  $J_0 = \sum_{i=1}^2 (J_{id} + J_{il})$ ,  $J_i = J_{id} - J_{il}$ . In the case of metal wires in the first approximation  $Z_{id} = Rd + jX_{id}$ ,  $R_d = 80 \tan^2(kL_0/2)$ ,  $X_{id} = 120 \ln(2L_0/a_{ei}) \cot kL_0$ ,  $jX_{il}(L_i, b_i) = -j120 \ln(b_i/a) \cot kL_i$ , where  $a_{ei} = \sqrt{ab_i}$  is the equivalent radius of a dipole.

If each element of a log-periodic antenna is the radiator with concentrated capacitive loads, and the loads are changed along a radiator axis in accordance with linear law  $J(z) = J(0)(L - |z|)$ , i.e., a current along each radiator is the in-phase current, then (see Chapter 1)

$$R_d = 20 k^2 L_0^2, X_{id} = -120 \ln(2L_0/a_{ei})/kL_0, jX_{il} = -j120 \ln(b_i/a)/kL_i.$$

The field of each radiator depends on its structure and location in an antenna. If the radiator arm is manufactured in the form of straight metallic wire, the current along it is distributed by the sinusoidal law  $J(z) = J(0) \sin k(L - |z|)$ . In this case

the far field of the radiator is equal to  $E = \frac{AJ(0)}{\sin\theta} [\cos(kL \cos\theta) - \cos kL]$ ,

where,  $A = j \frac{60}{\sin kL} \cdot \frac{\exp(-jkR)}{R}$ ,  $k$  is the propagation constant,  $R$  is the distance to the observation point. If the concentrated capacitive loads are included along the axis of the radiator, and these loads create in it the in-phase current, distributed along this axis by the linear law, the far field of the radiator is equal to

$$E = \frac{AJ(0) \sin\theta}{\cos^2\theta} [1 - \cos(kL \cos\theta)].$$

Consider an influence of the radiator location on the far field by way of a specific example of the antenna, shown in Fig. 31. The arm length of the middle (active) radiator is equal to 0.3 м, i.e., the wave length of the its first (series) resonance is equal to 1.2 м. Let radii of all radiators are the same and are equal to 0.001 м and the magnitude  $\tau$  is 0.9. It is obvious that the maximal radiation of the antenna should be directed to the right, toward the radiator 2. Since the radiator 1 is located from the left of the active radiator 0, at a distance  $b_1$  from it, then the its field under angle  $\theta$  lags behind the active radiator field, firstly by  $kb_1$  in phase (in accordance with the time of the signal propagation from the active radiator to the passive radiator 1) and



secondly by  $kb_1/\sin \theta$  in phase (in accordance with the time of the signal propagation in the opposite direction, from the radiator 1 to the active radiator). At that the signal of the radiator 1 must come to the active radiator at the same angle  $\theta$ , i.e., it travels the distance  $b_1/\sin \theta$  and not the distance  $b_1$ . The total difference of phases is equal to

$$\psi_1 = -kb_1 (1 + \sin \theta)/\sin \theta.$$

Similarly, in the case of radiator 2, this phase difference is equal to

$$\psi_2 = -kb_2 (\sin \theta - 1)/\sin \theta.$$

In accordance with aforesaid one can calculate the total field of the antenna structure, shown in Fig. 31, with in-phase current distribution. Under angle  $\theta$  this field is equal to

$$E = \frac{AJ(0) \sin \theta}{\cos^2 \theta} \sum_{i=1}^2 e_i \left\{ \left( \frac{1}{4Z_{id}} + \frac{1}{2Z_{il}} \right) [1 - \cos (kL_0 \cos \langle \theta - \theta_0 \rangle)] + \right. \\ \left. + [1/(4Z_{id}) - 1/(2Z_{il})] \exp(j\psi_i) [1 - \cos (kL_1 \cos \theta)] \right\}.$$

The directivity magnitude is determined by the expression

$$D = |E(\pi/2)|^2 \sum_{n=1}^N [|E(\theta_n)|^2 \Delta \sin \theta_n],$$

where  $\Delta$  is the interval between neighboring values  $\theta_n$ , and  $N$  is the number of these intervals between  $\theta = 0$  and  $\theta = \pi/2$ .

The results of calculating directivity of the structure, presented in Fig. 31, depending on an electrical length  $kL_0$  of the arm of an active radiator are given in Fig. 32 (curve 1). This curve shows the directivity of the structure with in-phase currents in each element. The directivity of the structure with sinusoidal currents is given for comparison by means of a curve 2. It is known that radiators with concentrated loads distributed in accordance with linear or exponential law along each arm allow us to ensure a high level of matching with a cable in the range with an overlap ratio of the order 10. Therefore, graphics are made so that to show the structure directivity in the range from  $kL_0 = \pi$  to  $kL_0 = 10\pi$ .

Radiation of neighboring elements of log-periodic antenna with the arm length 0.27 m and 0.333 m respectively requires calculating fields in the structures presented in Fig. 29. Results of these calculations are given in Fig. 32: curve 3 corresponds to Fig. 33a, curve 4 - to Fig. 33b.

The directivity magnitudes in Fig. 32 for specific values  $kL$  correspond to the same frequencies, i.e., the same values of  $kL$  correspond to the elements of equal length in the all three schemes (for example, to the elements with the arm length 0.3 m). The figure shows that the directivity magnitudes at the same  $kL$  are close to each other. This is natural, since the directivity in each scheme increases slowly with increasing frequency. Small increasing the active radiator length causes at the same  $kL$  the small increase of the resonant wavelength, i.e., the small decrease of the resonance frequency and the directivity.

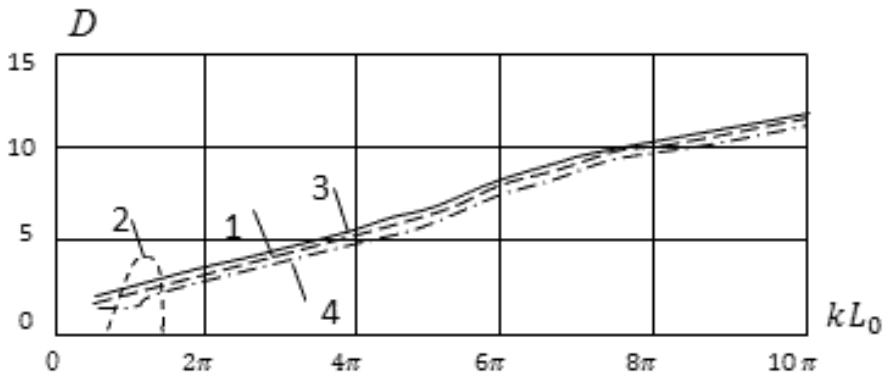


Fig. 32: Directivity of antennas consisting of three radiators.

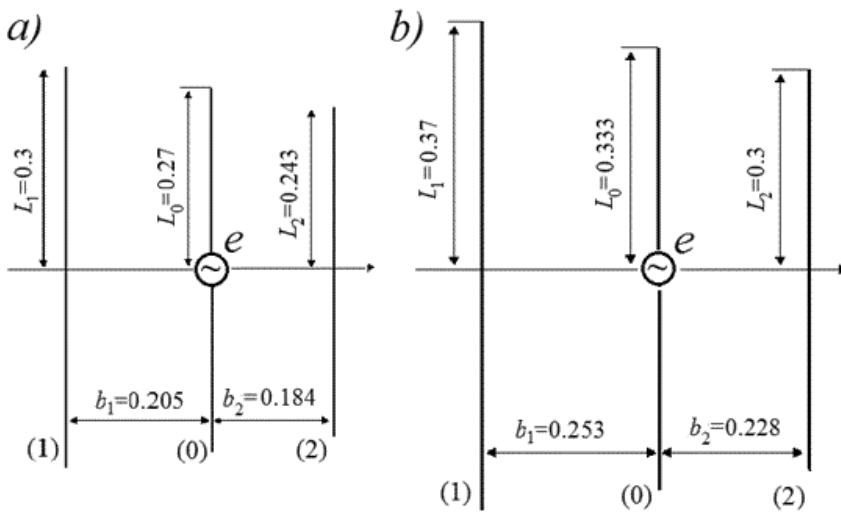
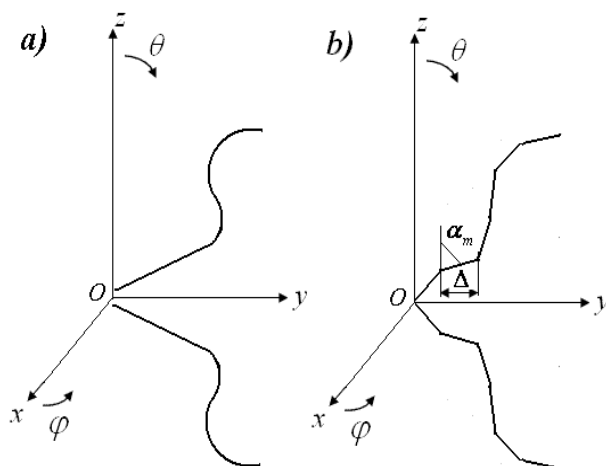


Fig. 33: Structures from reduced [(a)] and enlarged [(b)] radiators.

The obtained results show that each active radiator with in-phase current, included in the structure of the log-periodic antenna, provides high radiation directivity in a wide frequency range. Neighboring radiators have similar directivity magnitude. The direction of the radiation is the same. A signal propagates along the distribution line from short elements to the long dipoles (in Figures 31 and 33 from the right to the left), the radiated signal propagates in the opposite direction. The total path difference is quite large. For example, for the signal radiated by a half-wave neighboring radiator it is equal to  $0.38 \lambda$ , i.e., it is close to a half wavelength. Crossing wires of the distribution line in an interval between the elements permits to reduce dramatically this path difference.

We summarize the analysis of the log-periodic antenna. Known log-periodic antenna with sinusoidal current distribution in the radiators have a property of automatic currents "cut-off", i.e., a separate antenna segment (active region) radiates a signal in a narrow frequency band. Outside this band and outside the borders of



**Fig. 34:** Symmetrical radiator of an arbitrary geometry in the shape of a curve (a) and broken (b) line.

the active region the signal decays rapidly. Wide frequency range is provided by a large antenna length, which is equal to the sum of the lengths of the active regions. Reduction of the antenna length by disturbing a geometric progression led to a sharp deterioration of electrical characteristics.

The more effective methods are firstly a two-fold use of each active region by an application of linear-spiral radiators and secondly an employment of an asymmetrical log-periodic antenna with coaxial distribution line. These methods allow decreasing the antenna length by 25–30%.

Replacement of the metal radiators by the radiators with concentrated capacitive loads provides reusable active area and allows us to obtain a high directivity in a wide frequency range, using a simple structure with three radiators. Results obtained with the help of the method of electrostatic analogy may be used for solving optimization problem by methods of mathematical programming. Increasing the radiators number in the structure may allow dramatically increasing its directivity. These results open a promising direction of improving electrical characteristics and reducing dimensions of log-periodic antennas and require serious work to realize this opportunity.

## 6. Curvilinear Radiator

In the previous sections the synthesis problem of a straight radiator with concentrated loads is regarded. Together with loads the radiator shape substantially affects antennas characteristics, in particular its directivity. The title of this Section is related with this topic.

This problem unlike the previous one it is solved for the single frequency (or for the single electrical length of the radiator). A thin curvilinear radiator of an arbitrary geometry is situated in the vertical plane, e.g., in plane  $zOy$  of rectangular coordinate system (Fig. 34a). Directivity is defined in the direction of the axis  $y$ . Selecting the radiator shape is limited by the necessity to exclude super directivity, i.e., by a need

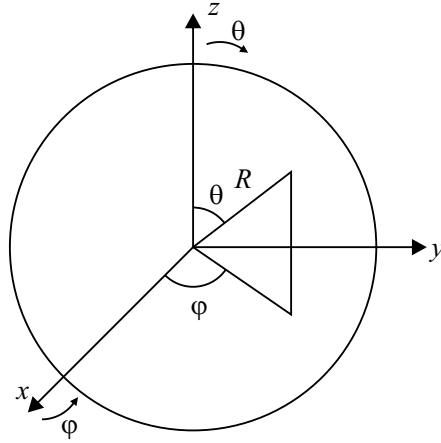


Fig. 35: An antenna in the shape of sphere.

to decrease the reactance of an antenna. The reason for such restriction is negative properties, which impede the realization of small-sized antennas with high directivity.

A rigorous analysis of the super directivity problem is given in [15]. This analysis studies an antenna in a shape of sphere (Fig. 35), in which only surface currents exist. It is assumed that the field has a circular symmetry relative the axis  $z$ , as well as it is symmetrical with respect to the equatorial plane. This simplification means a radiation concentration in the  $E$ -plane and a circular directional pattern in  $H$ -plane. Simplification of solved problem does not interfere to make the most general conclusions about the features of small antennas with high directivity.

Under these conditions the electromagnetic field in a spherical coordinates system has only three components, which are not equal to zero:  $E_R$ ,  $E_\theta$  and  $H_\varphi$ . Maxwell's equations take the form:

$$\begin{aligned} \frac{1}{R \sin \theta} \frac{\partial(H_\varphi \sin \theta)}{\partial \theta} &= j\omega \varepsilon_0 E_R, -\frac{1}{R} \frac{\partial(RH_\theta)}{\partial R} = j\omega \varepsilon_0 E_R, -\frac{1}{R} \left[ \frac{\partial(RH_\theta)}{\partial R} - \frac{\partial E_R}{\partial \theta} \right] \\ &= j\omega \mu_0 H_\varphi. \end{aligned}$$

Substituting  $E_R$  and  $E_\theta$  from the first two equations in the third equation and introducing a potential function  $U$ :

$$H_\varphi = \frac{1}{R} \frac{\partial U}{\partial \theta},$$

we obtain an equation

$$\frac{\partial^2 U}{\partial R^2} + \frac{1}{R^2 \sin \theta} \frac{\partial}{\partial \theta} \left( \sin \theta \frac{\partial U}{\partial \theta} \right) + k^2 U = 0.$$

Applying the method of separating variables (the eigenfunction method), in accordance with which

$$U = \mathfrak{R}(R) \Theta(\theta),$$

we come as a result to following two equations:

$$\frac{d^2 \mathfrak{R}}{dR^2} + \left[ k^2 + \frac{n(n+1)}{R^2} \right] R = 0, \quad \frac{1}{\sin \theta} \frac{d}{d\theta} \left( \sin \theta \frac{\partial \Theta}{\partial \theta} \right) + n(n+1) \Theta = 0.$$

They have solutions in the form of Hankel functions of the second kind of order  $n+1/2$   $\mathfrak{R}(R) = C_n \sqrt{R} H_{n+1/2}^{(2)}(kR)$  and of the Legendre polynomials  $\Theta(\theta) = P_n(\cos \theta)$ . Thus  $U = \sqrt{R} \sum_{n=0}^{\infty} C_n H_{n+1/2}^{(2)}(kR) P_n(\cos \theta)$ , i.e.,  $H_\varphi = \frac{1}{\sqrt{R}} \sum_{n=1}^{\infty} C_n H_{n+1/2}^{(2)}(kR) \frac{dP_n(\cos \theta)}{d\theta}$ .

In his turn

$$E_\theta = \frac{1}{\omega \varepsilon_0 R^{3/2}} \sum_{n=1}^{\infty} C_n \frac{\partial}{\partial R} [R H_{n+1/2}^{(2)}(kR)] \frac{dP_n(\cos \theta)}{d\theta}.$$

Indices  $n$  in these expressions must take only the odd values in order to satisfy the condition of the field symmetry with respect to the equatorial plane.

Replacing at large distances from the radiator, i.e., at large values of  $kR$ , the Hankel functions by their asymptotic magnitudes, we find the far field

$$H_\varphi = \sqrt{\frac{2}{\pi}} \frac{\exp(-jkR)}{R} \sum_{n=1}^N (-1)^{n+1/2} C_n \frac{dP_n(\cos \theta)}{d\theta}, \quad E_\theta = \sqrt{\mu_0/\varepsilon_0} H_\varphi,$$

where  $N \leq kR/2$ . If to substitute the fields into the expression for directivity

$$D = \frac{4\pi R^2 [\vec{E} \vec{H}]_{n \max}}{\oint_S [(\vec{E} \vec{H})_n] dS}, \quad (7.42)$$

and to calculate the factors, corresponding to the maximum directivity, we find

$$D_{\max} = 2 \sum_{n=1}^N [\bar{P}_n^{(1)}(0)]^2, \quad (7.43)$$

where  $\bar{P}_n^{(1)}(\cos \theta) = \sqrt{\frac{2n+1}{2n(n+1)}} P_n^{(1)}(\cos \theta)$ ,  $P_n^{(1)}(\cos \theta) = \frac{dP_n(\cos \theta)}{d\theta}$ . From (7.43)

it follows that the directivity increases with the increasing number of the series terms and does not depend on the antenna dimensions. The total current on the sphere surface ( $R = a$ ) is equal to

$$H_\varphi|_{R=0} = 2\pi a J_0 \sin \theta = 2\pi \sqrt{a} E_{\max} \sin \theta \sum_{n=1}^N \sqrt{\frac{2n+1}{2n(n+1)}} \frac{(-1)^{n/2} \bar{P}_n^{(1)}(0)}{\sum_{n=1}^N [\bar{P}_n^{(1)}(0)]^2} H_{n+1/2}^{(2)}(ka) P_n^{(1)}(\cos \theta). \quad (7.44)$$

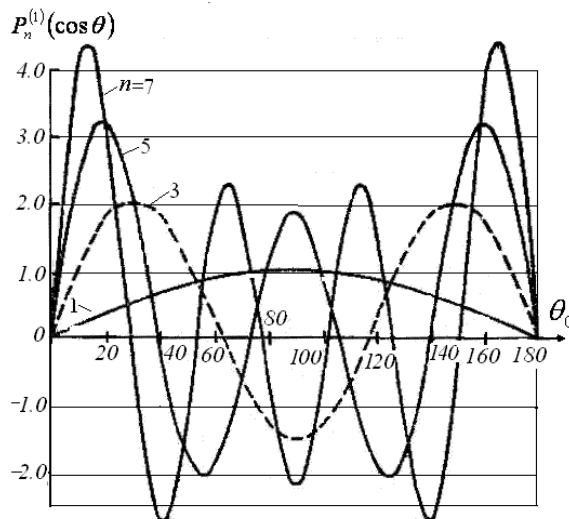

 Fig. 36: The graph of function  $P_n^{(1)}(\cos \theta)$ .

Table 4: Values of Hankel Function

$n$	$ka = 1$	$ka = 2$	$ka = 3$	$ka = 4$
1	0.2403 + j0.4311	0.3474 + j0.2797	0.2758 - j0.0502	0.0926 - j0.1836
3	0.0072 + j0.8764	0.0527 + j1.1843	0.1213 + j0.4054	0.1829 + j0.1744
5	0.0001 + j797.44	0.0021 + j14.834	0.0131 + j1.7929	0.0413 + j0.5288
7	0.0000 + j1.12·10 <sup>5</sup>	0.0001 + j416.15	0.0006 + j2.4352	0.0040 + j3.1818
9	0.0000 + j2.83·10 <sup>7</sup>	0.0000 + j35183	0.0000 + j609.72	0.0001 + j42.676

A graph of the function  $P_n^{(1)}(\cos \theta)$  for some values of  $n$  is given in Fig. 36. The values of the functions  $H_{n+1/2}^{(2)}(ka)$  for the same  $n$  are shown in Table 4. As it is seen from Fig. 36, the individual components of the series (7.43) are currents with different phases on short segments of an argument  $\theta$ , wherein the number of different segments is equal to the index  $n$ . Obviously, that the greater number of segments with currents of different phases, the less the radiated field for the same total current and the greater currents are required order to obtain the field of sufficient magnitude. That is confirmed by Table 4. The greater  $n$  when the same  $ka$ , the greater the absolute value of the current of each segment, which is moreover almost purely reactive.

Performed analysis shows that, in principle, a high directivity can be obtained in a relatively small-sized antenna. But this antenna must necessarily be variably-phase. With growing directivity, the number of alternations increases and anti-phase segments become shorter. Great reactive currents are inherent in this antenna. These currents must be distributed on individual segments with high precision. Great reactive currents associated with high  $Q$  and low stability of a system lead to low efficiency and a narrow bandwidth. Such systems require use of powerful transmitters. In consequence of these negative characteristics, creation of super directive antennas of small dimensions becomes impossible.

Analogous results are given in [27, 1].

We return to the optimization of a radiator with a flat curvilinear profile [10]. In accordance with (7.42)

$$D = \frac{4\pi |\vec{F}(\theta_0, \varphi_0)|^2}{\int_0^{2\pi} \int_0^\pi |\vec{F}(\theta, \varphi)|^2 \sin\theta d\theta d\varphi},$$

where  $\vec{F}(\theta, \varphi)$  is a vector directional pattern of the radiator,  $\theta_0$  and  $\varphi_0$  are angular coordinates defining the direction of maximum radiation. For the radiator located in the plane  $zOy$  components of the current in spherical coordinates system are

$$J_x(l) = 0, J_y(l) = J(l) \sin \alpha, J_z(l) = J(l) \cos \alpha.$$

Here  $l$  is coordinate along the radiator,  $\alpha$  is a value of an angle  $\theta$  in the radiator point with the coordinate  $l$ . Components of the radiator pattern with arm length equal to  $L$  are

$$F_y(\theta, \varphi) = \int_{-L}^L J(l) \sin \alpha \exp[jk(y \sin \theta \sin \varphi + z \cos \theta)] dl,$$

$$F_z(\theta, \varphi) = \int_{-L}^L J(l) \sin \alpha \exp[jk(y \sin \theta \sin \varphi + z \cos \theta)] dl,$$

Placing the radiator in a vertical plane permit to simplify the procedure of directivity calculation and optimization. We consider that the directivity is equal to the product

$$D = D_\varphi D_\theta,$$

where

$$D_\varphi = 1, D_\theta = \frac{2|F_\theta(\theta_0, \varphi_0)|^2}{\int_0^\pi |F_\theta(\theta, \varphi_0)|^2 \sin\theta d\theta}.$$

In order to exclude the effect of the super directivity, the directivity is divided into reactivity coefficient:

$$D_1 = \frac{D}{\Gamma} = \frac{|F_\theta(\theta_0, \varphi_0)|^2}{4\pi \int_0^L |J(l)|^2 dl},$$

Minimization of the functional allows to find the shape of the curve, provided the maximal directivity for a given arm length  $L$ . The mentioned minimization is accomplished by two ways. First way was used in [18]. The radiator arm was replaced by a broken line consisting of  $M$  straight segments with identical length  $\Delta = L/M$  (see Fig. 36b). The directional pattern of this radiator is calculated by the formula

$$E_\theta(\theta, \varphi) = \sum_{m=1}^M \left[ e^{jk\Delta \sum_{i=1}^{m-1} \cos(\alpha_i - \theta)} \cos(\alpha_m - \theta) * \int_0^\Delta J(l_m) e^{jkl_m \cos(\alpha_m - \theta)} dl_m \right].$$

Here the integral is replaced by the sum of the integrals along the segments,  $l_m$  is the coordinate along  $m$ th segment. The first exponent determines the current phase at

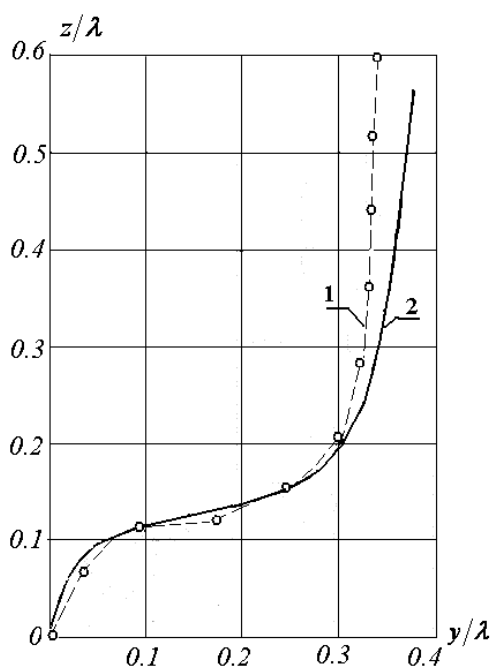


Fig. 37: Optimum configuration of the arm with length  $0.75\lambda$ , calculated by the first 1) and the second (2) versions.

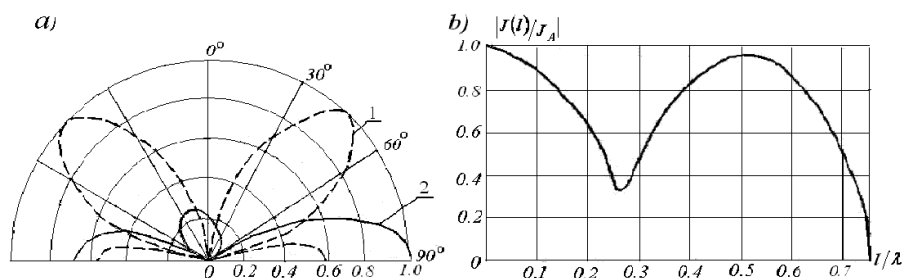


Fig. 38: The directional patterns in the vertical plane (a) and the curve of the current distribution along the radiator (b).

the segment beginning, and the second exponent—along the segment. Each integral over segment contributes its share to the radiation. It is assumed that the current distribution along the entire wire is sinusoidal, i.e., on the segment  $m$  we obtain

$$J(l_m) = J_A \frac{\sin[k\Delta(M - m + 1 - l_m/\Delta)]}{\sin kl},$$

where  $J_A$  is the current in the radiator feed point.

Calculation of integrals allows obtaining a rather cumbersome formula for  $F_\theta(\theta, \varphi)$ . Actually, that is a function of one variable— $\alpha$ . Selecting this function is performed by trial-and-error method. Optimal geometry for the arm of length  $0.75\lambda$ ,



found when  $M = 10$ , is shown in Fig. 37 (curve 1). The calculated magnitude of the directivity is equal to 6.2.

The second version of the calculation [19] did not confirm this result. Apparently, a significant error was caused by using sinusoidal distribution not along each segment, but along the entire broken line. In the second calculation the equation for the current along the antenna has been written in matrix form. A curvilinear radiator was represented as a set of short dipoles connected in series. The segments forming the short dipoles are not considered to be straight, but selected in the form of cubic splines. That permits to decrease the number of segments and to approximate more accurately the shape of the curve. The piecewise constant (pulse) functions are used as the basis functions for the current, and this choice apparently reduces the calculation accuracy as compared with using piecewise sinusoidal functions. The shape of antenna axis is determined depending on the obtained magnitude of directivity. The calculation was performed for the curvilinear antenna with arm length  $0.75\lambda$ , divided into three segments with lengths  $0.0714\lambda$ ,  $0.4286\lambda$  and  $0.25\lambda$ . Antenna radius is 2 mm. Optimum configuration of the arm is shown in Fig. 37 (curve 2). The calculated magnitude of the directivity is equal to 4.9. The directional patterns in the vertical plane and the curve of the current distribution along the radiator are shown in Fig. 38. Curve 1 corresponds to the directional pattern of the straight radiator with arm length  $0.75\lambda$ , curve 2 corresponds to that of the curvilinear radiator with the same arm length.

Let us compare this result with the directivity of the symmetrical straight vertical radiator. The directivity of the straight dipole with the arm length  $0.75\lambda$  is close to 1. Maximal directivity of this dipole is obtained when the arm length is equal to  $0.62\lambda$ . This directivity is equal to 3.2. Thus, the optimal directivity of curvilinear radiator with the arm length  $0.75\lambda$  is significantly higher than the directivity of straight dipole with the same arm length and one and half times higher than the maximum directivity of the straight dipole. This result is obtained by reducing the vertical projection of the segments with negative current (of the segments, in which current flows in the opposite direction).

Indeed, comparing the versions of straight and curvilinear dipoles, one can easily verify that the vertical projection of the curvilinear dipole with arm length  $0.75\lambda$  is significantly decreased. From this point of view, it is useful to compare the results of this Section with the results of capacitors using. It should be emphasized that the reactance of capacitors has frequency-dependent character. This allows create in-phase currents in antenna in a wide frequency band and thereby ensures the high characteristics, similar to a certain extent with characteristics in the area of series resonance of radiator. Curvilinear radiator of constant length and shape does not have such a frequency-dependent character, i.e., allows to get a positive result in one frequency only.

These critical remarks should not detract from usefulness of considered work. The idea of antenna characteristics optimization is important itself, irrespective of the antenna parameters, selected for its embodiment into practice by searching the optimal values of these parameters. In accordance with the terminology, presented in Section 2, a set of changed parameters is called by a vector. A few options were considered as the elements of such vector: magnitudes of concentrated loads, executed

in the form of simple elements (this option is described in Section 2), the shape of a thin antenna (option presented in this Section), the lengths of the straight rods in Yagi-Uda antenna (see Section 7). These variants are known, because they permit to obtain a useful result. In addition, it is necessary to remember that optimizing shape of a thin curvilinear radiator was accomplished more than 30 years ago, during the endless and futile debates about the possibility of practical using abstract theoretical distributions of the current along the wire.

At present, the shape selection can be executed at a higher level, in a frequency band instead of one frequency, with a sinusoidal current distribution along the increased number of short dipoles. It is expedient also replacing location of the antenna wire in one vertical plane by its placement in three-dimensional space. That will increase the number of freedom degrees and can provide new and unexpected results.

## 7. Director-type Antenna

In this Section a problem of optimizing end-fire antenna array (Yagi-Uda antenna) is considered. It is one of the most well-known types of directional antennas, in particular of VHF antennas. The standard version of this antenna, consisting of an active dipole, one or two reflectors and several equidistantly located directors of identical length is used for many years. Results of generalizing experimental data about these antennas and recommendations on selecting their geometric dimensions were given in [20]. Constantly experimental data are showing that there is opportunity for significant increasing directivity, for expanding operating bandwidth and for lowering level of side lobes, if to select correctly the lengths of dipoles and the distances between them. But experimental optimization of such antennas is accomplished at the cost of long time and big money, since this optimization requires the creation of a reliable mock-up with variable geometry and performance of numerous measurements of high quality.

In accordance with that Yagi antenna was among the first antennas, for which the optimization program has been specifically designed. Work on the program was brought to the final results.

The task of optimization of antenna arrays with passive dipoles as a rigorous task of mathematical programming was formulated in [21]. In [22] the task of creating end-fire array with maximal directivity was divided on two tasks: the choice of directors' lengths at the beginning and the choice of distances between directors after that. Most completely the problem was solved in [10], where independent selection of lengths and distances was used, and modern methods of mathematical programming were employed.

The antenna circuit is shown in Fig. 39a, the general view of a standard antenna with vertical polarization is given in Fig. 39b. In this case, the optimization problem has been formulated in the following way. It is required to determine the dipoles' lengths  $2L_i$  (here  $i$  is the dipole number,  $L_i$  is the length of its arm) and their coordinates  $d_i$  along the axis of the antenna, providing the maximal directivity in the direction

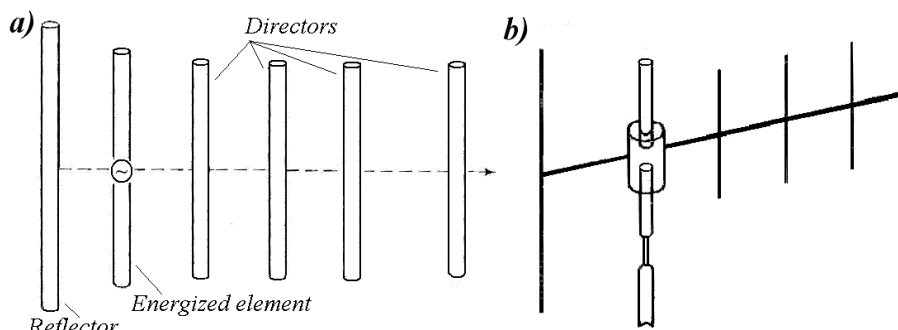


**Fig. 39:** Circuit of Yagi antenna (a) and general view of a standard antenna with vertical polarization (b).

of said axis for a given number  $N$  of the dipoles and under the concrete restrictions to the total antenna length, the dipoles' lengths, and the distances between adjacent dipoles.

Comparison of this problem with definition of the mathematical programming problem in the general case (see Section 2) shows that the objective function is presented here in the form of a partial functional, i.e., as the error' function of a single characteristic (directivity). Vector  $\vec{x}$  of parameters is presented by magnitudes  $L_i$  and  $d_i$ . The objective function is written in the form

$$F(\vec{x}) = \frac{1}{D(\vec{x})} + \alpha F_p(\vec{x} - \vec{y}),$$

where  $D(\vec{x})$  is the magnitude of directivity,  $F_p(\vec{x} - \vec{y})$  is penalty function,  $\vec{y}$  is the vector of allowable values of optimized parameters,  $\alpha$  is penalty factor.

The error function in this case was constructed using the criterion of Powell [23], which does not require the calculation of derivatives during changing direction of vector  $\vec{x}$ . New direction of this vector must be chosen on each iteration in accordance with the direction of maximal rise of the directivity. When analyzing the antenna characteristics, it is considered that the antenna consists of thin cylindrical wires, the current distribution along which obeys to the system of Hallen's equations:

$$\int_{-L_i}^{L_i} J_i(z_i) \sum_{j=1}^N G_{ij}(|z_j - z_i|) dz_i = -\frac{j}{Z_0} \left( C_i \cos kz_i + \frac{e_i}{2} \sin k|z_i| \right), \quad i = 1, 2, \dots, N. \quad (7.45)$$

Here  $J_i(z_i)$  and  $e_i$  are function of current distribution and extraneous emf on dipole  $i$  (emf of the passive dipole is zero),  $G_{ij} = \frac{\exp(-jkR_{ij})}{4\pi R_{ij}}$  is Green's function,  $R_{ij} = \sqrt{d_{ij}^2 + (z_j + z_i)^2}$  is a distance between the dipole points  $i$  and  $j$ ,  $Z_0 = 120\pi$  is a wave impedance of a free space. Comparing (7.45) and (4.5), it is easy to see that here Hallen's integral equation with approximate kernel is used.

The magnitude of current is sought in the form of an expansion in terms of spatial harmonics

$$J_i(z_i) = \sum_{m=1}^M I_{im} f_{im}(z_i),$$

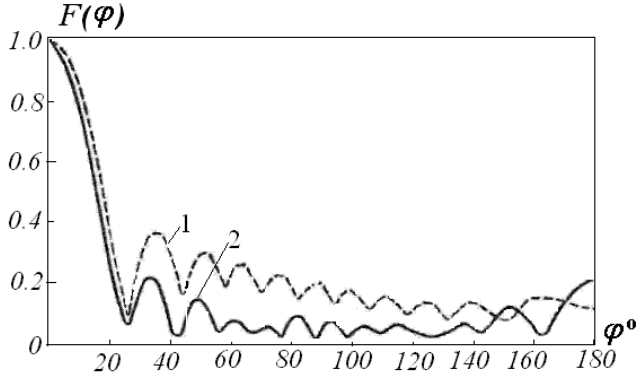


Fig. 40: Initial (1) and optimum (2) antenna patterns with fifteen dipoles.

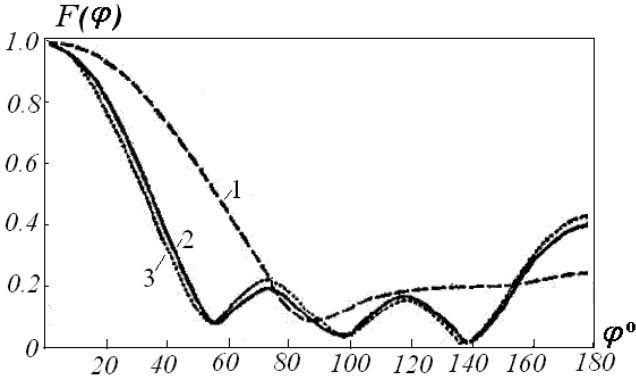


Fig. 41: Initial (1) and optimum directional pattern of the antenna with four dipoles for three (2) and four (3) harmonics.

where  $I_{im}$  is the complex amplitude of the harmonic  $m$  of the dipole  $i$ ,  $M$  is number of harmonics. Power functions  $f_{im}(z_i) = (1 - |z_i|/L_i)^m$  of Popovich [23] and trigonometric harmonics of King [25]

$$f_{im}(z_i) = \begin{cases} \sin k(L_{il} - |z_i|), & i = 1, \\ \cos \frac{kz_i}{m-1} - \cos \frac{kL_i}{m-1}, & m \geq 2 \end{cases}$$

are used as spatial harmonics (if the dipole is excited, also the first harmonic it is taken into consideration). The problem is reduced to the solution of written in matrix form system of linear algebraic equations for currents along the antenna segments. Knowing the currents of the dipoles, one may find the field in the far region and directivity in the direction of an antenna axis.

In [21] and [10] the results, obtained for antennas with three, four and fifteen dipoles are presented. Canonical array, described in [20], is taken as the first approximation of the array with fifteen dipoles. Selecting geometrical dimensions of this array in accordance with the described above procedure permitted to double

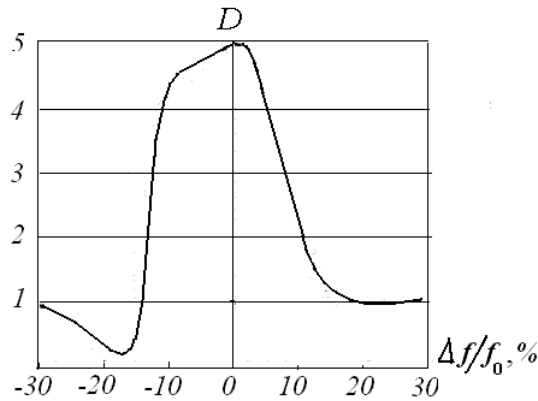


Fig. 42: Frequency characteristic of antenna with three dipoles.

Table 5: Characteristics of the End-Fire Arrays.

<i>N</i>	<i>D<sub>max</sub></i>	<i>SLL</i>	<i>Z<sub>A1</sub></i>	<i>Z<sub>A</sub></i>	<i>Z<sub>A2</sub></i>	$\Delta f/f_0, \%$	<i>Length</i>
4	14.48	0.43	16.2 + j27.5	6.0 + j91.2	9.4 + j145.2	-5.3...+2.8	0.76 λ
5	18.77	0.36	34.9 - j74.5	4.1 - j25.5	4.4 - j3.2	-6.3...+1.8	1.27 λ
6	21.69	0.31	26/2 - j78.6	3.0 - j36.1	2.1 - j19.4	-7.3...+1.3	1.6 λ
7	24.43	0.31	13.6 - j16.6	3.6 + j33.3	3.8 + j65.0	-5.5...+2.0	1.6 λ
8	24.04	0.35	28.7 - j53.9	2.6 - j3.5	2.3 + j18.2	-7.0...+1.5	1.6 λ
6	24.39	0.32	29.7 - j9.7	6.9 + j41.2	6.8 + j73.4	-5.5...+1.5	1.66 λ
7	25.31	0.27	6.9 - j211.7	0.8 - j180.6	1.9 - j172.5	-7.5...+1.0	1.8 λ
8	25.19	0.28	4.9 - j214.2	0.7 - j182.6	0.1 - j173.7	-7.5...+1.5	1.8 λ

its maximum directivity. Initial (1) and optimum (2) directional patterns of array are shown in Fig. 40.

The initial dimensions of the antenna with four dipoles were taken in accordance with the dimensions of a standard receiving television antenna. Optimization of the antenna dimensions led to directivity increase by 95%. Its directional patterns in the H-plane are shown in Fig. 41. Here 1 is initial directional pattern, 2 and 3 are optimum directional patterns for three and four current harmonics respectively. As is seen from Fig. 41, the inclusion of the fourth harmonic improves the calculated directional pattern. However, a further increase the number of harmonics does not affect the result.

In the calculations of the antenna with three dipoles (Fig. 42) two problems were included into objective function: increasing the directivity and the expansion of the operating bandwidth. Optimization allowed to increase the directivity in one and half times and to expand the bandwidth by 23%. Comparison of optimization results for the antenna with six dipoles with the results, obtained in [20], showed the advantage of the method described in [21]. Antenna directivity was increased by 4% and the length of the antenna was decreased by 0.04 λ.

**Table 6:** Amplitudes and Phases of Dipoles Currents.

N	Number of dipoles							
	7				8			
	Array length							
	1.6 $\lambda$		1.8 $\lambda$		1.6 $\lambda$		1.8 $\lambda$	
	$J_A$	$\varphi_A$	$J_A$	$\varphi_A$	$J_A$	$\varphi_A$	$J_A$	$\varphi_A$
1	0.339	-41.7	38.25	-34.4	2.520	92.4	35.63	-34.6
2	0.534	124.0	53.18	126.4	1.926	-106.3	48.54	126.5
3	0.748	-69.1	65.79	-63.9	1.866	-101.7	62.41	-64.4
4	1.011	98.1	95.50	105.9	3.923	62.6	83.39	105.0
5	0.312	118.7	210.2	-85.6	1.502	99.8	33.58	-93.4
6	1.792	-83.7	332.2	89.7	12.55	-127.6	176.8	-84.8
7	1.128	92.2	31.02	-101.8	13.76	22.6	328.6	89.8
8	-	-	-	-	4.610	-132.6	25.5	-104.8

During the ongoing research of the end-fire arrays other characteristics of arrays were calculated together with directivity, in particular an input impedance of an excited dipole, a level of side lobes, the distribution of amplitudes and phases of the currents along the array. These characteristics can be measured on a real mock up, i.e., calculation can be compared with experimental result. The frequency dependence of these magnitudes are genuine characteristics of antenna array, while, for example, the quality factor can be estimated only indirectly.

Results of the synthesis of end-fire arrays are presented in Table 5. Here  $N$  is the number of the dipoles,  $D_{max}$  is the maximum directivity,  $SLL$  is the level of side lobes,  $Z_{A1}$ ,  $Z_A$  and  $Z_{A2}$  are the input impedances at the lower, main, and upper frequency of the range accordingly,  $\Delta f/f_0$  is the ratio of the bandwidth to the main frequency. The bandwidth is defined as width of the band with half-directivity. Maximum lengths of the first five arrays are bounded by the magnitude  $1.6\lambda$ , and lengths of the other arrays—by the magnitude  $1.8\lambda$ .

Calculations show that with increasing frequency the directivity changes faster than with decreasing, and the real part of input impedance the opposite. When a number of dipoles is fixed, increasing antenna length causes the directivity increase, until the length does not exceed a certain critical value (see the examples of arrays). When a length of an antenna is fixed, increasing the number of passive dipoles leads to an increase of the directivity, but not always. The frequency bandwidth of antennas is 7–9%, which is sufficient for most applications. Low input impedance makes difficult the matching of antennas with a standard cable. It is the main their drawback.

In Table 6 the amplitudes (in amperes) and phases (in degrees) of currents in the dipoles' middles are presented. One can see that these amplitudes and phases of currents change along the array. Directivity of antenna array exceeds the restrictions, found Hansen-Woodward, i.e., these arrays should be considered as super directive arrays. The shape of directional patterns near the maximum is similar to a shape, which is given by expression  $F(\varphi) = \sin^8(\varphi/2)$ .

The results presented in this Section and in the first part of a chapter, show high potential opportunities of the mathematical programming method for improvement of the antennas characteristics.

## 8. Microstrip Antennas with In-phase Current Distribution

In Chapter 6 it was said about the importance of expanding a frequency range and improving the characteristics of microstrip antennas. The solution of these problems primarily depends on the nature of a current distribution along a particular antenna.

As was shown in Section 3.2, to calculate an effective length and a radiation's resistance of a vertical linear antenna, one must define the component  $E_\theta$  ( $\pi/2$ ) of electrical field created by this radiator in the horizontal direction. As is known, the effective length of a metal dipole with an arm length  $L$  is equal to  $l_e = \frac{2}{k} \tan \frac{kL}{2}$ , and the radiation resistance is  $R_\Sigma = 20k^2 l_e^2 = 80 \tan^2 \frac{kL}{2}$ . If  $L = \lambda/4$ , then  $l_e = 2/k$ ,  $R_\Sigma = 80$ . When  $L > \lambda/4$ , the value  $R_\Sigma$  grows with increasing  $L$ , but the corresponding expression becomes very approximate. Simultaneously with the growth of  $R_\Sigma$  the reactive component of an input impedance increases, and the input current of the antenna decreases. At  $L > \lambda/2$   $R_\Sigma$  begins to decrease, since segments with anti-phase currents appear along the antenna length. If  $L > \frac{\lambda}{4}$  the directivity  $D$  starts to grow. But an increase of  $D$  can lead to a decrease in the communication range, if the signal in a horizontal direction decreases. To quantify such a result, it was introduced the new characteristic—pattern factor PF (see Section 2). When the arm length is  $\lambda/4$ , its magnitude is equal to  $PF_1 = \int_{\pi/3}^{\pi/2} \sin \theta d\theta = 0.5$ . With growth  $L$  this factor begins to decrease, sharply limiting the range of operation frequencies.

In a linear antenna with an inductive surface impedance, the current distribution remains sinusoidal, but the wave slows down and the propagation constant  $k_1$  increases. Calculations show that for the same geometric length, the radiation's resistance of an antenna with a constant inductive impedance is somewhat greater than the radiation's resistance of a metal antenna, and for the same electrical length, it is much less.

In-phase current distributions created by capacitive loads connected at regular intervals along the entire length of the antenna are of particular interest. In the case of a linear distribution, the current amplitude decreases uniformly from the generator to the free ends of the radiator:

$$J_1(z) = J(0)(1 - |z|/L),$$

and  $R_\Sigma = 20k^2 L^2$ . In this case  $R_\Sigma$  grows continuously with increasing  $L$ . At that the values  $D$  and  $PF$  do not change, i.e., with an increase in the radiator length the field and the radiation's resistance grow within the frequency band, in which the in-phase distribution is preserved. In the case of an exponential in-phase current distribution along the radiator the distribution function is equal to  $f(z) = (e^{-\alpha z} - e^{-\alpha L})/(1 - e^{-\alpha L})$ , and the resistance of radiation is  $R_\Sigma = 80 k^2/\alpha^2$ .

The reactive component of an input impedance of a microstrip antenna is proportional to a total wave impedance, which depends on the permittivity of a substrate and was determined in Section 6.7.

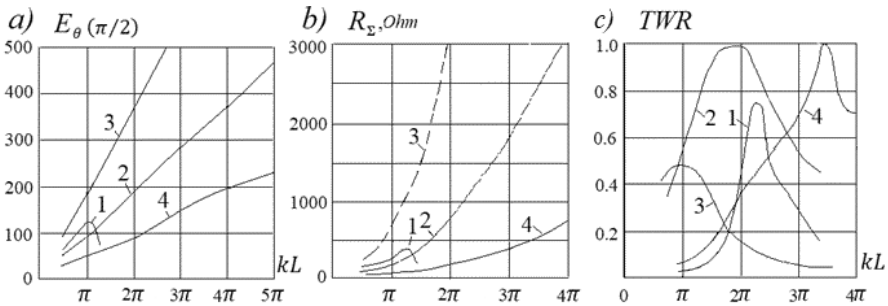


Fig. 43: Field (a), radiation resistance (b) and  $TWR$  (c) of micro-strip antenna with different current distribution.

As is shown in Section 1, the wave impedance changes depending from the distribution. In the case of a linear in-phase distribution the reactive component of an input impedance decreases when an antenna length decreases, and that significantly changes a matching level with a signal source.

Figure 43 demonstrates result of characteristics' calculation for asymmetrical linear metal radiators (monopoles) with the same dimensions depending on the current distributions. The characteristics presented for four variants of the currents distribution: sinusoidal (1), in-phase with a linear amplitude distribution (2), in-phase with an exponential distribution and the decrement  $\alpha = 1/L$  (3) and in-phase with an exponential distribution and the decrement  $\alpha = 4/L$  (4). The radiators with an arm length 1 m and a radius 0.01 m are excited by the cable with a wave impedance 60 Ohm. The resistances of radiators are given in Fig. 43b, travelling wave ratio ( $TWR$ ), from which an operation frequency band depends—in Fig. 43c.

These results were obtained in [26]. They show that antennas with in-phase current distribution in the transmit mode provide the high electrical characteristics in the wide frequency range, including the range, which used for operation with sinusoidal distribution. They confirm advantages of applying the in-phase current distribution. Other options of loads allow to operate in different ranges, using short waves, which length is much less than the length of an antenna arm, i.e., at frequencies where a sinusoidal distribution is not applicable.

The signal level of the vertical radiator at angles close to the earth's surface with increasing frequency grows with the general growth of the field. This circumstance is very important for ensuring reliable radio communications over long distances. These properties are equally valid for both electric and magnetic radiators. Antennas with switchable loads make it possible to operate in all need ranges.

Obtained results allow us to analyze the performances of microstrip antennas and to suggest methods for improving their characteristics. Their main disadvantage is low efficiency and narrow frequency range. The small thickness of the substrate leads to losses in a substrate and reduces efficiency.

Despite the individual structural elements that distinguish microstrip antennas from other radiators, and the features of electrical characteristics caused by these elements, a sober look at the operation of these antennas shows that in principle they little differ from ordinary radiators. And therefore, to improve their performance, one



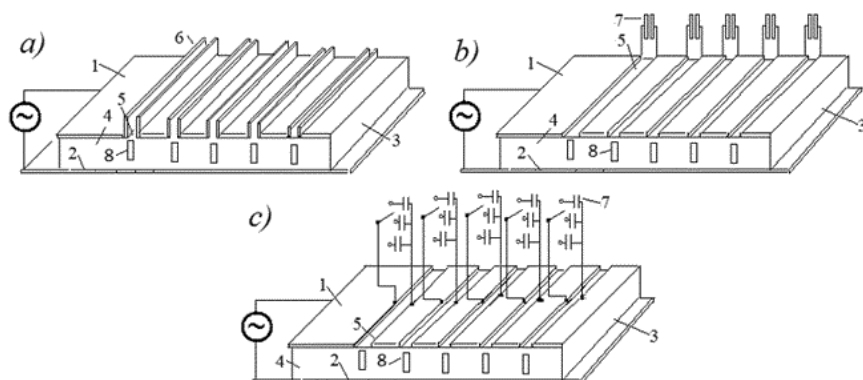


**Fig. 44:** Designs of micro-strip antenna: first option (a), second option (b), third option (c). 1 – metal strip, 2 – ground plane, 3 – substrate, 4 – side of substrate.

must use the usual methods. The current in a microstrip antenna is distributed along a sinusoid, as in a conventional linear radiator.

A linear antenna with a sinusoidal current distribution is equivalent to a resonant circuit operating in a narrow frequency range. To expand the frequency range of such a structure, it is necessary in particular to lower its  $Q$  factor, i.e., increase the resistance of radiation and losses. In the case of a microstrip antenna, this method can be implemented by using a two-story structure, in which the upper antenna (second floor) connects to the main (first floor), provides additional radiation and partially extends the operating range (see, for example, [27]). But a significant expansion of the operating range is possible only by creating in a linear radiator an in-phase current distribution with the help of capacitive loads.

Capacitive loads, located along the axis of a linear electrical radiator, make it possible to provide over the entire its length a current close to the in-phase in a wide frequency range. Amplitude of in-phase current decrease toward antenna ends in a linear or exponential law. As a result, constant loads allow several times to expand a frequency range with a required matching level. Changing of loads by means of their switching greatly improve this result. In accordance with the duality principle the inductive loads connected along the slot provide similar result in a magnetic radiator.

This method can be applied in a microstrip antenna. Figure 44 shows three options of such an antenna with capacitive and inductive loads located along its axis. The capacitive loads are installed on a metal plate 1 and are made in the form of transverse slots 5 with metal selvages 6 (see Fig. 44a) or with capacitors 7 (Fig. 44b). The inductive loads are made in the form of metal tapes 8 and are placed on the substrates' sides 4. The third option (Fig. 44c) makes it possible to switch capacitive loads and change operating ranges.

The use of capacitive loads in an electric radiator of the microstrip antenna makes it possible to expand the operating range and significantly improve the characteristics of the antenna. Calculating the wave impedance of a metal radiator, identical to the slot in shape and size, shows that magnetic radiator of the microstrip antenna at the currently used sizes has little effect on the magnitude of the radiated signal. To improve the field of the magnetic radiator, it is necessary to increase the thickness of the microstrip antenna.

# References

- [1] Hallen, E. (1938). Theoretical investigations into the transmitting and receiving qualities of antennae. *Nova Acta Regiae Soc. Sci. Upsaliensis*, IV(2): 1–44.
- [2] Levin, B.M. (2013). *The Theory of Thin Antennas and Its Use in Antenna Engineering*. Bentham Science Publishers.
- [3] Wu, T.T. and King, R.W.P. (1958). The cylindrical antenna with non-reflecting resistive loading. *IEEE Transactions on Antennas and Propagation*, AP-6(2): 197–201.
- [4] Levin, B.M. (1998). Monopole and dipole antennas for marine-vehicle radio communication. *St.-Petersburg: Abris* (in Russian).
- [5] Levin, B.M. and Yakovlev, A.D. (1985). Antenna with loads as impedance radiator with impedance changing along its length. *Radiotechnics and Electronics Engineering*, 30(1): 25–33 (in Russian).
- [6] Levin, B.M. (1990). Use of loads for creating a given current distribution along a dipole. *Radiotechnics and Electronics Engineering*, 35(8): 1581–1589 (in Russian).
- [7] Himmelblau, D. (1972). *Applied Nonlinear Programming*. New York: McGraw-Hill.
- [8] Neyman, L.R. and Kalantarov, P.L. (1959). *Theoretical Background of Electro Engineering*, Part 3. Moscow – Leningrad (in Russian).
- [9] Iossel, Yu. Ya., Kochanov, E.S. and Strunsky, M.G. (1981). *Calculation of Electrical Capacitance*. Leningrad: Energoisdat (in Russian).
- [10] Chaplin, A.F., Buchazky, M.D. and Mihailov, M. Yu. (1983). Optimization of director-type antennas. *Radiotechnics*, 7: 79–82 (in Russian).
- [11] Levin, B.M. (2017). Director antennas with in-phase currents. *Proc. of Conf. ICATT'17, Kyiv*, 110–113.
- [12] Carrel, R.L. (1961). The design of log-periodic dipole antennas. *IRE Intern. Convention Record*, part 1: 61–75.
- [13] De Vito, G. and Strassa, G.B. (1973). Comments on the design of log-periodic dipole antennas. *IEEE Transactions on Antennas and Propagation*, AP-21(3): 303–309.
- [14] Yakovlev, A.F. and Pyatnenkov, A.E. (2007). Wide-band directional antennas arrays from dipoles. *S.-Petersburg* (in Russian).
- [15] Fradin, A.Z. (1977). *Antenna-Feeder Devices*. Moscow: Communication (in Russian).
- [16] Yaru, N. (1951). A note of super-gain antenna arrays. *Proceedings IRE*, 9: 1081–1085.
- [17] Bloch, A., Medhurst, R.G. and Pool, S.D. (1953). A new approach to the design of super-directive aerial arrays. *Proceedings IEE – Part I*, 67: 303–314.
- [18] Galichin, O.I. (1980). Optimum geometry of radiator. *Proc. of Chelyabinsk Polytechnic Institute*, 255: 110–114 (in Russian).
- [19] Galichin, O.I. and Seregin, V.P. (1982). Synthesis of antenna shape for a given directivity pattern. *Proc. of Chelyabinsk Polytechnic Institute*, 273: 75–78 (in Russian).
- [20] Ehrenspeck, H.W. and Poehler, H. (1959). A new method for obtaining maximum gain from Yagi antennas. *IRE Transactions on Antennas and Propagation*, AP-7(4): 379–386.
- [21] Chaplin, A.F. (1969). Synthesis of arrays of passive radiators, *Izvestiya Vuzov - Radioelectronics*, 6: 559–562 (in Russian).
- [22] Chen, C.A. and Cheng, D.K. (1975). Optimum element lengths for Yagi-Uda arrays. *IEEE Transactions on Antennas and Propagation*, AP-23(1): 8–15.
- [23] Powell, M.J.D. (1964). An efficient method for finding the minimum of a function of several variables without calculating derivatives. *Computer Journal*, 7: 155–162.
- [24] Popovic, B.D. (1970). Polynomial approximation of current along thin symmetrical cylindrical dipoles. *Proceedings of IEE*, 5: 873–878.
- [25] King, R.W.P., Mack, R.B. and Sandler, S.S. (1968). *Arrays of Cylindrical Dipoles*. New York: Cambridge University Press.
- [26] Levin, B.M. (2022). About microstrip antennas. *Applied Science and Innovative Research*, 6(3): 1–20.
- [27] Croq, F. and Pozar, D.M. (1991). Millimeter-wave design of wide-band aperture coupled stacked microstrip antennas. *IEEE Transactions on Antennas and Propagation*, AP-39(12): 1770–1776.

# Some Types of Antennas and Cables

## 1. Loop and Folded Antenna with Capacitors

As shown in Chapter 7, the use in a linear antenna of concentrated capacitive loads, evenly spaced along the antenna wire, allows to create in the antenna an in-phase current distribution, the amplitude of which decreases linearly or exponentially towards the free ends of the antenna. In-phase distribution can significantly improve the electrical characteristics of linear and V-radiators. In this regard, it is advisable to consider the possibility of using the in-phase current distribution in other radiators, for example, in loop ones.

Chapter 4 discusses two options of loop radiators - circular and rectangular. In both cases, the wires of loops are connected to each other at the opposite end from the generator, and the current of each wire at this point is maximum. The currents at the ends of the linear antenna tend to zero. Therefore, the wire of the loop at the opposite end must be cut. The symmetrical structure of the resulting radiator allows

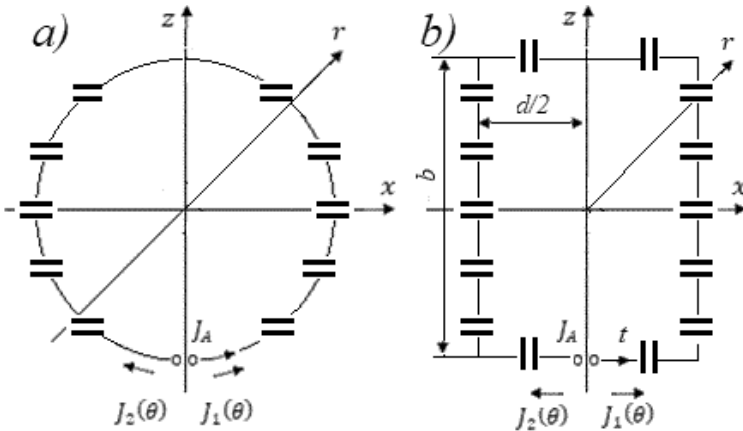


Fig. 1: Circular (a) and rectangular (b) loop antenna with capacitors.

us to ensure the preservation of the most important property of the loop antenna—the existence of a direction of zero reception.

Structures of an obtained rectangular and circular loop antennas with capacitive loads are shown in Fig. 1. In the case of linear in-phase distribution, the current in the antenna wire is distributed according to the linear law (7.8). This means that the expression  $J(t) = \frac{J_A}{\cos kL} (1 - |t|/L)$  is valid for the current in the circular loop. Then the field of the right wire of the radiator in the direction of the axis  $x$  is equal to

$$E_\theta = j30kR \frac{J_A}{\cos kL} \frac{e^{jk(R-r)}}{r} \int_0^\pi (1 + \theta/\pi) \cos \theta d\theta = j60kR \frac{J_A}{\pi \cos kL} \frac{e^{jk(R-r)}}{r}.$$

The field of the left wire in the indicated direction is small compared to the field of the right wire (see Chapter 4). Therefore, in the first approximation, the field of the left wire can be neglected. The effective length of an asymmetric radiator excited at the base by a generator with a current  $J_A$  is equal to

$$h_e = \int_0^\pi (1 + \theta/\pi) \cos \theta d\theta = \frac{1}{k \cos kL} \int_0^\pi \left[ \cos \theta + \frac{1}{\pi} (\theta \cos \theta) \right] d\theta =$$

$$\frac{1}{k \cos kL} \left( \sin \theta + \frac{1}{\pi} \cos \theta \right) \Big|_0^\pi = -\frac{2}{\pi k \cos kL}.$$

The radiation resistance of such a radiator is equal to

$$R_\Sigma = 40k^2 h_e^2 = 16.2/\cos^2 kL.$$

In the case of a rectangular loop antenna, the dependence of the current on the coordinate along the wire remains valid, but the coordinate  $t$  is measured along the rectangular perimeter. The radiation of horizontal wires in the first approximation can be neglected, since the fields of the segments located on different sides of the vertical axis of symmetry are mutually compensated. The fields of the vertical segments in the horizontal direction are

$$E_\theta = j30k \frac{J_A}{\cos kL} \frac{e^{jk(d/2-r)}}{r} \int_{d/2}^{L-d/2} (1 + t/L) dt.$$

Here,  $L = d + b$ . The effective length of the right wire, excited in the foundation by the generator with current  $J_A$ , is equal to

$$h_e = \frac{1}{k \cos kL} \left[ L - d + \frac{(L - d/2)^2 - d^2/4}{2L} \right] = \frac{1}{k \cos kL} (L - 3d/2).$$

Considering the left wire, the effective length of the asymmetric rectangular radiator is

$$h_e = \frac{e^{-kd}}{k \cos kL} (L - 3d/2).$$

The wire antenna without capacitors, similar to loop and folded radiators, was suggested for solving specific technical problems and described in [1]. The authors called this antenna by 'self-grounded Bow-Tie antenna'. The name chosen by the authors can hardly be considered successful, but the numerous experimental results presented in the article deserve unconditional interest.

This antenna can be considered as one of the variants of the folded antenna described in Section 1.5 of the present book. In Fig. 2a it is shown the circuit of an antenna, equivalent to the original structure.

The antenna has two parallel vertical plates connected at the ends and may be performed in two versions (Fig. 2b): in the first version the right (unexcited) wire is divided by the gap, in the second version the gap is absent. In accordance with the known calculation's method each folded antenna consists from two devices: a symmetrical linear radiator and a two-wire long line (Fig. 2c).

In [2] the characteristics of the antenna, described in the article [1], were re-analyzed and the results compared with those of the authors. To simplify the calculations and improve their accuracy, the model of the studied antenna and its location were partially changed. Taking into account the large distance between the antenna and the ground surface and the resulting low effect of the ground on the characteristics, the linear radiator was, as usual, located vertically. The metal plates are replaced with wires, and the slightly curved wires were made straight. The dimensions of the elements (in millimeters) correspond to the dimensions of the variant with  $\alpha = 60^\circ$ . At the same time, the materials of the article [1] are used with the greatest possible accuracy. In addition, in [2] the results of using in such an antenna an in-phase current distribution, created with the help of capacitive loads, were considered, and the characteristics of an antenna with such current distribution along the wires were compared with the characteristics of an antenna with a sinusoidal current distribution.

As can be seen from Fig. 2a, in this case the radiator is made of two branches of metal wires (three wires in each branch), located at a distance  $\rho \approx 30$  mm from each other. Each branch at the same time is a conductor of the two-wire long line. If the wire radius is equal to  $a = 2$  mm, then the equivalent radiator radius in the first approximation is  $a_e = \sqrt[6]{6a\rho^5} \approx 30$  mm, the wave impedance of a radiator is  $W_R = 120 \ln \frac{2L}{a_e e} = 120 \cdot 0,45 = 54$  Ohm (here  $L = 62 + 12,5$  mm is the length of the radiator arm,  $e = 2,718$  is the base of natural logarithms). The reactive component of the input impedance is

$$jX_R = -j54 \cot kL,$$

where  $k$  is the wave propagation constant along the radiator. The conductors (branches) of the long line are located at a distance  $D = 25$  mm from each other, each conductor consists of three wires with a radius  $a = 2$  mm. The capacitance  $C$  between the conductors is equal to the sum of nine capacitances between the individual wires:  $C = 9 (\pi \epsilon_0) \ln (D/a)$ , where  $\epsilon_0 = \frac{1}{36\pi} \cdot 10^{-9}$  is the absolute dielectric constant of air. The wave impedance of a long line is  $W_l = \frac{1}{cC}$ , where  $c = 3 \cdot 10^8$  m/s is the speed of light speed, that is,  $W_l = 33,7$  Ohm,  $jX_l = jW_l \tan kL$ .

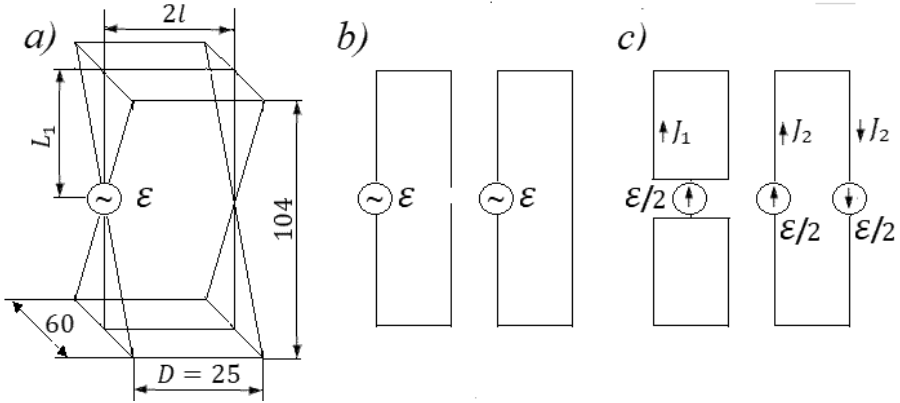


Fig. 2: The studied folded antenna: a – the structure, b – two versions, c - the equivalent circuit.

Let us determine the electrical characteristics of the radiator and the long line, whose are shown in Fig. 2c. As can be seen from Fig. 2a, each arm of a metal radiator with a length  $L$  consists of two segments: the vertical segment with length  $L_1$  and the horizontal segment with length  $l$ . Assuming that the strength of the electric field  $E_\theta$  of the horizontal segment is small and is largely compensated by the field of the opposite segment, we calculate the field of the vertical segment, proceeding from its analogy with the Hertz dipole field, i.e., in accordance with the well-known expression

$$E_\theta = AJ(0) \frac{\sin \theta}{\sin kL} \int_{-L_1}^{L_1} \sin k(L - |z|) \exp(jkz \cos \theta) dz. \quad (8.1)$$

Here  $A = j30k \frac{\exp(-jkR)}{R}$ , where  $R$  is the distance from the integration point to the observation point,  $J(0)$  is the generator current. The current distribution along the radiator is considered to be sinusoidal. If to replace the variables  $z_1 = -z$  in the integral over the lower antenna arm, it is easy to arrive at the expression

$$E_\theta = 2AJ(0) \frac{\sin \theta}{\sin kL} \int_0^{L_1} \sin k(L - z) \cos(kz \cos \theta) dz.$$

Replacing the trigonometric functions by exponential ones, we obtain

$$E_\theta = AJ(0) \frac{\sin \theta}{2j \sin kL} [e^{jk(L-z)} - e^{-jk(L-z)}] \cdot [e^{jkz \cos \theta} + e^{-jkz \cos \theta}] dz.$$

whence, after integration and reduction of similar terms

$$E_\theta = \frac{2AJ(0)}{\sin kL} [\cos kl \cos (kL_1 \cos \theta) - \cos kL - \cos \theta \sin kl \sin (kL_1 \cos \theta)]$$

For  $\theta = \pi/2$

$$E_\theta = \frac{2AJ(0)}{k \sin kL} (\cos kl \cos kL_1 - \cos kL).$$

whence, taking into account that  $L = l + L_1$ , we obtain for the effective length of the radiator

$$l_{e1} = \frac{2}{k} \left( \frac{\cos kl \cos kL_1}{\sin kL} - \cot kL \right).$$

Knowing the magnitude of  $l_{e1}$ , it is easy to determine the radiation's resistance of a linear radiator in accordance with the method described in Section 3.3:

$$R_{\Sigma 1} = 20k^2 l_{e1}^2.$$

The obtained results make it possible to determine the current  $J_1$  at the input of the excited conductor. As follows from Fig. 2c, the emf  $e$  of the generator, exciting the radiator, is half the input emf, and the radiator current is divided in half between the antenna branches, located at a distance  $2l$  from each other. It means that

$$J_1 = \frac{e}{4}(R_{\Sigma 1} + jX_R).$$

It should be remembered that the excited conductor of the radiator simultaneously serves as one of the long line's conductors. Since the line conductors at the upper end of the antenna are interconnected, the currents along these wires are distributed according to the cosine law. They are the same in the magnitude and opposite in sign. Therefore, we will neglect the influence of their radiation's resistance on the input impedance of the antenna. As for the reactive component  $jX_p$  then, as can be seen from

Figure 2b, it is equal to the sum of the input reactive components of two short-circuited at the end long lines with length  $L$  (each long line consists from the wire and the surface of the zero potential), i.e.,  $X_l = W_l \tan kL$ . This means that the current  $J_2$ , created in the line wire by the generator  $e/2$ , is equal to

$$J_2 = \frac{e}{2} / Z_l = e / (2jW_l \tan kL).$$

The antenna input impedance is calculated by dividing the exciting emf to the sum of the currents  $J_1$  and  $J_2$ :

$$Z_A = e / (J_1 + J_2).$$

The described calculation method allows us to determine the main electrical characteristics of the antenna: the radiation's resistance  $R_{\Sigma 1}$  of the linear radiator; the reactive component  $jX_R$  of its input impedance; the reactive impedance of the long line. With their help one can to determine the currents magnitudes  $J_1$  at the input of the excited conductor and the currents' magnitudes  $J_2$ , created in the wires of a long line, as well as the antenna input impedance.

The active and reactive components of the antenna input impedance are shown in Fig. 3a. As can be seen from the figure, the reactive component sharply increases near  $L/\lambda = 0.2$  and changes sign twice. Operation in this part of the range is unlikely. Calculations show that an increase in the distance between the excited and unexcited antenna conductors does not allow us to weaken this disadvantage.

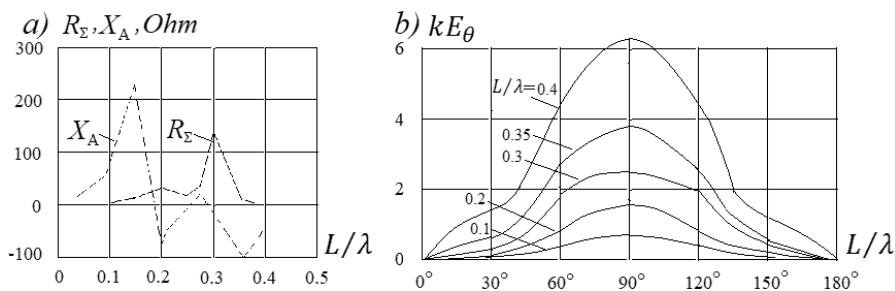


**Fig. 3:** Electrical characteristic of folded antenna with sinusoidal currents: a) input impedance, b) vertical directional pattern.

Using the above expressions, it is possible to calculate the directional patterns of the radiator in the vertical plane. In Fig. 3b the directional patterns of the excited radiator are plotted in a rectangular coordinates system for different values  $L/\lambda$ . The directional pattern of a passive radiator has the similar shape. To calculate the total field in the given direction, it is necessary to add the fields of both radiators in allowance the distances between them, which leads to an increase in the field of the passive radiator in its direction and to weakening of its field in the opposite direction, in view of the phase difference between radiators fields. This circumstance complicates the adjustment. In general, from the obtained results, it follows that using the antenna under consideration, it is possible to provide the high electrical characteristics, but only on limited sections of the range.

As already said, the electrical performance of an antenna can be improved by creating an in-phase current distribution with help of capacitive loads. This distribution can be obtained by including concentrated capacitive loads along the antenna. In this case, the capacitances of the loads, uniformly located along the wire, should decrease towards the free ends of the radiator according to a linear or exponential law.

Such loads can be used in the considered antenna. But their application in this antenna is associated with fundamental limitations. In a usual folded antenna, the current distribution law depends on the surface impedance and does not depend on the boundary conditions (on the point of emf inclusion and the loads at the antenna ends). In the given case the vertical wires are simultaneously the wires of both radiator and line, i.e., the concentrated elements determine the same current distribution law in both circuits. In a linear radiator with the indicated loads, the current decreases in the direction from the generator to the free ends of the wires. In a short-circuited long line, the current at the end of the line has maximum. It is impossible to combine two different distributions in one wire using the same concentrated loads. The only possible option is to replace the short-circuited line with an open-ended line. In this case, the scheme of dividing the antenna into a radiator and a long line, shown in Fig. 2 must change. The circuit of the changed antenna is shown in Fig. 4.

If the current is distributed along the radiator according to a linear law  $J(z) = J(0)(1 - |z|/L)$ , then the field of the vertical segment of the radiator, similarly to (8.1), is



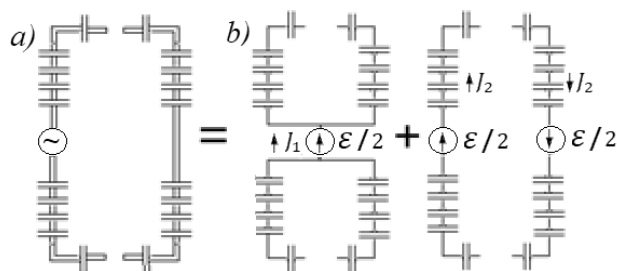


**Fig. 4:** Structure (a) and equivalent circuit (b) of folded antenna with in-phase currents.

$$E_{\theta} = 2AJ(0) \sin \theta \int_0^{L_1} (1 - |z|/L) \cos(kz \cos \theta) dz.$$

As a result of integration, we obtain

$$E_{\theta} = 2AJ(0) \sin \theta \left\{ \frac{\sin(kz \cos \theta)}{k \cos \theta} - \frac{1}{L} \left[ \frac{\cos(kz \cos \theta)}{k^2 \cos^2 \theta} + \frac{z \sin(kz \cos \theta)}{k \cos \theta} \right] \right\} \Big|_0^{L_1}.$$

In particular, for  $\theta = \pi/2$

$$E_{\theta} = \frac{2AJ(0)}{kL} l \sin kL_1 \left[ 1 + \tan \frac{kL_1}{2} / (kl) \right],$$

i.e., the effective length of the radiator is

$$l_{e2} = \frac{2l}{kL} \sin kL_1 \left[ 1 + \tan \frac{kL_1}{2} / (kl) \right],$$

The input impedance of an antenna with in-phase currents is shown in Fig. 5. As can be seen from the figure, the active and reactive components of the input impedance have in this case much smoother character. The directional patterns of each radiator of such an antenna are also shown in Fig. 5.

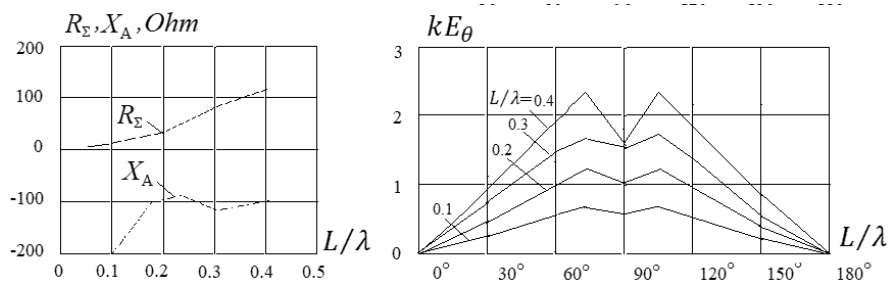


**Fig. 5:** Electrical characteristics of folded antennas with in-phase current: a) input impedance, b) vertical directional pattern.

The developed methods for calculating antennas make it possible to successfully analyze the characteristics of new versions of folded radiator, open at the ends, with capacitors (see Chapter 1).

## 2. Multi-tiered Antennas

Vertical linear radiators, for example whip antennas, are widely used for a short-wave radio communication of mobile objects. They take up little space and do not interfere with overview. Their disadvantage is that the maximum radiation is directed horizontally only at small electrical length of the antenna. With the growth of an electrical length the horizontal signal decreases. If the antenna height  $L$  is greater than  $0.7\lambda$ , a main lobe of a vertical directional pattern separates from a ground, and the radiation in the horizontal direction drops sharply. Varying the height, for example by a telescopic construction, allows to improve the antenna characteristics. But such mechanical tuning consumes a time and complicates the design of the antenna. Folded structures allow creating an antenna, in which the length of radiating segment is changing without changing the geometric dimensions of the device [3].

In the simplest embodiment (Fig. 6), such an antenna is designed for operation in two frequency bands (like the telescopic antenna, which may have two geometrical heights during operation). The antenna is made as two-tiered and consists of two radiators, which are located one above the other and connected. The upper radiator is linear, the lower radiator is folded. Exciting emfs  $e_1$  and  $e_2$  are placed in both wires of the folded radiator and may vary in amplitude and phase by means of tuning circuit.

If antenna operates in the first frequency band, emfs have the identical phase, creating currents in one direction in both wires of folded radiator. These currents form the current of linear radiator. As a result, the field is created by the currents,

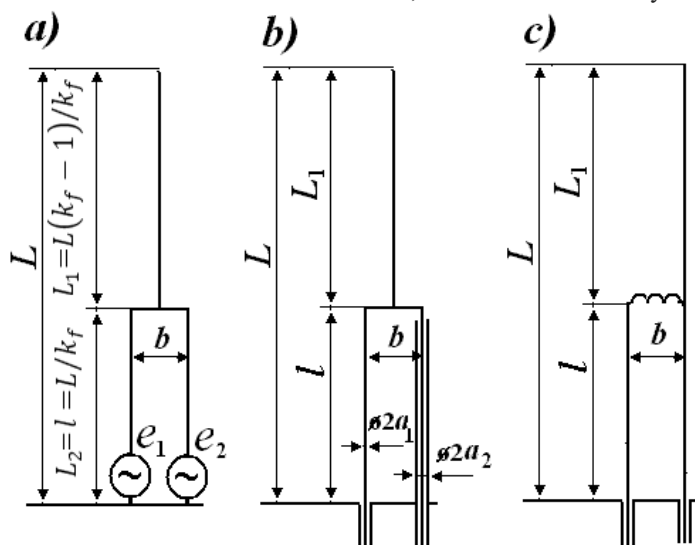


Fig. 6: Two-tiered antenna: a – common circuit, b – with coaxial cable, c – with reactive load.

distributed along the entire antenna length, and the height of radiating segment is equal to the total height of the antenna.

If the antenna operates in the second frequency band, the current is created only in the wires of the folded radiator. With this aim exciting emfs are included in anti-phase, and their magnitudes are chosen so that the potential at the point of joining of the linear radiator to folded radiator is zero. This eliminates the immediate excitation of the linear radiator. The upper segment of the antenna, consisting of one wire, can be excited by electromagnetic fields of the currents, flowing along the wires of the folded radiator. However, if the length of the upper segment is far from the resonance (is not a multiple of  $\lambda/2$ ), the current along this segment is small, i.e., the height of the radiating section of the antenna is equal to the height of the folded radiator.

Changing the height of the radiator allows provision of the operation in two frequency bands. If the overlap ratio in each frequency band is equal to  $k_f$ , the total overlap ratio is equal to  $k_f^2$ . The height of the folded radiator is chosen to be

$$l = L/k_f.$$

The considered circuit of the antenna can be generalized for use in  $N$  bands of frequency instead of two bands. For this, the number of tiers of the antenna should be increased to  $N$ . The two upper tiers are similar with the described embodiment. The lower ends of each wire of the folded radiator are connected with the upper points of the folded radiator of the next (third) tier, etc. Overall frequency overlap ratio of  $N$ -tiered antenna is equal to  $k_f^N$ . The heights of the lower tier and the rest tiers are given by expressions

$$L_n = \begin{cases} L/k_f^{n-1}, & n = N, \\ \frac{L(k_f - 1)}{k_f^n}, & n \neq N, \end{cases}$$

where  $n$  is the tier number, counting from the top.

Multi-tiered antenna creates a new prospect for the creation of a broadband antenna. In this direction the most significant results were obtained earlier by means of connecting concentrated capacitive loads along the radiator and their optimization. Calculations show (see Section 7.3) that the capacitive loads allow extending the antenna range in the direction of higher frequencies with a sufficiently high level of matching, ensuring overlap frequency ratio of the order of 10. But the required vertical directional pattern in the lower part of a frequency range may not work out. Using a multi-tiered structure and capacitive loads in the wires of each tier ensures in a wide range both high level of matching and desired directional pattern.

We return to the two-tiered variant of the antenna, more precisely to its excitation in anti-phase mode. In order that antenna may radiate, it is necessary to provide asymmetry in the folded radiator, i.e., to obtain different amplitudes of the currents in the left and right branches of the radiator. With this aim one must accomplish one wire in the form of a coaxial cable (see Fig. 6b), i.e., to include generator

$e_2$  not in the lower, but in the upper point of the wire. Another way of creating an asymmetry is connection of a reactive load in one of the wires (see Fig. 6c). In the case of asymmetry not only the anti-phase, but also in-phase currents will flow in the branches of the folded radiator. In-phase currents are caused by the presence of the ground. Exactly these in-phase currents create radiation. However, for the sake of simplicity we shall conventionally call by anti-phase mode the mode of antenna operation when the potential at the point, in which the linear radiator joins to folded radiator, is zero.

In order to analyze the two-tiered antenna we apply the theory of electrically coupled long lines, described in Section 1.3. This theory allows to find the currents and potentials along each wire of line and emf of generators providing the required operation mode. In this case, the equivalent line (Fig. 7) is considered in the general form—with two generators in one of the branches and two complex loads.

The set of equations (1.37) for the three wires in this case takes the form:

$$\begin{aligned} i_1 &= I_1 \cos kz_1 + j[U_1/W_{11} - U_2/W_{12}] \sin kz_1, u_1 = U_1 \cos kz_1 + j(\rho_{11} I_1 + \rho_{12} I_2) \sin kz_1, \\ i_2 &= I_2 \cos kz_1 + j[U_2/W_{22} - U_1/W_{12}] \sin kz_1, u_2 = U_2 \cos kz_1 + j(\rho_{12} I_1 + \rho_{22} I_2) \sin kz_1, \\ i_3 &= I_3 \cos kz_3 + j(U_3/W_{33}) \sin kz_3, u_3 = U_3 \cos kz_3 + j\rho_{33} I_3 \sin kz_3. \end{aligned} \quad (8.2)$$

The boundary conditions for the currents and potentials are

$$\begin{aligned} i_3|_{z_3=0} &= 0, i_1 + i_2|_{z_1=0} = i_3|_{z_3=L}, u_1|_{z_1=l} = e_1, u_2|_{z_1=l} = e_2, \\ u_1 - Z_1 i_1|_{z_1=0} &= u_2 - Z_2 i_2|_{z_1=0} + e_3 = u_3|_{z_1=L}. \end{aligned} \quad (8.3)$$

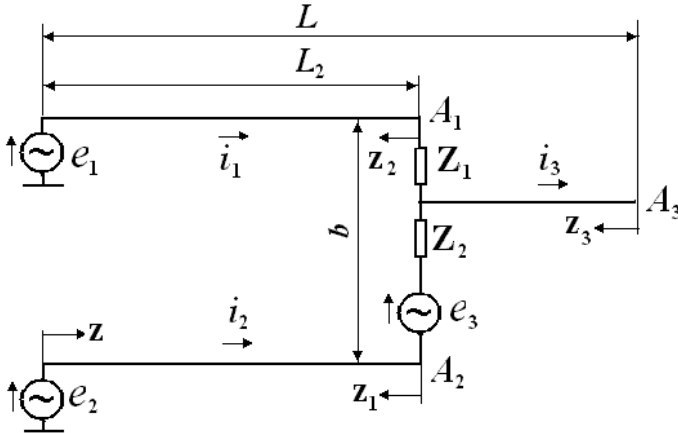


Fig. 7: Equivalent asymmetric line.

Equalities (8.2) and boundary conditions (8.3) are the set of equations with six unknown magnitudes  $U_i, I_i$  ( $i = 1, 2, 3$ ). Substituting (8.2) into (8.3), we obtain:

$$\begin{aligned}
 I_3 &= 0, I_2 = -I_1 + J(U_3/W_{33}) \sin k(L-l), U_1 = Z_1 I_1 + U_3 \cos k(L-l), \\
 U_2 &= -e_3 - Z_2 I_1 + U_3 \cos k(L-l)[1 + j(Z_2/W_{33}) \tan k(L-l)], \\
 e_1 &= I_1 \cos kl[Z_1 + j(\rho_{11} - \rho_{12}) \tan kl] + U_3 \cos kl \cos k(L-l) \left[ 1 - \frac{\rho_{12}}{W_{33}} \tan kl \tan k(L-l) \right], \\
 e_2 &= -e_3 \cos kl - I_1 \cos kl[Z_2 + j(\rho_{11} - \rho_{12}) \tan kl] + U_3 \cos kl \cos k(L-l) * \\
 &\quad \left[ 1 - \frac{\rho_{22} - jz_2}{W_{33}} \tan kl \tan k(L-l) \right]. \tag{8.4}
 \end{aligned}$$

The rest two formulas permit to express the magnitudes  $I_1$  and  $U_3$  through emf of generators. But corresponding expressions are cumbersome, are not used for further analysis and are not presented here. The previous four equalities after substituting into (8.2) allow expressing the current distribution along each wire as a function of magnitudes  $I_1$  and  $U_3$ :

$$\begin{aligned}
 i_1(z) &= I_1 \cos k(L-z) [1 + j(Z_1/W_{11} + Z_2/W_{12}) \tan k(l-z)] + je_3 \sin k(l-z)/W_{12} + \\
 &\quad U_3 [j(1/W_{11} - 1/W_{12}) \cos k(L-l) + Z_2 \sin k(L-l)/(W_{12} W_{33})] \sin k(L-z), \\
 i_2(z) &= -I_1 \cos k(L-z) [1 + j(Z_1/W_{12} + Z_2/W_{22}) \tan k(l-z)] - je_3 \sin k(L-z)/W_{22} + \\
 &\quad U_3 [j(1/W_{22} - 1/W_{12}) \cos k(L-l) \\
 &\quad - Z_2 \sin k(L-l)/(W_{22} W_{33}) + j \sin k(L-l) \cot k(L-z)/W_{33}] \sin k(L-z). \\
 i_3(z) &= jU_3 \sin k(L-z)/W_{33}. \tag{8.5}
 \end{aligned}$$

Further we consider the specific embodiments of antennas as partial cases of general equivalent circuit. Circuit of two-tiered antenna with a coaxial cable is shown in Fig. 6b. Here a few of elements of the overall circuit is absent, i.e.,

$$Z_1 = Z_2 = e_2 = 0.$$

In anti-phase mode in accordance with the boundary condition  $u_3|_{z=L-l} = 0$  we find that  $u_3 = 0$ . Then from (8.4) it follows that emfs of generators are equals to

$$e_1 = j(\rho_{11} - \rho_{12}) I_1 \sin kl, e_3 = -j(\rho_{22} - \rho_{12}) I_1 \tan kl = -j \frac{\rho_{22} - \rho_{12}}{\rho_{11} - \rho_{12}} \sec kl.$$

It is necessary to emphasize that the relationship between emf of two generators is an obligatory condition for providing anti-phase mode in the antenna. Currents along the antenna wires in this mode according to (8.5) are

$$\begin{aligned} i_1(z) &= I_1 \cos k(l-z) + \frac{\rho_{22} - \rho_{12}}{W_{12}} I_1 \tan kl \sin k(l-z), \\ i_2(z) &= -I_1 \cos k(l-z) - \frac{\rho_{22} - \rho_{12}}{W_{22}} I_1 \tan kl \sin k(l-z), \quad i_3(z) = 0. \end{aligned} \quad (8.6)$$

Expressions (8.6) confirm that the currents along the first and the second wires contain in-phase and anti-phase components. The total antenna current (sum of wires currents) varies along antenna similarly to the current along the linear radiator with the length  $l$ :

$$i_1(z) + i_2(z) = -\frac{(\rho_{22} - \rho_{12})(\rho_{11} - \rho_{12})}{\rho_{11}\rho_{22} - \rho_{12}^2} I_1 \tan kl \sin k(l-z). \quad (8.7)$$

Here it is taken into account that (see Section 1.3)

$$\frac{1}{W_{22}} = \frac{\rho_{11}}{\rho_{11}\rho_{22} - \rho_{12}^2}, \quad \frac{1}{W_{12}} = \frac{\rho_{12}}{\rho_{11}\rho_{22} - \rho_{12}^2}.$$

The current distribution along the antenna wires in the anti-phase mode is shown in Fig. 8a. The boundary between the components of current in each wire is given by a dotted line, and the total current of the wire and the total current of the antenna are given by solid curves. The impedance on the output of each generator, exciting asymmetric transmission line, is equal to

$$\begin{aligned} jX_{A1} &= \frac{e_1}{i_1(0)} = j(\rho_{11} - \rho_{12}) \tan kl \left[ 1 + \frac{\rho_{22} - \rho_{12}}{W_{12}} \tan^2 kl \right]^{-1}, \\ jX_{A3} &= \frac{e_3}{i_2(l)} = j(\rho_{22} - \rho_{12}) \tan kl. \end{aligned} \quad (8.8)$$

These expressions allow to determine approximately the reactive component of the loading impedance of each generator (like the formula for the input impedance of an equivalent two-wire transmission line, which allows determining approximately the reactive component of the input impedance of a linear antenna).

From the viewpoint of radiation, as seen from (8.6) and Fig. 8a, the antenna in anti-phase mode consists of two parallel radiators of the height  $l$  with in-phase currents in the base

$$i_1^{(i)} = \frac{\rho_{22} - \rho_{12}}{W_{12}} I_1 \tan kl \sin kl, \quad i_2^{(i)} = -\frac{\rho_{22} - \rho_{12}}{W_{22}} I_1 \tan kl \sin kl.$$

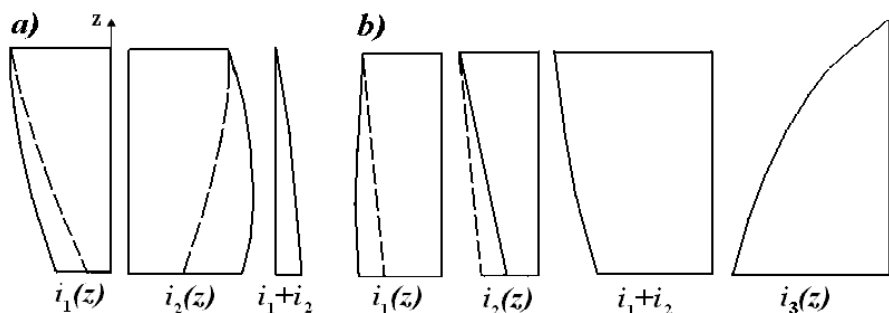


Fig. 8: Currents in the two-tiered antenna with a coaxial cable in anti-phase (a) and in-phase (b) modes.

The resistance of each radiator consists of self and mutual resistance (the last one is multiplied by the ratio of the currents). In particular, for the first radiator we write:

$$R_{A1} = R_{11} + R_{12} i_2^{(1)}(0)/i_1^{(1)}(0), \quad (8.9)$$

where  $R_{11}$  is self-resistance,  $R_{12}$  is the mutual resistance, at that  $R_{12} \approx R_{11}$ , since the radiator heights are the same and the distance between radiators is small in comparison with wave length. Thus,

$$R_{A1} = R_{11} (1 - W_{12}/W_{22}), R_{A2} = R_{11} (1 - W_{22}/W_{12}). \quad (8.10)$$

In anti-phase mode the electric field strength in the far field and the directional pattern coincides with similar characteristics of conventional linear radiator with a height  $l$ . Expressions (8.6) – (8.10) are sufficiently simple and allow determining the influence of antenna geometric dimensions upon the current magnitude in each wire and upon the electrical characteristics of the radiator. More precisely the input impedance of the antenna can be calculated by using an algorithm of calculation, based on the integral equation for the current, the Moment Method and the systems of piecewise sinusoidal basis functions.

Let's move on to an analysis of the in-phase mode. For the implementation of this mode, one must ensure equality of potentials in both branches of the folded radiator, i.e.,

$$u_1(z) = u_2(z).$$

Applying this condition to the set of equations (8.2), we find:

$$e_1 = jI_1 \frac{\rho_{11}\rho_{22} - \rho_{12}^2}{\rho_{22} - \rho_{12}} \sin kl - jI_1 W_{33}, \quad \frac{\rho_{11} + \rho_{22} - 2\rho_{12}}{\rho_{22} - \rho_{12}} \cos k(L-l), \quad e_3 = e_1 \sec kl.$$

Currents along the wires consist in this case only of the in-phase components:

$$i_1(z) + i_2(z) = I_1 \left\{ W_{33} \frac{\rho_{11} + \rho_{22} - 2\rho_{12}}{\rho_{11}\rho_{22} - \rho_{12}^2} \cot k(L-l) \sin k(l-z) \right.$$

$$+ \frac{\rho_{11} - \rho_{12}}{\rho_{22} - \rho_{12}} \tan kl \sin k(l - z) + \left( 1 + \frac{\rho_{11} - \rho_{12}}{\rho_{22} - \rho_{12}} \right) \cos k(L - l) \Bigg\},$$

$$i_3(z) = I_1 \left( 1 + \frac{\rho_{11} - \rho_{12}}{\rho_{22} - \rho_{12}} \right) \frac{\sin k(L - z)}{\sin k(L - l)}. \quad (8.11)$$

The current distribution along the wires is shown in Fig. 8b. Impedances on the output of each generator, exciting asymmetric transmission line, are  $jX_{A1} = e_1/i_1(0)$ ,  $jX_{A3} = e_3/i_2(l)$ , i.e.,

$$X_{A1} = \frac{\rho_{11}\rho_{22} - \rho_{12}^2}{\rho_{22} - \rho_{12}} \tan kl$$

$$1 - W_{33} \frac{\rho_{11} + \rho_{22} - 2\rho_{12}}{\rho_{11}\rho_{22} - \rho_{12}^2} \cot kl \cot k(L - l)$$


---


$$1 + \frac{W_{33}}{W_{11}} \frac{\rho_{11} + \rho_{22} - 2\rho_{12}}{\rho_{22} - \rho_{12}} \tan kl \cot k(L - l) - \frac{\rho_{12}}{\rho_{22} - \rho_{12}} \tan^2 kl$$

$$jX_{A3} = j \frac{\rho_{11}\rho_{22} - \rho_{12}^2}{\rho_{11} - \rho_{12}} \tan kl \left[ 1 - W_{33} \frac{\rho_{11} + \rho_{22} - 2\rho_{12}}{\rho_{11}\rho_{22} - \rho_{12}^2} \cot kl \cot k(L - l) \right].$$

The resistance is calculated according to formulas like (8.9). But  $R_{11}$  is the resistance of the radiator of height  $L$ , the current along which is determined by (8.11). Since the derivative of the current has discontinuity on the border of segments, the calculation should use the technique described in Section 1.2, i.e., should consider the discontinuity of the current's derivative. Correspondingly for the asymmetrical radiator, using expression (1.26) instead of expression (1.25), it is necessary to write

$$E_z(J) = -j \frac{15}{k} \left\{ \frac{2 \exp(-jkR_0)}{R_0} \frac{dJ(0)}{dz} - \left[ \frac{\exp(-jkR_{11})}{R_{11}} + \frac{\exp(-jkR_{12})}{R_{12}} \right] \frac{dJ(L)}{dz} + \right.$$

$$\left. \sum_{m=1}^M \left[ \frac{\exp(-jkR_{m1})}{R_{m1}} \frac{\exp(-jkR_{m2})}{R_{m2}} \right] \left[ \frac{dJ(l_m + 0)}{dz} + \frac{dJ(l_m - 0)}{dz} \right] \right\},$$

Here  $R_{m1}$  and  $R_{m2}$  are the distances from observation point to the segments' borders in the upper and lower arms of the radiator,  $M$  is number of borders,  $\frac{dJ(l_m + 0)}{dz}$  and  $\frac{dJ(l_m - 0)}{dz}$  are magnitudes of derivatives for the currents from the left and the right of point  $z = l_m$ .

It should be noted that for the same diameters of the antenna wires the formulas become far simpler.

As an example of a two-tiered antenna with coaxial cable we consider the antenna with dimensions (in meters):  $L = 1.0$ ,  $l = 0.39$ ,  $b = 0.037$ ,  $a_1 = 0.002$ ,



$a_2 = 0.025$ . Here,  $b$  is distance between the axes of the wires of the folded radiator,  $a_1$  and  $a_2$  are radii of the wires (see Fig. 6b). Calculation of antenna characteristics was accomplished by means of the Moment method.

Figure 9 shows the calculated curves for the directional patterns in the vertical planes—in the in-phase (a) and anti-phase (b) modes. Model of antenna was made in full size. The results of experimental verification are given for frequencies 150 and 300 MHz. As can be seen from the figures, the coincidence of the calculation and experiment is quite satisfactory. The high level of radiation in the direction perpendicular to the axis of the radiator (along the ground) is provided in the frequency range with overlap ratio equal 2. However, in the anti-phase mode, when the length of a third wire (of the upper segment of the antenna) is a multiple of half the wavelength, i.e., at frequencies 245 and 490 MHz, the main lobe of the directional pattern is located at a large angle to the horizontal. Here the current along the third wire is too large. The dimensions of the antenna must be chosen so that the resonance frequencies were lying outside the operating range.

Figure 10 shows the current distribution along the antenna wires in the anti-phase mode, including the current distribution along the left wire and the connecting bridge between the wires of the folded radiator. Also, the current distribution along the right wire and the upper (third) wire is presented. These distributions of currents are a graphic illustration of the processes in the anti-phase mode of the two-tiered antenna. The results are given at four frequencies, including frequencies 245 and 490 MHz, where the main lobe is located at a large angle to the horizon, since the current of the third (upper) wire is too great.

The circuit of two-tiered antenna with a reactive load is shown in Fig. 6c. Here a few of the elements of an overall circuit are absent also, i.e.,  $Z_2 = e_3 = 0$ . Let us assume that  $\rho_{11} = \rho_{22}$ . In the anti-phase mode, the boundary condition  $u_3|_{z=L-l} = 0$  should be executed. This means that the emfs of generators are connected by the relationship  $e_2 = -e_1 + Z_1 I_1 \cos kl$ , and the currents along the antenna wires in this mode are equal to

$$i_1(z) + i_2(z) = jZ_1 I_1 W_{33} \frac{1}{\rho_{11} + \rho_{12}} \sin k(l-z), \quad i_3(z) = 0.$$

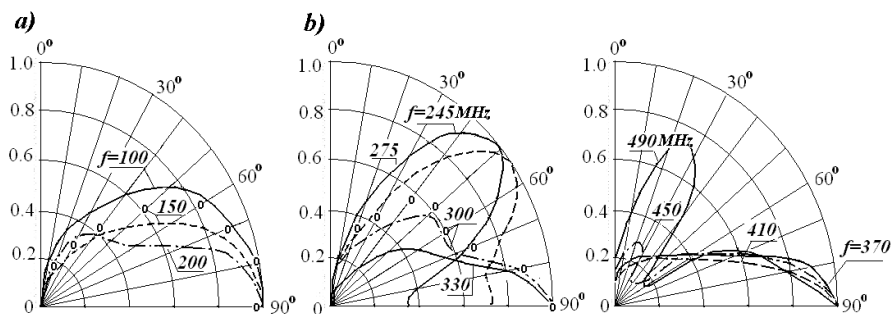
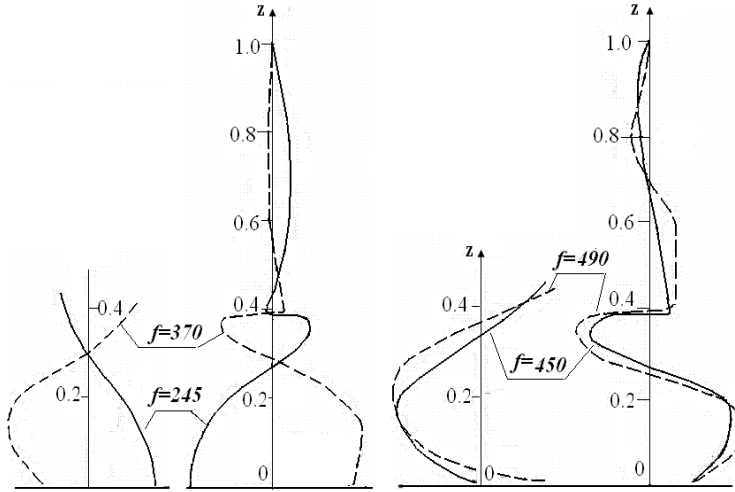


Fig. 9. Directional patterns of antenna in the vertical plane in the in-phase (a) and anti-phase (b) modes.



**Fig. 10:** Current distribution along the wires of two-tiered antenna with coaxial cable at four frequencies (in anti-phase mode).

Reactive components of generators' load are

$$jX_{A1} = \frac{Z_1 + j(\rho_{11} - \rho_{12}) \tan kl}{1 + jZ_1 \tan kl/W_{11}}, \quad jX_{A2} = \frac{j(\rho_{11} - \rho_{12}) \tan kl}{1 + jZ_1 \tan kl/W_{12}}.$$

Resistances are calculated in accordance with (8.10), and

$$i_2^{(i)}(0)/i_1^{(i)}(0) = W_{11}/W_{12}.$$

The in-phase mode has salient features. Since a load is connected in the upper section of the folded radiator, it is impossible to produce the equality of voltages in both its wires. Let us assume that

$$u_1(z) - u_2(z) = U \cos k(l - z).$$

For executing this condition, it is necessary that

$$e_2 = e_1 - Z_1 I_1 \cos kl.$$

The currents along the wires are calculated in accordance with expressions

$$i_1(z) + i_2(z) = 2I_1 \cos k(l - z) + \frac{4I_1 W_{33}}{\rho_{11} + \rho_{12}} \cot k(L - l) \sin k(l - z) + j \frac{Z_1 I_1}{\rho_{11} + \rho_{12}} \sin k(l - z),$$

$$i_3(z) = 2I_1 \frac{\sin k(L - z)}{\sin k(L - l)}.$$

Reactive impedances of generators' load are

$$jX_{A1} = \frac{Z_1 + j(\rho_{11} + \rho_{12}) \tan kl - 2jW_{33} \cot k(L-l)}{1 + jZ_1 \tan kl/W_{11} + 2W_{33} \tan kl \cot k(L-l)/(\rho_{11} + \rho_{12})},$$

$$jX_{A2} = \frac{j(\rho_{11} + \rho_{12}) \tan kl - 2jW_{33} \cot k(L-l)}{1 - jZ_1 \tan kl/W_{12} + 2W_{33} \tan kl \cot k(L-l)/(\rho_{11} + \rho_{12})}.$$

The current distribution along the wires of the antenna with the reactive load in the in-phase and anti-phase modes is shown in Fig. 11. In-phase currents are designated by symbol (i), anti-phase currents are designated by symbol (a).

Summarizing the results presented in this Section, one should make the following conclusion. The principle of changing electrical height of the radiator without changing its geometric dimensions, realized in the circuit of two-tiered antenna, is very promising, quite efficient and requires careful study to implement it in real structures.

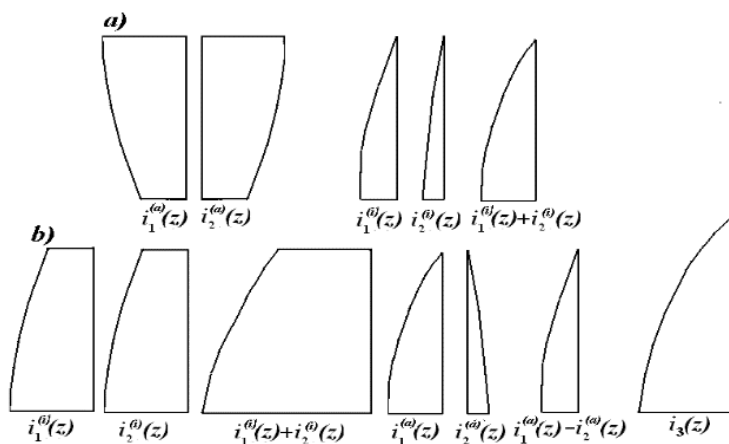


Fig. 11: Currents in the antenna with the reactive load in anti-phase (a) and in-phase (b) modes.

### 3. Antennas for Underground Communication

Reliable underground radio communication is required for many applications, e.g., for communication between people, working below ground and on the ground surface [4, 5]. The need for such communication is especially obvious in the case of underground accident, for example, in the mines.

In addition to the need in communication between an underground zone and a ground surface, a channel between two subterranean points is also often required. This channel is more complicated, and its difficulties rise due to the fact that the signal, radiated by an underground source, is subjected to strong attenuation. Besides that, it propagates in two ways [6, 7]. The first pathway goes in a vertical direction to the earth surface, located above the transmitting antenna. After that the signal propagates in air along the earth surface, and finally, passing vertically downwards through earth

layers, reaches the receiving antenna. The second pathway is horizontal, i.e., the signal propagates through the earth in a horizontal direction.

The ratio between the two signals at the receiving point depends on a distance between the correspondents, on a placement depth of transmitter and receiver, and on electromagnetic characteristics of the ground layers along the channel. As a rule, the signal, propagating by the first way, is greater. On the other hand, the signal, propagating by the second way, may be used in order to secure observation of underground channel and detecting its change. In that case the second signal must be substantially greater than the first signal. Or it is necessary be able to extract the second signal from the mixture of signals.

Losses in the earth dramatically increase at high frequencies, and the signal, propagating through the earth, is quickly attenuated. Using low frequencies requires radiating structures of large dimensions. Proceeding from these contradictory requirements, one must find a compromise solution. When developing an underground communication system, it is necessary also to take into consideration that a horizontal component of the signal propagating in the earth is attenuated slower than a vertical component. Since the efficiency of an antenna, located next to the earth, is small, it is expedient to create a big air cavity around the transmitting antenna. It should be also noted that the presence of a metal sheet underneath of the transmitting antenna increases the first signal, propagating in air along the earth, and hence placement of a metal sheet under the antenna is harmful for the system of observation. Published works show that currently it is possible to create an underground communication at a distance of 10 km by means of a transmitter of power 100–200 W, operating at frequencies 150–200 kHz [8].

To increase the signal magnitude, the transmitting antenna must be directional. For this purpose, it is expedient to use the antenna with a high directivity or the antenna array. If an antenna array consists of active dipoles, then changing phases of their emf allows us to change the direction of the radiation. The antennas are placed in air cavities located in the earth. Based on foregoing, the placement of the transmitting and receiving radiators in such a system may look as shown in Fig. 12.

Chapter 1 presents expressions (1.21) and (1.22) for the linear current and electric field of a symmetrical electric radiator located in free space. The field in the earth has peculiarities, since the ground is a medium with relatively high conductivity. Therefore, as it is rightly pointed out in [7], due to the high attenuation of electromagnetic waves for calculating fields in earth it is necessary to use rigorous expressions. The rigorous approach used in [7] made it possible to compare the results of using a sinusoidal and cosine distribution of the linear current in the radiator.

The electric current along a perfectly conducting filament, used as a model of a symmetrical radiator, is equal to

$$J(\zeta) = J(0) \frac{\sin[k(L - |\zeta|) + \varphi]}{\sin(kL + \varphi)}. \quad (8.12)$$

If in the expression (8.12)  $\varphi = 0$ , the current is distributed in accordance with the sinusoidal law (Fig. 13a). At  $\varphi = \pi/2$  this distribution has the shape of the cosine (Fig. 13b).

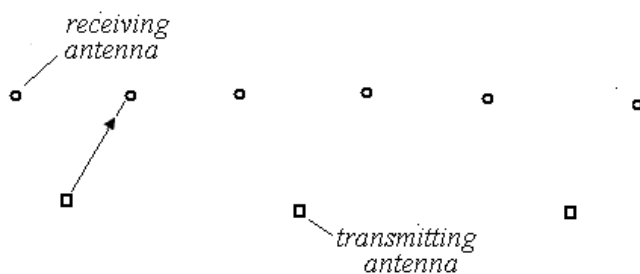


Fig. 12: Placement of transmitting and receiving antennas.

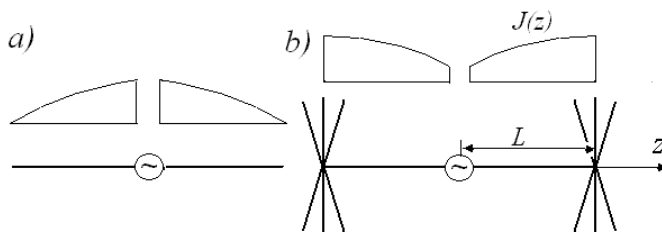


Fig. 13: Sinusoidal (a) and cosine (b) current distributions along the radiator arm.

In accordance with Maxwell's equations  $z$ -component of an electrical field in the system of cylindrical coordinates  $(\rho, \varphi, z)$  is calculated by means (1.22). Using relations between derivatives  $R$  and  $R_+$  with respect to  $\zeta$  and  $z$  and integrating the expression by parts twice, we come to (1.23). The field of the radiator is maximum in an equatorial plane ( $z = 0$ ) and is equal to

$$E_0 = j \frac{60J(0)}{\varepsilon_r \sin(kL + \varphi)} \left[ \sin \varphi (1 + jkR_{01}) L \frac{\exp(-jkR_{01})}{R_{01}^3} - k \cos \varphi \frac{\exp(-jkR_{01})}{R_{01}} + k \cos(kL + \varphi) \frac{\exp(-jk\rho)}{\rho} \right],$$

where  $\varepsilon_r$  is a relative dielectric permittivity of the medium,  $R_{01} = \sqrt{\zeta^2 + \rho^2}$ , and  $\rho$  is the distance from an observation point to a middle of the radiator. This expression considers that  $k/(4\pi\omega\varepsilon_0) = 30$ .

The magnitude of the field depends on  $\varphi$ , i.e., from the law of current distribution along the radiator. If a distance from an antenna is several kilometers, the main component of the field is close to  $1/\rho$ . The fields in this region are far fields. Losses in the earth lead to increased dielectric permittivity and decreased signals. The signal magnitude depends on the multiplier  $\exp(-jk\rho)$ , where  $k$  is equal to

$$k = \omega \sqrt{\varepsilon\mu(1 - j\sigma/\omega\varepsilon)}.$$

Here  $\varepsilon$ ,  $\mu$  and  $\sqrt{\varepsilon\mu}$  are permittivity, permeability, and propagation constant in a lossless medium,  $\sigma$  is a medium conductivity. Since the wavelength in a lossless medium is  $\lambda = \lambda_0/\sqrt{\varepsilon_r}$ , where  $\lambda_0$  is the wavelength in a free space, then  $k = \omega \sqrt{\varepsilon\mu} \sqrt{1 - j60 \lambda_0 \sigma / \sqrt{\varepsilon_r}}$ . It is seen that for the real earth conductivity the second term under the square root is much greater than the first term, i.e.,

$$k = \omega \sqrt{\varepsilon\mu} (1 - j) \sqrt{30 \lambda_0 \sigma / \varepsilon_r}.$$

Hence it follows that the signal, which propagates through ground, decays exponentially, and a decrement is equal to  $\alpha = 2\pi (\sqrt{\varepsilon_r}/\lambda_0) \sqrt{30 \lambda_0 \sigma / \varepsilon_r} = 2\pi \sqrt{30 \sigma / \lambda_0}$ . If  $\sigma = 0.5 \text{ S/m}$ ,  $\lambda_0 = 200 \text{ m}$ , then  $\alpha = 1.72 \frac{1}{\text{m}}$ , i.e., on the distance  $\rho = 10 \text{ m}$  from the antenna the signal attenuates in  $\exp(\alpha\rho) = 3 \cdot 10^7$  times.

Let us compare the fields magnitudes, created in the far region by radiators with sinusoidal and cosine current distribution. Assuming, that the input currents of the radiators in both cases have the same amplitudes and introducing the notation  $A = -j60J(0)\exp(-jk\rho)/\varepsilon_r$ , we obtain at  $\varphi = 0$  (sinusoidal distribution) and  $\varphi = \pi/2$  (cosine distribution) accordingly

$$E_{0I} = A \frac{k(1 - \cos kL)}{\rho \sin kL}, \quad E_{0II} = \frac{A}{\cos kL} \left( \frac{L}{\rho^3} + j \frac{kL}{\rho^2} - \frac{k \sin kL}{\rho} \right).$$

If  $\lambda_0 = 200$ ,  $L = 50$ ,  $\rho = 2000$ , the fields are equal to  $E_{0I} \approx 0.4A$ ,  $E_{0II} \approx A$ .

To provide a cosine current distribution or distribution close to it, one must decide the complicated task of creating wires' structure on the antenna ends or realize a good contact with the ground. Temporarily leaving this task to the side, we shall consider electrical characteristics of a radiator with such current distribution depending on arm length of the radiator. An antenna input impedance is equal to  $Z_A = R_\Sigma + jX_A$ , and in the first approximation one can write for the linear radiator:

$$R_\Sigma = 20(kh_e)^2, \quad X_A = jW \tan kL.$$

Here  $W = 120[\ln(2L/a) - 1]$  is the wave impedance,  $L$  is the arm length,  $a$  is the arm radius. Since  $J_A(\zeta) = J_A(0) \cos k(L - |z|)/\cos kL$ , the effective length  $h_e$  of the radiator is equal to

$$h_e = \frac{2}{J_A(0)} \int_0^L J_A(z) dz = \frac{2}{k} \tan kL.$$

Let, for example,  $\lambda = 200$ ,  $a = 0.1$  (dimensions are given in meters). If  $L = 0.15\lambda = 30$ , then  $jX_A = j892$ ,  $h_e = 2.75/k$ ,  $R_\Sigma = 151$ . When wave impedance  $W_c$  of the cable is equal to 100, the reflectivity  $\rho = \sqrt{[(R_\Sigma - W_c)^2 + X_A^2]/[(R_\Sigma + W_c)^2 + X_A^2]} = 96$ , and standing wave ratio is equal to  $SWR = (1 + \rho)/(1 - \rho) = 49$ . If  $L = 0.2\lambda = 40$ , then  $jX_A = j2102$ ,  $h_e = 6.16k$ ,  $R_\Sigma = 759$ ,  $\rho = 0.97$ ,  $SWR = 66$ . Obviously, both options with this level of matching are unacceptable, and the situation is even worse, when the arm length is close to a quarter of the wavelength, i.e., the cosine distribution has no advantages over the sinusoidal one. In addition to the matching problem, it is necessary to consider that the difference between the fields created by antennas with sinusoidal and cosine current distributions at the same radiation power is relatively small and that the field quickly decreases with distance. Therefore, using the cosine distribution is inappropriate.

Published works show that currently it is possible to provide underground communication at a distance 10 km using a transmitter with a power of 100–200 W, operating at frequencies of 150–200 kHz [8].

To reduce the size of the antenna, one can use a flat self-complementary antenna with rotational symmetry, for example with three metal dipoles (see Fig. 14). Each arm of such an antenna consists of three plates. As a result, firstly, the wave impedance of an antenna is significantly lower than that of a flat self-complementary antenna with a single-plate arm. This antenna allows for a high level of matching with standard cable. The antenna arm at the frequency of a first series resonance is shorter than a quarter of the wavelength, i.e., the dimensions of the antenna can be reduced. Since the signal must be horizontally polarized, the antenna is located along the horizontal axis and lies in a vertical plane perpendicular to the direction on the receiving antenna.

Another possible type of radiator is a curvilinear V-dipole with capacitive loads.

An analysis of the design that can be used for underground communication shows that the implementation of this communication system is possible. For this option, it is advisable to use mid frequencies. To transmit the signal, it is necessary to use an antenna array consisting of two or three horizontal emitters. A new type of directional antenna can be used as a horizontal emitter: a flat self-complementary antenna with rotational symmetry or a curved V-dipole with capacitive loads.

The results of the work on creating an underground communication system confirm the possibility of creating a monitoring system for underground communication channels. For inspection purposes, the area can be divided into

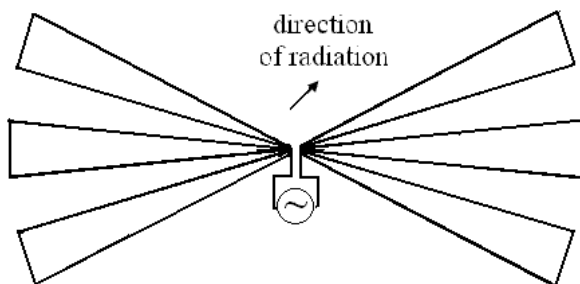


Fig. 14: The circuit of the flat self-complementary antenna with rotational symmetry.

sections about ten kilometers long, on the boundaries of which receiving and transmitting centers should be located. The transmitter of the surveillance system, like the transmitters of the underground radio communication system, must create a signal of sufficient magnitude, i.e., operate at frequencies of 150–200 kHz, and have a power of about 1 kW. A receiver located in a nearby center must ensure that changes in the received signal are recorded. The need to divide the inspection zone into sections is associated with a sharp attenuation of the underground signal with distance. Therefore, for example, doubling the communication range requires, as shown earlier, a multiple increase in the power of the generated signal. A reasonable choice of the length of the controlled section allows you to make the solution of the problem real.

The choice of transmitting antenna option must consider the conflicting requirements for underground communications systems described at the beginning of this section regarding the frequency and polarization of the radiated signal, as well as the placement and characteristics of the transmitting antenna. To weaken the interfering signal, which propagates in air along the earth surface, one can install on the earth near the transmitter an additional antenna, radiating an additional signal in antiphase with the main signal. In contrast to the short and rectangular main (underground) signal, the additional signal must be long and slowly decrease to compensate for the interfering signal at the right time and ensure that the main signal is fixed.

Compliance with other requirements for the signal frequency, transmitter power, transmitting antenna (array), and structure of the transmitting center should ensure that the neighboring center receives a high-quality and intelligible signal. The difference in operating frequencies in different parts of the inspection zone should ensure simultaneous control in all areas. A significant excess of the signal level over the required minimum guarantees the receipt of high-quality and reliable information.

#### **4. Antenna for Coast Radio Center**

Antenna for coast radio center provides a communication with the ships in the ranges of high and medium frequencies. The project of this antenna was developed based on the theory of self-complementary antennas in two versions—plane and volumetric. Both variants were intended for creating the antenna with the height 50 m and wide (the distance between supports) 100 m. In the high-frequency region antenna characteristics are like characteristics of the self-complementary structure. In the medium-frequency region this antenna is a variant of the folded radiator. First embodiment (see Fig. 15a) provides bi-directional radiation and the second one (see Fig. 15b)—unidirectional radiation with increased directivity.

Figure 15a shows a wire structure, used in the calculation of the flat vertical antenna. Dimensions are given in meters. It is considered that the ground is perfectly conducting and the antenna structure is symmetric with respect to its surface. The central vertical wire is located along an axis of the antenna symmetry. The antenna consists of two sectors (upper and lower), and it allows reducing the size of mutual impedances' matrix. Each wire is regarded as an insulated conductor (circuit), which adjoins in the end point to the central or to the other side wire.



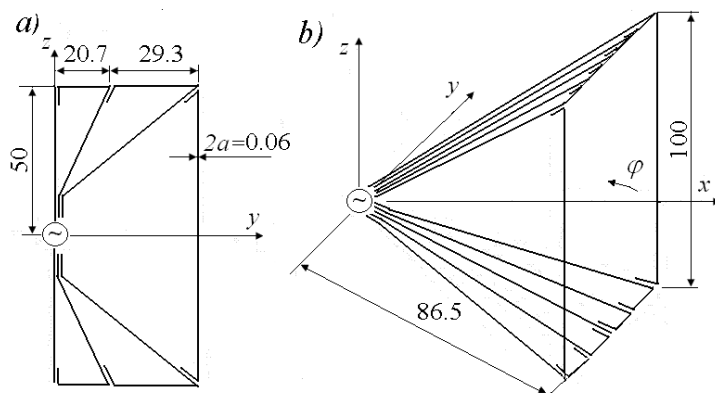


**Fig. 15:** Wire structures for calculation of the flat (a) and volumetric (b) antennas.

Input characteristics of the flat vertical antenna are presented in Fig. 16a, the directional pattern in the horizontal and vertical planes are given in Figs. 16b and Fig. 16c. TWR is calculated in a cable with wave impedance 75 ohms. Together with the calculated curves in the figure the experimental values, obtained on the model, executed in the scale of 1:50, are shown by points (in the form of squares, circles, and triangles). The coincidence of the calculated and experimental data in the first part of the range is quite good, in the second part it is rather qualitative. The directional pattern in the horizontal plane has a shape of an oval, elongated in a direction perpendicular to the antenna plane. The width of the main lobe on the level of 0.7 at frequencies up to 3 MHz is more  $80^\circ$ . In the vertical plane the directional pattern is flattened and has a width from 20 to  $40^\circ$ .

The results of calculation and experiment show that an increasing the number of wires in the antenna allows to reduce the reactive component of the input impedance and to raise the level of TWR. It is expedient to connect the wires of triangular radiator with each other by horizontal connecting links. Increasing diameters of side shunts (supports) also helps to improve matching.

The experimental TWR in the cable, which feeds the antenna in the form of a triangular radiator from nine wires is presented in Fig. 17. Curve 1 corresponds to the antenna option with one additional horizontal connecting link, curve 2—with four connecting links. Curve 3 is given for the antenna with four connecting links and with a diameter of each support increased to 0.7 m. The last option allows to obtain TWR more 0.4 at the frequencies from 0.9 to 5.3 MHz with overlap ratio, equal to 5.9. This option was recommended to realization.

Using of the volumetric antenna with an inclined triangular radiator allows us to create unidirectional radiation and to expand the range to the side of lower frequencies. The wire structure used for the calculation of this antenna is shown in Fig. 15b, and electrical characteristics are presented in Fig. 18. From the drawings it is seen that increasing dimensions of a triangular radiator shifts the resonances to left. Radiation is increased in the direction of the triangle's inclination. Directional patterns in mutually perpendicular vertical planes are substantially different from each other.

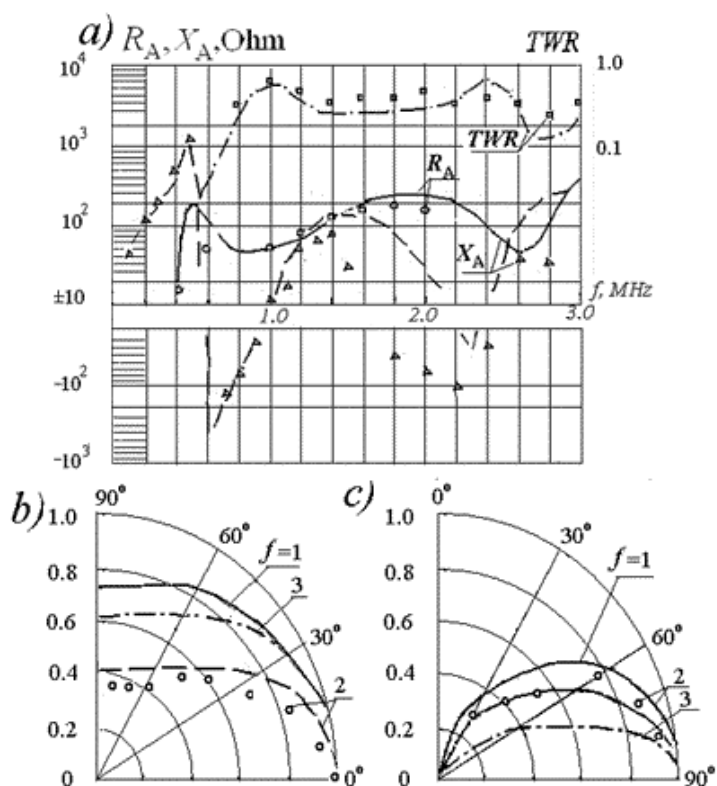


Fig 16: The input impedance (a) and the directional patterns of the flat vertical antenna in horizontal (b) and vertical (c) planes.

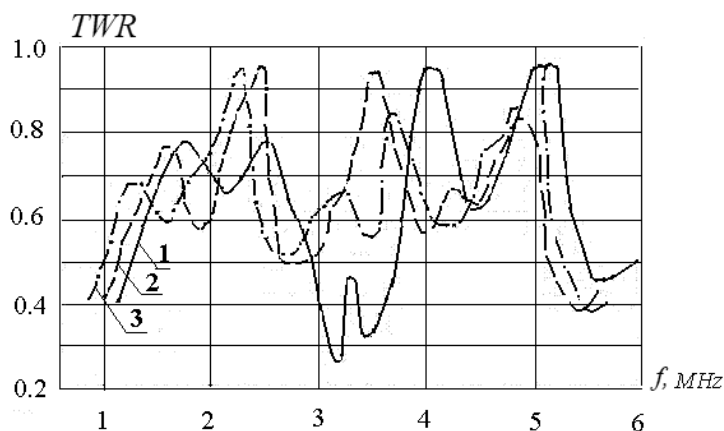
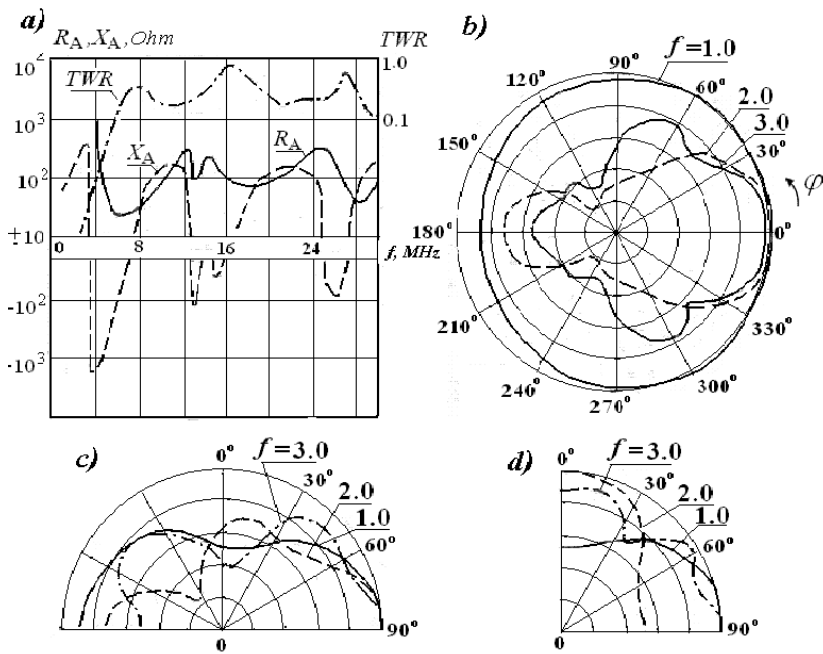


Fig. 17: Experimental TWR of different antenna variants.

Table 1 shows directivity of the flat and the volumetric antenna (relative to isotropic radiator).



**Fig. 18:** The input impedance (a), and the directional patterns in horizontal (b) and vertical planes  $xOz$  (c) and  $yOz$  (d).

**Table 1:** Maximal Directivities of Antennas.

Type of antenna	$f = 2 \text{ MHz}$	$3 \text{ MHz}$
flat	5.9	6.4
volumetric	7.1	6.9

The antenna for the coast radio center was developed by a group of specialists headed by V. K. Pevzner and described in the book [9].

### 5. Ship's Antennas for Medium Frequency Waves

Antennas are widely used for a variety of purposes and in the most diverse areas of our lives. These purposes and areas of use necessitate the development of products that correspond to an application of antennas. The most important area of antennas uses a radio communication and broadcasting. A peculiar installation place for antennas are ships and vessels for various purposes. This following Sections are devoted to the analysis of the features of antennas used in ship conditions for the radio communication and broadcasting.

The main ship's antenna is an antenna operating in the range of the medium-frequency waves. With allowance for peculiarity of their propagation, these electromagnetic waves should be directed along the earth surface and have a vertical polarization. In the horizontal plane, the directional pattern of the antenna should be close to circular. The efficiency of the main antenna should be sufficient to create

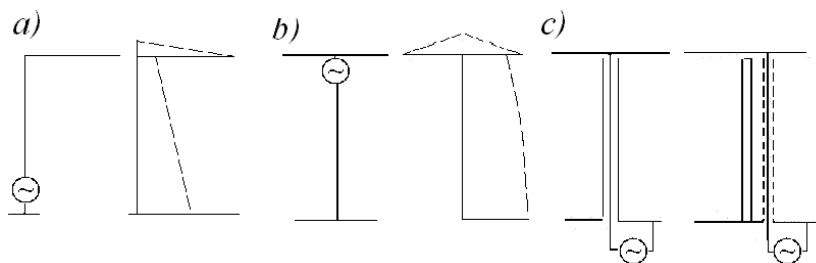


**Fig. 19:** The main ship's wire antennas and the current distribution along it: a—with excitation in a low point, b—with an upper excitation, c—placement of the antenna feeder inside and outside the mast.

an electric field with a voltage 50 microvolt/m at a distance 150 miles from the ship when the main radio transmitter of the ship connected to the antenna.

As a rule, the height of the ship's antenna is small in comparison with a wavelength, i.e., the resistance of radiation is small, and that leads to low efficiency. Accordingly, the main task of developing new medium-frequency antenna is the increase of its effective height. Therefore, the antennas with capacitive loading at the upper end are widespread. Their loading is fabricated in the form of a horizontal wire structure and permits to improve (to make more uniform) current distribution along the vertical wire of antenna to increase its effective height and resistance of radiation.

Such an antenna is excited as a rule in the base. The antenna is named inverted *L* antenna. Its circuit and a distribution of a current amplitude along the wires are given in Fig. 19a. The vertical segment may be single-wire, multi-wire or fan-shaped, and it as a rule consists of several wires placed in one vertical plane, located in parallel or convergent to an excitation point. This segment is connected to an end or to a middle of a horizontal loading. Accordingly, antenna has inverted *L* or *T*-shape.

Along with the antenna excitation in a bottom point (in the base), one can use the circuit of the upper excitation, when a radio transmitter is connected to the bottom end of a wire located inside the mast or inside a special feeder. The upper end of the wire is connected to a horizontal loading (Fig. 19b, c). In this case, the outer surface of the mast acts as a radiator, the internal surface of the mast and a central wire form the feeder. Such a circuit of antenna excitation does not give particular advantages, although the effective height of the antenna in this case significantly increases and is close to the height of the mast. But a long feeder reduces the load's resistance of a transmitter, i.e., decreases a positive effect created by the upper excitation. To weaken the feeder influence, one must increase the mast diameter.

The effective antenna height increases with increasing length and width of the loading. To increase the loading's efficiency without changing its length. one must to replace the usual structure of the parallel wires with the meandering loading, described in Section 1.8. A calculating method for electrical characteristics of an antenna with the meandering loading and results of applying such a loading are given in [9].

Disadvantages of wire antennas are obvious: they require a second mast, which hinders cargo operations. They are torn in stormy conditions. In addition, the mast, near which the vertical antenna wire, excited in a lower point, is suspended, not only plays a role of a support but also creates an additional parasitic capacitance between the antenna and the ground, reducing the resistance of a radiation. The calculating

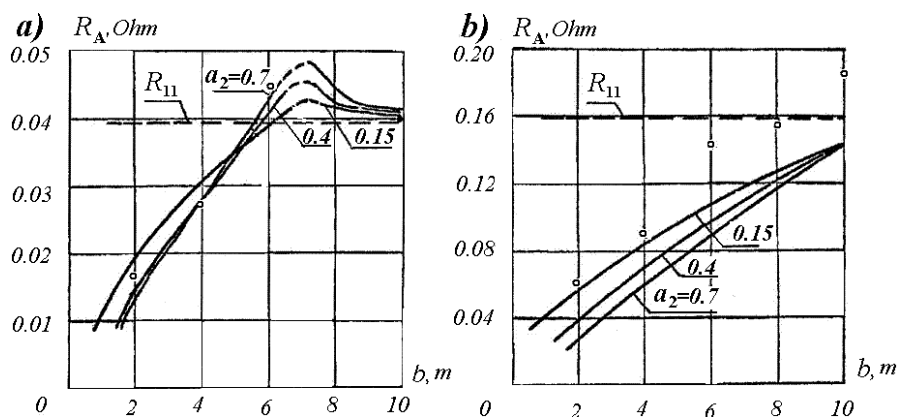


Fig. 20: Dependence of the radiation's resistance of the wire antenna on the distance to the mast.

resistance of a radiation for an antenna, located in parallel to the mast, is described in [10]. It is based on a theory of a folded radiator. Figure 20 shows the results of calculating the radiation's resistance for antennas 6.5 and 13 m height at a frequency 0.46 MHz depending on a distance  $b$  between the antenna and the mast for different radii  $a_2$  of the mast (all dimensions are indicated in meters). The radius of the antenna wire is equal to  $a_1 = 3.7 \cdot 10^{-3}$  m. The points in the figure give the results of an experimental check, when the mast radius is equal to  $a_2 = 0.4$  m. For comparison, the graphs show the radiation's resistance  $R_{11}$  for an isolated antenna.

It is seen from the figure that active component of the antenna input impedance drops sharply when the distance between the antenna and the mast is small. Horizontal loading weakens the influence of the mast. But in this case also it is necessary to move the antenna away from the mast as far as possible (from 4 to 8 m, depending from the mast height).

The small radiation's resistance and low efficiency are not sole drawbacks of wires antennas. One must be added to them such drawback as a wide variation range of the input impedance, which hampers standardization of antennas and complicates the onboard equipment. Besides, an antenna often hinders cargo operations. A storm or an ice formation can tear the vertical segment or the horizontal loading of the antenna. The antenna may require mounting of a second mast, which is not necessary for contemporary ship.

For this reason, antenna-masts have found their use as the main ships' antennas. At first, three variants of such antennas appeared: 1) with guy ropes, 2) free-standing and 3) placed on the mast. The first variant was dropped soon because of the large area occupied by the antenna. Therefore, in the first stage free-standing (self-supporting) antenna-masts were built, but they were used only on great ships. Further, in order to reduce the cost of the antennas and to their use on the ships of small and medium tonnage, the antenna-mast with inductive-capacitive load was designed. It is mounted on the existent ship mast.

The circuit of this antenna is presented in Fig. 21a. It is an antenna with an open vertical wire, excited in the lower point. This means that this antenna differs from inverted  $L$  antenna only by the type of loading. The loading is created in the

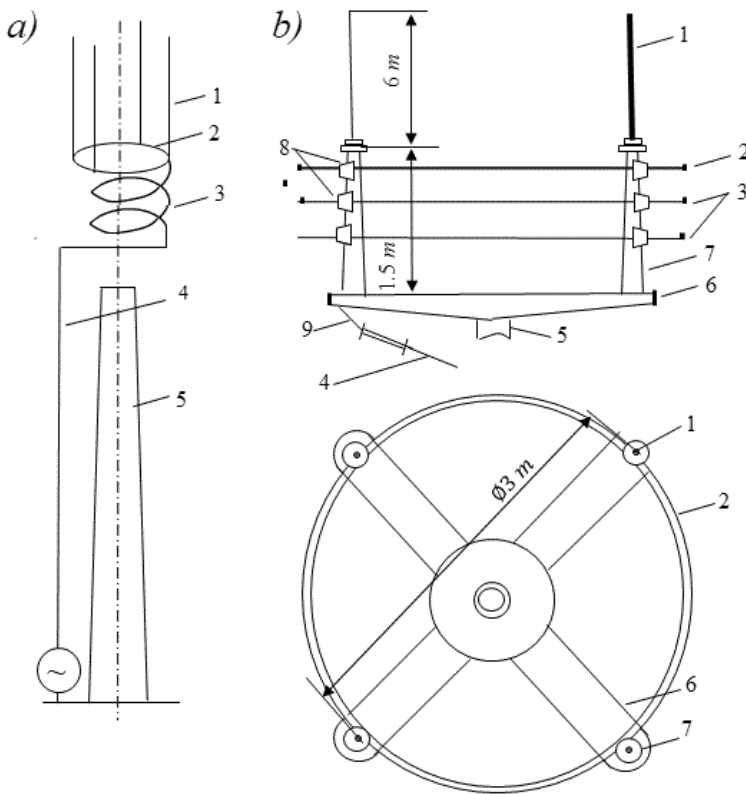


**Fig. 21:** Antenna with inductive-capacitive load: a – circuit, b – design of the load  
 1 – whip antenna, 2 – conducting ring, 3 – two-turn volumetric spiral, 4 – open vertical wire, 5 – mast,  
 6 – work platform, 7 – dielectric column, 8 – base insulator, 9 – rod insulator.

form of a vertical structure, which is the extension of the mast. The mast acts as a support. As a result, a geometric height of the antenna is significantly greater than the mast height. Increasing the effective height of the antenna caused by increasing its geometric height improves all its electrical characteristics. Besides, this antenna can be installed on a board of exploited ship. An antenna option with an upper excitation is also possible.

As shown in Fig. 21b, the antenna loading consists of four whip antennas connected in the base by a conductive ring, and a two-turn volumetric spiral, which is included in series with the system of whip antennas. The system of four whip antennas is equivalent to a thick metal radiator with a great capacitance and a low wave impedance. The spiral increases the electrical length of the antenna. The system of whip antennas creates the capacitive component of the load. The two-turn volumetric spiral creates the inductive component of it. Both elements decrease the input reactance of the antenna and increase its effective height and the radiation's resistance.

Use of whip antennas allows, if necessary, to incline them and decrease the total height of the structure. In the case of necessity, there is the possibility of access

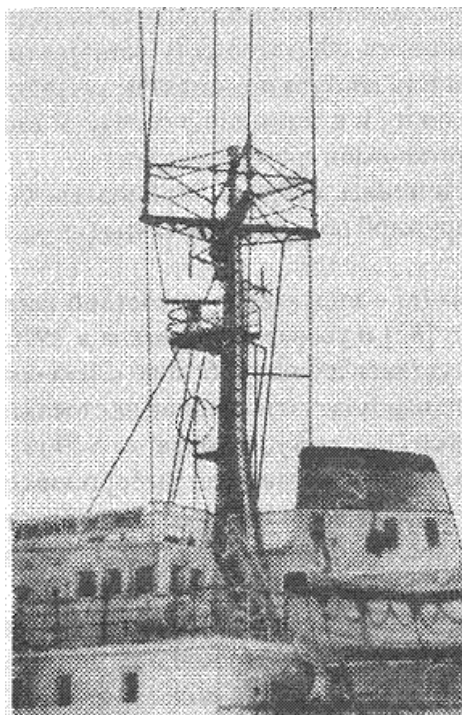


**Fig. 22:** Antenna-mast with inductive-capacitive load on the upper bridge of cargo ship '*Konstantin Shestakov*'.

to elements of the antenna load at the time of parking the ship in a port and in a calm weather. The lightning-conductor (spark gap) is installed at the antenna wire upstream of the transmitter room.

The antenna-mast with inductive-capacitive load was proposed in 1967 [11] and was improved in 1970 [12]. The antenna prototype was mounted on the board of cargo ship '*Konstantin Shestakov*' with displacement 3500 ton (Fig. 22). Antenna is placed on a ship's upper bridge, on the mast of a height 9.5 m and diameter 0.3 m. The total antenna height is about 16 m. The static capacitance of an antenna is equal to 442 pF, the self-wave length is 240 m, and the resistance at frequency 400 kHz is  $4.3\Omega$ . In 1968–1969, the antenna passed comprehensive operational tests. They showed that the antenna fully meets the Maritime Register requirements, including a level of intensity of the created field.

In subsequent years, antennas of a similar type were developed in other countries (Fig. 23, dimensions are given in meters). They include the Norwegian antenna AS9 (the antenna option with possible inclination is named AS9ST) and antenna 938G-1 of the firm Collins, USA. The capacitive loads in them, as in the described antenna, consist of whip antennas installed on the mast top. The inductive load is made in the form of a coil or spiral, connected in series with a system of whip antennas and with a vertical wire. Antennas are fabricated as free-standing structures of fiberglass and have the total height about 15.3 m. Combining these antennas with a conventional ship mast is not provided.

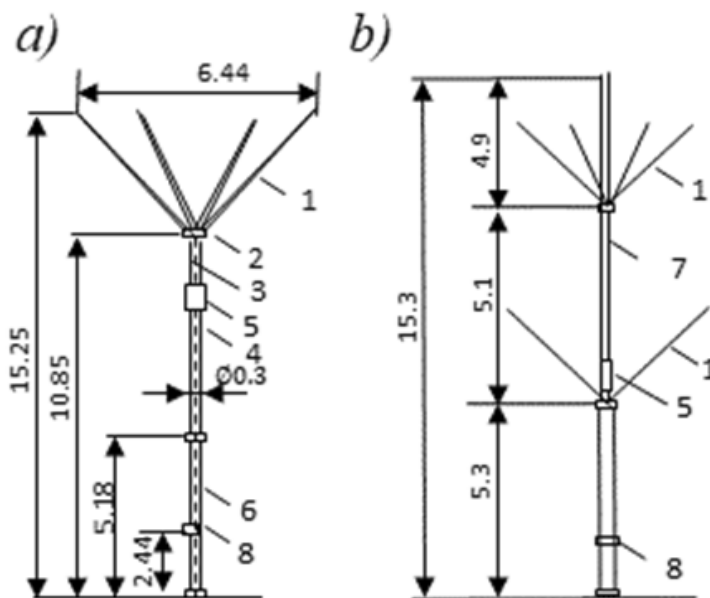


Fig. 23: Antennas-masts with inductive-capacitive load: a – 938G-1, b – AS9

1 – whip antenna of fiberglass with wicker copper mesh, 2 – bronze cap, 3 – central copper wire, 4 – fiberglass mast, 5 – inductance, 6 – aluminum tube, 7 – fiberglass tube, 8 – antenna lead-in.

The calculating method of the electrical characteristics of the antenna-mast (using the example of an antenna-mast with inductive-capacitive load) is described in [9]. Also, the antenna test results are given there.

In principle different version of a main antenna was developed for ships, where the masts are absent and replaced by superstructures of a tower-type. The antenna general view is shown in Fig. 24. This is the antenna with an upper feeding. The antenna consists of an excited metal structure (tower) and two wire cylinders 13–15 m long and about 0.5 m in diameter. The cylinders play the role of an antenna loading and are made of six parallel wires that are located along the cylinder generatrices and converge at the ends. Cylinders can be located at the same height at an angle from  $0^\circ$  to  $20^\circ$  to the horizontal and from  $20^\circ$  to  $50^\circ$  to each other. If there is no space for such placement, then the cylinders can be located one below the other with an angle between them from  $10^\circ$  to  $30^\circ$ . The upper ends of the cylinders are fixed to a support cross-beam or bracket through insulators. The lower ends are fixed to the excited structure (also through insulators). Using flexible jumpers, the ends of the cylinders are connected to each other and to a cable. To reduce losses in the cable, an end cascade or remote resonant circuit of the radio transmitter should be located near the excitation point of the antenna. The distance between a side surface of the cylinder and the metal superstructure must not be less than 3 m.

The described antenna was installed on one of the navy ships. The tests carried out confirmed its prospect and showed that the antenna has a high level of matching and an acceptable directional pattern, which are implemented if during installation of the antenna on the ship to observe above restrictions. The advantage of this antenna is



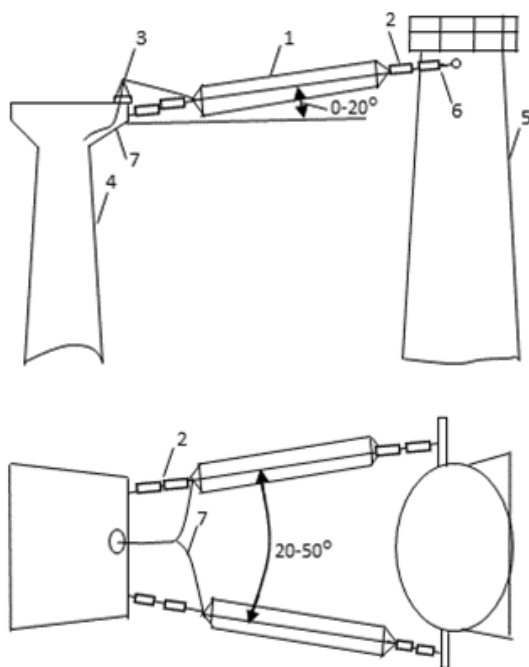


**Fig. 24:** Antenna with load in the form of two wire cylinders

1 - wire cylinder, 2 - insulator circuit, 3 - coupling, 4 - excited structure, 5 - support tower, 6 - connector, 7 - cable.

the absence of resistive elements in its design, and resulting in the antenna efficiency close to 1.

To ensure the safety of navigation, ships in addition to stationary antennas must be equipped with antennas that can be deployed and used in emergency situations. Such an emergency antenna should be kept fully prepared for an immediate installation. For this purpose, pneumatic and ballistic antennas can be used. In both cases, the antenna is a vertical radiator excited in the base.

In a pneumatic antenna [13] the radiator is a flexible wire that is supported in a vertical position using one or more rubber containers (Fig. 25a). Containers are made of a flexible, durable and airtight material. When the compressor delivers a compressed air to the container, then, thanks to the guiding metal pipe, the antenna is promoted and assumes a vertical position. After this, it is only necessary to maintain the desired pressure in the container according to the signal of a special sensor (Fig. 25b). The air pressure must be sufficient to maintain the antenna upright. In the folded position, the shell of container is wound on a drum of a winch. Upon transition to the operating position, the compressor increases the air pressure inside the container, forcing the shell to rise upward and gradually increase the antenna height. A height adjustment is made by turning the drum (Fig. 25c).

To operate in the medium wave range, the pneumatic antenna should have a height of about 20 m. In order to improve the electrical characteristics and increase the stability of the shell, one can overlay a metal mesh on the shell or replace the vertical wire with several wires.

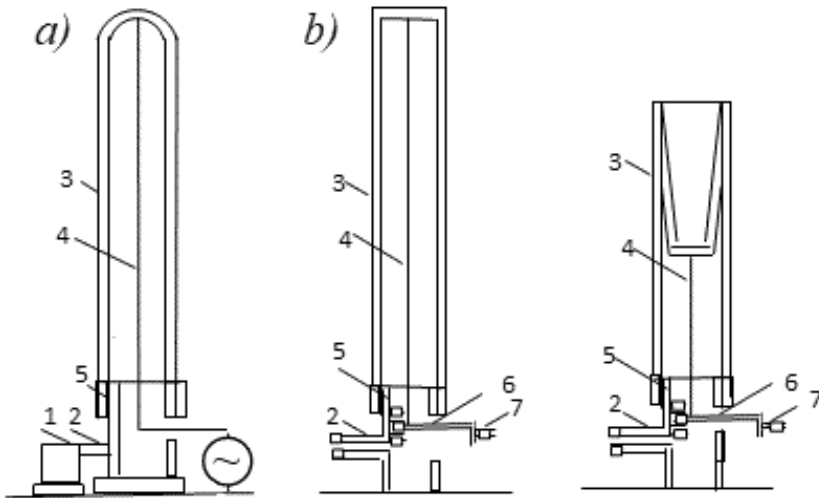


**Fig. 25:** Pneumatic antenna (a), its deployment mechanism (b), and a height adjustment (c)  
1 - compressor, 2 - tube, 3 - container, 4 - flexible wire, 5 - base, 6 - drum, 7 - handle of winch.

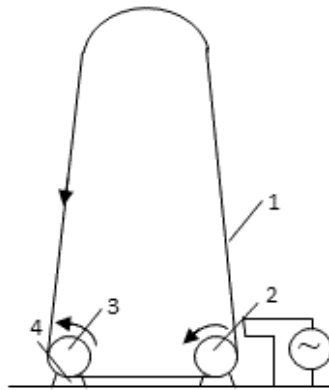


**Fig. 26:** Circuit of ballistic antenna  
1 - filament, 2 - motor with a pulley (catapult), 3 - receiving pulley, 4 - insulator.

Another variant of the deployable emergency antenna is a ballistic antenna [14]. An antenna circuit is shown in Fig. 26. A flexible filament closed in a ring is thrown out with the help of a catapult (rotating pulley 2 mounted on the motor axis), forming an ascending branch of the antenna. Another pulley accepts the filament arriving in a descending branch. The catapult and accepted pulley are isolated from the ground. A high-frequency energy is transmitted to the antenna by means of an inductive coupling.

As a filament, one can use a metal hawser with washers or discs mounted on it. Such the filament has an increased aerodynamic drag, which allows to reduce the speed of the filament, without threatening the stability of the antenna. In another embodiment, the radiator is made of high strength elastomer with a complex cross-

sectional profile. It is twisted along the longitudinal axis by an angle  $n\pi$  (of the Möbius loop type) and is covered with a metal layer with a thickness of 0.01–0.1 mm ( $10^{-5} - 10^{-4}$  m). This design permits to implement an antenna with a height of several tens of meters or more. The design provides fast ascent and descent. Changing the height of the antenna is done by changing the relative position of the additional rollers along which the filament is moved.

Concluding the Section devoted to medium wave antennas for the ships, it is necessary to summarize what has been said. At first glance, this Section is devoted to the relatively narrow field of antennas application, and these antennas are used to solve a simple problem. But, as follows from the foregoing, this task entails a variety of side problems associated with the placement of antennas on the object and the influence of operating conditions. To solve the problems caused side effects, sometimes a strict approach is required at the highest scientific level. One of these problems is the mutual influence of the radiators located on the mast one above the other. It is discussed in Section 8.

## 6. Short-wave Antennas

In ship radio communications, a range of short (decameter) waves is widely used. Its peculiarity is the operational change of working frequencies. The need for such a change is caused by daily and seasonal changes of the state of the ionosphere. In addition, the choice of the operating frequency depends on the ship's location, the extent of the radio communication line, the level of sun activity, etc. Therefore, it is necessary to operate practically in almost the entire high-frequency range. The use on ships in the range of decameter waves of wide-range radio transmitters based on power amplifiers with distributed amplification simplifies the operation of radio transmitters and the automation of their control. But at the same time, it is necessary that the load impedance of the transmitter lies within the specified limits. These limits are much narrower than the limits necessary for the operation of transmitters with resonant amplification.

Therefore, the use of wide-range transmitters is impossible without wide-range antennas. Also, without wide-range antennas it is impossible to accomplish an automation of radio communication. Thus, the first requirement to a ships' shortwave antennas is a wide operating range. To operate in a wide frequency range, it is necessary to ensure high electrical characteristics at each operating frequency. The directional pattern of antenna in the horizontal plane should be close to circular one. As for the vertical plane, the greatest range of radio communication during signal propagation by a surface (terrestrial) and spatial beam is obtained in the case of a maximal radiation in the horizontal direction or under small angles to the horizon, when the pattern factor is close to 1. In this direction, maximal radiation should be ensured. In [15] the results of statistical processing of various communication lines are presented (Fig. 5.36). On their basis one can establish the optimal relationships between the signal frequency, the angle of maximum radiation, and the width of the directional pattern in the vertical plane. Each curve in the figure shows the probability  $p$  of the event when the elevation angle  $\theta_1$  hit into the interval  $\theta \leq \theta_1 \leq 90^\circ$ . As can be seen from the figure, the hatched region covers 80% of the angles  $\theta_1$ .

Therefore, it is necessary that the width of the main lobe of the directional pattern corresponds to the width of the shaded area, and the direction of maximal radiation is defined by a curve passing in the middle of this region ( $p = 50\%$ ). With increasing frequency, the angle of rise of the main lobe above the earth's surface should decrease. Of course, using a real antenna, it is difficult to obtain such a dependence of the directional pattern on frequency. However, the general trend is clear: the main radiation in the decameter range should be directed under angles from  $0^\circ$  to  $40^\circ$  to the horizon.

The choice of polarization of the radiated signal is associated with the shape of directional pattern. Horizontal antennas create weak radiation in the horizontal direction. Mirroring in the ground multiplies the signal of a horizontal antenna located at a height  $h$  above the ground by the value  $\sin(kh \cos \theta)$ , i.e., sharply attenuates the signal. Horizontally polarized waves during propagation along the sea surface decay faster than vertically polarized ones. Therefore, the ships primarily use vertical polarized antennas. An exception is log-periodic antennas, which are installed at a great height above the deck, that weakens the influence of the earth. The low efficiency of the antenna leads not only to useless energy losses, but also limits the allowable power. As a result, simultaneous operation of several transmitters on one antenna becomes impossible, and that does not allow to decrease us the number of antennas. A wide-range antenna with high characteristics at all frequencies solves this problem. Thus, the second requirement to a ship's shortwave antenna is the presence of high electrical characteristics at each operating frequency.

In accordance with a third requirement the ship's shortwave antenna must have a free-standing design. As a rule, only the free-standing design can provide the antenna characteristics independent on the type and size of the ship. Therefore, a wide-range shortwave antenna should have just such a design. Based on the real possibilities of placement, the maximum height of the structure should not exceed 10–12 m.

Consider the specific options for the used antennas. Although whip antennas cannot be called wide-range, they are widely used for short-wave radio communication. The antennas used in the US Navy were described in detail in [16]. Aluminum and fiberglass rod antennas are widely used on the ships. The aluminum rods NT-66046 and NT-66047 consisting of four or five elements, are mounted on feedthrough insulators and have a total height of 8.5 and 10.6 m (see Fig. 27a). Plastic glass antennas AS-2537/SR and AS-2537A/SR consist of two elements inserted or screwed into each other (Fig. 27b). The total antenna height is 10.5 or 10.6 m. The radiator is made in the form of a wire or a metal strip of beryllium bronze, reinforced with fiberglass. The lower element is mounted on an insulator inserted in a metal foundation. Power is supplied to the contact located above the insulator. Antennas have a small diameter and a high impedance. For example, the diameter of the NT-66047 antenna is 7.6 cm at the base.

The transverse dimension of the AS-2807/SRC antenna is increased. The antenna is made in the form of three hollow aluminum boxes of square cross-section, the lower one of which is mounted on a base insulator inserted into a metal foundation (Fig. 27c). The antenna height is equal to 10.6 m, the width at the base and the top is 0.3 and 0.025 m. The operating range in the transmission mode is from 2 to 32 MHz.

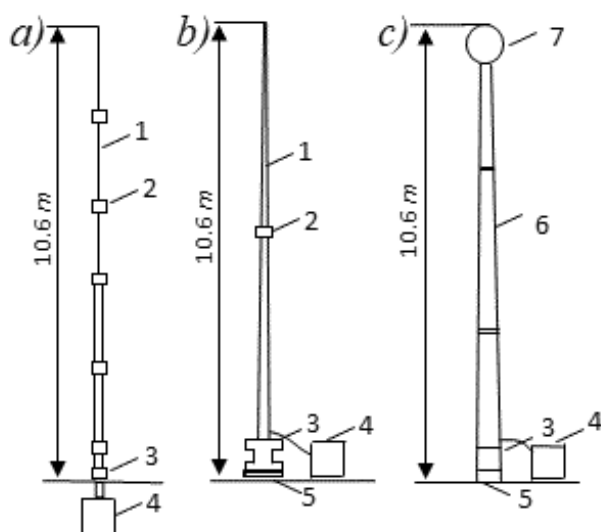


**Fig. 27:** Ship antennas of HF range NT-66047 (a), AS-2537A/SR (b) and AS-2807/SRC (c)  
 1 – element, 2 – screw tie, 3 – insulator, 4 – matching device, 5 – base, 6 – aluminum box, 7 – damper,  
 8 – feedthrough insulator.

At the base of each antenna, a matching device is installed that provides  $TWR$  in the cable of at least 0.3.

Whip antennas of the indicated length do not have in the vertical plane the desired directional pattern in the upper part of high-frequency range. A tunable matching device allows to obtain the required  $TWR$  in the cable, but this device takes time for tuning and does not allow to quickly change the frequency of the radio transmitter. As already mentioned, whip antennas with such properties cannot be considered wide-range ones.

The task of creating wide-range antennas with a high level of matching requires a reduction of the antenna wave impedance. As follows from (7.35),  $TWR$  is maximal, if the reactive component of an input impedance is small and an active component is close to the wave impedance of a cable. It is possible to reduce the antenna wave impedance by increasing its transverse dimensions. To the mass and windage of the resulting design were not excessive, one may replace the cylindrical antenna by the antenna of several wires. Around the rod antenna a wire system can be installed. An example of such a volume radiator is the AS-2805/SRC antenna, described in the book [16]. It is based on the AS-2807/SRC rod radiator, around which a four-wire construction is installed (Fig. 28a). The wires are stretched between the top (upper boundary) of the second aluminum element and the spacers. The antenna height is 10.6 m, the width at the base is 2.45 m. The operating range is from 4 to 12 MHz. The matching device in the housing with a side of 0.3 m is installed near the antenna and connected to it with a flexible jumper.

To improving the matching level, one can use two rods. For example, the OE-214/U antenna consists of two AS-2807 rod antennas (Fig. 28b) installed at a common site at a distance 3 m from each other and connected by flexible jumpers to

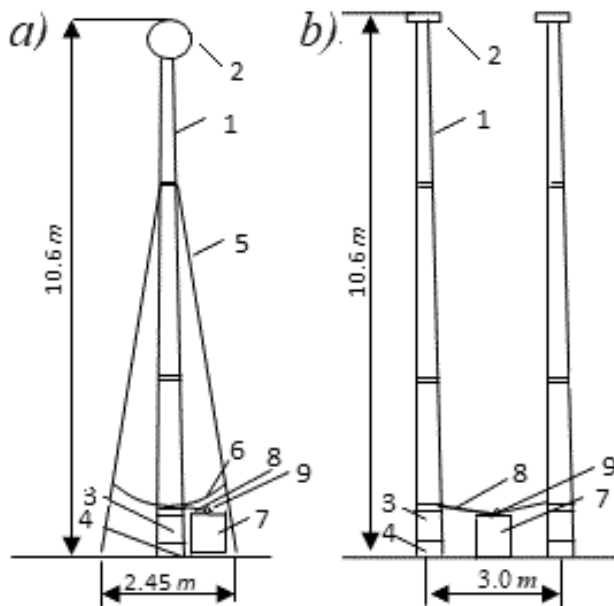


**Fig. 28:** Volumetric radiators AS-2805/SRC (a) and OE-214/U (b), based on one and two rods  
 1 – aluminum element (box), 2 – damper, 3 and 9 – insulators, 4 – base, 5 – wire, 6 – connecting wire,  
 7 – matching device, 8 – jumper.

a common matching device. Bulkier versions of volumetric antennas with different heights are created based on metal mast with a disk, to which a cylindrical or conical multi-wire radiator is suspended. The radiator can be installed around the ship's mast. It is fabricated of insulated from the mast wires, joined with each other, and connected to the central conductor of a cable (Fig. 29a). If necessary, such an antenna can be made separately from the mast and adjusted in height [17]. For this, wires of variable length are stretched along the generatrices of a cylinder or cone between the disk mounted on a top of the central rod and the drum of the winch, to which an internal conductor of a cable is connected using a spring contact. The central rod itself can also be made expanding, for example, telescopic (Fig. 29b).

In the idle position, the telescopic elements are inserted into each other, and the wires are wound on the drum. When lifting the antenna, the rod is extended, and the wires are wound from the drum. When lowering the antenna, the wires are wound on the drum and wherein pull the upper element of the telescopic structure. The tracking drive allows to extend the antenna to the desired height in accordance with the operating frequency.

This antenna is an example of a tunable radiator, whose height changes with a change of the operating frequency that allows to provide optimal electrical characteristics at each frequency. In the idle position, the antenna dimensions are small, simplifying the task of storage and transportation. An unfolding antenna also can be built in the form of thin-walled elastic profiles or telescopic structures. Using the force, one can give to the thin-walled elastic profiles the shape of a flat tape and in this form to twist them into a roll. The antennas, in which the elastic

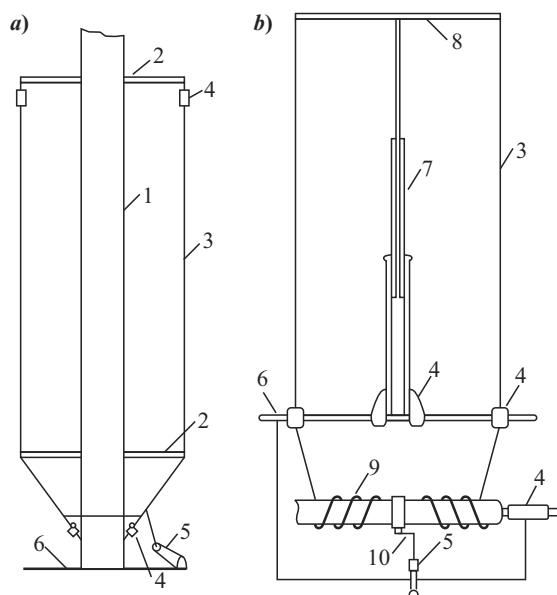


**Fig. 29:** Stationary (a) and expanding (b) volumetric radiators

1 – mast, 2 – spacer, 3 – wire, 4 – insulator, 5 – cable, 6 – deck, 7 – telescopic element, 8 – disk, 9 – drum, 10 – spring contact.

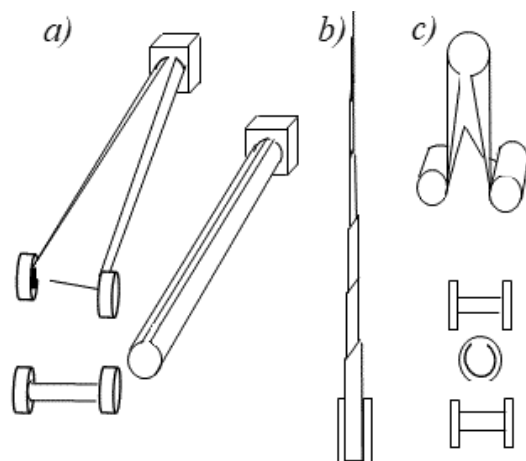


**Fig. 30:** Self-unfolding antennas with a grooved (a) and a spiral (b) profile, from two elements (c).

profiles are used, are named tape antennas. If necessary, the profiles are deployed due to the energy stored during twisting and acquire a given shape. Therefore, a thin-walled profile can be used as unfolding transformable elastic element. Antennas based on such elements are described in [18] and are presented in Fig. 30a. One end of the elastic element is rigidly fixed to the insulator, and the other is twisted on a drum equipped with a locking device (pin). In pulling out the pin, the antenna unfolds and assumes the operating position. As shown in Fig. 30b, the elastic element

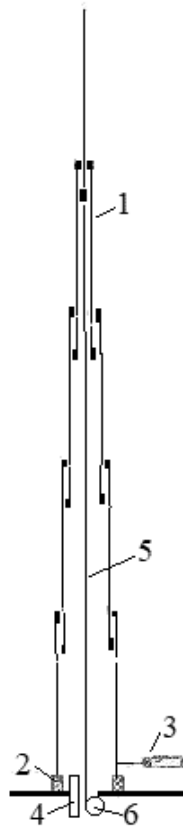


**Fig. 31:** Pneumatic mechanism for lifting telescopic antenna

1 – element, 2 – insulator, 3 – cable, 4 – tube for air supply, 5 – hawser, 6 – drum.

may have a spiral profile. The drum, on which the elastic element is twisting, is connected through the gearbox with the drive. With the help of the drive, the height of the antenna can be adjusted. To increase the rigidity of the structure, the antenna can be fabricated from two or more elastic elements, twisted on different drums (Fig. 30c). At that the diameter of the profile of the internal tape must be greater than the diameter of the profile of the outer tape [19].

Another variant of the unfolding antenna is a telescopic design. This is a system of telescopic hollow elements inserted one into the other and divided by the insulators. The central conductor of the cable is connected to the lower (fixed) element of the antenna, and the outer shell is connected to the body of the object. Locking mechanisms and contact brushes are installed on the upper ends of the telescopic elements. To raise and to lower the telescopic antenna one can use various types of drives: cable, rack, pneumatic and other types. The circuit of a pneumatic drive is shown in Fig. 31. This drive uses compressed air for lifting the antenna. To lower the antenna, one can use a hawser, one end of which is connected to the upper element of the antenna, and the other is wound on a drum [20].



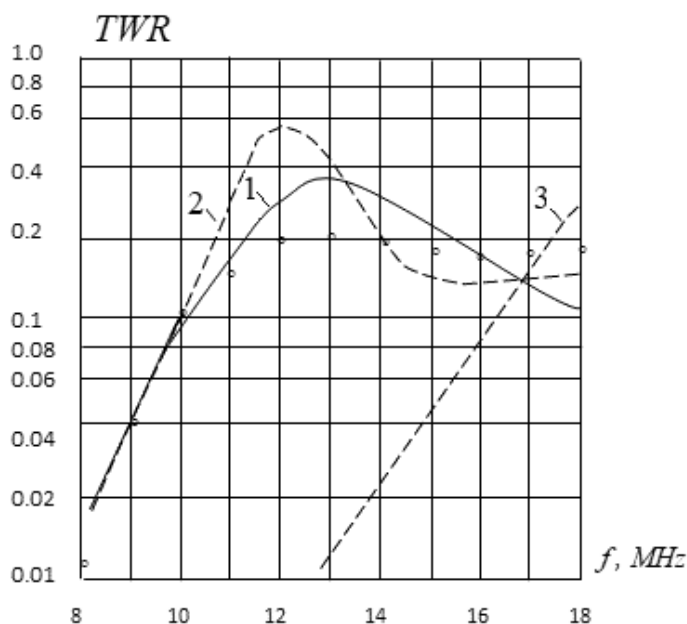


**Fig. 32:** *TWR* of the impedance antenna 3.5 m high (1) and of the rods with the height 6 m (2) and 3.5 m (3).

A smooth change of height when changing the operating frequency complicates the design of the antenna and its control system, increases the tuning time, and reduces an operational reliability. Therefore, in practice, a stepped extension system is often used with several fixed heights selected in the way that to reduce dips of *TWR* curve in the cable. Unfortunately, this approach helps poorly. A significant improvement of electrical characteristics can be achieved by creating an impedance radiator on the base of an expanding telescopic design. For this, a metallic disk is mounted on the top end of each telescopic element. Figure 32 demonstrates the positive effect of such a replacement by means of comparing the matching level of three antennas: (1) an impedance antenna 3.5 m high with a central rod of a diameter 0.02 m and a disk of a radius 0.3 m (curve 1), (2) a metal antenna 6 m high and a diameter 0.02 m (curve 2), (3) a metal antenna 3.5 m high and a diameter 0.02 m (curve 3). The circles in the figure show the results of an experimental check of the first antenna. From the figure it follows that *TWR* of the antenna with the disks is significantly higher than *TWR* of the rod with the same height and approaches to *TWR* of the rod with the double high.

Antennas with discs can be used on small ships, including river passenger one. They may be fabricated in the form of a lightweight, durable and, if necessary, folding designs.

Volumetric and unfolding antennas permit improve the electrical characteristics of antennas, in particular ship ones, but they do not solve the problem of creating non-tunable wide-range antennas. In the course of solving this problem, a method based on the use of concentrated loads was considered. First, resistive loads were examined [21], and then complex impedances in the form of a resistor and an

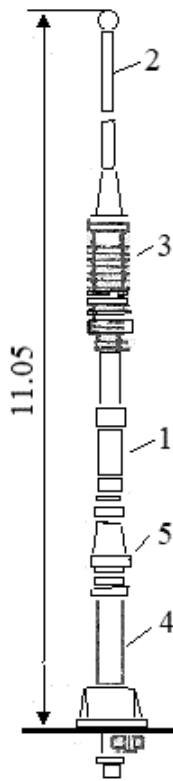


**Fig. 33:** Antenna with a complex load  
1 – trunk, 2 – rod, 3 – absorber, 4 – transformer, 5 – surface insulator.

inductance coil, connected in parallel. The reason for the transition to complex load was the hope of reducing losses and increasing an efficiency. One of the design options for an antenna with such a load is a multi-radiator antenna with a complex impedance load described in Section 1.4. Other option is presented in [22]. The general view of this antenna is shown in Fig. 33.

In the antenna structure it was used the broadband absorber with a maximum dissipation power  $1.5\text{ kW}$ . It executed in the form of coaxial line with spiral wires of resistive materials. This absorber ensures a uniform power dissipation. The absorber input is located at a height of  $2/3 L$  from the ground, where  $L$  is the height of the antenna. The purpose of its inclusion is to provide the traveling wave mode on a lower segment of the antenna. The operating frequency range of the described antenna is from 4 to 25.6 MHz. A similar antenna circuit designed to operate at frequencies from 2 to 12 MHz was proposed in [23].

Low efficiency is a very serious disadvantage of antennas with resistive load. Therefore, they quickly became outdate in antenna technology. The way out was found in Hallen's proposal to use purely reactive capacitive loads included along the entire length of the linear antenna, and to create an in-phase current distribution with help of these loads. The results obtained during the analysis and development of this proposal are described in detail in the Chapter 7.

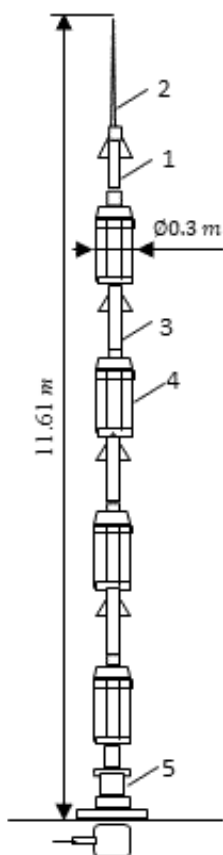


**Fig. 34:** Antenna K674-3 with capacitive loads.  
1 – tube, 2 – rod, 3 – dielectric insert, 4 – wires structure, 5 – insulator.

A general view of the antenna K674-3, based on a circuit of a linear radiator with capacitive loads, is shown in Fig. 34. The antenna is made in two versions: tunable and non-tunable. The first option provides a higher level of matching and an increased pattern factor. In this option switches used for changing capacitive loads without changing the dimensions of the antenna and its components. Loads are performed in the form of lumped elements (capacitors). The antenna height is close to 12 m. Its trunk consists from steel tubes. To increase the antenna diameter, around each steel tube the wires structures, located along the generatrices of cylinders, are installed. They are fabricated from stranded wires and connected to the ends of the tubes. As a result, the antenna diameter increases to 0.3 m, that makes possible to increase the *TWR* to 0.4 at frequencies from 6 to 30 MHz and to 0.45 at frequencies from 30 to 60 MHz.

Loads and switches are placed inside the dielectric inserts connecting the metal tubes of the trunk. Switching is done on the distance. The connectors of control circuits are installed in the base of the antenna and inside the inserts. They are open during operation of the antenna with the connected radio transmitter. When switching

capacitors, they are closed sequentially starting from the base of the antenna. That permits to prevent shunting of the loads and the insulator by control wires.

By reducing the requirements for electrical characteristics, the number of sub ranges can be reduced or tuning canceled altogether. A non-tunable antenna with capacitive loads provides *TWR* at least 0.2 at frequencies from 8 to 20 MHz and at least 0.3 at frequencies from 20 to 60 MHz. In the middle and upper part of the range (from 24 to 30 and from 45 to 60 MHz under small angles to the horizon, the signal decreases significantly.

At the end of the Section, one must say a few words about the great folded antennas, which sometimes named by loop antennas. They are used on longer waves. The principle of their action is based on the excitation of individual elements of ship structures: masts, towers, various columns, and others. Their application facilitates the solution of the problem of radiators placement, the relevance of which is caused with the reducing free territory on ships.

A great folded antenna consists of a grounded design (e.g., a superstructure) and a system of thin conductors located in parallel to this design or at a slight angle to it. In fact, this is an asymmetric folded radiator of conductors with different diameters. The exciting conductor is made from the wires, and the second conductor is the metal superstructure. The study of electromagnetic waves in systems consisting of parallel thin conductors is the subject of article [24]. In [24] it is shown that one can divide the current in each conductor of such a structure into in-phase and anti-phase and consider the entire structure as a combination of a linear radiator and non-radiating long lines. An example of a more complex structure of this type is an asymmetric multi-folded radiator.

A general view of one variant of a great folded antenna with lower excitation is shown in Fig. 35. The conductors are made of metal tubes or wires and are placed on insulators along the metal superstructure at 0.4–1.0 m from it. The upper ends of conductors are connected to this structure. The lower ends are combined and with help of flexible jumper connected to the cable through a coupling. As is seen from figure, two antennas (A1 and A2) are installed on one superstructure.

Fan-shaped antennas built according to the circuit with upper excitation are designed for operating with wide-range radio transmitters. Using a similar scheme, the dual fan-shaped antennas, which built in the USA and described in [16], are manufactured. One of them is antenna AS-2803/SRC, made of two fans. Each fan consists from three wires, located in one plane. A general view of antennas of this type is shown in Fig. 36.

The previous two Sections of Chapter 8 are devoted to ship antennas of the medium frequencies and high frequencies and to questions about development of these antennas, proceeding from the conditions of their use and the present level of their characteristics. From the point of view of a logical sequence of exposition, we should further pass to directional antennas of the high frequencies, considering the diversity of these antennas and the importance of their use. The use of directional antennas on ships is an effective method of increasing the range and reliability of short-wave radio communications. These antennas create predominant signal radiation in a required direction.

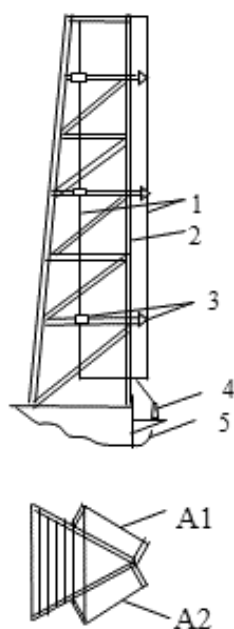


**Fig. 35:** Great folded antenna.

1 – exciting conductor, 2 – mast, 3 – insulator, 4 – coupling, 5 – cable.

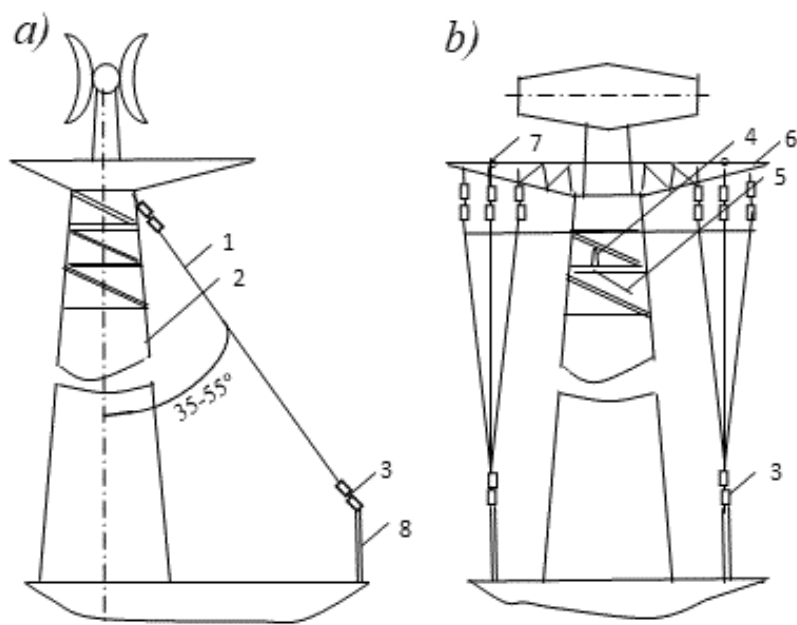


**Fig. 36:** Great folded antenna with upper excitation

1 – exciting conductor, 2 – tower, 3 – insulator, 4 – coupling, 5 – cable, 6 – ray, 7 – connector, 8 – rod.

To provide radio communications at different times and at any latitude, the directional antenna must operate in a wide frequency range and have high electrical characteristics: an appropriate level of matching and acceptable efficiency. In the vertical plane, the main radiation should be directed at angles from  $0^\circ$  to  $40^\circ$  to the horizon. In the horizontal plane, the directional pattern should not be too narrow so as not to lose communication due to the pitching of the ship in stormy weather or because of the deviation of the beam from an arc of large radius connecting the points of the correspondents' location. The level of the side lobes determines the amount of interference to closely located receiving antennas, as well as the reverse echo magnitude, which troubles communication in the shortwave range.

To provide the main radiation in accordance with the direction to the correspondent and the course of the ship, two methods are used. The first of them is the mechanical rotation of a directional antenna (for example, log-periodic one) around a vertical axis. The second option is the electrical control of the directional pattern of a stationary antenna (for example, phased array antenna) by changing the amplitudes and phases of the currents in its elements.

Many pages of this book already were devoted to directional antennas, due to their importance. Methods of calculating directional characteristics and methods of increasing directivity are discussed in Chapters 5 and 7.

The most effective and at the same time the most complex directional antenna of the decameter range is the log-periodic antenna. The large size of log-periodic antennas prevents their widespread use on ships. They are installed only on large ships with high stability. The log-periodic antenna AS-2874/SRC is used on US Navy landing craft [16]. This is a rotating horizontal antenna, which is mounted on a special pedestal at the top of the tower. In the pedestal there are the motor for rotating the antenna around its axis, a selsyn-sensor of turning angle and a rotating joint for connecting the antenna to the cable located inside the tower.

The scheme of this antenna is shown in Fig. 37. The antenna consists of the carrier boom 1 with the distribution line inside it, ten radiators 2 and the matching device 3. To reduce the sweeping radius, the long radiators are shortened with help of inductors 4 and capacitive loads 5. To reduce vibration, each radiator is equipped with a damper and a connects at the end with neighboring elements. This allows to work in strong winds. The structural elements of the antenna are made of aluminum and fiberglass.

In Section 7.5 the new and almost unknown results obtained by A.F. Yakovlev on the way to improve the performance and reduce the dimensions of the log-periodic antenna are described. These results are presented in [25]. The main achievement of the author is the development of an asymmetric coaxial log-periodic antenna, which the author named the log-periodic monopole antenna (LPMA) by analogy with the LPDA (log-periodic dipole antenna). Also, in the chapter 7 the method for synthesis of directional antennas with the optimal characteristics, named by the method of the electrostatic analogy, is described, and the results of its application to log-periodic antennas are presented.

The antenna array had got less attention. This array allows, on the one hand, to increase the electromagnetic field strength in the far zone without increasing the power of a radio transmitter, and on the other hand, to increase the total power

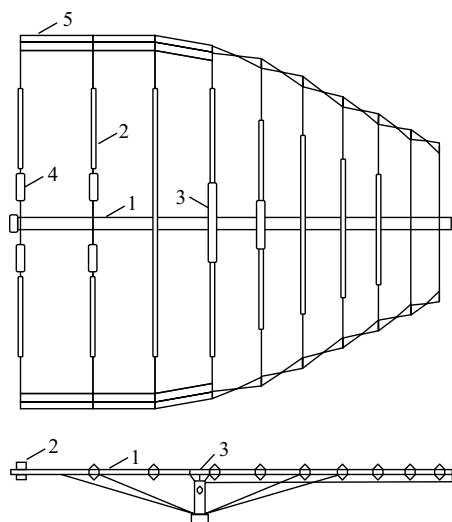


**Fig. 37:** Log-periodic antenna AS-2874/SRC

1 – carrying boom, 2 – radiator, 3 – matching device, 4 – inductor, 5 – capacitive load.

in the antenna array without exceeding a maximal allowable power in a separate radiator and a feeder. In a ship conditions, it is difficult to place an antenna system that occupies a significant area. Therefore, large flat antenna arrays are almost never found on ships. But the linear array of radiators can be placed along the ship board. Application of such array is very useful.

In principle, the array may consist of active and passive radiators. But the use of passive radiators requires the development of switched reactive impedances, which must be designed for high power and also tune in the frequency range. Adjustment of active radiators can be performed in pre-amplification stages, i.e., at a low power level. Therefore, preference should be given to the array from active radiators. It is also advisable to use uniform arrays, in which the currents' amplitudes in the radiators are the same, and the phases vary linearly. It is known that one can optimize the directional pattern of the antenna array, i.e., to select so the amplitudes of currents in the separate radiators that to reduce the width of the main lobe of the array and to low the level of the side lobes. However, the implementation of arrays with optimized directional patterns in a ship is difficult, since the influence of the surrounding metal bodies significantly distorts their shape.

As radiators in the phased array the wide-range antennas should be used. In Fig. 38 the recommended antenna array from eight radiators is shown. Along with the linear array an array of randomly located radiators, created from the existing antennas through their integration into a single antenna system, can be implemented on the ship. Under the conditions of the ship the calculated phase shifts should be adjusted, considering the actual placement of the antennas in accordance with the results of measurements on the model or in natural conditions.

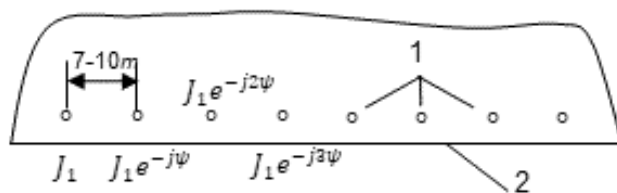


Fig. 38: Ship's antenna array: 1 – radiators, 2 – board of ship.

## 7. Antennas of Meter and Decimeter Waves

At high frequencies, radio communication is provided mainly in conditions of a direct visibility (radio waves decay rapidly beyond the horizon line). Such radio communication is of a high quality and reliability. Compared to lower frequencies, communication in the meter and decimeter ranges has several advantages. This is, in particular, an increase of the number of channels, a decrease of the power and dimensions of radio equipment, as well as a simplification of its designs.

Currently, two options of radio communication are used in the ranges at issue. The first is a direct communication between two objects, the second is a communication using a beam, reflected from a highly flying object. The requirements to the antennas used in both communication options have their own characteristics. If radio communication is carried out in conditions of a direct visibility, then to increase the distance the antennas must be raised above the ground. As a rule, they are placed on superstructures or masts and are connected to radio stations by long cables. Based on the conditions of placement, the antenna design should be as simple as possible, lightweight and durable, i.e., insensitive to mechanical loads—pitching, vibration, shock, etc. In this case, antennas with vertical polarization are mainly used. Radio communications through an artificial satellite primarily requires the antenna to provide a comprehensive azimuth and elevation overview. The second condition is to ensure a high gain. Both requirements fulfil by means of the use of rotary antennas with large directivity. Antenna for satellite communications is installing on the deck or on a special base, providing gyro stabilization. It must radiate and receive electromagnetic waves with a circular polarization.

Further the typical designs of ship antennas for various purposes, operating in the meter and decimeter ranges, are given. In Fig. 39 the variants of symmetric radiators (dipoles) are presented, in Fig. 40 variants of asymmetric radiators (monopoles) are shown.

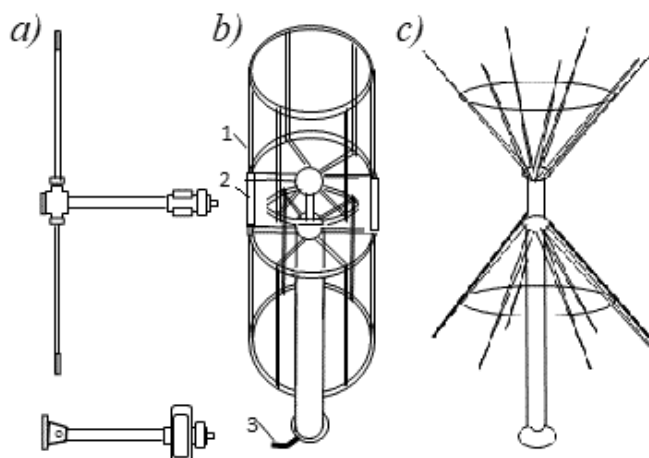
Discone antennas are given in Fig. 41, coaxial radiators are shown in Fig. 42.

Figure 43 demonstrates linear arrays with vertical polarization, Fig. 44 shows antennas with elliptical polarization.

In Fig. 45 and 46 two variants of radio buoy are given—with a whip antenna and with a multi-wire radiator in an inflatable shell.

Directional radiation in a wide frequency range is provided using a log-periodic antenna. Examples of such radiators are antennas of satellite communication *AS-2814* and *AS-2493* (Fig. 47).





**Fig. 39:** Symmetric radiators of the meter range: a – NT-66095, b – AS-2231, c – AS-2811  
1 – antenna wire, 2 – dielectric insert, 3 – cable.

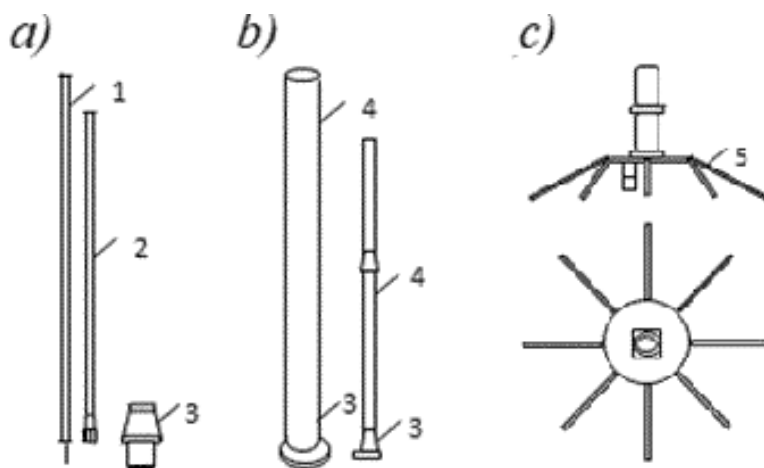


**Fig. 40:** Thin asymmetric radiators (monopoles): a – AS-1729, b – AS-3226, c – AS-390  
1 – upper rod, 2 – lower rod, 3 – insulator, 4 – fiberglass body, 5 – counterpoise.

## 8. Reciprocal Coupling between Coaxially Disposed Radiators

Section 2 of this chapter was entirely devoted to the antennas, which provides radiation in a plane perpendicular to an antenna axis in wide frequency range. In other words, serious attention was paid to the question of creating the vertical antenna with required directional pattern in the vertical plane. An issue of obtaining the required directional pattern in the horizontal plane is very often not less important. A solitary symmetric about axis vertical antenna has in the horizontal plane a circular directional pattern. But if two antennas are located nearby, then their mutual influence leads to

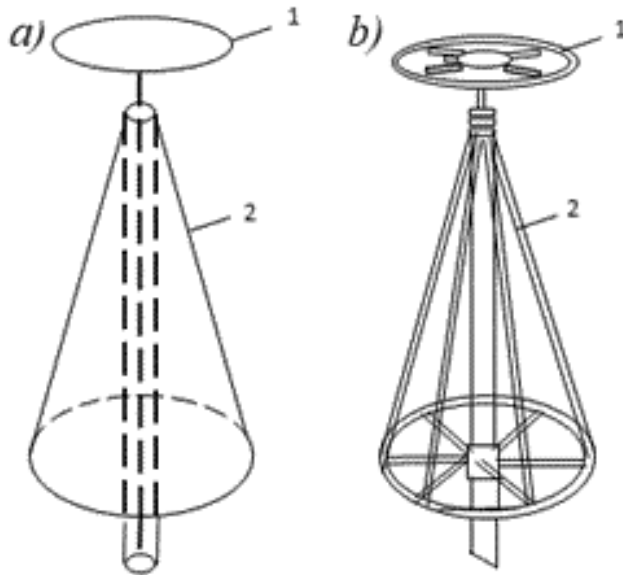


Fig. 41: Discone antennas: a – circuit, b – multi-wire construction  
1 – disc (counterpoise), 2 – cone.

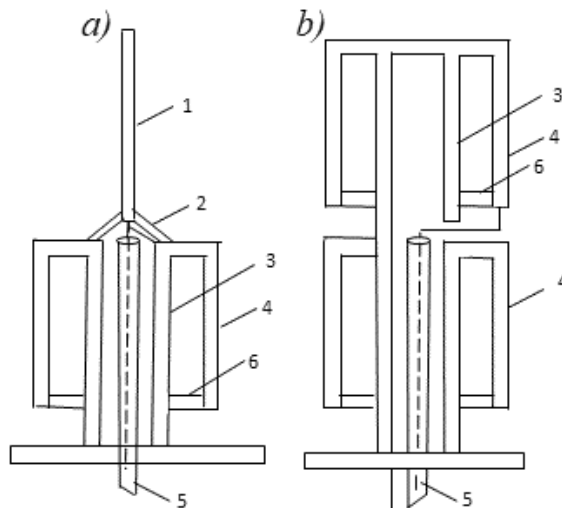
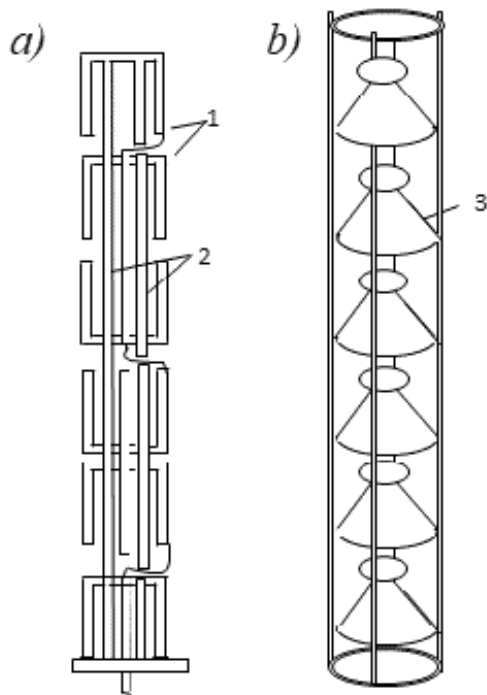


Fig. 42: Coaxial radiators with one (a) and two (b) quarter-wave arm  
1 – a rod, 2 – an insulator, 3 – rack, 4 – arm, 5 – cable, 6 – dielectric insert.

a deterioration of their electrical characteristics, to the distortion of their horizontal directional pattern.

At high frequencies, for example, in *VHF-UHF* ranges, the coaxial installation of antennas is used widely to decrease the mutual influence of vertical antennas located close to each other. This radiators arrangement greatly reduces their mutual influence. In addition, mast or other construction, on which antennas are mounted,



**Fig. 43:** Vertical linear arrays of coaxial (a) and discon (b) radiators  
1 – coaxial antenna, 2 – rack, 3 – housing of discon antenna.

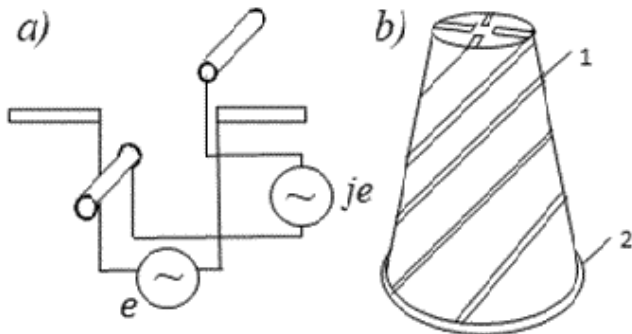


**Fig. 44:** Antennas with elliptical polarization: a – turnstile, b – four-way conical spiral  
1 – spiral, 2 – counterpoise.

is expensive structure and should be used to the utmost. In order to the mast did not affect the radiators properties, it must be made of dielectric material (plastic). But the mast is not the only cause of distorting characteristics of antennas. Also, one must reduce the influence of other metallic elements, for examples of the cables of antennas located above. A similar problem occurs when one must mount on the mast the phased antenna array, if in this array the flat vertical metal reflector, behind which it is possible to place the cables, is absent.

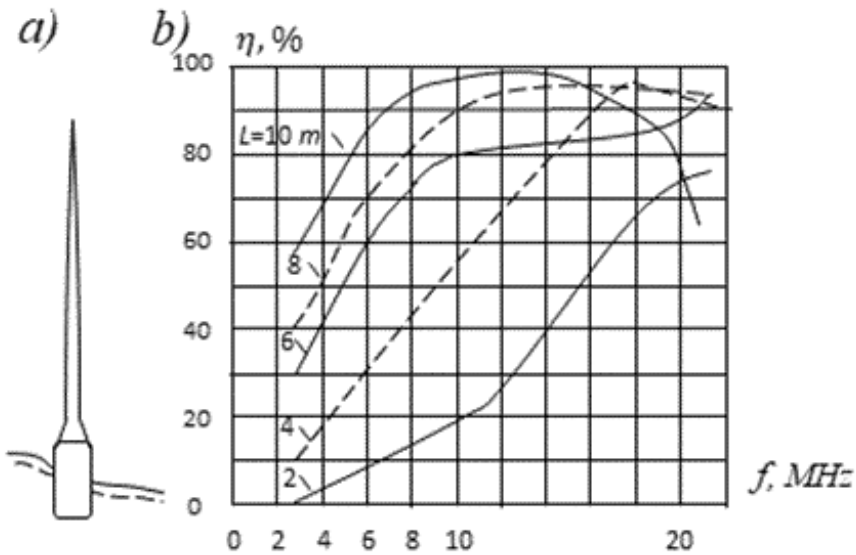


Fig. 45: Radio buoy with a whip antenna (a), and efficiency of an antenna and antenna tuner (b) as function of the whip height  $L$ .

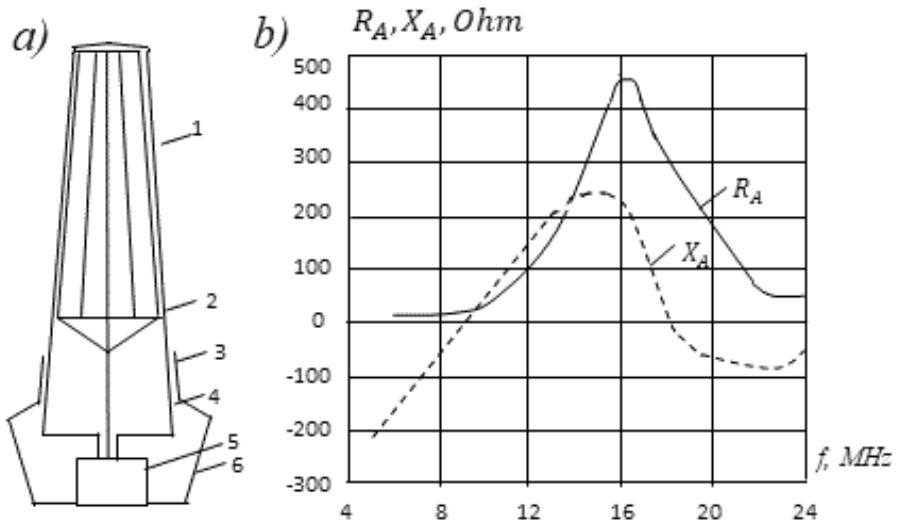
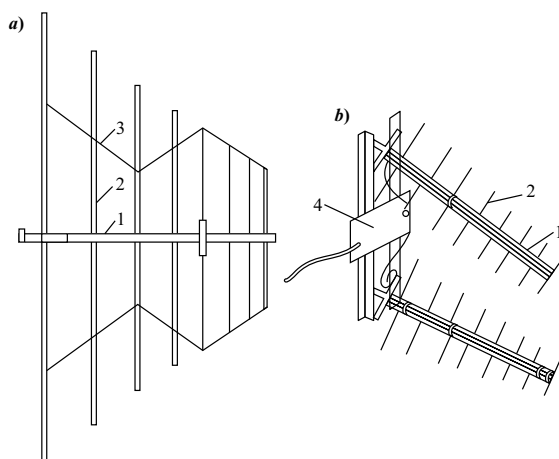


Fig. 46: Radio buoy with a multi-wire radiator in an inflatable shell (a), and input impedance of a multi-wire radiator (b). 1 – radiator, 2 – shell, 3 – screen, 4 – cup, 5 – radio transmitter, 6 – housing.

Considering the different ways of counteracting this unpleasant effect, it should be clearly understood that the placement of cables around the radiator is better than placing radiators around the cables, and that only one radiator should be in each storey. This method of solving the problem allows to reduce as much as possible the influence of cables on the radiator's properties and to bring nearer characteristics of an antenna mounted on a mast to the characteristics of an antenna in free space.



**Fig. 47:** Log-periodic antennas of satellite communication AS-2814 (a) and AS-2493 (b).  
1 – distribution line, 2 – radiator, 3 – flexible rope, 4 – power divider.

A typical placement of vertical radiators on the mast is presented in Fig. 48. Different options of placement of cables and other metal elements around radiators are considered in [26]. It assumes that dimensions of cable cross-section are not exceeded  $0.1\lambda$ . Results of analysis are given further for the following variants: (1) metal elements in the form of several rods, evenly located around the radiator (Fig. 49), (2) metal element in the shape of a meander, a horizontal segment of which lies in a plane passing through the radiator center; the midpoint of a segment coincides with this center (Fig. 50), (3) metal elements in the form of several metal rods, evenly located around each radiator; the upper and lower segments of the rods are displaced relative to one another by half of interval between the rods (Fig. 51), (4) metal element in the shape of a vertical cylindrical spiral (Fig. 52).

It is well known that the directional pattern of a vertical radiator 1, placed next to the mast 2 (see Fig. 48a) distorted the stronger, the more cross-section of the mast. Figure 48b shows the experimental directional patterns in the H-plane for the radiator located at a distance  $R = 0.19\lambda_{\max}$  from a vertical metal rod of height  $\lambda_{\max}$  with a cross section in the shape of a corner with a side  $0.025\lambda_{\max}$ . As can be seen from the figure, the directional patterns have areas where the signal level is sharply reduced (up to 0.3 of a maximum). It is unacceptable for antennas of mobile objects.

Directional pattern can be improved, if the radiator 1 is placed between two metal rods 2 (see Fig. 49a). Measurements show that the directional patterns of the radiator, located between the two rods of mentioned type at a distance  $R = 0.19\lambda_{\max}$  from each rod, remain uniform ( $E \geq 0.7 E_{\max}$ ) in the range from  $f_{\min}$  to  $1.5f_{\min}$  (see Fig. 49b).

Let the metal element 2 has the shape of a meander, and the midpoint of its horizontal segment coincides with the center of the radiator 1 (see Fig. 50a). It allows to improve the directional pattern of the radiator in H-plane in comparison with the pattern of radiator located next to the mast, and at the same time permits to reduce the impact of the metal element on the input impedance in comparison

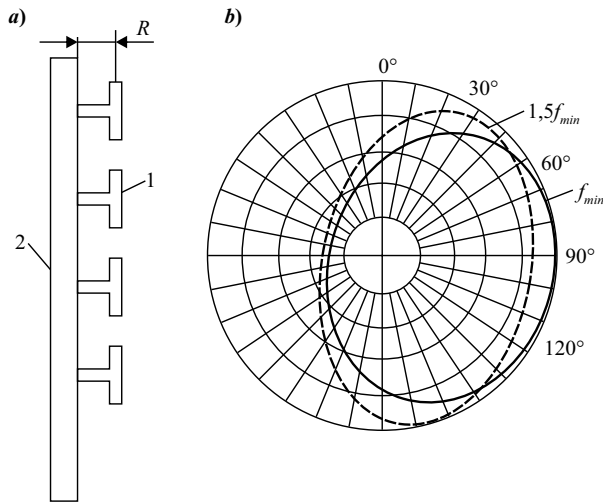


**Fig. 48:** Vertical radiators next to the mast (a) and their directional patterns in horizontal plane (b).

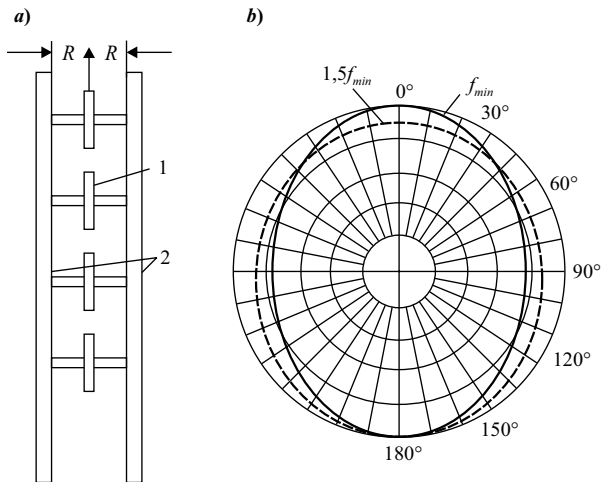


**Fig. 49:** Vertical radiators between two metal rods (a), and their directional patterns in horizontal plane (b).

with placement between the rods. As can be seen from Fig. 50a, in using this metal element, fabricated of rods of mentioned type, with a length of horizontal segment  $2R = 0.38\lambda$  the directional pattern remains uniform in the frequency range from  $f_{min}$  to  $1.5f_{min}$ .

The variant shown in Fig. 51a is a modification of the variant shown in Fig. 50a. This variant allows to increase the number of metal elements. As the measurements show, the more a number  $M$  of metal rods, placed around the radiator, the wider the frequency range, in which the directional pattern is close to the circular. On the other hand, increasing  $M$  and decreasing the radius  $R$  of free space around the radiator causes a growth of its input impedances and troubles matching with a cable. Figure 51b contains experimental data about the growth of the active component

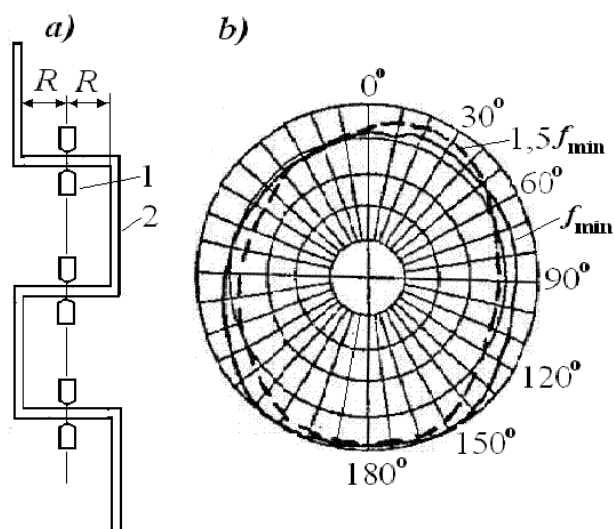


**Fig. 50:** Metal element in the shape of a meander (a) and directional patterns of the radiator in horizontal plane (b).

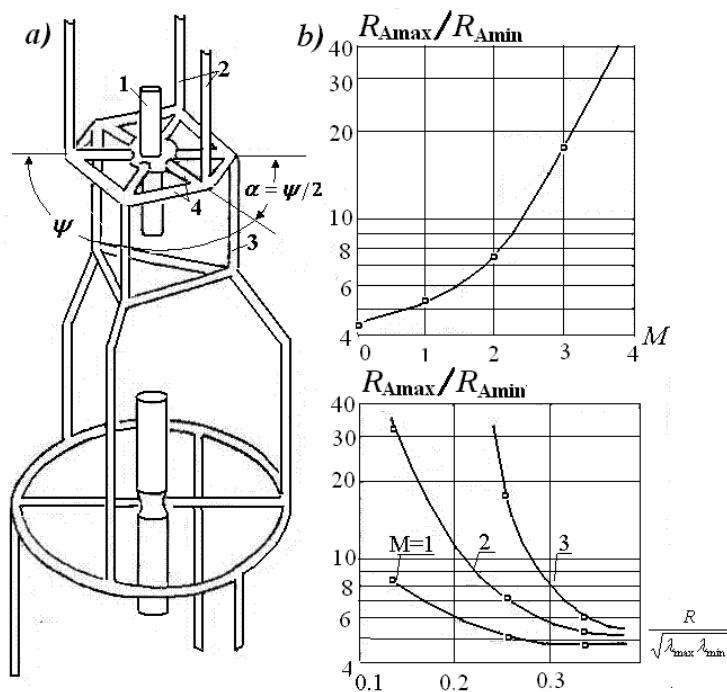


**Fig. 51:** Metal elements in the form of several metal rods (a) and the radiator resistance as a function of  $R$  and  $M$  (b).

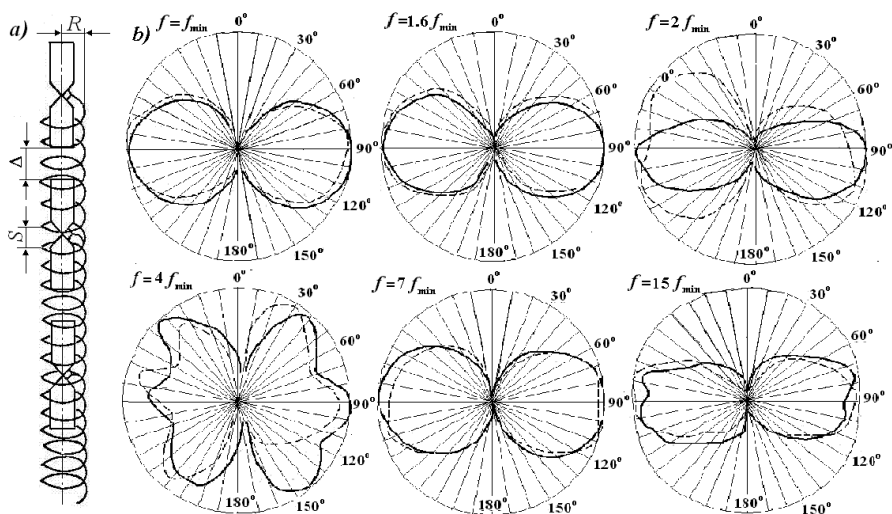


Fig. 52: Metal element in the shape of a cylindrical spiral (a) and experimental directional patterns in a vertical plane (b).

of the input impedance as a function of  $R$  and  $M$  in the range from  $f_{\min}$  to  $4f_{\min}$ . As the curves show, to avoid large transverse dimensions of the structure and growth of input impedances and  $SWR$ , it is need that the radius of free space was equal to  $R = 0.33\sqrt{\lambda_{\max}\lambda_{\min}}$  and  $M$  was not less than three.

To expand the frequency range of the radiator, surrounded by vertical rods, the rods must be divided by a plane passing through the middle of each radiator (see Fig. 51a) onto the upper (2) and lower (3) segments. Further they should be shifted relative to each other by half of interval between the rods (by an angle  $\alpha = \psi/2 = \pi/M$ ). The effect of this change on the directional pattern coincides with the result of doubling the number of vertical rods ( $M_e = 2M$ ) and does not increase  $SWR$ . The links 4 connect the rods with each other and the radiator center.

Experiments show that these elements from metal rods with a cross-section in the shape of a corner with a side  $0.01\lambda_{\max}$  allow to obtain the uniform directional pattern in the H-plane ( $E \geq 0.7E_{\max}$ ).

These elements almost do not affect on the directional pattern in E-plane. They as a rule increase  $SWR$  in comparison with the radiator located in the free space not more than 12% in a wide frequency range from  $f_{\min}$  to  $4f_{\min}$ , if  $M_e = 2M = 6$  and  $R = 0.33\sqrt{\lambda_{\max}\lambda_{\min}}$ .

Metal element in the shape of a vertical cylindrical spiral (see Fig. 52a) deserves special attention, since the spiral has minimal effect on the electrical characteristics of vertical radiators. It is expedient to choose close values of a spiral pitch  $S$  and a spiral radius  $R$ , since with a growth of  $S/R$  the spiral begins to damage radiator characteristics, and with decreasing  $S/R$  a cable, placed into a cylindrical spiral, becomes too long, and this leads to large losses in the cable and a great weight of the device.



Measured characteristics of radiators with  $SWR \leq 2$  showed that the spiral with  $S \approx R$  at an average level of  $SWR$  has very weak effect on the directional pattern in H-plane (less than 2 dB).  $SWR$  increases no more than 15 per cents. The radiation's resistance changes when  $R/\lambda = 0.04 \div 0.6$  ( $\lambda_{max}/\lambda_{min} = 0.15$ ), but the radiator may be used in a wide frequency range, if the spiral parameters ( $\lambda_{max}/\lambda_{min} = 0.15$ ), but the radiator may be used in a wide frequency range, if the spiral parameters do not change.

Figure 52b compares vertical directional patterns of the radiator located in free space (solid lines) and along the axis of spiral made of a cable with an outer diameter  $0.0033\lambda_{max}$  (dotted lines). Figure 53 presents the results of measuring mutual coupling between two identical radiators located along the axis of spiral with  $R = S = 0.04\lambda_{max}$  at a distance  $\Delta$ , which is equal to  $0.1\lambda_{max}$  and  $0.2\lambda_{max}$ . In a wide frequency range, the magnitude of mutual coupling between the radiators is close to the same magnitude for the radiators located in the free space. It is very substantial from the point of electromagnetic compatibility.

The results of calculating input impedances and directional patterns in a system of two radiators are presented for following three variants of the cable placement (Figure 54): a—the cable is absent, b—the cable is placed vertically (excluding the short horizontal segment), c—the cable is placed along the cylindrical spiral and the mentioned radial segment. The cylinder radius and the distance between the structure axis and the vertical cable are taken the same and equal to  $0.042\lambda_{max}$ . These results demonstrate the weak effect of a spiral cable upon the electrical characteristics of radiators.

The equivalent circuits of the radiating structures for each variant are shown in Fig. 54. It is considered that the upper radiator is passive and short-circuited in the middle. Radii of all wires for the sake of simplicity are taken equal to the radius of the passive radiator ( $0.0027\lambda_{max}$ ).

Figure 55a shows curves for  $TWR$  of the lower radiator in a range  $\lambda_{max}/\lambda_{min} = 4$  ( $S = R$ ). As seen from the figure, placement of the cable along the cylindrical spiral (variant c) allows to obtain a higher level of matching. The calculated directional patterns in the horizontal plane for different variants of the cable placement

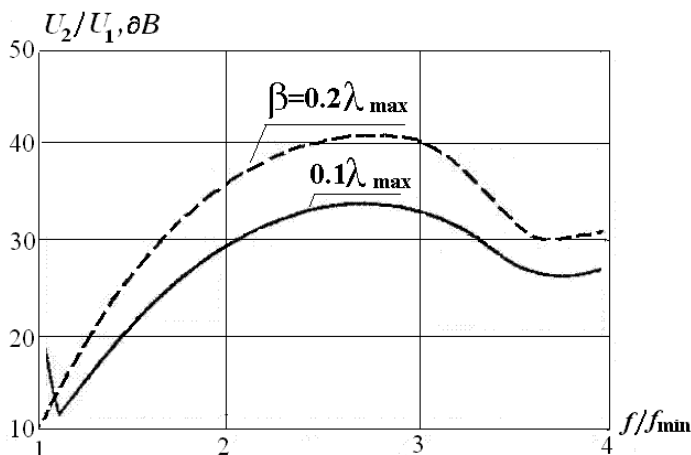


Fig. 53: Mutual coupling between radiators located along a spiral axis.

and different diameters of the spiral are given in Fig. 55b. The minimal values  $f(\varphi) = E/E_{\max}$  of the directional patterns are given in Table 2. Figures and table clearly confirm that the placement of the cable along the cylindrical spiral allows to weaken significantly the distortions of the directional patterns.

Results of analyzing characteristics of antennas located in the form of several floors show that the arrangement of cables along the cylindrical spiral, axis of which coincides with axis of radiators, facilitates the solution of problem of their electromagnetic compatibility.

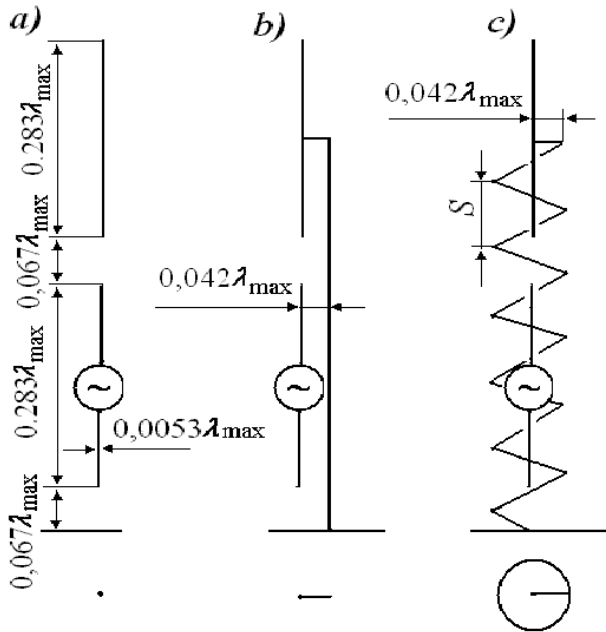


Fig. 54: Three variants of the cable placement.

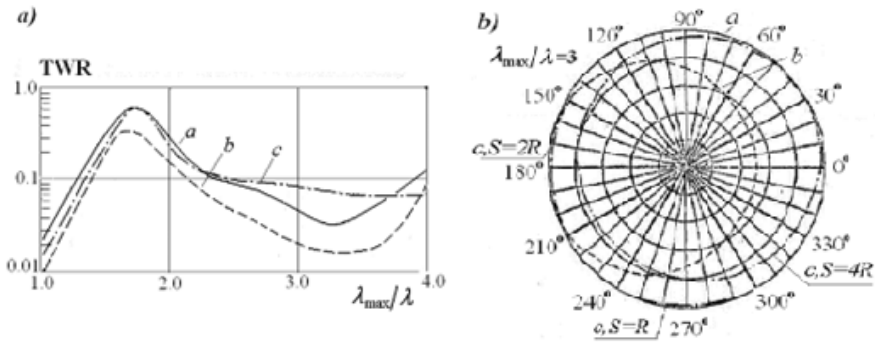


Fig. 55: Level of matching (a) and directional patterns (b) of lower radiator.

**Table 2:** Minimal Values of Directional Patterns.

$\lambda_{max}/\lambda$	Variant <i>a</i>	Variant <i>b</i>	Variant <i>c</i>		
			<i>S</i> = <i>R</i>	<i>S</i> = 2 <i>R</i>	<i>S</i> = 4 <i>R</i>
1.0	1.0	0.786	1.0		
1.5	1.0	0.705	0.997		
2.0	1.0	0.600	0.999	0.994	0.905
2.5	1.0	0.554	0.997		
3.0	1.0	0.514	0.985	0.986	0.749
3.5	1.0	0.462	0.991		
4.0	1.0	0.424	0.982		

9. Multi-wire Cables

The theory of coupled lines, described in Section 1.4, permitted to show, that the mutual coupling between lines in multi-conductor cables results in the emergence of the electromagnetic interference (crosstalk) in communication channels, and that an asymmetry of excitation and loads causes the emergence of the common mode currents in the lines.

In order to determine the signal magnitude at the end of a multi-conductor cable located inside a metal shield it is necessary to define the electrical characteristics of the lines. The magnitude of voltage across a load placed at the end of an adjacent line can be used as a measure of such a distortion [27]. The rigorous method of calculating the mutual coupling between lines enables the development of a simple and effective procedure of preventing interference.

Electromagnetic interference in communication channels (imbalance of a cable) is caused not only by the cable asymmetry, but also by asymmetry of excitation and load, which provokes the emergence of the in-phase currents in cables (common mode currents). The rigorous calculation method of the electrical characteristics of multi-conductor cables enables to determine these currents. Compensation of the in-phase currents allows us to decrease the electromagnetic radiation and susceptibility to the external fields. The rigorous method is applied first for calculating characteristics of a two-wire line located inside a metal screen and then for mutual coupling between lines. It is considered that the lines are uniform, the electromagnetic waves are transverse (TEM), and the cable diameter is small in comparison with the wavelength.

A single pair of wires (twisted pair) inside a metal cylinder can be modeled as two wires of radius *a*, situated at a distance *b* from each other inside a metal cylinder with radius *R* and length *L* (Fig. 56). If wire radius *a* and distance *b* in multi-conductor cables are small in comparison with the cylinder radius *R*, i.e., *a*, *b* << *R*, so the wave impedance of the line is constant along its length (the wave impedance varies along the line, if the axial lines of the cylinder and the twisted pair do not coincide, and the inequality of *b* and *R* is not true). Also, we assume that the wires are straight and consider account the twisting by increasing length *L* of the equivalent line.

Because a pitch of a spiral, along which each wire is located, is greater than the diameter *b* of the spiral, inductance  $\Lambda$  per unit length undergoes a slight change at the

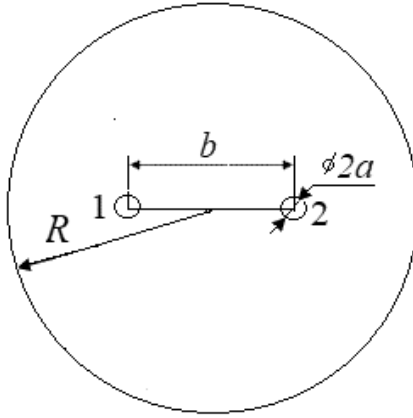


Fig. 56: Two wires inside a cylinder.

replacement of a spiral wire by a straight wire. The wire capacitance per unit length also small depends on the spiral pitch, i.e., twisting wires has no effect on the wave impedances of a structure.

But the asymmetrical location of the line in a real cable can cause a change of the wave impedance and of the input impedance of the two-wire line. It is one of a cause of the cable asymmetry. The implementation of each two-wire line in the form of a twisted pair (spiral), is another cause of the cable asymmetry. The twisted pair causes a difference of the average distances between different wires and the mutual coupling (cross talk) between two two-wire lines surrounded by a common screen, even if the exciting emf of each line and the line load are symmetric.

The equivalent circuit for a single line inside the screen is shown in Fig. 57. The two-wire line is located above the ground (inside a metal cylinder). The current and the potential along the wire  $n$  of an asymmetrical line of  $N$  parallel wires situated above ground, in the general case, are determined by an expression (1.34). The boundary conditions for the currents and potentials in this circuit are

$$i_1(0) + i_2(0) = 0, u_1(0) = u_2(0) + i_1(0)Z, i_1(L) + i_2(L) = 0, u_1(L) = e + u_2(L). \quad (8.13)$$

Here,  $Z$  is the impedance of the long line's load. Sequentially substituting expressions (5.5) in the first and second equalities of the set (8.13), we obtain

$$I_2 = -I_1, U_2 = -I_1 Z.$$

Taking into consideration formulas for  $1/W_{ik}$ , presented in Section 1.3, we find from the third equation of the set (8.13) that

$$U_1 = I_1 Z \left( \frac{1}{W_{22}} - \frac{1}{W_{12}} \right) \left( \frac{1}{W_{11}} + \frac{1}{W_{22}} - \frac{2}{W_{12}} \right) = I_1 Z \frac{\rho_{11} - \rho_{12}}{\rho_{11} + \rho_{22} - 2\rho_{12}}.$$

And from the fourth equation follows

$$I_1 = e/[Z \cos kL + j(\rho_{11} + \rho_{22} - 2\rho_{12}) \sin kL].$$

The input impedance of a two-wire line inside a metal screen (the load impedance of generator  $e$ ) is  $Z_1 = e/i_1(L)$ . Substituting magnitude  $i_1(L)$  from expression (1.34) and using the relationships between  $e, I_1, I_2, U_1, U_2$ , we find that

$$Z_1 = W \frac{Z + jW \tan kL}{W + jZ \tan kL}, \quad (8.14)$$

where  $W = \rho_{11} + \rho_{22} - 2\rho_{12}$ .

The expression (8.14) coincides with the expression for the input impedance of a two-wire long line that has no losses and is loaded at the end by impedance  $Z$ . The line is located in free space and has the wave impedance  $W$ . The asymmetry of line leads to a difference of the electro-dynamics and electrostatics wave impedances of the wires ( $\rho_{11} \neq \rho_{22}, \rho W_{11} \neq W_{22}$ ). The calculation of currents  $i_1(z)$  and  $i_2(z)$  shows that the currents in a two-wire line are identical in magnitude and opposite in sign:

$$i_1(z) = -i_2(z) = I_1 \cos kz + jI_1 (Z/W) \sin kz.$$

In these wires there are only anti-phase currents. In-phase currents absent, because the emf and load impedance are included between the line wires. The in-phase currents can be appeared in the connection of an additional emf or an additional load between one of wires of this line and the screen.

To determine the potential coefficients  $\alpha_{ms}$ , one should consider the following facts. If the system consists of two identical conductors (a wire and its image) and the structure is electrically neutral, the mutual partial capacitance coincides with the capacitance between the conductors [28] and is equal to

$$C = 1/[2(\alpha_{11} - \alpha_{12})],$$

where  $\alpha_{11}$  is the own potential coefficient, and  $\alpha_{12}$  is the potential coefficient of the image. The capacitance between the conductor and the ground is twice as much the capacitance between two conductors:  $C_l = 2C$ . For two wires of radius  $a$ , located inside the metal cylinder of a radius  $R$  at a distance  $b$  from each other, symmetrically with respect to the cylinder axes (see Fig. 55), we can write, using expression (4.20) from [28],

$$\alpha_{11} = \alpha_{22} = \frac{1}{2\pi\epsilon} \cosh^{-1} \frac{R^2 + a^2 - b^2/4}{2Ra}.$$

Here  $\epsilon$  is the permittivity of the medium inside the cable. If wire radius  $a$  and distance  $b$  are small in comparison with the cylinder radius  $R$ , then, in the air,  $\rho_{11} = \rho_{22} \approx 60 \ln(R/a)$ . Similarly, using expression (4.22) from [28], we find:  $\rho_{12} \approx 60 \ln(R/\sqrt{ab})$ , i.e., the wave impedance of a lossless two-wire line, symmetrically situated inside a metal cylinder, is a half of the wave impedance of the same line in the free space:  $W_0 = \rho_{11} + \rho_{22} - 2\rho_{12} \approx 60 \ln(b/a)$ .

If the wires inside a metal cylinder of a radius  $R$  are located asymmetrically, e.g., they are displaced to the right by distance  $\Delta$  (Fig. 57), then

$$\alpha_{11} = \frac{1}{2\pi\epsilon} \cosh^{-1} \frac{R^2 + a^2 - (b/2 - \Delta)^2}{2Ra},$$

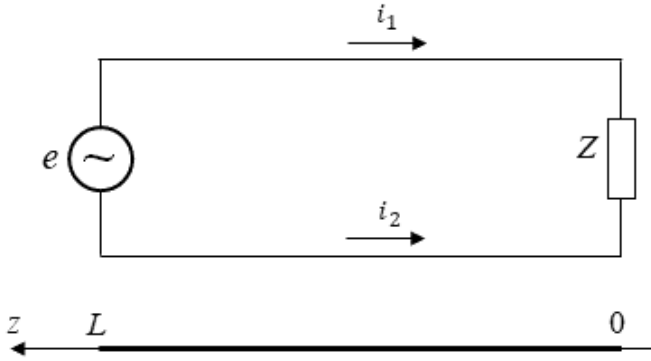


Fig. 57: The equivalent circuit of a single line inside a screen.

so, at  $a, b \ll R$

$$\alpha_{11} = \frac{1}{2\pi\epsilon} \ln \left\{ \frac{R}{a} \left[ 1 + \frac{\Delta(b-\Delta)}{R^2} \right] \right\} = \frac{1}{2\pi\epsilon} \left[ \ln \frac{R}{a} + \frac{\Delta(b-\Delta)}{R^2} \right],$$

$$\alpha_{22} = \frac{1}{2\pi\epsilon} \left[ \ln \frac{R}{a} - \frac{\Delta(b+\Delta)}{R^2} \right].$$

In this case, the wave impedance of the line is

$$W = W_0 - \frac{120\Delta^2}{R^2}. \quad (8.15)$$

That is one of the possible causes of changing the wave impedance of the long lines inside the screen.

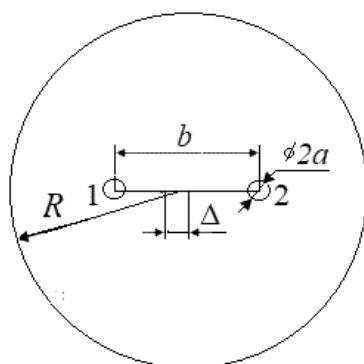
If the distance between the wires is increased by value  $\Delta$ , then at  $\Delta \ll b$

$$\rho_{12} \approx 60 \ln \frac{R^2}{\sqrt{a(b+\Delta)}} \approx 60 \left( \ln \frac{R}{\sqrt{ab}} - \frac{\Delta}{2b} \right). \quad (8.16)$$

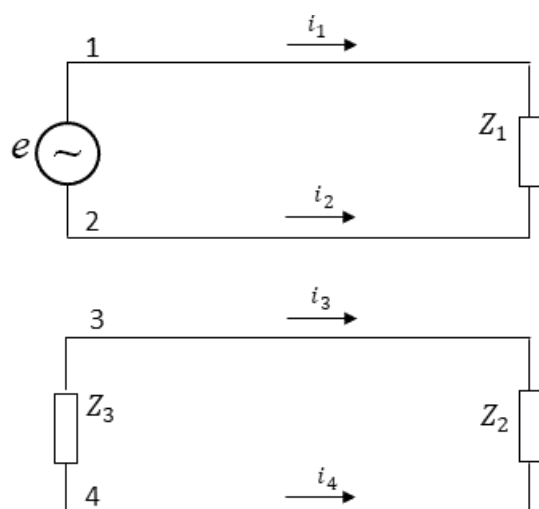
This is the second cause. As can be seen from these results, a change of the distance between wires has a greater effect on the wave impedance of the line than a displacement of wire relative to the cylinder axis.

Figure 59 shows the equivalent circuit of two coupled two-wire lines inside a screen. One of the lines is excited by generator  $e$  and is loaded by complex impedance  $Z_1$ . The loads  $Z_2$  and  $Z_3$  are connected in the wires at both ends of the other line. It is necessary to emphasize that such circuit has the most general nature. If, for example, generator  $e_1$  is located at the end of the second line (at point  $z = L$ ), the currents and voltages created by generator  $e$  are calculated considering that the input impedance of generator  $e_1$  is equal to  $Z_3$ .

As was stated at the beginning of this Section, cable asymmetry leads to a mutual coupling between two two-wire lines, i.e., to interconnection and cross talk. The reason of such asymmetry is the structure of each two-wire line. This structure has a shape of a twisted pair (spiral). In Fig. 60 the cross-section of two twisted-pairs is shown.



**Fig. 58:** Offset wires inside a cylinder.



**Fig. 59:** The equivalent circuit of two coupled lines placed inside a screen.

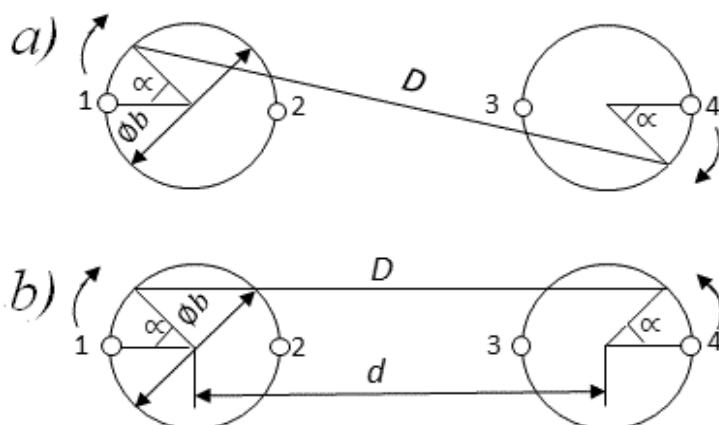


**Fig. 60:** Distance between wires 1 and 4 at the same (a) and opposite (b) direction winding of wire 4.

The line conductors are placed in different points of a given cross-section. That placement changes during winding and depends on the initial cross-section of the cable and on the variant of winding. If, for example, in the initial cross-section the ends of spirals 1 and 3 are located in it the initial point of cross-section and the ends of spirals 2 and 4 are displaced along the perimeter by  $\pi$  from this point, it means that the distance between wires 1 and 3 (and also between wires 2 and 4) is  $D_{13} = D_{24} = d$  along all length of the cable, whereas the distance between wires 1 and 4 (and also between wires 2 and 3) varies along wires from  $d + b$  to  $d - b$ . For example, the distance between wires 1 and 4 (see Fig. 60a) is

$$D_{14} = \sqrt{(d + b \cos \alpha)^2 + b^2 \sin^2 \alpha} \approx d + b \cos \alpha + (b \sin \alpha)^2 / (2d)$$

(here  $\alpha$  is angular displacement of points 1 and 4 along the perimeter of cross-section), i.e., the average distance between these wires,

$$(D_{14})_0 = \frac{1}{\pi} \int_0^\pi D d\alpha = d + \frac{b^2}{4d}$$

differs from distance  $d$ . The potential coefficients as well as the electrodynamic and electrostatic wave impedances vary accordingly.

If, at the initial cross-section of the cable, the ends of spirals 3 and 4 are displaced along the perimeter of cross-section by  $\pi/2$  and  $3\pi/2$  from the initial point, respectively, the distance between wire 1 and wire 3 (or wire 4) is

$$D_{13} \approx d + \frac{b}{2} (\cos \alpha + \sin \alpha) + \frac{b^2}{8d} (\sin \alpha - \cos \alpha)^2,$$

$$D_{14} \approx d + \frac{b}{2} (\cos \alpha - \sin \alpha) + \frac{b^2}{8d} (\sin \alpha + \cos \alpha)^2.$$

The average distance between the wires in this case is

$$(D_{13})_0 \approx d + \frac{b}{\pi} + \frac{b^2}{8d}, \quad (D_{14})_0 \approx d - \frac{b}{\pi} + \frac{b^2}{8d},$$

i.e., the displacement of the spiral ends of the two-wire line by  $\pi/2$  changes substantially the average distance between wires. Difference between  $(D_{13})_0$  and  $(D_{14})_0$  increases from value  $b^2/4d$  to  $2b/\pi$ , where  $b \ll d$ . In order for the average distance  $D_0$  between wires 1 and 4 does not differ from  $d$ , it is necessary to wind wire 4 in the opposite direction to the direction winding of other wires. In this case (see Fig. 60b)

$$D = d + b \cos \alpha, \quad D_0 = d. \quad (8.17)$$

The electrodynamic wave impedances of the structure at the same direction winding are

$$\begin{aligned} \rho_{11} = \rho_{22} = \rho_{33} = \rho_{44} = \rho_1 = 60 \ln(R/a), \quad \rho_{12} = \rho_{34} = \rho_2 = 60 \ln(R/\sqrt{ab}), \\ \rho_{13} = \rho_{24} = \rho_3 = 60 \ln(R/\sqrt{ab}), \quad \rho_{14} = \rho_{23} = \rho_4 = 60 \ln[R/\sqrt{a(d + b^2\pi/(4d))}], \end{aligned}$$



In the case of lines located at finite distance  $H$  from the cable axis, we find

$$\rho_1 = 60 \ln \frac{R(1 - H^2/R^2)}{a}.$$

These expressions for other quantity  $\rho_n$  remain valid. This means that the wave impedance of a two wire line, which has no losses and is situated inside a metal cylinder at a distance  $H$  from its axis, is in accordance with equation for  $W$ :

$$W = 60 \ln [b(1 - H^2/R^2)^2/a],$$

i.e., the wave impedance of this line decreases as the result of its displacement from the cable axis. When  $H$  is small and equal to  $\Delta$ , we arrive at the expression (8.14). Since the electrostatic wave impedances are

$$W_{ns} = \begin{cases} \Delta_N/\Delta_{ns}, & n = s, \\ -\Delta_N/\Delta_{ns}, & n \neq s, \end{cases}$$

where  $\Delta_N = |\rho_{ns}|$  is the  $N \times N$  determinant, and  $\Delta_{ns}$  is the cofactor of the determinant  $\Delta_N$ . For a structure made of four wires

$$\begin{aligned} W_{11} = W_{22} = W_{33} = W_{44} = W_1 = \Delta_4/\Delta_{11}, \quad W_{12} = W_{34} = W_2 = -\Delta_4/\Delta_{12}, \\ W_{13} = W_{24} = W_3 = -\Delta_4/\Delta_{13}, \quad W_{14} = W_{23} = W_4 = -\Delta_4/\Delta_{14}. \end{aligned}$$

The current and potential of wire  $n$  of an asymmetric line, consisting of  $N$  parallel wires, located above ground, found from expressions (1.34). The boundary conditions for the currents and voltages in the circuit, shown in Fig. 57, are

$$\begin{aligned} i_1(0) + i_2(0) = i_3(0) + i_4(0) = i_1(L) + i_2(L) = i_3(L) + i_4(L) = 0, \quad u_1(0) = u_2(0) + i_1(0) Z_1, \\ u_3(0) = u_4(0) + i_3(0) Z_2, \quad u_1(L) = u_2(L) + e, \quad u_3(L) = u_4(L) + i_3(L) Z_3. \end{aligned}$$

Substituting expressions (1.34) for the currents and voltages in these equations, we find

$$I_1 = \frac{e}{Z_1 \cos kL + 2j[\rho_1 - \rho_2 + (\rho_3 - \rho_4)A] \sin kL}, \quad I_3 = AI_1, \quad (8.18)$$

where

$$A = \frac{4(\rho_3 - \rho_4) + Z_1 Z_3 (1/W_3 - 1/W_4)}{-4(\rho_1 - \rho_2) + Z_2 Z_3 (1/W_1 + 1/W_2) + j2(Z_2 - Z_3) \cot kL}.$$

If  $\rho_3 = \rho_4$  (and, accordingly,  $W = W_4$ ), then  $A = 0$ , the current at the beginning of the second long line is zero. In this case, the presence of the second two-wire long line has no effect on the first line. This result obviously corroborates the fact that the asymmetry of cable leads in mutual coupling (crosstalk) between two two-wire lines.

Knowing all parameters in expressions (1.34), one can calculate the load impedance of the generator  $e$ :

$$Z_l = \frac{e}{i_1(L)} = 2 \frac{Z_1 + 2j[\rho_1 - \rho_2 + A(\rho_3 - \rho_4)] \tan kL}{2 + j[Z_1(1/(W_1 + 1/W_2) - AZ_2(1/W_3 - 1/W_4)) \tan kL]}$$

and the currents in the wires of the second (unexcited) line:

$$i_3(z) = I_1 A \cos kz + j I_1/2 [AZ_2(1/W_1 + 1/W_2) - Z_1(1/W_3 - 1/W_4)] \sin kz, \quad i_4(z) = -i_3(z).$$

The sum of the currents is zero, i.e., as in the case of a single long line placed into the screen, the in-phase current absent since the emf and the loads located only between wires of each line. The voltages across passive loads are

$$V_1 = i_1(0) Z_1 = I_1 Z_1 \quad V_2 = i_3(0) Z_2 = I_1 A Z_2,$$

$$V_3 = i_3(L) Z_3 = I_1 Z_3 \{A \cos kL + j0.5[AZ_2(1/W_1 + 1/W_2) - Z_1(1/(W_3 - 1/W_4))] \sin kL\},$$

As an example, consider a structure from two pairs of wires inside the screen with sizes (in millimeters):  $a = 0.2$ ,  $b = 0.5$ ,  $d = 2$ ,  $R = 2$ . If the loads are identical and equal to 100 Ohm, ratio  $A$  of the currents at the beginning of the second and first line is equal to 0.13. If the loads magnitudes are equal to the wave impedance of the single two-wire line inside the metal screen, i.e., 55 Ohm, the currents ratio is substantially increased ( $A = -0.76$ ). The absolute values of the currents depending on  $kz$  are plotted in Fig. 61. Here,  $k$  is the propagation constant of a wave in a medium,  $z$  is the coordinate along the line (see Fig. 59).

Consider the effect of loads placed between the wires and the screen, using a two-wire line as an example (Fig. 62). It differs from the circuit shown in Fig. 56 by connection of its wires near the generator to a screen through the complex impedance  $Z_1$  or  $Z_2$ . Their magnitudes depend on the circuit of a long line's excitation. In a real circuit in the capacity of exciting emf can act the secondary winding of the transformer. In this case impedances  $Z_1$  and  $Z_2$  are stray capacitances between the secondary winding and a cable screen.

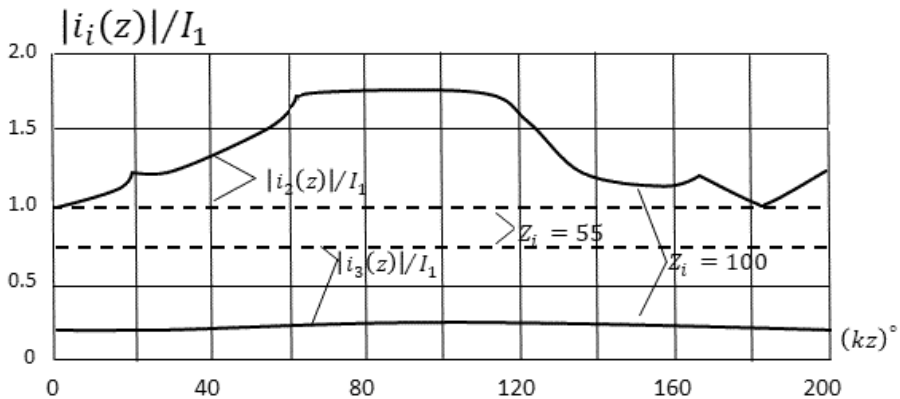
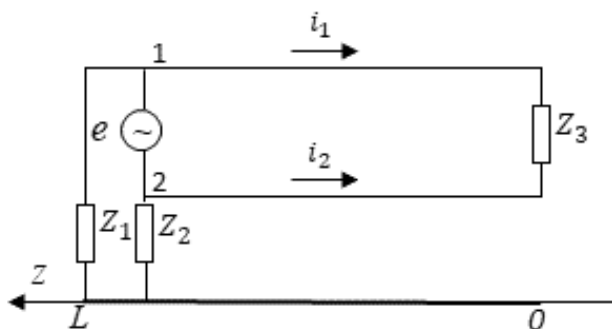


Fig. 61: The absolute values of the currents in the excited and unexcited wires.



**Fig. 62:** The equivalent circuit of a single line with loads connected between the wires and the screen.

The boundary conditions for the currents and potentials in the circuit, shown in Fig. 62, have the form

$$\begin{aligned} i_1(0) + i_2(0) &= 0, & u_1(0) &= u_2(0) + i_1(0)Z, \\ i_1(L) + i_2(L) + u_1(L)/Z_1 + u_2(L)/Z_2 &= 0, & u_1(L) &= e + u_2(L). \end{aligned} \quad (8.19)$$

Substituting expression (1.34) in the equations (8.19), we find the input impedance of a two-wire line

$$\begin{aligned} Z_l &= \frac{e}{i_1(L) + \frac{u_1(L)}{Z_1}} \\ &= \frac{Z \cos kL + j(\rho_{11} + \rho_{22} - 2\rho_{12})}{1 + \frac{U_1}{I_1} \left[ \frac{1}{Z_1} + j \left( \frac{1}{W_1} - \frac{1}{W_2} \right) \tan kL \right] + j \left[ \frac{Z}{W_{12}} + \frac{\rho_{11} - \rho_{22}}{Z_1} \right] \tan kL}, \end{aligned} \quad (8.20)$$

and the sum of the currents in the line wires is

$$i_s(z) = i_1(z) + i_2(z) = jI_1 \left[ Z \left( \frac{1}{W_{12}} - \frac{1}{W_{22}} \right) + \frac{U_1}{I_1} \left( \frac{1}{W_{11}} + \frac{1}{W_{22}} - \frac{2}{W_{12}} \right) \right] \sin kz. \quad (8.21)$$

Therefore, the placement of the loads between the wires and the screen leads to the appearance of the in-phase current in the wires and the current along the inner surface of the cable screen, equal in magnitude but opposite in direction. For two wires of the same radius situated symmetrically to the cylinder axis

$$Z_l = [Z + 2j(\rho_1 - \rho_2) \tan kL]/B,$$

where

$$B = 1 + j \frac{Z\rho_2}{\rho_1^2 - \rho_2^2} \tan kL + j \frac{1}{2(\rho_1 - \rho_2)} [Z + (\rho_1 + \rho_2)C]$$

$$+ \frac{1}{2Z_1} [Z + (\rho_1 + \rho_2)C + 2j(\rho_1 - \rho_2) \tan kL],$$

and

$$i_s(z) = j \frac{eC \sin kz}{Z \cos kL + j2(\rho_1 - \rho_2) \sin kL}.$$

It is not difficult to convince that, if  $\frac{1}{z_1} = \frac{1}{z_2} = 0$ , quantity  $C$  is zero and the expressions for  $U_1$  and  $Z_1$  coincide with the similar expressions for the circuit without loads. From the presented results it is easy to obtain also the expressions for the circuit with one load, if for example,  $\frac{1}{z_2} = 0$ .

The above analysis confirms that the cause of the appearance of in-phase currents in wires of line is the asymmetry of its excitation produced for example by the secondary transformer winding. Asymmetry of loads at  $z = 0$ , i.e., at the far end of line, produces similar results. The in-phase currents in the excited line create the in-phase currents in wires of the adjacent unexcited line, even if it is totally symmetric (with respect to ground and the excited line). Removal of the excitation and load asymmetry in the excited line results in the disappearance of these currents in wires of both lines.

In order to reduce or eliminate the in-phase currents, it is necessary to violate the asymmetry, e.g., to neutralize the effect of stray capacitances to ground (to the cable screen). To this end, in [29] it was proposed to compensate the current through stray capacitance with the current equal in magnitude and opposite in direction, which is created by an additional transformer winding.

As is shown in the Section 1.3, the theory of electrically coupled lines is based on the telegraph equations and on the relationship between the potential coefficients and the coefficients of electrostatic induction. In the case, when the wires and the medium have no losses, electrostatic  $W_{ns}$  and electrodynamic  $\rho_{ns}$  wave impedances between wires  $n$  and  $s$  are real-valued quantities, and  $k$  is the propagation constant of the wave in the medium.

As follows from the above, electrodynamic wave impedance  $\rho_{ns}$  is proportional to the own or mutual inductance of wires segment, i.e., is proportional to the reactance, which is connected in series with wires. Electrostatic wave impedance  $W_{ns}$  is proportional to the mutual capacitance between wires, i.e., to the susceptance between them. Therefore, it is expedient to connect the resistance of losses in a wire (e.g., the skin-effect loss) in series with the inductance and the leakage conductance—in parallel with the mutual capacitance.

In order to take into account, the loss in the medium and in the wires, one must consider that wave impedances  $W_{ns}$  and  $\rho_{ns}$  and the propagation constant  $k$  are complex values. If the inductance of the wire  $n$  per unit of its length is  $\Lambda_0$  and its active resistance is  $R_0$ , its impedance per unit length is  $j\rho_{nn} = j\omega\Lambda_0 + R_0$ , i.e., the own electrodynamic wave impedance of a loss wire is equal to

$$\rho_{nn} = \rho_0 (1 - jR_0/\rho_0),$$

where  $\rho_0 = \omega\Lambda_0$  is electrodynamic wave impedance in the absence of losses,  $R_0$  is total loss resistance in the wire  $n$  and in the metal screen per unit length.

For the mutual electrodynamic wave impedance between wires  $n$  and  $s$ , we obtain

$$\rho_{ns} = \rho_{ns0} (1 - jR_{ns0}/\rho_{ns0}),$$

where  $\rho_{ns0} = \omega M_{ns0}$ ,  $M_{ns0}$  is the mutual inductance between wires  $n$  and  $s$  per unit length, and  $R_{ns0}$  is the loss resistance in both wires per unit length.

Similarly, for the admittance between wires  $n$  and  $s$  per unit length we find:  $jW_{ns} = j\omega C_{ns0} + G_{ns0}$  i.e., the electrostatic wave impedance in a medium with losses is

$$W_{ns} = W_{ns0} (1 - jG_{ns0}/W_{ns0})$$

where  $W_{ns0} = \omega C_{ns0}$ . Here  $C_{ns0}$  and  $G_{ns0}$  are the mutual partial capacitance and the leakage conductance between wires  $n$  and  $s$  per unit length. Thus, the evaluation of the electrical performances of the coupled lines with losses can use the results previously received for the lossless lines by substitution of the complex wave impedances into obtained earlier expressions. Here, the losses in wires and losses in an imperfectly conducting metallic tube (screen) is considered.

A rigorous method for the calculation of characteristics of two-wire lines inside a metal screen allows to revise the mechanism of mutual coupling between lines in multi-conductor cables and to determine the values of voltage (interferences) across impedances located at the beginning and the end of the adjacent line at the given power in the main line. The reason of cross talks is the asymmetry of the cable structure (the different average distant between wires) and, accordingly, the asymmetric wave impedances. The asymmetry decrease reduces cross talks in multi-conductor cables, i.e., allows to increase the carrying capacity of a channel. This is true also for multi-conductor connectors.

The reason of the emergence of the in-phase currents in the lines of a multi-conductor cable is the asymmetry of excitation and loads. As it was noted, the compensation of this asymmetry permits to decrease the EM radiation and to reduce its susceptibility to external fields.

## References

- [1] Yang, J. and Kishk, A. (2012). A novel low-profile compact-directional ultra-wideband antenna: the self-grounded bow-tie antenna. *IEEE Transactions on Antennas and Propagation*. AP-60(3): 1214–1220.
- [2] Levin, B.M. (2021). About the new folded antenna. *Proc. of 25th Intern. Seminar/Workshop on DIPED, Tbilisi*, 141–145.
- [3] Levin, B.M. and Yakovlev, A.F. (1992). About one method of widening an antenna operation range. *Radiotechnics and Electronics Engineering*, 1: 55–64 (in Russian).
- [4] Doluchanov, M.P. (1972). *Wave Propagation*. Moscow: Communication (in Russian).
- [5] Wait J.R. (1981). *Wave Pergamon Theory*. New York: Pergamon.
- [6] Doluchanov, M.P. (1970). Underground wave propagation. *Radio*, 1: 42–43 (in Russian).
- [7] Drabkin, A.L. (1987). Wireless transmission of information in underground conditions. *Radiotechnics*, 5: 68–70 (in Russian).
- [8] Yazishin, V.I. (2011). *Underground Radio Communication in Mines (bibliographic index)*. Kharkov (in Russian).

- [9] Levin, B.M. (1998). Monopole and dipole antennas for marine-vehicle radio communications. S.-Petersburg: Абрис (in Russian).
- [10] Levin, B.M. (2019). Wide-range and Multi-frequency Antennas. London, New York: CRC Press.
- [11] Vershkov, M.V., Levin, B.M. et al. (1967). Antenna-mast. Patent of USSR 191651. Bulletin of Inventions, 4 (in Russian).
- [12] Vershkov, M.V., Levin, B.M. et al. (1973). Antenna-mast. Patent of USSR 328824. Bulletin of Inventions, 45 (in Russian).
- [13] Aizenberg, G.Z. and Uriyadko, V.N. (1959). Vertical linear radiator. Patent of USSR 122500, Bulletin of Inventions, 18 (in Russian).
- [14] Pirogov, A.A. (1972). On the prospects for the use of ballistic antennas. Radiotechnics, 1: 83–84 (in Russian).
- [15] Stark, A. (1980). Optimum pattern shape of a short-wave antennas from radio link computations. Proc. of Intern. Symposium on Antenna and Propagation, Quebec, 1: 306–307.
- [16] Low, P.E. (1983). Shipboard antennas. Dedham, MA: Artech House.
- [17] Vershkov, M.V., Levin, B.M. and Feldman, Ya. M. (1973). Антенна. Patent of USSR 341388. Bulletin of Inventions, 45 (in Russian).
- [18] Berry, T.G. and Kline, T.F. Self-extending antenna. Patent of USA 3467328.
- [19] Dmitrievsky, N.M. and Polinov, Yu. S. (1966). Extending antenna. Patent of USSR 185970, Bulletin of Inventions, 18 (in Russian).
- [20] McCorcle, M. Submarine mounted telescopic antenna. Patent of USA 3158865.
- [21] Altshuler, E.E. (1961). The travelling-wave linear antenna. IRE Transactions on Antennas and Propagation, 9: 324–329.
- [22] Gole, R.M., Drabkin, R.L. and Mirotvorsky, O.B. (1985). Antenna. Patent of USSR 380229. Bulletin of Inventions, 47 (in Russian).
- [23] Halpern, B. and Mittra, R. (1985). Broadband whip antennas for use in HF communications. Proc. of IEEE Symposium on Antennas and Propagation, Canada: 763–767.
- [24] Leontovich, M.A. (1945). Theory of forced electromagnetic oscillations in thin conductors of arbitrary cross-section and its applications to calculation of some antennas. Proc. of NII MPSS, 1: 1 (in Russian).
- [25] Yakovlev, A.F. and Pyatnenkov, A.E. (2007). Wide-Band Directional Antennas Arrays from Dipoles. S.-Petersburg (in Russian).
- [26] Yakovlev, A.F. and Levin, B.M. (1996). Reducing of the cable download effect on the characteristics of vertical aligned radiators and the reciprocal coupling between them. Proc. of 13th Intern. Wroclaw Symp. on Electromagn. Compatibility: 123–126.
- [27] Valenti, C. (2002). NEXT and FEXT models for twisted-pair North American loop plant. IEEE Journal Select. Areas Commun., 5: 893–900.
- [28] Iossel, Yu. Ya., Kochanov, E.S. and Strunsky, M.G. (1981). Calculation of electrical capacitance. Leningrad: Energoisdat (in Russian).
- [29] Cochrane, D. (2001). Passive cancellation of common-mode electromagnetic interference in switching power converters. M.S. Thesis, Virginia Polytechnic Inst. State Univ.: Blacksburg.



# Taylor & Francis

Taylor & Francis Group

<http://taylorandfrancis.com>

# Types of Antennas

---

asymmetrical antenna  
ballistic antenna  
cage antenna  
circular loop antenna  
complementary antenna  
conic antenna  
dipole antenna  
director-type antenna  
fan-shaped antenna  
flat antenna  
folded antenna  
impedance antenna  
log-periodic antenna  
microstrip antenna  
monopole antenna  
multi-folded antenna  
multi-radiator antenna  
multi-tiered antenna  
multi-wire antenna  
parabolic antenna  
rectangular loop antenna  
self-complementary antenna  
ship's antenna  
slot antenna  
symmetrical antenna  
transparent antenna  
two-tiered antenna  
V-antenna  
whip antenna



# Index

## A

anechoni chamber 106, 148, 292, 293, 295–297, 329–333  
 antenna effective height 42, 114, 222, 256, 359, 475, 477  
 antenna-mast 252, 476, 478, 479  
 arbitrary geometry 434  
 Array 74, 80, 108, 141–143, 146–148, 178, 179, 198, 247, 250, 251, 280–282, 285–288, 290, 291, 297–300, 327, 370, 376–380, 382, 424, 441, 443–445, 467, 470, 471, 493–495, 498,  
 asymmetrical antenna 1, 2, 12–14, 19, 21–24, 41, 60, 61, 91, 159, 168, 169, 229, 313, 315, 316, 320, 331, 369, 393, 405, 428, 429, 439, 447, 463, 507  
 asymmetrical long line 1, 2, 12–14, 19, 21–24, 41, 60, 61, 91, 159, 167, 168, 231, 313, 315, 316, 320, 331, 369, 393, 405, 427, 428, 429, 432, 446, 464, 506, 507  
 average potential 22, 42

## B

ballistic antenna 479, 480, 481  
 Boundary 2, 11, 14, 15, 19, 33, 42, 43, 46, 48, 53, 54, 65, 67, 69–71, 75, 81, 87, 88, 90, 93, 96, 106, 115, 130, 140, 145, 146, 151, 157, 160, 164, 169, 183, 199, 203, 210, 211, 234, 238, 245, 255, 272–274, 276–278, 307–309, 312, 321, 333, 340, 341, 367, 374, 384, 455, 459–461, 464, 484, 507, 512, 514  
 bracket 258–261  
 broadside array 141, 142, 148, 149

## C

cage antenna 16–18  
 capacitors 85, 391, 399, 448, 450, 456  
 cellular phone 41, 301, 307, 313, 320, 322  
 circular loop antenna 5, 6, 8, 9, 30, 60, 77, 78, 80, 82–84, 93–97, 99, 101, 106, 113–115, 117, 119, 120, 122, 123, 145, 150, 153, 157, 163, 178, 186, 193, 203, 218–224, 227, 229, 231, 246, 247, 250, 252, 261, 272–274, 276, 277, 279, 280, 289, 290, 296, 302, 311, 315,

329, 330, 332, 348, 349, 350, 352, 355, 358, 361–363, 365, 368, 370, 372, 375, 376, 379, 435, 450, 451, 474, 482, 495, 496, 501  
 coast radio center 471  
 coaxial chamber 24, 28, 97, 102, 171, 201, 279, 315, 329–334, 336, 338, 342, 347, 350, 351, 362, 363, 368, 370, 371, 375, 427–429, 434, 457, 458, 460, 462, 463, 465, 489, 493, 495–498  
 coaxial connectors 330  
 coaxial line 28, 171, 330, 370, 371, 428, 489  
 coaxial log-periodic 428, 429, 493  
 compensation 300, 302  
 complementary antenna 53, 77–80, 91–94, 96, 97, 99, 100–104, 106, 108, 109, 113, 117, 355, 358, 363, 370–373, 415, 423, 470, 471  
 complex potential 268, 272, 307, 329  
 Components 2, 8–10, 28, 35, 38, 39, 60, 70, 71, 85, 97, 101, 105, 108, 109, 119, 120, 122, 127, 128/, 137, 152–155, 164, 165, 169, 200, 2014, 204, 209, 210, 218, 225, 229–232, 246, 260, 269, 272, 302, 306, 313–315, 330, 331, 333, 357, 358, 374, 377, 401, 405, 424, 434, 436, 437, 454, 456, 461–463, 465, 489  
 concentrated loads 58  
 conformal transformations 109  
 conic antenna 104–105, 115  
 conical 93–95, 97–103, 114–117, 330, 343, 348, 349, 352, 356, 358, 362, 368, 371, 485, 498  
 conjugate gradients 402  
 constant surface impedance 53, 157, 169, 208, 385  
 cross-beam 261–263  
 Current distribution 1, 2, 5–7, 9–11, 15, 17, 25, 34, 41, 49, 53–55, 57, 58, 62, 69, 81, 88, 89, 90, 107, 117, 124, 135, 140, 147, 156–160, 169, 202, 205, 206, 211, 212, 214, 219, 233, 234, 235, 237, 239, 241, 242, 245, 246, 255, 257, 264, 306, 377, 384–401, 404, 405, 410–414, 417, 431, 432, 438–441, 445–447, 450, 452, 453, 455, 461–466, 468, 469, 474, 475, 489  
 current distribution 385, 390, 393, 411  
 curvilinear 96, 141, 215, 216, 270, 358, 359, 363, 364, 367, 434, 440, 441, 470

cylindrical 2, 4–6, 8, 18, 54, 58, 60, 82, 94, 96,  
97, 109–111, 113, 114, 117, 121, 122, 153,  
184, 187, 189, 193, 194, 196, 198, 234, 238,  
247, 248, 264, 265, 270, 272, 274, 280, 302,  
304, 308, 315, 330–336, 338–342, 348–351,  
356, 358–360, 362, 364, 367, 368, 372, 384,  
427, 441, 448, 468, 483, 484, 499, 503, 505

## D

dark spot 308, 309, 312  
dielectric cylinder 276, 341, 343  
dipole antenna 1, 6, 10, 11, 41, 55, 84, 86, 99,  
100, 106, 113, 119–121, 123, 125, 127, 128,  
130, 143, 144, 147, 155, 178, 180, 184, 187,  
189, 191, 193–197, 217–219, 244, 245, 280,  
302, 307, 311, 313–316, 318, 319, 350, 351,  
363, 367, 371, 373, 375, 378, 385, 387, 392,  
397–400, 412, 413, 416, 417, 422–427, 431,  
440, 441–443, 445, 446, 448, 453, 470, 493  
directional pattern 18, 41, 64, 75, 80, 83, 99, 120,  
121, 124, 140, 141, 178, 207, 216, 217, 221,  
222, 247, 248, 250–253, 256–258, 260–264,  
266, 281, 286, 287–291, 294–298, 300–302,  
311–313, 317, 382, 384, 387, 392, 397, 401,  
410, 426, 435, 438, 440, 443, 444, 455, 457,  
458, 459, 462, 464, 472, 474, 479, 482–484,  
493, 494, 496, 497, 500, 501, 503, 504  
directivity 93, 96, 97, 99, 120, 121, 140, 141,  
145, 149, 215, 236, 246–248, 264, 266, 267,  
280, 284–286, 288–291, 293, 295, 320, 321,  
363, 370, 385, 387, 413, 414, 420–422, 427,  
428, 430, 432–438, 440–446, 467, 471, 473,  
493, 495  
director-type antenna 416, 417, 419–421, 430,  
441  
discon 498  
discs 488

## E

effective length 61, 69, 75, 90, 124, 128, 130,  
133–135, 178, 193, 207, 210, 212, 217, 218,  
221, 222, 316, 388, 446, 451, 454, 456, 469  
electromagnetic compatibility 40, 504, 505  
electrostatic analogy 415, 416, 419, 428, 432  
electrostatic field 13, 66, 333, 344, 415, 416, 419,  
428, 432, 515  
electrostatic induction 13, 66, 344, 515

## F

fan-shaped antenna 475, 491  
ferrite shell 61  
flat antenna 87, 91, 101, 104, 107–109, 111, 115  
folded antenna 1, 12, 18, 23–29, 33–41, 65,  
67–73, 160, 168, 171, 173–175, 201, 254,

303, 314–318, 416, 430, 450, 452, 453,  
455–459, 462, 464, 466, 471, 475, 479, 490,  
491, 492

folded radiators 11, 12, 18, 23–29, 35–41, 65,  
67–73, 159, 160, 166, 171–175, 200, 254,  
303, 314–318, 418, 431, 450, 452, 453,  
455–459, 462, 464–465, 471, 476, 480, 491,  
492

frequency overlap ratio 108, 406, 407, 420, 458

## G

gain 74, 99, 104, 120, 121, 140–142, 145, 146,  
148, 149, 181, 252, 288, 290, 292, 295–297,  
300, 327, 363, 495  
goniometric antenna 217  
great folded antenna 491, 492

## H

horizontal load 11–13, 15, 41, 48, 59, 60, 99, 110,  
111, 113, 123, 125, 128, 133, 135, 139, 173,  
178, 217, 220, 222, 223, 232–234, 247–254,  
258–266, 281, 282, 288, 290, 291, 293–295,  
297–300, 301, 302, 309, 310, 311, 317, 323,  
324, 363, 364, 366, 367, 428, 445, 451, 453,  
457, 458, 464, 467, 470–475, 478, 482, 491,  
493, 497–503, 505  
Howe 69, 324

## I

impedance antenna 5, 11–19, 21, 22, 26–32, 34,  
35, 37–43, 46–48, 50, 53–109, 104–114,  
116, 117, 120, 121, 123, 127–137, 140,  
152–160, 163, 164, 166, 169, 171–178, 180,  
188, 189, 191–201, 202, 204–214, 218, 219,  
222, 229, 234, 235, 242, 245–248, 252,  
254–257, 260, 261, 264, 292, 303–306,  
314–317, 319, 322, 323, 329–334, 349–353,  
355–358, 362, 368, 369, 371–375, 377, 378,  
384–386, 388, 389, 392–397, 400, 401, 405,  
406, 414, 418–427, 442–448, 452, 454–456,  
461, 462, 469–474, 476, 482–484, 487, 488,  
499, 500, 503, 506–509, 512–516  
impedance long line 5, 11–19, 21, 22, 26–32, 34,  
35, 37–43, 46–48, 50, 53–73, 77, 79, 80–95,  
97–104, 107–109, 111–114, 116, 117, 120,  
121, 123, 127, 129–139, 152–158, 160, 161,  
164, 167, 168, 171–178, 180, 188, 189,  
191–198, 201, 202, 204–214, 218, 219, 223,  
231, 234–236, 242, 245–248, 252, 254, 292,  
303–306, 314–317, 319, 322, 323, 329–334,  
349, 350, 352, 353, 355–358, 362, 368, 369,  
371–375, 377, 378, 384–386, 388, 389,  
392–397, 400, 401, 405, 406, 414, 416, 417,  
421–427, 441, 443–446, 448, 452, 454–457,  
469–472, 474–476, 482, 483, 487, 488, 489,  
500, 501, 506–509, 511–516

in the ground 99, 152, 156, 161, 163, 164,  
166–169, 171–173, 357, 371, 373, 482

induced emf 15, 21, 35, 68, 121, 137, 138, 139,  
140, 152–157, 160, 161, 177, 189, 193, 194,  
198, 206, 214, 239, 241, 245–247, 268

inductive-capacitive load 476–479

in-phase 26, 27, 35, 67, 135, 146, 179, 180, 233,  
234, 236–239, 288, 290, 298, 303, 306, 315,  
317, 318, 333, 384–390, 393, 395, 399, 400,  
405, 411, 413, 414, 418–421, 428, 430–432,  
440, 445–447, 450–452, 455–457, 459,  
461–466, 489, 491, 506, 508, 513–516,

in-phase current distribution 393, 432, 446, 447

in-phase linear 239

input impedance 5, 11, 14, 15, 17, 18, 21, 26–30,  
32, 34, 35, 37–39, 42, 43, 46–48, 50, 55,  
56, 58–61, 67, 68–73, 77, 79, 80, 82, 84,  
85, 90, 92, 93, 95, 97, 98, 101–104, 107,  
108, 121, 127, 136, 137, 152–157, 160, 163,  
164, 171–175, 178, 180, 188, 189, 191–197,  
201, 202, 204, 205, 208–214, 218, 229, 235,  
247, 248, 252, 254, 256, 257, 260, 261, 264,  
303–305, 315–317, 319, 322, 323, 333, 352,  
353, 355–358, 362, 368, 369, 371, 374, 377,  
384, 388, 389, 392, 395, 396, 414, 418, 422,  
423–425, 427, 445–447, 452, 454, 456, 447,  
452, 454, 456, 461, 462, 469, 472–474, 476,  
484, 500, 503, 507–509, 514

inverted L antenna 42, 47, 48, 475, 476

## K

Kirchhoff equation 245

## L

Leontovich equation 87, 127, 136, 156, 160, 186,  
194, 195, 196, 203, 231, 234, 238

linear radiator 5, 14, 15, 17, 21, 22, 24–26, 28,  
29, 32, 35, 53, 71, 123, 124, 134, 140, 141,  
145, 161, 175, 183, 194, 196, 218, 221, 238,  
246, 280, 302–304, 307, 308, 317, 374, 384,  
393, 397, 377, 400, 4185, 419, 420, 430,  
434, 440, 441, 448, 452, 454, 455, 457–459,  
461, 462, 469, 490, 491

Load 3, 12, 13, 17–23, 30, 31, 37, 41–44, 46–51,  
64, 67, 84, 131, 158, 159, 177, 178, 193,  
205, 210, 234–239, 245, 252, 254, 303, 330,  
345, 377–379, 381, 384, 390–392, 394, 397,  
399, 400, 401, 405, 410, 458, 459, 464–466,  
476–480, 482, 488, 489, 494, 506–508, 512,  
515

log-periodic antenna 74, 106, 415, 421–424,  
426–434, 483, 493, 491, 494, 495, 500

Long line 6, 10, 11, 15–18, 21–23, 25–33, 35, 37,  
40, 53, 55–58, 62, 65, 68, 71, 79, 82, 94, 97,  
100, 107, 136, 155, 157, 158, 160, 168–173,  
175, 188, 191, 195, 196, 2085, 212, 217,

219, 231, 255, 276, 280, 303, 317, 333, 341,  
346, 349, 352, 358, 362, 367–369, 371–374,  
377, 385, 386, 388, 389, 392, 393, 395, 396,  
409, 410, 411, 414, 416, 417, 430, 452–454,  
456, 457, 508, 512, 513

loop antenna 82, 84–86, 120, 216–230, 326, 330,  
450–452, 482, 491

Los, ses 60, 85, 88, 90, 107, 121, 131, 152, 155,  
156, 161–166, 168–173, 195, 208, 209, 308,  
319, 332–334, 428, 447, 467,

loss resistance 21, 61, 152, 156, 161, 166–169,  
171–173, 258, 516

## M

magnetic antenna 1–3, 8, 53, 54, 60, 61, 71, 72,  
74, 75, 77–85, 92, 96, 100, 101, 120, 122,  
123, 150, 152, 161–167, 169, 171, 203, 208,  
218, 268, 307, 330–332, 334, 358, 362, 368,  
371, 415, 447, 448

magneto-dielectric shell 54, 59

matching level 42, 121, 358, 385, 447, 448, 484,  
488

mathematical programming 400, 401, 403, 405,  
410, 411, 428, 432, 441, 445

Maxwell equation 73, 150, 217, 274, 415

metal radiator 77, 128

metal superstructure 248, 250, 412, 479, 491

microstrip antenna 179, 370–382, 446–448

moments 18, 139, 241

monopole antenna 1, 2, 10, 11, 25–28, 32–35,  
37–41, 55, 58, 70, 90, 130, 162, 166, 167,  
171–173, 221, 229, 231, 247, 250, 251, 303,  
304, 315, 316–319, 373, 374, 385, 388, 407,  
410, 427, 428, 493

multi-folded antenna 18, 35, 36, 38, 40, 41, 166,  
172, 173, 314–318, 491

multi-radiator antenna 15–19, 21–23, 160, 489

multi-tiered antenna 410, 457, 458

multi-wire antenna 12, 15–18, 200, 367, 475,  
485, 495, 497, 499, 506

## P

parabolic antenna 96–100, 114, 115, 117, 178,  
243, 244, 297, 358, 359, 360–362, 366,  
368, 377

pattern factor 121, 236, 237, 287, 363, 401, 407,  
420, 421, 446, 482, 490

permeability 59–61, 71, 72, 75, 83, 87, 123, 163,  
208, 224, 258, 332, 340, 367, 468

permittivity 30, 59, 61, 72, 75, 106, 110, 123,  
163, 208, 218, 271–273, 275, 276, 278, 279,  
302, 307, 308, 330, 334, 335, 338, 339, 341,  
342, 346, 365, 369, 371, 372, 374, 376,  
379–381, 417, 446, 468, 508

PIFA 319–321

pillar 256, 257, 260, 262  
 plane-parallel 93, 270, 272, 346, 360, 367, 368, 376  
 pneumatic antenna 480, 481, 487  
 Pocklington's equation 215  
 potential coefficient 13–15, 22, 23, 31, 335, 340, 341, 508  
 Poynting vector 153  
 Principle of complementarity 92, 420  
 Principle of duality 74, 92, 350, 415  
 Principle of mutual compensation 41  
 Principle of similarity 73, 74, 415  
 Principle of superposition 25, 198  
 propagation constant 3, 12, 15, 17, 55, 57, 59, 60, 62, 63, 70, 81–84, 86, 89, 123, 128, 130, 131, 133, 135, 155–158, 172, 173, 204, 206, 208, 209, 211, 233–235, 255, 298, 332, 333, 369, 372–374, 385, 391–393, 397, 399, 400, 405, 410, 413, 418, 431, 446, 452, 468, 513, 515

## Q

quasi-Tchebyscheff 401, 407

## R

radiation resistance 35, 121, 129, 181, 254, 316, 445, 447, 476  
 rectangular loop antenna 82, 90, 96, 102, 111, 119, 141, 143, 167, 214, 216, 222–224, 227, 228, 230, 233, 269–271, 281, 282, 288, 314, 355, 357–359, 363, 365, 370, 371, 380, 414, 434, 450, 451, 455, 471  
 reflectivity 91, 97, 98, 101–103, 115, 470  
 reflector array 178, 179, 297, 376, 377, 416, 424, 441, 498  
 resistive coating 86, 87, 89, 131, 133, 135, 315, 353, 356, 358, 405, 480, 488, 489  
 root-mean-square 401, 407, 411  
 rotation symmetry 108, 113

## S

self-complementary antenna 74, 78, 91–94, 96, 97, 99, 100–104, 106, 108, 109, 113, 117, 355, 358, 363, 370–373, 415, 423, 470, 471  
 self-expanding 486  
 shifted feed point 167, 168  
 ship's antenna 246, 251, 225, 254, 258, 261, 474, 475, 478, 482, 483, 485, 495  
 sinusoidal 4, 6, 9, 10, 14, 34, 49, 55, 57, 81, 84, 88, 90, 123, 124, 128, 130, 131, 135, 137, 149, 150, 154–157, 187, 188, 190, 196, 197, 200, 205, 211, 213, 219, 233, 234–239, 244, 245, 247, 318, 384, 385, 387, 388, 392, 393, 405, 413, 414, 417, 419, 431, 432, 438, 440, 446, 447, 452, 453, 455, 462, 468, 469, 470

slot antenna 9, 74–86, 92–97, 101, 102, 106, 108, 110, 112–117, 230, 350–358, 362, 371–373, 377, 381, 382, 423, 424, 448  
 slowing 60, 71, 129, 133, 331, 376, 426  
 Spiral 58, 92, 95, 329–335, 337, 338–343, 352, 353, 426, 443, 432, 476, 477, 485, 486, 488, 498, 499, 504–507, 509, 511  
 standing wave ratio 97, 98, 101, 102, 105, 319, 470  
 steepest descent 402  
 stepped long line 7, 15, 56–58, 63, 108, 130, 135, 158, 212, 230, 386, 388, 397, 398, 414, 487  
 successive approximation 185  
 surface impedance 384  
 symmetrical antenna 1, 2, 6, 10, 12, 55, 75, 78, 93, 95, 96, 99, 100, 102, 104–106, 114, 115, 135, 153, 155, 157, 160, 198, 216, 224, 233–235, 247, 265–267, 280, 290, 315, 318, 319, 329, 331, 333, 352, 360, 368, 370, 372–374, 376, 414, 424, 428, 434, 439, 435, 440, 450, 452, 467  
 Synthesis of antennas of wide-band antennas 410  
 Synthesis of antennas with required current distribution 385, 393, 404, 411

## T

telegraph 11, 12, 15, 54, 65, 80, 88, 515  
 telescopic antenna 457, 485–488  
 Theorem about oscillating power 149  
 Theorem of equivalence 2, 54  
 Theorem of Floquet 308  
 Theorem of reciprocity 154, 177  
 Theorem of uniqueness 94, 109, 271, 272, 347, 359, 364  
 three-wire 39, 40, 42, 43, 49  
 transparent antenna 87–92, 133, 135  
 travelling wave ratio 319, 401, 446  
 trough 82, 263–267  
 two media 273, 274, 278, 280, 307, 308, 338, 341, 374  
 two radiators 78, 80, 89, 138, 140, 198–201, 206, 213, 298, 300, 302, 304, 305, 311, 323–326, 457, 504  
 two-row array 282, 285, 286  
 two-story 380, 381, 448  
 two-tiered antenna 457, 458, 459, 463–466

## U

underground 466, 467, 470, 471, 516  
 uniform array 15, 19, 56, 58, 66, 79, 82, 90, 95, 97, 101, 107, 114, 141, 146, 148, 149, 205, 250, 282, 290, 297, 330, 331, 352, 355, 356, 362, 369, 373, 386–389, 393, 397, 407, 415, 446, 455, 475, 489, 494, 500, 501, 503, 506  
 uniform excitation 146, 148, 149

uniform long line 15, 56, 66, 79, 90, 94, 97, 100,  
101, 107, 114, 117, 146, 148, 149, 205, 250,  
282, 290, 297, 330, 331, 352, 355, 356, 362,  
369, 373, 388, 389, 407, 474, 488, 493, 500,  
501, 506

upper excitation 491, 492

## V

---

V-antenna 95, 231–233, 397, 399, 412

volumetric antenna 4, 16, 99, 101, 113, 114, 120,  
268, 358, 361, 362, 471–474, 477, 485, 486,  
488

V-radiators 421

## W

---

wave impedance 11, 17, 26, 30, 31, 37, 41, 55,  
56, 57, 59, 71, 79, 81, 91, 92, 94, 97, 98,  
100–104, 107–109, 112–114, 116, 117, 120,  
123, 130, 136, 138, 175, 188, 191, 219, 223,

235, 236, 292, 303, 315, 319, 329, 330, 333,  
349–352, 355–358, 362, 369, 372–375, 377,  
378, 388, 394, 400, 401, 405, 424–427, 441,  
446, 448, 452, 470, 471, 476, 483, 506, 508,  
509, 511–513, 215, 516

weak field 40, 140

whip antenna 247, 248, 249, 252, 253, 255,  
258–262, 264, 405, 407, 457, 477–479, 483,  
484, 495, 499

wires 2, 6, 10–17, 19, 20, 22–33, 35, 37–44,  
46–51, 53–55, 65–67, 69, 71, 79, 80, 92,  
93, 96, 99, 100, 108, 109, 160, 164, 168,  
169, 171–173, 185, 198, 201, 214, 215, 219,  
220–223, 230, 231, 234, 236, 243, 246–248,  
250, 252, 258–261, 264, 265, 270, 272, 273,  
276, 277, 279, 280, 303, 305, 306, 314–318,  
329–343, 345, 346, 350, 351, 358–360, 362,  
365–371, 374, 393, 397, 405, 410, 413, 416–  
418, 422–425, 427, 430, 432, 441, 450–452,  
454–456, 458–466, 469, 472, 474, 475, 478,  
480, 483, 484, 488–491, 504, 506–516